Concepts of Theoretical Solid State Physics[1]

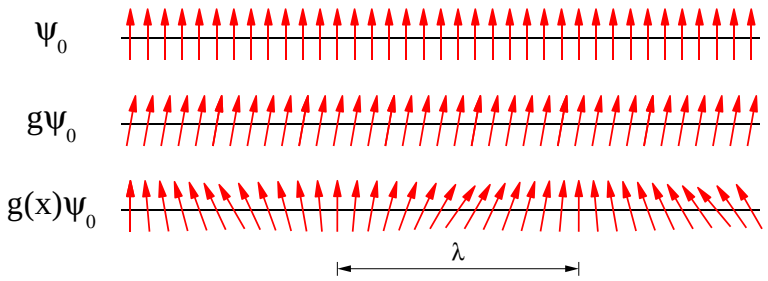

Alexander Altland and Ben Simons

Chapter 1

Collective Excitations: From Particles to Fields

The goal of this section is to introduce some fundamental concepts of classical field theory in the framework of a simple model of lattice dynamics. In doing so, we will become acquainted with the notion of a continuum action, elementary excitations, collective modes, symmetries and universality — concepts which will pervade the rest of the course.

One of the more remarkable facts about condensed matter physics is that phenomenology of phantastic complexity is born out of a Hamiltonian that does not look particularly impressive. Indeed, it is not in the least difficult to write down microscopic "condensed matter Hamiltonians" of reasonable generality. E.g. a prototypical metal might be described by

$$\begin{aligned} H &= H_{\rm e} + H_{\rm i} + H_{\rm ei}\,, \\ H_{\rm e} &= \sum_i \frac{\mathbf{p}_i^2}{2m} + \sum_{i\neq j} V_{\rm ee}(\mathbf{r}_i - \mathbf{r}_j), \\ H_{\rm i} &= \sum_I \frac{\mathbf{P}_I^2}{2M} + \sum_{I\neq J} V_{\rm ii}(\mathbf{R}_I - \mathbf{R}_J), \\ H_{\rm ei} &= \sum_{iI} V_{\rm ei}(\mathbf{R}_I - \mathbf{r}_i), \end{aligned} \tag{1.1}$$

where, $\mathbf{r}_i$ ($\mathbf{R}_I$) are the coordinates of $i, I = 1, \ldots, N$ valence electrons (ion cores) and $H_{\rm e}, H_{\rm i}$, and $H_{\rm ei}$ describe the dynamics of electrons, ions and the interaction of electrons and ions, respectively. (For details of the notation, see Fig. 1.1.) Of course, the Hamiltonian (9.30) can be made "more realistic", e.g. by remembering that electrons and ions carry spin, adding disorder or introducing host lattices with multi-atomic unit-cells, however for developing our present line of thought the prototype H will do fine.

The fact that an innocuously looking Hamiltonian like (9.30) is capable of generating a vast panopticum of metallic phenomenology can be read in reverse order: one will normally not be able to make theoretical progress by approaching the problem in an "ab

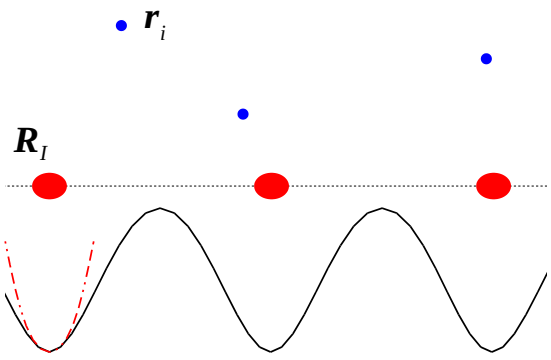

Figure 1.1: One-dimensional cartoon of a (metallic) solid. Positively charged ions located at positions $\mathbf{R}_I$ are sourrounded by a conduction electron cloud (electron coordinates denoted by $\mathbf{r}_i$). Both electrons and ions are free to move, as described by the kinetic energy terms $\sum \mathbf{p}_i^2/(2m)$ and $\sum \mathbf{P}_i^2/(2M)$ of Eq. (9.30), respectively. While, the motion of the ions is massively constrained by the lattice potential $V_{\rm ii}$ (indicated by solid lines) the dynamics of the electrons is affected by their mutual interaction ($V_{\rm ee}$) and the interaction with the core ions ($V_{\rm ei}$).

initio" manner, i.e. an approach that treats all microscopic constituents as equally relevant degrees of freedom. But how then, *can* successful analytical approaches be developed? Much of the answer to this question lies in a number of basic principles inherent to generic condensed matter systems

1. **Structural reducibility** of the problem. Which simply means that not all compounds of the Hamiltonian (9.30) need to be treated simultaneously. E.g. when the interest is foremostly in the vibrational motion of the ion lattice, the dynamics of the electron system can often be neglected or, at least, be treated in a simplistic manner. Similarly, much of the dynamics of the electrons is independent of the ion lattice, etc.

2. In the majority of condensed matter applications one is not so much interested in the full profile of a given system but rather in its energetically low lying dynamics. This is partly motivated by practical aspects (In daily life, iron is normaly encoutered at room temperature and not at its melting point.), partly by the tendency of large systems to behave "universal" at low temperatures. **Universality** means that systems differing in microscopic detail (e.g. different types of interaction potentials, ion species etc.) exhibit identical collective behaviour. As a physicist, one will normally seek for unifying principles in collective phenomena rather than to describe the specialties of individual species. Hence the fundamental importance of the universality priniciple. However, universality is equally important in the *practice* of condensed matter theory. It implies, e.g., that at low temperatures, details of the functional form of microscopic interaction potentials are of secondary importance, i.e. that one may employ *simple* model Hamiltonians.

3. For most systems of interest, the number of degrees of freedom, N, is formidably large, e.g. $N = \mathcal{O}(10^{23})$. However, contrary to the first impression, the magnitude of this figure is rather an advantage. The reason is that in addressing condensed matter problems we may make use of the **concepts of statistics** and that (precisely due to the largeness of N) statistical errors tend to be negligibly small[1].

4. Finally, condensed matter systems typically possess a number of intrinsic **symmetries**. E.g. our prototype Hamiltonian above is invariant under simultaneous translation and rotation of all coordinates which expresses the global Galilei invariance of the system (a continuous set of symmetries). Spin rotation invariance (continuous) and time reversal invariance (discrete) are other examples of frequently encountered symmetries. The general importance of symmetries needs no stressing: symmetries entail conservation laws and conservation laws simplify any problem. Yet in condensed matter physics, symmetries are "even more" important. The point is that a conserved observable is generally tied to an energetically low-lying excitation. In the universal low temperature regimes we will typically be interested in, it is precisely the dynamics of these low level excitations that governs the gross behaviour of the system. In subsequent section, the sequence "symmetry $\rightarrow$ conservation law $\rightarrow$ low-lying excitations" will be encountered time and again. At any rate, identification of the fundamental symmetries will typically be step no.1 in the analysis of a solid state system.

Employing a chain of harmonically bound atoms as an example, we next attempt to illustrate how such principles can be applied to construct "effective low energy" models of solid state systems. I.e. models that are universal, encapsulate the essential low energy dynamics, and can be related to experimentally observable data. We will also observe that the low energy dynamics[2] of large systems naturally relates to concepts of **field theory**; In a way, this and the next few chapters represent a first introduction to the use of field theoretical methods in solid state physics.

1.1 Classical Harmonic Chain: Phonons

Coming back to our prototype Hamiltonian (9.30), let us focus on dynamical behaviour of the positively charged *core ions* constituting the host lattice. For the moment, let us neglect the fact that atoms are quantum objects, i.e. treat the ions as *classical*. To further simplify the problem, we consider an atomic chain rather than a generic d-dimensional solid. I.e. the positions of the ions are given by a sequence of points with average spacing a. Relying on the reduction principle (1.) we next argue that to understand the behaviour

[1] The importance of this point is illustrated by the empirical observation that the most resistive system classes in physical sciences are of *medium* (and not large) scale. E.g. metallic clusters, medium size nuclei or large atoms consist of $\mathcal{O}(10^{1-2})$ fundamental constituents. Such problems are well beyond the reach of few body quantum mechanics while not yet accessible to reliable statistical modelling. Often the only viable path to approaching systems of this type is massive use of phenomenology.

[2] In this course we will focus on the *dynamical* behaviour of large systems, as opposed to *static* structural properties. E.g., we will not address questions related to the formation of definite crystallographic structures in solid state systems.

of the ions the dynamics of the conduction electronic sector of is of secondary importance, i.e. we set $H_{\rm e} = H_{\rm ei} = 0$.

At striktly zero temperature, the system of ions will be frozen out, i.e. the one-dimensional ion coordinates $R_I \equiv \bar{R}_I = Ia$ define a regularly spaced array. Any deviation from a perfectly regular configuration has to be payed for by a prize in potential energy. For low enough temperatures (priniciple 3.), this energy will be approximately quadratic in the small deviation from the equilibrium position (the dashed line in Fig. 1.1.) The reduced low energy **Hamiltonian**[3] of our system then reads

$$H = \sum_{I=1}^{N} \left(\frac{P_I^2}{2M} + \frac{k_s}{2}(R_I - R_{I+1} - a)^2 \right), \tag{1.2}$$

where the coefficient k_s determines the steepness of the lattice potential. Notice that H can be interpreted as the Hamiltonian of N particles of mass M elastically connected by springs with spring constant k_s (see Fig. 1.2).

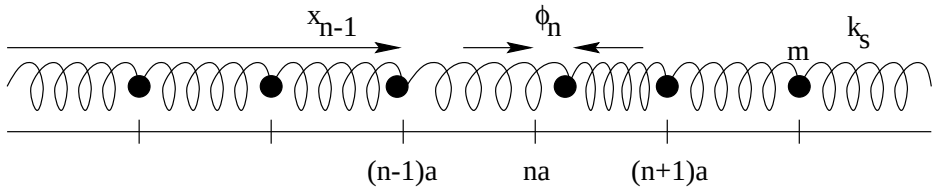

Figure 1.2: Toy model of a one-dimensional solid: A chain of elastically bound massive point particles. `change` $x \leftrightarrow R$

1.1.1 Lagrangian Formulation and Equations of Motion

What are the elementary low energy excitations of th is system? To answer this question we might, in prinicple, solve Hamiltons equations of motion; this is possible because H is quadratic in all its coordinates. However, we must keep in mind that few of the problems encountered in general solid state physics enjoy this property. Further, it seems unlikely that the low energy dynamics of a macroscopically large chain – which we know from our experience will be governed by *large scale* wave type excitations – is adequately described in terms of an "atomistic" language; the relevant degrees of freedom will be of different type. Rather what we should do is make much more excessive use from our basic principles 1.-4. Notably, we have so far neither payed attention to the intrinsic symmetry of the problem nor to the fact that N is large.

[3] Sir William Rowan Hamilton 1805-1865; a mathematician credited with the discovery of quaternions, the first non-commutative algebra to be studied. He also invented important new methods in Mechanics.

Now comes a very imporant point: To reduce a microscopically formulated model down to an effective low energy model, the Hamiltonian is often not a very convenient starting point. It is usually more efficient to start out from an *action*. As usual, the **Lagrangian action**[4] of our system is defined as

$$S = \int_0^T L(R, \dot{R}) dt,$$

where $(R, \dot{R}) \equiv \{R_I, \dot{R}_I\}$ symbolically represents the set of all coordinates and their time derivatives. The **Lagrangian** L related to the Hamiltonian (1.2) is given by

$$L = T - U = \sum_{I=1}^{N} \left(\frac{P_I^2}{2M} - \frac{k_s}{2}(R_I - R_{I+1} - a)^2 \right), \tag{1.3}$$

where T and U stand for kinetic and potential energy, respectively.

▷ EXERCISE. Recapitulate the connection between Hamiltonian and Lagrangian in N-particle classical mechanics.

For convenience we assume that our atomic chain has the topology of a ring, i.e. adopt periodic boundary conditions $R_{N+1} = R_1$. Further, anticipating that the effect of lattice vibrations on the solid is weak (i.e. long-range atomic order is maintained) we assume that the deviation from the equilibrium position is small ($|R_I(t) - \bar{R}_I| \ll a$), i.e. the integrity of the solid is maintained. With $R_I(t) = \bar{R}_I + \phi_I(t)$ ($\phi_{I+1} = \phi_1$) the Lagrangian (1.3) simplifies to

$$L = \sum_{I=1}^{N} \left(\frac{M}{2}\dot{\phi}_I^2 - \frac{k_s}{2}\left(\phi_{I+1} - \phi_I\right)^2 \right).$$

To make further progress, we now use that we are not concerned with the behaviour of our system on 'atomic' scales. (In any case, for such purposes a modelling like the one above would be much too primitive!) Rather, we are interested in experimentally observable behaviour that manifests itself on macroscopic length scales (principle 2.). For example, one might wish to study the specific heat of the solid in the limit of infinitely many atoms (or at least a macroscopically large number, $O(10^{23})$). Under these conditions, microscopic models can usually be substantially simplified (principle 3.). In particular it is often permissible to subject a discrete lattice model to a so-called **continuum limit**, i.e. to neglect the discreteness of the microscopic entities of the system and to describe it in terms of effective continuum degrees of freedom.

[4] Joseph-Louis Lagrange 1736-1813; Lagrange was a mathematician who excelled in all fields of analysis, number theory, analytical, and celestial mechanics. In 1788 he published Mécanique analytique, which summarised all the work done in the field of mechanics since the time of Newton and is notable for its use of the theory of differential equations. In it he transformed mechanics into a branch of mathematical analysis.

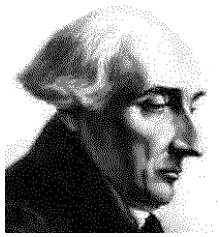

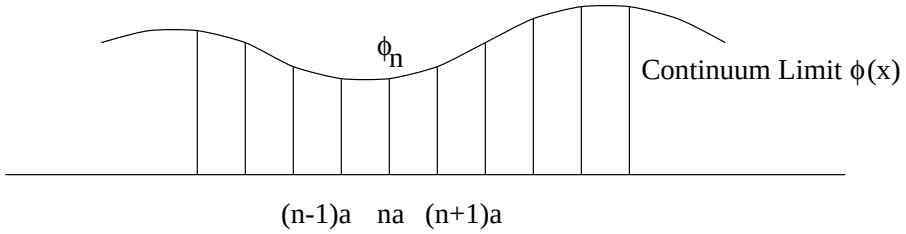

Figure 1.3: Continuum limit of the harmonic chain. For clarity, the (horizontal) distortion of the point particles has been plotted against the vertical.

In the present case, taking a continuum limit amounts to describing the lattice fluctuations ϕ_I in terms of smooth functions of a continuous variable x (Fig. 1.3). Clearly such a description makes sense only if relative fluctuations on atomic scales are weak. (Otherwise the smoothness condition would be violated.) However, if this condition is met – as it will be for sufficiently large values of the stiffness constant k_s – the continuum description is much more powerful than the discrete encoding in terms of the 'vector' $\{\phi_I\}$. All steps we need to take to go from the Lagrangian to concrete physical predictions will be much easier to formulate.

Introducing continuum degrees of freedom $\phi(x)$, and applying a first order Taylor expansion,[5] we define

$$\phi_I \to a^{1/2}\phi(x)\Big|_{x=Ia}, \qquad \phi_{I+1}-\phi_I \to a^{3/2}\partial_x\phi(x)\Big|_{x=Ia}, \qquad \sum_{I=1}^{N} \longrightarrow \frac{1}{a}\int_0^L dx,$$

where $L = Na$. Note that, as defined, the functions $\phi(x,t)$ have dimensionality $[\text{Length}]^{1/2}$. Expressed in terms of the new degrees of freedom, the continuum limit of the Lagrangian then reads

$$L[\phi] = \int_0^L dx\ \mathcal{L}(\phi, \partial_x\phi, \dot{\phi}), \qquad \mathcal{L}(\phi, \partial_x\phi, \dot{\phi}) = \frac{m}{2}\dot{\phi}^2 - \frac{k_s a^2}{2}(\partial_x\phi)^2, \tag{1.4}$$

where the **Lagrangian density** $\mathcal{L}$ has dimensionality [energy]/[length] and we have designated the particle mass by the more common symbol $m \equiv M$. Similarly, the classical action assumes the continuum form

$$\boxed{S[\phi] = \int dt\ L[\phi] = \int dt \int_0^L dx\ \mathcal{L}(\phi, \partial_x\phi, \dot{\phi}).} \tag{1.5}$$

We have thus succeeded in abandoning the N-point particle description in favour of one involving *continuous* degrees of freedom, a **(classical) field**. The dynamics of the latter is specified by the **functionals** L and S which represent the continuum generalisations of the discrete classical Lagrangian and action, respectively.

▷ INFO. The continuum variable ϕ is our first encounter with a *field*. Before proceeding with our example, let us pause to make some preliminary remarks on the general definition of

[5] Indeed, for reasons that will become clear, higher order contributions to the Taylor expansion are immaterial in the long-range continuum limit.

these objectcs. This will help to place the subsequent discussion of the atomic chain into a larger context.

Mathematically speaking, a field is a mapping

$$\begin{aligned} \phi: \quad & M \to T, \\ & z \mapsto \phi(t), \end{aligned}$$

from a certain manifold M, often called the 'base manifold', into a target or field manifold T, see Fig. 1.4. In our present example, $M = [0, L] \times [0, T] \subset \mathbb{R}^2$ is the product of intervals in space and time, and $T = \mathbb{R}$ is the real numbers. In general applications, the base manifold will be a (subset of) some d-dimensional space-like manifold $\mathcal{R}$ multiplied by a time-like interval: $M \subset \mathcal{R} \times \mathbb{R}$. (E.g. in our present example, $\mathcal{R} \simeq S_1$ is isomorphic to the unit circle S_1.) Sometimes, especially in problems relating to statistical mechanics, $M \subset \mathcal{R}$ is just spacelike. However, we are always free to assume that *locally* M is isomorphic to some subsset of $d+1$- or d-dimensional real vector space. In contrast, the target manifold can be just *any* (differentiable) manifold. From real or complex numbers, over vectorspaces and groups to the fanciest objects of mathematical physics.

In applied field theory, fields do not appear as final objects but rather as input to *functionals* (see Fig. 1.4) Mathematically, a functional $S : \phi \mapsto S[\phi] \in \mathbb{R}$ is a mapping that that takes a field as its argument and maps it into the real numbers. The functional profile $S[\phi]$ essentially determines the character of a field theory. Notice that the argument of a functional is commonly indicated in angular brackets $[\,.\,]$.

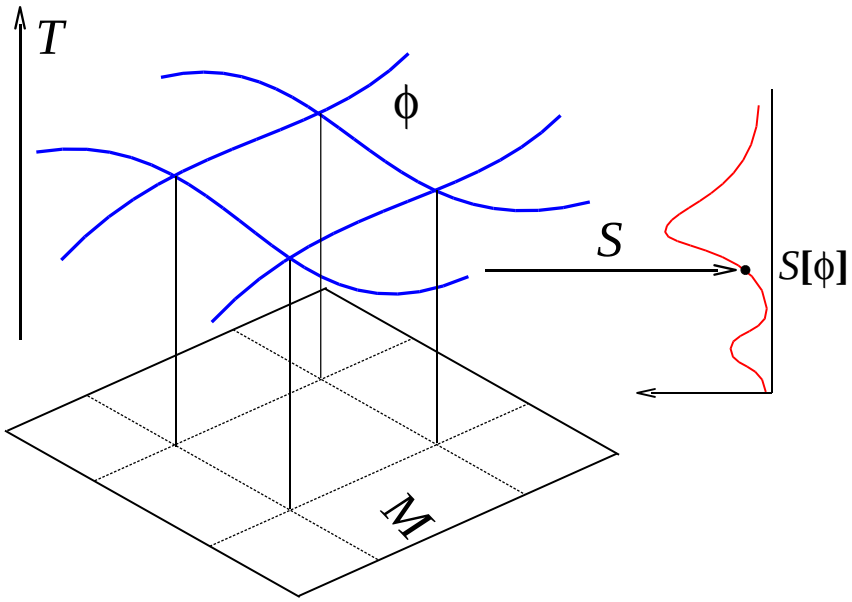

Figure 1.4: Schematic vizualization of a field: a mapping ϕ from a base manifold M into a target space T (here the real numbers, but T can be more complicated). A functional assigns to each ϕ a real number $S[\phi]$. The grid embedded into M indicates that fields in condensed matter physics arise as continuum limits of discrete mappings.

While these formulations may appear unneccessarily abstract, remembering the dry mathematical backbone of the theory often helps to avoid confusion. At any rate, it takes some time and practice to get used to the concept of fields and functionals. Conceptual difficulties

in handling these objects can be overcome by remembering that any field in condensed matter physics arises as the limit of a *discrete* mapping. E.g. in our example, the field $\phi(x)$ obtained as continuum approximation of the discrete vector $\{\phi_I\} \in \mathbb{R}^N$; the function*al* $L[\phi]$ is the continuum limit of the functi*on* $L : \mathbb{R}^N \to \mathbb{R}$, etc. While in practical calculations fields are usually easier to handle than their discrete analogs, it is sometimes easier to think about problems of field theory in a discrete language. Within the disrcrete picture, the mathematical aparatus of field theory reduces to finite dimensional calculus.

Although Eq. (1.4) contains the full information about the model, we have not yet learned much about its actual behaviour. To extract concrete physical information from Eq. (1.4) we need to derive **equations of motion**. At first sight, it may not be entirely clear what is meant by the term 'equations of motion' in the context of an infinite dimensional model: The equations of motion relevant for the present problem obtain as generalization of the conventional Lagrange equations of N-particle classical mechanics to a model with infinitely many degrees of freedom. To derive these equations we need to generalize Hamilton's extremal principle, i.e. the route from an action to the associated equations of motion, to infinite dimensions. As a warmup, let us briefly recapitulate how the extremal principle worked for a system with one degree of freedom:

Suppose the dynamics of a classical *point* particle with coordinate $x(t)$ is described by the classical Lagrangian $L(x, \dot{x})$, and action $S[x] = \int dt L(x, \dot{x})$. **Hamilton's extremal principle** states that the configurations $x(t)$ that are *actually realised* are those that extremise the action $\delta S[x] = 0$. This means that for any smooth curve $t \mapsto y(t)$,

$$\lim_{\epsilon \to 0} \frac{1}{\epsilon}(S[x + \epsilon y] - S[x]) = 0. \tag{1.6}$$

I.e. to first order in ϵ the action has to remain invariant. Applying this condition, one finds that it is fulfilled if and only if x solves **Lagrange's equation of motion**

$$\boxed{\frac{d}{dt}(\partial_{\dot{x}} L) - \partial_x L = 0.} \tag{1.7}$$

▷ Exercise. Recapitulate the derivation of (1.7) from the classical action.

In Eq. (1.5) we are dealing with a system of infinitely many degrees of freedom $\phi(x, t)$. Yet Hamilton's principle is general and we may see what happens if (1.5) is subjected to an extremal principle analogous to Eq. (1.6). To do so, we substitute

$$\phi(x, t) \to \phi(x, t) + \epsilon\eta(x, t)$$

into Eq. (1.5) and demand vanishing of the first order contribution to an expansion in ϵ (see Fig. 1.5). When applied to the specific Lagrangian (1.4), substituting the 'varied' field leads to

$$S[\phi + \epsilon\eta] = S[\phi] + \epsilon \int dt \int_0^L dx \left(m\dot{\phi}\dot{\eta} - k_s a^2 \partial_x \phi \partial_x \eta \right) + \mathcal{O}(\epsilon^2).$$

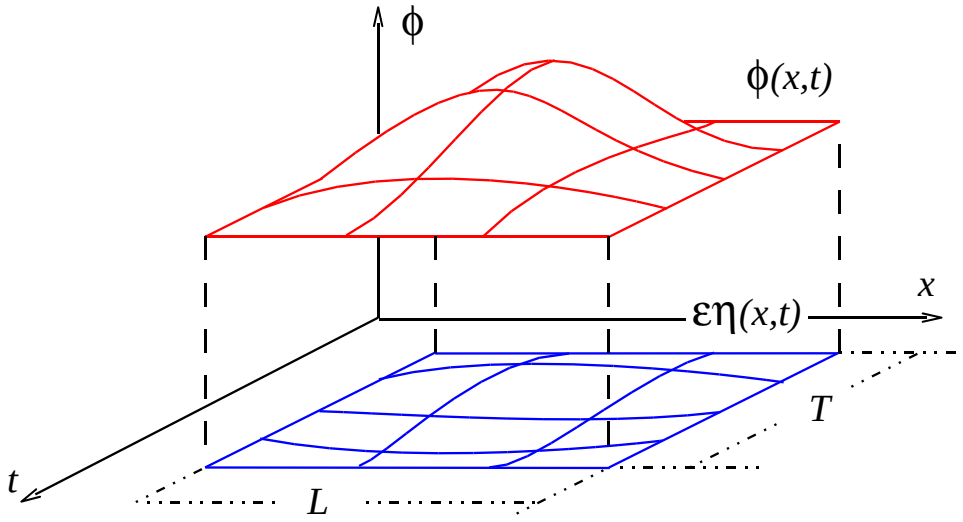

Figure 1.5: Schematic diagram showing the variation of the field associated with the action functional. Notice that the variation $\epsilon\eta$ is supposed to vanish on the boundaries of the base $M = [0, L] \times [0, T]$.

Integrating by parts and demanding that the contribution linear in ϵ vanishes, one obtains

$$\int dt \int dx \left(m\ddot{\phi} - k_s a^2 \partial_x^2 \phi \right) \eta = 0.$$

(Notice that the boundary terms vanish identically.) Now, since η was defined to be an arbitrary smooth function, the integral above can only vanish if the term in parentheses is globally vanishing. Thus the equation of motion takes the form of a **wave equation**

$$\boxed{\left(m\partial_t^2 - k_s a^2 \partial_x^2\right) \phi = 0.} \tag{1.8}$$

The solutions of Eq. (1.8) have the general form $\phi_+(x-vt)+\phi_-(x+vt)$ where $v = a\sqrt{k_s/m}$, and $\phi_\pm$ are arbitrary smooth functions of the argument. From this we can deduce that the basic low energy **elementary excitations** of our model are lattice vibrations propagating as **sound waves** to the left or right at a constant velocity v (see Fig. 1.6)[6]. The trivial behaviour of our model is of course a direct consequence of its simplistic definition – no dissipation, dispersion or other non-trivial ingredients. Adding these refinements leads to the general classical theory of lattice vibrations (see, e.g., Ref. [**?**]). Finally, notice that the elementary excitations of the chain have little in common with its "microscopic" constitutents (i.e. the atomic oscillators.) They rather are **collective excitations**, i.e. excitations comprising a macroscopically large number of microscopic degrees of freedom.

▷ INFO. The 'relevant' excitations of a condensed matter system can but need not be of collective type. E.g. the interacting electron gas, a system to be discussed in detail below, supports microscopic excitations – viz. charged quasi-particles standing in 1-1 correspondence

[6]Striktly speaking the modeling of our system enforces a periodicity constraint $\phi_\pm(x + L) = \phi_\pm(x)$. However, in the limit of a large system, this aspect becomes inessential.

with the electrons of the original microscopic system – and collective excitations – plasmon modes of large wavelength. The nature of the fundamental excitations is often far from obvious from the microscopic definition of a model. In fact, the mere *identification* of the relevant excitations often represents the most important step in the solution of a condensed matter problem.

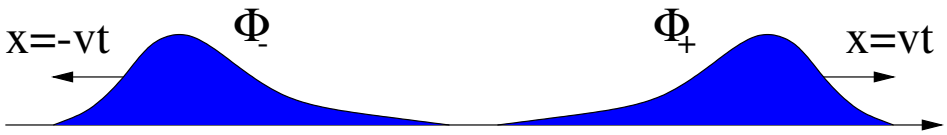

Figure 1.6: Visualisation of the fundamental left and right moving excitations of the classical harmonic chain.

1.1.2 Hamiltonian Formulation

An important characteristic of any excitation is its *energy*. How much energy is stored in the sound waves of the harmonic chain? To address this question, we need to switch back to a Hamiltonian formulation. This is, again, done by generalizing standard manipulations from point mechanics to the continuum. Remembering that for a Lagrangian, $L(x, \dot{x})$ of a point particle, $p \equiv \partial_{\dot{x}} L$ is the momentum conjugate to the coordinate x, we consider the Lagrangian *density* and define

$$\boxed{\pi \equiv \frac{\partial \mathcal{L}(\phi, \partial_x \phi, \dot{\phi})}{\partial \dot{\phi}} \quad .} \tag{1.9}$$

as the **canonical momentum** associated to ϕ. (In the field theory literature it is popular to denote the momentum by Greek letters.) In common with ϕ the momentum π is a continuum degree of freedom. At each space point it may take an independent value. Notice that $\pi(x)$ is nothing other than the continuum generalization of the lattice momentum P_I of Eq. (1.2). (I.e. applied to P_I, a continuum approximation like $\phi_I \to \phi(x)$ would produce $\pi(x)$.)

The **Hamiltonian density** is then defined as usual through Legendre transformation,

$$\boxed{\mathcal{H}(\phi, \partial_x \phi, \pi) = \left(\pi \dot{\phi} - \mathcal{L}(\phi, \partial_x \phi, \dot{\phi}) \right) \Big|_{\dot{\phi} = \dot{\phi}(\phi, \pi)}} \,, \tag{1.10}$$

from where the full Hamiltonian obtains as $H = \int_0^L \mathcal{H} dx$.

▷ EXERCISE. Verify that the transition $L \to H$ is a straightforward continuum generalization of the Legendre transformation of the N-particle Lagrangian $L(\{\phi_I\}, \{\dot{\phi}_I\})$.

Having introduced a Hamiltonian, we are in a position to determine the energy of sound waves. Application of (1.9) and (1.10) to the Lagrangian of the atomic chain yields $\pi(x,t) = m\dot{\phi}(x,t)$ and

$$H[\pi,\phi] = \int dx \left(\frac{1}{2m}\pi^2 + \frac{k_s a^2}{2}\partial_x\phi\partial_x\phi \right). \tag{1.11}$$

We next evaluate this function on a sound wave, i.e. on a specific solution of the equations of motion. Considering for definiteness a right-moving excitation, $\phi(x,t) = \phi_+(x-vt)$, we find $\pi(x,t) = -mv\partial_x\phi_+(x-vt)$ and

$$H[\pi,\phi] = k_s a^2 \int dx[\partial_x\phi_+(x-vt)]^2 = k_s a^2 \int dx[\partial_x\phi_+(x)]^2,$$

i.e. a positive definite time independent expression as one would expect.

Notice an interesting feature of the energy functional: in the limit of an infintelty shallow excitation, $\partial_x\phi_+ \to 0$, the energy vanishes. This brings the **symmetry** principle, 4.), not considered so far, onto the stage: The Hamiltonian of an atomic chain is invariant under simultaneous translation of all atom coordinates by a fixed increment: $\phi_I \to \phi_I + \delta$, where δ is constant. This expresses the fact that a global translation of the solid as a whole does not affect the internal energy. Now, the ground state of any specific realization of the solid will be defined through a static array of atoms, each located at a fixed coordinate $R_I = Ia \Rightarrow \phi_I = 0$. We say that the translational symmetry is "spontaneously broken", i.e. the solid has to decide where exactly it wants to rest. However, spontaneous breakdown of a symmetry does not imply that the symmetry disappeared, on the contrary: Infinite wavelength deviations from the pre-assigned ground state come close to global translations of (macroscopically large portions of) the solid and, therefore, cost a vanishingly small amount of energy. This is the reason for the vanishing of the sound wave energy in the limit $\partial_x\phi \to 0$. It is also our first encounter with the aforementioned phenomenon that symmetries lead to the formation of soft, i.e. low-energy excitations. A much more systematic exposition of these connections will be given in chapter ** below.

To conclude our discussion of the classical harmonic chain, let us consider the **specific heat**, i.e. a quantity directly accessible to experimental measurement. An rought estimate of this quantity can readily be obtained from our initial harmonic Hamiltonian (1.2). According to the principles of statistical mechanics, the thermodynamic energy density is given by

$$u = \frac{1}{L}\frac{\int d\Gamma e^{-\beta H} H}{\int d\Gamma e^{-\beta H}} = -\frac{1}{L}\partial_\beta \ln\left(\int d\Gamma e^{-\beta H} \right),$$

where $\beta = 1/T$, $\mathcal{Z} \equiv \int d\Gamma e^{-\beta H}$ is the **Boltzmann partition function**[7] and the phase

[7] Ludwig Boltzmann 1844-1906: physicist whose greatest achievement was in the development of statistical mechanics, which explains and predicts how the properties of atoms (such as mass, charge, and structure) determine the visible properties of matter (such as viscosity, thermal conductivity, and diffusion).

space volume element

$$d\Gamma = \prod_{I=1}^{N} dR_I dP_I.$$

The specific heat then obtains as $c = \partial_T u$. To determine the temperature dependence of this quantity, we use that upon rescaling integration variables,

$$R_I \to \beta^{-1/2} X_I \qquad P_I \to \beta^{-1/2} Y_I,$$

the exponent $\beta H(R,P) \to H(X,Y)$ becomes independent of temperature. (Notice that this relies on the quadratic dependence of H on both R and P.) The integration measure transforms as $d\Gamma \to \beta^{-N} \prod_{I=1}^{N} dX_I dY_I \equiv \beta^{-1} d\Gamma'$. Expressed in terms of the rescaled variables, the energy density reads as

$$u = -\frac{1}{L}\partial_\beta \ln\left(\beta^{-N} K\right) = \rho T,$$

where $\rho = \frac{N}{L}$ is the density of atoms and we have used that the constant $K \equiv \int d\Gamma' e^{-H(X,Y)}$ is independent of temperature. We thus find a temperature independent specific heat $c = \rho$. Notice that c is fully universal, i.e. independent of the material constants M and k_s determining H. (IN fact, we could have anticipated this result from the equipartition theorem of classical mechanics, i.e. the law that in a system with N degrees of freedom the energy scales like $U = NT$.)

How do these findings compare with experiment? Fig. 1.7 shows the specific heat of various insulatoring, semiconducing and metalic solids[8]. For large temperatures, the specific heat approaches a constant value, in accord with our so far analysis. However, for lower temperatures, drastic deviations from $c = \text{const.}$ occur. The strong temperature dependence invalidates attempts to explain the deviations by inaccurate modeling. It is rather indicative of a *quantum phenomenon*. Indeed, we have so far totally neglected the quantum nature of the atomic oscillators. In the next chapter we will cure this defficiency and discuss how the the effective low energy theory of the harmonic chain can be promoted to a quantum field theory. However, before proceeding with the development of the theory let us pause to introduce a number of mathematical concepts that surfaced above in a way that survives generalization to more interesting problems.

1.2 Functional Analysis and Variational Principles

Let us revisit the derivation of the equations of motion (1.8). Although straightforward, the calculation was neither efficient, nor did it reveal general structures. In fact, what we did — expanding explicitly to first order in the variational parameter ϵ — had the same status as evaluating derivatives by explicitly taking limits: $f'(x) = \lim_{\epsilon\to 0}(f(x+\epsilon) - f(x))/\epsilon$. Moreover, the derivation made explicit use of the particular form of the Lagrangian, thereby being of limited use with regard to a general understanding of the construction scheme. Given the importance attached to extremal principles in all of field

[8] In metals, the specific heat due to lattice vibrations exceeds the specfic heat of the free conduction electron for temperatures larger than a few Kelvin.

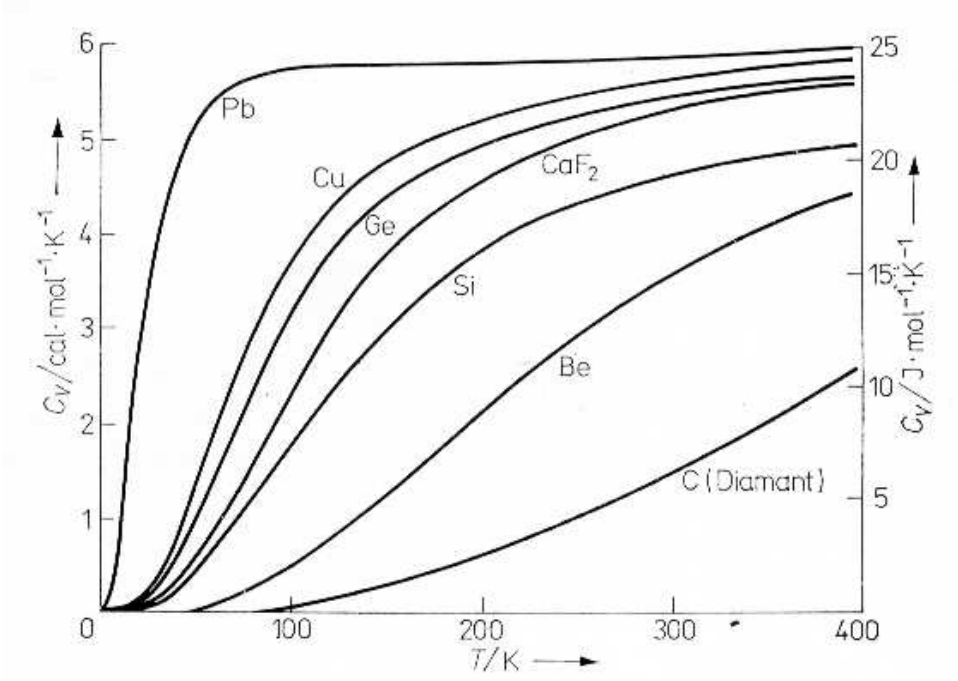

Figure 1.7: Specific heat c of various different solids. At large temperatures, the specific heat approaches a constant value, as predicted by the analysis of the classical harmonic model system. However, for small temperatures, deviations from $c = \text{const.}$ are grave: quantum effects.

theory, it is worthwhile investing some effort in constructing a more efficient scheme for general variational analysis of continuum theories. In order to carry out this program we first need to introduce a mathematical tool of functional analysis, viz. the concept of functional differentiation.

In working with functionals, one is often concerned with how a given functional behaves under (small) variations of its argument function. where h is an 'infinitely small' increment function. In ordinary analysis, questions of this type are commonly addressed by exploring *derivatives*, i.e. what we need to do is generalize the concept of a derivative to functionals. This is achieved by the following definition: A functional F is called differentiable if

$$F[f + \epsilon g] - F[f] = \epsilon DF_f[g] + \mathcal{O}(\epsilon^2),$$

where the **differential** DF_f is a linear functional (i.e. one with $DF_f[g_1 + g_2] = DF_f[g_1] + DF_f[g_2]$), ϵ a small parameter and g an arbitrary function. The subscript indicates that the differential generally depends on the 'base argument' f. A functional F is said to be **stationary** on f, iff $DF_f = 0$.

In principle, the definition above answers our question for a stationarity condition. However, to make actual use of the definition, we still need to know how to compute the differential DF and how to relate the differentiability criterion to the concepts of ordinary calculus. In order to understand how answers to these questions can be systematically found, it is helpful to temporarily return to a discrete way of thinking, i.e. to interpret the argument f of a functional $F[f]$ as the limit $N \to \infty$ of a discrete vector $\mathbf{f} =$

$\{f_n \equiv f(x_n), n = 1, \ldots N\}$, where $\{x_n\}$ denotes a discretisation of the support of $\mathbf{f}$ (c.f. Fig. 1.3 $\phi \leftrightarrow f$). Prior to taking the continuum limit, $N \to \infty$, $\mathbf{f}$ has the status of a N-dimensional vector and $F(\mathbf{f})$ is a function defined over N-dimensional space. After the continuum limit, $\mathbf{f} \to f$ becomes a function itself and $F(\mathbf{f}) \to F[f]$ becomes a functional.

Now, within the discrete picture it is clear how the variational behaviour of functions is to be analysed. E.g. the condition that for all ϵ and all vectors $\mathbf{g}$, the linear expansion of $F(\mathbf{f} + \epsilon\mathbf{g})$ ought to vanish, is simply to say that the ordinary differential, $dF_{\mathbf{f}}$, defined through

$$F(\mathbf{f} + \epsilon\mathbf{g}) = F(\mathbf{f}) + \epsilon dF_{\mathbf{f}}\,\mathbf{g} + \mathcal{O}(\epsilon^2)$$

must be zero. In practice, one often expresses conditions of this type in terms of a certain basis. E.g. in a Cartesian basis of N unit vectors, $\hat{\mathbf{e}}_n$, $n = 1, \ldots, N$,

$$dF_{\mathbf{f}}\,\mathbf{g} \equiv \langle \boldsymbol{\nabla} F_{\mathbf{f}}, \mathbf{g} \rangle,$$

where $\langle \mathbf{g}, \mathbf{f} \rangle \equiv \sum_{n=1}^{N} f_n g_n$ is the standard scalar product, $\boldsymbol{\nabla} F|_{\mathbf{f}} = \{\partial_{f_n} F\}$ the gradient and $\partial_{f_n} F$ the partial derivative defined through

$$\partial_{f_n} F(\mathbf{f}) \equiv \lim_{\epsilon \to 0} \frac{1}{\epsilon} \left[F(\mathbf{f} + \epsilon \hat{\mathbf{e}}_n) - F(\mathbf{f}) \right]. \tag{1.12}$$

From these identities, the differential is identified as

$$dF_{\mathbf{f}}\,\mathbf{g} = \sum_n \partial_{f_n} F(\mathbf{f}) g_n. \tag{1.13}$$

Vanishing of the differential amounts to vanishing of all partial derivatives $\partial_{f_n} F = 0$.

Eqs. (1.12) and (1.13) can now be straightforwardly generalized by taking continuum limits. In the continuum limit, the summation defining the finite dimensional scalar product becomes an integral,

$$\sum_{n=1}^{N} f_n g_n \to \int dx f(x) g(x).$$

The analog of the n-th unit vector is a δ-distribution,

$$\mathbf{e}_n \to \delta_y,$$

where $\delta_y(x) = \delta(x - y)$, as can be seen from the following correspondence,

$$\begin{aligned} f_n &\stackrel{!}{=} \sum_m f_m (e_n)_m \to \\ f(y) &\stackrel{!}{=} \int dx f(x) \delta_y(x). \end{aligned}$$

Here $(e_n)_m = \delta_{nm}$ stands for the m-th component of the n-th unit vector. The correspondence (unit vector $\leftrightarrow$ δ-distribution) is easy to memorize: While the components of $\mathbf{e}_n$ vanish, save for the n-th component that equals unity, δ_y is a function that vanishes

everywhere, save for y where it equals *infinity*. That a unit component is replaced by 'infinity' has to do with the fact that the support of the δ-distribution is infinitely narrow. I.e. to obtain a unit-normalized integral $\int \delta_y$, the function must be singular.

As a consequence of these identities, the continuum version of (1.13), i.e. the continuum differential, is given by

$$dF_f[g] = \int dx \frac{\delta F[f]}{\delta f(x)} g(x), \tag{1.14}$$

where the generalization of the partial derivative,

$$\frac{\delta F[f]}{\delta f(x)} \equiv \lim_{\epsilon \to 0} \frac{1}{\epsilon} \left(F[f + \epsilon \delta_x] - F[f] \right). \tag{1.15}$$

is commonly denoted by a curly δ instead of ∂.

Eqs. (1.14) and (1.15) establish the conceptual connection between ordinary and functional differentiation. Notice, that we have not yet learned how to *practically* calculate the differential, i.e. evaluate expressions like (1.15) for concrete functionals. Nevertheless, the identities above are very useful. They enable us to generalize more complex derivative operations of ordinary calculus by straightforward transcription. E.g. the generalisation of the standard chain rule,

$$\partial_{f_n} F(\mathbf{g}(\mathbf{f})) = \sum_m \partial_{g_m} F(\mathbf{g})|_{\mathbf{g}=\mathbf{g}(\mathbf{f})} \partial_{f_n} g_m(\mathbf{f})$$

reads

$$\frac{\delta F[g[f]]}{\delta f(x)} = \int dy \left. \frac{\delta F[g]}{\delta g(y)} \right|_{g=g[f]} \frac{\delta g(y)[f]}{\delta f(x)}. \tag{1.16}$$

Here $g[f]$ is the continuum generalization of an $\mathbb{R}^m$-valued function, $\mathbf{g} : \mathbb{R}^n \to \mathbb{R}^m$, i.e. a function whose components $g(y)[f]$ are functionals by themselves. Furthermore, given some functional $F[f]$, we can Taylor expand it as

$$F[f] = F[0] + \int dx_1 \frac{\delta F[f]}{\delta f(x_1)} f(x_1) + \int dx_1 \int dx_2 \, \frac{1}{2} \frac{\delta^2 F[f]}{\delta f(x_2) \delta f(x_1)} f(x_1) f(x_2) + \cdots, \tag{1.17}$$

where

$$\frac{\delta^2 F[f]}{\delta f(x_2) \delta f(x_1)} = \lim_{\epsilon_{1,2} \to 0} \frac{1}{\epsilon_1 \epsilon_2} \left(F[f + \epsilon_1 \delta_{x_1} + \epsilon_2 \delta_{x_2}] - F[f] \right)$$

generalizes a two-fold partial derivative. The validity of these identities can be made plausible by applying the transcription table 1.1 to the corresponding relations of standard calculus. To actually verify the formulae, one has to take the continuum limit of each step taken in the proof of the discrete counterparts. At any rate, experience shows that it takes some time to get used to the concept of functional differentiation. However, after some practice it will become clear that this operation is not only extremely useful but also as easy to handle as conventional partial differentiation.

entity	discrete	continuum
argument	vector $\mathbf{f}$	function f
function(al)	multi-dimensional function $F(\mathbf{f})$	functional $F[f]$
differential	$dF_{\mathbf{f}}\mathbf{g}$	$DF_f[g]$
Cartesian basis	$\hat{\mathbf{e}}_n$	δ_x
scalar product, $\langle\ ,\ \rangle$	$\sum_n f_n g_n$	$\int dx f(x)g(x)$
'partial derivative'	$\partial_{f_n} F(\mathbf{f})$	$\dfrac{\delta F[f]}{\delta f(x)}$

Table 1.1: Summary of basic definitions of discrete and continuum calculus.

We finally address the question how to compute the functional differential for the functionals commonly encountered in field theory. What we will use is that in all but a few cases, these functionals are of the structure,

$$S[\phi] = \int dt L(\phi(t), \dot{\phi}(t)),$$

where L is an ordinary function. To establish contact with the discussion of the previous sections, we have changed the notation, $F \to S$, $f \to \phi$, $x \to t$. The essential point is that the information carried by the functional is encoded in an local *function*. In general applications both, the field manifold and the base manifold will be higher dimensional. However, the functional S will still be described by a certain functi*on* L.

Owing to the specific form of S, the *functional* derivative can be related to an *ordinary* derivative of the function L. To achieve this, all what we have to do is evaluate the general definition (1.14) on the functional S:

$$\begin{aligned} S[\phi + \epsilon\theta] - S[\phi] &= \int dt \left[L(\phi + \epsilon\theta, \dot{\phi} + \dot{\epsilon}\theta) - L(\phi, \dot{\phi}) \right] = \\ &= \int dt \left[\frac{\partial L}{\partial \phi}\theta + \frac{\partial L}{\partial \dot{\phi}}\dot{\theta} \right] \epsilon + O(\epsilon^2) = \int dt \left[\frac{\partial L}{\partial \phi} - \frac{d}{dt}\frac{\partial L}{\partial \dot{\phi}} \right] \theta\epsilon + O(\epsilon^2). \end{aligned} \tag{1.18}$$

Comparison with (1.14) identifies the functional derivative as

$$\frac{\delta S[\phi]}{\delta \phi(t)} = \frac{\partial L}{\partial \phi(t)} - \frac{d}{dt}\frac{\partial L}{\partial \dot{\phi}(t)}. \tag{1.19}$$

This equation answers our initial question of the stationarity of functionals: The functional is stationary, if its differential vanishes. According to (3.26), this is guaranteed if the rhs of Eq. (1.19) vanishes for all t. Conversly, if the differential vanishes, Eq. (3.26) must vanish for all smooth functions g. This requires vanishing of the rhs of Eq. (1.19) *for all* t. We thus conclude that vanishing of the rhs of (1.19) is a sufficient and necessary condition for the stationarity of the functional S. Needless to say that

$$\forall t: \qquad \frac{\partial L}{\partial \phi(t)} - \frac{d}{dt}\frac{\partial L}{\partial \dot{\phi}(t)} = 0 \tag{1.20}$$

is the familiar Euler-Lagrange equation.

▷ EXERCISE. Consider a one-dimensional classical continuum system. The action functional is then given by $S[\phi] = \int dxdt\mathcal{L}(\phi, \partial_x\phi, \dot{\phi})$, i.e. the Lagrangian density $\mathcal{L}$ assumes the role of the function L above. Show that the generalization of Eq. (1.20) produces the Euler-Lagrange equations

$$\frac{\delta S[\phi]}{\delta\phi(x,t)} = \frac{\partial\mathcal{L}}{\partial\phi} - \frac{d}{dt}\frac{\partial\mathcal{L}}{\partial\dot{\phi}} - \frac{d}{dx}\frac{\partial\mathcal{L}}{\partial(\partial_x\phi)} = 0. \tag{1.21}$$

▷ EXERCISE. Write down the equation of motion corresponding to the Lagrangian density $\mathcal{L} = \mathcal{L}(\phi, \partial_x^2\phi, \dot{\phi})$.

Eq. (1.21) represents the generalisation of Lagrange's equation of motion of point mechanics to classical one-dimensional field theory. Notice that the equation is invariant under exchange of space and time coordinates. This is because, mathematically, we are varying a functional that depends on fields ϕ and first derivatives $\partial_\mu\phi, \mu = x, t$, i.e. mathematics does not care about the fact that in *classical* mechanics space and time play fundamentally different roles. However, the structural symmetry of the equations is more than mathematical coincidence! E.g. in relativistic theories, space and time appear in a unified manner and a sensible variational equation *must* reflect this feature. To make this structure more explicit, let us introduce a two component vector $x_\mu, \mu = 0, 1$ with $x_0 = t$ and $x_1 = x$. Eq. (1.21) then assumes the form

$$\frac{\delta S[\phi]}{\delta\phi(\mathbf{x})} = \frac{\partial\mathcal{L}}{\partial\phi} - \partial_\mu\frac{\partial\mathcal{L}}{\partial(\partial_\mu\phi)} = 0. \tag{1.22}$$

which not only expresses space-time symmetry but also is easy to remember.

▷ EXERCISE. Assume we were dealing with a field $\phi : \mathbb{R}^d \times \mathbb{R} \to \mathbb{R}, (\mathbf{x}, t) \mapsto \phi(\mathbf{x}, t)$ defined over a $d+1$-dimensional base manifold and an associated functional $L[\phi, \partial_{x_i}\phi, \partial_t\phi]$. Defining x_μ by $x_0 = t$ and $x_{\mu=1,2,\ldots d} = x_{1,2,\ldots d}$ show that Eq. (1.23) is the equation of motion, i.e that the equation survives generalization to higher dimensional problems.

Finally, we will frequently, encounter problems where the field manifold T is more complex than the real numbers. (For example, $T \subset \mathbb{R}^N$ might be a subset of an N-dimensional vector space.) Suppose, we had parameterized a field $\phi \in T$ through some coordinates ϕ^i, $i = 1, \ldots N$. The Lagrangian $\mathcal{L}(\phi^i, \partial_\mu\phi^i)$ would then be a function of the coefficients of the fields and their derivatives. The variational principle demands that the action be stationary under variation of all field components *individually*. This produces N independent variational equations,

$$\boxed{\frac{\delta S[\phi]}{\delta\phi^i(\mathbf{x})} = \frac{\partial\mathcal{L}}{\partial\phi^i} - \partial_\mu\frac{\partial\mathcal{L}}{\partial(\partial_\mu\phi^i)} = 0, \qquad i = 1, \ldots, N.} \tag{1.23}$$

Eq. (1.23) expresses the variational principle in its most general form.

▷ EXERCISE. Verify this equation by varying the action $S[\phi] = \int \mathcal{L}(\phi^i, \partial_\mu \phi^i)$ wrt the field components $\phi^i(\mathbf{x})$.

In the next section we will illustrate how the general variational principle (1.23) works on a higher dimensional problem:

1.3 Maxwell Theory from Variational Principles

As a second example, let us consider *the* archetype of classical field theory, classical electrodynamics. The idea not only is to exemplify the application of continuum variational principles on a problem we are all well acquainted with but also to illustrate the unifying potential of the approach: That problems as different as the low-lying vibrational modes of a solid and electrodynamics can be described by almost identical language indicates that we are dealing with a useful formalism.

Specifically, what we wish to explore is how the equations of motion of electrodynamics, the inhomogeneous Maxwell[9] eqution,

$$\begin{aligned} \nabla \cdot \mathbf{E} &= \rho, \\ \nabla \times \mathbf{B} - \partial_t \mathbf{E} &= \mathbf{j}, \end{aligned} \tag{1.24}$$

can be obtained from variational principles. (For simplicity, we restrict ourselves to a vacuum theory, i.e. $\mathbf{E} = \mathbf{D}$ and $\mathbf{B} = \mathbf{H}$. Further, we have set the velocity of light to unity, $c = 1$. Within the framework of the variational principle the *homogeneous* equations,

$$\begin{aligned} \nabla \times \mathbf{E} + \partial_t \mathbf{B} &= 0, \\ \nabla \cdot \mathbf{B} &= 0, \end{aligned} \tag{1.25}$$

are regarded as ab initio constraints imposed on the 'degrees of freedom' $\mathbf{E}$ and $\mathbf{B}$.) What we need to describe Maxwell theory by variational principle is 1.) a set of suitable 'generalized coordinates' and 2.) an action. As for coordinates, the natural choice will be the coefficients of the electromagnetic (EM) 4-potential, $A = \{A_\mu\}$, where $A_0 = \phi$ is the scalar and $A_{\mu=1,2,3} = -A_{1,2,3}$ (the negative of) the vector potential. The potential A is unconstrained and uniquely determines the fields $\mathbf{E}$ and $\mathbf{B}$ through the standard equations $\mathbf{E} = -\nabla\phi - \partial_t \mathbf{A}$ and $\mathbf{B} = \nabla \times \mathbf{A}$. (In fact, the set of coordinates A_μ is 'overly free', in the

[9]

James C. Maxwell 1831-1879; Amongst many other achievements in the fields of physics and mathematics, he is credited with the formulation of the theory of electromagnetism.

sense that gauge transformations $A_\mu \to A_\mu + \partial_\mu \Gamma$, where Γ is a function, leave the physical fields invariant. We will comment on this point later on.) The connection between A and the physical fields can be expressed in a more symmetric way by introducing the EM field tensor,

$$F = \{F_{\mu\nu}\} = \begin{bmatrix} 0 & E_1 & E_2 & E_3 \\ -E_1 & 0 & -B_3 & B_2 \\ -E_2 & B_3 & 0 & -B_1 \\ -E_3 & -B_2 & B_1 & 0 \end{bmatrix} . \tag{1.26}$$

The relation between fields and potential now reads $F_{\mu\nu} = \partial_\mu A_\nu - \partial_\nu A_\mu$, where, as above, $\partial_0 = \partial_t$ and $\partial_{\mu=1,2,3} = \nabla_{1,2,3}$.

▷ EXERCISE. Check that this connection follows from the definition of the vector potential. To verify that the constraint (1.25) is automatically included in the definition (1.26), compute the construct

$$\partial_\lambda F_{\mu\nu} + \partial_\mu F_{\nu\lambda} + \partial_\nu F_{\lambda\mu},$$

where $(\lambda\nu\mu)$ are arbitrary but *different* integers drawn from the set $(0, 1, 2, 3)$. This produces four different terms, identified as the lhs of (1.25). Evaluation of the same construct on $F_{\mu\nu} \equiv \partial_\mu A_\nu - \partial_\nu A_\mu$ produces zero by the symmetry of the right hand side.

As for the structure of the action $S[A]$ we can proceed in different ways. One option would be to regard Maxwell's equations as fundamental, i.e. to *postulate* an action that produces these equations upon variation (similarly to the situation in classical mechanics, were the action functional was *designed* so as to reproduce Newton's equations.) However, we can also be a little bit more ambitious and ask whether the structure of the action can be motivated independently of Maxwells equations. In fact, there is just one principle in electrodynamics equally 'fundamental' as Maxwells equations, *symmetry*: A theory of electromagnetism must be Lorentz-invariant, i.e. invariant under relativistic coordinate transformations.

▷ INFO. Referring for a thorough discussion of relativistic theories to chapter * below, let us briefly recapitulate the notion of **Lorentz invariance**[10]: Suppose we are given a 4-vector X_μ. A linear coordinate transformation $X_\mu \to X'_\mu \equiv T_{\mu\nu} X_\nu$ is a Lorentz transformation if it leaves the 4-metric

$$g = \{g^{\mu\nu}\} = \begin{bmatrix} 1 & & & \\ & -1 & & \\ & & -1 & \\ & & & -1 \end{bmatrix} \tag{1.27}$$

[10] Hendrik Antoon Lorentz 1853-1928; 1902 Nobel Laureate in Physics (with Pieter Zeeman) in recognition of the extraordinary service they rendered by their researches into the influence of magnetism upon radiation phenomena.

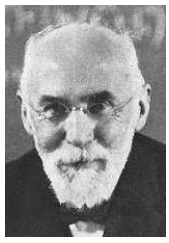

invariant: $T^T g T = g$. To concisely formulate the invariance properties of relativistic theories, is is common to introduce the notion of raised and lowered indices. Defining $X^\mu \equiv g^{\mu\nu} X_\nu$, Lorentz invariance is expressed as $X^\mu X_\mu = X^{\mu\prime} X'_\mu$.

Aided by the symmetry criterion, we can try to conjecture the structure of the action from three basic presumptions, all independent from Maxwell's equations: The action should be invariant under (a) Lorentz transformations, (b) gauge transformations, and (c) simple. The most elementary choice compatible with these conditions is

$$S[A] = \int d^4x \left(c_1 F_{\mu\nu} F^{\mu\nu} + c_2 A_\mu j^\mu \right), \tag{1.28}$$

where the measure $d^4x = \prod_\mu dx_\mu = dt dx_1 dx_2 dx_3$, the 4-current j_μ is defined through $j_0 = \rho$ and $j_{\mu=1,2,3} = j_{1,2,3}$, and $c_{1,2}$ are undetermined constants. Up to quadratic order in A, Eq. (1.28) defines, in fact, the only possible structure consisetent with gauge and Lorentz invariance.

▷ EXERCISE. Using the continuity equation $\partial_\mu j^\mu = 0$, verify that the Aj-coupling is gauge invariant. Hint: integrate by parts. Verify that a contribution like $\int A_\mu A^\mu$ would *not* be gauge invariant.

Having defined a trial action, we can apply the variational principle, i.e. Eq. (1.23), to compute equations of motion. In the present context, the role of the field ϕ is taken over by the four-components of A. Variation of the action w.r.t. A_μ obtains four equations of motion,

$$\frac{\partial \mathcal{L}}{\partial A_\mu} - \partial_\nu \frac{\partial \mathcal{L}}{\partial(\partial_\nu A_\mu)} = 0, \qquad \mu = 0, \ldots, 3, \tag{1.29}$$

where the Lagrangian density is defined through $S = \int d^4x \mathcal{L}$.

▷ EXERCISE. Following the logics of section 1.2, verify that, irrespective of the form of the Lagrangian $\mathcal{L}(A_\mu, \partial_\nu A_\mu)$, the generalization of Eq. (1.23) to a vectorial field, $\phi \to A_\mu$, is given by (1.29).

With our specific form of $\mathcal{L}$, it is straightforward to verify that $\partial_{A_\mu} \mathcal{L} = c_2 j^\mu$ and $\partial_{\partial_\nu A_\mu} \mathcal{L} = -4 c_1 F^{\mu\nu}$. Substituion of these building blocks into the equations of motion finally yields

$$4 c_1 \partial^\nu F_{\nu\mu} = c_2 j_\mu .$$

Comparing this with the definition of the field tensor (1.26) and setting $\frac{c_1}{c_2} = \frac{1}{4}$ we arrive the Maxwell equations (1.24). and

$$\boxed{S[A] = \int d^4x \left(\frac{1}{4} F_{\mu\nu} F^{\mu\nu} + A_\mu j^\mu \right),} \tag{1.30}$$

as the final result for the **Lagrangian action of the electromagnetic field**. Here we have fixed the overall multiplicative constant $c_1 = c_2/4$, not determined by the variational principle, by requiring that the Hamiltonian density associated to $\mathcal{L}$ coincides with the known energy of the EM field. (See the problem section.)

▷ EXERCISE. Verify the statements made in the previous paragraph.

At first sight, this result does not at all look spectacular; After all, Maxwell's equations can be found on p1 of most text books on electrodynamics. However, a second thought shows that what we have achieved is actually quite remarkable. The only piece of input that went into the construction was symmetry. This was enough to fix the algebraic structure of Maxwell's equations unambigously. We have thus proven that Maxwell's equations are relatvistically invariant, a fact not obvious from the equations itself. Further we have shown that (1.24) are the *only* equations of motion linear in the current/density distribution and consistent with the invariance principle. One might object that in addition to symmetry we also imposed an ad hoc 'simplicity' criterion on the action $S[A]$. However, later on we will see that that was motivated by more than mere aesthetic principles.

Finally, notice that the symmetry oriented modelling that led to (1.28) stands exemplaric for a popular construction scheme in modern field theory. The symmetry oriented approach stands complementary to the "microscopic" formulation exemplified in section 1.1. Roughly speaking, these are the two principal approaches to constructing effective low energy field theories:

- ▷ The **microscopic** route: Starting from a microscopically defined system, one projects out the degrees of freedom one believes relevant for the low energy dyanmics. Ideally, this 'belief' is backed up by a small expansion parameter stabilizing the mathematical parts of the analysis.
  pro: The method is rigorous and fixes the resulting field theory completely.
  contra: The microscopic route is slow and, for sufficiently complex systems, not even viable.

- ▷ The **phenomenological** route: Given a physical system one has already decided what its relevant degrees of freedom are. (Sometimes this has to be done on the basis of mere phenomenological reasoning.) The structure of the effectic low energy action is then usually fixed by symmetries.
  pro: The method is fast and elegant.
  contra: It is less explicit than the microscopic approach. Most importantly, it does fix the coefficients of the different contributions to the action.

1.4 Summary and Outlook

We have introduced some basic concepts of field theoretical modelling in condensed matter physics. Starting from a microscopic model Hamiltonian, we have exemplified how principles of universality and symmetry can be applied to destill effective continuum theories capturing the low energy content of the system. We have formulated such theories in the

language of Langrangian and Hamiltonian continuum mechanics, respectively, and shown how variational principles can be applied to extract concrete physical information. Also, we have seen that field theory provides a unifying framework whereby analogies between seemingly different physical systems can be uncovered.

In the next chapter we will discuss how the formalism of classical field theory is promoted to the quantum level.

1.5 Problem Set

1.5.1 Questions on Collective Modes and Field Theories

Q1 In obtaining the spectrum of collective phonon excitations for the lattice Lagrangian (??), a continuum approximation was employed. However, since the degrees of freedom are coupled linearly, the equations of motion can be solved explicitly, even for the discrete model. By constructing the equations of motion, identify the **normal modes** of the system and obtain the exact spectrum of excitations. Identify the limit in which the spectrum of the discrete lattice model coincides with that obtained for the continuum approximation of the model. In what limit does the continuum approximation fail and why?

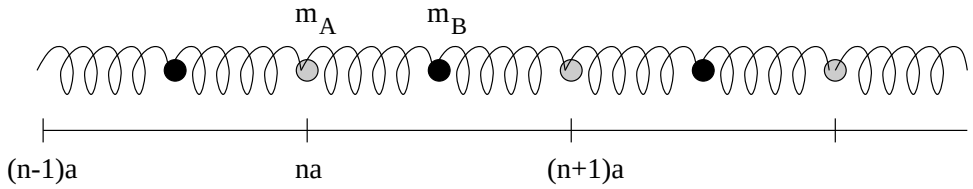

Figure 1.8: Lattice with two atoms of mass m_A and m_B per unit cell.

Q2 In lattices with two atoms (of different mass m_A and m_B) per unit cell (see fig. 1.8) the spectrum of elementary excitations splits into an **acoustic** and **optic** branch. For this model, show that the lattice Lagrangian can be written as

$$L = \sum_{n=1}^{N} \left[\frac{m_A}{2}(\dot{\phi}_n^{(A)})^2 + \frac{m_B}{2}(\dot{\phi}_n^{(B)})^2 - \frac{k_s}{2}\left(\phi_{n+1}^{(A)} - \phi_n^{(B)}\right)^2 - \frac{k_s}{2}\left(\phi_n^{(B)} - \phi_n^{(A)}\right)^2 \right].$$

Applying the Euler-Lagrange equation, obtain the equations of motion. Taking the boundary conditions to be periodic, and switching to Fourier representation, show that the exact (i.e. discrete) spectrum can be obtained from the 2×2 secular equation for each k value

$$\det \begin{vmatrix} m_A\omega_k^2 - 2k_s & k_s(1+e^{ika}) \\ k_s(1+e^{-ika}) & m_B\omega_k^2 - 2k_s \end{vmatrix} = 0.$$

By finding an expression for the spectrum, obtain the asymptotic dependence as $k \to 0$. In this limit, describe qualitatively the symmetry of the normal modes.

Q3 Electrodynamics can be described by Maxwell's equations or, equivalently, by wave type equations for the vector potential. *In the Lorentz gauge*, $\partial_t \phi = \nabla \cdot \mathbf{A}$, these equations read

$$(\partial_t^2 - \Delta)\phi = \rho,$$
$$(\partial_t^2 - \Delta)\mathbf{A} = \mathbf{j},$$

where $\Delta = \nabla \cdot \nabla$ is the three-dimensional Laplace operator. Using relativistially covariant notation, the form of the equations can be compressed further to

$$\partial_\mu \partial^\mu A = j, \qquad \partial_\mu \partial^\mu A = 0.$$

Starting from the Lagrangian action,

$$S[A] = \int d^4x \left(\frac{1}{4} F_{\mu\nu} F^{\mu\nu} + A_\mu j^\mu \right),$$

obtain these equations by applying the variational prinicple. Compare the Lorentz gauge representation of the action of the field with the action of the elastic chain. What are the differences/parallels?

Q4 Consider the electormagnetic field in the absence of matter, $j = 0$. Verify that the total energy stored in the field is given by $H \equiv \int d^3x \mathcal{H}(\mathbf{x})$ where

$$\mathcal{H}(\mathbf{x}) = \mathbf{E}^2(\mathbf{x}) + \mathbf{B}^2(\mathbf{x}),$$

is the familiar expression for the EM energy density. Hint: Use the vacuum form of Maxwell's equations and that for an infinite system the energy is defined only up to surface terms.

1.5.2 Answers

A1 Applying the Euler-Lagrange equation $d_t(\partial_{\dot{\phi}_n} L) - \partial_{\phi_n} L = 0$ to the discrete Lagrangian of the lattice model we find the N equations of motion which take the form of a three-term difference equation,

$$m\ddot{\phi}_n = k_s \left(\phi_{n+1} - 2\phi_n + \phi_{n-1}\right).$$

As in the continuum theory, the latter can be brought to diagonal form by turning to the Fourier representation. Applying the Ansatz

$$\phi_n(t) = \frac{1}{\sqrt{N}} \sum_k e^{i(\omega_k t - kna)} \phi_k$$

where the discrete quasi-momentum $k = 2\pi m/Na$ take values from the range $m = [-N/2, N/2]$ (i.e. the first Brillouin Zone), we find

$$\left[m\omega_k^2 - 2k_s \left(1 - \cos(ka)\right)\right] \phi_k = 0.$$

From this equation we obtain the dispersion relation

$$\omega_k = 2\sqrt{k_s/m} |\sin(ka/2)|.$$

In the limit $k \to 0$, this result collapses to the linear dispersion relation $\omega_k = v|k|$ obtained from the continuum theory. This can be understood simply by comparing the wavelength of the lattice vibration $\lambda = 2\pi/k$ with the lattice spacing a. When $\lambda \gg a$, the *relative* displacement of the atomic sites is small and the continuum approximation is justified. When $\lambda \sim a$, the relative displacement is large and the continuum theory becomes inapplicable.

In the two-dimensional generalisation the displacement takes the form of a two-component vector $\phi_{\mathbf{n}}$. In this case, the discrete Lagrangian assumes the form

$$L = \sum_{\mathbf{n}} \left[\frac{1}{2} m\dot{\phi}_{\mathbf{n}}^2 + \sum_{i=x,y} \frac{1}{2} k_s \left(\phi_{\mathbf{n}+\hat{\mathbf{e}}_i} - \phi_{\mathbf{n}}\right)^2\right].$$

In this case, the Euler-Lagrange equations lead to the difference equation

$$m\phi_{\mathbf{n}} = \sum_{i=x,y} k_s \left(\phi_{\mathbf{n}+\hat{\mathbf{e}}_i} - 2\phi_{\mathbf{n}} + \phi_{\mathbf{n}-\hat{\mathbf{e}}_i}\right),$$

with the soloution $\omega_{\mathbf{k}} = 2\sqrt{k_s/m}(\sin^2(k_x a) + \sin^2(k_y a))^{1/2}$. In the low-energy limit, the spectrum reduces to the relativistic form $\omega_{\mathbf{k}} = v|\mathbf{k}|$.

A2 Applying the Euler-Lagrange equations we obtain the $2 \times N$ coupled equations of motion

$$\begin{aligned} m_A \ddot{\phi}_n^{(A)} &= k_s \left(\phi_n^{(B)} - 2\phi_n^{(A)} + \phi_{n-1}^{(B)}\right), \\ m_B \ddot{\phi}_n^{(B)} &= k_s \left(\phi_{n+1}^{(A)} - 2\phi_n^{(B)} + \phi_n^{(A)}\right). \end{aligned}$$

Applying the Ansatz $\phi_n^{(A/B)} = (1/\sqrt{N})\sum_k e^{i(\omega_k t - kna)}\phi_k^{(A/B)}$, we obtain

$$\begin{pmatrix} m_A\omega_k^2 - 2k_s & k_s(1+e^{ika}) \\ k_s(1+e^{-ika}) & m_B\omega_k^2 - 2k_s \end{pmatrix} \begin{pmatrix} \phi_k^{(A)} \\ \phi_k^{(B)} \end{pmatrix} = 0.$$

Diagonalizing the 2×2 matrix we obtain the secular equation shown in the question and from which we obtain the dispersion relation (see Fig. 1.9)

$$\omega_k^{(\pm)} = \omega_0 \left[1 \pm \left(1 - \frac{4m_A m_B}{(m_A+m_B)^2}\sin^2(ka/2)\right)^{1/2}\right]^{1/2}.$$

where $\omega_0 = \sqrt{k_s/\mu}$ where $\mu = 1/(m_A^{-1}+m_B^{-1})$ denotes the reduced mass. It is instructive to note how the standard phonon dispersion relation is recovered when the masses are set equal.

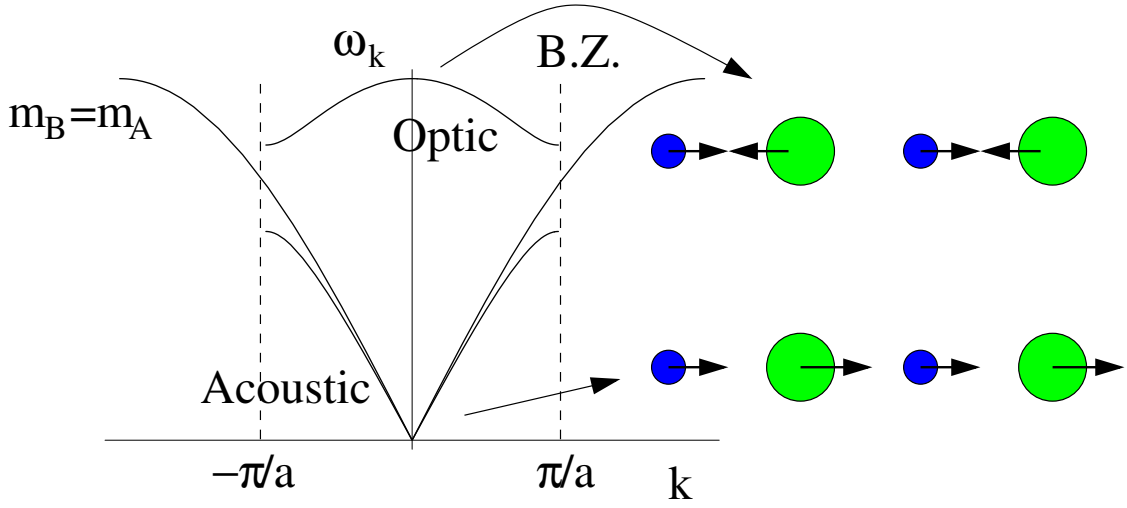

Figure 1.9: Spectrum of the two-atom discrete linear chain. Note that when $m_A = m_B$ we recover the spectrum of the single atom chain with period $a/2$. For $m_A \neq m_B$, a gap opens at the Brillounin zone boundary. The lower energy band is known as the acoustic branch where atoms in each unit cell move in phase. The higher energy optic branch involves atoms in each cell moving in antiphase.

An expansion in the limit $k \to 0$ yields

$$\omega_k^{(\pm)} \to \omega_0 \begin{cases} \sqrt{2}\left(1 - \dfrac{m_A m_B}{8(m_A+m_B)^2}(ka)^2\right) + O(k^4) \\ \sqrt{\dfrac{m_A m_B}{2}}\dfrac{1}{(m_A+m_B)}|ka| + O(k^3) \end{cases}$$

from which we deduce that the lower branch describes acoustic phonons with a linear dispersion relation, while the optic phonons are massive with a quadratic spectrum.

A3 Using that $F_{\mu\nu} = \partial_\mu A_\nu - \partial_\nu A_\mu$ and integrating by parts the action assumes the form

$$S[A] = \int d^4x \left(-\frac{1}{2}A_\nu\left[\partial_\mu\partial^\mu A^\nu - \partial_\mu\partial^\nu A^\mu\right] + j_\mu A^\mu\right).$$

Due to the Lorentz gauge condition, the second contribution in the angular brackets vanishes and we obtain

$$S[A] = \int d^4x \left(\frac{1}{2} \partial_\mu A_\nu \partial^\mu A^\nu + j_\mu A^\mu \right),$$

where we have again integrated by parts. Application of the general variational equation (1.23) finally obtains the wave equation.

A4 Following the canonical prescription, we consider the Lagrangian density,

$$\begin{aligned} \mathcal{L} = -\frac{1}{4} F_{\mu\nu} F^{\mu\nu} = \frac{1}{4} (\partial_\mu A_\nu - \partial_\nu A_\mu)(\partial^\mu A^\nu - \partial^\nu A^\mu) = \\ = \frac{1}{2} \sum_{i=1}^{3} (\partial_0 A_i - \partial_i A_0)(\partial_0 A_i - \partial_i A_0) - \frac{1}{4} \sum_{i,j=1}^{3} (\partial_i A_j - \partial_j A_i)(\partial_i A_j - \partial_j A_i), \end{aligned}$$

where we have lowered all indices on account of introducing minus signs in the first group of terms. We next determine the components of the canoncial momentum through $\pi_\mu = \partial_0 A_\mu \mathcal{L}$:

$$\begin{aligned} \pi_0 &= 0, \\ \pi_i &= \partial_0 A_i - \partial_i A_0 = E_i. \end{aligned}$$

Using that $\partial_i A_j - \partial_j A_i$ is a component of the magnetic field, the Hamiltonian density can now be written as

$$\begin{aligned} \tilde{\mathcal{H}} = \pi_\mu \partial_0 A_\mu - \mathcal{L} = \frac{1}{2} (2\mathbf{E} \cdot \partial_0 \mathbf{A} - \mathbf{E}^2 + \mathbf{B}^2) \stackrel{1)}{=} \\ \stackrel{1)}{=} \frac{1}{2} (2\mathbf{E} \cdot \nabla\phi + \mathbf{E}^2 + \mathbf{B}^2) \stackrel{2)}{=} \frac{1}{2} (2[\mathbf{E} \cdot \nabla\phi + \nabla \cdot \mathbf{E}\phi] + \mathbf{E}^2 + \mathbf{B}^2) \\ \stackrel{3)}{=} \frac{1}{2} (2\nabla \cdot (\mathbf{E}\phi) + \mathbf{E}^2 + \mathbf{B}^2), \end{aligned}$$

where 1) is based on addition and subtraction of a a term $2\mathbf{E}\cdot\nabla\phi$, 2) on $\nabla\cdot\mathbf{E} = 0$ and 3) on the identity $\nabla\cdot(\mathbf{a}f) = \nabla\cdot\mathbf{a}f + \mathbf{a}\cdot\nabla f$ (valid for general vector (scalar) functions $\mathbf{a}$ (f)). Substitution of this expression into the definition of the Hamiltonian yields

$$H = \frac{1}{2} \int d^3x \left(2\nabla \cdot (\mathbf{E}\phi) + \mathbf{E}^2 + \mathbf{B}^2 \right) = \frac{1}{2} \int d^3x \left(\mathbf{E}^2 + \mathbf{B}^2 \right),$$

where we have used that the contribution $\nabla \cdot (\mathbf{E}\phi)$ is a surface term that vanishes upon integration by parts.

Chapter 2

From Classical to Quantum Fields

The concept of field quantization is introduced. Again employing the atomic chain and the electromagnetic field as examples, we will explore how excitations in the continuum Hilbert space acquire the meaning of quantum 'particles'.

In the previous chapter we had seen that at low temperatures the excitation profile of the classical atomic chain differs drastically from what is observed in experiment. Generally, in condensed matter physics, low energy phenonmena with pronounced temperature sensitivity are indicative of a quantum mechanism at work. To introduce and exempify a general procedure whereby quantum mechanics can be incorportated into continuum models, we next consider the low energy physics of the

2.1 Quantum Chain

The first question to ask is a conceptual one: in which way can a model like Eq. (1.4) be quantised in general? As a matter of fact there exists a standard procedure of quantising continuum theories which closely resembles the quantisation of Hamiltonian point mechanics: Consider the defining equation (1.9) and (1.10) for the canonical momentum and the Hamiltonian, respectively. Classically, the momentum $\pi(x)$ and the coordinate $\phi(x)$ are canonically conjugate variables: $\{\pi(x), \phi(x')\} = \delta(x-x')$ where $\{\ ,\ \}$ is the Poisson bracket and the δ-function arises through continuum generalization of the discrete identity $\{P_I, R_{I'}\} = \delta_{II'}$, $I, I' = 1, \ldots N$. The theory is quantized by generalization of the canonical quantization prodedure for the discrete pair of conjugate coordinates (R_I, P_I) to the continuum: (i) promote $\phi(x)$ and $\pi(x)$ to operators: $\phi \mapsto \hat{\phi}$, $\pi \mapsto \hat{\pi}$, and (ii) generalize the canonical commutation relation $[P_I, R_{I'}] = -i\hbar\delta_{II'}$ to[1]

$$\boxed{[\hat{\pi}(x), \hat{\phi}(x')] = -i\hbar\delta(x-x')\ .} \tag{2.1}$$

[1]Note that the dimensionality of both the quantum and classical continuum fields is compatible with the dimensionality of the Dirac δ-function, $[\delta(x-x')] = [\text{Length}]^{-1}$, i.e. $[\phi(x)] = [\phi_I] \cdot [\text{Length}]^{-1/2}$ and similarly for π.

Operator-valued functions like $\hat{\phi}$ and $\hat{\pi}$ are generally referred to as **quantum fields**. For clarity, the relevant relations between canonically conjugate classical and quantum fields are summarized in Tab. 2.1.

	classical	quantum
discrete	$\{P_I, R_{I'}\} = \delta_{II'}$	$[P_I, R_{I'}] = -i\hbar\delta_{II'}$
continuum	$\{\pi(x), \phi(x')\} = \delta(x - x')$	$[\hat{\pi}(x), \hat{\phi}(x')] = -i\hbar\delta(x - x')$

Table 2.1: Relations between discrete and continuum canonically conjugate variables/operators

▷ INFO. By introducing quantum fields, we have left the conceptual framework laid on page 6: Being operator valued, the quantized field no longer represents a mapping into an ordinary differentiable manifold[2]. It is thus legitimate to ask why we bothered to give a lengthy exposition of fields as 'ordinary' functions. The reason is that in the not too distant future, after the framework of field functional integration has been introduced, we will be back on the comfortable ground of the definition of page 6.

Employing these definitions, the classical Hamilonian density (1.10) becomes the quantum operator

$$\hat{\mathcal{H}}(\hat{\phi}, \hat{\pi}) = \frac{1}{2m}\hat{\pi}^2 + \frac{k_s a^2}{2}(\partial_x \hat{\phi})^2. \tag{2.2}$$

The Hamiltonian above represents a quantum field theoretical *formulation* of the problem but not yet a *solution*. In fact, the development of a spectrum of methods for the analysis of quantum field theoretical models will represent a major part of this text. At this point the objective is merely to exemplify how physical information can be extracted from models like (2.2). As a word of precaution, let us mention that the following manipulations, while mathematically not difficult, are conceptually deep. To disentangle different aspects of the problem, we will first concentrate on plain operational aspects. 'What has really happened' will then be discussed in section * below.

As with any function, operator valued functions can be represented in a variety of different ways. In particular they can be subjected to a Fourier transform,

$$\begin{Bmatrix} \hat{\phi}_k \\ \hat{\pi}_k \end{Bmatrix} \equiv \frac{1}{L^{1/2}} \int_0^L dx\; e^{\{\mp ikx} \begin{Bmatrix} \hat{\phi}(x) \\ \hat{\pi}(x) \end{Bmatrix}, \qquad \begin{Bmatrix} \hat{\phi}(x) \\ \hat{\pi}(x) \end{Bmatrix} = \frac{1}{L^{1/2}} \sum_k e^{\{\pm ikx} \begin{Bmatrix} \hat{\phi}_k \\ \hat{\pi}_k \end{Bmatrix}, \tag{2.3}$$

where $\sum_k$ represents the sum over all Fourier coefficients indexed by quantised momenta $k = 2\pi m/L$, $m \in \mathcal{Z}$. (Do not confuse the momenta k with the 'operator momentum' $\hat{\pi}$!) Note that the *real* classical field $\phi(x)$ quantises to an *Hermitian* quantum field $\hat{\phi}(x)$

[2] At least if we ignore the mathematical subtlety that a linear operator can be interpreted as element of a certain manifold, too.

implying that $\hat{\phi}_k = \hat{\phi}^\dagger_{-k}$ (and similarly for $\hat{\pi}_k$). The Fourier representation of the canonical commutation relations reads

$$[\hat{\pi}_k, \hat{\phi}_{k'}] = -i\hbar\delta_{kk'} \tag{2.4}$$

▷ EXERCISE. Verify this identity.

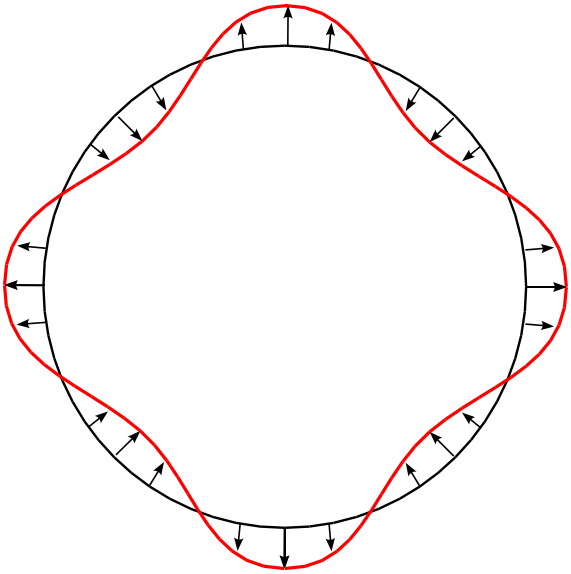

Figure 2.1: Schematic visualisation of the oscillator mode $k = 8\pi/L$ of the harmonic chain. Arrows indicate the distortion of individual atoms (for clarity plotted in the vertical direction.)

When expressed in the Fourier representation, making use of the identity

$$\int dx\ (\partial\hat{\phi})^2 = \sum_{k,k'}(-ik\hat{\phi}_k)(-ik'\hat{\phi}_{k'})\ \overbrace{\frac{1}{L}\int dx e^{-i(k+k')x}}^{\delta_{k+k',0}} = \sum_k k^2\hat{\phi}_k\hat{\phi}_{-k} = \sum_k k^2|\hat{\phi}_k|^2$$

together with a similar relation for $\int dx\ \hat{\pi}^2$, the Hamiltonian assumes the near diagonal form

$$\hat{H} = \sum_k \left[\frac{1}{2m}\hat{\pi}_k\hat{\pi}_{-k} + \frac{m\omega_k^2}{2}\hat{\phi}_k\hat{\phi}_{-k}\right], \tag{2.5}$$

where $\omega_k = v|k|$ and $v = \sqrt{\frac{k_s}{m}}a$ denotes the classical sound velocity. In this form, the Hamiltonian can be identified as nothing but a superposition of independent **harmonic oscillators**.[3] This result is actually not difficult to understand (see Fig. 2.1): Classically,

[3] The only difference to the canoncial form of an oscillator Hamiltonian $\hat{H} = \frac{\hat{p}^2}{2m} + \frac{m\omega^2}{2}\hat{x}^2$ is the presence of the sub-indices k and $-k$. (Which is a consequence of $\hat{\phi}^\dagger_k = \hat{\phi}_{-k}$.) As we will show momentarily, this difference is completely inessential.

the system supports a discrete set of wave excitations, each indexed by a wave number $k = 2\pi m/L$. Within the quantum picture, each of these excitations is described by an oscillator Hamilton operator with k-dependent frequency. (However, it is important not to confuse the atomic constituents, also oscillators albeit coupled ones, with the independent *collective* oscillator modes described by $\hat{H}$.)

The description above, albeit perfectly valid still suffers from a defficiency: What we are doing, see Fig. 2.1, amounts to explicitly describing the effective low energy excitations of the system (the waves) in terms of their microscopic constituents (the atoms). Indeed the different contributions to $\hat{H}$ keeps track of details of the microscopic oscillator dynamics of individual k-modes. However, it would be much more desirable to develop a picture where the relevant excitations of the system, the waves, appear as fundamental units, without explicit account of underlying microscopic details. (Like, e.g. in hydrodynamics information is encoded in terms of collective density variables rather than through individual molecules.) As a preparation to the construction of this improved formulation of the system let us temporarily focus on a single oscillator mode.

2.1.1 Harmonic Oscillator Revisited

Consider a standard harmonic oscillator (HO) Hamiltonian defined through

$$\hat{H} = \frac{1}{2m}\hat{p}^2 + \frac{m\omega^2}{2}\hat{x}^2.$$

The few first energy levels $\epsilon_n = \omega\left(n + \frac{1}{2}\right)$ and the associated Hermite-polynomial eigenfunctions are displayed schematically in Fig. 2.2. (To simplify the notation we henceforth set $\hbar = 1$.)

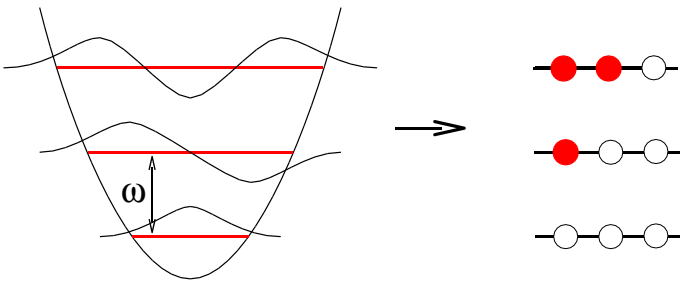

Figure 2.2: Schematic diagram showing the low lying energy levels/states of the harmonic oscillator.

In quantum mechanics, the HO has, of course, the status of a single-particle problem. However, the fact that the energy levels are *equi-distant* suggests an alternative interpretation: Think of a given energy state ϵ_n as an accumulation of n elementary entities, or **quasi-particles**, each having energy ω. What can be said about the features of these new objects? First, they are structureless, i.e. the only 'quantum number' identifying the quasiparticles is their energy ω. (Otherwise n-particle states formed of the quasi-particles would not be equi-distant.) This implies that the quasi-particles must be *bosons*. (The same state ω can be occupied by more than one particle, see Fig. 2.2.)

This idea can be formulated in quantitative terms by employing the formalism of so-called ladder-operators: Define a pair of Hermitian adjoint operators through

$$\hat{a} \equiv \sqrt{\frac{m\omega}{2}} \left(\hat{x} + \frac{i}{m\omega} \hat{p} \right), \qquad \hat{a}^\dagger \equiv \sqrt{\frac{m\omega}{2}} \left(\hat{x} - \frac{i}{m\omega} \hat{p} \right).$$

(Up to a factor of i,) the transformation $(\hat{x}, \hat{p}) \to (\hat{a}, \hat{a}^\dagger)$, is canonical, i.e. the new operators obey the canonical commutation relation

$$[\hat{a}, \hat{a}^\dagger] = 1. \tag{2.6}$$

More importantly, the a-representation of the Hamiltonian is very simple, viz.

$$\hat{H} = \omega \left(\hat{a}^\dagger \hat{a} + \frac{1}{2} \right), \tag{2.7}$$

as can be checked by direct substitution. Suppose now, we had been given a zero eigenvalue state $|0\rangle$ of the operator $\hat{a}$: $\hat{a}|0\rangle = 0$. As a direct consequence, $\hat{H}|0\rangle = \frac{\omega}{2}|0\rangle$, i.e. $|0\rangle$ is identified as the ground state of the oscillator[4]. The complete hierarchy of higher energy states can now generated by setting

$$|n\rangle \equiv \frac{1}{(n!)^{1/2}} \hat{a}^{\dagger n} |0\rangle.$$

▷ EXERCISE. Using the canonical commutation relation, verify that $\hat{H}|n\rangle = \omega(n + 1/2)|n\rangle$ and $\langle n|n\rangle = 1$.

So far, what we have achieved is constructing yet another way of solving the HO-problem. However, the 'real' advantage of the a-representation is that it naturally affords a many particle interpretation: Temporarily forgetting about the original definition of the oscillator, let us *declare* $|0\rangle$ to represent a 'vacuum' state, i.e. a state with zero particles present. Next, imagine that $\hat{a}^\dagger|0\rangle$ was a state with a single featureless particle (the operator $\hat{a}^\dagger$ does not carry any quantum number labels) of energy ω. Similarly, $\hat{a}^{\dagger n}|0\rangle$ is considered as a many body state with n of these particles, i.e. within the new picture, $\hat{a}^\dagger$ is an operator that creates particles. The total energy of these states is given by $\omega \times$ (occupation number). Indeed, it is straightforward to verify that $\hat{a}^\dagger \hat{a}|n\rangle = n|n\rangle$, i.e. the Hamiltonian basically counts the number of particles. The new interpretation, while at first sight unfamiliarly looking, is internally consistent. In particular it does what we had asked for above, i.e. interpreting the excited states of the HO as an superposition of independent structureless entities.

The representation above illustrates the possibility to think about individual quantum problems in complementary pictures. This principle finds innumerable applications in modern condensed matter physics. To get used to it one has to realize that interpreting

[4] ... as can be verified by explicit construction: Going into a real space representation one solves $[x + \partial_x/(m\omega)]\langle x|0\rangle$ to $\langle x|0\rangle = \sqrt{\frac{2\pi}{m\omega}} e^{-x^2 m\omega/2}$ which is the well known ground state wave function of the oscillator.

a give system in different directions is by no means heretic but, rather, stands in the best spirit of quantum mechanics. Indeed, it is one of the prime principles of quantum theories that there is no such thing like 'the real system' underneath the surface of phenomenology. The only thing that matters is observable phenomena. For example, we will see later on that the 'ficticious' quasi-particle states of oscillator systems *behave* like 'real' particles, i.e. they have dynamics, they can interact, be detected experimentally etc. From a quantum point of view there is actually no fundamental difference between these objects and 'real' particles.

2.1.2 Quasi-Particle Interpretation of the Quantum Chain

Turning back to the oscillator chain, we transform the Hamiltonian (2.5) to a form analogous to (2.7). This is achieved by defining the ladder operators[5]

$$\hat{a}_k \equiv \sqrt{\frac{m\omega_k}{2}}\left(\hat{\phi}_k + i\frac{1}{m\omega_k}\hat{\pi}_{-k}\right), \qquad \hat{a}_k^\dagger \equiv \sqrt{\frac{m\omega_k}{2}}\left(\hat{\phi}_{-k} - i\frac{1}{m\omega_k}\hat{\pi}_k\right).$$

With this definition, applying the commutation relations (2.4), one finds that the ladder

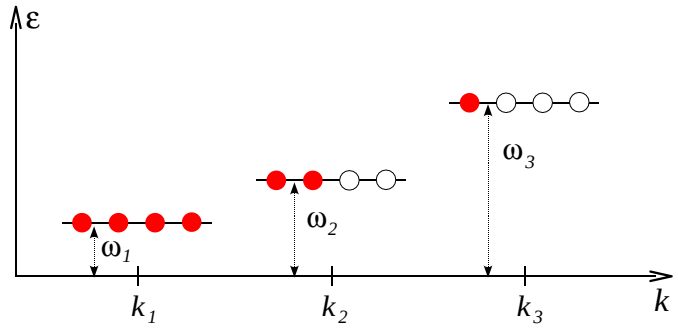

Figure 2.3: Schematic diagram visualizing an excited state of the chain. The number of created quasi-particles decreases with increasing energy ω_k.

operators obey commutation relations generalizing (2.6):

$$[a_k, a_{k'}^\dagger] = \delta_{kk'}, \qquad [a_k, a_{k'}] = [a_k^\dagger, a_{k'}^\dagger] = 0. \tag{2.8}$$

Expressing the operators $(\hat{\phi}_k, \hat{\pi}_k)$ in terms of $(\hat{a}_k, \hat{a}_k^\dagger)$ it is now straightforward to bring the Hamiltonian into the quasi-particle oscillator form

$$\hat{H} = \sum_k \hbar\omega_k \left(a_k^\dagger a_k + \frac{1}{2}\right). \tag{2.9}$$

Equations (2.9) and (2.8) represent the final result of our analysis. The Hamiltonian $\hat{H}$ takes the form of a sum of harmonic oscillators with characteristic frequencies ω_k. Notice

[5] As for the consistency of these definitions, recall that $\hat{\phi}_k^\dagger = \hat{\phi}_{-k}$ and $\hat{\pi}_k^\dagger = \hat{\pi}_{-k}$. Under these conditions the second of the definitions below indeed follows from the first upon taking the Hermitian adjoint.

that $\omega_k =\!\!\rightarrow 0$ in the limit of fluctuations with long wavelength, $k \to 0$. Excitations with this property are generally called **massless excitations**.

An excited state of the system is represented through a set $(n_1, n_2, \ldots)$ of n_k quasi-particles with energy ω_k. Physically, the quasi-particles of the harmonic chain are to be identified with the **phonon modes** of the solid. A plot ot 'real' phonon excitation energies is shown in Fig. 2.4. Notice that at low momenta, $\omega_k \sim |k|$ in agreement with our simplistic model and in spite of the fact that the spectrum was recorded for a three-dimensional solid with non-trivial unit cell (universality!). While linear dispersion was a feature already of the classical sound waves, the low temperature specific heat behaves altogether non-classical: It is left as an (answered) excercise to verify that the quantum nature of the phonons resolves the problem with the low temperature profile of the specific heat discussed in section 1.1.2. For further discussion of phonon modes in atomic lattices we refer to Kittel, Chapter 2.

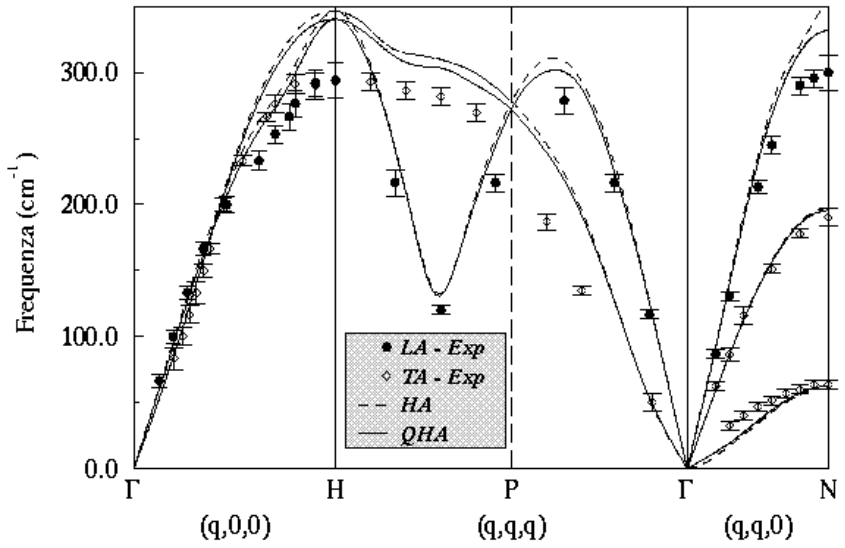

Figure 2.4: Typical phonon spectra of a crystal with a BCC lattice. The data is sensitive to both longitudinal (LA) and transverse (TA) acoustic phonons. Notice that for small momenta, the dispersion is linear.

2.2 Quantum Electrodynamics

The generality of the procedure outlined above suggests that the quantization of the EM field action (1.30) proceeds in analogy to the discussion of the phonon system. However, there are are a number *practical* differences which make quantization of the EM field a much harder (but also more interesting!) experience: First, the vectorial character of the vector potential, in combination with the imperative condition of relativistic covariance, gives the problem a non-trivial internal geometry. Closely related, the gauge freedom of the vector potential introduces redundant degrees of freedom whose removal on the quantum level is not easily achieved. E.g. quantization in a setting where *only* physical

degrees of freedom – i.e. the two polarization directions of the transverse photon field – are kept is technically cumbersome, the reason being that the relevant gauge condition is not relativistically covariant. In contrast, a manifestly covariant scheme, while technically more convenient, introduces spurious 'ghost degrees of freedom' which are difficult to get rid of. In order to not get caught up in a discussion of these problems we will not discuss the problem of EM field quantization in full detail[6].

On the other hand, the quantum aspects of the photon field play a much too important role in various areas of condensed matter physics to drop the problem altogether. We will therefore aim at an intermediate exposition, largely insensitive to the problems outlined above but sufficiently general to illustrate the main priniciples.

2.2.1 Wave Guide Quantization

Consider the Lagrangian of the matter-free EM field, $L = -\frac{1}{4}\int d^3x F_{\mu\nu}F^{\mu\nu}$. As a first step towards quantization of this system we fix a gauge. E.g., in the absence of charge a particularly convenient choice is the Coulomb gauge, $\nabla \cdot \mathbf{A} = 0$, plus vanishing of the scalar component, $\phi = 0$. Keep in mind that once a gauge has been set we cannot expect further results to display 'gauge invariance'.

Using the gauge conditions and integrating by parts one verifies that the Lagrangian assumes the form

$$L = \frac{1}{2}\int d^3x \left[\partial_t \mathbf{A} \cdot \partial_t \mathbf{A} + \mathbf{A} \cdot \Delta \mathbf{A}\right]. \tag{2.10}$$

In analogy to our discussion of the atomic chain, one would next proceed to 'decouple' the theory by expanding in terms of eigenfunctions of the Laplace operator. The *difference* to our previous discussion is that we are dealing (i) with the full three-dimensional Laplacian (instead of a simple second derivative) acting on (ii) the vectorial quantity $\mathbf{A}$ which is (iii) subject to the constraint $\nabla \cdot \mathbf{A} = 0$. It is these aspects which lead to the complications outlined above.

We can navigate around these difficulties by considering problems where the system geometry reduces the complexity of the eigenvlue problem. This restriction is less artificial than it might appear. E.g. in anisotropic electromagnetic wave guides, systems of undisputable *technological* relevance, the solutions of the eigenvalue equation can be formulated as[7]

$$\Delta \mathbf{R}_k(\mathbf{x}) = \lambda_k \mathbf{R}_k(\mathbf{x}), \tag{2.11}$$

where $k \in \mathbb{R}$ is a *one-dimensional* index parameter and the vector-valued functions $\mathbf{R}_k$ are real and ortho-normalized, $\int \mathbf{R}_k \cdot \mathbf{R}'_k = \delta_{kk'}$. The dependence of the eigenvalues λ_k on k depends on details of the geometry (see Eq. (2.14) below) and needs not be specified for the moment.

[6] Readers interested to learn more about this very important problem are deferred to one of several excellent introductions, e.g. the book by Ryder.

[7] More precisely, one should say that (2.11) defines the set of eigenfunctions relevant for the low energy dynamics of the wave guide. More complex eigenfunctions of the Laplace operator exist but they carry much higher energy.

▷ INFO. An **electrodynamic wave guide** is a quasi one-dimensional cavity with metallic boundaries (cf. Fig. 2.5.) The great practical advantage of wave guides is that they are very good at confining EM waves. At large frequencies where the wavelengths are of order meters or less radiation loss in conventional conductors are high. In these frequency domains, hollow conductors provide the only practical way of transmitting radiation.

EM field propagation inside a wave guide is constrained by boundary conditions. E.g., assuming the walls of the system to be perfectly conducting,

$$\mathbf{E}_{\parallel}(\mathbf{x}_{\mathrm{b}}) = 0, \tag{2.12}$$
$$\mathbf{B}_{\perp}(\mathbf{x}_{\mathrm{b}}) = 0, \tag{2.13}$$

where $\mathbf{x}_{\mathrm{b}}$ is a point at the system boundary and $\mathbf{E}_{\parallel}$ ($\mathbf{B}_{\perp}$) is the parallel (perpendicular) component of the electric (magnetic) field.

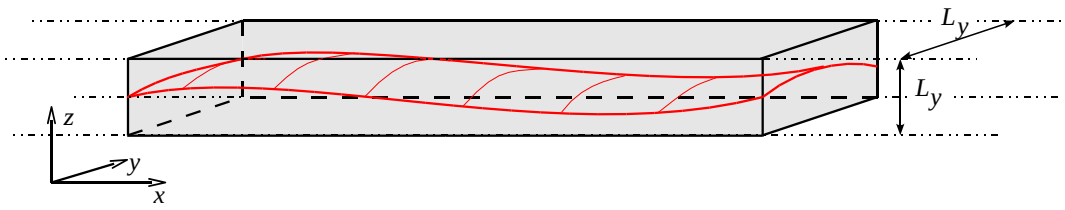

Figure 2.5: Rectangular EM wave guide. The structure of the eigenmodes of the EM field is determined by boundary conditions at the walls of the cavity.

For concreteness, and turning back to our problem of field quantization, let us consider a cavity with uniform rectangular cross section $L_y \times L_z$. To conveniently represent the Lagrangian of the system, we wish to express the vector potential in terms of eigenfunctions $\mathbf{R}_{\mathbf{k}}$ that are consistent with the boundary conditions (2.12). A complete set of functions fulfilling this condition is given by

$$\mathbf{R}_{\mathbf{k}} = \mathcal{N}_k \begin{pmatrix} c_1 \cos(k_x x)\sin(k_y y)\sin(k_z z) \\ c_2 \sin(k_x x)\cos(k_y y)\sin(k_z z) \\ c_3 \sin(k_x x)\sin(k_y y)\cos(k_z z) \end{pmatrix}.$$

Here, $k_i = n_i \pi / L_i$, $n_i \in \mathbb{N}$, $i = x, y, z$, $\mathcal{N}_k$ is a factor normalizing $\mathbf{R}_{\mathbf{k}}$ to unity, and the coefficients c_i are subject to the condition $c_1 k_x + c_2 k_y + c_3 k_z = 0$. Indeed, it is straightforward to verify that a general superposition of the type $\mathbf{A}(\mathbf{x}, t) \equiv \sum_{\mathbf{k}} \alpha_{\mathbf{k}}(t) \mathbf{R}_{\mathbf{k}}(\mathbf{x})$, $\alpha_{\mathbf{k}}(t) \in \mathbb{R}$, is divergenceless, and generates an EM field compatible with (2.12). Substitution of $\mathbf{R}_{\mathbf{k}}$ into (2.11) identifies the eigenvalues to

$$\lambda_{\mathbf{k}} = -(k_x^2 + k_y^2 + k_z^2).$$

In the physics and electro-engineering literature, eigenfunctions of the Laplace operator in a quasi one-dimensional geometry are commonly denoted as **modes**. As we will see shortly, the energy of a mode (i.e. the Hamiltonian evaluated on a specific mode configuration) grows with $|\lambda_{\mathbf{k}}|$; In cases where one is interested in the low energy dynamics of the EM field, only configurations with small $|\lambda_{\mathbf{k}}|$ are relevant. E.g. let us consider a massively anisotropic wave guide with $L_z < L_y \ll L_x$. In this case the modes with smallest $|\lambda_k|$ are those with $k_z = 0$, $k_y = \pi / L_y$ and $k_x \equiv k \ll L_{z,y}^{-1}$. (Why is it not possible to set *both* k_y and k_z to zero?) With this choice,

$$\lambda_k = -\left(k^2 + \left(\frac{\pi}{L_y}\right)^2\right) \tag{2.14}$$

and a scalar index k suffices to label both eigenvalues and eigenfunctions R_k. A cartoon of the spatial structure the functions $\mathbf{R}_k$ is shown in Fig. 2.5. The dynamical properties of these configurations will be discussed in the text.

Turning back to the problem posed by (2.10) and (2.11), we expand the vector potential in terms of eigenfunctions R_k,

$$\mathbf{A}(\mathbf{x},t) = \sum_k \alpha_k(t)\mathbf{R}_k(\mathbf{x}),$$

where the sum runs over all allowed values of the index parameter k. (E.g. in a wave guide, $k \in \frac{\pi}{L}n$, $n \in \mathbb{N}$ where L is the length of the guide.) Substituting this expansion into (2.10) and using the normalization properties of the $\mathbf{R}_k$, we obtain

$$L = \frac{1}{2}\sum_k \left(\dot{\alpha}_k^2 + \lambda_k \alpha_k^2\right),$$

i.e. a decoupled representation where the system is described in terms of independent dynamical systems with coordinates α_k. From this point on, quantization proceeds along the lines of the standard algorithm: Define momenta through $\pi_k = \partial_{\dot{\alpha}_k} L = \dot{\alpha}_k$. This produces the Hamiltonian $H = \sum_k (\pi_k\pi_k - (\lambda_k/2)\alpha_k\alpha_k)$. We next quantize by promoting $\alpha_k \to \hat{\alpha}_k$ and $\pi_k \to \hat{\pi}_k$ to operators and declaring $[\hat{\pi}_k, \hat{\alpha}_{k'}] = -i\delta_{kk'}$. The quantum Hamilton operator, again of harmonic oscillator type, then reads

$$\hat{H} = \sum_k \left(\frac{1}{2m}\hat{\pi}_k\hat{\pi}_k + \frac{m\omega_k^2}{2}\hat{\alpha}_k\hat{\alpha}_k\right),$$

where the 'mass' parameter $m = 1$ and $\omega_k = |\lambda_k|$. Following the same logics as in section 2.1.2, we define ladder operators

$$a_k \equiv \sqrt{\frac{m\omega_k}{2}}\left(\hat{\alpha}_k + \frac{i}{m\omega_k}\hat{\pi}_k\right), \qquad a_k^\dagger \equiv \sqrt{\frac{m\omega_k}{2}}\left(\hat{\alpha}_k - \frac{i}{m\omega_k}\hat{\pi}_k\right),$$

whereupon the Hamiltonian assumes its final form

$$\hat{H} = \sum_k \omega_k\left(a_k^\dagger\hat{a}_k + \frac{1}{2}\right). \tag{2.15}$$

For the specific problem of the first excited mode in a wave guide of witdth L_y, $\omega_k = [k^2 + (\pi/L_y)^2]^{1/2}$. Eq. (2.15) represents our final result for the quantum Hamiltonian of the EM wave guide. Before concluding this section let us make a few comments on the structure of the result:

- ▷ First, notice that the construction above almost completely paralleld our previous discussion of the harmonic chain[8]. The close structural simiarity between the two

[8] Technically, the only technical is that instead of index pairs $(k,-k)$ all indices (k,k) are equal and positive. This can be traced back to the fact that we have expanded in terms of the *real* eigenfunctions of the closed wave guide instead of the *complex* eigenfunctions of the circular oscillator chain. At any rate, the difference is largely inessential.

systems roots in the fact that the free field Lagrangian (2.10) is quadratic and, therefore, bound to map onto an oscillator type Hamiltonian. That we obtained a simple *one-dimensional* superposition of oscillators is due to the boundary conditions specific to a narrow wave guide. For less restrictive geometries, e.g. free space, a more complex superposition of vectorial degrees of freedom in three-dimensional space would have been obtained. However, the principal mapping of the free EM field onto a superposition of oscillators is independent of geometry.

- ▷ Physically, the quantum excitations described by (2.15) are, of course, the **photons** of the EM field. The unfamilar appearance of the dispersion relation ω_k is again a peculiarity of the wave guide. However, in the limit of large longitudinal wave numbers $k \gg L_y^{-1}$, the dispersion approaches $\omega_k \sim |k|$, i.e. the relativistic dispersion of the photon field. Also notice that, due to the equality of the Hamiltonians (2.9) and (2.15), all what had been said about the behaviour of the phonon modes of the atomic chain carries over to the photon modes of the wave guide.

- ▷ As with their phononic analog, the oscillators described by (2.15) exhibit zero point fluctuations. It is a fascinating aspect of quantum electrodynamics that these oscillations, caused by quantization of *the* most relativistic field, surface at various points of non-relativistic physics. In the next section two prominent manifestations of zero point fluctuations in condensed matter physics will be briefly discussed.

2.2.2 The Quantum Vacuum

One of the most prominent manifestations of vacuum fluctuations is the **Casimir effect**[9]: Two parallel conducting plates embedded into the vacuum excert an attractive force on each other. This phenomenon is believed to be of some relevance for, e.g., colloidal chemistry. Namely the force balance of hydrophobic suspensions of particles, sized $0.1 - 1\mu$m, in electrolytes. At least it is problems of this type which prompted Casimir to his famous analysis of the idealized vacuum problem. Qualitatively, the origin of the Casimir force is readily understood (See our poor attempt at an illustration, Fig. 2.6.): Like their classical analog, quantum photons exert a certain radiation pressure on macroscopic media. The difference to the classical case is that, due to zero point oscillations, even the quantum *vaccuum* is capable of creating radiation pressure. For a single conducting body embedded into the infinite vacuum, the net pressure vanishes by symmetry. However, for two parallel plates, the situation is different. Mode quantization arguments similar to the ones used in the previous section show that the density of quantum modes between the plates is lower than in the half infinite outer spaces. Hence, the force (density) created by outer space exceeds the counter pressure from the inside; The plates 'attract' each

[9]

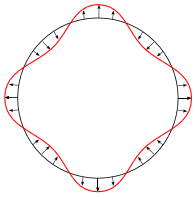

Casimir.

other. For a quantiative formulation of this picture, see problem XX. A second important

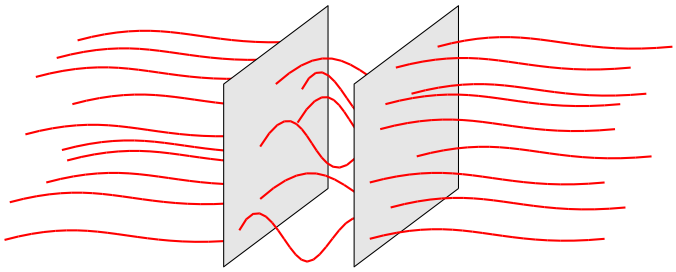

Figure 2.6: Very schematic attempt to illustrate the principle behind the casimir effect. Mode quantization implies that the density of EM field modes between two parallel plates in a vacuum is lower than in outer space. Consequently, the radiation pressure from the outside exceeds the counter pressure from the inside and the plates feel an attractive force.

phenonmenon where vacuum fluctuations play some role is **Van der Waals forces**[10]: Neutral atoms or molecules attract each other by a potential that, at small separation r, scales like r^{-6}. Early microscopic attempts to classically explain the origin of the phenomenon produced results for the attraction force that, in conflict with experimental finding, were strongly temperature dependent. It was considered a major breakthrough of the new quantum mechanics when London[11] proposed a model whereby a temperature independent r^{-6}-law was obtained. The essence of Londons idea is easily explained: Imagine each of the atoms/molecules as an oscillator. The zero point motion of these oscillators, measured in terms of some coordinate x, creates a dipole moment of strength $\sim x$. At close distances, the systems interact through a dipole-dipole interaction. Writing down coupled oscillator equations (see problem XX), one readily obtains a lowering of the ground state energy by a contribution $V(r) \sim r^{-6}$.

However, there is a subtle point about the seemingly innocous coupling of the *quantum* oscillator to the *classical* Coulomb potential. Close inspection (see Milonni's book for details) shows that to maintain the quantum commutation relations of the oscillator degrees of freedom, the EM field must not be assumed entirely classical. In fact, once the quantum nature of the EM field has entered the stage, it becomes possible to explain the force without need for phenomenological introduction of atomic oscillator degrees of

10 Johannes Diderik van der Waals 1837-1923, 1910 Nobel Laureate in physics in recognition of his work on the state equation of non-ideal gases.

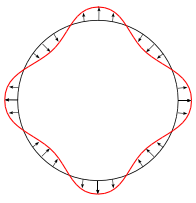

11 Fritz Wolfgang London 1900-1954, famous for his work on van der Waals forces and his phenomenological theory of superconductivity (in collaboration with his brother Heinz, 1907-1970.)

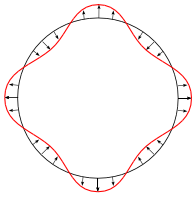

freedom:

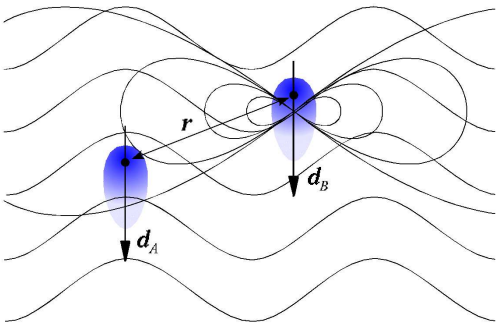

Figure 2.7: On the creation of van der Waals forces by EM vacuum fluctuations. An atom or molecule B is exposed to fluctuations of the EM quantum vacuum (visualized by wavy lines.) This leads to the creation of a dipole element $\mathbf{d}_B$. A closeby partner atom A sees both the vacuum amplitude and the dipole field created by $\mathbf{d}_B$. The cooperation of the two field strengths leads to a net lowering of the energy of A.

Consider an atom A exposed to an electric field $\mathbf{E}$. The field gives rise to the atomic Stark[12] effect, i.e. a level shift of order $W \sim \alpha\langle \mathbf{E}(\mathbf{x}_A) \cdot \mathbf{E}(\mathbf{x} - A)\rangle$, where α is the atomic polarizability, $\mathbf{E} = \partial_t \mathbf{A}$ is the *operator* representing the EM field, and $\langle \ldots \rangle$ a quantum expectation value.

For an atom in the empty vacuum $\mathbf{E} \equiv \mathbf{E}_0$ is determined by the zero point amplitude of the quantum oscillator field. However, in the neighbourhood of a second atom B, the field amplitude is different. The point is that the zero point amplitude $\mathbf{E}_0$ induces a dipole element $\mathbf{d}_B \propto \alpha \mathbf{E}_0(\mathbf{x}_B)$. This dipole creates a field $\mathbf{E}_B$ which contributes to the total field amplitude felt by atom A: $\mathbf{E}(\mathbf{x}_A) = (\mathbf{E}_0 + \mathbf{E}_B)(\mathbf{x}_A)$ (see Fig. 2.7.) The dominant contribution to the level shift due to the proximity of B is then given by

$$V(\mathbf{r}) = W - \alpha\langle \mathbf{E}_0(\mathbf{x}_A) \cdot \mathbf{E}_0(\mathbf{x}_A)\rangle \sim \alpha\langle \mathbf{E}_0(\mathbf{x}_A) \cdot \mathbf{E}_B(\mathbf{x}_B) \sim \alpha^2 \langle \mathbf{E}_0^T(\mathbf{x}_A)\mathbf{A}(\mathbf{r})\mathbf{E}(\mathbf{x}_B)\rangle, \tag{2.16}$$

where $\mathbf{r} \equiv \mathbf{r}_B - \mathbf{r}_A$ and $\mathbf{A}(\mathbf{r})$ is a matrix kernel describing the geometric details of the dipole interaction. (We have subtracted the vacuum level shift because it represents an undetectable offset.) Notice (2.16) predicts the van der Waals interaction to be proportional to the square of the zero point field amplitude.

Unfortunatelty, the quantiatitve evaluation of the matrix element, involving a geometric average over all polarization directions of the quantum field amplitude is somewhat involved. As a final result of a calculation (detailed, e.g., in Millnors book, section 3.11.)

---

[12] Johannes Stark 1874-1957, Nobel laureate 1919 for his discovery of the Stark effect in 1913. Otherwise, one of the worst characters of Nazi German science. In 1937 accused Heisenberg of cooperating with jews. It took the personal intervention of Himmler, Reichsführer SS (!), to get Heisenberg out of trouble.

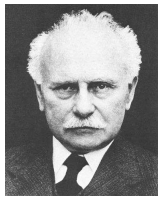

one obtains

$$V(\mathbf{r}) = -\frac{3\omega_0\alpha^2}{4r^6}, \tag{2.17}$$

where ω_0 is the transition frequency between the ground state and the first excited state of the atom. (This paramter enters the result through the dependence of the microscopic polarizability on the transition frequencies.)

2.3 Summary and Outlook

In this chapter we have introduced the general algorithm whereby classical continuum theories are quantized. Employing the elementary harmonic oscillator as a prototypical example we have seen that the Hilbert spaces of these theories afford different interpretations. Of particular use was a quasi-particle picture whereby the collective excitations of the continuum theories acquired the status of elementary particles.

Suspiciously, both examples discussed in this text, the harmonic quantum chain and free quantum electrodynamics, led to exactly solvable, **free field theories**. However, it takes only little imagination to foresee that only few continuum theories will be as simple. E.g. the exact solvability of the atomic chain would have been lost had we included higher order contributions in the expansion in powers of the lattice distortion amplitude. Such terms would hinder the free wave-like propagation of the phonon modes. Put differently, phonons would begin to scatter off each other or interact. Similarly, the free status of electrodynamics is lost once the EM field is allowed to interact with a matter field. Needless to say, **interacting field theories** are infinitely more complex, but also more interesting, than the systems considered so far.

Technically, we have seen that the phonon/photon interpretation of the field theories discussed in this chapter could conveniently be formulated in terms of ladder operators. However, the applications discussed so far provide only a glimpse on the full spectrum of advantages of this language. In fact, the formalism of ladder operators, commonly denoted as 'second quantization', represents a central, and historically the oldest element of quantum field theory. The next chapter is devoted to a more comprehensive discussion of both the formal aspects and applications of this language.

2.4 Problem Set

Q1 Applying the Euler-Lagrange equation, obtain the equation of motion of the Lagrangian densities:

1. $\mathcal{L}[\phi, \dot{\phi}, \partial_x \phi] = \frac{m\dot{\phi}^2}{2} - \frac{k_s a^2}{2}(\partial_x \phi)^2 - \frac{m^*}{2}\omega^2\phi^2$
2. $\mathcal{L}[\phi, \dot{\phi}, \partial_x^2 \phi] = \frac{m\dot{\phi}^2}{2} - \frac{\kappa}{2}\left(\partial_x^2 \phi\right)^2$
3. $\mathcal{L}[\phi, \dot{\phi}] = \frac{m\dot{\phi}^2}{2} - \frac{m^*}{2}\omega^2\phi^2 - \frac{\eta}{4}\phi^4$
4. $\mathcal{L}[\{\dot{\phi}_i\}, \{\partial_x \phi_i\}] = \sum_{i=1}^{n}\left[\frac{m}{2}\dot{\phi}_i^2 - \frac{1}{2}k_s a^2(\partial_x \phi_i)^2\right]$
5. $\mathcal{L}[\dot{\phi}, \partial_x \phi] = \frac{m}{2}|\dot{\phi}|^2 - \frac{1}{2}k_s a^2|\partial_x \phi|^2$

[Note that in 5. the field ϕ is complex.] Cast the Lagrangian density 4. in a more compact form by making use of a relativistic 4-vector notation. Starting with the Lagrangian 2., obtain the Hamiltonian density. Introducing canonical commutation relations, quantise the Hamiltonian.

Q2 Following the discussion in the lectures, a periodic one-dimensional quantum elastic chain of length L is expressed by the Hamiltonian

$$\hat{H} = \int dx \left[\frac{1}{2m}\hat{\pi}^2 + \frac{k_s a^2}{2}(\partial_x \hat{\phi})^2\right]$$

where the field operators obey the canonical commutation relations

$$\left[\hat{\pi}(x), \hat{\phi}(x')\right] = -i\hbar\delta(x - x').$$

(a) Defining the Fourier representation,

$$\begin{Bmatrix} \hat{\phi}_k \\ \hat{\pi}_k \end{Bmatrix} \equiv \frac{1}{L^{1/2}}\int_0^L dx e^{\{\mp ikx}\begin{Bmatrix} \hat{\phi}(x) \\ \hat{\pi}(x) \end{Bmatrix}, \qquad \begin{Bmatrix} \hat{\phi}(x) \\ \hat{\pi}(x) \end{Bmatrix} = \frac{1}{L^{1/2}}\sum_k e^{\{\pm ikx}\begin{Bmatrix} \hat{\phi}_k \\ \hat{\pi}_k \end{Bmatrix},$$

where $\sum_k$ represents the sum over all quantised quasi-momenta $k = 2\pi m/L$, $m \in \mathcal{Z}$, show that the field operators obey the commutation relations $[\hat{\pi}_k, \hat{\phi}_{k'}] = -i\hbar\delta_{kk'}$.

(b) In the Fourier representation, show that the Hamiltonian takes the form

$$\hat{H} = \sum_k \left[\frac{1}{2m}\hat{\pi}_k\hat{\pi}_{-k} + \frac{k_s a^2}{2}k^2\hat{\phi}_k\hat{\phi}_{-k}\right].$$

(c) Defining

$$a_k \equiv \sqrt{\frac{m\omega_k}{2\hbar}}\left(\hat{\phi}_k + i\frac{1}{m\omega_k}\hat{\pi}_{-k}\right)$$

where $\omega_k = a(k_s/m)^{1/2}|k| = v|k|$ show that the field operators obey the canonical commutation relations $[a_k, a_{k'}^\dagger] = \delta_{kk'}$, and $[a_k, a_{k'}] = 0$.

(d) Finally, with this definition, show that the Hamiltonian can be expressed in the form

$$\hat{H} = \sum_k \hbar\omega_k \left(a_k^\dagger a_k + \frac{1}{2} \right).$$

Q3 Londons phenomenological approach to explaining the van der Waals force starts out from the Hamiltonian

$$\hat{H} = \frac{\hat{p}_1^2}{2m} + \frac{\hat{p}_1^2}{2m} + \frac{m\omega_o^2}{2}(\hat{x}_1^2 + \hat{x}_2^2) + mK\hat{x}_1\hat{x}_2,$$

where $\hat{x}_i$ is the coordinate of an oscillator phenomenologically representing one of two atoms $i = 1, 2$. The atoms are coupled through a dipole-dipole interaction, where the dipole operators are proportional to $\hat{x}_i$ and $K = qe^2/(mr^3)$ encapsulates the details of the interaction. Here r denotes the distance between the atoms and q is a dipole-dipole orientation factor.

Compute the spectrum of the two-particle system described by $\hat{H}$ and verify that the dipole coupling leads to a lowering

$$V(r) = \frac{K^2}{8\omega_o^3}$$

of the ground state energy. Using that the classical polarizability of an oscillator is given by $\alpha = e^2/(m\omega^2)$ this becomes $V = \frac{q^2\omega\alpha^2}{8r^6}$. Finally, using that the directional average of the geometric factor q^2 equals 2 and multiplying by three to account for the three dimensional character of a 'real' atomic oscillator, we recover the result (2.17).

2.4.1 Answers

A1 To complete this problem, one must generalise the Euler-Lagrange equation derived in lectures. E.g., for case 2., a variation of the action obtains

$$\begin{aligned}\delta S &= \int \left[\mathcal{L}(\dot{\phi}+\epsilon\dot{\eta}, \partial_x^2\phi + \epsilon\partial_x^2\eta) - \mathcal{L}(\dot{\phi}, \partial_x^2\phi)\right] \\ &= \epsilon \int \left[\dot{\eta}\partial_{\dot{\phi}}\mathcal{L} + \partial_x^2\eta\partial_{\partial_x^2\phi}\mathcal{L}\right] = \epsilon \int \eta\left[-d_t\partial_{\dot{\phi}}\mathcal{L} + d_x^2\left(\partial_{\partial_x^2\phi}\mathcal{L}\right)\right]\end{aligned}$$

from which we obtain the Euler-Lagrange equation

$$-d_t\partial_{\dot{\phi}}\mathcal{L} + d_x^2\left(\partial_{\partial_x^2\phi}\mathcal{L}\right) = 0.$$

Applied to the Lagrangian functionals at hand, one finds the equation of motion

1. $\ddot{\phi} - \dfrac{k_s a^2}{m}\partial_x^2\phi + \omega^2\phi = 0,$
2. $\ddot{\phi} + \dfrac{\kappa}{m}\partial_x^4\phi = 0,$
3. $\ddot{\phi} + \omega^2\phi + \dfrac{\eta}{m}\phi^3 = 0$
4. $\ddot{\phi}_i - \dfrac{k_s a^2}{m}\partial_x^2\phi_i = 0.$

Finally, turning to case 5., it is necessary to generalise the Euler-Lagrange equation to account for complex fields. Since the real and imaginary parts fluctuate independently, we can consider a variation of each independently. Separating $\phi = \phi' + i\phi''$ into its real and imaginary parts, and applying a variation to each component, one obtains

$$\ddot{\phi}' - \frac{k_s a^2}{m}\partial_x^2\phi' = 0, \qquad \ddot{\phi}'' - \frac{k_s a^2}{m}\partial_x^2\phi'' = 0.$$

In fact, this result shows that the components ϕ and the complex conjugate ϕ^* can be treated as independent. A variation of the action with respect to ϕ^* obtains

5. $\ddot{\phi} - \dfrac{k_s a^2}{m}\partial_x^2\phi = 0.$

For case 2. the momentum conjugate to the field ϕ is given by

$$\phi = \partial_{\dot{\phi}}\mathcal{L} = m\dot{\phi}.$$

The Hamiltonian corresponding to case 2. is given by

$$\mathcal{H} = \pi\dot{\phi} - \mathcal{L} = \frac{\pi^2}{2m} + \frac{k_s a^2}{2}(\partial_x^2\phi)^2.$$

Applying the canonical commutation relations $[\hat{\pi}(x), \hat{\phi}(x')] = -i\hbar\delta(x-x')$, and promoting the classical fields to operators, one obtains the quantum Hamiltonian. In Fourier space, the Hamiltonian takes the same form as that discussed in lectures with $q^2 \mapsto q^4$.

A2 (a) Using the definition provided, together with the canonical commutation relations of the field operators, one obtains

$$[\hat{\pi}_k, \hat{\phi}_{k'}] = \frac{1}{L}\int_0^L dx \int_0^L dx' e^{-ikx+ik'x'} \overbrace{[\hat{\pi}(x), \hat{\phi}(x')]}^{-i\hbar\delta(x-x')}$$
$$= -i\hbar \overbrace{\frac{1}{L}\int_0^L dx\ e^{-i(k-k')x'}}^{\delta_{kk'}} = -i\hbar\delta_{kk'}.$$

(b) Again, using the definition, the kinetic component of the Hamiltonian takes the form

$$\int_0^L dx\ \frac{\hat{\pi}^2}{2m} = \sum_{kk'}\frac{1}{L}\int_0^L dx\ e^{i(k+k')x}\frac{1}{2m}\ \hat{\pi}_k\hat{\pi}_{k'} = \sum_k \frac{1}{2m}\hat{\pi}_k\hat{\pi}_{-k}.$$

Similarly, applied to the potential component one obtains the Hamiltonian as advertised.

(c) Using the commutation relation derived above, one finds

$$[a_k, a^\dagger_{k'}] = \frac{i}{2\hbar}\left([\hat{\phi}_{-k}, \hat{\pi}_{-k'}] - [\hat{\pi}_k\hat{\phi}_{k'}]\right) = \delta_{kk'}, \qquad [a^\dagger_k, a^\dagger_{k'}] = 0.$$

(d) Inverting the expression for the field operators, one finds

$$\hat{\phi}_k = \left(\frac{\hbar}{2m\omega_k}\right)^{1/2}\left(a_k + a^\dagger_{-k}\right), \qquad \hat{\pi}_k = i\left(\frac{m\hbar\omega_k}{2}\right)^{1/2}\left(a^\dagger_k - a_{-k}\right).$$

Using the identity

$$\frac{1}{2m}\left(\hat{\pi}_k\hat{\pi}_{-k} + \hat{\pi}_{-k}\hat{\pi}_k\right) + \frac{k_s a^2}{2}k^2\left(\hat{\phi}_k\hat{\phi}_{-k} + \hat{\phi}_{-k}\hat{\phi}_k\right)$$
$$= \frac{1}{2}\hbar\omega_k\left(a^\dagger_k a_k + a_k a^\dagger_k + a^\dagger_{-k}a_{-k} + a_{-k}a^\dagger_{-k}\right).$$

together with the commutation relations, we obtain the harmonic oscillator Hamiltonian.

A3 We begin by formulating the potential $\hat{U}$ of the oscillator system in a matrix notation, $\hat{U} = \hat{\mathbf{x}}^T A\hat{\mathbf{x}}$, where $\hat{\mathbf{x}}^T = (\hat{x}_1, \hat{x}_2)^T$ and

$$A = \frac{m}{2}\begin{pmatrix}\omega^2 & K\\ K & \omega^2\end{pmatrix}.$$

Diagonalizing the matrix, $A = UDU^T$ and transforming coordinates $\mathbf{x} \to U^T\mathbf{x} = \mathbf{x}'$, the system decouples into two independent oscillators,

$$\hat{H} = \sum_{i=1,2}\left(\frac{\hat{p}_i^{2\prime}}{2m} + \frac{m\omega_i^2}{2}\hat{x}_i^{2\prime}\right),$$

where the new characteristic frequencies $\omega_{1/2} = \frac{m}{2}(\omega_o^2 \pm K)^{1/2}$ are determined by the eigenvalues of the matrix D. The ground state of this system is given by

$$E_0 = \frac{1}{2}(\omega_1 + \omega_2) \approx \omega_o - \frac{K^2}{8\omega_o^3},$$

which lies by an amount $V = -\frac{K^2}{8\omega_o^3}$ lower than the energy of the isolated atoms.

Chapter 3

Second Quantisation

The aim of this section is to introduce and apply the method of second quantisation. The first part of the section focuses on methodology and notation, while the remainder is devoted to applications. We will investigate the physics of charge density wave propagation in one-dimensional quantum wires, spin waves in a quantum Heisenberg (anti)ferromagnet, the weakly interacting Bose gas, and the electron-phonon interaction. In later chapters most of these problem classes will be revisited from different perspectives.

In the previous chapter we have encountered two field theories that could conveniently be represented in the language of 'second quantization', i.e. a formulation based on the algebra of certain ladder operators $\hat{a}_k$[1]. There have been two remarkable facts about this formulation: First, second quantization provided a compact way of representing the *many body* quasi-particle space of excitations in these systems. (There was no need to explicitly symmetrize many particle states as would be the case in the formalism of 'ordinary' many body quantum mechanics.) Second, the properties of the ladder operators were encoded in a simple set of commutation relations (cf. Eq. 2.8) rather than in some explicit Hilbert space representation.

Apart from a certain aesthetic appeal, these observations would not be of much relevance if it were not for the fact that the formulation can be generalized to a comprehensive and highly efficient formulation of many body quantum mechanics *in general*. In fact, second quantization can be considered the first major cornerstone on which the theoretical framework of quantum field theory was built. As such, extensive introductions to the concept can be found throughout the literature (see, e.g., Feynman [**?**]). We will therefore not develop the formalism in full mathematical rigour but rather proceed pragmatically by first motivating and introducing its basic elements, followed by a discussion of the 'second quantized' version of standard operations of quantum mechanics (taking matrix elements,

[1] In the opinion of the authors the denotation 'second quantization' is chosen unfortunately. Historically, this denotation was motivated by the observation that the ladder operator algebra fosters an interpretation of quantum excitations as discrete 'quantized' units. Fundamentally, however, there is no such thing like 'two' superimposed quantization steps in single- or many-particle quantum mechanics. What we are dealing with is basically a problem-adjusted representation of the 'first and only quantized' theory.

changing bases, representing operators etc.) The second part of the chaper will be concerned with developing fluency in the method by addressing a number of applications. Readers familiar with the formalism may directly proceed to these sections.

3.1 Introduction to Second Quantization

3.1.1 Motivation

We begin our discussion by recapitulating some fundamental notions of many body quantum mechanics, as formualted in the traditional language of symmetrized/anti-symmetrized wave functions. Consider the (normalised) set of wavefunctions $|\psi_n\rangle$ of some single-particle Hamiltonian $\hat{H}$,

$$\hat{H}|\psi_\lambda\rangle = \epsilon_\lambda|\psi_\lambda\rangle.$$

where ϵ_λ are the eigenvalues. With this definition, the normalized 2-particle wavefunction of two fermions (bosons) populating the levels λ and $\lambda' \neq \lambda$ given by the anti-symmetrized (symmetrized) product

$$\psi_F(x_1, x_2) = \frac{1}{\sqrt{2}}\left(\psi_\lambda(x_1)\psi_{\lambda'}(x_2) - \psi_{\lambda'}(x_1)\psi_\lambda(x_2)\right),$$
$$\psi_B(x_1, x_2) = \frac{1}{\sqrt{2}}\left(\psi_\lambda(x_1)\psi_{\lambda'}(x_2) + \psi_{\lambda'}(x_1)\psi_\lambda(x_2)\right).$$

In the Dirac Bracket representation,

$$|\lambda, \lambda'\rangle_{F(B)} \equiv \frac{1}{\sqrt{2}}\left(|\psi_\lambda\rangle \otimes |\psi_{\lambda'}\rangle - \zeta|\psi_{\lambda'}\rangle \otimes |\psi_\lambda\rangle\right), \tag{3.1}$$

where $\zeta = 1$ for fermions while $\zeta = -1$ for bosons[2]. Note that the explicit symmetrization of the wave functions is necessitated by quantum mechanical **indistinguishability**: For (fermions) bosons the wave function has to be anti-symmetric (symmetric) under particle exchange. More generally, an appropriately symmetrized N-particle wavefunction is expressed in the form

$$\boxed{|\lambda_1, \lambda_2, \ldots \lambda_N\rangle \equiv \frac{1}{\sqrt{N!\prod_{\lambda=0}^{\infty} n_\lambda!}} \sum_{\mathcal{P}} (-\zeta)^{(1-\text{par}\,\mathcal{P})/2} |\psi_{\lambda_{\mathcal{P}1}}\rangle \otimes |\psi_{\lambda_{\mathcal{P}2}}\rangle \ldots \otimes |\psi_{\lambda_{\mathcal{P}N}}\rangle} \tag{3.2}$$

where n_λ is the total number of particles in state λ (for fermions, Pauli exclusion enforces the constraint $n_\lambda = 1$) – see fig. 3.1. The summation runs over all $N!$ permutations of the

[2]

Enrico Fermi 1901-1954 (left) and Satyendranath Bose 1894-1974 (right): Fermi was made 1938 Nobel Laureate in Physics for his demonstrations of the existence of new radioactive elements produced by neutron irradiation, and for his related discovery of nuclear reactions brought about by slow neutrons.

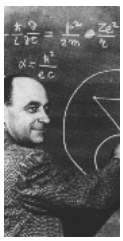

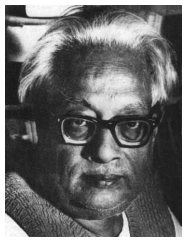

set of quantum numbers $\{\lambda_1, \ldots \lambda_N\}$, and $\mathrm{par}\,\mathcal{P}$ denotes the parity of the permutation $\mathcal{P}$. ($\mathrm{par}\,\mathcal{P} = 1(-1)$ if the number of transpositions of two elements which brings the permutation $(\mathcal{P}_1, \mathcal{P}_2, \cdots \mathcal{P}_N)$ back to its original form $(1, 2, \cdots N)$ is even (odd)). The prefactor $1/\sqrt{N! \prod_\lambda n_\lambda!}$ normalises the many-body wave function. In the fermionic case, the many-body wavefunction is known as a **Slater determinant**. Finally notice that it will be useful to assume the quantum numbers $\{\lambda_i\}$ defining the state $|\lambda_1, \lambda_2, \ldots, \lambda_N\rangle$ to be ordered according to some convention. (E.g. for $\lambda_i = x_i$ a one-dimensional coordinate representation we might order according to $x_1 \leq x_2 \leq \ldots \leq x_N$.) Any initially non-ordered state can be brought into an ordered form at the cost of, at most, a minus sign.

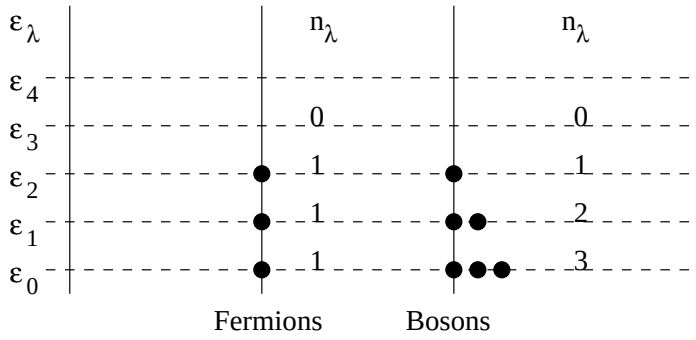

Figure 3.1: Schematic diagram showing occupation numbers for a generic fermion and boson system.

While representations like (3.2) *can* be used to represent the full Hilbert space[3] of many body quantum mechanics, a moments thought shows that this formulation is not in the least convenient:

- ▷ It takes little imagination to anticipate that actual working in the language of (3.2) will be difficult. E.g to compute the overlap of two wave function one needs to form $(N!)^2$ different products.
- ▷ The representation is tailor made to problems with fixed particle number N. However, we know from statistical mechanics that for $N = \mathcal{O}(10^{23})$ it is much more convenient to work in a grand canonical formulation whereby N is allowed to fluctuate. Closely related,
- ▷ In applications one will often ask questions like, "What is the amplitude for injection of a particle into the system at a certain space-time coordinate (x_1, t_1) followed by annihilation at some later time (x_2, t_2)". Ideally, one would work with a representation that supports the intuition afforded by thinking in terms of such processes. I.e.

[3] David Hilbert 1862-1943; His work in geometry had the greatest influence in that area after Euclid. A systematic study of the axioms of Euclidean geometry led Hilbert to propose 21 such axioms and he analysed their significance. He contributed to many areas of mathematics.

a representation where the quantum numbers of of *individual* quasi-particles rather than the entangled set the quantum numbers of *all* constitutents are fundamental.

The 'second quantized' formulation of many body quantum mechanics, as introduced in the next subsection, does not suffer from these deficits.

3.1.2 The Apparatus of Second Quantization

We begin the construction of a more efficient formulation of many body quantum mechanics with a few abstract definitions: Let $|\Omega\rangle$ denote a normalized reference state lying in the full many body Hilbert space. $|\Omega\rangle$ will be called the **vacuum state**; Physically, it represents an 'empty' state with no quasi-particles present. Next introduce a set of **field operators** a_λ together with their adjoints $a_\lambda^\dagger$, as follows:[4]

$$\boxed{a_\lambda|\Omega\rangle = 0, \qquad \mathcal{N}\prod_{i=1}^{N} a_{\lambda_i}^\dagger|\Omega\rangle = |\lambda_1, \lambda_2, \ldots \lambda_N\rangle,} \tag{3.3}$$

where the normalization factor

$$\mathcal{N} \equiv \frac{1}{\sqrt{\prod_\lambda n_\lambda!}}.$$

(Notice that due to $1! = 1$, $\mathcal{N} = 1$ in the fermionic case.) These definitions are far from innocent and deserve some qualification. Firstly, in order not to be at conflict with the symmetry of the wavefunction, the operators a_λ have to fulfill the commutation relations

$$\boxed{\left[a_\lambda, a_\mu^\dagger\right]_\zeta = \delta_{\lambda,\mu}, \qquad \left[a_\lambda, a_\mu\right]_\zeta = 0, \qquad \left[a_\lambda^\dagger, a_\mu^\dagger\right]_\zeta = 0,} \tag{3.4}$$

where $[\hat{A}, \hat{B}]_\zeta \equiv \hat{A}\hat{B} + \zeta\hat{B}\hat{A}$ is the commutator (anti-commutator) for bosons (fermions). The most straightforward way to understand this condition is to check that the definition $|\lambda, \mu\rangle = a_\lambda^\dagger a_\mu^\dagger|\Omega\rangle$ and property $|\lambda, \mu\rangle = -\zeta|\mu, \lambda\rangle$ in fact necessitate the last two identies of (3.4). To verify the consistency of the first commutator relation, compute its expectation value in the vaccuum state:

$$\delta_{\lambda\mu} \overset{(3.3)}{=} \langle\Omega|a_\lambda a_\mu^\dagger|\Omega\rangle = \langle\Omega|(-\zeta)a_\mu^\dagger a_\lambda + [a_\lambda, a_\mu^\dagger]_\zeta|\Omega\rangle \overset{(3.3)}{=} \langle\Omega|[a_\lambda, a_\mu^\dagger]_\zeta|\Omega\rangle.$$

Since the vacuum state is normalized, $\langle\Omega|\Omega\rangle$, consistency with a c-number valued commutator $[a_\lambda, a_\mu^\dagger]_\zeta = \delta_{\lambda\mu}$ has been verified.

▷ EXERCISE. Verify the general validity of the identity $[a_\lambda, a_\mu^\dagger]_\zeta = \delta_{\lambda\mu}$ by taking its matrix element between arbitrary states $|\lambda_1, \ldots, \lambda_N\rangle$ and $\langle\mu_N, \ldots, \mu_1|$. Hints: Represent the reference states through (3.3) and use the known orthonormality properties of many body wavefunctions. To understand the general principle, consider the case $N = 1$, first. (A detailed exposition of the proof can be found in Negele and Orland, section 1.4.)

[4] As before, it will be convenient to represent these operators without a circumflex.

Yet even if the consistency of (3.4) is understood, the definitions above remain non-trivial. Actually, quite a strong statement has been made: For *any* N, the N-body wavefunction can be generated by application of a set of N-*independent* **creation operators** $a^\dagger_\lambda$ to a unique vacuum state. The operator algebra (3.4) entails that the states generated through (3.3) have all characteristic properties of N-body wave functions including, for instance, the correct symmetrisation and normalisation. For the details of the *proof* of the equivalence of the representations (3.2) on the one hand and (3.3) and (3.4) on the other hand we refer to one of several pedagogical expositions in the literature (e.g. the book by Negele and Orland.) Here, taking a pragmatic point of view, we will assume the validity of Eqs. (3.3) and (3.4) and explore what kind of description of many body quantum mechanics results.

We first notice that the second quantized formulation is taylor made to addressing problems with varying particle number. To see this, let $\mathcal{F}_N$ be the Hilbert space of states with fixed particle number N, i.e. the linear span of all states $|\lambda_1, \cdots \lambda_N\rangle = \mathcal{N} \prod_{i=1}^N a^\dagger_{\lambda_i} |\Omega\rangle$ obtained by N fold application of opertors $a^\dagger$ to the vaccuum state. The full space containing *all* many body states (regardless of the particle number) is called the **Fock space**, $\mathcal{F}$. It is defined as the direct sum $\mathcal{F} \equiv \oplus_{N=1}^\infty \mathcal{F}_N$ (see Fig. 3.2) of all subspaces $\mathcal{F}_N$. A general state $|\phi\rangle$ of the Fock space is, therefore, a linear combination of states with any number of particles. While the operator algebra (3.4) does not close in individual $\mathcal{F}_N$'s, it does so in $\mathcal{F}$. Indeed, application of a creation operator, $a^\dagger_\lambda : \mathcal{F}_N \to \mathcal{F}_{N+1}$ increases the particle number while the conjugate operators, also called **annihilation operators** $a_\lambda : \mathcal{F}_N \to \mathcal{F}_{N-1}$ lower the particle number (cf. Fig. 3.2.)

▷ EXERCISE. Use the commutation relations (3.4) to verify the last statement.

Finally, notice that the formalism of second quantization provides us with a language tailor made to the description of quantum *fields*. To appreciate this point, let us assume that our reference states $|\lambda\rangle \equiv |\mathbf{x}\rangle$ define a real space basis. (For basis changes in connection with second quantized operators, see below.) We then have one pair of canonically conjugate operators, $(a_\mathbf{x}, a^\dagger_\mathbf{x})$, for each point in space. Each operator-pair describes – as exemplified in chapter 2 – a *single* quantum degree of freedom (alias a field amplitude) living at $\mathbf{x}$. (For the description of a quantum degree of freedom in terms of opearators $(a, a^\dagger)$, remember section 2.1.1.) The (continuum) assembly of operators $\{a_\mathbf{x}, a^\dagger_\mathbf{x}\}$ describes the quantum field. To turn these rather abstract definitions into a valuable tool

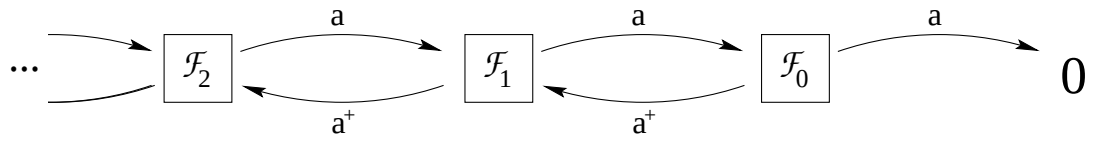

Figure 3.2: Visualisation of the generation of the Fock-subspaces $\mathcal{F}_N$ by repeated action of creation operators onto the vacuum space $\mathcal{F}_0$.

for practical computations we need to put them into relation with standard operations performed in quantum mechanics. In particular we have to specify how changes from one single particle basis $\{\lambda\}$ to another $\{\tilde{\lambda}\}$ affect the operator algebra $\{a_\lambda\}$, and in which

way standard operators of (many-body) quantum mechanics can be represented in terms of the a's:

▷ **Change of basis:** Using the resoluation of identity $\mathrm{id} = \sum_{\lambda=0}^{\infty} |\lambda\rangle\langle\lambda|$, the relations $|\tilde{\lambda}\rangle = \sum_\lambda |\lambda\rangle\langle\lambda|\tilde{\lambda}\rangle$, $|\lambda\rangle \equiv a_\lambda^\dagger|\Omega\rangle$, and $|\tilde{\lambda}\rangle \equiv a_{\tilde{\lambda}}^\dagger|\Omega\rangle$ immediately give rise to the transformation law

$$\boxed{a_{\tilde{\lambda}}^\dagger = \sum_\lambda \langle\lambda|\tilde{\lambda}\rangle a_\lambda^\dagger, \qquad a_{\tilde{\lambda}} = \sum_\lambda \langle\tilde{\lambda}|\lambda\rangle a_\lambda} \tag{3.5}$$

In many applications we are not dealing with a set of discrete quantum numbers (spin, quantised momenta, etc) but rather with a continuum (a continuous position coordinate, say). In these cases, the quantum numbers are commonly denoted in a bracket notation $a_\lambda \rightsquigarrow a(x) = \sum_\lambda \langle x|\lambda\rangle a_\lambda$ and the summations appearing in the transformation formula above become integrals.

Example: The transformation from the coordinate to the momentum representation in a finite one-dimensional system of length L would read

$$a_k = \int_0^L dx\ \langle k|x\rangle a(x), \qquad \langle k|x\rangle \equiv \langle x|k\rangle^* = \frac{1}{L^{1/2}} e^{-ikx}. \tag{3.6}$$

▷ **Representation of operators (one-body):** Single particle or one-body operators $\hat{\mathcal{O}}_1$ acting in the N-particle Hilbert space $\mathcal{F}_N$ generally take the form $\hat{\mathcal{O}}_1 = \sum_{n=1}^N \hat{o}_n$, where $\hat{o}_n$ is an ordinary single particle operator acting on the nth particle. A typical example is the kinetic energy operator $\hat{T} = \sum_n \hat{p}_n^2/2m$, where $\hat{p}_n$ is the momentum operator acting on the nth particle. Other examples include the one-particle potential operator $\hat{V} = \sum_n V(\hat{x}_n)$, where $V(x)$ is a scalar potential, the total spin-operator $\sum_n \hat{\mathbf{S}}_n$, etc. Since we have seen that by applying field operators to the vacuum space we can generate the Fock space in general and any N-particle Hilbert space in particular, it must be possible to represent any operator $\hat{\mathcal{O}}_1$ in an a-representation.

Now, although the representation of n-body operators is afterall quite straightforward, the construction can, at first sight seem daunting. A convenient way of finding such a representation is to express the operator in terms of a basis in which it is diagonal, and only later transform to an arbitrary basis. For this purpose it is useful to define **occupation number operator**

$$\boxed{\hat{n}_\lambda = a_\lambda^\dagger a_\lambda} \tag{3.7}$$

with the property that, for bosons or fermions, (exercise)

$$\hat{n}_\lambda\ (a_\lambda^\dagger)^n|\Omega\rangle = n\ (a_\lambda^\dagger)^n|\Omega\rangle.$$

I.e. the state $(a_\lambda^\dagger)^n|\Omega\rangle$ is an eigenstate of the number operator with eigenvalue n. When acting upon a state $|\lambda_1, \lambda_2, \cdots \lambda_N\rangle$, it is a straightforward exercise to show that the number operator obtains

$$\hat{n}_\lambda|\lambda_1, \lambda_2, \cdots \lambda_N\rangle = \mathcal{N} a_\lambda^\dagger a_\lambda \prod_{i=1}^N a_{\lambda_i}^\dagger|\Omega\rangle = \sum_{i=1}^N \delta_{\lambda\lambda_i}|\lambda_1, \lambda_2, \cdots \lambda_N\rangle.$$

The number operator simply counts the number of particles in state λ. Let us now consider a one-body operator, $\hat{\mathcal{O}}_1$, which is diagonal in the basis $|\lambda\rangle$, $\hat{o} = \sum_\lambda o_\lambda |\lambda\rangle\langle\lambda|$, $o_\lambda = \langle\lambda|\hat{o}|\lambda\rangle$. With this definition, one finds

$$\begin{aligned}\langle\lambda'_1, \cdots \lambda'_N|\hat{\mathcal{O}}_1|\lambda_1, \cdots \lambda_N\rangle &= \left(\sum_{i=1}^{N} o_{\lambda_i}\right)\langle\lambda'_1, \cdots \lambda'_N|\lambda_1, \cdots \lambda_N\rangle \\ &= \langle\lambda'_1, \cdots \lambda'_N|\sum_{\lambda=0}^{\infty} o_\lambda \hat{n}_\lambda|\lambda_1, \cdots \lambda_N\rangle.\end{aligned}$$

Since this equality holds for any set of states, we obtain the operator or second quantised representation

$$\hat{\mathcal{O}}_1 = \sum_{\lambda=0}^{\infty} o_\lambda \hat{n}_\lambda = \sum_{\lambda=0}^{\infty}\langle\lambda|\hat{o}|\lambda\rangle a^\dagger_\lambda a_\lambda.$$

The result is straightforward; a one-body operator engages a single particle at a time — the others are just spectators. In the diagonal representation, one simply counts the number of particles in a state λ and multiplies by the corresponding eigenvalue of the one-body operator. Finally, by transforming from the diagonal representation to a general basis, one obtains the general result,

$$\boxed{\hat{\mathcal{O}}_1 = \sum_{\mu\nu}\langle\mu|\hat{o}|\nu\rangle a^\dagger_\mu a_\nu.} \tag{3.8}$$

Let us illustrate this formula on a few examples: The **spin operator** is given by

$$\hat{\mathbf{S}} = \sum_{\lambda\alpha\alpha'} a^\dagger_{\lambda\alpha'}\mathbf{S}_{\alpha'\alpha}a_{\lambda\alpha}, \qquad \mathbf{S}_{\alpha\alpha'} = \frac{1}{2}\boldsymbol{\sigma}_{\alpha\alpha'} \tag{3.9}$$

where $\alpha = \uparrow, \downarrow$ is the spin-quantum number, λ denotes the set of additional quantum numbers (e.g. lattice site), and $\boldsymbol{\sigma}$ denote the vector of Pauli[5] spin matrices

$$\sigma_x = \begin{pmatrix} 0 & 1 \\ 1 & 0 \end{pmatrix}, \quad \sigma_y = \begin{pmatrix} 0 & -i \\ i & 0 \end{pmatrix}, \quad \sigma_z = \begin{pmatrix} 1 & 0 \\ 0 & -1 \end{pmatrix}. \tag{3.10}$$

Second quantised in the position representation, the **one-body Hamiltonian** is given as a sum of kinetic and potential energy as

$$\boxed{\hat{H} = \int dx\; a^\dagger(x)\left[\frac{\hat{p}^2}{2m} + V(x)\right]a(x)} \tag{3.11}$$

[5]

Wolfgang Pauli 1900-1958: 1945 Nobel Laureate in Physics for the discovery of the Exclusion Principle, also called the Pauli Principle.

where $\hat{p} = -i\hbar\partial_x$. (The latter is easily proved by expressing the kinetic energy in the momentum representation in which it is diagonal.) The **local density operator**, $\hat{\rho}(x)$ measuring the particle density at a certain coordinate x is simply given by

$$\hat{\rho}(x) = a^\dagger(x)a(x). \tag{3.12}$$

Finally, the **total occupation number operator**, obtained by integrating over the particle density, is defined as

$$\hat{N} = \int dx\; a^\dagger(x)a(x).$$

In a theory with discrete quantum numbers, this operator assumes the form

$$\hat{N} = \sum_\lambda a^\dagger_\lambda a_\lambda.$$

▷ **Representation of operators (two-body):** Two-body operators $\hat{\mathcal{O}}_2$ are needed to describe pairwise interactions between particles. Although pair-interaction potentials are straightforwardly included into classical many-body theories their embedding into conventional many-body quantum mechanics is made awkwardly cumbersome by particle indistinguishability. As compared to the conventional description, the formulation of interaction processes within the language of second quantisation is *much* easier. Referring to the literature for details (see also problem set 3.4) we here merely outline the basic strategy underlying the introduction of a second quantised formulation of interaction operators.

Owing to the fact that only two particles are simultaneously involved in a pair interaction process, a general two-body operator $\hat{\mathcal{O}}_2$ can be completely characterised in terms of its action on two particle states. Using (3.2) with $N = 2$, any operator $\mathcal{O}_2$ can be represented in terms of its matrix elements

$$\boxed{\mathcal{O}_{\mu,\mu',\lambda,\lambda'} \equiv \langle \mu, \mu' | \hat{\mathcal{O}}_2 | \lambda, \lambda' \rangle.}$$

One next computes the matrix element

$$\langle \mu_1, \ldots \mu_N | \hat{\mathcal{O}}_2 | \lambda_1, \ldots \lambda_N \rangle$$

between two general N-body states in terms of two-body elements $\mathcal{O}_{\mu,\mu',\lambda,\lambda'}$ and confirms that the resulting expression is reproduced when

$$\boxed{\hat{\mathcal{O}}_2 = \sum_{\lambda\lambda'\mu\mu'} \mathcal{O}_{\mu,\mu',\lambda,\lambda'} a^\dagger_\mu a^\dagger_{\mu'} a_\lambda a_{\lambda'}} \tag{3.13}$$

is sandwiched between the second quantised representation (3.3) of the many-body wave functions. These calculations, though easily formulated in principle, are quite cumbersome in practice. Fortunately, though, there is normally no need to maneuver

through the general scheme outlined above: In the vast majority of cases, two-body interaction operators are given as the product of two *single* particle operators. E.g. the **Coulomb interaction**, $\hat{V} = \frac{1}{2}\int d^dx_1 d^dx_2 \hat{\rho}(\mathbf{x}_1)V(\mathbf{x}_1-\mathbf{x}_2)\hat{\rho}(\mathbf{x}_2)$ where $\hat{\rho}(\mathbf{x}_i)$ is the single particle density operator at coordinate $\mathbf{x}_i$ and $V(\mathbf{x}_1-\mathbf{x}_2)$ the Coulomb potential. But we already know how to second quantize the density operator: $\hat{\rho}(\mathbf{x}) = a^\dagger(\mathbf{x})a(\mathbf{x})$. This implies that the second quantized representation of the Coulomb interaction in a system of charged fermions is given by:

$$\hat{V} = \frac{1}{2}\int d^dx \int d^dx'\ a^\dagger(\mathbf{x})a(\mathbf{x})V(\mathbf{x}-\mathbf{x}')a^\dagger(\mathbf{x}')a(\mathbf{x}').$$

Another important interaction, frequently encountered in problems of quantum magnetism, is $\hat{V} = \mathrm{tr}\,(\hat{\mathbf{S}}(\mathbf{x})\cdot\hat{\mathbf{S}}(\mathbf{x}'))$, i.e. a **spin-spin interaction**. From our discussion of the second quantized representation of $\hat{\mathbf{S}}$ above we infer that

$$\hat{V} = \sum_{\alpha\alpha'\beta\beta'} a^\dagger_\alpha(\mathbf{x})\mathbf{S}_{\alpha\beta}a_\beta(\mathbf{x})\ a^\dagger_{\alpha'}(\mathbf{x}')\mathbf{S}_{\alpha'\beta'}a_{\beta'}(\mathbf{x}'). \tag{3.14}$$

This completes our formal introduction to the method of second quantisation. To make these concepts seem less abstract, the remainder of this chapter applies this method to a variety of problems. Although second quantisation is a representation, and not a solution, its application often leads to a considerable simplification of the analysis of many-particle systems. To emphasize this fact, and to practice the manipulation of second quantised operators, we will discuss a number of applications of different physical background.

3.2 Applications of Second Quantisation

Starting from the prototype Hamiltonian (9.30), in chapter 1 we had explored aspects of the ion dynamics of a metallic condensed matter system. In much of the rest of this course we will concentrate on the complementary sector, the dynamics of the conduction electrons. To get a grip on this problem, and following the first of the principles discussed in chapter 1, we begin by reducing the full Hamiltonian to a form that contains the essential elements of the electronic dynamics. The reduced Hamiltonian will certainly be determined by the pure electronic sub-Hamiltonian H_e but also by the interaction between the electrons and the positively charged ionic background lattice. On the other hand, it is likely that both lattice distortions due to the motion of the ions and the ion-ion interaction couple only indirectly. (Exercise: state a prmominent example where the electronic sector is *crucially* influenced by the dynamics of the host lattice.) To a first approximation, we thus describe the electronic system through

$$\begin{aligned}\hat{H} &= \hat{H}_0 + \hat{V}_{\mathrm{ee}} = \\ &= \int d\mathbf{r}\ a^\dagger_\sigma(\mathbf{r})\left[\frac{\hat{\mathbf{p}}^2}{2m} + V(\mathbf{r})\right]a_\sigma(\mathbf{r}) + \frac{1}{2}\int d\mathbf{r}\int d\mathbf{r}'\ a^\dagger_\sigma(\mathbf{r})a_\sigma(\mathbf{r})V(\mathbf{r}-\mathbf{r}')a^\dagger_{\sigma'}(\mathbf{r}')a_{\sigma'}(\mathbf{r}'),\end{aligned} \tag{3.15}$$

where $V(\mathbf{r}) = \sum_I V_{\mathrm{ei}}(\mathbf{R}_I - \mathbf{r})$ and the coordinates of the lattice ions are presumed fixed. For completeness, we have also equipped the electrons with a spin index, $\sigma = \pm 1/2$. The

Hamiltonian (3.28) defines the problem of the interacting electron gas embedded into a solid state system.

Now comes an intriguing point: If you open a research paper on the dynamics of the electronic system, notably the *interacting* electronic system, you ususally find the lattice potential V swept under the carpet: Either the non-interacting part of the Hamiltonian is presumed to be diagonalized by simple plane waves, as would be the case for $V = 0$, or the lattice potential is presumed to be so strong that it confines the electrons to a discrete set of hopping centers. In either case, V does not appear explicitly. To understand the philosophy behind these simplifications, and to set the stage for our later discussion of the interaction contribution $V_{\rm ee}$, we need to recapitulate some aspect of the problem of

3.2.1 Electrons in a Periodic Potential

Let us for a moment switch off the interaction, $V_{\rm ee}$, and consider the single-particle Hamiltonian of electrons in a periodic potential, Eq. (3.11). As we know from Bloch's theorem[6], eigenstates of this Hamiltonian can be represented in the form of Bloch waves

$$\psi_{\mathbf{k}n}(\mathbf{r}) = e^{i\mathbf{k}\cdot\mathbf{r}} u_{\mathbf{k}n}(\mathbf{r}),$$

where the components of the crystal momentum $\mathbf{k}$, $k_i \in [-\pi/a, \pi/a]$ and we have assumed that the periodicity of the lattice potential is the same in all directions, $V(\mathbf{r}+a\mathbf{e}_i) = V(\mathbf{r})$. The index n labels the energy bands of the solid and the functions $u_{\mathbf{k}n}(\mathbf{r} + a\mathbf{e}_i) = u_{\mathbf{k}n}(\mathbf{r})$ are lattice periodic.

Now, there are two complementary classes of materials where the general structure of the Bloch functions can be significantly simplified:

Nearly Free Electron Systems

For certain metals, notably metals in the groups I-IV of the periodic table, electrons behave as if they were 'nearly free', i.e. oblivious of the potential created by the positively charged ions. Losely speaking, the prime reason for this behaviour is that electrons in those metals are highly mobile and, therefore, good at screening the ionic background potential. In nearly free electron compounds, complete neglect of the lattice potential is usually a good approximation (as long as one stays clear of the boundaries of the tight binding zone, $k_i = \pi/a$.) In practice, this means that we are permitted to set $u = 1$ and regard the eigenstates of the non-interacting Hamiltonian as plane waves. This motivates to represent the field operators in momentum space, (3.6), whereupon the non-interacting part of the Hamiltonian becomes

$$H_0 = \sum_{\mathbf{k}} a^\dagger_{\mathbf{k}\sigma}(k^2/2m)a_{\mathbf{k}\sigma}. \tag{3.16}$$

[6] Felix Bloch 1905-1983: 1952 Nobel Laureate in Physics for the development (with Edward M. Purcell) of new methods for nuclear magnetic precision measurements and discoveries in connection therewith.

Turning to the Coulomb interaction we first note that the Fourier representaton of the interaction operator (??) is given by

$$\hat{V}_{\rm ee} = \frac{1}{2L^d} \sum_{\mathbf{k},\mathbf{k}',\mathbf{q}} a^\dagger_{\mathbf{k}-\mathbf{q}\sigma} a_{\mathbf{k}\sigma} V(q) a^\dagger_{\mathbf{k}'+\mathbf{q}\sigma'} a_{\mathbf{k}'\sigma'}, \tag{3.17}$$

where

$$V(q) = \frac{e^2}{q^2} \tag{3.18}$$

is the Fourier transform of the Coulomb potential $V(r) = e^2/r$ and we have added spin. Now, this expression neglects the fact that in ionized solids, the negative charge density of the electron cloud will be largely compensated by the charge density $\rho_0(\mathbf{x})$ of the positively ionized background: $\hat{\rho}(\mathbf{x}) = a^\dagger(\mathbf{x})a(\mathbf{x}) - \rho_0(\mathbf{x})$. An effective interaction operator accounting for this mechanism reads as

$$\hat{V}_{\rm ee} = \frac{1}{2L^d} \sum_{\mathbf{k},\mathbf{k}',\mathbf{q}} (a^\dagger_{\mathbf{k}-\mathbf{q}\sigma} a_{\mathbf{k}\sigma} - \rho_0 \delta_{\mathbf{q},0}) V(q) (a^\dagger_{\mathbf{k}'+\mathbf{q}\sigma'} a_{\mathbf{k}'\sigma'} - \rho_0 \delta_{\mathbf{q},0}).$$

where we have assumed that the positive charge density is (a) classical (described by a function) and (b) smeared out to an constant background – the **jellium model**. Notice that overall charge neutrality of the system requires that

$$\langle \hat{N} \rangle = L^d \rho_0, \tag{3.19}$$

where, in principle, the expectation value $\langle \ldots \rangle$ should be taken in any system-state with a fixed number of particles. However, neglecting particle number fluctuations inherent to the grand canonical ensemble, it is customary to promote (3.19) to an approximate *operator identity*: $\hat{N} \simeq L^d \rho_0$. This assumption can be built into our formalism by re-adopting () as an interaction operator where, however, the zero momentum component of the Coulomb interaction potential $V(q) \to V(q)(1 - \delta_{q,0}$ is explicitly removed. The charge neutrality ensuring factor $1 - \delta_{q,0}$ is usually not indicated in the notation but understood implicitly.

The interaction described by (3.2.1) can be illustrated graphically, as shown in the figure (For a more elaborate discussion of such diagrams, see section XX below.): Two electrons with momenta $\mathbf{k} - \mathbf{q}$ and $\mathbf{k}' + \mathbf{q}$, respectively are annihilated on account of the creation of a 'new' pair or electrons with momenta $\mathbf{k}$ and $\mathbf{k}'$. Alternatively, and perhaps more physically, we can think of the process as scattering of an electron from momentum $\mathbf{k}-\mathbf{q}$ into a new momentum state $\mathbf{k}$. Momentum conservation implies a similar scattering process $\mathbf{k}' + \mathbf{q} \to \mathbf{k}'$ experienced by a partner electron.

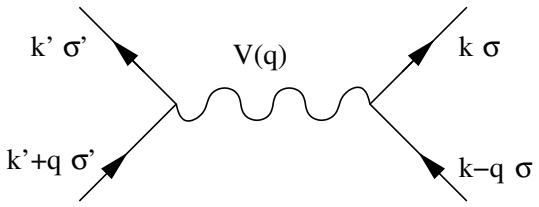

In concrete applications of low temperature condensed matter physics one will consider the system (3.28) at low excitation energies. The solution of such problems is naturally organized around the zero temperature ground state as a reference platform. However, the accurate calculation of the ground state energy of (3.28) is a complicated problem of many body physics that cannot be solved in closed form. Therefore, assuming that interactinons will not substantially alter the ground state of the free problem (3.16) one usually uses the latter as a reference state.

▷ INFO. Referring for a more qualified discussion to section 6.2 below, a preliminary justification of this assumption can be given as follows: Suppose the density of our electron gas is such that each of its N particles occupies an average volume of $\mathcal{O}(a^d)$. The average kinetic energy per particle is then estimated as $T \sim \frac{1}{ma^2}$, while the Coulomb interaction potential will scale like $V \sim e^2/a$. Thus, for $a \ll a_0$ much smaller than the **Bohr radius** $a_0 = e^2/m$, the interaction contribution is much smaller than the average kinteic energy. In other words, for the *dense* electron gas the interaction energy can, indeed, be treated as a perturbation. Unfortunately, for most metals $a \simeq a_0$ and neither high- nor low-density approximations are really justified.

The ground state of the system inhabited by N non-interacting particles can readily be inferred from (3.16). The Pauli principle implies that all energy states $\epsilon_{\mathbf{k}} = k^2/2m$ will be uniformly occupied up to a cutoff **Fermi energy**, E_F. Specifically, for a system of size L, allowed momentum states $\mathbf{k}$ have components $k_i = 2\pi n_i/L$, $n_i \in \mathbb{Z}$. The summation extends up to momenta with $|\mathbf{k}| \leq k_F$, where the **Fermi momentum**, k_F, is defined through $k_F^2/(2m) = E_F$, see Fig. 3.3. The relation between the Fermi momentum and the occupation number can be established by dividing the volume of the **Fermi sphere**, $V_F \sim k_F^d$ through the momentum space volume per mode, $\Delta = (2\pi/L)^d$, $N = V_F/\Delta = C(k_F L)^d$, where C is a dimensionless geometry dependent constant.

In the language of second quantization, the ground state can now be represented as

$$|\Omega\rangle \equiv \mathcal{N} \prod_{k<k_F,\sigma} a^\dagger_{\mathbf{k}\sigma}|\tilde{\Omega}\rangle, \tag{3.20}$$

where $|\tilde{\Omega}\rangle$ denotes the state with zero electrons present. We anticipate that low temperature physical phenomena will be governed by energetically low-lying excitations superimposed on $|0\rangle$. Therefore, remembering the philosophy whereby excitations rather than microscopic constituents play a prime role, one would like to declare the filled Fermi sea, $|0\rangle \equiv |\Omega\rangle$ (rather than $|\tilde{\Omega}\rangle$) to be the 'physical vacuum' of the theory. To make this compatible with the language of second quantization, we need to identify a new operator algebra $c_{\mathbf{k}\sigma}, c^\dagger_{\mathbf{k}\sigma}$ such that the new operators $c_{\mathbf{k}\sigma}$ annihilate the Fermi sea. This can easily be achieved by defining,

$$c^\dagger_{\mathbf{k}\sigma} = \begin{cases} a^\dagger_{\mathbf{k}\sigma} & , k > k_F \\ a_{\mathbf{k}\sigma} & , k \leq k_F \end{cases}, \qquad c_{\mathbf{k}\sigma} = \begin{cases} a_{\mathbf{k}\sigma} & , k > k_F \\ a^\dagger_{\mathbf{k}\sigma} & , k \leq k_F \end{cases}, \tag{3.21}$$

It is straightforward to verify, that $c_{\mathbf{k}\sigma}|\Omega\rangle = 0$ and that the canonical commutation relations are preserved.

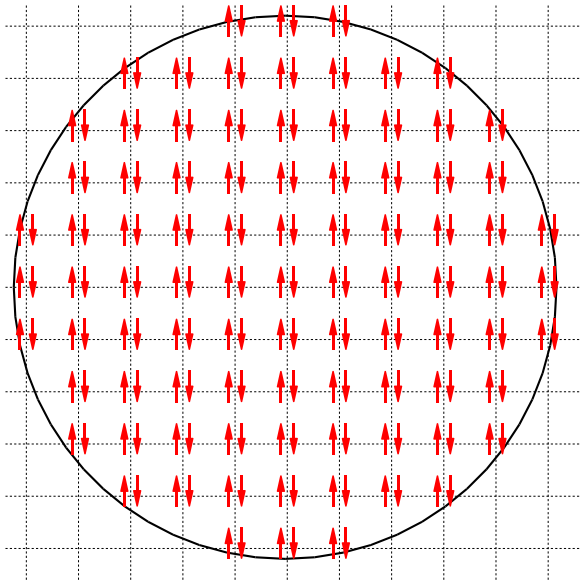

Figure 3.3: Cartoon of the two-dimensional Fermi sphere. Each momentum state is filled by two electrons of opposite spin.

The Hamiltonian defined through (3.16) and (3.2.1), represented in terms of the operator algebra (3.21) and the vacuum (3.20), forms the basis of the theory interactions in *highly mobile* electron compounds. The role of interactions in this system will be discussed in sections XX.

We next turn our attention to a complementary class of electronic systems, i.e. systems the where the lattice potential confining the electrons is stong. In such situations, realized, e.g. in transition metal oxides, a description based on 'almost localized' electron states will be used to represent the Hamiltonian (3.28):

Tight Binding Systems

Imagine a situation where, on average, electrons are 'tightly bound' to the lattice centers. In such systems, it is convenient to expand the theory in terms of the local basis of **Wannier states**

$$|\psi_{\mathbf{R}n}\rangle \equiv \frac{1}{\sqrt{N}} \sum_{\mathbf{k}}^{\text{B.Z.}} e^{-i\mathbf{k}\cdot\mathbf{R}} |\psi_{\mathbf{k}n}\rangle, \qquad |\psi_{\mathbf{k}n}\rangle = \frac{1}{\sqrt{N}} \sum_{\mathbf{R}} e^{i\mathbf{k}\cdot\mathbf{R}} |\psi_{\mathbf{R}n}\rangle, \tag{3.22}$$

where $\mathbf{R}$ are the coordinates of the lattice centres and $\sum_k^{\text{B.Z.}}$ stands for a summation over all momenta $k_i = n_i \frac{2\pi}{L} \in [0, 2\pi/a]$ in the first Brillouin zone. For a system with vanishingly weak inter-atomic overlap, i.e. a lattice where V approaches a superposition of independent atomic potentials, the Wannier function $\psi_{\mathbf{R}n}(\mathbf{r}) \equiv \langle \mathbf{r}|\psi_{\mathbf{R}n}\rangle$ equals the nth orbital of an isolated atom centered at coordinate $\mathbf{R}$. However, for finite inter-atomic coupling, i.e. a 'real' solid, the N formerly degenerate states labeled by n split to form an energy band (see Fig. 3.4.) In this case, the Wannier functions differ from isolated atomic orbitals. Also notice that, unlike the Bloch functions, the Wannier functions are not eigenfunctions of the lattice Hamiltonian.

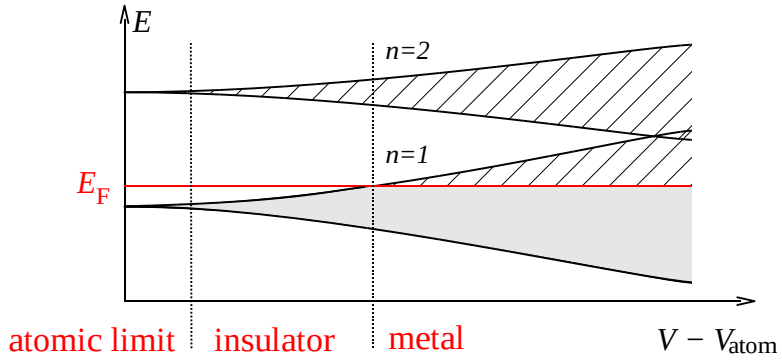

Figure 3.4: Energy bands in a solid. For an asymptotically weakly bound solid, the energy levels are N-fold degenerate and coincide with the bound state levels of isolated atom-potentials $V_{\rm atom}$. For finite inter-atomic coupling, levels split to form bands. If the Fermi energy lies within a band the system is a metal, otherwise an insulator.

In cases where the Fermi energy is situated between two energetically separated bands, we are dealing with an insulator. However, in the complementary case, i.e. the Fermi energy located within a band, the system is metallic. Ignoring the complications that arise when bands begin to *overlap*, we henceforth focus on metallic systems where the Fermi energy is located within a definite band n_0.

We next ask, how the Wannier-language can be employed to obtain a problem adjusted representation of the general Hamiltonian (3.28). The first thing to be noticed is that the Wannier states $\{|\psi_{\mathbf{R}n}\rangle\}$ form an orthonormal basis of the single particle Hilbert space, i.e. the transformation between the real-space and the Wannier representation,

$$|\mathbf{r}\rangle = \sum_{\mathbf{R}} \langle \psi_{\mathbf{R}} | \mathbf{r} \rangle \; |\psi_{\mathbf{R}}\rangle = \sum_{\mathbf{R}} \psi^*_{\mathbf{R}}(\mathbf{r}) \; |\psi_{\mathbf{R}}\rangle$$

is unitary. (Here we have dropped the band-index summation, because we will only be interested in contributions coming from the 'metallic' band n_0.) As such, it induces a transformation

$$a^\dagger_\sigma(\mathbf{r}) = \sum_{\mathbf{R}} \psi^*_{\mathbf{R}}(\mathbf{r}) a^\dagger_{\mathbf{R}\sigma} \equiv \sum_i \psi^*_{\mathbf{R}_i}(\mathbf{r}) a^\dagger_{i\sigma} \tag{3.23}$$

between the real space and the Wannier state operator basis, respectively. In the second representation, following a convention commonly used in the literature, we have labeled the lattice center coordinates $\mathbf{R} \equiv \mathbf{R}_i$ by a counting index $i = 1, \ldots, N$. Similarly, the unitary transformation between Bloch- and Wannier-states, (3.22), induces an operator transformation

$$a^\dagger_{\mathbf{k}\sigma} = \frac{1}{\sqrt{N}} \sum_i e^{i\mathbf{k}\cdot\mathbf{R}_i} a^\dagger_{i\sigma} \tag{3.24}$$

We can now use the transformation formulae (3.23) and (3.24) to formulate a Wannier-representation of the Hamiltonian (3.28). Using that the Bloch states diagonalize the

single particle component H_0, we obtain

$$H_0 = \int d\mathbf{r}\; a^\dagger_\sigma(\mathbf{r}) \left[\frac{\hat{\mathbf{p}}^2}{2m} + V(\mathbf{r})\right] a_\sigma(\mathbf{r}) = \sum_{\mathbf{k}\sigma} a^\dagger_{\mathbf{k}\sigma}\epsilon_k a_{\mathbf{k}\sigma} =$$
$$\overset{(3.24)}{=} \frac{1}{N}\sum_{ii'}\sum_{\mathbf{k}} e^{i\mathbf{k}(\mathbf{R}_i - \mathbf{R}_{i'})}\epsilon_k\; a^\dagger_{i\sigma}a_{i'\sigma} \equiv \sum_{ii'} a^\dagger_{i\sigma}\, t_{ii'}\, a_{i'\sigma},$$

where we have defined $t_{ii'} = \frac{1}{N}\sum_{\mathbf{k}} e^{i\mathbf{k}(\mathbf{R}_i - \mathbf{R}_{i'})}\epsilon_k$. The new representation of H_0 describes **electron hopping** from one lattice center i to another. The strength of the hopping amplitude $t_{ii'}$ is controlled by the effective overlap of neighbouring atoms. In the atomic limit, where the levels $\epsilon_k = $ const. are degenerate, $t_{ii'} = \delta_{ii'}$ and no inter-atomic transport is possible. The tight binding representation is useful, if $t_{i\neq i'}$ is non-vanishing but so weak that only nearest neighbour hopping effectively contributes.

▷ EXERCISE. Assuming a square lattice and that

$$t_{ii'} = \begin{cases} t, & i, i' \text{ nearest neighbours,} \\ 0, & \text{otherwise,} \end{cases}$$

diagonalize the two-dimensional hopping Hamiltonian H_0. (Hint: Re-express the Hamiltonian in terms of Bloch operators, (3.24).) Show that the eigenvalues are given by

$$\epsilon_{\mathbf{k}} = 2t(\cos(k_x a) + \cos(k_y a)), \tag{3.25}$$

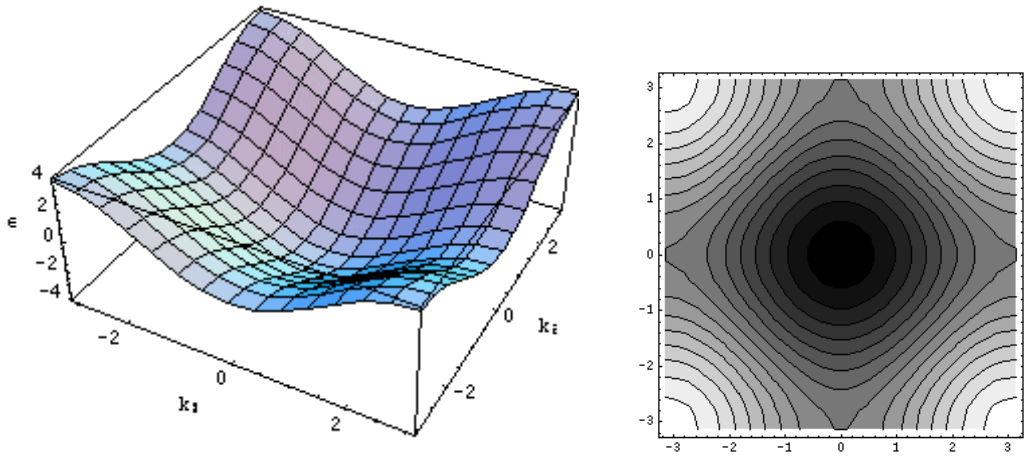

Figure 3.5: Left: Plot of the dispersion relation (3.25). Right: Contour plot of the same function. Notice that for a half filled band, $E_F = 0$, the Fermi surface becomes rectangular.

Turning to the interaction component V_{ee}, we use the transformation (3.23) to obtain

$$V_{\text{ee}} = \sum_{ii'jj'} U_{ii'jj'}\; a^\dagger_{i\sigma}a_{j\sigma}a^\dagger_{i'\sigma'}a_{j'\sigma'},$$

where the matrix element

$$U_{ii'jj'} = \frac{1}{2}\int d\mathbf{r}d\mathbf{r}'\psi^*_{\mathbf{R}_i}(\mathbf{r})\psi_{\mathbf{R}_j}(\mathbf{r})V(\mathbf{r}-\mathbf{r}')\psi^*_{\mathbf{R}_{i'}}(\mathbf{r}')\psi_{\mathbf{R}_{j'}}(\mathbf{r}'). \tag{3.26}$$

The combination of the contributions H_0 and $V_{\rm ee}$

$$\boxed{H = \sum_{ii'} a^\dagger_{i\sigma}\, t_{ii'}\, a_{i'\sigma} + \sum_{ii'jj'} U_{ii'jj'}\; a^\dagger_{i\sigma}a_{j\sigma}a^\dagger_{i'\sigma'}a_{j'\sigma'}} \tag{3.27}$$

defines the **tight binding representation** of the interaction Hamiltonian.

Hamiltonians of the type (3.27) stand at the basis of innumerable analyses of interacting electronic systems, notably *strongly* interacting systems. Various aspects of such problems will be discussed in later chapters. Before leaving this section, and without going into any detail, let us try to anticipate a little bit and give some preliminary impression of the diversity of interaction phenomena generated by the second contribution to (3.27).

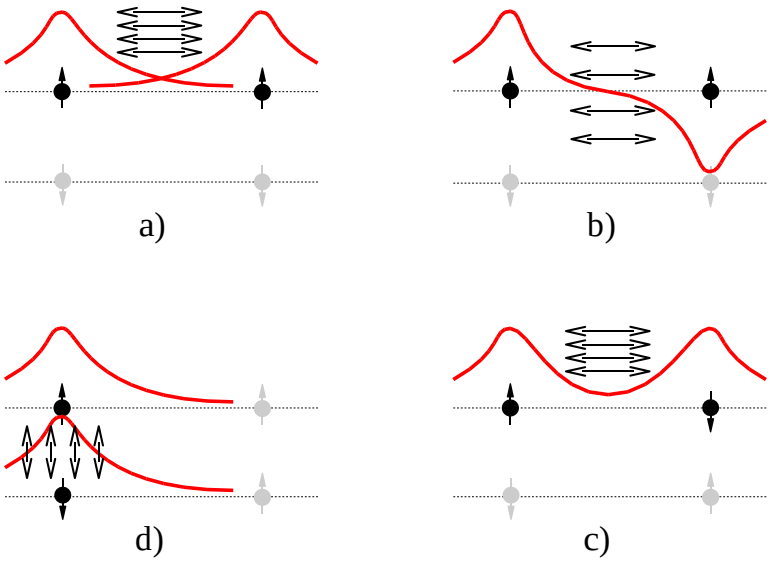

Figure 3.6: Different types of interaction mechanisms induced by the tight binding interaction $V_{\rm ee}$. Red lines symbolically indicate wave function envelopes. a) Direct Coulomb interaction between neighbouring sites. Accounting for the exchange interaction, parallel alignment of spins b) is preferred on account of the antisymmetry of the spatial wave function. In contrast, for anti-parallel spin-configurations c) the wave function amplitude in the repulsion zone is enhanced. d) Coulomb interaction between electrons of opposite spin populating the same site.

On the face of it, the interacting contribution to the Hamiltonian does not look in the least transparent. To get some better understanding of the physical meaning of the matrix elements $U_{ii'j'}$, the spatial structure of the Wannier functions has to be taken into account. Following the general philosophy of this section, we will assume that the

electrons are tightly bound, i.e. the Wannier functions short ranged. We will thus focus on contributions to $U_{ii'jj'}$ where the indices are either equal, or, at most, nearest neighbours. Focusing on the most relevant of these matrix elements, a number of physically different contributions can be identified:

▷ The **direct terms** $U_{iii'i'} \equiv V_{ii'}$ involve integrals over square moduli of Wannier functions and couple *density fluctuations* at neighbouring sites,

$$\sum_{i \neq i'} V_{ii'} \hat{n}_i \hat{n}_{i'},$$

where $\hat{n}_i = \sum_\sigma a^\dagger_{i\sigma} a_{i\sigma}$. This contribution accounts for the – essentially classical – interaction between charges localized at neighbouring sites, see Fig. In certain materials, interactions of this type have the capacity to induce global instabilities in the charge distribution, so called *charge density* instabilities. An example of such a phenomenon will be discussed in section XX.

▷ A second important contribution derives from the **exchange coupling** which induce magnetic correlations among the electronic spins. Setting $J^F_{ij} \equiv U_{ijji}$, and making use of the identity derived in problem set 3.4, we obtain

$$\sum_{i \neq j} U_{ijji}\, a^\dagger_{i\sigma} a_{j\sigma} a^\dagger_{j\sigma'} a_{i\sigma'} = -2 \sum_{i \neq j} J^F_{ij} \left(\hat{\mathbf{S}}_i \cdot \hat{\mathbf{S}}_j + \frac{1}{4} \hat{n}_i \hat{n}_j \right).$$

Such contributions tend to induce weak **ferromagnetic coupling** of neighbouring spins (i.e. $J_F > 0$). The fact that an effective *magnetic* coupling is born out of the *electric* interaction between quantum particles is easily understood as follows: Consider two electrons inhabiting neighbouring sites. The Coulomb repulsion between the particles is minimized if the orbital two particle wave function is antisymmetric and, therefore, has low amplitude in the interaction zone between the particles. Since the overall wavefunction must be antisymmetric, the energetically favoured real-space configuration enforces a symmetric alignment of the two spins.

As a rule, magnetic interactions in solids are usually generated as an indirect manifestation of the much stronger Coulomb interaction. This mechanism is familiar from atomic physics where it is manifest as **Hund's rule**.

▷ However, in the so-called **atomic limit** where the atoms are well-separated and the overlap between neighbouring orbitals is weak, the matrix elements t_{ij} and J^F_{ij} are exponentially small in the interatomic separation. In this limit, the 'on-site' Coulomb or **Hubbard interaction**, U_{iiii},

$$\sum_{i\sigma\sigma'} U_{iiii} a^\dagger_{i\sigma} a_{i\sigma} a^\dagger_{i\sigma'} a_{i\sigma'} = \sum_{i\sigma\sigma'} \left(U \hat{n}_{i\uparrow} \hat{n}_{i\downarrow} - \frac{U}{2} \hat{n}_i \right)$$

where $U \equiv 2U_{iiii}$, generates the dominant interaction mechanism, see Fig. 3.6, d).

In the literature, the Hamiltonian reduced to the on-site interaction,

$$\boxed{H = \sum_{\langle ii' \rangle} a^\dagger_{i\sigma}\, t_{ii'}\, a_{i'\sigma} + U \sum_i \hat{n}_{i\uparrow}\hat{n}_{i\downarrow}} \tag{3.28}$$

goes under the name **Hubbard Hamiltonian**. (We have omitted the contribution $\sim \frac{U}{2}\sum_i \hat{n}_i$ as it merely generates a trivial shift of the chemical potential.) The notation $\langle ii' \rangle$ indicates that the summation extends over nearest neighbour lattice sites.

In hindsight, a model of this structure could have been guessed on phenomenological grounds from the outset. Electrons tunnel between atomic orbitals localised on individual lattice sites and experience a local Coulomb interaction with other electrons. Deceptive in its simplicity, the Hubbard model is acknowledged as a paradigm of strongly interacting electronic systems. Yet, after forty years of (often intense) investigation, the phase diagram of the Hubbard model is still only poorly understood. We will turn back to the discussion of this model system in chapter X.

This concludes our first introduction to interacting electronic model systems. Notice that, so far, we have merely discussed ways to destill reduced model systems from the initial Hamiltonian (3.28). However, save for the two examples of free field theories analysed in chapter 2, we have not yet learned how methods of second quantisation can be applied to actually solve problems. Filling this gap, we will next illustrate the application of the method on a prominent, and essentially interacting problem.

3.2.2 Interacting Fermions in One Dimension

Within the context of many body physics, a theory is termed **free** if it is quadratic in the creation/annihilation operators, i.e. $H \sim \sum_{\mu\nu} a^\dagger_\mu H_{\mu\nu} a_\nu$, where H may be a finite or inifinite dimensional matrix. Such models are termed 'solvable' in the sense that the solution of the problem amounts to diagonalization of the matrix $H_{\mu\nu}$. However, only few models of interest belong to this category. In general, interaction contributions of $\mathcal{O}(a^4)$ are present and, therefore, complete solutions out of reach.

Yet there are a few precious examples of genuinely interacting systems which are amenable to (nearly) exact solution schemes. In this section we discuss an important representative of such a system class, viz. the one-dimensional interacting electron gas. The analysis of this system is not only physically interesting but also will provide us with opportunity to practice working with the second quantized operator formalism on a deeper level than before.

Qualitative Discussion

Consider the nearly free electron Hamiltonian (3.16) and (3.2.1) reduced to a one-dimensional environment:

$$\hat{H} = \sum_k a_k^\dagger \left(\frac{k^2}{2m} - \mu \right) a_k + \frac{1}{2L} \sum_{kk'q} a_{k-q}^\dagger a_k V(q) a_{k'+q}^\dagger a_{k'}, \tag{3.29}$$

where, for simplicity, we are neglecting spin degrees of freedom. Further, following a standard convention, the chemical potential $\mu \equiv E_F$ has been absorbed into the definition of the Hamilton operator. At first sight, the model Hamiltonian (3.29) may appear like an overly simplistic reduction of the generic d-dimensional problem. However, there is more to the problem (3.29):

Effectively one-dimensional interacting fermion systems are realized in a number of material classes. E.g. certain **organic molecules** (e.g. the Bechgaard salt, $(TMTSF)_2PF_6$, where $TMTSF$ stands for the tetramethyl-tetraselenafulvalene) or **carbon nanotubes** (see Fig. 3.7) are surrounded by clouds of mobile electrons. At low temperatures, the circumferential degrees of freedom are frozen out, while density variations in the longitudinal direction are still possible (cf. Fig. 3.9, right.) Another realization is provided by so-called **semiconductor quantum wires**. In the vicinity of planar boundaries between different semiconductor compounds (e.g. $GaAs$ vs. $GaAlAs$) it comes to the formation of nearly perfectly *two*-dimensional conducting electron systems. Referring for a more substantial discussion of such systems to chapter XX, we here merely mention that by additional application of electrostatic fields one can manufacture narrow potential 'grooves', i.e. quasi one-dimensional structures in which electron motion in transverse direction is impeded by a massive potential gradient (Fig. 3.9, left.) At sufficiently low Fermi energies, only the lowest eigenstate of the transverse Schroedinger problem (the lowest 'quantum mode') is populated and we are left with a striktly one-dimensional electron system. There are other realizations, like edge modes in **quantum Hall systems**, so-called **stripe phases** in high tempterature superconductors, or certain **inorganic crystals** but we shall not discuss these here.

What makes the one-dimensional Fermion system physically interesting is that it exhibits a number of unique features, not observed in higher dimensions. The origin of these peculiarities can easily be understood from a simple qualitative picture: Imagine interacting fermions confined to a line. All they can do to optimize their configuration is push each other around, thereby creating *density distortions*. In contrast, in higher-dimensional systems, electrons are free to avoid contact by moving around each other. A slightly different formulation of the same picture can be given in momentum space: The Fermi 'sphere' of the one-dimensional system is defined through the interval $[-k_F, k_F]$ of filled momentum states; The Fermi 'surface' consists of two *isolated* points $\{k_F, -k_F\}$ (cf. Fig. 3.10.) This is to be compared with the continuous and simply connected Fermi surfaces of higher dimensional systems. It takes little imagination to anticipate that an extended Fermi sphere provides more phase space to two-particle interaction processes than the two isolated Fermi energy sectors of the $1d$-system.

Finally, the one-dimensional electron system represents a rare exeption of an *interacting* system that can be solved under no more than a few, and physically weak, simplifying

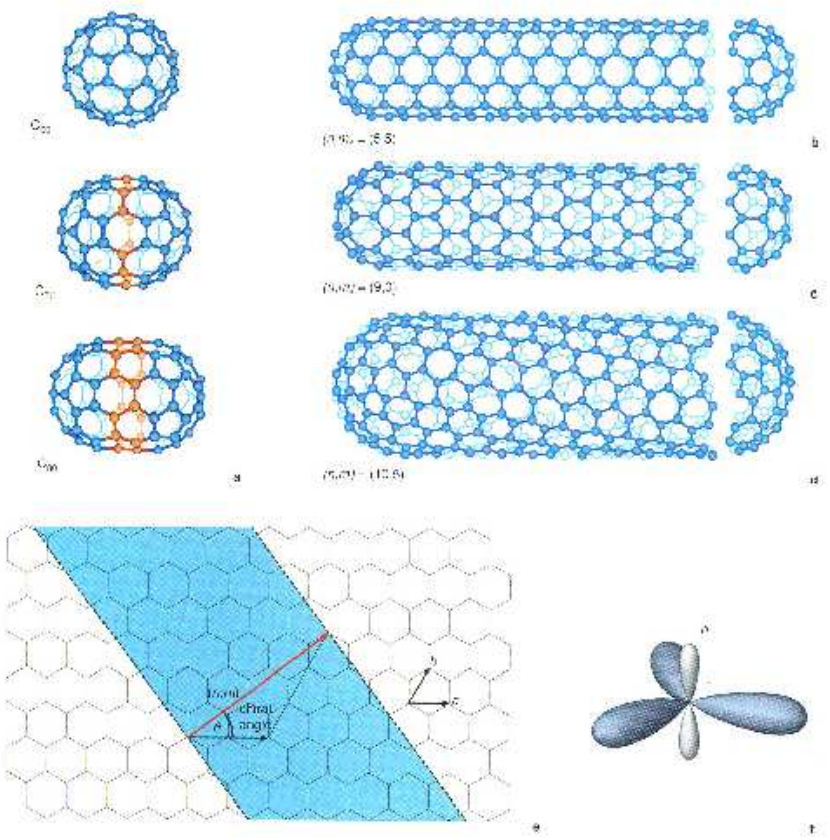

Figure 3.7: On the molecular structure of carbon nanotubes. Essentially, carbon nanotubes are elongated versions of **buckminsterfullerenes**, (i.e. spherical or near-spherical 'cages' of sp_2-hybridized carbon.) Alternatively, one can think of nanotubes as cylindrically wrapped up graphite sheets. The fine-structure of the molecule depends on how the graphite is 'rolled' to a cylinder. (See the three alternatives to the right.) The p-orbital electrons of the sp_2-hybirdized carbon atoms sourround the cylinder like a cloud of mobile charge carriers.

assumptions. This makes i a precious test system on which non-perturbative quantum manifestions of many body interactions can be explored.

Quantitative Analysis

We now proceed to develop a quantitative picture of the charge density excitations of the one-dimensional electron system. Anticipating that at low temperatures the relevant dynamics will take place in the vicinity of the two Fermi points $\{+k_F, -k_F\}$, the Hamiltonian (3.29) can be reduced further to an effective Hamiltonian describing the propagation of left and right moving excitations. To this end, we first introduce the notation,

$$a^\dagger_{k_F+q} \equiv a^\dagger_{Rq}, \qquad a^\dagger_{-k_F+q} \equiv a^\dagger_{Lq}, \qquad |q| \ll k_F,$$

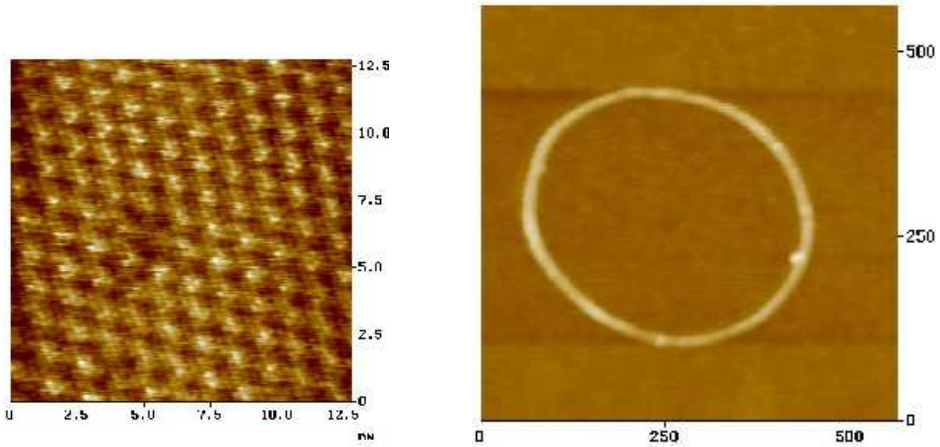

Figure 3.8: Two computer tomographic images of carbon nanotubes. The picture on the left is of atomic resolution.

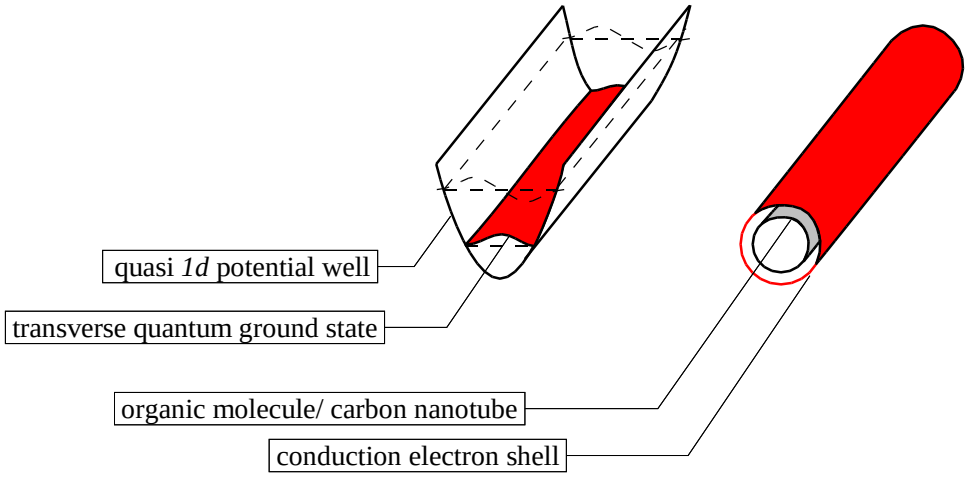

Figure 3.9: Schematic sketch of a number of realizations of one-dimensional electron systems.

where the subscripts L/R indicate that an operator $a^\dagger_{(+/-)k_F+q}$ creates an electron that moves to the left/right with velocity $\simeq \pm v_F \equiv k_F/m$. We next observe (cf. Fig. 3.10) that in the immediate vicinity of the Fermi points, the dispersion relation is approximately linear,

$$\frac{(\pm k_F + q)^2}{2m} - \mu \approx \pm v_F q,$$

implying that the non-interacting part of the Hamiltonian can be represented as,

$$\hat{H}_0 \simeq - \sum_{s=L,R} \tilde{\sum_q} a^\dagger_{sq}\, \sigma_s v_F q\, a_{sq}, \tag{3.30}$$

where $\sigma_s = (+/-)$ for $s = L/R$ and the notation $\tilde{\sum}$ indicates that in order for the effective Fermi surface description to make sense, the summation over momenta has to be truncated

at some cutoff momentum: $\tilde{\sum}_k \equiv \sum_{|k|<\Gamma}$, where Γ is a momentum beyond which the linearization of the dispersion relation no longer represents a good approximation.

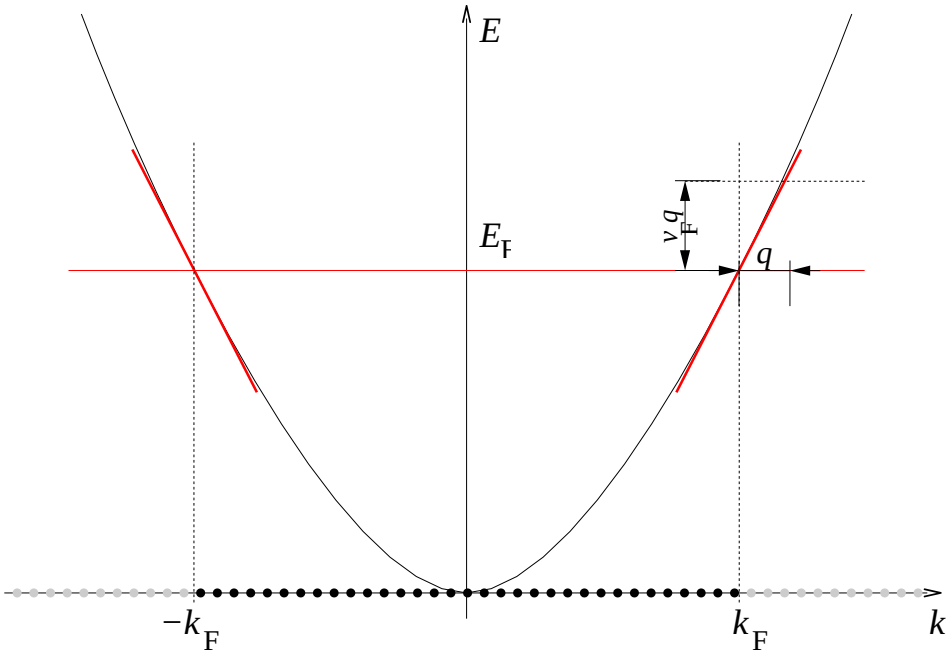

Figure 3.10: On the dispersion k-space structure of the one-dimensional electron gas.

Turning to the interacting part of the Hamiltonian, we first define the notation

$$\hat{\rho}_{sq} = \tilde{\sum}_k a^\dagger_{sk+q} a_{sk}. \tag{3.31}$$

Importantly, the definition of these operators is not just motivated by notational convenience. It is straightforward to verify (exercise) that $\hat{\rho}_s(q)$ obtains as the Fourier transform of the density operator $\hat{\rho}(x)$ defined in (3.12), if the summation over momenta k in the Fourier decomposition (3.6) is restricted to the Γ-vicintiy of $\pm k_F$. In other words, $\hat{\rho}_{sq}$ measures density fluctutations of characteristic wavelength q^{-1} supported by electronic excitations with characteristic momentum $\pm k_F$ (see Fig. 3.11, left.) From our heuristic argument above, suggesting charge density modulations to be the basic excitations of the one-dimensional electron gas, we expect the operators $\hat{\rho}_{sq}$ to represent the central degrees of freedom of the theory.

Represented in terms of the density operators, the interaction contribution of the Hamiltonian reads as

$$\hat{V}_{\rm ee} = \frac{1}{2L}\sum_{kk'q} a^\dagger_{k-q} a_k V(q) a^\dagger_{k'+q} a_{k'} \equiv \frac{1}{2L}\sum_{qs}\left[g_4 \hat{\rho}_{sq}\hat{\rho}_{s-q} + g_2 \hat{\rho}_{sq}\hat{\rho}_{\bar{s}-q}\right], \tag{3.32}$$

where $\bar{s} = R/L$ for $s = L/R$ and the constants g_2 and g_4 measure the strength of the interaction at characteristic momentum $q = 0$ and $q = 2k_F$, respectively[7]. (With the notation $g_{2,4}$ we follow a common literature convention.)

[7] In fact, the relation between the coupling constants $g_{2,4}$ and the momentum Fourier transform of

▷ INFO. Working with second quantized theories, one frequently needs to compute commutators of operators $\hat{A}(a, a^\dagger)$ polynomial in the elementary boson/fermion operators of the theory. (E.g. $\hat{A} = aa^\dagger$, $\hat{A} = aaa^\dagger a^\dagger$, etc. where we have ommitted the quantum number subscripts generally carried by a and $a^\dagger$.) Such type of operations are made easier by a number of operations of elementary **commutator algebra**. The most basic identity, from which all sorts of other formulae can be generated recursively, is

$$\boxed{[\hat{A}, \hat{B}\hat{C}]_\pm = [\hat{A}, \hat{B}]_\pm \hat{C} \mp \hat{B}[\hat{A}, \hat{C}]_\pm.} \tag{3.33}$$

Iteration of this equation for *boson operators* a,$a^\dagger$ shows that

$$[a^\dagger, a^n] = (n-1)a^{n-1}. \tag{3.34}$$

(Due to $a^2 = 0$ in the fermionic case, there is no fermion analog of this equation.) Taylor expansion then shows that for any analytic function $F(a)$,

$$[a^\dagger, F(a)] = F'(a).$$

Another useful formula is

$$a^\dagger F(aa^\dagger) = F(a^\dagger a)a^\dagger,$$

which is also verified by series expansion.

So far, we have merely re-written parts of the Hamiltonian in terms of density operators. Ultimately, however, we wish to arrive at a representation whereby these operators, instead of the original electron operators, represent the fundamental degrees of freedom of the theory. Since the definition of the ρ's involves the square of two Fermi operators, we expect the densitiy operators to resemble *bosonic* excitations. Thus, as a first and essential step towards the construction of the new picture, we explore the commutation relations between the operators $\hat{\rho}_{sq}$.

From the definition (3.31) and the auxiliary identity (3.33) it is straightforward to verify that

$$[\hat{\rho}_{sq}, \hat{\rho}_{s'(-q')}] = \delta_{ss'} \tilde{\sum_k} (a^\dagger_{sk+q} a_{sk+q'} - a^\dagger_{sk+q-q'} a_{sk}).$$

As it stands, this relation is certainly not of much practical use. To make further progress, we need to resort to a (weak) approximation: The point we exploit is that ultimately we will want to compute some observables and this will involve quantum averages $\langle\Omega| \ldots |\Omega\rangle$ taken in the ground state of the theory. To simplify the structure of the theory, we thus replace the rhs of the relation by its ground state expectation value:

$$[\hat{\rho}_{sq}, \hat{\rho}_{s'}(-q')] \approx \delta_{ss'} \tilde{\sum_k} \langle\Omega| a^\dagger_{sk+q} a_{sk+q'} - a^\dagger_{sk+q-q'} a_{sk} |\Omega\rangle =$$

$$= \delta_{ss'}\delta_{qq'} \tilde{\sum_k} \langle\Omega| \hat{n}_{sk+q} - \hat{n}_{sk} |\Omega\rangle.$$

V is not entirely straightforward. The reason is that to the summation $\sum_{kk'q}$ terms with $(k, k', q) \simeq (\pm k_F, \pm k_F, \leq \Gamma)$ but also with $(k, k', q) \simeq (\pm k_F, \mp k_F, 2k_F)$ contribute (See Ref.[] for a detailed discussion.) When adequately ordered (exercise), these contributions can be arranged to the rhs of (3.32). At any rate, the only point that matters for our present discussion is that the interaction *can* be represented through density operators with positive constants $g_{2,4}$ determined by the interaction strength.

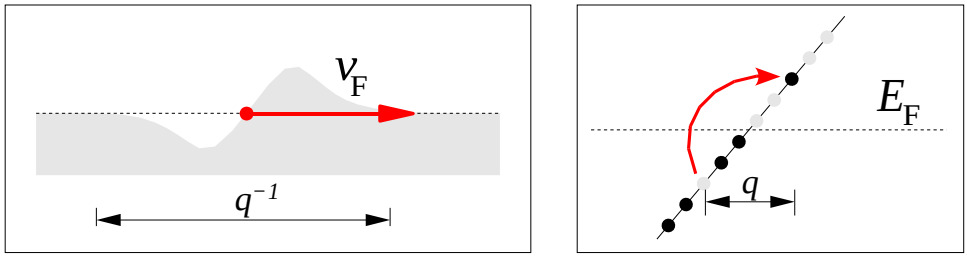

Figure 3.11: Two different interpretations of the excitations created by the density operators $\hat{\rho}_{sq}$. Left: Real space; $\hat{\rho}_{sq}$ creates density modulations of characteristic wave length q^{-1} and characteristic velocity v_F. Right: Momentum space; Application of $\hat{\rho}_{sq}$ onto the ground state exites electrons from states k to $k+q$. This creates particle-hole excitations of energy $\epsilon_{k+q}-\epsilon_k = v_F q$ *independent* of the paricle/hole momentum k. Both particles and holes forming the excitation travel with the same velocity v_F implying that the excitation does not disperse (decay).

where $\hat{n}_{sk} = a^\dagger_{sk} a_{sk}$ and we have used that $\langle\Omega|a^\dagger_{sk} a_{sk'}|\Omega\rangle = \delta_{kk'}$. This is an uncontrolled approximation but it is expected to becomce the better the closer we stay to the zero temperature ground state $|\Omega\rangle$ of the theory (i.e. at low excitation energies.).

▷ EXERCISE. Try to critically form an opinion on the validy of the approximation.

At first glance, it looks like the rhs of our simplified commutator relation actually vanishes. A simple shift of the summation index, $\tilde{\sum}_k \langle\Omega|\hat{n}_{sk+q}|\Omega\rangle \stackrel{?}{=} \tilde{\sum}_k \langle\Omega|\hat{n}_{sk}|\Omega\rangle$ seems to show that the two terms contributing to the sum cancel. However, this argument is certainly too naive. It ignores that our summation is limited by a cutoff momentum Γ. Since the shift $k \to k-q$ changes the cutoff the speculation above is invalid.

To obtain a better result, let us consider the case $s = R$ and $q > 0$. What we know is that in the ground state, all states with momentum $k < 0$ are occupied while all states with $k \geq 0$ are empty. This implies that

$$\tilde{\sum}_k \langle\Omega|\hat{n}_{Rk+q} - \hat{n}_{Rk}|\Omega\rangle = \left(\sum_{-\Gamma<k<-q} + \sum_{-q<k\leq 0} + \sum_{0<k<\Gamma}\right) \langle\Omega|\hat{n}_{Rk+q} - \hat{n}_{Rk}|\Omega\rangle =$$
$$= \sum_{-q\leq k\leq 0} \underbrace{\langle\Omega|\hat{n}_{Rk+q} - \hat{n}_{Rk}|\Omega\rangle}_{1} = -\frac{qL}{2\pi},$$

wher in the last identity we have used that a momentum interval of size q contains $q/(2\pi/L)$ quantized momentum states. Similar reasoning for $s = L$ shows that the effective form of the commutator relation reads as

$$[\hat{\rho}_{sq}, \hat{\rho}_{s'-q'}] = \delta_{ss'}\delta_{qq'}\sigma_s \frac{qL}{2\pi}. \tag{3.35}$$

Now, if it where not for the q-dependence of the rhs of this relation we would indeed have found (approximate) bosonic commutation relations. To make the connection to bosons

explicit, we define

$$b_q \equiv \left(\frac{2\pi}{Lq}\right)^{1/2} \hat{\rho}_{Lq}, \qquad b_q^\dagger \equiv \left(\frac{2\pi}{Lq}\right)^{1/2} \hat{\rho}_{L-q}, \tag{3.36}$$

$$b_{-q} \equiv \left(\frac{2\pi}{Lq}\right)^{1/2} \hat{\rho}_{R-q}, \qquad b_{-q}^\dagger \equiv \left(\frac{2\pi}{Lq}\right)^{1/2} \hat{\rho}_{Rq}, \tag{3.37}$$

where $q > 0$. The newly defined operators b_q obey canonical commutation relations (exercise), i.e. we have indeed found that, apart from the scaling factors $\sqrt{2\pi/qL}$, the density excitations of the system are bosonic particles.

Expressed in terms of the b's, the interaction part of the Hamiltonian reads as (exercise),

$$V_{\text{ee}} = \frac{1}{2\pi} \sum_{q>0} q \begin{pmatrix} b_q & b_{-q}^\dagger \end{pmatrix} \begin{pmatrix} g_4 & g_2 \\ g_2 & g_4 \end{pmatrix} \cdot \begin{pmatrix} b_q^\dagger \\ b_{-q} \end{pmatrix}$$

Notice that we have succeeded in representing a genuine two body interaction, i.e. a contribution that usually renders a model un-solvable in terms of a quadratic representation.

However, the free boson representation of the interaction term will be of little use as long as we have not managed to express the kinetic part of the Hamiltonian, H_0, in terms of b's, too. There are various ways of achieving this goal. The most straightforward route, i.e. direct construction of a representation of H_0 in terms of bose operators, is cumbersome in practice. However, there exists a much more efficient way which is based on somewhat indirect reasoning: As follows from the discussion of section 3.1.2, the properties of second quantized operators are essentially fixed by their commutation relations[8]. So, what we are going to do is search for an operator $H_0(b, b^\dagger)$ that has the same commutation relations with the boson operators $(b, b^\dagger)$ as the original kinetic energy operator $H_0(a, a^\dagger)$. Using (3.30), the definition (3.31), and the auxiliary identity (3.33) it is straightforward to verify that

$$[\hat{H}_0, \hat{\rho}_{sq}] = q v_F \sigma_s \hat{\rho}_{sq}.$$

On the other hand, using (3.35) one finds that the same commutation relations hold with the operator

$$\hat{H}_0' = \frac{2\pi v_F}{L} \sum_{qs} \rho_{sq} \rho_{s-q},$$

i.e., $[\hat{H}_0', \hat{\rho}_{sq}] = q v_F \sigma_s \hat{\rho}_{sq}$. Following the logics of our argument we thus identify $\hat{H}_0 = \hat{H}_0'$ (up to inessential constants) and use H_0' for the non-interacting Hamiltonian.

▷ EXERCISE. To gain confidence the in the identification $H_0 = H_0' + \text{const.}$, and to show that the undetermined constant actually equalls zero, determine the energy expectation value

[8] This argument can be made quantitative by group theoretical reasoning: Eqs. (3.3) and (3.4) define the irreducible representation of an operator algebra. An *algebra* because [,] defines a product in the space of generators $\{a_\lambda, a_\lambda^\dagger\}$, a *representation* because the operators act in a vector space (viz. Fock space $\mathcal{F}$), which is *irreducible* because all states $|\lambda_1, \ldots, \lambda_N\rangle \in \mathcal{F}$ can be reached by iterative application of operators onto a unique reference state (e.g. $|\Omega\rangle$). Under these conditions, Schur's Lemma – to be discussed in more detail in section XX below – states that two operators A_1 and A_2 sharing identical commutation relations with all $\{a_\lambda, a_\lambda^\dagger\}$ are equal up to a constant.

of the state $|\Psi_{sq}\rangle \equiv \hat{\rho}_{sq}|\Omega\rangle$ both as $\langle\Psi_{sq}|\hat{H}_0|\Psi_{sq}\rangle$ and as $\langle\Psi_{sq}|\hat{H}_0'|\Psi_{sq}\rangle$. Show that the two expressions coincide.

Finally, expressing the ρ's in terms of the bose operators (3.36) and adding the interaction contribution $V_{\rm ee}$ we arrive at the effective Hamiltonian

$$\hat{H} = \sum_{q>0} q \begin{pmatrix} b_q & b_{-q}^\dagger \end{pmatrix} \begin{pmatrix} v_F + \frac{g_4}{2\pi} & \frac{g_2}{2\pi} \\ \frac{g_2}{2\pi} & v_F + \frac{g_4}{2\pi} \end{pmatrix} \begin{pmatrix} b_q^\dagger \\ b_{-q} \end{pmatrix}. \tag{3.38}$$

We have thus succeeded to map the full interacting problem onto a *free* bosonic theory. The mapping $a \to \hat{\rho} \to b$ is our first example of **bosonization**. Bosonization techniques play an important role in 2(=1 space +1 time)-dimensional field theory in general. Conversely, it is sometimes useful to represent a boson problem in terms of fermions via **fermionization**. One may wonder why it is possible at all to effortlessly represent the low lying excitations of a gas of *fermions* in terms of *bosons*. **Fermi-Bose transmutability** is indeed a peculiarity of one-dimensional quantum systems: Particles confined to a line cannot pass around each other. That means that the whole issue of sign factors arising upon interchange of particle coordinates does not arise and much of the exclusion type characteristics of the Fermi system are inactivated. A more systematic formulation of Fermi $\leftrightarrow$ Bose transformations will be discussed in chapter XX below.

Now, there is one last problem that needs to be overcome to actually solve the problem. In chapter 1, we had learned how to interpret Hamiltonians of the structure $\sum_q b_q^\dagger b_q$ as superpositions of harmonic oscillators. However, in our present problem terms of the type $b_q b_{-q}$ and $b_{-q}^\dagger b_q^\dagger$ appear. To get back to familiar terrain, we need to eliminate these terms. However, before doing so, it is intstructive to discuss the physical meaning of the problem.

We first recapitulate that the total number operator of a theory described by operators $\{b_\lambda^\dagger, b_\lambda\}$ is given by $\hat{N} = \sum_\lambda b_\lambda^\dagger b_\lambda$. Now, if the Hamiltonian has the form $\hat{H} = \sum_{\mu\nu} b_\mu^\dagger H_{\mu\nu} b_\nu$, the total number operator commutes with $\hat{H}$, i.e. $[\hat{N}, \hat{H}] = 0$ (exercise). This means that $\hat{H}$ and $\hat{N}$ can be simultaneously diagonalized, or, in more physical terms, that the Hamiltonian does not create or annihilate particles. More generally, any Hamiltonian in which operators appear as monomials containing equal numbers of creators and annihilators (e.g. $bb^\dagger bb^\dagger$, $bbbb^\dagger b^\dagger b^\dagger$) has this property. This is because any operator of this structure creates as many particles as it annihilates. In problems, were the total number of particles is conserved (e.g. the theory of interacting electrons in an isolated piece of metal), the Hamiltonian is bound to have this structure. Conversely, in situations where the number of excitations is not fixed (e.g. a theory of photons or phonons) particle number violating terms like bb or $b^\dagger b^\dagger$ can appear. Such a situation is realized in our present problem; the number of density excitations in an electronic system is certainly not a conserved quantity which explains why contributions like $b_q b_{-q}$ appear in $\hat{H}_0$.

To eliminate the non-particle number conserving contributions we should, somehow, transform the matrix

$$K \equiv \begin{pmatrix} v_F + \frac{g_4}{2\pi} & \frac{g_2}{2\pi} \\ \frac{g_2}{2\pi} & v_F + \frac{g_4}{2\pi} \end{pmatrix}$$

to a diagonal structure. Transformations of K can be generated by transforming the

operators b_q and $b_q^\dagger$ to a different representation. Specifically, with

$$\Psi_q \equiv \begin{pmatrix} b_q^\dagger \\ b_{-q} \end{pmatrix},$$

we may define $\Psi'_q \equiv T\Psi_q$, where T is a 2×2 matrix acting on the two components of Ψ. (Since K does not depend on q, T can be chosen to have the same property.) After the transformation, the Hamiltonian will have the form

$$H = \sum_{q>0} \Psi_q^\dagger K \Psi_q \to \sum_{q>0} \Psi_q'^\dagger \underbrace{T^\dagger K T}_{K'} \Psi'_q, \tag{3.39}$$

with a new matrix $K' \equiv T^\dagger K T$. We will seek for a transformation T that makes K' diagonal. However, an important point to be kept in mind is that not all 2×2 matrices T qualify as transformations: We must ensure that the transformed 'vector' again has the structure

$$\Psi'_q \equiv \begin{pmatrix} b_q^{\dagger\prime} \\ b'_{-q} \end{pmatrix},$$

with a boson creator/annihilator in the first/second component. Remembering that the algebraic properties of the operators b are specified through commutation relations, this condition can be cast in mathematical form by demanding that the commutator

$$[\Psi_{qi}, \Psi_{qj}^\dagger] = (\sigma_3)_{ij} \stackrel{!}{=} [\Psi'_{qi}, \Psi_{qj}'^\dagger]$$

be invariant under transformation. Here, σ_3 is the third of the Pauli matrices

$$\sigma_1 = \begin{pmatrix} & 1 \\ 1 & \end{pmatrix}, \qquad \sigma_2 = \begin{pmatrix} & -i \\ i & \end{pmatrix}, \qquad \sigma_3 = \begin{pmatrix} 1 & \\ & -1 \end{pmatrix}, \tag{3.40}$$

and $i = 1, 2$ labels the components of Ψ. Using that $\Psi' = T\Psi$, this condition is seen to be equivalent to the pseudo unitarity condition,

$$T^\dagger \sigma_3 T \stackrel{!}{=} \sigma_3.$$

Having understood this, we are in a position to find a transformation that brings the matrix K' to a 2×2 diagonal form. Multiplication of the definition $K' = T^\dagger K T$ by σ_3 leads to

$$T^\dagger K T = K' \Leftrightarrow \underbrace{\sigma_3 T^\dagger \sigma_3}_{T^{-1}} \sigma_3 K T = \sigma_3 K'.$$

This means that the matrix $\sigma_3 K'$ is obtained by a *similarity* transformation $T^{-1}(\ldots)T$ from the matrix $\sigma_3 K$, or, in other words, that the matrix $\sigma_3 K'$ contains the eigenvalues $\pm u$ of $\sigma_3 K$ on its diagonal[9]. However, the eigenvalues of

$$\sigma_3 K = \begin{pmatrix} v_F + \frac{g_4}{2\pi} & \frac{g_2}{2\pi} \\ -\frac{g_2}{2\pi} & -v_F - \frac{g_4}{2\pi} \end{pmatrix},$$

[9] That the eigenvalues sum to 0 follows from the fact that the trace, $\mathrm{tr}(\sigma_3 K) = 0$.

are readily computed as

$$u = \frac{1}{2\pi}\left[(2\pi v_F + g_4)^2 - g_2^2\right]^{1/2}. \tag{3.41}$$

Thus, with $\sigma_3 K' = \sigma_3 u$ we arrive at $K' = u \cdot \mathrm{id.}$, where 'id.' stands for the unit matrix[10]. Substitution of this result into (3.39) finally leads to $\hat{H} = u \sum_{q>0} q \Psi_q'^{\dagger} \Psi_q'$, or using that $\Psi_q'^{\dagger}\Psi_q' = b_q b_q^{\dagger} + b_{-q} b_{-q}^{\dagger} + 1$,

$$\hat{H} = \sum_q u|q|\, b_q^{\dagger} b_q, \tag{3.42}$$

where we have ignored an overall constant and omitted the prime on our new bose operators. In the literature, the transformation procedure just outlined is called a **Bogoliubov transformation**[11] . Transformations of this type are frequently applied quantum magnetism, superconductivity, or, more generally, in all problems where the particle number is not conserved. Notice that the possibility to transform to a representation $\sim b^{\dagger} b$ does, of course, not imply that miraculously the theory has become particle number conserving. The new *quasi-particle* operators b are related to the original bose operators through a transformation that mixes b and $b^{\dagger}$. While the quasi-particle number is conserved, the number of original density exicitations is not.

Eqs. (3.41) and ((3.42) represent our final solution of the problem of spinless interacting fermions in one dimension. We have managed to map the problem onto a form analogous to our previous results (2.9) and (2.15) for the phonon and the photon system, respectively. All what had been said about these Hamiltonians equally applies to (3.42): The basic excitations of the $1d$ fermion system are waves, i.e. excitations with linear dispersion $\omega = u|q|$. In the present context, they are termed **charge density waves (CDW)**. The bose creation operators describing these excitations are, apart from Bogoliubov transformation and a momentum dependent scaling factor $(2\pi/Lq)^{1/2}$ equivalent to the density operators of the electron gas. For a non-interacting system, $g_2 = g_4 = 0$, the CDW propagates with the velocity of the Fermi-particles, v_F. A ficticious interaction not coupling between particles of opposite Fermi momentum, $g_2 = 0, g_4 \neq 0$, speed up the CDW. Heuristically, this can be interpreted as an 'acceleration process' whereby a charge density wave electrostatically pushes its own charge front. In contrast, interactions between left and right movers, $g_2 \neq 0$, diminish the velocity, i.e. due to the Coulomb interaction it is difficult for distortions of opposite velocity to penetrate each other. (Notice

[10] Explicit knowledge of the transformation matrix T, i.e. knowledge of the relation between the operators b and b', is not needed for our construction. However, for the sake of completeness, we mention that

$$T = \begin{pmatrix} \cosh\theta_k & \sinh\theta_k \\ \sinh\theta_k & \cosh\theta_k \end{pmatrix}$$

with $\tanh(2\theta) = \frac{g_2}{2\pi v_F + g_4}$ does the job.

[11] N. N. Bogoliubov 1909-1992: Theoretical physcists aclaimed for his works in nonlinear mechanics, statistical physics, theory of superfluidity and superconductivity, Quantum field theory, renormalization group theory, proof of dispersion relations, and elementary particle theory.

that for a theory with $g_2 = 0$ no Bogoliubov transformation would be needed to diagonalize the Hamiltonian, i.e. in this case undisturbedly left and right moving waves would be the basic excitations of the theory.) While there is general consensus about CDW's being a basic excitation of the interacting electron gas, these waves have never so far been observed in experiment. There are, however, lots of indirect manifestations of their existence. We will come back to this point, after the spinfull model has been discussed in chapter XX. However, for the moment we conclude the discussion of the one-dimensional interacting Fermi system and turn to an entirely different problem.

3.2.3 Quantum Spin Chains

In the previous section, the emphasis has been on *charging effects* generated by the Coulomb interaction. However, as we have seen in section 3.2.1 Coulomb correlations may also lead to the indirect generation of *magnetic* interactions, both of ferromagnetic and anti-ferromagnetic[12] type. In one dimension, one can account for these mechanisms by adding to our previously structureless electrons a spin degree of freedom. This leads to the so-called **Tomonaga-Luttinger liquid**, a system governed by the co-existence of collective spin- and charge-excitations. Needless to say that the dynamics of this system is more complex than that of the pure CDW-system discussed above. We will turn back to the discussion of this problem in section XX below. However, to get a first survey of phenomena brought about by quantum-magnetic correlations, it is instructive to begin by considering systems where the charge degrees of freedom are frozen and only spin-excitations remain. Such systems are realized through quantum spin chains or, more generally, higher-dimensional quantum spin lattices. Beginning with the case of the ferromagnetic spin chain it is the intent of the present section to explore aspects of the low-energy physics of such systems.

Quantum Ferromagnet

The quantum Heisenberg[13] ferromagnet is specified by the Hamiltonian

$$\boxed{\hat{H} = -J \sum_{\langle mn \rangle} \hat{\mathbf{S}}_m \cdot \hat{\mathbf{S}}_n} \tag{3.43}$$

[12] As a matter of fact, the generation of anti-ferromagnetic correlations from the Hubbard model has not been demonstrated so far. Borroughing from our discussion of chapter XX below, we here merely mention that for a half filled tight binding band, the Hubbard model is governed by anti-ferromagnetic correlations.

[13] Werner Heisenberg 1901-1976: 1932 Nobel Laureate in Physics for the creation of quantum mechanics, the application of which has, *inter alia*, led to the discovery of the allotropic forms of hydrogen.

where $J > 0$, $\langle mn \rangle$ denotes summation over neighbouring sites of a lattice and $\hat{S}^i$ represents the ith component of a quantum mechanical spin operator at site n. In section 3.1.2 (cf. Eq. (3.9)) we had represented the operator $\hat{\mathbf{S}}_m$ in terms of spin-full electrons. However, one can conceive situations where the spin sitting at site m is carried by a different object (e.g. an atom with non-vanishing magnetic moment). At any rate, for the purposes of our present discussion, we need not specify the concrete realization of the spin. All we need to know is that the operators S^i_m, defined through the SU(2) commutator algebra

$$[\hat{S}^i_m, \hat{S}^j_n] = i\delta_{mn}\epsilon^{ijk} S^k_n, \tag{3.44}$$

represent *some* quantum spin sitting at site m. Notice, that these spins need not be $1/2$ but can have any interger or half-integer value S.

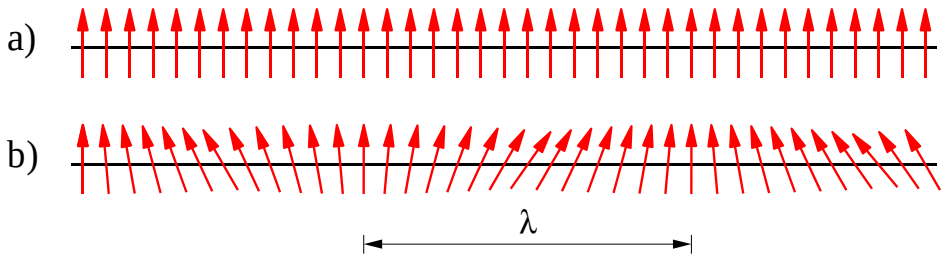

Figure 3.12: a) perfectly aligned ground state of the Heisenberg ferromagnet. b) Low lying excitations arise as long wavelength fluctuations around the mean orientation axis.

Now, due to the positivity of the coupling constant J, the Hamiltonian favours configurations where the spins at neighbouring sites are aligned in the same direction (cf. Fig. 3.12.) A ground state of the system is given by

$$|\Omega\rangle \equiv \otimes_m |\uparrow_m\rangle,$$

where $|\uparrow_m\rangle$ represents a state with maximal spin-z component: $S^3_m|\uparrow_m\rangle = S|\uparrow_m\rangle$. We have written 'a' ground state instead of 'the' ground state, because the system is highly degenerate: A simultaneous change of the orientation of all spins does not change the ground state energy, i.e. the system posesses a global rotation symmetry.

▷ EXERCISE. Compute the energy expectation value of the state $|\Omega\rangle$. Defining *global* spin operators through

$$\hat{S}^i \equiv \sum_m \hat{S}^i_m, \tag{3.45}$$

consider the state $|\boldsymbol{\alpha}\rangle \equiv \exp(i\boldsymbol{\alpha}\cdot\hat{\mathbf{S}})|\Omega\rangle$, where $\boldsymbol{\alpha}$ is a three-component vector of angles $\alpha_i \in [0, 2\pi]$. Verify that the state $\boldsymbol{\alpha}$ is degenerate with $|\Omega\rangle$. Explicitly compute the state $|(\pi/2, 0, 0)\rangle$. Convince yourself that for general $\boldsymbol{\alpha}$, $|\boldsymbol{\alpha}\rangle$ can be interpreted as a a state with rotated quantization axis.

As with our previous examples, we expect that a global continuous symmetry will entail the presence of energetically low-lying exciations. Indeed, it is obvious that a in the limit of long wavelength λ, a weak distortion of a groundstate configuration (cf. Fig.

3.12 b)) will cost vanishingly small energy. To quantitatively explore the physics of these **spin-waves**, we adopt a 'semiclassical' picture, where the spin $S \gg 1$ is assumed to be large. In this limit, the rotation of the spins around the ground state configuration becomes similar to the rotation of a classical magnetic moment.

▷ INFO. To better understand the mechanism behind the **semiclassical approximation**, consider the Heisenberg uncertainty relation,

$$\Delta S^i \Delta S^j \leq |\langle [\hat{S}^i, \hat{S}^j] \rangle| = \epsilon^{ijk} \langle \hat{S}^k \rangle,$$

where ΔS^i is the rms of the quantum uncertainty of spin component i. Using that $|\langle \hat{S}^k \rangle| \leq S$, we obtain for the relative uncertainty, $\Delta S^i / S$,

$$\frac{\Delta S^i}{S} \frac{\Delta S^j}{S} \leq \frac{S}{S^2} \overset{S \gg 1}{\longrightarrow} 0.$$

I.e. for $S \gg 1$, quantum fluctuations of the spin become less important.

In the limit of large S, and at low excitation energies, it is natural to describe the ordered phase in terms of small fluctuations of the spins around their expectation values (c.f. the description of the ordered phase of a crystal in terms of small fluctuations of the atoms around the ordered lattice sites). These fluctuations are conveniently represented in terms of spin raising and lowering operators: With $\hat{S}^{\pm}_m \equiv \frac{1}{2}(S^1_m \pm i S^2_m)$, it is straightforward to verify that

$$[\hat{S}^3_m, \hat{S}^{\pm}_n] = \pm \delta_{mn} S^{\pm}_m, \qquad [\hat{S}^+_m, \hat{S}^-_n] = 2\delta_{mn} S^3_m. \tag{3.46}$$

It is straightforward to verify that application of $\hat{S}^{-(+)}_m$ lowers (increases) the z-expectation value of the spin at site m by one. To actually make use of the fact that deviations around $|\Omega\rangle$ are small, a representation known as the **Holstein-Primakoff transformation**[14] was introduced in which the spin operators $\hat{S}^{\pm}$, $\hat{S}$ are specified in terms of boson creation and annihilation operators $a^\dagger$ and a:

$$\begin{aligned} \hat{S}^-_m &= (2S)^{1/2} a^\dagger_m \left(1 - \frac{a^\dagger_m a_m}{2S}\right)^{1/2}, \\ \hat{S}^+_m &= (2S)^{1/2} \left(1 - \frac{a^\dagger_m a_m}{2S}\right)^{1/2} a_m, \\ \hat{S}^3_m &= S - a^\dagger_m a_m. \end{aligned}$$

Using the auxiliary identities summarized on page 71, it is a straightforward exercise to show that the spin operators obey the commutation relations (3.46). The utility of this representation is clear when the spin is large $S \gg 1$. An expansion in powers of $1/S$ gives

$$\hat{S}^z_m = S - a^\dagger_m a_m, \qquad \hat{S}^-_m \simeq (2S)^{1/2} a^\dagger_m, \qquad \hat{S}^+ \simeq (2S)^{1/2} a_m.$$

[14] T. Holstein and H. Primakoff, Phys. Rev. **58**, 1908 (1940).

In this approximation, the Heisenberg Hamiltonian takes the form

$$\begin{aligned}\hat{H} &= -J\sum_{\langle mn\rangle}\left\{\hat{S}^3_m\hat{S}^3_n+\frac{1}{2}\left(\hat{S}^+_m\hat{S}^-_n+\hat{S}^-_m\hat{S}^+_n\right)\right\}\\ &= -J\sum_{\langle mn\rangle}\left\{S^2+S\left(a^\dagger_m a_n+a_m a^\dagger_n-a^\dagger_m a_m-a^\dagger_n a_n\right)+O(S^0)\right\}\\ &= -J\sum_{m}\left\{S^2-2Sa^\dagger_m a_m+S\left(a^\dagger_m a_{m+1}+\text{h.c.}\right)+O(S^0)\right\}.\end{aligned}$$

Keeping fluctuations at leading order in S, the quadratic Hamiltonian can be diagonalised by Fourier transformation. In this case, it is convenient to impose periodic boundary conditions: $\hat{S}_{m+N}=\hat{S}_m$, and $a_{m+N}=a_m$, where N denotes the total number of lattice sites. Defining

$$a_k=\frac{1}{\sqrt{N}}\sum_{n=1}^{N}e^{ikn}a_n,\qquad a_n=\frac{1}{\sqrt{N}}\sum_{k}^{\text{B.Z.}}e^{-ikn}a_k,\qquad \left[a_k,a^\dagger_{k'}\right]=\delta_{kk'},$$

the Hamiltonian for a one-dimensional lattice takes the form (exercise)

$$\boxed{\hat{H}=-JNS^2+\sum_{k}^{\text{B.Z.}}\hbar\omega_k a^\dagger_k a_k+O(S^0)} \tag{3.47}$$

where $\hbar\omega_k=2JS(1-\cos k)=4JS\sin^2(k/2)$ represents the dispersion relation. In particular, in the limit $k\to 0$, the energy of the elementary excitations goes to zero, $\hbar\omega_k\to JSk^2$. These massless low-energy excitations, known as **magnons**, describe the elementary spin-wave excitations of the ferromagnet. Taking into account terms at higher order in the parameter $1/S$, one finds interactions between the magnons.

How do these theoretical predictions compare with experiment? Figure 3.13 (a) shows the dispersion relation measured for a ferromagnetic material. At low values of momenta q, the dispersion relation is shown to be quadratic in agreement with our low-energy theory.

Quantum Antiferromagnet

Having explored the elementary excitation spectrum of the ferromagnet, we now turn to the discussion of the Heisenberg antiferromagnet

$$\boxed{\hat{H}=J\sum_{\langle mn\rangle}\hat{\mathbf{S}}_m\cdot\hat{\mathbf{S}}_n,}$$

where, again, $J>0$. In nature, antiferromagnetic phases mostly occur in the context of strongly correlated electron systems. E.g. high-temperature superconductors at low doping usually exhibit antiferromagnetic correlations. Indeed, we will see later on in chapter XX that the electronic Hubbard model close to half filling, a model generally regarded as

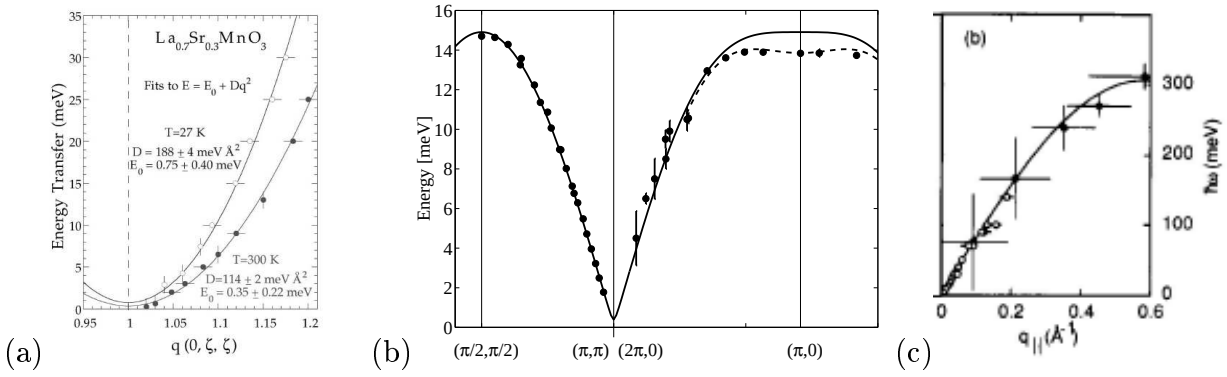

Figure 3.13: Measurements of the spin-wave dispersion relations for various ferro- and antiferromagnetic materials. (a) The ferromagnetic material $La_{0.7}Sr_{0.3}MnO_3$, (b) the antiferromagnetic metal-organic compound $Cu(DCOO)_2{\cdot}4D_2O$, where 'D' is 'Deuteron' (taken from H.M. Ronnow et al., cond-mat/0101238, and (c) the antiferromagnet Mott insulator La_2CuO_4. When doped away from stoichiometry, the latter becomes a high temperature superconductor.

a 'good' descriptor of the cuprate CuO_2 planes, is an antiferromagnetic insulator. (For an oversimplified explanation of how antiferromagnetic correlations can be born out of Hubbard type systems, see the problem set of this chapter.)

Although $\hat{H}$ differs from its ferromagnetic relative 'only' by a global change in the coupling constant, the differences in the physics are drastic. First, the phenomenology displayed by the anti-ferromagnetic $\hat{H}$ depends sensitively on the morphology of underlying lattice: For a **bipartite lattice**, i.e. one which can be segmented into two inter-penetrating A and B (cf. Fig. 3.14 a)), the ground states of the Heisenberg antiferromagnet adopt a staggered spin configuration, known as a **Néel state**[15] , where *all* neighbouring spins are antiparallel. Again the ground state is degenerate, i.e. a global rotation of all spins by the same amount does not change the energy. In contrast, on non-bipartite lattices such as the triangular lattice shown in Fig. 3.14 b), no spin arrangement can be found wherein which each bond recovers the full exchange energy J. Spin models of this kind are said to be **frustrated** (see Problem set 3.4).

Turning back to the case of one-dimension, we first notice that a chain is trivially bipartite. However, in contrast to the ferromagnetic model, the classical Néel ground states of the chain (see Fig. 3.15) are not *exact* eigenstate of the quantum Hamiltonian. Nevertheless, when $S \gg 1$, the classical ground state serves as a useful reference state from which fluctuations can be examined within the Holstein-Primakoff representation.

Before expanding the Hamiltonian in terms of bosonic operators, it is convenient to apply a canonical transformation to the Hamiltonian in which the spins on one sublattice,

---

[15] Louis Néel 1904-, 1970 Nobel Laureate in physics for fundamental work and discoveries concerning antiferromagnetism and ferrimagnetism which have led to important applications in solid state physics

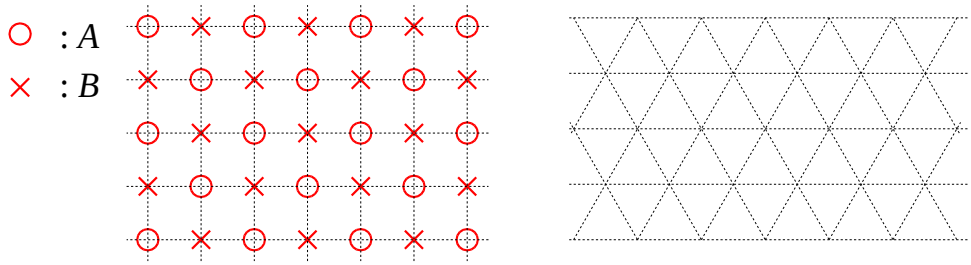

Figure 3.14: a) Example of a two-dimensional bipartite lattice. b) a non-bipartite lattice; no anti-ferromagnetic occupation possible.

say B, are rotated through 180^o about the 1-axis, i.e. $S^1_B \to \widetilde{S}^1_B = S^1_B$, $S^2_B \to \widetilde{S}^2_B = -S^2_B$, and $S^3_B \to \widetilde{S}^3_B = -S^3_B$. I.e. when represented in terms of the new operators, the Néel ground state looks like a ferromagnetic state, with all spins aligned. We expect that a gradual distortion of this state will produce the antiferromagnetic analog of the spin-waves discussed in the previous section.

Represented in terms of the transformed operators, the Hamiltonian reads as

$$\hat{H} = -J \sum_{\langle mn \rangle} \left[S^3_m \widetilde{S}^3_n - \frac{1}{2} \left(S^+_m \widetilde{S}^+_n + S^-_m \widetilde{S}^-_n \right) \right].$$

Once again, applying the semiclassically approximated Holstein-Primakoff transformation, $S^-_m \simeq (2S)^{1/2} a^\dagger_m$, $\widetilde{S}^-_n \simeq (2S)^{1/2} a^\dagger_n$, etc., we obtain the Hamiltonian

$$\hat{H} = -NJS^2 + JS \sum_{\langle mn \rangle} \left[a^\dagger_m a_m + a^\dagger_n a_n + a_m a_n + a^\dagger_m a^\dagger_n \right] + O(S^0).$$

At first sight the structure of this Hamiltonian, albeit quadratic in the Bose operators, looks akward. However, after a Fourier transformation, $a_m = N^{-1/2} \sum_k e^{-ikx_m} a_k$ it assumes the more accessible form

$$\hat{H} = -NJS(S+1) + JS \sum_k \begin{pmatrix} a^\dagger_k & a_{-k} \end{pmatrix} \begin{pmatrix} 1 & \gamma_k \\ \gamma_k & 1 \end{pmatrix} \begin{pmatrix} a_k \\ a^\dagger_{-k} \end{pmatrix} + O(S^0),$$

where $\gamma_k = \cos k$. Apart from the definition of the matrix kernel between the bose operators, $\hat{H}$ is equivalent to the Hamiltonian (3.38) discussed in connection with charge density waves. Performing exactly the same steps as on pp 75 the non-particle number conserving contributions $a^\dagger a^\dagger$ can be removed by Bogoliubov transformation. As before, the transformated Hamiltonian assumes a diagonal form,

$$\boxed{\hat{H} = -NJS^2 + 2JS \sum_k |\sin k| \left[\alpha^\dagger_k \alpha_k + \frac{1}{2} \right]} \tag{3.48}$$

Thus, in contrast to the ferromagnet, the spin-wave excitations of the antiferromagnetic model display a *linear spectrum* in the limit $k \to 0$.

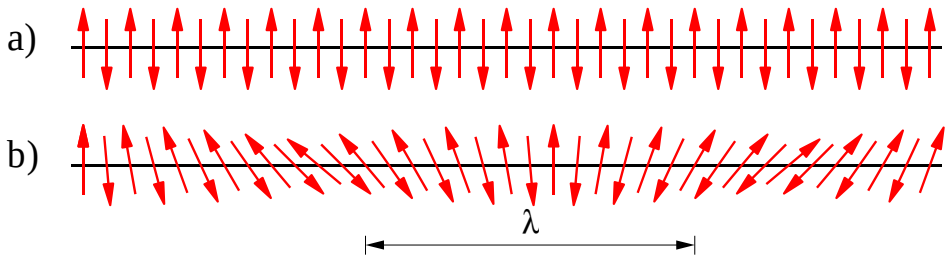

Figure 3.15: a) Néel ground state configuration of the spin chain. b) Cartoon of an antiferromagnetic spin-wave.

Experimental date for the spin-wave dispersion of two antiferrmagnetic substances is shown in Fig. 3.13. Despite having a moment of $S = 1/2$, the experiment reveals a linear dispersion at low momenta indicating that the large spin expansion captures the qualitative features of the low spin physics.

3.3 Summary and Outlook

This concludes our preliminary discussion of applications of second quantization. Additional, and interesting examples can be found in problem set 3.4.

In this chapter, we have introduced second quantization as a tool wherby problems of many body quantum mechanics can be attacked much more efficiently than by the traditional language of symmetrized many body wave functions. We have discussed how the two approaches are related to each other and how the standard operatations of quantum mechanics can be performed by second quantized methods.

Turning to applications, one notices that our so far list of applications contained problems that were either non-interacting from the outset, or could be reduced to quadratic operator structure by a number of suitable manipulations. However, we carefully avoided to touch interacting problems were no such reductions are possible. Yet it should be clear already at this stage of our discussion that completely or nearly solvable systems represent only a small minority of the problem classes encountered in condensed matter physics. But what can be done in situations where interactions, i.e. operator contributions of fourth or higher order, are present and *no* tricks like bosonization can be played? In the fourties, fifities and sixties it became an industry to address such problems by ever more sophisticated techniques of *perturbation theory*. Importantly, interacting problems of many body physics are either fundamentally inaccessible to perturbation theory, or they neccessitate perturbative analyses of *infinite* order in the interaction contribution(s). I.e. situations were a satisfactory result can be obtained by obtained by first or second order perturbation theory are exeptional.

Within second quantization, large order perturbative expansions in interaction operators leads to complex polynomials of creation and annihilation operators. Quantum expectation values taken of such structures can be computed by a reductive algorithm, known as **Wick's theorem**. However, from to date's point of view, formulating perturbation theory in this way is not very efficient. More importantly, problems that are

principally non-perturbative have moved into the focus of interest.

To understand the language of modern condensed matter physics, we thus need to develop another layer of theory, known as **field integration**. In essence, field integration is a concept generalizing the effective action approach of chapter 1 to the quantum level. However, before discussing quantum *field* theory, we should understand how the concept works in principle, i.e. on the level of point particle quantum mechanics. This will be the subject of the next chapter.

3.4 Problem Set

3.4.1 Questions on the Second Quantisation

Q1 (a) Starting with the commutation relation for bosonic creation $a^\dagger$ and annihilation operators a

$$\left[a, a^\dagger\right] = 1,$$

show that

$$[a^\dagger a, a] = -a, \qquad [a^\dagger a, a^\dagger] = a^\dagger.$$

Using this result, show that, if $|\alpha\rangle$ represents an eigenstate of the operator $a^\dagger a$ with eigenvalue α, $a|\alpha\rangle$ is also an eigenstate with eigenvalue $\alpha - 1$ (unless $a|\alpha\rangle = 0$). Similarly, show that $a^\dagger|\alpha\rangle$ is an eigenstate with eigenvalue $\alpha + 1$.

(b) If $|\alpha\rangle$ represents a normalised eigenstate of the operator $a^\dagger a$ with eigenvalue α for all $\alpha \geq 0$, show that

$$\begin{aligned} a|\alpha\rangle &= \sqrt{n}|\alpha - 1\rangle \\ a^\dagger|\alpha\rangle &= \sqrt{n+1}|\alpha + 1\rangle \end{aligned}$$

Defining as the normalised vacuum $|\Omega\rangle$ the normalised state that is anniliated by the operator a, show that $|n\rangle = (1/\sqrt{n!})(a^\dagger)^n|\Omega\rangle$ is a normalised eigenstate of $a^\dagger a$ with eigenvalue n.

(c) Assuming the operators a and $a^\dagger$ obey Fermionic anticommutation relations, repeat (a) and (b).

Q2 Starting from first principles, show that the second quantised representation of the one-body kinetic energy operator is given by

$$\hat{T} = \int d^d x a^\dagger(x) \frac{\hat{p}^2}{2m} a(x).$$

[Hint: Remember that the representation is most easily obtained from the basis in which the operator is diagonal.]

Q3 †In the diagonal basis $|\lambda\rangle$, a two-body operator is defined by

$$\hat{\mathcal{O}}_2|\lambda\lambda'\rangle = o_{\lambda\lambda'}|\lambda\lambda'\rangle.$$

E.g., for the two-body pairwise interaction potential $\hat{O}_2 = \sum_{ij} V(\hat{r}_i - \hat{r}_j)$, the diagonal basis is the real space basis $|r\rangle$. In the diagonal basis, show that

$$\langle\lambda'_1 \cdots \lambda'_N|\hat{\mathcal{O}}_2|\lambda_1 \cdots \lambda_N\rangle = \langle\lambda'_1 \cdots \lambda'_N|\frac{1}{2}\sum_{i\neq j}^{N} o_{\lambda_i\lambda_j}\hat{P}_{\lambda_i\lambda_j}|\lambda_1 \cdots \lambda_N\rangle,$$

where the operator

$$\hat{P}_{\lambda\lambda'} = \hat{n}_\lambda \hat{n}_{\lambda'} - \delta_{\lambda,\lambda'}\hat{n}_\lambda,$$

with $\hat{n}$ representing the number operator, counts the total number of pairs of particles in the states $|\lambda\rangle$ and $|\lambda'\rangle$. (Note that this number is different depending on whether or not $|\lambda\rangle = |\lambda'\rangle$.) With this question you might find it useful to consult Negele and Orland [**?**] or Feynman [**?**]. Using this result, show that, in second quantised notation, the two-body operator takes the form

$$\hat{\mathcal{O}}_2 = \frac{1}{2}\sum_{\lambda\lambda'}\langle\lambda\lambda'|\mathcal{O}_2|\lambda\lambda'\rangle a^\dagger_\lambda a^\dagger_{\lambda'} a_{\lambda'} a_\lambda.$$

Note that, for a pairwise interaction in real space, this result implies that

$$\hat{V} = \frac{1}{2}\int d^d x \int d^d x' a^\dagger(x) a^\dagger(x') V(x-x') a(x) a(x'),$$

where $V(x)$ is the function characterising the dependence of the interaction on the distance between the particles.

Q4 Transforming to the Fourier basis, diagonalise the non-interacting three-dimensional cubic lattice tight-binding Hamiltonian

$$\hat{H}^{(0)} = -\sum_{\langle \mathbf{mn}\rangle} t_{\mathbf{mn}} c^\dagger_{\mathbf{m}\sigma} c_{\mathbf{n}\sigma},$$

where the matrix elements $t_{\mathbf{mn}}$ take the positive real value t between neighbouring sites and zero otherwise. Comment on how this result compares to the spectrum of the Heisenberg ferromagnet.

Q5 Making use of the Pauli matrix identity $\boldsymbol{\sigma}_{\alpha\beta}\cdot\boldsymbol{\sigma}_{\gamma\delta} = 2\delta_{\alpha\delta}\delta_{\beta\gamma} - \delta_{\alpha\beta}\delta_{\gamma\delta}$ (where '$\cdot$' denotes the scalar or dot product), prove that

$$\hat{\mathbf{S}}_m \cdot \hat{\mathbf{S}}_n = -\frac{1}{2} c^\dagger_{m\alpha} c^\dagger_{n\beta} c_{m\beta} c_{n\alpha} - \frac{1}{4}\hat{n}_m \hat{n}_n$$

where $\hat{\mathbf{S}}_n = c^\dagger_{m\alpha}\sigma_{\alpha\beta}c_{m\beta}/2$ denotes the spin operator, $\hat{n}_m = c^\dagger_{m\alpha}c_{m\alpha}$ represents the total number operator on site m, and the summation over repeated spin indicies is assumed. (Here assume that lattice sites m and n are distinct.)

Q6 †**Hubbard Model**: The aim of this question is to explore the stability of the antiferromagnetic ground state of the half-filled Hubbard model by studying a toy system exactly.

(a) A system comprised of two lattice sites can accommodate up to a maximum of four electrons (spin up and spin down on each site). If the system is half-filled, i.e. the total system accommodates just two electrons, write down the six eigenstates states of the local Hubbard interaction (c.f. section **??**)

$$\hat{H}_U = U\sum_i n_{i\uparrow} n_{i\downarrow}.$$

Adding a hopping matrix element and exchange interaction between the neighbouring sites

$$\hat{H} = \hat{H}_U + \sum_{\langle ij \rangle} \left[-t c^\dagger_{i\sigma} c_{j\sigma} + \frac{V}{2} c^\dagger_{i\sigma} c^\dagger_{j\sigma'} c_{i\sigma'} c_{j\sigma} \right],$$

explain why two of the six eigenstates of $\hat{H}_U$ remain eigenstates of $\hat{H}$.

[The remainder of this problem is simplified by adopting a judicious convention for the fermionic ordering of the two-electron basis states.]

(b) Remembering the anticommutation relations of the electron operators, find the matrix elements between the remaining four states and thereby obtain the exact eigenvalues and eigenvectors of the complete Hamiltonian. [Hint: The form of the 4×4 Hamiltonian should suggest a unitary transformation which partially diagonalises the Hamiltonian reducing it to a 2×2 problem. I.e. the calculation of the secular equation associated with the 4×4 Hamiltonian is unnecessary.] Classify the eigenstates according to their total spin.

(c) Sketch the *phase diagram* of the model as a function of the dimensionless parameters U/t and V/t. In particular, note the region where the singlet ground state becomes unstable to the formation of a spin polarised ferromagnetic state. How does this phase diagram compare with the intuition drawn from the analysis of the Hubbard Hamiltonian in the limit of large U/t discussed in lectures?

Q7 †**Nagaoka Ferromagnetism**: At $U = \infty$, all 2^N states of the half-filled Hubbard model are degenerate — each site is occupied by a single electron of arbitrary spin. This degeneracy is lifted by the removal of a single electron from the lower Hubbard band (or, equivalently, the addition of a vacancy or hole). In such a case, there is a theorem due to Nagaoka[16] that, on a bipartite lattice, the ground state is ferromagnetic. The aim of this question is to explicitly test this prediction by applying the Hubbard model at $U = \infty$ to a square plaquette. For a four site plaquette with three electrons determine the eigenspectrum within the manifold (a) $S^z_{\rm total} = 3/2$, and (b) $S^z_{\rm total} = 1/2$. In each case, determine the total spin of the ground state. [Hint: In (b) there are a total of 12 basis states — you will find it useful to arrange these states in the order in which they are generated by application of the Hamiltonian.]

Q8 Starting with the definition

$$\hat{S}^- = (2S)^{1/2} a^\dagger \left(1 - \frac{a^\dagger a}{2S} \right)^{1/2},$$

confirm the validity of the Holstein-Primakoff transformation by explicitly checking the commutation relations of the spin raising and lowering operators.

[16] Y. Nagaoka, Phys. Rev. **147**, 392 (1966).

Q9 †**Frustration**: On a bipartite lattice (i.e. one in which the neighbours of one sublattice belong to the other sublattice), the ground state (known as a Néel state) of a classical antiferromagnet can adopt a staggered spin configuration in which the exchange energy is maximised. Lattices which can not be classified in this way are said to be frustrated — the maximal exchange energy associated with each bond can not be recovered. *Using only symmetry arguments*, specify one of the possible ground states of a classical three site triangular lattice antiferromagnet. (Note that the invariance of the Hamiltonian under a global rotation of the spins means that the there is manifold of continuous degeneracy in the ground state.) Using this result, construct one of the classical ground states of the infinite triangular lattice.

Q10 Confirm that the bosonic commutation relations of the operators a and $a^\dagger$ are preserved by the Bogoluibov transformation,

$$\begin{pmatrix} \alpha \\ \alpha^\dagger \end{pmatrix} = \begin{pmatrix} \cosh\theta & \sinh\theta \\ \sinh\theta & \cosh\theta \end{pmatrix} \begin{pmatrix} a \\ a^\dagger \end{pmatrix}.$$

Q11 (a) Making use of the spin commutation relation, $[S_i^\alpha, S_j^\beta] = i\delta_{ij}\epsilon^{\alpha\beta\gamma}S_i^\gamma$, apply the identity

$$i\hbar\dot{\hat{\mathbf{S}}}_i = [\hat{\mathbf{S}}_i, \hat{H}]$$

to express the equation of motion of a spin in a nearest neighbour spin S one-dimensional Heisenberg ferromagnet as a difference equation.

(b) Interpreting the spins as *classical* vectors, and taking the continuum limit, show that the equation of motion of the *hydrodynamic modes* takes the form

$$\hbar\dot{\mathbf{S}} = 2Ja^2\mathbf{S}\times\partial^2\mathbf{S},$$

where a denotes the lattice spacing. [Hint: Going to the continuum limit, apply a Taylor expansion to the spins viz. $S_{i+1} = S_i + a\partial S_i + \cdots$.]

(c) Parameterising the spin as

$$\mathbf{S} = \left(c\cos(kx-\omega t), c\sin(kx-\omega t), \sqrt{S^2-c^2}\right),$$

solve this equation. Sketch a 'snapshot' configuration of the spins in a spin chain.

Q12 †**Valence Bond Solid**: Starting with the spin 1/2 **Majumdar-Ghosh Hamiltonian**

$$\hat{H}_{\rm MG} = \frac{4|J|}{3}\sum_{n=1}^{N}\left(\hat{\mathbf{S}}_n\cdot\hat{\mathbf{S}}_{n+1} + \frac{1}{2}\hat{\mathbf{S}}_n\cdot\hat{\mathbf{S}}_{n+2}\right) + \frac{N}{2},$$

where the total number of sites N is even, and $\hat{\mathbf{S}}_{N+1} = \hat{\mathbf{S}}_1$, show that the two dimer or valence bond states

$$|0_\pm\rangle = \prod_{n=1}^{N/2}\frac{1}{\sqrt{2}}\left(|\uparrow_{2n}\rangle\otimes|\downarrow_{2n\pm1}\rangle - |\downarrow_{2n}\rangle\otimes|\uparrow_{2n\pm1}\rangle\right),$$

are exact eigenstates. [Hint: Try to recast the Hamiltonian in terms of the total spin of a triad $\hat{\mathbf{J}}_n = \hat{\mathbf{S}}_{n-1} + \hat{\mathbf{S}}_n + \hat{\mathbf{S}}_{n+1}$, and consider what this representation implies.] In fact these states represent the ground states of the Hamiltonian. Suggest what would happen if the total number of sites was odd.

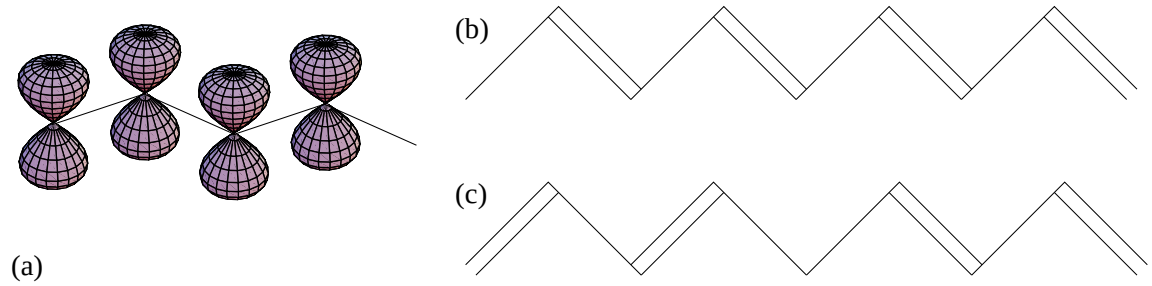

Figure 3.16: (a) Schematic diagram showing the π-bonding orbitals in long chain polyacetylene. (b) One of the configurations of the Peirels distorted chain. The double bonds represent the short links of the lattice. (c) A topological defect separating a two domains of the ordered phase.

Q13 Su-Shrieffer-Heeger Model[17] of the conducting polymers: Polyacetylene consists of bonded CH groups forming an isomeric long chain polymer. According to molecular orbital theory, the carbon atoms are expected to be sp^2 hybridised suggesting a planar configuration of the molecule. An unpaired electron is expected to occupy a single p-orbital which points out of the plane. The weak overlap of the p-orbitals delocalise the electrons into a π-conduction band (c.f. the benzene molecule) — see fig. 3.16a. Therefore, according to the nearly free electron theory, one might expect the half-filled conduction band of a polyacetylene chain to be metallic. However, the energy of a half-filled band of a one-dimension system can always be lowered by imposing a periodic lattice distortion known as the **Peirels instability** (see fig. 3.16b). One can think of an enhanced probability of finding the π electron on the short bond where the orbital overlap is stronger — the "double bond". The aim of this problem is to explore the instability.

(a) At its simplest level, the conduction band of polyacetylene can be modelled by a simple Hamiltonian, due to Su-Shrieffer-Heeger, in which the hopping matrix elements of the electrons are modulated by the lattice distortion of the atoms. Taking the displacement for the atomic sites to be u_n, and treating their dynamics

17

Alan J. Heeger: 2000 Nobel Laureate in Physics with Alan G. MacDiarmid, and Hideki Shirakawa for the discovery and development of conductive polymers.

as classical, the effective Hamiltonian takes the form

$$\hat{H} \;=\; -t\sum_{n=1}^{N}(1+u_n)\left[c^{\dagger}_{n\sigma}c_{n+1\sigma}+\text{h.c.}\right]+\sum_{n=1}^{N}\frac{k_s}{2}\left(u_{n+1}-u_n\right)^2,$$

where, for simplicity, the boundary conditions are taken to be periodic, and summation over the spins σ is assumed. The first term describes the hopping of electrons between neighbouring sites with a matrix element modulated by the periodic distortion of the bond-length, while the last term represents the associated increase in the elastic energy. Taking the lattice distortion to be periodic, $u_n = (-1)^n\alpha$, the Hamiltonian takes the form

$$\hat{H} = -t\sum_{n=1}^{N}(1+(-1)^n\alpha)\left[c^{\dagger}_{n\sigma}c_{n+1\sigma}+\text{h.c.}\right]+\frac{Nk_s\alpha^2}{2}.$$

Taking the *number of sites to be even*, diagonalise the Hamiltonian. [Hint: the lattice distortion lowers the symmetry of the lattice. The Hamiltonian is most easily diagonalised by distinguishing the two sites of the sublattice — i.e. doubling the size of the elementary unit cell.] Show that the Peierls distortion of the lattice opens a gap in the spectrum at the Fermi level of the half-filled system.

(b) By estimating the total electronic and elastic energy of the half-filled band (i.e. an average of one electron per lattice site), show that the one-dimensional system is always unstable towards the Peirels distortion. To complete this calculation, you will need the approximate formula for the (elliptic) integral,

$$\int_{-\pi/2}^{\pi/2}dk\left(1-\left(1-\alpha^2\right)\sin^2 k\right)^{1/2}\simeq 2+(a_1-b_1\ln\alpha^2)\alpha^2+O(\alpha^2\ln\alpha^2)$$

where a_1 and b_1 are (unspecified) numerical constants.

†(c) For an even number of sites, the Peierls instability has two degenerate configurations (see fig. 3.16b) — ABABAB.. and BABABA... Comment on the qualitative form of the ground state lattice configuration if the number of sites is odd (c.f. fig. 3.16c). Explain why such configurations give rise to mid-gap states.

Q14 In the **Schwinger boson representation**,[18] the quantum mechanical spin is expressed in terms of two bosonic operators a, and b in the form

$$\hat{S}^{+}=a^{\dagger}b,\qquad \hat{S}^{-}=(\hat{S}^{+})^{\dagger},\qquad \hat{S}^{z}=\frac{1}{2}\left(a^{\dagger}a-b^{\dagger}b\right).$$

18

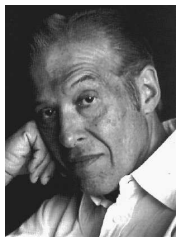

Julian Schwinger: 1965 Nobel Laureate in Physics with Sin-Itiro Tomonaga and Richard P. Feynman, for their fundamental work in quantum electrodynamics, with deep-ploughing consequences for the physics of elementary particles.

(a) Show that this definition is consistent with the commutation relations for spin: $[\hat{S}^+, \hat{S}^-] = 2\hat{S}^z$.

(b) Using the bosonic commutation relations, show that

$$|S, m\rangle = \frac{(a^\dagger)^{S+m}}{\sqrt{(S+m)!}} \frac{(b^\dagger)^{S-m}}{\sqrt{(S-m)!}} |\Omega\rangle,$$

is compatible with the definition of an eigenstate of the total spin operator $\mathbf{S}^2$ and S^z. Here $|\Omega\rangle$ denotes the vacuum of the Schwinger bosons, and the total spin S defines the physical subspace

$$\{|n_a, n_b\rangle : n_a + n_b = 2S\}.$$

Q15 †**The Jordan-Wigner Transformation**: So far we have shown how the algebra of quantum mechanical spin can be expressed using boson operators — c.f. the Holstein-Primakoff transformation and the Schwinger representation. In this problem we show that a representation for spin 1/2 can be obtained in terms of Fermion operators. Specifically, let us represent an up spin as a particle and a down spin as the vacuum, viz.

$$|\uparrow\rangle \equiv |1\rangle = f^\dagger |0\rangle,$$
$$|\downarrow\rangle \equiv |0\rangle = f|1\rangle.$$

In this representation the spin raising and lowering operators are expressed in the form $\hat{S}^+ = f^\dagger$ and $\hat{S}^- = f$, while $\hat{S}^z = f^\dagger f - 1/2$.

(a) With this definition, confirm that the spins obey the algebra $[\hat{S}^+, \hat{S}^-] = 2\hat{S}^z$.

However, there is a problem: spins on different sites commute while fermion operators anticommute, e.g.

$$S_i^+ S_j^+ = S_j^+ S_i^+, \qquad \text{but} \quad f_i^\dagger f_j^\dagger = -f_j^\dagger f_i^\dagger.$$

To obtain a faithful spin representation, it is necessary cancel this unwanted sign. Although a general procedure is hard to formulate, in one dimension this can be achieved by a non-linear transformation, viz.

$$\hat{S}_l^+ = f_l^\dagger e^{i\pi \sum_{j<l} \hat{n}_j}, \qquad \hat{S}_l^- = e^{-i\pi \sum_{j<l} \hat{n}_j} f_l, \qquad \hat{S}_l^z = f_l^\dagger f_l - \frac{1}{2}.$$

Operationally, this seemingly complicated transformation is straightforward: in one dimension, the particles can be ordered on the line. By counting the number of particles 'to the left' we can assign an overall phase of $+1$ or -1 to a given configuration and thereby transmute the particles into a fermions. (Put differently, the exchange to two fermions induces a sign change which is compensated by the factor arising from the phase — the 'Jordan-Wigner string'.)

(b) Using the Jordan-Wigner representation, show that

$$\hat{S}_m^+ \hat{S}_{m+1}^- = f_m^\dagger f_{m+1}.$$

(c) For the spin 1/2 anisotropic quantum Heisenberg spin chain, the spin Hamiltonian assumes the form

$$\hat{H} = -\sum_n \left[J_z \hat{S}^z_n \hat{S}^z_{n+1} + \frac{J_\perp}{2} \left(\hat{S}^+_n \hat{S}^-_{n+1} + \hat{S}^-_n \hat{S}^+_{n+1} \right) \right]$$

Turning to the Jordan-Wigner representation, show that the Hamiltonian can be cast in the form

$$\hat{H} = \sum_n \left[\frac{J_\perp}{2} \left(f^\dagger_n f_{n+1} + \text{h.c.} \right) + J_z \left(\frac{1}{4} - f^\dagger_n f_n + f^\dagger_n f_n f^\dagger_{n+1} f_{n+1} \right) \right]$$

(d) The mapping above shows that the one-dimensional quantum spin 1/2 XY-model (i.e. $J_z = 0$) can be diagonalised as a non-interacting theory of spinless fermions. In this case, show that the spectrum assumes the form

$$\epsilon(k) = -J_\perp \cos ka$$

3.4.2 Answers

A1 (a) Making use of the commutation relations for bosons, one finds

$$a^\dagger aa = a(a^\dagger a - 1), \qquad a^\dagger aa^\dagger = a^\dagger(1 + a^\dagger a)$$

from which the results follow. Using these results, one finds that, providing $a|\alpha\rangle \neq 0$,

$$\begin{aligned} a^\dagger a\ a|\alpha\rangle &= a(a^\dagger a - 1)|\alpha\rangle = (\alpha - 1)a|\alpha\rangle \\ a^\dagger a\ a^\dagger|\alpha\rangle &= a^\dagger(1 + a^\dagger a)|\alpha\rangle = (1 + \alpha)a^\dagger|\alpha\rangle \end{aligned}$$

(b) If $|\alpha\rangle$ is a normalised eigenstate of $a^\dagger a$ with eigenvalue α, the norm of state created by the action of the creation operator is given by

$$||a^\dagger|\alpha\rangle|| \equiv \sqrt{\langle\alpha|aa^\dagger|\alpha\rangle} = \sqrt{\langle\alpha|a^\dagger a + 1|\alpha\rangle} = \sqrt{n+1}.$$

Similarly, the norm of state created by the action of the annihilation operator is given by

$$||a|\alpha\rangle|| \equiv \sqrt{\langle\alpha|a^\dagger a|\alpha\rangle} = \sqrt{n}.$$

Therefore, if we define $|\alpha + 1\rangle$ and $|\alpha - 1\rangle$ as the normalised eigenstates of the operator $a^\dagger a$ with eigenvalue $\alpha + 1$ and $\alpha - 1$ respectively, one finds

$$\begin{aligned} a|\alpha\rangle &= \sqrt{n}|\alpha - 1\rangle \\ a^\dagger|\alpha\rangle &= \sqrt{n+1}|\alpha + 1\rangle \end{aligned}$$

Defining as the vacuum $|\Omega\rangle$ the normalised state that is anniliated by the operator a, an application of the result above shows the state $|n\rangle = (1/\sqrt{n!})(a^\dagger)^n|\Omega\rangle$ to be a normalised eigenstate of $a^\dagger a$ with eigenvalue n.

(c) If the operators obey anticommutation relations, one finds

$$a^\dagger aa = a(1 - a^\dagger a), \qquad a^\dagger aa^\dagger = a^\dagger(1 - a^\dagger a)$$

from which one obtains

$$[a^\dagger a, a]_+ = a, \qquad [a^\dagger a, a^\dagger]_+ = a^\dagger.$$

Using these results, one finds that, providing $a|\alpha\rangle \neq 0$ and $a^\dagger|\alpha\rangle \neq 0$,

$$\begin{aligned} a^\dagger a\ a|\alpha\rangle &= a(1 - a^\dagger a)|\alpha\rangle = (1 - \alpha)a|\alpha\rangle \\ a^\dagger a\ a^\dagger|\alpha\rangle &= a^\dagger(1 - a^\dagger a)|\alpha\rangle = (1 - \alpha)a^\dagger|\alpha\rangle \end{aligned}$$

If $|\alpha\rangle$ is a normalised eigenstate of $a^\dagger a$ with eigenvalue α, the norm of state created by the action of the creation operator is given by

$$||a^\dagger|\alpha\rangle|| \equiv \sqrt{\langle\alpha|aa^\dagger|\alpha\rangle} = \sqrt{\langle\alpha|1 - a^\dagger a|\alpha\rangle} = \sqrt{1-n}.$$

Similarly, the norm of state created by the action of the annihilation operator is given by

$$||a|\alpha\rangle|| \equiv \sqrt{\langle\alpha|a^\dagger a|\alpha\rangle} = \sqrt{n}.$$

Therefore, if we define $|\alpha+1\rangle$ and $|\alpha-1\rangle$ as the normalised eigenstates of the operator $a^\dagger a$ with eigenvalue $\alpha+1$ and $\alpha-1$ respectively, one finds

$$\begin{aligned} a|\alpha\rangle &= \sqrt{n}|\alpha-1\rangle \\ a^\dagger|\alpha\rangle &= \sqrt{1-n}|\alpha+1\rangle \end{aligned}$$

Now, using the fact that $(a^\dagger)^2 = 0$, it is clear that there are only two possible states: the (normalised) vacuum state $|\Omega\rangle$ which is anniliated by the operator a, and the state with a single particle $|1\rangle = a^\dagger|\Omega\rangle$.

A2 The kinetic energy operator is diagonal in the momentum basis. Following the analysis in the text, the corresponding second quantised one-body operator is given by

$$\hat{T} = \sum_p \frac{p^2}{2m} a_p^\dagger a_p.$$

Transforming to the coordinate representation, $a_p = L^{-1/2}\int_0^L dx e^{ipx} a(x)$, one obtains

$$\hat{T} = \frac{1}{L}\sum_p \frac{p^2}{2m}\int_0^L dy \int_0^L dx e^{ip(x-y)} a^\dagger(y)a(x).$$

Expressing factor p^2 as a derivative of the exponential factor, and integrating by parts, one obtains the required

A3 Since the two-body operator is diagonal in the basis $|\lambda\rangle$, the matrix elements of $\hat{\mathcal{O}}_2$ can be expressed in the form

$$\begin{aligned} \langle\lambda_1'\cdots\lambda_N'|\hat{\mathcal{O}}_2|\lambda_1\cdots\lambda_N\rangle &= \sum_{\mathcal{P}}(-\zeta)^{\mathcal{P}} c_{\rm norm} \sum_{i\neq j}\prod_{k\neq i,k\neq j}\langle\lambda_{\mathcal{P}_k}|\lambda_i\rangle\langle\lambda_{\mathcal{P}_i'}\lambda_{\mathcal{P}_j'}|\hat{\mathcal{O}}_2|\lambda_i\lambda_j\rangle \\ &= \left(\frac{1}{2}\sum_{i\neq j}^{N} o_{\lambda_i\lambda_j}\right)\langle\lambda_1'\cdots\lambda_N'|\lambda_1\cdots\lambda_N\rangle \end{aligned}$$

where, as in the text, $c_{\rm norm}$ represents the (unimportant) normalisation factor, and $\mathcal{P}$ represents the parity of the configuration. The factor $\sum_{i\neq j} o_{\lambda_i\lambda_j}/2$ represents the sum over all distinct pairs of particles present in the state $|\lambda_1\cdots\lambda_N\rangle$. We therefore need to construct and operator $\hat{P}_{\lambda_i\lambda_j}$ which counts the number of pairs of particles in the states $|\lambda_i\rangle$ and $|\lambda_j\rangle$. If $|\lambda_i\rangle \neq |\lambda_j\rangle$ (i.e. they represent different states), the number of pairs is $n_i n_j$, otherwise the number of pairs is $n_i(n_i-1)$. Hence, the corresponding operator may be written as

$$\hat{P}_{\lambda\lambda'} = \hat{n}_\lambda\hat{n}_{\lambda'} - \delta_{\lambda,\lambda'}\hat{n}_\lambda \equiv a_\lambda^\dagger a_{\lambda'}^\dagger a_{\lambda'} a_\lambda.$$

We therefore have that

$$\langle \lambda_1' \cdots \lambda_N' | \hat{\mathcal{O}}_2 | \lambda_1 \cdots \lambda_N \rangle = \langle \lambda_1' \cdots \lambda_N' | \frac{1}{2} \sum_{i \neq j}^{N} o_{\lambda_i \lambda_j} \hat{P}_{\lambda_i \lambda_j} | \lambda_1 \cdots \lambda_N \rangle,$$

and hence

$$\hat{\mathcal{O}}_2 = \frac{1}{2} \sum_{\lambda \lambda'} \langle \lambda \lambda' | \mathcal{O}_2 | \lambda \lambda' \rangle a_\lambda^\dagger a_{\lambda'}^\dagger a_{\lambda'} a_\lambda.$$

Transforming to an arbitrary basis, we obtain

$$\hat{\mathcal{O}}_2 = \frac{1}{2} \sum_{\lambda \mu \nu \rho} \langle \lambda \mu | \mathcal{O}_2 | \nu \rho \rangle a_\lambda^\dagger a_\mu^\dagger a_\nu a_\rho.$$

A4 A Hamiltonian which is translationally invariant is easily diagonalised in the Fourier representation. Setting $c_{\mathbf{m}\sigma}^\dagger = (1/N^{d/2}) \sum_{\mathbf{k}} e^{i\mathbf{k}\cdot\mathbf{m}} c_{\mathbf{k}\sigma}^\dagger$, the Hamiltonian takes the form

$$\hat{H}^{(0)} = \sum_{\mathbf{k}}^{\text{B.Z.}} \sum_{\sigma} \epsilon_{\mathbf{k}} c_{\mathbf{k}\sigma}^\dagger c_{\mathbf{k}\sigma},$$

where $\epsilon_{\mathbf{k}} = -t \sum_{i=x,y,z} e^{i\mathbf{k}\cdot\hat{\mathbf{e}}_i}$, with the sum running over neighbouring lattice vectors $\hat{\mathbf{e}}_i$, and the lattice spacing is taken to be unity.

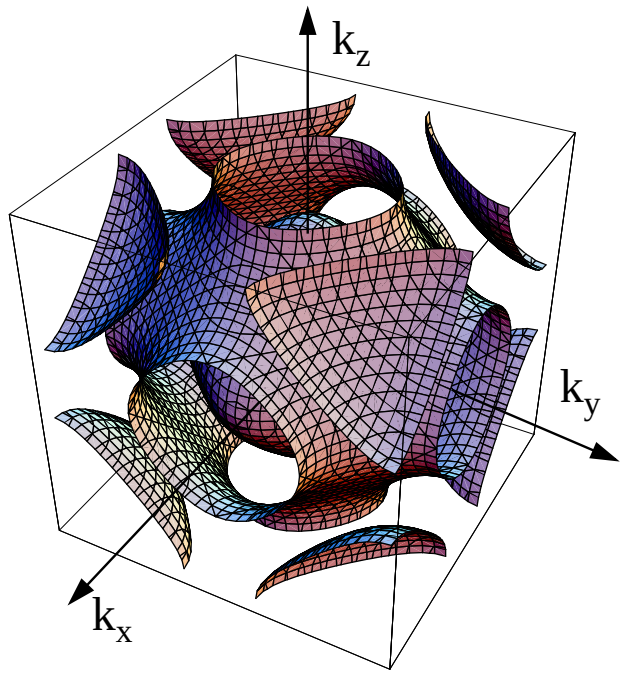

Figure 3.17: Contours of constant energy shown for the spectrum of the three-dimensional cubic lattice.

A5 Applying the fermionic representation of spin 1/2, $\hat{\mathbf{S}} = c^\dagger_\alpha \boldsymbol{\sigma}_{\alpha\beta} c_\beta/2$, and making use of the identity given in the question, we have

$$\hat{\mathbf{S}}_i \cdot \hat{\mathbf{S}}_j = \frac{1}{4} c^\dagger_{i\alpha} c_{i\beta} c^\dagger_{j\gamma} c_{j\delta} \boldsymbol{\sigma}_{\alpha\beta} \cdot \boldsymbol{\sigma}_{\gamma\delta} = \frac{1}{4}\left(2 c^\dagger_{i\alpha} c_{i\beta} c^\dagger_{j\beta} c_{j\alpha} - n_i n_j\right).$$

Rearranging this expression (and noting that $i \neq j$) we obtain the required identity.

A6 (a) In the two-site model at half-filling (i.e. one electron per site), the Hubbard interaction $\hat{H}_U$ has six eigenstates. Of these, the two spin polarised states $c^\dagger_{2\downarrow} c^\dagger_{1\downarrow}|0\rangle$ and $c^\dagger_{2\uparrow} c^\dagger_{1\uparrow}|0\rangle$ are eigenstates of the full Hamiltonian $\hat{H}$ each with eigenvalue $-V$. The remain four eigenstates

$$\begin{aligned} |s_1\rangle &= c^\dagger_{1\uparrow} c^\dagger_{2\downarrow}|0\rangle, \quad |s_2\rangle = c^\dagger_{2\uparrow} c^\dagger_{1\downarrow}|0\rangle, \\ |d_1\rangle &= c^\dagger_{1\uparrow} c^\dagger_{1\downarrow}|0\rangle, \quad |d_2\rangle = c^\dagger_{2\uparrow} c^\dagger_{2\downarrow}|0\rangle, \end{aligned}$$

serve as a convenient basis.

(b) Within this basis, matrix elements of the Hamiltonian $\hat{H}$ take the symmetric form

$$\hat{H} = \begin{pmatrix} 0 & V & -t & -t \\ V & 0 & -t & -t \\ -t & -t & U & 0 \\ -t & -t & 0 & U \end{pmatrix}.$$

This suggests applying the unitary transformation

$$\begin{pmatrix} U & 0 \\ 0 & U \end{pmatrix} \hat{H} \begin{pmatrix} U^\dagger & 0 \\ 0 & U^\dagger \end{pmatrix} = \begin{pmatrix} V & 0 & -2t & 0 \\ 0 & -V & 0 & 0 \\ -2t & 0 & U & 0 \\ 0 & 0 & 0 & U \end{pmatrix}, \quad U = \frac{1}{\sqrt{2}} \begin{pmatrix} 1 & 1 \\ 1 & -1 \end{pmatrix},$$

wherein we find that $|s_1\rangle - |s_2\rangle$ and $|d_1\rangle - |d_2\rangle$ are eigenstates with eigenvalues of $-V$ and U respectively. The former can be identified as the spin $S_z = 0$ triplet state accompanying the two spin polarised states. The remaining basis states $|s_1\rangle + |s_2\rangle$ and $|d_1\rangle + |d_2\rangle$ are mixed by the matrix elements of the Hamiltonian. Diagonalising the 2×2 matrix, the eigenvectors and eigenvalues take the form

$$\frac{1}{2}\left[V + U \pm \frac{(V-U)}{\cos\theta}\right], \qquad \begin{pmatrix} \cos\theta & \sin\theta \\ \sin\theta & -\cos\theta \end{pmatrix} \begin{pmatrix} |s_1\rangle + |s_2\rangle \\ |d_1\rangle + |d_2\rangle \end{pmatrix},$$

where $2\theta = -\tan^{-1}[4t/(U-V)]$.

(c) Taking $U \gg [V, t]$ and expanding, the lowest energy states of this pair is seen to be predominantly singlet, $|s_1\rangle + |s_2\rangle$, with eigenvalue $V - J$, where $J = 4t^2/U$. This state remains the overall ground state for $V < 2J$ while for $V > 2J$ the ferromagnetic exchange interaction wins and the degenerate triplet states become ground states with energy $-V$ (see fig. 3.18).

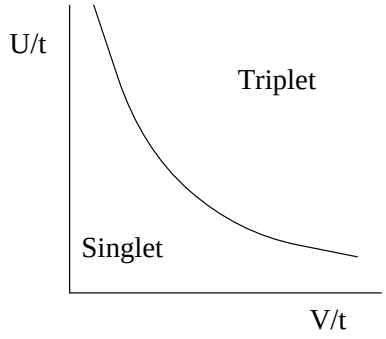

Figure 3.18: Qualitative phase diagram showing the crossover from the singlet to the triplet ground state. The latter can be regarded as the Hund's rule dominated phase while the former represents the '*spin liquid*' or low spin phase.

A7 (a) In the subspace $S_z = 3/2$, there exists a total of four basis states — after specifying the position of the hole, the positions of the up-spins are determined. Under the action of the infinite U Hubbard Hamiltonian, $\hat{H} = -t \sum_{\langle ij \rangle} \hat{P}_s c^\dagger_{i\sigma} c_{i\sigma} \hat{P}_s$, where $\hat{P}_s$ projects out states of double occupancy,[19] the vacancy moves around the plaquette permuting the spins. The corresponding tight-binding Hamiltonian is

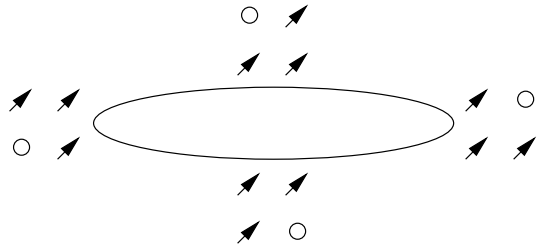

isomorphic to that of a single particle on a four site lattice with periodic boundary conditions. The corresponding spectrum is given by $\epsilon_n = -2t\cos(2n\pi/4)$, $n = 1, \cdots 4$, and all states including the ground state is, by construction, ferromagnetic.

(b) In the subspace $S_z = 1/2$, there exist a total of 12 basis states — after specifying one of a possible 4 positions of the hole, there are total of 3 sites at which one can place a down spin, while the remaining sites must host the up spin. Repeated application of the Hamiltonian to a given basis state traces out the entire subspace — the vacancy must traverse the plaquette 3 times before recovering the original spin configuration (a circuit known as a **Trugman cycle**). The corresponding Hamiltonian is isomorphic to that of a single particle on a twelve site lattice with periodic boundary conditions. The corresponding spectrum is given by $\epsilon_n = -2t\cos(2n\pi/12)$, $n = 1, \cdots 12$. In particular, the ground state involves a uniform superposition of all twelve basis states and is, therefore, a state of maximal spin in accord with Nagaoka's theorem. (In fact, we could have generated the ground state by operating the total spin lowering operator on the ground state from part (a).)

[19] Note that in part (a) the projection operator is made superfluous by the Pauli exclusion principle.

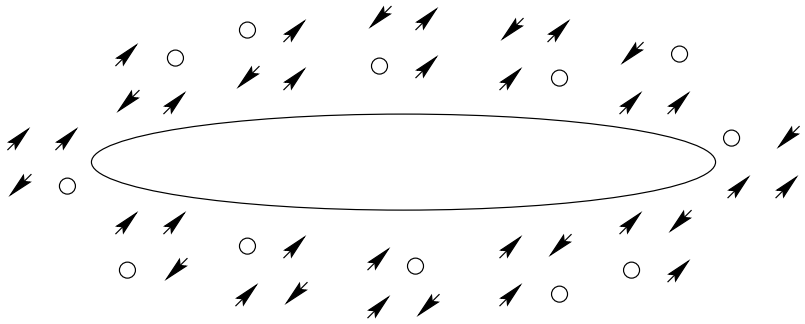

A8 Substituting the definition of the spin raising and lowering operators using the Holstein-Primakoff transformation, the commutator is obtained as

$$\begin{aligned}\frac{1}{2S}[\hat{S}^+,\hat{S}^-] &= \left(1-\frac{a^\dagger a}{2S}\right)^{1/2} aa^\dagger \left(1-\frac{a^\dagger a}{2S}\right)^{1/2} - a^\dagger\left(1-\frac{a^\dagger a}{2S}\right)a \\ &= \left(1-\frac{a^\dagger a}{2S}\right) + a^\dagger a\left(1-\frac{a^\dagger a}{2S}\right) - a^\dagger a + \frac{a^\dagger a^\dagger aa}{2S} \\ &= 1-\frac{a^\dagger a}{S}.\end{aligned}$$

With $S^z = S - a^\dagger a$, we obtain the required commutation relation $[\hat{S}^+,\hat{S}^-] = 2S^z$.

A9 By symmetry, the maximal exchange energy that can be recovered is obtained when the spins are maximally anti-aligned, i.e. at 120^o to each other. Using the spin orientation of a single triangle, the two-dimensional triangular lattice can be tessilated with all spins aligned at 120^o to the neighbours.

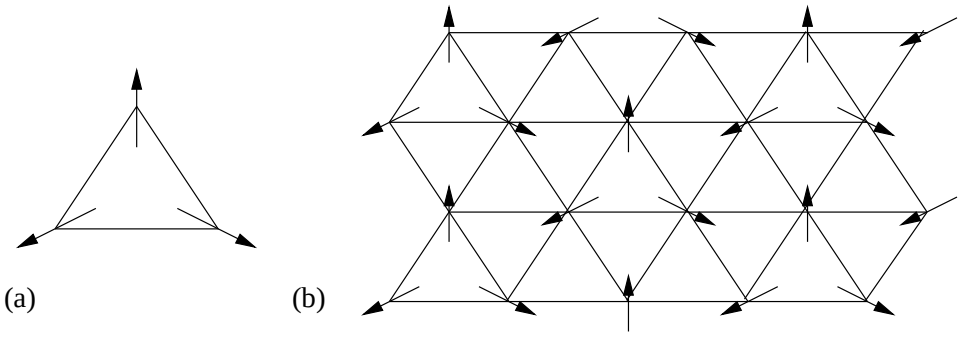

A10 To confirm the validity of the Bogoluibov transformation let us consider the commutation relations of α:

$$\begin{aligned}\left[\alpha,\alpha^\dagger\right] &= \left[\cosh\theta\ a + \sinh\theta\ a^\dagger, \cosh\theta\ a^\dagger + \sinh\theta\ a\right] \\ &= \cosh^2\theta\left[a,a^\dagger\right] + \sinh^2\theta\left[a^\dagger,a\right] \\ &= \cosh^2\theta - \sinh^2\theta = 1.\end{aligned}$$

as required.

A11 (a) Making use of the equation of motion $i\hbar\dot{\hat{\mathbf{S}}}_i = [\hat{\mathbf{S}}_i, \hat{H}]$, and the commutation relation $[S_i^\alpha, S_j^\beta] = i\delta_{ij}\epsilon^{\alpha\beta\gamma}S_i^\gamma$, we obtain

$$i\hbar\dot{\hat{\mathbf{S}}}_i = 2Ji\hat{\mathbf{S}}_i \times \left(\hat{\mathbf{S}}_{i+1} + \hat{\mathbf{S}}_{i-1}\right)$$

(b) Interpreting the spins as classical vectors, and applying the Taylor expansion $\mathbf{S}_{i+1} \mapsto \mathbf{S}(x+a) = \mathbf{S} + a\partial\mathbf{S} + (a^2/2)\partial^2\mathbf{S} + \cdots$, we obtain the classical equation of motion

$$\hbar\dot{\mathbf{S}} = 2Ja^2\mathbf{S} \times \partial^2\mathbf{S}.$$

Substituting, we find that

$$\mathbf{S} = \left(c\cos(kx - \omega t), c\sin(kx - \omega t), \sqrt{S^2 - c^2}\right),$$

satisfies the equation of motion with $\hbar\omega = 2J(ka)^2$.

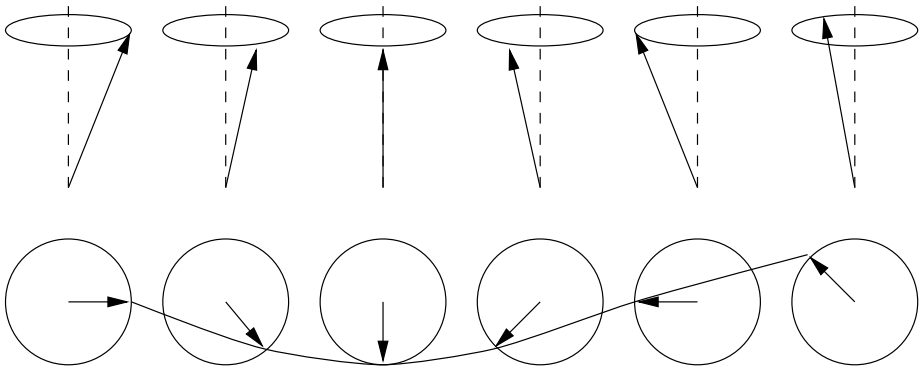

Figure 3.19: Spin-wave dispersion.

(c) The corresponding spin wave solution has the form shown in fig 3.19.

A12 Defining the total spin on a triad $\hat{\mathbf{J}}_n = \hat{\mathbf{S}}_{n-1} + \hat{\mathbf{S}}_n + \hat{\mathbf{S}}_{n+1}$, the Hamiltonian can be recast in the form

$$\hat{H}_{\rm MG} = |J| \sum_{n=1}^{N} \hat{\mathcal{P}}_{3/2}(n-1, 1, n+1),$$

where $\hat{\mathcal{P}}_{3/2}(n-1, n, n+1) = (\hat{\mathbf{J}}_n^2 - 3/4)/3$ annihilates any state with total spin $J = 1/2$ of the triad. Since in any three sites, two of the spins are in a singlet, there can be no components of $J = 3/2$ on any triad. Therefore the dimer states are eigenstates of zero energy. Now since $\hat{\mathcal{P}}_{3/2}$ is positive definite, these states must be the ground states.

A13 (a) Since each unit cell is of twice the dimension of the original lattice, we begin by recasting the Hamiltonian in the sublattice form

$$\hat{H} = -t \sum_{m=1,\sigma}^{N/2} \left\{(1+\alpha)\left[c_{m\sigma}^\dagger b_{m\sigma} + \text{h.c.}\right] + (1-\alpha)\left[b_{m\sigma}^\dagger a_{m+1\sigma} + \text{h.c.}\right]\right\} + \frac{Nk_s\alpha^2}{2}.$$

Switching to the Fourier basis, $a_m = \sqrt{2/N}\sum_k e^{2ikm}a_k$ (similarly b_m), where k takes $N/2$ values uniformly on the interval $[-\pi/2, \pi/2]$, the Hamiltonian takes the form

$$\hat{H} = \frac{Nka^2}{2}\alpha^2 \\ -t\sum_k \begin{pmatrix} a^\dagger_{k\sigma} & b^\dagger_{k\sigma} \end{pmatrix} \begin{pmatrix} 0 & (1+\alpha)+(1-\alpha)e^{2ik} \\ (1+\alpha)+(1-\alpha)e^{-2ik} & 0 \end{pmatrix} \begin{pmatrix} a_{k\sigma} \\ b_{k\sigma} \end{pmatrix}.$$

Diagonalising the 2×2 Hamiltonian, we obtain the spectrum

$$\epsilon(k) = \pm 2t\left[\cos^2 k + \alpha^2 \sin^2 k\right]^{1/2}.$$

Reassuringly, in the limit $\alpha \to 0$, we obtain the cos spectrum of the undistorted problem, while in the limit $\alpha \to 1$, pairs of monomers become decoupled and we obtain a massively degenerate bonding and antibonding spectrum.

(b) According to the formula given in the text, the total shift in energy is given by

$$\delta\epsilon = -4t(a_1 - b_1 \ln\alpha^2)\alpha^2 + \frac{Nk_s\alpha^2}{2}$$

Maximising the energy gain with respect to α, one finds that the stable configuration is found when

$$\alpha^2 = \exp\left[\frac{a_1}{b_1} - 1 - \frac{Nk_s\alpha^2}{8tb_1}\right]$$

(c) If the number of sites is odd, the Peirels distortion is inevitably frustrated — a configuration that starts ABABAB must finish as BABABA. The result is that the polymer chain must accommodate a **topological excitation**. The excitation is said to be topological because the defect can not be removed by a smooth continuous deformation — it is like a dislocation line in a crystal. It's effect on the spectrum of the model is to introduce a state that lies within the band gap of the material.

The consideration of an odd number of sites forces a topological defect into the system. However, even if the number of sites is even, one can create low energy topological excitations of the system either by doping (see fig. 3.16c), or by the creation of **excitons**, particle-hole excitations of the system. Indeed, such topological excitations can dominate the transport properties of the system.

As a footnote, one should add that the particular model considered above is somewhat over-simplified. It seems likely that Coulomb interactions play a dominant role in driving the Peirels instability in Polyacetylene. However, the qualitative interpretation of the existence of topological excitations is born out by experiment.

A14 (a) Using the commutation relation for bosons, one finds.

$$\begin{aligned} [\hat{S}^+, \hat{S}^-] &= a^\dagger b\, b^\dagger a - b^\dagger a\, a^\dagger b \\ &= a^\dagger a b b^\dagger - a a^\dagger b^\dagger b \\ &= a^\dagger a(b^\dagger b + 1) - (a^\dagger a + 1)b^\dagger b \\ &= a^\dagger a - b^\dagger b = 2\hat{S}^z \end{aligned}$$

(b) Using the identities for boson operators:

$$a|n\rangle = \sqrt{n}|n-1\rangle, \qquad a^\dagger|n\rangle = \sqrt{n+1}|n+1\rangle$$

where $|n\rangle = (1/\sqrt{n})(a^\dagger)^n|\Omega\rangle$, one finds

$$\begin{aligned}
\hat{S}^+|S,m\rangle &= a^\dagger b|n_a = S+m, n_b = S-m\rangle \\
&= \sqrt{S+m+1}\sqrt{S-m}|n_a = S+m+1, n_b = S-m-1\rangle \\
&= \sqrt{S+m+1}\sqrt{S-m}|S,m+1\rangle, \\
\hat{S}^-|S,m\rangle &= b^\dagger a|n_a = S+m, n_b = S-m\rangle \\
&= \sqrt{S+m}\sqrt{S-m+1}|n_a = S+m-1, n_b = S-m+1\rangle \\
&= \sqrt{S+m}\sqrt{S-m+1}|S,m-1\rangle.
\end{aligned}$$

Using these results one finds

$$\begin{aligned}
\hat{S}^+\hat{S}^-|S,m\rangle &= \sqrt{S+m}\sqrt{S-m+1}\ \hat{S}^+|S,m-1\rangle \\
&= (S+m)(S-m+1)|S,m\rangle \\
\hat{S}^-\hat{S}^+|S,m\rangle &= \sqrt{S+m+1}\sqrt{S-m}\ \hat{S}^-|S,m+1\rangle \\
&= (S+m+1)(S-m)|S,m\rangle.
\end{aligned}$$

Similarly, one finds

$$\begin{aligned}
\hat{S}^z|S,m\rangle &= \frac{1}{2}(n_a - n_b)|n_a = S+m, n_b = S-m\rangle \\
&= \frac{1}{2}\left[(S+m)-(S-m)\right]|S,m\rangle = m|S,m\rangle,
\end{aligned}$$

showing $|S,m\rangle$ to be an eigenstate of the operator $\hat{S}^z$ with eigenvalue m. Finally, using the identity

$$\hat{\mathbf{S}}^2 = \left(\hat{S}^z\right)^2 + \frac{1}{2}\left(\hat{S}^+\hat{S}^- + \hat{S}^-\hat{S}^+\right)$$

one obtains

$$\begin{aligned}
\hat{\mathbf{S}}^2|S,m\rangle &= \left[m^2 + \frac{1}{2}\left((S+m)(S-m+1) + (S+m+1)(S-m)\right)\right]|S,m\rangle \\
&= S(S+1)|S,m\rangle
\end{aligned}$$

as required. As with the Holstein-Primakoff representation, the Schwinger boson represents yet another representation of quantum mechanical spin. Which representation is most convenient for the analysis of quantum spin models depends sensitively on the nature of the microscopic Hamiltonian.

A15 (a) Using the fermionic anticommutation relations, one finds

$$\begin{aligned}
[\hat{S}^+, \hat{S}^-]_- &= [f^\dagger, f]_- = f^\dagger f - f f^\dagger \\
&= 2f^\dagger f - 1 = 2\hat{S}^z.
\end{aligned}$$

(b) Using the fact that the number operators on different sites commute, one finds

$$\hat{S}_m^+ \hat{S}_{m+1}^- = f_m^\dagger e^{i\pi \sum_{j<m} n_j} e^{-i\pi \sum_{l<m+1} n_l} f_{m+1} = f_m^\dagger e^{-i\pi n_m} f_{m+1} = f_m^\dagger f_{m+1}$$

where here we have made use of the fact that, for fermionic particles

$$f_m^\dagger e^{-i\pi n_m} \equiv f_m^\dagger.$$

(c) The fermion representation is simply obtained by substitution.

(d) With $J_z = 0$, the spin Hamiltonian assumes the form of a non-interacting tight-binding Hamiltonian

$$\hat{H} = \frac{J_\perp}{2} \sum_n \left(f_n^\dagger f_{n+1} + \text{h.c.} \right).$$

This Hamiltonian, which has been encountered previously, is diagonalised in the Fourier space after which one obtains the cosine band dispersion.

Chapter 4

Feynman Path Integral

The goal of this chapter is to introduce and apply the Feynman path integral. Particular emphasis is placed on establishing the interconnections between the quantum mechanical path integral, classical Hamiltonian mechanics and classical statistical mechanics. Three extended examples are discussed in the text: the Feynman path integral of a quantum particle in a single well, tunneling in a double well, and quantum mechanical spin. These examples form the basis for several applications to different areas of physics in the problem sets including random walks and the equilibrium statistical mechanics of polymer chains, dissipation in macroscopic quantum tunnelling, and the path integral approach in finance!

In this chapter we will temporarily leave behind many-body physics and second quantisation and, at least superficially, return to ordinary single-particle quantum mechanics. However, by establishing the path integral approach for ordinary quantum mechanics, we will also set the stage for the introduction of functional field integral methods for many-body theory explored in the next chapter. We will in fact see that the path integral not only represents a gateway to higher dimensional functional integral methods but, when looked at from an appropriate point of view, already represents a field theoretical approach in its own right. Exploiting this connection, various techniques and concepts of field theory, viz. stationary phase analyses of functional integrals, the Euclidean formulation of field theory, instanton techniques and the role of topological concepts in field theory, will be motivated and introduced in this chapter

4.1 The Path Integral – General Formalism

Broadly speaking, there are two basic approaches to the formulation of quantum mechanics: the 'operator approach' based on the canonical quantisation of physical observables together with the associated operator algebra, and the Feynman path integral.[1] Whereas

[1] For a general introduction to the Feynman path integral, one can refer to one of the many standard texts including Refs.[?, ?, ?, ?] or, indeed, turn to the original paper, R. P. Feynman, Rev. Mod. Phys. **20**, 367 (1948).

canonical quantisation is usually taught first in elementary courses on quantum mechanics, path integrals seem to have acquired the reputation of being a sophisticated concept that is better reserved for advanced courses. Yet this treatment seems hardly justified! In fact, the path integral formulation has many advantages most of which explicitly support an intuitive understanding of quantum mechanics. Moreover, integrals — even the infinite dimensional ones encountered below — are hardly any more abstract than infinite dimensional linear operators. Further merits of the path integral include:

- ▷ Whereas the classical limit is not always easy to retrieve within the canonical formulation of quantum mechanics, it constantly remains visible in the path integral approach. In other words, the path integral makes explicit use of classical mechanics as a basic 'platform' on which to construct a theory of quantum fluctuations. The classical solutions of Hamilton's equation of motion always remain a central ingredient of the formalism. (For this reason, path integration has turned out to be an indispensable tool in fields such as **quantum chaos** where the quantum manifestations of classically non-trivial behaviour are investigated.)

- ▷ Path integrals allow for an efficient formulation of *non-perturbative* approaches to the solution of quantum mechanical problems. For example, the 'instanton' formulation of quantum tunnelling discussed below — whose extension to continuum theories has led to some of the most powerful concepts of quantum field theory — makes extensive use of the classical equations of motion when it is tailored to a path integral formulation.

- ▷ The Feynman path integral represents a prototype of the higher dimensional functional field integrals to be introduced in the next chapter. However,

- ▷ even in its non-continuum, 'zero-dimensional' form discussed in this chapter, the path integral is of relevance to various applications in many body physics. The reason is that in a number of applications, including superconductivity and -fluidity, the modern field of few-electron electronics, and others, a macroscopically large number of degrees of freedom 'locks' to form a single collective variable. (E.g. to a first approximation the phase information carried by the order parameter field in moderatly large superconducting grains can often be described in terms of a *single* phase degree of freedom, i.e. a 'quantum particle' living on the complex unit circle.) Path integral techniques have proven ideally suited to the analysis of such systems.

But what then is the basic idea of this approach? More then any other formulation of quantum mechanics, the path integral formalism is based on connections to classical

Richard P. Feynman 1918-1988, 1965 Nobel Laureate in Physics (with Sin-Itiro Tomonaga, and Julian Schwinger) for fundamental work in quantum electrodynamics, with deep-ploughing consequences for the physics of elementary particles.

mechanics. The variational approach of employed in chapter ?? relied on the fact that classically allowed trajectories in configuration space extermize an action functional. A principal constraint to be imposed on any such trajectory is energy conservation. Now, we know that quantum particles, have a little bit more freedom than their classical counterparts. E.g. energy conservation can be violated by an amount ΔE over time scales $\sim \hbar/\Delta E$ ($\hbar$ re-installed throughout this chapter.) The connection to action principles of classical mechanics becomes particularly apparent in problems of quantum tunneling: A particle of energy E may tunnel through a potential barrier of height $V > E$. However, this process is penalized by a damping factor $\sim \exp\left(-i\hbar^{-1}\int_{\text{barrier}} dxp\right)$, where $p = \sqrt{2m(E-V)}$, i.e. the exponent of the (imaginary) action associated to the classically forbidden path.

These observations motivate the idea of a new formulation of quantum propagation: Could it be that, as in classical mechanics, the quantum amplitude A for propagation between any two points in coordinate space is again controlled by the action functional? However, in a relaxed sense where not just a single extremal path $x_{\text{cl}}(t)$ but an entire manifold of neighbouring paths contribute. More specifically, one might speculate that the amplitude obtains as $A \sim \sum_{x(t)} \exp(-i\hbar^{-1}S[x])$, where $\sum_{x(t)}$ symbolically stands for a summation over all paths compatible with the initial conditions of the problem and S is the *classical* action. Although at this stage we know nothing about possibilities to formally justify this ansatz, some features of quantum mechanics would obviously be born out correctly: In the classical limit, $\hbar \to 0$ the set of paths $x(t)$ effectively contributing to the sum would collapse to the extremal, or classical path $x_{\text{cl}}(t)$. This is because any non-extremal configurations would be weighed by rapidly oscillatory phases $\sim -iS/\hbar$ and, therefore, average to zero[2]. Second, quantum tunneling would be a natural element of the theory. I.e. non-classical paths do contribute to the net-amplitude, however at the cost of a damping factor specified by the imaginary action, as in the traditional formulation.

Fortunately, no fundamentally novel 'picture' of quantum mechanics needs to be declared to promote the idea of a path 'integral' $\sum_{x(t)} \exp(-i\hbar^{-1}S[x])$ to a working theory. As we will see in the next section, the new formulation can quantitatively be developed from the save ground of canonical quantization.

4.2 Construction of the Path Integral

All information about any autonomous[3] quantum mechanical system is contained in the matrix elements of its time evolution operator. A formal integration of the time-dependent Schrödinger equation

$$i\hbar\partial_t|\Psi\rangle = \hat{H}|\Psi\rangle \tag{4.1}$$

[2] More precisely, in the limit of small $\hbar$, the path sum can be evaluated by saddle point methods, as detailed in section XX below.

[3] A system is called **autonomous** if its Hamiltonian does not explicitly depend on time. Actually the construction of the path integral can be straightforwardly extended so as to include time-dependent problems. However, in order to keep the introductory discussion as simple as possible, here we assume time-independence.

obtains the time evolution operator

$$|\Psi(t')\rangle = \hat{U}(t',t)|\Psi(t)\rangle, \qquad \hat{U}(t',t) = e^{-\frac{i}{\hbar}\hat{H}(t'-t)}\Theta(t'-t) \tag{4.2}$$

The action of the operator $\hat{U}(t'-t)$ describes dynamical evolution under the influence of the Hamiltonian from a time t to time t'. Causality implies that $t' > t$ as indicated by the step or Heaviside Θ-function. In the real space representation we can write

$$\Psi(q',t') = \langle q'|\Psi(t')\rangle = \langle q'|\hat{U}(t',t)\Psi(t)\rangle = \int dq\; U(q',t';q,t)\Psi(q,t),$$

where

$$U(q',t';q,t) = \langle q'|e^{-\frac{i}{\hbar}\hat{H}(t'-t)}|q\rangle\Theta(t'-t)$$

defines the (q',q) component of the time evolution operator. As the matrix element expresses the probability amplitude for a particle to propagate between points q and q' in a time $t'-t$, it is sometimes known as the **propagator** of the theory.

The basic idea behind Feynman's path integral approach is easy to formulate. Rather than attacking the Schrödinger equation governing the time evolution for general times t, one may first attempt to solve the much simpler problem of describing the time evolution for infinitesimally small times Δt. In order to formulate this idea quantitatively we first 'divide' the time evolution operator into $N \gg 1$ discrete 'time steps',

$$e^{-i\hat{H}t/\hbar} = \left[e^{-i\hat{H}\Delta t/\hbar}\right]^N, \tag{4.3}$$

where $\Delta t = t/N$. Albeit nothing more than a formal rewriting of E.q. (4.2), the representation (4.3) has the advantage that the exponents of each of the factors $e^{-i\hat{H}\Delta t/\hbar}$ are small. (More precisely, if Δt is much smaller than the (reciprocal of the) eigenvalues of the Hamiltonian in the regime of physical interest, the exponents are small in comparison with unity and can be treated perturbatively.) A first simplification arising from this fact is that the exponentials can be factorised into two pieces each of which can be readily diagonalised. To achieve this factorisation, we make use of the identity

$$\boxed{e^{\hat{A}+\hat{B}} = e^{\hat{A}}e^{\hat{B}}e^{-\frac{1}{2}[\hat{A},\hat{B}]}} \tag{4.4}$$

valid in the case where the commutator $[\hat{A},\hat{B}]$ commutes with the operators $\hat{A}$ and $\hat{B}$.

▷ INFO. Eq. (4.4) is a particular case of a so-called **Baker-Campbell-Hausdorff (BCH) formula**. BCH formulae play an important role in the theory of Lie-groups and thereby in various areas of physics. Here we do not give a proof of Eq. (4.4) since, for the purpose of constructing the path integral, it suffices to check (4.4) perturbatively, i.e. to assume that $\hat{A}$ and $\hat{B}$ are in some sense small and to show that the identity holds to leading order in an expansion in these operators.

———————————————————————

Applying Eq. (4.4) to the Hamiltonian we obtain

$$e^{-i\hat{H}\Delta t/\hbar} = e^{-i\hat{T}\Delta t/\hbar}e^{-i\hat{V}\Delta t/\hbar} + O(\Delta t^2),$$

where the Hamiltonian $\hat{H} = \hat{T} + \hat{V}$ is the sum of a kinetic energy $\hat{T} = \hat{p}^2/2m$, and some potential energy operator $\hat{V}$.[4] (The following analysis, restricted for simplicity to a one-dimensional Hamiltonian, is easily generalised to arbitrary spatial dimensional.) The key advantage of this factorisation is that the eigenstates of each of the factors $e^{-i\hat{T}\Delta t/\hbar}$ and $e^{-i\hat{V}\Delta t/\hbar}$ are known independently. To exploit this fact we consider the time evolution operator factorised as a product,

$$\begin{aligned}\left\langle q_F \left| \left[e^{-i\hat{H}\Delta t/\hbar}\right]^N \right| q_I \right\rangle \\ \simeq \left\langle q_F \left| \wedge e^{-i\hat{T}\Delta t/\hbar}e^{-i\hat{V}\Delta t/\hbar} \wedge e^{-i\hat{T}\Delta t/\hbar}e^{-i\hat{V}\Delta t/\hbar} \wedge \cdots \wedge e^{-i\hat{T}\Delta t/\hbar}e^{-i\hat{V}\Delta t/\hbar} \right| q_I \right\rangle\end{aligned} \tag{4.5}$$

and insert at each of the positions indicated by a $\wedge$ the resolution of identity

$$\text{id.} = \int dq_n \int dp_n |q_n\rangle\langle q_n|p_n\rangle\langle p_n|, \tag{4.6}$$

where $|q_n\rangle$ and $|p_n\rangle$ represent a complete set of position and momentum eigenstates respectively, and $n = 1, \ldots, N$ serves as an index keeping track of the time steps at which the unit operator is inserted. The rational behind the particular choice (4.6) is clear. The unit operator is arranged in such a way that both $\hat{T}$ and $\hat{V}$ act on the corresponding eigenstates. Inserting (4.6) into (4.5), and using that

$$\langle q|p\rangle = \langle p|q\rangle^* = \frac{1}{2\pi\hbar}e^{iqp/\hbar},$$

we obtain

$$\begin{aligned}\left\langle q_F \left| e^{-i\hat{H}t/\hbar} \right| q_I \right\rangle \\ = \int_{q_N=q_F, q_0=q_I} \prod_{n=1}^{N-1} dq_n \prod_{n=1}^{N} \frac{dp_n}{2\pi\hbar} e^{-i\frac{\Delta t}{\hbar}\sum_{n=0}^{N-1}\left(V(q_n)+T(p_{n+1})-p_{n+1}\frac{q_{n+1}-q_n}{\Delta t}\right)}.\end{aligned} \tag{4.7}$$

Thus, the matrix element of the time evolution operator has been expressed as a $2N-1$ dimensional integral over eigenvalues. Up to corrections of higher order in $V\Delta t/\hbar$ and $T\Delta t/\hbar$, the expression (4.7) is exact. At each 'time step' $t_n = n\Delta t$, $n = 1, \ldots, N$ we are integrating over a pair of coordinates $\mathbf{x}_n \equiv (q_n, p_n)$ parametrising the **classical phase space**. Taken together, the points $\{\mathbf{x}_n\}$ form a N-point discretization of a path in this space (see Fig. 4.1).

[4] Although the Ansatz (4.2) already covers a wide class of quantum mechanical problems, many applications of practical importance (e.g. Hamiltonians involving spin or magnetic fields, etc.) do not fit into this framework. For a general exposition covering all its applications we refer to the literature e.g. to Schulman's book [**?**].

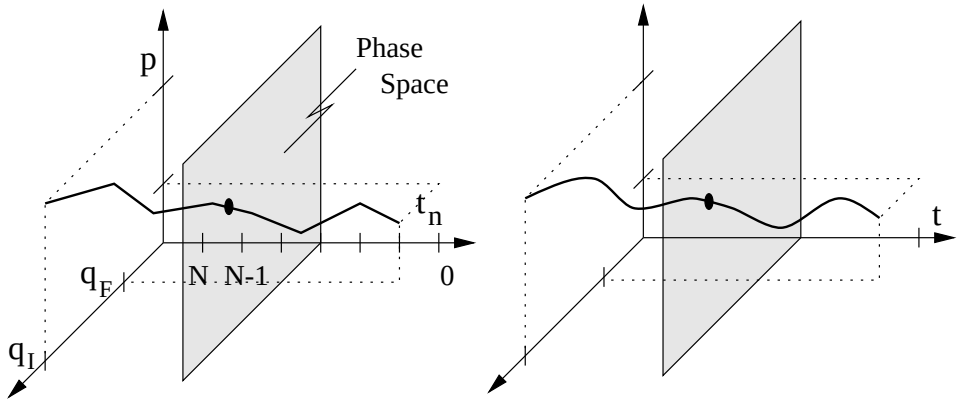

Figure 4.1: Left: visualisation of a set of phase space points contributing to the discrete time configuration integral (4.7). Right: in the continuum limit, the set of points becomes a smooth curve.

To make further progress, we need to develop some intuition for the behaviour of the integral (4.7). We first notice that rapid fluctuations of the integration arguments $\mathbf{x}_n$ as a function of the index n are strongly inhibited by the structure of the integrand. When taken together, contributions for which $(q_{n+1}-q_n)p_{n+1} > O(\hbar)$ (i.e. when the phase of the exponential exceeds 2π) tend to lead to a 'random phase cancellation'. In the language of wave mechanics, the 'incoherent' superposition of different Feynman paths destructively interferes. The *smooth* variation of the paths which contribute significantly motivate the application of a continuum limit analogous to that employed in chapter 1.

To be specific, sending $N \to \infty$ whilst keeping $t = N\Delta t$ fixed, the formerly discrete set $t_n = n\Delta t,\ n = 1, \ldots, N$ becomes dense on the time interval $[0, t]$, and the set of phase space points $\{\mathbf{x}_n\}$ becomes a continuous curve $\mathbf{x}(t)$. In the same limit we have

$$\begin{aligned}
\Delta t \sum_{n=0}^{N-1} &\longrightarrow \int_0^t dt', \\
\frac{q_{n+1}-q_n}{\Delta t} &\longrightarrow \partial_{t'} q\Big|_{t'=t_n} \equiv \dot{q}|_{t'=t_n}, \\
V(q_n) + T(p_{n+1}) &\longrightarrow (T(p|_{t'=t_n}) + V(q|_{t'=t_n})) \equiv H(\mathbf{x}|_{t'=t_n}), \\
\int \prod_{\substack{n=1 \\ q_N=q_F, q_0=q_I}}^{N-1} dq_n \prod_{n=1}^{N} \frac{dp_n}{2\pi\hbar} &\longrightarrow \lim_{N\to\infty} \int \prod_{\substack{n=1 \\ q_N=q_F, q_0=q_I}}^{N-1} dq_n \prod_{n=1}^{N} \frac{dp_n}{2\pi\hbar} \equiv \int_{\substack{q(t)=q_F \\ q(0)=q_I}} D(q,p).
\end{aligned}$$

In third line, H denotes the *classical* Hamiltonian. In the limit $N \to \infty$, the fact that kinetic and potential energies are evaluated at neighbouring time slices, n and $n+1$, becomes irrelevant.[5] The fourth line *defines* the integration measure of the integral.

[5] To see this formally, one may Taylor expand $T(p_{n+1}) = T(p(t'+\Delta t))|_{t'=n\Delta t}$ around $p(t')$. For smooth $p(t')$ all but the zeroth order contribution, $T(p(t'))$ scale with powers of Δt, thereby becoming irrelevant. Note, however, that all these arguments are based on the assertion that the dominant contributions to the path integral are smooth in the sense $q_{n+1} - q_n \sim O(\Delta t)$. A closer inspection, however, shows that in fact $q_{n+1} - q_n \sim O(\sqrt{\Delta t})$ [?]. In some cases, the most prominent one being the quantum mechanics of

Integrals extending over infinite dimensional integration measures like $D(q,p)$ are generally called **functional integrals** (recall our discussion of functionals in chapter 1). The question of how functional integration can rigorously be defined is far from innocent and represents a subject of current, and partly controversial mathematical research. In this lecture course — as in most applications in physics — we take a pragmatic point of view and deal with the infinite dimensional integration naively unless mathematical problems arise (which actually won't be the case!).

Applying these conventions to Eq. (4.7) we obtain as a final result

$$\boxed{\left\langle q_F \left| e^{-i\hat{H}t/\hbar} \right| q_I \right\rangle = \int_{\substack{q(t)=q_F \\ q(0)=q_I}} D(q,p) \exp\left[\frac{i}{\hbar}\int_0^t dt' \left(p\dot{q} - H(p,q)\right)\right].} \tag{4.8}$$

Eq. (4.8) represents the **Hamiltonian formulation of the path integral**: the integration extends over all possible paths through the classical phase space of the system which begin and end at the same *configuration* points q_I and q_F respectively (c.f. Fig. 4.1). The contribution of each path is weighted with its Hamiltonian action.

▷ INFO. Remembering the connection of the Hamiltonian to the Lagrangian through the Legendre transform, $H(p,q) = p\dot{q} - L(p,q)$, the **classical action** of a trajectory $t \mapsto q(t)$ is given by

$$S = \int_0^t dt\ L(q,\dot{q}) = \int_0^t dt\ \left[p\dot{q} - H(p,q)\right].$$

Before we turn to the discussion of the path integral (4.8), we first recast the integral in an alternative form which will be both convenient in various applications and physically instructive. The search for an alternative formulation is motivated by the observation of the close resemblance of (4.8) with the Hamiltonian formulation of classical mechanics. Given that, classically, Hamiltonian and *Lagrangian* mechanics can equally be employed to describe dynamical evolution, it is natural to seek a Lagrangian analog of (4.8). Indeed, a Lagrangian form of the path integral not only exists but can be straightforwardly obtained from (4.8) by Gaussian integration.

To make this point clear, let us rewrite the integral in a way that emphasises its dependence on the momentum variable p:

$$\left\langle q_F \left| e^{-i\hat{H}t/\hbar} \right| q_I \right\rangle = \int_{\substack{q(t)=q_F \\ q(0)=q_I}} Dq\ e^{-\frac{i}{\hbar}\int_0^t dt' V(q)} \int Dp\ e^{-\frac{i}{\hbar}\int_0^t dt' \left(\frac{p^2}{2m} - p\dot{q}\right)}. \tag{4.9}$$

The exponent of the integral is quadratic in the momentum variable or, equivalently, the integral is Gaussian in p.

a particle in a magnetic field, the lowered power of Δt spoils the naive form of the continuity argument above, and more care must be applied in taking the continuum limit. In cases where a 'new' path integral description of a quantum mechanical problem is developed, it is imperative to delay taking the continuum limit until the fluctuation behaviour of the discrete integral across individual time slices has been thoroughly examined.

▷ INFO. Apart from a few rare exceptions, all integrals encountered in this course will be **Gaussian**. In most cases the dimension of the integrals will be large if not infinite. Yet after a bit of practice it will become clear that high dimensional representatives of Gaussian integrals are no more difficult to handle than their one-dimensional counterparts. In consideration of the important role Gaussian integrals play in field theory, a compendium summarising the most important Gaussian integral formulae has been added as an Appendix to this section.

Carrying out the integration by means of Eq. (4.42), we obtain

$$\boxed{\left\langle q_F \left| e^{-i\hat{H}t/\hbar} \right| q_I \right\rangle = \int_{\substack{q(t)=q_F \\ q(0)=q_I}} Dq \ \exp\left[\frac{i}{\hbar}\int_0^t dt' L(q,\dot{q})\right].} \tag{4.10}$$

where $L(q,\dot{q}) = m\dot{q}^2/2 - V(q)$ represents the classical Lagrangian, and

$$Dq \to \widetilde{D}q = \lim_{N\to\infty}\left(\frac{Nm}{it2\pi\hbar}\right)^{N/2}\prod_{n=1}^{N-1} dq_n$$

is the functional measure of the remaining q-integration. Strictly speaking, the (finite-dimensional) integral formula (4.42) is not directly applicable to the infinite dimensional Gaussian integral (4.9). This, however, does not represent a substantial problem as we can always re-discretise the integral (4.9), apply (4.42), and re-install the continuum limit after integration.

$$\int Dp\, e^{-\frac{i}{\hbar}\int_0^t dt'\left(\frac{p^2}{2m}-pq\right)} = \lim_{N\to\infty}\int\prod_{n=1}^{N}\frac{dp_n}{2\pi\hbar}e^{-i\frac{t}{N\hbar}\sum_{n=1}^{N}\left(\frac{p_n^2}{2m}-p_n\Delta q_n\right)} =$$

$$= \lim_{N\to\infty}\prod_{n=1}^{N}\left(\frac{Nm}{it2\pi\hbar}\right)^{1/2} e^{i\frac{t}{\hbar N}\sum_{n=1}^{N}\frac{m}{2}(\Delta q_n)^2} = \lim_{N\to\infty}\prod_{n=1}^{N}\left(\frac{Nm}{it2\pi\hbar}\right)^{1/2} e^{\frac{i}{\hbar}\int_0^t dt'\frac{m}{2}(\partial_{t'}q)^2},$$

where $\Delta q_n \equiv (N/t)(q_{n+1} - q_n)$.

Eqs. (4.8) and (4.10) represent the central results of this section. A quantum mechanical transition amplitude has been expressed in terms of an infinite dimensional integral extending over paths through phase space (4.8) or coordinate space (4.10). All paths begin (end) at the initial (final) coordinate of the matrix element. Each path is weighted by its *classical* action. Notice in particular that the quantum transition amplitude has been cast in a form which does not contain quantum mechanical operators. Nonetheless, quantum mechanics is still fully present! The point is that the integration extends over *all* paths and not just the subset of solutions of the classical equations of motions. (The distinguished role classical paths play in the path integral will be discussed in section 4.2.2.) The two forms of the path integral, (4.8) and (4.10), represent the formal implementation of the 'alternative picture' of quantum mechanics proposed heuristically in the beginning of the chapter.

Before turning to specific applications of the path integral, let us stay with the general structure of the formalism and identify two fundamental connections of the path integral to *classical point mechanics* and *classical and quantum Statistical Mechanics*.

4.2.1 Path Integral and Statistical Mechanics

The path integral reveals a connection between quantum mechanics and classical (and quantum) statistical mechanics whose importance to all areas of field theory and statistical physics can hardly be exaggerated. To reveal this link, let us for a moment forget about quantum mechanics and consider a perfectly classical, one-dimensional continuum model describing a 'flexible string', held under constant tension, and confined to a 'gutter-like potential' (as shown in Fig. 4.2). Transverse fluctuations of the string are penalised by the line tension in the string, and by the external potential.

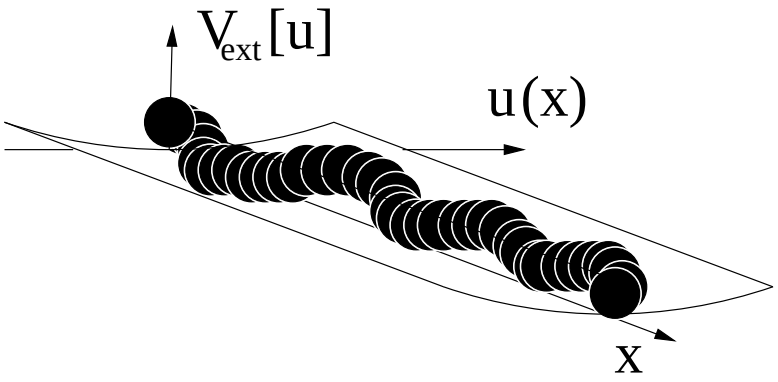

Figure 4.2: A string held under tension and confined to a potential well $V[u]$. (Compare this model to the phonon model discussed in chapter 1.)

Assuming that the transverse displacement of the string $u(x)$ is small, the potential energy stored in the string separates into two parts. The first arises form the line tension stored in the string, and the second comes from the external potential. Starting with the former, a transverse fluctuation of a line segment of length dx by an amount du, leads to a potential energy of magnitude $\delta V_t = T[(dx^2 + du^2)^{1/2} - dx] \simeq T dx (\partial_x u)^2/2$, where T denotes the tension. Integrated over the length of the string, one obtains

$$V_T[\partial_x u] \equiv \int \delta V_T = \frac{1}{2}\int_0^L dx\; T\,(\partial_x u(x))^2\,. \tag{4.11}$$

The second contribution arising from the external potential is given by

$$V_{\rm ext}[u] \equiv \int_0^L dx\; V[u(x)]. \tag{4.12}$$

Adding the two contributions (4.11) and (4.12) we find that the total energy of the string is given by

$$V = V_T + V_{\rm ext} = \int_0^L dx \left[\frac{T}{2}\,(\partial_x u)^2 + V(u)\right].$$

(Exercise: Find an expression for the kinetic energy contribution assuming that the string has a mass per unit length of m.)

According to the general prinicples of statistical mechanics the equilibrium properties of a system are encoded in the partition function $\mathcal{Z} = \mathrm{tr}\left[e^{-\beta V}\right]$, where 'tr' denotes a summation over all possible configurations of the system and V is the total potential energy functional. Applied to the present case, $\mathrm{tr} \to \int Du$, where $\int Du$ stands for the functional integration over all configurations of the string $u(x)$, $x \in [0, L]$. Thus, the partition function of the string is given by

$$\mathcal{Z} = \int Du \ \exp\left[-\beta \int_0^L dx \left(\frac{T}{2}(\partial_x u)^2 + V(u)\right)\right]. \tag{4.13}$$

▷ EXERCISE. How does this model compare to the continuum model of lattice vibrations discussed in chapter 1?

Comparing this result with Eq. (4.10) we deduce that the partition function of the *classical* system coincides with the *quantum mechanical* amplitude

$$\mathcal{Z} = \int dq \left\langle q \left| e^{i\hat{S}[q]/\hbar} \right| q \right\rangle \Big|_{t=-iL}$$

evaluated for imaginary 'time' $\tau \equiv L \equiv it$ and 'temperature' $\hbar$. (Here we have assumed that our string is subject to periodic boundary conditions.)

To see this explicitly, let us assume we had had reasons to consider quantum propagation in imaginary time, i.e. $e^{-it\hat{H}/\hbar} \to e^{-\tau\hat{H}/\hbar}$, or $t \to -i\tau$. (Assuming convergence, i.e. positivity of the eigenvalues of $\hat{H}$,) a construction scheme perfectly analogous to the one outlined in section 4.1 would have led to a path integral formula of the structure (4.10). Formally, the only differece would be that (a) the Lagrangian would be integrated along the imaginary time axis $t' \to -i\tau' \in [0, -i\tau]$ and (b) a change of the sign of the kinetic energy term ($(\partial_{t'} q)^2 \to -(\partial_{\tau'} q)^2$). After a suitable exchange of variables, $\tau \to L, \hbar \to T$, the coincidence of the resulting expression with the partition function (4.13) is clear.

The connection between quantum mechanics and classical statistical mechanics outlined above generalises to higher dimensions: There are tight analogies between quantum field theories in d dimensions and classical statistical mechanics in $d + 1$. (The equality of the path integral above with the one-dimensional statistical model is the $d = 0$ version of this connection.) In fact, this connection turned out to be of the major driving forces behind the success of path integral techniques in modern field theory/statistical mechanics. It offered, for the first time, a possibility to draw connections between systems which before had seemed to be unrelated. E.g. the long range behaviour of the classical two-dimensional Ising model, a paradigm of an exactly solvable system in classical mechanics, turned out to be closely related to the quantum Ising *chain*, etc.

However, the concept of imaginary times not only provides a bridge between quantum and classical statistical mechanics but also plays a role within a purely quantum mechanical context. Consider the *quantum* partition function of a *single particle* quantum mechanical system,

$$\mathcal{Z} = \mathrm{tr}\left[e^{-\beta\hat{H}}\right] = \int dq \left\langle q \left| e^{-\beta\hat{H}} \right| q \right\rangle$$

The partition function can be interpreted as the transition amplitude $\sim \langle q|e^{-i\hat{H}t/\hbar}|q\rangle$ evaluated at an imaginary time $t = -i\hbar\beta$. Thus, real time dynamics and quantum statistical mechanics can be treated on the same footing, provided that we allow for the appearance of imaginary times.

Later we will see that the concept of imaginary or even generalized complex times plays an important role in all of field theory. There is even some nomenclature regarding imaginary times. The transformation $t \to -i\tau$ is denoted as a **Wick rotation** (alluding to the fact that a multiplication with the imaginary unit can be interpreted as a $\pi/2$-rotation in the complex plane). Imaginary time representations of Lagrangian actions are denoted as **Euclidean actions**[6] whereas the standard (real time) forms are called **Minkowski actions**.

▷ INFO. The origin of these denotations can be understood by considering the structure of the action of, say, the phonon model (1.4). Forgetting for a moment about the magnitude of the coupling constants, we see that the action has the structure $\sim x_\mu g^{\mu\nu} x_\nu$, where $\mu = 0, 1$, the vector $x_\mu = \partial_\mu \phi$ and

$$g = \begin{pmatrix} -1 & \\ & 1 \end{pmatrix}$$

is the two dimensional version of a Minkowski metric. (In three spatial dimensions, g would take the form of the standard Minkowski metric of special relativity.) Wick rotating time, the -1 in the metric changes sign and g becomes a positive definite Euclidean metric. The nature of this transformation motivates the notation above.

Once one has grown accustomed to the idea that interpretating time as an imaginary quantity can be useful, yet more general concepts can be conceived. E.g. one may contemplate quantum propagation along temporal contours that are neither purely real or imaginary but *generally complex*. Indeed, we will see below, that path integrals with curvelinear integration contours in the complex 'time plane' find many applications in statistical and quantum field theory.

4.2.2 Path Integral and Classical Mechanics: The Semiclassical Approximation

In deriving the two path integrals (4.8) and (4.10) no approximations have been made. Yet the vast majority of quantum mechanical problems cannot be solved in closed form, and it would be hoping for too much to expect that within the path integral approach this situation would be any different. In fact no more than the path integrals of problems with

[6] Euclid of Alexandria ca. 325 BC-265 BC: the most prominent mathematician of antiquity best known for his treatise on mathematics "The Elements". The long lasting nature of "The Elements" must make Euclid the leading mathematics teacher of all time. However little is known of Euclid's life except that he taught at Alexandria in Egypt.

a quadratic Hamiltonian — corresponding to the quantum mechanical harmonic oscillator and generalisations thereof — can be carried out in closed form. Yet what counts more than the (rare) availability of exact solutions is the flexibility with which *approximation* schemes can be developed. As for the path integral formulation, it is particularly strong in cases where **semiclassical limits of quantum theories** are explored. By 'semiclassical limit' we mean $\hbar \to 0$, i.e. the case where the theory is expected to be largely governed by classical structures with quantum fluctuations superimposed.

To see more formally how classical structures enter the path integral approach, let us explore Eqs. (4.8) and (4.10) in the limit of small $\hbar$. In this case the path integrals are dominated by path configurations with stationary action. (Non-stationary contributions to the integral imply massive phase fluctuations which largely average to zero.) Now, since the exponents of the two path integrals (4.8) and (4.10) are just the classical action functionals in their Hamiltonian respectively Lagrangian form, the path configurations extremising the path integrals are just the solutions of the classical equations of motion,

$$\begin{aligned} \text{Hamiltonian}: \quad & \delta S[\bar{x}] = 0 \quad \Rightarrow d_t \bar{\mathbf{x}} = \{H(\bar{\mathbf{x}}), \bar{\mathbf{x}}\} \equiv \partial_{\bar{p}} \bar{\mathbf{x}} \partial_{\bar{q}} H - \partial_{\bar{q}} \bar{\mathbf{p}} \partial_{\bar{q}} H, \\ \text{Lagrangian}: \quad & \delta S[\bar{q}] = 0 \quad \Rightarrow \left(d_t \partial_{\dot{\bar{q}}} - \partial_{\bar{q}}\right) L(\bar{q}, \dot{\bar{q}}) = 0. \end{aligned} \tag{4.14}$$

These equations are to be solved subject to the boundary conditions $\bar{q}(0) = q_I$ and $\bar{q}(t) = q_F$. (Note that these boundary conditions do not uniquely specify a solution, i.e. in general there are many solutions to the equations (4.14). Exercise: Invent examples!)

Now the very fact that the stationary phase configurations are classical does not imply that quantum mechanics has disappeared completely. As with saddle-point approximations in general, it is not just the saddle-point itself that matters but also the fluctuations around it. At least it is necessary to integrate out Gaussian (quadratic) fluctuations around the point of stationary phase. In the case of the path integral, fluctuations of the action around the stationary phase configurations involve non-classical (in that they do not solve the classical equations of motion) trajectories through phase or coordinate space.

Before exploring how this mechanism works in detail, let us consider the stationary phase analysis of a functional integrals in general.

▷ INFO. **Stationary Phase Approximation**: Consider a general functional integral

$$\int Dx e^{-F[x]}, \tag{4.15}$$

where $Dx = \lim_{N\to\infty} \prod_{n=1}^{N} dx_n$ represents a functional measure resulting from taking the continuum limit of some finite dimensional integration space, and the 'action' $F[x]$ may be an arbitrary functional (leading to convergence of the integral). The function resulting from taking the limit of infinitely many discretisation points, $\{x_n\}$ is denoted by $x : t \mapsto x(t)$ (where t plays the role of the formerly discrete index n.)

Evaluating the integral above within a stationary phase approximation amounts to performing the following steps:

1. Find the 'points' of stationary phase, i.e. configurations $\bar{x}$ qualified by the condition of vanishing functional derivative,

$$\frac{\delta F[\bar{x}]}{\delta \bar{x}} \equiv \lim_{\epsilon \to 0} \frac{F[x(t) + \epsilon y(t)] - F[x(t)]}{\epsilon} = 0.$$

There may be one or many solutions. For clarity, we first discuss the case of just one stationary phase configuration $\bar{x}$.

2. Expand the functional to second order around $\bar{x}$ (cf. Eq. (1.17)),

$$F[x] = F[\bar{x}+y] = F[\bar{x}] + \frac{1}{2}\int dt \int dt' y(t') A(t,t') y(t) + \dots \tag{4.16}$$

where

$$A(t,t') = \left.\frac{\delta^2 F[x]}{\delta x(t)\delta x(t')}\right|_{x=\bar{x}}$$

is the second functional derivative. Due to the stationarity of $\bar{x}$ no first order contribution appears.

3. Check that the *operator* $\hat{A} \equiv \{A(t,t')\}$ is positive definite. If it is not, there is a problem — the integration over the Gaussian fluctuations y below diverges. For positive $\hat{A}$, however, the functional integral over y can be performed and we obtain

$$\int Dx\; e^{-F[x]} \simeq e^{-F[\bar{x}]}\; \det\left(\frac{\hat{A}}{2\pi}\right)^{-1/2},$$

(c.f. the discussion in section 4.5.4, and Eq. (4.48)).

4. Finally, if there are many stationary phase configurations, $\bar{x}_i$, the individual contributions have to be added:

$$\int Dx\; e^{-F[x]} \simeq \sum_i e^{-F[\bar{x}_i]}\; \det\left(\frac{\hat{A}_i}{2\pi}\right)^{-1/2}. \tag{4.17}$$

Eq. (4.17) represents the most general form of the stationary phase evaluation of a (real) functional integral.

Applied to the Lagrangian form of the Feynman path integral, this program can be implimented directly. Defining $r(t) = q(t) - \bar{q}(t)$ as the deviation of a general path, $q(t)$, from a nearby classical path, $\bar{q}(t)$ (see Fig. 4.3), and assuming for simplicity that only one classical solution connecting q_I with q_F in time t exists, a stationary phase analysis obtains

$$\left\langle q_F \left| e^{-i\hat{H}t/\hbar} \right| q_I \right\rangle \simeq e^{iS[\bar{q}]/\hbar} \int_{r(0)=r(t)=0} Dr \exp\left[\frac{i}{2\hbar}\int_0^t dt' \int dt'' r(t')\left.\frac{\delta^2 S[q]}{\delta q(t')\delta q(t'')}\right|_{q=\bar{q}} r(t'')\right] \tag{4.18}$$

for the Gaussian approximation to the path integral (c.f. Eq. (4.16)). For potential type Lagrangians,

$$L(q,\dot{q}) = \frac{m}{2}\dot{q}^2 - V(q),$$

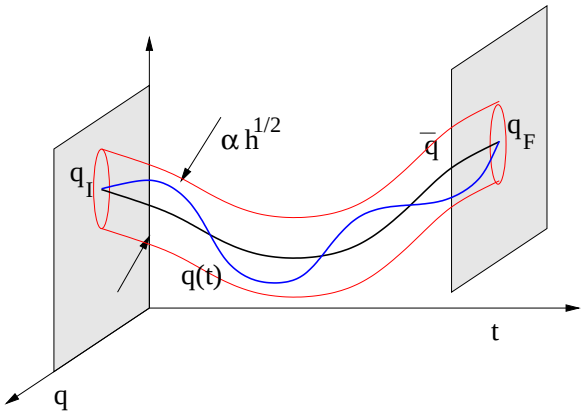

Figure 4.3: Quantum fluctuations around a classical path in coordinate space (here we assume a set of two-dimensional coordinates). Non-classical paths q fluctuating around a classical solution $\bar{q}$ typically extend a distance $O(h^{1/2})$. *All* paths begin and end at q_I and q_F, respectively.

the second functional derivative of the action can be straightforwardly computed by means of the rules of functional differentiation formulated in section 1. Alternatively, one can obtain this result by simply expanding the action as a Taylor series in the deviation $r(t)$. The result is (exercise!)

$$\frac{1}{2}\int_0^t dt \int dt' r(t) \left.\frac{\delta^2 S[q]}{\delta q(t)\delta q(t')}\right|_{q=\bar{q}} r(t') = -\frac{1}{2}\int dt\; r(t)\left[m\partial_t^2 + V''(\bar{q}(t))\right] r(t), \qquad (4.19)$$

where $V''(\bar{q}(t))$ is the ordinary (second) derivative of the potential function evaluated at $\bar{q}(t)$. Thus, the Gaussian integration over r yields the square root of the determinant of $m\partial_t^2 + V''(\bar{q}(t))$ — interpreted as an operator acting in the space of functions $r(t)$ with boundary conditions $r(0) = r(t) = 0$. (Note that, as we are dealing with a differential operator, the issue of boundary conditions is crucial.)

▷ INFO. More generally, we obtain

$$\left\langle q_F \left| e^{-i\hat{H}t/\hbar} \right| q_I \right\rangle \simeq \det\left(\frac{i}{2\pi\hbar}\frac{\partial^2 S[\bar{q}]}{\partial q_I \partial q_F}\right)^{1/2} e^{\frac{i}{\hbar}S[\bar{q}]} \qquad (4.20)$$

as the final result for the semiclassical evaluation of the transition amplitude. (In cases where there is more than one classical solution, the individual contributions have to be added.) To derive this expression, one shows that the operator controlling the quadratic action (4.19) fulfills some differential relations which can, again, be related back to the classical action. While a detailed formulation of this calculation (see, e.g., [**?**], pp94) is beyond the scope of the present text, the heuristic interpretation of the result is straightforward (see Fig. 4.4):

According to the rules of quantum mechanics $P(q_F, q_I, t) = \left|\left\langle q_F \left| e^{-i\hat{H}t/\hbar} \right| q_I \right\rangle\right|^2$ is the probability for a particle starting at coordinate q_I to arrive at coordinate q_F after time t. The semiclassical analysis predicts that

$$P(q_F, q_I, t) = \left|\det\left(\frac{1}{2\pi\hbar}\frac{\partial^2 S[\bar{q}]}{\partial q_I \partial q_F}\right)\right|.$$

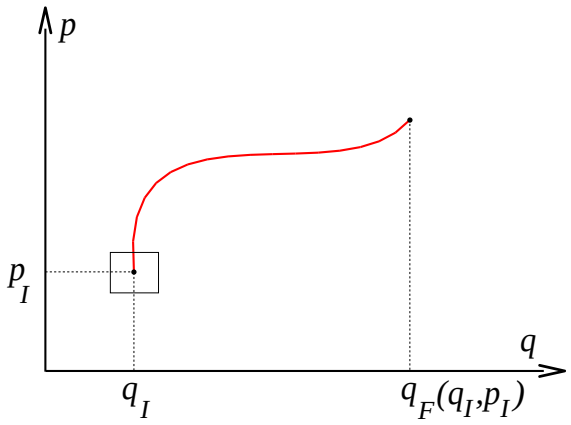

Figure 4.4: Trajectory in two-dimensional phase space. For fixed initial coordinate q_I, the final coordinate $q_F(q_I, p_I)$ becomes a function of the initial momentum. In quantum mechanics, the Planck cell $\hbar^d$ (indicated by the rectangle) limits the accuracy at which the initial coordinate can be set.

To understand this prediction, notice that for fixed inital coordinate q_I the final coordinate $q_F(q_I, p_I)$ becomes a function of the initial *momentum* p_I. The classical probability density $p(q_I, q_F)$ can then be related to the probabilty density $\tilde{p}(q_I, p_I)$ for a particle to leave at the initial phase space coordinate (q_I, p_I) according to

$$p(q_I, q_F) dq_I dq_F = p(q_I, q_F) \left| \det \left(\frac{\partial q_F}{\partial p_I} \right) \right| dq_I dp_I = \tilde{p}(q_I, p_I) dq_I dp_I .$$

Now, when we say that our particle actually left at the a phase space coordinate (q_I, p_I), $\tilde{p}$ becomes singular at (q_I, p_I) while being zero everywhere else. In quantum mechanics, however, all we can say is that our particle was initially confined to a *Planck cell* centered around (q_I, p_I): $\tilde{p}(q_I, p_I) = 1/(2\pi\hbar)^d$. We thus conclude that

$$p(q_I, q_F) = \left| \det \left(\frac{\partial p_I}{\partial q_F} \right) \right| \hbar^{-d} .$$

Finally, noticing that $p_I = -\partial_{q_I} S$ we arrive at

$$p(q_I, q_F) = \left| \det \left(-\frac{1}{2\pi\hbar} \frac{\partial^2 S}{\partial q_I \partial q_F} \right) \right| \hbar^{-d} ,$$

which is the result of the semiclassical analysis.

In deriving (4.20) we have restricted ourselves to the consideration of *quadratic* fluctuations around the classical paths — the essence of the semiclassical approximation. Under what conditions is this approximation justified? Unfortunately there is no rigorous and generally applicable answer to this question: For finite $\hbar$, the quality of the approximation depends largely on the sensitivity of the action to path variations. Whether or not the approximation is legitimate, is a question that has to be judged from case to case. However, the *asymptotic* stability of the semiclassical approximation in the limit $\hbar \to 0$, can be deduced simply from power counting. From the structure of (4.20) it is clear that the typical magnitude of fluctuations r scales like $r \sim (\hbar/\delta_q^2 S)^{1/2}$, where $\delta_q^2 S$ is a symbolic shorthand for the functional variation of the action.

(Variations larger than that lead to phase fluctuations $> 2\pi$, thereby being negligible.) Non Gaussian contributions to the action would have the structure $\sim \hbar^{-1} r^n \delta_q^n S$, $n > 2$. For a typical r, this is of the order $\sim \delta_q^n S/(\delta_q^2 S)^{n/2} \hbar^{n/2-1}$. Since the S-dependent factors are classical ($\hbar$-independent) these contributions scale to zero as $\hbar \to 0$.

This concludes the conceptual part of the chapter. Before turning to the discussion of applications, and for future reference, let us briefly recapitulate the main steps taken in constructing the path integral:

4.2.3 Construction Recipe

Consider a general quantum transition amplitude $\langle \psi | e^{-i\hat{H}t/\hbar} | \psi' \rangle$, where t may be real, purely imaginary or generally complex. To construct a functional integral representation:

1. Partition the time interval into $N \gg 1$ steps,

$$e^{-i\hat{H}t/\hbar} = \left[e^{-i\hat{H}\Delta t/\hbar} \right]^N, \qquad \Delta t = t/N.$$

2. Regroup the operator content appearing in the expansion of each factor $e^{i\hat{H}\Delta t/\hbar}$ according to

$$e^{-i\hat{H}\Delta t/\hbar} = 1 + \Delta t \sum_{mn} c_{mn} \hat{A}^m \hat{B}^n + O(\Delta t^2),$$

   where the eigenstates $|a\rangle, |b\rangle$ of $\hat{A}, \hat{B}$ are known and the coefficients c_{mn}'s are c-numbers. (In the quantum-mechanical application above $\hat{A} = \hat{p}$, $\hat{B} = \hat{q}$.)

3. Insert resolutions of identity according to

$$\begin{aligned} e^{-i\hat{H}\Delta t/\hbar} &\to \sum_{a,b} |a\rangle\langle a| \left(1 + \Delta t \sum_{mn} c_{mn} \hat{A}^m \hat{B}^n + O(\Delta t^2) \right) |b\rangle\langle b| \\ &= \sum_{a,b} |a\rangle\langle a| e^{-iH(a,b)\Delta t/\hbar} |b\rangle\langle b| + O(\Delta t^2), \end{aligned}$$

   where $H(a,b)$ is the Hamiltonian evaluated at the eigenvalues of $\hat{A}$ and $\hat{B}$.

4. Regroup terms in the exponent: due to the 'mismatch' of the eigenstates at neighbouring time slices n and $n+1$, not only the Hamiltonians $H(a,b)$, but also sums over differences of eigenvalues appear (c.f. the last term in the action (4.7)).

5. Take the continuum limit.

4.3 Applications of the Feynman Path Integral

Having introduced the general machinery of path integration we now turn to the discussion of three specific examples: a quantum low energy particle in a well, tunnelling in a double well environment, and the semiclassical trace formulae in quantum chaos. In the second example we will become acquainted with instanton techniques and the role of topology in field theory.

The simplest example of a quantum mechanical problem is that of a *free* particle ($\hat{H} = \hat{p}^2/2m$). Within the framework of the path integral this example, which can be straightforwardly dealt with by elementary means, is far from trivial. As such, the derivation of the free particle propagator is often treated as a first example in the literature. Here the derivation of the one-dimensional transition amplitude is left as an exercise (see Problem set 4.6), the result of which gives[7]

$$\boxed{G_{\rm free}(q_F, q_I; t) \equiv \left\langle q_F \left| e^{-i\hat{p}^2 t/2m\hbar} \right| q_I \right\rangle \Theta(t) = \left(\frac{m}{2\pi i\hbar t}\right)^{1/2} \exp\left[\frac{i}{\hbar}\frac{m(q_F - q_I)^2}{2t}\right] \Theta(t)} \tag{4.21}$$

where the Heaviside Θ-function explicitly indicates that we are considering positive times only.

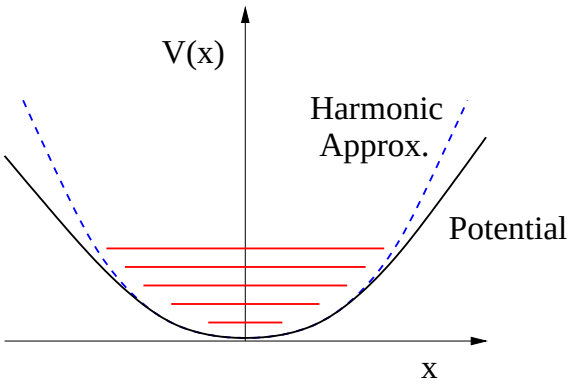

Figure 4.5: Solid: Potential well. Dashed: Quadratic fit approximating the potential shape close to the minimum.

4.3.1 Quantum Particle in a Well

Let us now proceed to a somewhat less trivial case and consider a quantum particle in a one-dimensional potential well (see Fig. 4.5). The discussion of this example will illustrate how the semiclassical evaluation scheme discussed above works in practice. For simplicity we assume the potential to be symmetric, $V(q) = V(-q)$ with $V(0) = 0$. The quantity we wish to compute is the probability amplitude to stay at the origin,

$$G(0,0;t) \equiv \left\langle q_F = 0 \left| e^{-i\hat{H}t/\hbar} \right| q_I = 0 \right\rangle \Theta(t),$$

[7] Compare this result to the solution of a classical diffusion equation.

where $\hat{H} = \hat{p}^2/2m + \hat{V}$. The path integral representation (4.10) of the transition amplitude is given by

$$G(0,0;t) = \int_{q(t)=q(0)=0} Dq \exp\left[\frac{i}{\hbar}\int_0^t dt' L(q,\dot{q})\right],$$

where $L = m\dot{q}^2/2 - V(q)$ represents the Lagrangian.

We wish to evaluate the path integral within the semiclassical approximation above. Accordingly, we must first find solutions to the classical equations of motion. Minimising the action with respect to variations of $q(t)$, we obtain the Euler-Lagrange equations from which we obtain the equation of motion

$$m\ddot{q} = -V'(q),$$

where $V'(q) \equiv \partial_q V(q)$. According to the Feynman path integral, this equation must be solved subject to the boundary conditions $q(t) = q(0) = 0$. One solution is obvious:

$$\bar{q}(t) = 0.$$

Assuming that this is in fact the only solution,[8] we obtain (c.f. Eqs. (4.18) and (4.19))

$$G(0,0;t) \simeq \int_{r(0)=r(t)=0} Dr \exp\left[-\frac{i}{\hbar}\int_0^t dt' r(t')\frac{m}{2}\left(\partial_{t'}^2 + \omega^2\right) r(t')\right],$$

where, by definition, $m\omega^2 \equiv V''(0)$ is the second derivative of the potential at the origin.[9] Note that, in this case, the contribution from the saddle-point solution $S[\bar{q}] = 0$. Following the discussion in section 4.5.4, Gaussian functional integration over r, then leads to

$$G(0,0;t) \simeq J\mathrm{det}\left(-\frac{m}{2}\partial_t^2 - \frac{m\omega^2}{2}\right)^{-1/2},$$

where the prefactor J absorbs various constant prefactors.

Operator determinants are usually most conveniently obtained by presenting them as a product over eigenvalues. In the present case, the eigenvalues ϵ_n are determined by the equation

$$\left(-\frac{m}{2}\partial_t^2 - \frac{m\omega^2}{2}\right) r_n = \epsilon_n r_n,$$

which is to be solved subject to the boundary condition $r_n(t) = r_n(0) = 0$. A complete set of solutions to this equation is given by (remember the structure of the Schrödinger equation of a particle in a one-dimensional box of width $L = t$!),

$$r_n(t') = \sin(n\pi t'/t), \quad n = 1, 2, \ldots,$$

[8] In general, this assumption is wrong. E.g. for smooth potentials, it is certainly reasonable to approximate $V(q)$ for small q by a harmonic oscillator potential, $V_{\mathrm{osc.}}(q) = m\omega^2 q^2/2$. For times t that are commensurate with π/ω, one has periodic solutions, $\bar{q}(t) \propto \sin(\omega t)$ that start out from the origin at time 0 and revisit it just at the right time t. In the next section we will see why the restriction to just the trivial solution was nonetheless legitimate (for arbitrary times t).

[9] Those who are uncomfortable with functional differentiation can arrive at the same expression simply by substituting $q(t) = \bar{q} + r(t)$ into the action and expanding.

with eigenvalues $\epsilon_n = m((n\pi/t)^2 - \omega^2)/2$. Thus,

$$\det\left(-\frac{m}{2}\partial_t^2 - \frac{m\omega^2}{2}\right)^{-1/2} = \prod_{n=1}^{\infty}\left(\frac{m}{2}\left(\frac{n\pi}{t}\right)^2 - \frac{m\omega^2}{2}\right)^{-1/2}.$$

Now we still have the problem that we don't know the value of the infinite product (which even looks divergent for times commensurate with ω). Moreover the value of the constant J has yet to be properly determined. To solve these difficulties, we exploit the fact that (a) we do know the transition amplitude (4.21) of the *free* particle, and (b) the latter coincides with the G in the special case where the potential $V \equiv 0$. In other words, had we computed $G_{\rm free}$ via the path integral, we would have obtained the same constant J and, more importantly, an infinite product like the one above, but with $\omega = 0$. This implies that the propagator can be expressed as

$$G(0,0;t) \equiv \frac{G(0,0;t)}{G_{\rm free}(0,0;t)} G_{\rm free}(0,0;t) = \prod_{n=1}^{\infty}\left[1 - \left(\frac{\omega t}{n\pi}\right)^2\right]^{-1/2}\left(\frac{m}{2\pi i\hbar t}\right)^{1/2}\Theta(t).$$

With the help of the mathematical identity

$$\prod_{n=1}^{\infty}[1 - (x/n\pi)^2]^{-1} = x/\sin x, \tag{4.22}$$

we finally arrive at

$$G(0,0;t) \simeq \sqrt{\frac{m\omega}{2\pi i\hbar \sin(\omega t)}}\Theta(t). \tag{4.23}$$

In fact $G(0,0;t)$ coincides *exactly* with the result we would have obtained within a full quantum mechanical calculation of the transition amplitude based on a parabolic (harmonic oscillator) approximation to the potential (see Problem Set 4.6). As a rule, the semiclassical approximation is exact for quadratic Hamiltonians. This is simply a consequence of the fact that for quadratic quantum Hamiltonians, the path integral is itself quadratic, i.e. higher order contributions to a semiclassical expansion do not exist. The calculation above also illustrates how coordinate space fluctuations around a completely static solution may install the zero-point fluctuation physics characteristic for quantum mechanical bound states.

4.3.2 Double Well Potential: Tunnelling and Instantons

As a second and physically richer application of the path integral let us consider the motion of a particle in a double well potential (see Fig. 4.6). Our aim will be to estimate the quantum probability amplitude for a particle to either stay at the bottom of one of the local minima *or* to go from one minimum to the other. In doing so, it is understood that the energy range accessible to the particle is well below the potential barrier height, i.e. quantum mechanical transfer between minima is by *tunnelling*. This is exactly what makes the problem more difficult than the one above: At first sight it is far from clear what kind of classical stationary phase solutions may serve as a basis for a description of

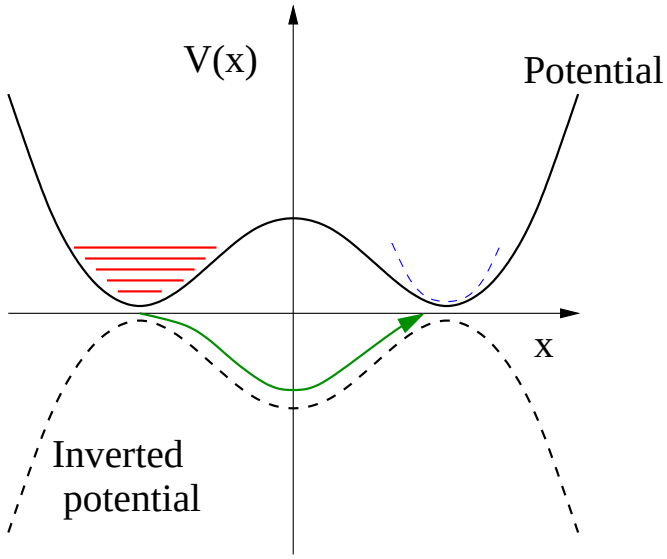

Figure 4.6: Solid: Double well potential. Dashed: Inverted potential

quantum tunnelling; there appear to be no classical paths connecting the two minima. Of course one may think of particles 'rolling' over the potential hill. Yet, these are singular and, by assumption, energetically not accessible.

The key to resolving these difficulties is an observation, already made above, that the time argument appearing in the path integral should be considered as a general complex quantity that can, according to convenience, be sent to basically any value in the complex plane. In the present case, a Wick rotation to imaginary times will reveal a stationary point of the action. At the end of the calculation, the *real* time amplitudes we seek can be straightforwardly obtained by analytic continuation.

▷ INFO. The mechanism of quantum double (or multiple) well tunneling plays a role in a number of problems of condensed matter physics. A prominent example is in the physics of amorphous solids such as **glasses**. A caricature of a glass is shown in Figure 4.7. The absence of long range order in the system implies that individual chemical bonds cannot assume their optimal binding lengths. For understretched bonds this leads to the formation of two approximately equal metastable minima around the ideal binding axis (see inset of Fig. 4.7). The energetically lowest excitations of the system are transitions of individual atoms between nearly degenerate minima of this type, i.e. flips of atoms around the binding axis. A prominent phenomenological model[10] describes the system by an *ensemble* of quantum double wells of random center height and width. This model effortlessly explains the existence of a vast system of metastable minima in the landscape of low-energy configurations of glassy systems.

To be specific, let us attempt to compute the transition amplitudes

$$G(a, \pm a; \tau) \equiv \left\langle \pm a \left| \exp\left[-\frac{\tau}{\hbar}\hat{H}\right] \right| a \right\rangle = G(-a, \mp a; \tau) \tag{4.24}$$

[10] P.W. Anderson, B.I. Halperin, and C.M. Varma, Phil. Mag. **25**, 1 (1971).

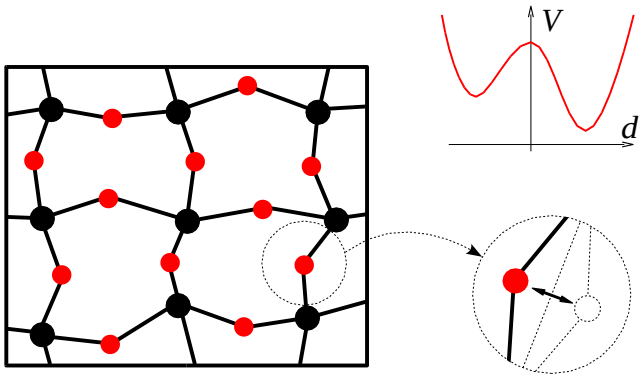

Figure 4.7: Cartoon of a glass. Atoms are arranged in an aperiodic pattern void of long-range order. The binding lengths between nearest neighbour atoms are over/understreched which leads to frustration and the formation of meta-stable minima. Presumably, the lowest excitations of the system are flips of individual atoms around the axes between next-nearest binding partners (inset.)

where $\pm a$ are the two minima of the potential. According to section 4.2.1, the **Euclidean path integral** formulation of the transition amplitudes is given by

$$\boxed{G(a,\pm a;\tau) = \int_{\substack{q(0)=\pm a \\ q(\tau)=a}} Dq \ \exp\left[-\frac{1}{\hbar}\int_0^\tau d\tau' \left(\frac{m}{2}\dot{q}^2 + V(q)\right)\right]} \tag{4.25}$$

where the function q now depends on imaginary time. From (4.25) we obtain the stationary phase equations

$$-m\ddot{q} + V'(q) = 0. \tag{4.26}$$

Thus, the result of the Wick rotation is to effectively *invert* the potential, $V \to -V$ (see Fig. 4.6, dashed). The crucial point is that within the inverted potential landscape the barrier has become a sink, i.e. within the new formulation, there *are* classical solutions connecting the two points, $\pm a$. More precisely, there are three different types of classical solutions which fulfil the condition to be at coordinates $\pm a$ at times 0 and/or τ: (a) The solution wherein the particle rests permanently at a,[11] (b) the corresponding solution staying at $-a$ and, most importantly, (c) the solution in which the particle leaves its initial position at $\pm a$, accelerates through the minimum at 0 and eventually reaches the final position $\mp a$ at τ. In computing the transition amplitudes, all three types of paths have to be taken into account. As for (a) and (b), by computing quantum fluctuations around these solutions we recover the physics of the zero-point motion described in section 4.3.1 for each well individually (Exercise: Convince yourself that this is true!). Now let us see what happens if the paths connecting the two coordinates are added to this picture.

[11] Note that the potential inversion answers a question that came up above, i.e. whether or not the classical solution staying at the bottom of the single well was actually the only one to be considered. Like the double well case, we could have treated the single well within an imaginary time representation, whereupon the well would have become a hill. Clearly there is just one classical solution being at two different times at the top of the bump, viz. the solution that stays there forever. By formulating the semiclassical expansion around that path we would have obtained (4.23) with $t \to -i\tau$, which, upon analytic continuation, would have led back to the real time result.

The Instanton Gas

The classical solution of the Euclidean equations of motion that connect the two potential maxima is called an **instanton solution**. A solution traversing the same path but in the opposite direction ('$-a \to a$' $\rightsquigarrow$ '$a \to -a$') is called an anti-instanton. The name 'instanton' was invented by 't Hooft[12] with the idea that these objects are very similar in their mathematical structure to 'solitons', particle-like solutions of classical field theories. However, unlike solitons, they are structures in time (albeit Euclidean time); thus the 'instant-'. As another etymographic remark, note that the syllable '-on' in 'instanton' hints to an interpretation of these states as a kind of particle. The background is that, as a function of the time coordinate, instantons are almost everywhere constant save a short region of variation (see below). Alluding to the interpretation of time as something akin to a spatial dimension, these states can be interpreted as a well-localised excitation or, according to standard field theoretical practice, a *particle*.[13]

To proceed, we must first compute the classical action associated with a single instanton solution. Multiplying (4.26) by $\dot{\bar{q}}$, integrating over time (i.e. performing the first integral of the equation of motion), and using the fact that at $\bar{q} = \pm a$, $\partial_\tau \bar{q} = V = 0$, we find

$$\frac{m}{2}\dot{\bar{q}}^2 = V(\bar{q}). \tag{4.27}$$

With this result, one obtains the instanton action

$$\begin{aligned} S_{\text{inst.}} &= \int_0^\tau d\tau' \left(\frac{m}{2}\dot{\bar{q}}^2 + V(\bar{q})\right) = \int_0^\tau d\tau' m\dot{\bar{q}}^2 \\ &= \int d\tau' \, \frac{d\bar{q}}{d\tau'}(m\dot{\bar{q}}) = \int_{-a}^{a} dq \; (2mV(q))^{1/2}. \end{aligned}$$

Secondly, let us explore the structure of the instanton as a function of time. Defining the second derivative of the potential at $\pm a$ by

$$V''(\pm a) = m\omega^2,$$

Eq. (4.27) implies that for large times (where the particle is close to the right maximum), $\dot{\bar{q}} = -\omega(\bar{q} - a)$ which integrates to

$$\bar{q}(\tau) \stackrel{\tau\to\infty}{\longrightarrow} a - e^{-\tau\omega}.$$

Thus the temporal extension of the instanton is set by the oscillator frequencies of the local potential minima (the maxima of the inverted potential) and, in cases where tunnelling takes place on time scales much larger than that, can be regarded as short (see Fig. 4.8).

Gerardus 't Hooft 1946- : 1999 Nobel Laureate in Physics for elucidating the quantum structure of electroweak interactions in physics.

[12]

[13] In addition to the original literature, the importance that has been attached to the instanton method has inspired a variety of excellent and pedagogical reviews of the field. Of these, the following are highly recommended: A. M. Polyakov, "Quark Confinement and Topology of Gauge Theories", Nucl. Phys. **B120**, 429 (1977) — see also Ref. [?]; S. Coleman, in "Aspects of Symmetry — Selected Erice Lectures", (CUP 1985) chapter 7

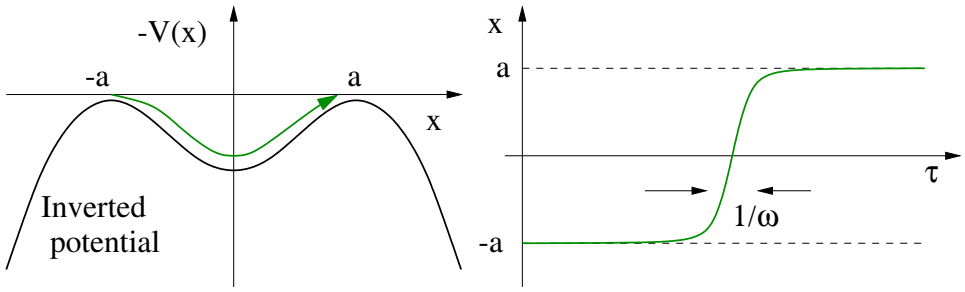

Figure 4.8: Single instanton configuration.

The confinement of the instanton configuration to a narrow interval of time has important implications — there must exist approximate solutions of the stationary equation involving further anti-instanton/instanton pairs (physically, the particle repeatedly bouncing to and fro). According to the general philosophy of the saddle-point scheme, the path integral is obtained by summing over all solutions of the saddle-point equations and hence over all instanton configurations. The summation over multi-instanton configurations — the so-called '**instanton gas**' — is substantially simplified by the fact that individual instantons have short temporal support (events of overlapping configurations are rare) and that not too many instantons can be accommodated in a finite time interval (the instanton gas is dilute). The actual density is dictated by the competition between the configurational 'entropy' (favouring high density), and the 'energetics', the exponential weight implied by the action (favouring low density).

In practice, multi-instanton configurations imply the transition amplitude

$$G(a,\pm a;\tau) \simeq \sum_{n \text{ even / odd}} K^n \int_0^\tau d\tau_1 \int_0^{\tau_1} d\tau_2 \cdots \int_0^{\tau_{n-1}} d\tau_n A_n(\tau_1,\ldots,\tau_n), \qquad (4.28)$$

where A_n denotes the amplitude associated with n instantons present, and we have taken into account the fact that in order to connect a with $\pm a$, the number of instantons must be even/odd. The n instanton bounces contributing to each A_n can take place at arbitrary times $\tau_i \in [0,\tau]$, $i = 1,\ldots,n$ and all these possibilities have to be added (i.e. integrated). K is a (dimensionful) constant absorbing the temporal dimension $[\text{time}]^n$ introduced by the time integrations,[14] and $A_n(\tau_1,\ldots,\tau_n)$ is the transition amplitude, evaluated within the semiclassical approximation around a configuration of n instanton bounces at times $0 \le \tau_1 < \tau_2 < \ldots < \tau_n \le \tau$ (see Fig. 4.9).

According to the general semiclassical principle, each amplitude $A_n = A_{n,\text{cl.}} \times A_{n,\text{qu.}}$ factorises into two parts, a classical contribution $A_{n,\text{cl.}}$ accounting for the action of the instanton configuration, and a quantum contribution $A_{n,\text{qu.}}$ resulting from quadratic fluctuations around the classical path. Focusing initially on $A_{n,\text{cl.}}$, we note that at intermediate times, $\tau_i \ll \tau' \ll \tau_{i+1}$, where the particle rests on top of either of the maxima at $\pm a$, no action accumulates (c.f. the previous section). However, each instanton bounce has a

[14] We restrict ourselves to a calculation of the transition amplitude with 'exponential accuracy', i.e. factors that do not depend exponentially on the transition time will be lumped into an overall prefactor which is not explicitly computed.

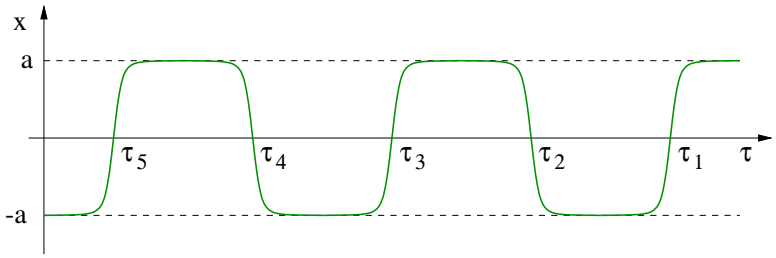

Figure 4.9: Dilute instanton gas configuration.

finite action $S_{\text{inst.}}$ (see Eq. (4.28)) and these contributions add up to give the full classical action,

$$A_{n,\text{cl.}}(\tau_1,\ldots,\tau_n) = e^{-nS_{\text{inst.}}/\hbar}, \tag{4.29}$$

which is independent of the time coordinates τ_i. (The individual instantons 'don't know of each other'; their action is independent of their relative position.)

As for the quantum factor $A_{n,\text{qu.}}$, there are, in principle, two contributions. Whilst the particle rests on either of the hills (the straight segments in Fig. 4.9), quadratic fluctuations around the classical (i.e. spatially constant) configuration play the same role as the quantum fluctuations considered in the previous section, the only difference being that we are working in a Wick rotated picture. There it was found that quantum fluctuations around a classical configuration that stays for a (real) time t at the bottom of the well result in a factor $\sqrt{1/\sin(\omega t)}$, (the remaining constants being absorbed into the prefactor K^n). Rotating to imaginary times, $t \to -i\tau$, we find that the quantum fluctuation accumulated during the stationary time $\tau_{i+1} - \tau_i$ is given by

$$\sqrt{1/\sin(-i\omega(\tau_{i+1}-\tau_i))} \sim e^{-\omega(\tau_{i+1}-\tau_i)/2},$$

where we have used the fact that, for the dilute configuration, the typical separation times between bounces are much larger than the inverse of the characteristic oscillator scales of each of the minima. (It takes the particle much longer to tunnel through a high barrier than to oscillate in either of the wells of the *real* potential.)

Now, in principle there are also fluctuations around the 'bouncing' segments of the path. However, due to the fact that a bounce takes a time of $O(\omega^{-1}) \ll \Delta\tau$, where $\Delta\tau$ represents the typical time *between* bounces, we neglect these contributions (which is to say that we absorb them into the prefactors K without explicit calculation. Within this approximation, setting $\tau_0 \equiv 0$, $\tau_{n+1} \equiv \tau$, the overall quantum fluctuation correction is given by

$$A_{n,\text{qu.}}(\tau_1,\ldots,\tau_n) = \prod_{i=0}^{n} e^{-\omega(\tau_{i+1}-\tau_i)/2} = e^{-\omega\tau/2}, \tag{4.30}$$

again independent of the particular spacing configuration $\{\tau_i\}$. Combining (4.29) and (4.30), we find

$$G(a,\pm a;\tau) \;\simeq\; \sum_{n \text{ even / odd}} K^n e^{-nS_{\text{inst.}}/\hbar} e^{-\omega\tau/2} \overbrace{\int_0^\tau d\tau_1 \int_0^{\tau_1} d\tau_2 \cdots \int_0^{\tau_{n-1}} d\tau_n}^{\tau^n/n!}$$

$$= e^{-\omega\tau/2} \sum_{n \text{ even / odd}} \frac{1}{n!} \left(\tau K e^{-S_{\text{inst.}}/\hbar}\right)^n .$$

Performing the summation, we finally obtain

$$\begin{aligned} G(a,a;\tau) &\simeq C e^{-\omega\tau/2} \cosh\left(\tau K e^{-S_{\text{inst.}}/\hbar}\right), \\ G(a,-a;\tau) &\simeq C e^{-\omega\tau/2} \sinh\left(\tau K e^{-S_{\text{inst.}}/\hbar}\right), \end{aligned} \tag{4.31}$$

where C is some factor that depends in a non-exponential way on the transition time.

Before we turn to a discussion of the physical content of this result, let us self-consistently check whether our central working hypothesis — the diluteness of the instanton gas — was actually correct. To this end, consider the representation of G in terms of the partial amplitudes, A_n:

$$G(a,\pm a;\tau) \sim \sum_{n \text{ even / odd}} \frac{1}{n!} \left(\tau K e^{-S_{\text{inst.}}/\hbar}\right)^n . \tag{4.32}$$

To determine the typical number of instantons $\bar{n}$ contributing to the sum, we use the general formula

$$\bar{n} = \langle n \rangle \equiv \frac{\sum_n n X^n/n!}{\sum_n X^n/n!} = X.$$

Application to (4.32) ($X = \tau K e^{-S_{\text{inst.}}/\hbar}$), gives

$$\bar{n} = \tau K e^{-S_{\text{inst.}}/\hbar}, \tag{4.33}$$

where the even/odd distinction is irrelevant as long as $\bar{n} \gg 1$. Eq. (4.33) states that the average instanton density, $\bar{n}/\tau = K e^{-S_{\text{inst.}}/\hbar}$ is both exponentially small in the instanton action $S_{\text{inst.}}$, and independent of τ confirming the validity of the diluteness assumption.

Finally, let us discuss how the form of the transition amplitude (4.31) can be understood in physical terms. To this end, re-consider the basic structure of the problem we are dealing with (see Fig. 4.10). While there is no coupling across the barrier, the Hamiltonian has two independent, oscillator like sets of low lying eigenstates sitting in the two local minima. Upon allowing for a weak inter-barrier coupling, the oscillator ground states (like all higher states) split into a doublet of a symmetric and an antisymmetric eigenstate, $|S\rangle$ and $|A\rangle$ with energies ϵ_A and ϵ_S, respectively. Focusing on the low energy sector formed by the ground state doublet, we can express the transition amplitudes (4.24) as

$$G(a,\pm a;\tau) \simeq \langle a | \Big[|S\rangle e^{-\epsilon_S \tau/\hbar} \langle S| + |A\rangle e^{-\epsilon_A \tau/\hbar} \langle A| \Big] | \pm a \rangle.$$

Assuming that, by symmetry,

$$|\langle a|S\rangle|^2 = |\langle -a|S\rangle|^2 = \frac{C}{2}, \qquad \langle a|A\rangle\langle A|-a\rangle = -|\langle a|A\rangle|^2 = -\frac{C}{2},$$

and setting $\epsilon_{A/S} = \hbar\omega/2 \pm \Delta\epsilon/2$, where $\Delta\epsilon$ is the tunnel-splitting, we obtain

$$G(a,\pm a;\tau) \simeq \frac{C}{2}\left(e^{-(\hbar\omega-\Delta\epsilon)\tau/2\hbar} \pm e^{-(\hbar\omega+\Delta\epsilon)\tau/2\hbar}\right) = C e^{-\omega\tau/2} \begin{cases} \cosh(\Delta\epsilon\tau/\hbar) \\ \sinh(\Delta\epsilon\tau/\hbar) \end{cases} .$$

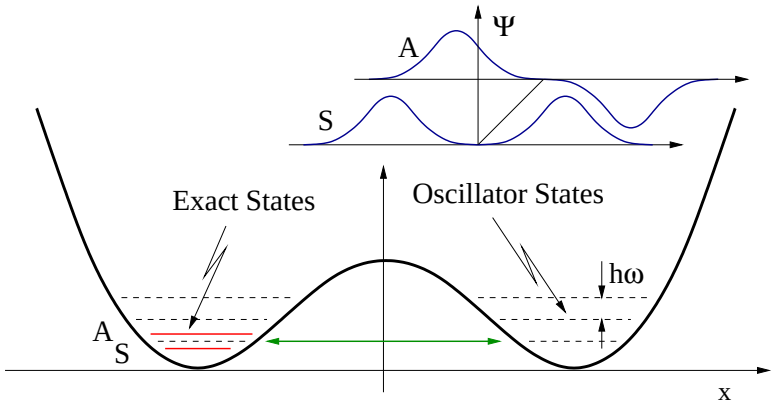

Figure 4.10: Quantum states in the double well: Dashed: Harmonic oscillator states. Solid: Exact eigenstates.

Comparing this expression with (4.31) the interpretation of the instanton calculation becomes clear. It describes the unperturbed energy spectra of the wells *with* account for tunnelling. Remarkably, the effect of tunnelling was obtained from a purely classical picture (formulated in imaginary time!). The instanton calculation also produced a prediction for the tunnel splitting of the energies, viz.

$$\Delta\epsilon = \hbar K \exp(-S_{\text{inst.}}/\hbar),$$

which, up to the prefactor, agrees with the result of a WKB-type analysis of the tunnel process.

Before leaving this section, two general remarks on instantons are in order:

- ▷ In hindsight, was the approximation scheme used above consistent? In particular, terms at second order in $\hbar$ were neglected, while terms non-perturbative in $\hbar$ (the instanton) were kept. Yet, the former typically give rise to a larger correction to the energy than the latter. However, the large perturbative shift affects the energies of the symmetric and antisymmetric state equally. The instanton contribution gives the *leading* correction to the splitting of the levels. It is the latter which is likely to be of more physical significance.

- ▷ Secondly, it may — legitimately — appear as though the development of the machinery above was a bit of an "overkill" for describing a simple tunnelling process. As a matter of fact, the basic result (4.31) could have been obtained in a much simpler way by elementary quantum mechanics (using, for example, the WKB method). Why then did we discuss instantons at length? One reason is that, even within a purely quantum mechanical framework, the instanton formulation of tunnelling is much stronger than WKB. The latter represents, by and large, an uncontrolled approximation. In general it is hard to tell whether WKB results are accurate or not. In contrast, the instanton approximation to the path integral is controlled by a number of well defined expansion parameters. E.g. by going beyond the semiclassical approximation and/or softening the diluteness assumption, the calculation of the transition amplitudes can, in principle, be driven to arbitrary accuracy.

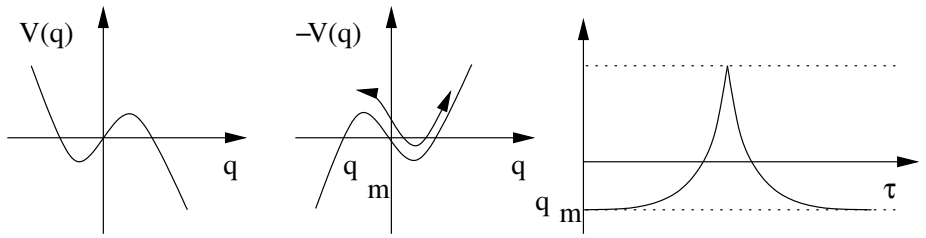

Figure 4.11: Effective potential showing a metastable minimum taken from problem set 4.6 together with the inverted potential and a sketch of a bounce solution. To obtain the tunnelling rate it is necessary to sum over a dilute gas of bounce trajectories.

A second, and for our purposes more important, motivation is that instanton techniques are of crucial importance within higher dimensional field theories (here we regard the path integral formulation of quantum mechanics as a 0 space +1 time = 1-dimensional field theory). The reason is that instantons are intrinsically non-perturbative objects, which is to say that instanton solutions to stationary phase equations describe a type of physics that cannot be obtained by a perturbative expansion around a non-instanton sector of the theory. (E.g. the bouncing orbits in the example above cannot be incorporated into the analysis by doing a kind of perturbative expansion around a trivial orbit.) This non-perturbative nature of instantons can be understood by topological reasoning:

▷ One of the features of the instanton analysis above was that the *number* of instantons involved was a stable quantity; 'stable' in the sense that by including perturbative fluctuations around the n instanton sector, say, one does not connect with the $n+1$ sector. Although no rigorous proof of this statement has been given, it should be heuristically clear: a trajectory involving n bounces between the hills of the inverted potential cannot be smoothly connected with one of a different number. Suppose for instance we would forcably attempt to interpolate between two paths with different bounce numbers: inevitably, some of the intermediate configurations would be charged with actions that are far apart from any stationary phase like value. Thus, the different instanton sectors are separated by an energetic barrier that cannot be penetrated by smooth interpolation and, in this sense, they are **topologically distinct**.

Unstable States and Bounces: False Vacuum

Before closing this section let us return to the instanton calculation to explore the quantum mechanical decay process of a metastable state. Figure 4.11 shows a potential $V(q)$ which has a metastable minimum at a coordinate q_m. Suppose we wish to estimate the "survival probability" of a particle trapped in the metastable minimum of the one-dimensional potential.

According to the path integral scheme, the survival probability, defined by the probability amplitude to remain at q_m, i.e. the propagator $G(q_m, q_m; t)$ can be evaluated by making use of the Euclidean time formulation of the Feynman path integral. As with the double well, in the Euclidean time formalism, the dominant contribution arises from the classical path minimising the action corresponding to the inverted potential (see figure. 4.11). However, in contrast to the double well potential, the classical solution takes the form of a 'bounce' (i.e. the particle spends only a short time away from zero). Put differently, in this case there is only one metastable minimum of the potential. Summing over all bounce solutions (note that in this case we have an exponential series — no even/odd parity effect), we obtain the survival probability

$$\boxed{G(q_m, q_m; \tau) = Ce^{-\omega\tau/2} \exp\left[\tau K e^{-S_{\rm inst}/\hbar}\right]}$$

Applying an analytic continuation to real time, we find

$$G(\theta_m, \theta_m; t) = Ce^{-i\omega t/2} \exp\left[-\frac{\Gamma}{2}t\right],$$

where the decay rate is given by $\Gamma/2 = |K|e^{-S_{\rm inst}/\hbar}$. (Note that on physical grounds we can see that K must be imaginary.[15])

4.3.3 Trace Formulae and Quantum Chaos

Introductory courses of classical mechanics usually conevey the impression that dynamical systems behave in a regular and, at least in principle, mathematically predictable way. However, we all know from our own experience that a major part of real life dynamical processes does not conform with this picture; Partly, or even fully chaotic motion (i.e. motion that depends in a singular and essentially un-predictable way on its intial conditions) is the rule rather than an exception. In view of the drastic differences in the observable behaviour of integrable and chaotic systems, respectively, the obvious question arises: In which way does the *quantum* phenomenology of chaotic systems differ from the integrable case? This question defines the field of **quantum chaos**.

Understanding signatures of classically chaotic motion in quantum mechanics is an issue not only of conceptual, but also of great practical relevance. An example of an application area where these aspects are vitally important is low-temperature electronic transport in condensed matter systems: The inevitable presence of impurities and imperfections in any macroscopic solid renders the long time dynamics of electronic charge carriers chaotic. Relying on a lose interpretation of the Heisenberg principle, $\Delta t \sim \hbar/\Delta E$, i.e. relation between *long* time dynamical behaviour and *small* scale structures in energy, one would expect that signatures of chaotic quantum dynamics are especially important in the low-energy, or low-temperature regimes one is usually interested in. This expectation has been confirmed for innumerable observables related to low temperature electronic transport in solid state systems.

[15] In fact, a more careful analysis shows that this estimate of the decay rate is too large by a factor of 2 (see Ref. [?]).

Impurity disordered conductors represent but one of a wide class of dynamical systems with long time chaotic dynamics. In fact, recent experimental advances have made possible to realize a panopticum of effctively *non-disordered* chaotic dynamical systems in condensed matter devices, too. E.g. employing modern semiconductor device technology, it has become possible to manufacture small two-dimensional conducting systems, of size $\mathcal{O}(< 1\mu\,\mathrm{m})$ and basically any geometric shape. In systems of that size, the number of imperfections can be reduced to a negligible minimum, i.e. electrons propagate along straight trajectories, as in a billiard. The smallness of the devices further implies that the ratio between Fermi wavelength and system size is of $\mathcal{O}(10^{-1} - 10^{-3})$. I.e. while semiclassical concepts will surely be applicable, the wave aspects of quantum propagation remain visible. In recent years, the experimental and theoretical study of electron transport in such *quantum billiards* has become a field of its own (for two applications, see Fig. xx.)

But how then *can* signatures of chaotic dynamics in quantum systems be sought? The most fundamental characteristic of a quantum system is its spectrum. Although not a *direct* observable, it determines the majority of properties accessible to measurement. On the other hand, it is clear that the manifestations of chaos we are looking for must relate back to the *classical* dynamical properties of the system. The question then is, *how can a link between classical mechanics and quantum spectra be drawn?* This problem is tailor made for analysis by path integral techniques.

Semiclassical Approximation to the Density of States

The tight connection between the path integral and classical mechanics should be evident from the foregoing sections. However, to get going on the problem posed above, we still need to understand how the path integral can be employed to analyse the spectrum of a quantum system. Spectral properties of quantum systems are described by the (single particle) **density of states**

$$\rho(\epsilon) = \sum_a \delta(\epsilon - \epsilon_a), \tag{4.34}$$

where $\{\epsilon_a\}$ is the set of energy levels. To compute the sum, one commonly employs a trick based on the **Dirac identity**,

$$\lim_{\delta \searrow 0} \frac{1}{x + i\delta} = -i\pi\delta(x) + \mathcal{P}\frac{1}{x}, \tag{4.35}$$

where $\mathcal{P}(1/x)$ stands for the principal part of $1/x$. Taking the imaginary part of (4.35), Eq. (4.34) can be represented as

$$\rho(\epsilon) = -\frac{1}{\pi}\,\mathrm{Im}\sum_a \frac{1}{\epsilon^+ - \epsilon_a} = -\frac{1}{\pi}\,\mathrm{Im\ tr}\left(\frac{1}{\epsilon^+ - \hat{H}}\right),$$

where ϵ^+ stands for $\epsilon + i\delta$ and a limit $\lim_{\delta\searrow 0}$ is implicit. Using the identity $1/x^+ = -i\int_0^t dt e^{ix^+}$ and representing the trace $\mathrm{tr}\,(\hat{A}) = \int dq\langle q|\hat{A}|q\rangle$ as a real space integral,

$$\rho(\epsilon) = \frac{1}{\pi\hbar}\int_0^\infty dt\,\mathrm{Re\,tr}\left(e^{i\hbar^{-1}(\epsilon^+ - \hat{H})t}\right) = \frac{1}{\pi}\,\mathrm{Re}\int_0^\infty dt\, e^{i\hbar^{-1}\epsilon^+ t}\int dq\langle q|e^{-i\hbar^{-1}\hat{H}t}|q\rangle \tag{4.36}$$

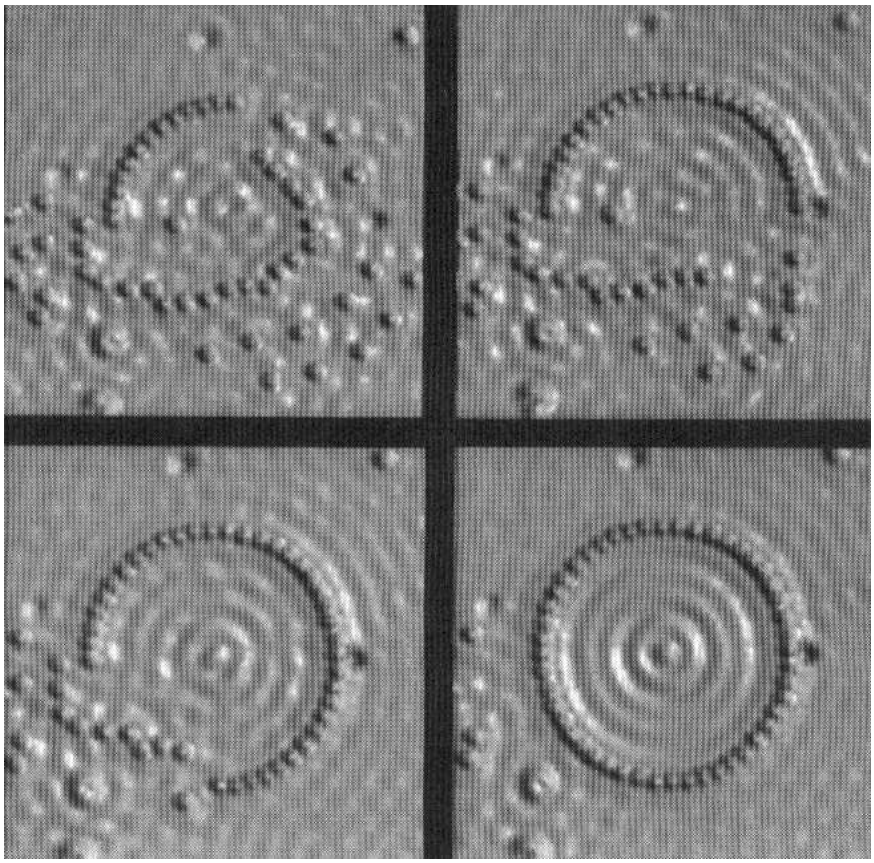

Figure 4.12: An artificially grown quantum 'chorral'. A scanning tunnel microscope (STM) is employed to move individual (!) iron atoms on a copper substrate. When the atoms are arranged to a near perfect circle, the electron motion inside the corral becomes classically integrable. In the present example, classical integrability entails an regular s-wave quantum ground state wave function, whose density distribution is clearly visible in the STM recording.

we have made the connection between the density of states and the quantum propagation amplitude explicit. (Exercise: Wy does the integral exist?)

Without going into full mathematical detail (see, e.g., Ref. [**?**] for a pedagogical presentation) we next outline how this integral is evaluated by path integral techniques and semiclassical approximation. Although some of the more tricky steps of the calculation are swept unter the carpet, the sketch will be accurate enough to make some beautiful connections between the spectral theory of chaotic quantum systems and classical chaotic dynamics manifest.

Substituting the semiclassical approximation (4.20) into (4.36), we obtain

$$\rho(\epsilon) \simeq \frac{1}{\pi}\,\mathrm{Re}\int_0^\infty dt\, e^{i\hbar^{-1}\epsilon^+ t}\int dq A[\bar{q}]e^{\frac{i}{\hbar}S[\bar{q}]},$$

where we have defined

$$A[\bar{q}] \equiv \det\left(\frac{i}{2\pi\hbar}\frac{\partial^2 S[\bar{q}]}{\partial q(0)\partial q(t)}\right)^{1/2}$$

and $\bar{q}$ is a *closed classical path* that begins at q at time 0 and ends at the same coordinate at time t. Again relying on the semiclassical condition $S[\bar{q}] \gg \hbar$, the integrals over q and t are now done in a stationary phase approximation. Beginning with the t integral, and noticing that $\partial_t S[\bar{q}] = -\epsilon_{\bar{q}}$ is the (conserved) energy of the path $\bar{q}$, we obtain the saddle point condition $\epsilon \stackrel{!}{=} \epsilon_{\bar{q}}$ and

$$\rho(\epsilon) \simeq \frac{1}{\pi} \mathrm{Re} \int dq\, A[\bar{q}_\epsilon] e^{\frac{i}{\hbar} S[\bar{q}_\epsilon]},$$

where the symbol $\bar{q}_\epsilon$ indicates that only paths $q \to q$ of energy ϵ are taken into account and the contribution coming from the quadratic integration around the saddle point has been absorbed into a re-definition of $A[\bar{q}_\epsilon]$. Turning to the q-integration, we use that

$$\partial_{q_i} S[\bar{q}] = -p_i, \qquad \partial_{q_f} S[\bar{q}] = p_f,$$

where $q_{i,f}$ are the initial and final coordinate of a path $\bar{q}$, and $p_{i,f}$ the initial and final momentum. Using these relations, the stationary phase condition assumes the form

$$0 \stackrel{!}{=} d_q S[\bar{q}_\epsilon] = \left(\partial_{q_i} + \partial_{q_f}\right) S[\bar{q}_\epsilon]|_{q_i = q_f = q} = p_f - p_i,$$

i.e. the stationarity of the integrand under the q-integration requires that initial and final momentum of the path $\bar{q}_\epsilon$ be identical. We thus find that the paths contributing to the integrated transition amplitude are not only periodic in coordinate space but even in *phase* space. Such paths are called **periodic orbits.** 'Periodic' because the path comes back to its initial phase space coordinate after a certain revolution time and, therefore, will be traversed repeatedly as time goes on (see the figure, where a periodic orbit α with initial coordinates $x = (p, q)$ is shown.)

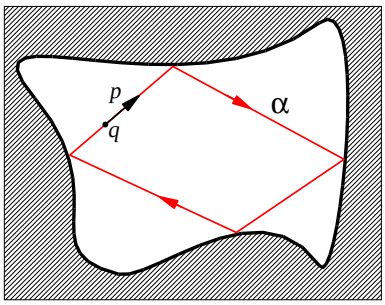

According to our analysis above, each coordinate point q lying on a periodic orbit is a stationary phase point of the q-integral. The stationary phase approximation of the integral can thus be formulated as

$$\rho(\epsilon) \simeq \frac{1}{\pi} \mathrm{Re} \int dq\, A[\bar{q}_\epsilon] e^{\frac{i}{\hbar} S[\bar{q}_\epsilon]} \simeq \sum_{n=1}^{\infty} \sum_{\alpha} \int_\alpha dq\, A_\alpha e^{\frac{i}{\hbar} n S_\alpha},$$

where $\sum_\alpha$ stands for a sum over all periodic orbits (of energy ϵ) and S_α is the action corresponding to *one* traversal of the orbit (all at fixed energy ϵ). The index n accounts for the fact, that, due to its periodicty, the orbit it can be traversed repeatedly, with total action nS_α. Further, $\int_\alpha dq$ is an integral over all coordinates lying on the orbit and we have again absorbed a contribution coming from the quadratic integration around the stationary phase points in the pre-exponential amplitude A_α.

Finally, noticing that $\int_\alpha dq \propto T_\alpha$, where T_p is the period of one traversal of the orbit (at energy ϵ), we arrive at the result

$$\boxed{\rho(\epsilon) \simeq \frac{1}{\pi} \mathrm{Re} \sum_{n=1}^{\infty} \sum_{\alpha} T_\alpha \, A_\alpha e^{\frac{i}{\hbar} n S_\alpha}.} \tag{4.37}$$

This is (a simplified[16]) representation of the famous **Gutzwiller trace formula**. The result is actually quite remarkable: The DoS, an observable of quantum significance, has been expressed entirely in terms of classical quantities.

An Application

Spectral analyses based on the trace formula (4.37) find many applications in condensed matter and atomic physics, quantum optics and other disciplines. By way of example we here mention a beautiful transport experiment measuring the spectra of chaotic semiconductor cavities[17].

[16] Had we carefully kept track of all determinants coming from the stationary phase integrals, the prefactor A_α would have read

$$A_\alpha = \frac{1}{\hbar} \frac{e^{i\frac{\pi}{2}\nu_\alpha}}{|\det M_\alpha^r - 1|^{\frac{1}{2}}},$$

where ν_α is the so-called Maslov index (an integer valued factor associated to singular points on the orbit, i.e. classical turning points) and M_α the **Monodromy matrix**. To understand the meaning of this object, notice that a phase space point $\bar{x}$ on a periodic orbit can be interpreted as a fixed point of the *classical* time evolution operator $U(T_\alpha)$: $U(T_\alpha, \bar{x}) = \bar{x}$, which is just to say that the orbit is periodic. As with any other smooth mapping, U can be linearized in the vicinity of its fixed points,

$$U(T_\alpha, \bar{x} + y) = \bar{x} + M_\alpha y,$$

where the linear operator M_α is the monodromy matrix. Evidently, M_α determines the stability of the orbit under small distortions which makes plausible that it appears as a controlling prefactor of the stationary phase DoS.

[17] T. M. Fromhold et al., Phys. Rev. Lett. **72**, 2608 (1994).

With the advent of modern semiconductor device technology it has become possible to manufacture artifical electronic potential wells of near microscopic width $\mathcal{O}(10^1\text{nm})$ and basically any geometry. Such devices are constructed by growing layers of different semiconductor compounds (typically $GaAs$, $GaAlAs$ or related materials) on top of each other. This obtains a stack of two-dimensionally extended slabs of semi-conductive material, a so-called a two-dimensional heterostructure. When the entire structure is subjected to an transverse voltage drop, the electronic bands of the sub-layers get distorted and a potential landscape tilted in transverse direction and two-dimensionally extended in the direction of the layer-planes results. (See the figure.) By suitable choice of thickness and constitution of the sub-layers, this setup can be used to manufacture two-dimensional **quantum wells** of the type shown schematically in Fig. 4.13.

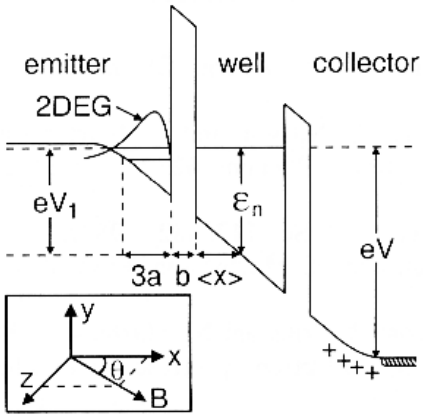

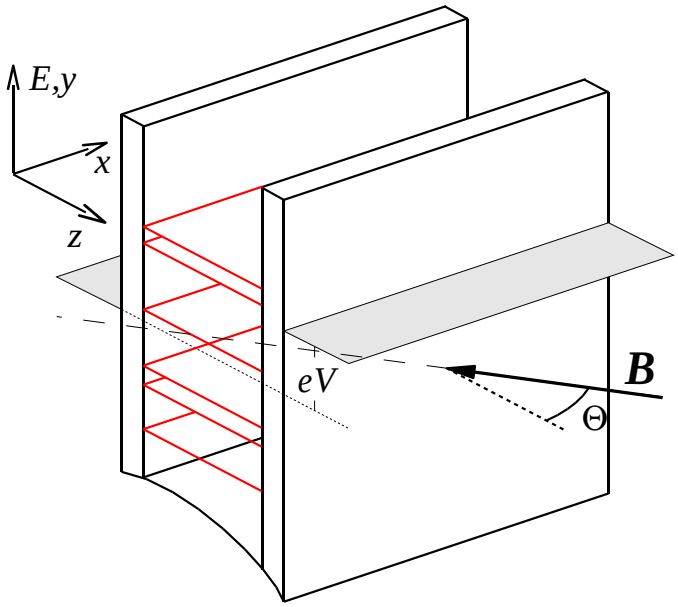

Figure 4.13: Schematic structure of a two-dimensional semiconductor quantum well.

Due to the presence of a potential drop V across the quantum well, electrons will want to flow from one side of the well (the 'emitter') to the other (the 'collector'). The quantum mechanics of this current flow consists of a two-step process: An electron with energy $E_F + eV$ tunnels from the emitter (in Fig. 4.13 indicated by the higher of the two shaded areas) onto an electronic level of the dot, and then escapes through the second barrier into the collector. The important point now is that the tunneling rate reaches a maximum when the dot contains a level $\approx E_F + eV$ resonant with the Fermi energy on the emitter side. Put differently, the tunneling *current* I is directly proportional to the

electronic DoS $\rho(E_F + eV)$ inside the well. This implies that the DoS of a quantum well can be monitored by measuring the (differential) conductance $g = dI/dV$ as a function of the bias voltage eV, or of the Fermi energy E_F. (In semiconductor devices, the value of the Fermi energy can by manipulated by adjustment of external electrodes.)

In the expermiental work by Fromhold et. al. the tunneling conductance of a well with chaotic dynamics was explored. How does one realize chaos in a well with two planar confining barriers (a priori a perfectly integrable system)? In the experiment this was achieved by subjecting the well to a tilted magnetic field (see Fig. 4.13). Chosing a coordinate system such that the field lies in the (x, z) plane, the single particle Hamiltonian describing the interior of the well can be written as

$$\hat{H} = \frac{1}{2m}(\hat{\mathbf{p}} - \mathbf{A})^2 + V(\hat{z}),$$

where $V(z)$ describes the z-dependent potential profile inside the well and

$$\mathbf{A} = B(0, x\cos\theta - z\sin\theta, 0)^T$$

is the vector potential of the magnetic field $\mathbf{B} = B(\sin\theta, 0, \cos\theta)^T$. Noticing that the momentum component k_y is a constant of motion, one makes the ansatz, $\psi(\mathbf{x}) = e^{ik_y y}\psi(x, z)$, to bring the stationary Schrödinger equation into the form

$$\hat{H}'\psi(x, z) = E\psi(x, z),$$

with Hamiltonian

$$\hat{H}_{\text{eff}} = \frac{1}{2m}(\hat{p}_x^2 + \hat{p}_z^2) + \hat{V}_{\text{eff}}(x, z)$$

and effective potential

$$\hat{V}_{\text{eff}} = \frac{1}{2m}(k_y - B\hat{x}\cos\theta - B\hat{z}\sin\theta)^2 + V(\hat{z}).$$

For a perpendicular magnetic field, $\theta = 0$, the system is integrable (which follows, e.g., from the fact that V_{eff} becomes separable, i.e. is the sum of an x- and a z-dependent contribution.) The same holds true in the case of a field parallel to the well, $\theta = 90$deg. For all intermediate values of θ, the dynamics is chaotic. In the figure to the right, the measured differential conductance (more precisely, the derivative dg/dV) is plotted as a function of the applied voltage V for various angles θ. (The specific assignment of tilt angles to conductance profiles is given by $\theta = 0\,\text{deg}$ (a), $\theta = 20\,\text{deg}$ (b), $\theta = 25\,\text{deg}$ (c), $\theta = 40\,\text{deg}$ (d), $\theta = 80\,\text{deg}$ (e), $\theta = 90\,\text{deg}$ (f).) For any given value of θ, the profile of dg/dV is characterized by an almost-periodic pattern of resonances. In some cases, e.g. (b), several periodicity patterns are observed for different values of the bias voltage. According to our discussion above, the resonant behaviour of the conductance follows from the existence of discrete energy levels inside the well. Since the extension of the well is much larger than the Fermi wave length of the conduction electrons, the structure of the electronic spectrum inside the well is amenable to semiclassical analysis. Indeed, it has been possible to attribute individual resonant periodicity intervals of dg/dV to isolated periodic orbits of the well. A few representatives of such orbits are shown in the figure. (Notice that the orbits shown in the topmost and bottom figure display the regularity characteristic for integrable cyclotron-type motion in a magnetic field.) For a more substantial discussion of the assignment of the conductance profile to individual orbits we refer to the book[?] or to the originial reference.

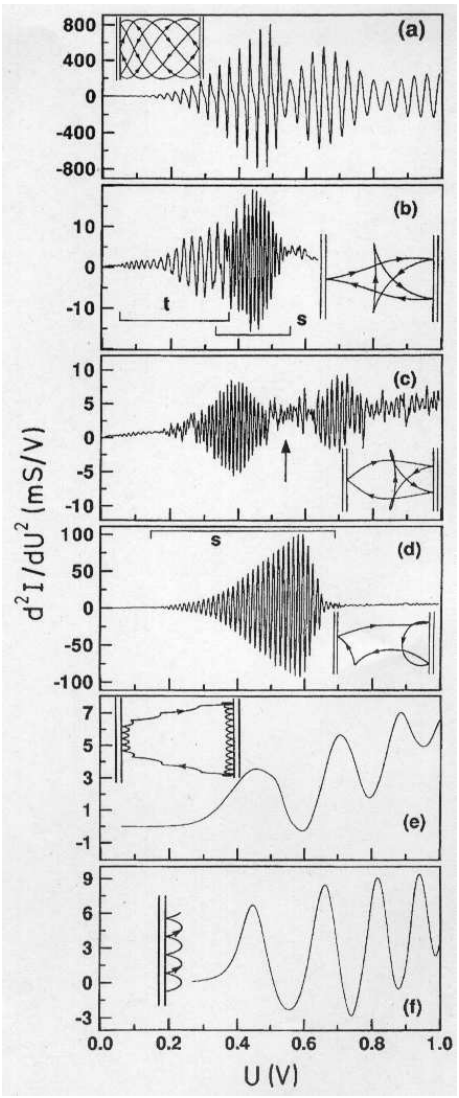

The experiment discussed above stands as an example for the application of semiclassical concepts to quantum transport in small electronic devices. (For a comprehensive discussion of semiclassics in condensed matter physics, see Refs. [?] and [?].) Here, the attribute 'small' means that the quantum wave coherence of the charge carriers inside the system remains experimentally visible, i.e. is not destroyed by the buildup of large-scale thermal decoherence as would be the case in an extended macroscopic systems. On the other hand, the devices are large enough to be amenable to semiclassical concepts, i.e. unlike an isolated atom or a nucleus they are not fully 'microscopic'. Systems of this type, standing intermediate between the classical physics of the macroscopic world and the microscopic limit of quantum mechanics have been dubbed **mesoscopic systems**.

The conductance measurement outlined above represents but one of hundreds of other experiments probing the mesoscopic regime. However, before discussing this fascinating subject in more detail (see chapter XX), we need to provide a number of additional

theoretical concepts, notably the method of functional *field* integration. The introduction of the field integral will be the subject the next chapter.

4.4 Summary and Outlook

In this chapter we have introduced the path integral formulation of quantum mechanics. An approach independent of, and, modulo certain mathematical imponderabilities related to continuum functional integration, equivalent to the standard route of canonical operator quantization. While a few exactly solvable quantum problems (e.g. the evolution of a free particle, the harmonic oscillator, and, intriguinly, spin) are more efficiently formulated by the standard approach, a spectrum of unique features make the path integral an indispensible tool of modern quantum mechanics: The path integral approach is highly intuitive, strong at the solution of non-perturbative problems, and tailor-made to formulation of semiclassical limits. Perhaps most importantly, we have seen that it provides a unifying link whereby quantum problems relate to classical statistical mechanics. Indeed, we found that the path integral of a quantum point particle is in many respects equivalent to the partition function of a classical one-dimensional continuum system. We hinted at a generalization of this prinicple, i.e. an equivalence priniciple relating d-dimensional quantum *field* theory to $d+1$-dimensional statistical mechanics. The importance of this connection in modern theoretical physics can hardly be exaggerated. However, before exploring this bridge, we first need to generalize the concept of path integration to quantum continuum problems. This will be the subject of the next chapter.

4.5 Appendix: Gaussian Integrals

In the development of functional methods in quantum and statistical field theory, the Gaussian[18] integral plays a pivotal role. In this Appendix important formulae on Gaussian integration are reviewed. We begin by discussing one-dimensional integrals, both real and complex. The basic ideas underlying the proofs of the one-dimensional formulae, will provide the key to the derivation of more complex, multi-dimensional and functional identities which will be used liberally throughout the remainder of the course.

4.5.1 One-dimensional Gaussian integrals

The basic ancestor of all Gaussian integrals is the identity

$$\boxed{\int_{-\infty}^{\infty} dx e^{-\frac{a}{2}x^2} = \sqrt{\frac{2\pi}{a}}, \qquad \text{Re } a > 0.} \tag{4.38}$$

In the sequel we will need various generalisations of Eq. (4.38). The first one is

$$\int_{-\infty}^{\infty} dx e^{-\frac{a}{2}x^2} x^2 = \sqrt{\frac{2\pi}{a}} \frac{1}{a},$$

a result easily proven either by substituting $a \to a + \epsilon$ in (4.38), and expanding both the left and the right side of the equation to leading order in ϵ, or by differentiation of (4.38). Often one encounters integrals where the exponent is not purely quadratic from the outset but rather contains both quadratic and linear pieces. The generalisation of (4.38) to this case reads

$$\int_{-\infty}^{\infty} dx e^{-\frac{a}{2}x^2 + bx} = \sqrt{\frac{2\pi}{a}} e^{\frac{b^2}{2a}}. \tag{4.39}$$

To prove this identity, one simply eliminates the linear term by means of the change of variables $x \to x + b/a$ — i.e. completing the square) — which transforms the exponent to

$$-\frac{a}{2}x^2 + bx \to -\frac{a}{2}x^2 + \frac{b^2}{2a}.$$

The constant factor scales out and we are left with Eq. (4.38). Note that (4.39) holds even for complex b. The reason is that by shifting the integration contour into the complex plane no singularities are encountered, i.e. the integral remains invariant.

The extension of (4.38) to the complex case reads

$$\int d(\bar{z}, z) e^{-\bar{z}wz} = \frac{\pi}{w}, \qquad \text{Re } w > 0,$$

---

[18] Johann Carl Friedrich Gauss 1777-1855: worked in a wide variety of fields in both mathematics and physics incuding number theory, analysis, differential geometry, geodesy, magnetism, astronomy and optics. Portrait taken from the German 10-Mark note.

where $\bar{z}$ represents the complex conjugate of z. Here, $\int d(\bar{z},z) \equiv \int_{-\infty}^{\infty} dxdy$ stands for the independent integration over the real and imaginary part of $z = x + iy$. The identity is easy to prove: Owing to the fact that $\bar{z}z = x^2 + y^2$, the integral factorizes into two pieces, each of which is equivalent to Eq. (4.38) with $a = w$. Similarly, the complex generalisation of Eq. (4.39) is given by

$$\int d(\bar{z},z) e^{-\bar{z}wz+\bar{u}z+\bar{z}v} = \frac{\pi}{w} e^{\frac{\bar{u}v}{w}}, \qquad \text{Re } w > 0. \tag{4.40}$$

What is important here is that $\bar{u}$ and v may be *independent* complex numbers; they need not be related to each other by complex conjugation. To prove (4.40) one substitutes $z = x + iy$ into the integrand. As a result one obtains two decoupled integrations (over x and y) each of which takes the form of (4.39) with a certain complex b. Performing the integrals and collecting terms one arrives at (4.40).

4.5.2 Gaussian integration in more than one dimension

All the integrals above have higher dimensional counterparts. Although the real and complex versions of the N-dimensional integral formulae can be derived in a perfectly analogous manner, it is better to discuss them seperately in order not to confuse the structure of the notation.

Real Case

The multi-dimensional generalisation of the prototype integral (4.38) reads

$$\int d\mathbf{v} e^{-\frac{1}{2}\mathbf{v}^T\mathbf{A}\mathbf{v}} = (2\pi)^{N/2} \det \mathbf{A}^{-1/2}, \tag{4.41}$$

where $\mathbf{A}$ is a positive definite real symmetric N-dimensional matrix and $\mathbf{v}$ is an N-component real vector. The proof makes use of the fact that $\mathbf{A}$ (by virtue of being symmetric) can be diagonalised by orthogonal transformation, $\mathbf{A} = \mathbf{O}^T\mathbf{D}\mathbf{O}$, where the matrix $\mathbf{O}$ is orthogonal, and all elements of the diagonal matrix $\mathbf{D}$ are positive. The matrix $\mathbf{O}$ can be absorbed into the integration vector by means of the variable transformation, $\mathbf{v} \mapsto \mathbf{O}\mathbf{v}$ which has unit Jacobian, $\det(\mathbf{O}) = 1$. As a result, we are left with a Gaussian integral with exponent $-\mathbf{v}^T\mathbf{D}\mathbf{v}/2$. Due to the diagonality of $\mathbf{D}$, the integral factorizes into N independent Gaussian integrals each of which gives a factor $\sqrt{2\pi/d_i}$, where d_i, $i = 1,\ldots,N$ is the ith entry of the matrix $\mathbf{D}$. Noticing that $\prod_{i=1}^{N} d_i = \det \mathbf{D} = \det \mathbf{A}$, we obtain (4.41).

The multi-dimensional generalization of (4.39) reads

$$\boxed{\int d\mathbf{v} e^{-\frac{1}{2}\mathbf{v}^T\mathbf{A}\mathbf{v}+\mathbf{j}^T\cdot\mathbf{v}} = (2\pi)^{N/2} \det \mathbf{A}^{-1/2} e^{\frac{1}{2}\mathbf{j}^T\mathbf{A}^{-1}\mathbf{j}}} \tag{4.42}$$

where $\mathbf{j}$ is an arbitrary N-component vector. Eq. (4.42) is proven by analogy to (4.39), i.e. by shifting the integration vector according to $\mathbf{v} \to \mathbf{v} + \mathbf{A}^{-1}\mathbf{j}$, which does not change the value of the integral but removes the linear term from the exponent,

$$-\frac{1}{2}\mathbf{v}^T\mathbf{A}\mathbf{v} + \mathbf{j}^T\cdot\mathbf{v} \to -\frac{1}{2}\mathbf{v}^T\mathbf{A}\mathbf{v} + \frac{1}{2}\mathbf{j}^T\mathbf{A}^{-1}\mathbf{j}.$$

The resulting integral is of type (4.41) and we arrive at (4.42). The integral (4.42) is not only of importance in its own right but also serves as a 'generator' of other useful integral identities. Applying the differentiation operation $\partial^2_{j_n j_m}|_{\mathbf{j}=0}$ to the left and the right hand side of Eq. (4.42), we obtain the identity

$$\int d\mathbf{v} e^{-\frac{1}{2}\mathbf{v}^T\mathbf{A}\mathbf{v}} v_n v_m = (2\pi)^{N/2} \det \mathbf{A}^{-1/2} A^{-1}_{nm}.$$

Interpreting the Gaussian as a probability distribution, this result can be more compactly formulated as

$$\langle v_n v_m \rangle = A^{-1}_{nm}, \tag{4.43}$$

where

$$\langle \ldots \rangle \equiv (2\pi)^{-N/2} \det \mathbf{A}^{1/2} \int d\mathbf{v} e^{-\frac{1}{2}\mathbf{v}^T\mathbf{A}\mathbf{v}} (\ldots). \tag{4.44}$$

The differentiation operation leading to (4.43) can be iterated: Differentiating four times, we get

$$\langle v_m v_n v_q v_p \rangle = A^{-1}_{mn} A^{-1}_{qp} + A^{-1}_{mq} A^{-1}_{np} + A^{-1}_{mp} A^{-1}_{nq}.$$

One way of memorising the structure of this — important — integral is that the Gaussian 'expectation' value $\langle v_m v_n v_p v_q \rangle$ is given by all 'pairings' of type (4.43) that can be formed from the four components v_m. This rule generalises to expectation values of arbitrary order: $2n$-fold differentiation of (4.42) yields

$$\boxed{\langle v_{i_1} v_{i_2} \ldots v_{i_{2n}} \rangle = \sum_{\substack{\text{all possible} \\ \text{pairings of} \{i_1, \ldots i_{2n}\}}} A^{-1}_{i_{k_1} i_{k_2}} \ldots A^{-1}_{i_{k_{2n-1}} i_{k_{2n}}}} \tag{4.45}$$

This result is the mathematical identity underlying **Wick's theorem** (for real bosonic fields).

4.5.3 Complex Case

The results above are straightforwardly extended to multidimensional complex Gaussian integrals. The complex version of (4.41) is given by

$$\int d(\mathbf{v}^\dagger, \mathbf{v}) e^{-\mathbf{v}^\dagger \mathbf{A} \mathbf{v}} = \pi^N \det \mathbf{A}^{-1}, \tag{4.46}$$

where $\mathbf{v}$ is a complex N-component vector, $d(\mathbf{v}^\dagger, \mathbf{v}) \equiv \prod_{i=1}^N d\mathrm{Re}\, v_i d\mathrm{Im}\, v_i$, and $\mathbf{A}$ is a complex matrix with positive definite Hermitian part. (Remember that every matrix can be decomposed into a Hermitian and an anti-Hermitian component, $\mathbf{A} = \frac{1}{2}(\mathbf{A} + \mathbf{A}^\dagger) + \frac{1}{2}(\mathbf{A} - \mathbf{A}^\dagger)$.) For Hermitian $\mathbf{A}$, the proof of (4.46) is analogous to (4.41), i.e. $\mathbf{A}$ is unitarily diagonalisable, $\mathbf{A} = \mathbf{U}^\dagger \mathbf{A} \mathbf{U}$; the matrices $\mathbf{U}$ can be transformed into $\mathbf{v}$, the resulting integral factorises, etc. For non-Hermitian $\mathbf{A}$ the proof is more elaborate and we

refer to the literature. The generalization of (4.46) to exponents with linear contributions reads

$$\boxed{\int d(\mathbf{v}^\dagger, \mathbf{v}) e^{-\mathbf{v}^\dagger \mathbf{A}\mathbf{v} + \mathbf{w}^\dagger \cdot \mathbf{v} + \mathbf{v}^\dagger \cdot \mathbf{w}'} = \pi^N \det \mathbf{A}^{-1} e^{\mathbf{w}^\dagger \mathbf{A}^{-1} \mathbf{w}'}} \tag{4.47}$$

Note that $\mathbf{w}$ and $\mathbf{w}'$ may be *independent* complex vectors. The proof of this identity follows that of (4.42), i.e. by shifting $\mathbf{v}^\dagger \to \mathbf{v}^\dagger + \mathbf{w}^\dagger$, $\mathbf{v} \to \mathbf{v} + \mathbf{w}'$. (For an explanation of why $\mathbf{v}$ and $\mathbf{v}^\dagger$ may be shifted independently of each other, c.f. the analyticity remarks made in connection with (4.40).) As with Eq. (4.42), Eq. (4.47) may also serve as a generator of related integral identities. Differentiating the integral twice according to $\partial^2_{w_n, w'_m}|_{\mathbf{w}=\mathbf{w}'=0}$ gives

$$\langle \bar{v}_n v_m \rangle = A^{-1}_{mn},$$

where

$$\langle \cdots \rangle \equiv \pi^{-N} \det \mathbf{A} \int d(\mathbf{v}^\dagger, \mathbf{v}) e^{-\mathbf{v}^\dagger \mathbf{A}\mathbf{v}} (\cdots).$$

The iteration to more than two derivatives gives

$$\langle \bar{v}_n \bar{v}_m v_p v_q \rangle = A^{-1}_{pm} A^{-1}_{qn} + A^{-1}_{pn} A^{-1}_{qm}$$

and, eventually,

$$\boxed{\langle \bar{v}_{i_1} \bar{v}_{i_2} \ldots \bar{v}_{i_n} v_{j_1} v_{j_2} \ldots v_{j_n} \rangle = \sum_P A^{-1}_{j_1 i_{P1}} \ldots A^{-1}_{j_n i_{Pn}}}$$

where $\sum_P$ represents for the sum over all permutations of N integers.

4.5.4 Gaussian Functional Integration

With this preparation, we are in a position to investigate the main practice of quantum and statistical field theory — the method of Gaussian functional integration. Turning to Eq. (4.42), let us suppose that the components of the vector $\mathbf{v}$ parameterise the weight of a field on the sites of a one-dimensional lattice. In the continuum limit, the set $\{v_i\}$ translates to a function $v(x)$, and the matrix A_{ij} is replaced by an **operator** kernel or **propagator** $A(x, x')$. In this limit, the natural generalisation of Eq. (4.42) is

$$\begin{aligned} \int Dv(x) \exp\left[-\frac{1}{2} \int dx\ dx' v(x) A(x, x') v(x') + \int dx\ j(x) v(x) \right] \\ \propto (\det A)^{-1/2} \exp\left[\frac{1}{2} \int dx\ dx'\ j(x) A^{-1}(x, x') j(x') \right], \end{aligned} \tag{4.48}$$

where the inverse kernel $A^{-1}(x, x')$ satisfies the equation

$$\boxed{\int dx'\ A(x, x') A^{-1}(x', x'') = \delta(x - x''),} \tag{4.49}$$

i.e. $A^{-1}(x,x')$ can be interpreted as the **Green function** of the operator $A(x,x')$. The notation $Dv(x)$ is used to denote the measure of the functional integral. Although the constant of proportionality, $(2\pi)^N$ left out of Eq. (4.48) is formally divergent in the thermodynamic limit $N \to \infty$, it does not affect averages that are obtained from derivatives of such integrals. E.g., for Gaussian distributed functions, Eq. (4.43) generalises to

$$\boxed{\langle v(x)v(x')\rangle = A^{-1}(x,x')}.$$

Accordingly, Eq. (4.45) becomes

$$\boxed{\langle v(x_1)v(x_2)\dots v(x_{2n})\rangle = \sum_{\substack{\text{all possible}\\ \text{pairings of}\{x_1,\dots x_{2n}\}}} A^{-1}(x_{k_1},x_{k_2})\dots A^{-1}(x_{k_{2n-1}},x_{k_{2n}}).} \tag{4.50}$$

The generalization of the other Gaussian averaging formulae discussed above should be obvious.

To make sense of Eq. (4.48) one must interpret the meaning of the determinant, $\det A$. When the variables entering the Gaussian integral were discrete, the latter simply represented the determinant of the (real symmetric) matrix. In the present case, one must interpret A as an Hermitian operator having an infinite set of eigenvalues. The determinant represents the product over this infinite set.

To make these ideas more tangeable, let us consider a particular example. In dealing with quantum fluctuations in the Feynman path integral, we encountered the quadratic form

$$S[r] = \int dt' \left[\frac{m}{2}\dot{r}^2 - \frac{m\omega^2}{2}r^2\right],$$

which, integrating by parts, implies an operator kernel

$$A(t,t') = -\frac{m}{2}\left(\partial_t^2 + \omega^2\right)\delta(t-t').$$

Substituting into Eq. (4.49) and integrating we obtain $-(m/2)(\partial_t^2+\omega^2)A^{-1}(t) = \delta(t)$. The eigenfunctions of the operator $A(t,t')$ are simply plane waves, with eigenvalues $\epsilon(k) = m(k^2+\omega^2)/2$, where k denotes the corresponding wavevector, and $\det A = \prod_k \epsilon(k)$. A discussion of how to evaluate the determinant in this case can be found in the text.

4.6 Problem Set

4.6.1 Questions on the Feynman Path Integral

The questions in this section are aimed at developing a fluency with the path integral technique while at the same time exploring novel applications of the method.

Q1 Free Particle: Starting from first principles (i.e. *without* using the Feynman path integral), derive the propagator $G_{\rm free}(q_F, q_I; t) \equiv \langle q_F|e^{i\hat{p}^2 t/2m\hbar}|q_I\rangle\Theta(t)$ for a free particle. Check your result against Eq. (4.21) and compare it to the Green function of the diffusion equation $(D\partial_q^2 - \partial_\tau)G(q,\tau) = \delta(\tau)\delta(q)$. [Hint: try expanding the propagator in eigenfunctions of the free particle Hamiltonian.]

Q2 Harmonic Oscillator: (a) Starting with the Feynman path integral, show that the propagator for the one-dimensional quantum Harmonic oscillator, $\hat{H} = \hat{p}^2/2m + m\omega^2 q^2/2$, takes the form

$$\langle q_F|e^{-i\hat{H}\bar{t}/\hbar}|q_I\rangle = \left(\frac{m\omega}{2\pi i\hbar \sin\omega\bar{t}}\right)^{1/2} \exp\left[\frac{i}{2\hbar}m\omega\left(\left[q_I^2+q_F^2\right]\cot\omega\bar{t} - \frac{2q_I q_F}{\sin\omega\bar{t}}\right)\right].$$

[Hint: To find the prefactor as an infinite product of Gaussian integrals use the formula $z/\sin z = \prod_{n=1}^{\infty}(1 - z^2/\pi^2 n^2)^{-1}$.] Explain why the propagator varies periodically in the time interval $\bar{t}$, and discuss the origin of the singularities at $\bar{t} = n\pi/\omega$, $n = 1, 2, \cdots$. Taking the frequency $\omega \to 0$, show that the propagator for the free particle is recovered.

[Warning: While the remainder of this question should not be conceptually difficult to understand, nor technically difficult to formulate, it is algebraically demanding.]

†(b) Show that, if initially the state of the oscillator is a Gaussian function centred at the origin, $\psi(q, t=0) = (2\pi a)^{-1/4}\exp[-q^2/4a]$, then it will remain a Gaussian at all subsequent times. Obtain the width $a(t)$ of the Gaussian wavepacket as a function of time. [Hint: Note that the propagator is a Green function — therefore, by forming a convolution of the propagator with $\psi(q, t=0)$, one can determine the full time evolution of the wavepacket — i.e. $\psi(q,t) = \int dq' \langle q|e^{-i\hat{H}t/\hbar}|q'\rangle\psi(q',0)$.]

†(c) Study the *semiclassical* limit for the oscillator. For this purpose, take the initial state to be of the form

$$\psi(q, t=0) = (2\pi a)^{-1/4}\exp\left[\frac{i}{\hbar}mvq - \frac{1}{4a}q^2\right],$$

which corresponds to a wavepacket centered at an initial position q_0 with a velocity v. Find the state at $t > 0$ and determine the mean position, mean velocity, and mean width of the wavepacket as a function of time.

Q3 Density Matrix: Using the results of the previous question, obtain the density matrix

$$\rho(q, q') = \langle q|e^{-\beta\hat{H}}|q'\rangle$$

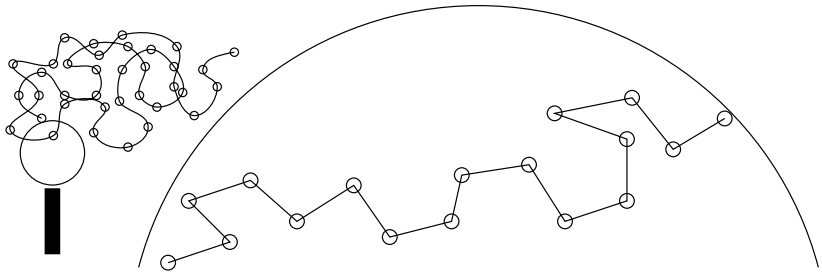

Figure 4.14: Freely jointed rod model of a single polymer chain.

for the oscillator at finite $\beta = 1/T$. Obtain and comment on the asymptotics: $T \ll \hbar\omega$ and $T \gg \hbar\omega$. [Hint: In the high temperature case, carry out the expansion in $\hbar\omega/T$ to second order.]

Q4 †**Classical Statistical Mechanics and Polymer Physics**: The field of polymer physics and soft condensed matter in general has benefited greatly from the application of field theoretic approaches. This trend perhaps began with the development of a theory of polymer dynamics within the framework of a statistical field theory. Borrowing formalism from the language of particle physics, Sir Sam Edwards[19] introduced a path integral approach which, with de Gennes and others established a complete theory of polymer dynamics.

At the crudest level, an ideal long-chain homopolymer (i.e. a polymer made up of identical monomers) can be modelled as a chain of rigid freely jointed rods (see Fig. 4.14). In equilibrium, the classical probability distribution function for the end-to-end distance $\mathbf{r}$ of a single N monomer chain in three dimensions is given by

$$P_N(\mathbf{r}) = \prod_{n=1}^{N} \int d^3\Delta\mathbf{r}_n \frac{1}{4\pi a^2} \delta\left(|\Delta\mathbf{r}_n| - a\right) \delta^{(3)}\left(\mathbf{r} - \sum_{n=1}^{N} \Delta\mathbf{r}_n\right),$$

where a represents the momoner length, and $4\pi a^2$ represents the normalisation. Such a simple model neglects 'excluded volume' effects from both 'self-interaction' of the chain, as well as interactions with neighbouring polymers in the melt.

[19] S. F. Edwards, Proc. Roy. Soc. Lond. **85**, 613 (1965); **88**, 265 (1966); **91**, 513 (1967); **92**, 9 (1967).

Sir Samuel Frederick Edwards 1928-, 1995 Boltzmann medal winner for providing a cornerstone to the modern theory of disordered systems. He was instrumental in bringing quantum field theory into statistical physics; he stimulated – and was at the forefront of – a new understanding of the statics and dynamics of polymeric systems, and he co-founded the subject of spin glasses.

Pierre-Gilles de Gennes 1932-, 1991 Nobel Laureate in Physics for discovering that methods developed for studying order phenomena in simple systems can be generalized to more complex forms of matter, in particular to liquid crystals and polymers.

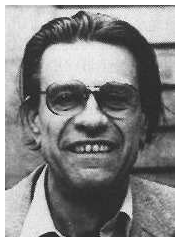

In the limit of large N, the distribution function can be easily shown (after Fourier transform, the integral can be performed exactly) to converge to the universal **random walk** result

$$P_N^{(0)}(\mathbf{r}) = \left(\frac{3}{2\pi N a^2}\right)^{3/2} \exp\left[-\frac{3\mathbf{r}^2}{2Na^2}\right].$$

Comparing this expression to the Euclidean time amplitude for a free quantum particle, the distribution function can be identified with the Feynman path integral

$$P_N^{(0)}(\mathbf{r}) = \int_{\substack{\mathbf{r}(0)=0 \\ \mathbf{r}(T)=\mathbf{r}}} D\mathbf{r} \exp\left[-\frac{1}{\hbar}\int_0^T d\tau \frac{m}{2}\dot{\mathbf{r}}^2\right],$$

where $T \mapsto Na$, and $m/\hbar \mapsto 3/a$. (This statement can be proved by explicit computation of the transmission amplitude — c.f. Q 1.) Although the end-to-end distribution agrees with the true polymer distribution for $|\mathbf{r}|/a \ll \sqrt{N}$, it is important to realise that the nature of the fluctuations in the two expressions is quite different. In the polymer expression, the length of each link $\Delta\mathbf{r}_n$ is fixed. For the free particle, each component fluctuates around zero mean with a mean square displacement $\langle(\Delta\mathbf{r}_n)^2\rangle = a\hbar/M \mapsto a^2/3$. Yet, if the end-to-end distance is small as compared to the completely stretched configuration, the distributions coincide. The aim of this question is to investigate the influence of rigidity on the form of the distribution function.

(a) Using the asymptotic form of the distribution function, determine the dependence of the second moment of the total length $\langle\mathbf{r}^2\rangle \equiv \int d\mathbf{r}\ \mathbf{r}^2 P_N^{(0)}(\mathbf{r})$ on the internal length of the chain Na. [Hint: remember that the integration runs over three dimensions.] How does this result compare with that for a Brownian random walk?

(b) The freely jointed chain model completely neglected steric constraints associated with a real polymer chain — a link would be prevented from retracing the path of its neighbour. In a crude approximation, this effect can be accommodated by incorporating a local rigidity for the polymer chain. At lowest order, the rigidity can be expressed in terms of the discrete (for the chain) or continuous (for the path integral) curvature through the potential

$$V_{\text{bend}} = \int_0^T d\tau \frac{\kappa}{2}\ddot{\mathbf{r}}^2$$

where κ represents the rigidity modulus (i.e. high values of the local curvature $\ddot{\mathbf{r}}$ are penalised).

Incorporating the potential into the path integral, show that the second moment of the end-to-end distance of the polymer chain can be expressed in the form

$$\langle(\mathbf{r}(T) - \mathbf{r}(0))^2\rangle = 4\hbar \int_{-\infty}^{\infty} \frac{d\omega}{2\pi} \frac{\sin^2(\omega T/2)}{m\omega^2 + \kappa\omega^4}.$$

[Hint: The average end-to-end distance can be expressed as a functional integral over all field configurations $\mathbf{r}(\tau)$ weighted by the total effective free energy or "action".

To evaluate the path integral you will find it convenient to regard the chain as one segment of an infinite chain thereby allowing the extension of the limits of the action to $\tau \in [-\infty, \infty]$. To evaluate the Gaussian functional integral, you will find it helpful to refer to section 4.5.4. Remember to include the normalisation of the classical average.]

(c) Evaluating this expression, obtain the long and short T asymptotics. Physically, how can one account for the different asymptotic scaling? Estimate the **persistence length** (i.e. the length over which the polymer remains rigid). [Hint: Evaluating the integral you may make use of the identity:

$$\int_{-\infty}^{\infty} \frac{d\omega}{2\pi} \frac{\sin^2(a\omega)}{\omega^2(1+\omega^2/\omega_0^2)} = \frac{a}{2}\left[1 - \frac{1}{2a\omega_0}\left(1 - e^{-2a\omega_0}\right)\right]. \qquad]$$

††(d) **Excluded volume effects**: Show that a non-local contact or self-interacting polymer chain, with

$$V_{\rm contact} = \frac{1}{2}\int_0^T d\tau d\tau' V_0 \delta^d\left(\mathbf{r}(\tau) - \mathbf{r}(\tau')\right),$$

can be mapped to a free particle moving in an Gaussian δ-correlated *imaginary* random quenched impurity distribution function. [Hint: Starting with the path integral of the free particle, integrate out the Gaussian impurity potential and show that the non-local contact interaction is induced.]

Phenomenological models of the type introduced above in the form of the functional field integral are known as **Ginzburg-Landau Models** . We will have more to say about such models at the end of chapter 5.

Q5 †**Confinement and Dissipation**: The macroscopic quantum tunnelling of a particle coupled to a set of external degrees of freedom gives rise to the phenomena of dissipation. The mechanism by which dissipation emerges has a natural interpretation within the framework of the Feynman path integral. The aim of this question is to derive and analyse the dissipative action.

A quantum particle of mass m is confined by a sinusoidal potential

$$U(q) = 2g\sin^2\left(\frac{\pi q}{q_0}\right).$$

(a) Employing the Euclidean (imaginary time) Feynman path integral,

$$\mathcal{Z} = \int Dq(\tau) e^{-S_{\rm part.}[q(\tau)]/\hbar}, \qquad S_{\rm part.}[q(\tau)] = \int_{-\infty}^{\infty} d\tau \left[\frac{m}{2}\dot{q}^2 + U(q)\right],$$

confirm by direct substitution that the maximal contribution to the propagator connecting two neighbouring degenerate minima ($q(\tau = -\infty) = 0$ and $q(\tau = \infty) = q_0$) is given by the instanton trajectory

$$\bar{q}(\tau) = \frac{2q_0}{\pi}\arctan\left(\exp\left[\omega_0\tau\right]\right), \qquad S[\bar{q}] = \frac{2}{\pi^2} m q_0^2 \omega_0,$$

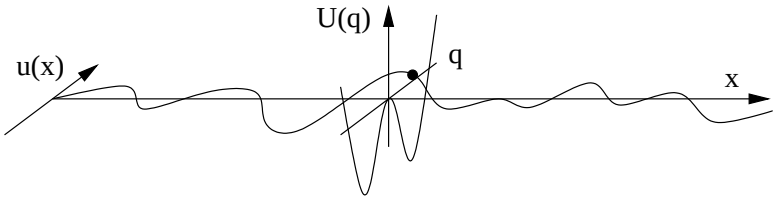

Figure 4.15: A particle confined by a periodic lattice potential and coupled to an infinite string.

where $\omega_0 = (2\pi/q_0)\sqrt{g/m}$. [NB: Although the equation of motion associated with the minimum of the Euclidean path integral is non-linear, the solution above is exact. It is known in the literature as a **soliton** configuration.]

(b) If the quantum particle is coupled at one point to an infinite "string" (see Fig. 4.15), the path integral is given by

$$\mathcal{Z} = \int Du(x,\tau) \int Dq(\tau)\, \delta\left(q(\tau) - u(\tau, x=0)\right) e^{-S_{\rm string}[u(x,\tau)]/\hbar - S_{\rm part.}[q(\tau)]/\hbar},$$

where the classical action of the string is given by (c.f. the action functional for phonons discussed in chapter 1.)

$$S_{\rm string}[u(x,\tau)] = \int_{-\infty}^{\infty} d\tau \int_{-\infty}^{\infty} dx \left[\frac{\rho}{2}\dot{u}^2 + \frac{\sigma}{2}\left(\frac{\partial u}{\partial x}\right)^2\right].$$

Here $\delta(q(\tau) - u(\tau, x=0))$ represents a functional δ-function which enforces the condition $q(\tau) = u(\tau, x=0)$ for all times τ. Operationally, it can be understood from the discretised form $\prod_n \delta(q(\tau_n) - u(\tau_n, x=0))$. The aim of the remainder of the problem is to investigate how the coupling of the particle to the external degrees of freedom (the string) influences the tunnelling probability.

By representing the functional δ-function as the functional integral

$$\delta(q(\tau) - u(\tau,0)) = \int Df(\tau) \exp\left[i\int_{-\infty}^{\infty} d\tau f(\tau)(q(\tau) - u(\tau,0))\right],$$

and performing the Gaussian integral over the Fourier components of the degrees of the freedom of the string, show that the dynamics of the particle is governed by the effective action

$$S_{\rm eff}[q] = S_{\rm part}[q] + \frac{\eta}{2}\int \frac{d\omega}{2\pi}|\omega||\widetilde{q}(\omega)|^2,$$

where $\eta = 2\sqrt{\rho\sigma}$, and $\widetilde{q}(\omega)$ denotes the Fourier transform

$$\widetilde{q}(\omega) = \int_{-\infty}^{\infty} dt\ q(t)e^{i\omega t}, \qquad q(t) = \int_{-\infty}^{\infty} \frac{d\omega}{2\pi}\widetilde{q}(\omega)e^{-i\omega t}.$$

[Hint: The calculation involves two separate functional integrations, the first over $\widetilde{u}(q,\omega)$, and the second over $f(\omega)$.]

(c) Treating the correction to the particle action as a perturbation, use your result from (a) to show that the effective action for an instanton-antinstanton pair

$$q(\tau) = \bar{q}(\tau + \bar{\tau}/2) - \bar{q}(\tau - \bar{\tau}/2),$$

where $\omega_0\bar{\tau} \gg 1$, is given *approximately* by

$$S_{\text{eff}}[q] = 2S_{\text{part}}[\bar{q}] - \frac{\eta q_0^2}{\pi}\ln(\omega_0\bar{\tau}).$$

[Hint: Note that, in finding the Fourier decomposition of $\bar{q}(\tau)$, a crude estimate is sufficient.]

(d) Using this result, estimate the typical separation of the pair, (i.e. interpret the overall action as an effective probability distribution function for $\bar{\tau}$ and evaluate $\langle\bar{\tau}\rangle = \int d\bar{\tau}\ \bar{\tau}e^{-S_{\text{eff}}}$). Comment on the implications of your result on the nature of the tunnelling probability.

Q6 Winding Numbers: Defining the Hamiltonian of a quantum particle confined to a ring by ($\hbar = 1$)

$$H = -\frac{1}{2I}\frac{\partial^2}{\partial\theta^2},$$

(a) Show that the quantum partition function is given by

$$\mathcal{Z} = \sum_{n=-\infty}^{\infty} \exp\left[-\beta\frac{n^2}{2I}\right] \tag{4.51}$$

where $\beta = 1/kT$.

(b) Cast as a Feynman Path integral, show that the quantum partition function takes the form

$$\mathcal{Z} = \int_0^{2\pi} d\theta \sum_{m=-\infty}^{\infty} \int_{\theta(0)=\theta}^{\theta(\beta)=\theta(0)+2\pi m} D\theta(\tau)\exp\left[-\frac{I}{2}\int_0^\beta d\tau\dot{\theta}^2\right].$$

(c) Minimising the Eulidean action with respect to θ, show that the path integral is minimised by the classical trajectories

$$\bar{\theta}(\tau) = \theta + 2\pi m\tau/\beta.$$

Parametrising a general path as $\theta(\tau) = \bar{\theta}(\tau) + \eta(\tau)$, where $\eta(\tau)$ is a path with no net winding, show that

$$\mathcal{Z} = 2\pi\mathcal{Z}_0 \sum_{m=-\infty}^{\infty} \exp\left[-\frac{I}{2}\frac{(2\pi m)^2}{\beta}\right], \tag{4.52}$$

where $\mathcal{Z}_0$ represents the quantum partition function for a free particle with open boundary conditions. Making use of the free particle propagator, show that $\mathcal{Z}_0 = \sqrt{I/2\pi\beta}$.

(d) Finally, making use of Poisson's summation formula,

$$\sum_{n=-\infty}^{\infty} h(n) = \sum_{m=-\infty}^{\infty} \int_{-\infty}^{\infty} d\phi h(\phi) e^{2\pi i m\phi},$$

show that Eq. (4.52) coincides with Eq. (4.51).

4.6.2 Answers

A1 Expanding the propagator in terms of the plain wave basis, we obtain

$$\begin{aligned}\langle q_F|e^{-i\hat{p}^2t/2m\hbar}|q_I\rangle &= \int_{-\infty}^{\infty} dp\langle q_F|p\rangle e^{-ip^2t/2m\hbar}\langle p|q_I\rangle \\ &= \int_{-\infty}^{\infty}\frac{dp}{2\pi\hbar}e^{ip(q_F-q_I)/\hbar}e^{-\tau p^2/2m\hbar} \\ &= \left(\frac{m}{2\pi i\hbar t}\right)e^{im(q_F-q_I)^2/2\hbar t},\end{aligned}$$

where $\tau \equiv -it$.

Equivalently, the free particle propagator is defined by

$$\left(i\hbar\partial_t - \frac{\hat{p}^2}{2m}\right)G(q,t) = \delta(q)\delta(t).$$

Setting $\hat{p} = -i\hbar\partial$, this result can be brought to the form of a standard diffusion propagator $(D\partial^2 - \partial_\tau)G(q,\tau) = \delta(q)\delta(\tau)$, by setting $D = \hbar^2/2m$, and applying the analytic continuation $\tau = it/\hbar$.

Focusing on the diffusion propagator, and applying a Fourier transform to the diffusion equation ($q \leftrightarrow k$, and $\tau \leftarrow \omega$), we obtain

$$G(k,\omega) = \frac{1}{i\omega - Dk^2}.$$

Fourier transforming back to real space and time, we obtain

$$G(q,\tau) = \frac{1}{(4\pi D\tau)^{1/2}}\exp\left[-\frac{q^2}{4D\tau}\right] = \left(\frac{m}{2\pi i\hbar t}\right)^{1/2}\exp\left[\frac{imq^2}{2\hbar t}\right].$$

A2 (a) The propagator is given by

$$\left\langle q_F|e^{-i\hat{H}\bar{t}/\hbar}|q_I\right\rangle = \int_{q(0)=q_I,q(\bar{t})=q_F} Dq(t)e^{iS[q(t)]/\hbar}, \qquad S = \int_0^{\bar{t}} dt\frac{m}{2}\left(\dot{q}^2 - \omega^2q^2\right).$$

Setting $q(t) = q_{\rm cl}(t) + \delta q(t)$ where $q_{\rm cl}(t)$ satisfies the classical equations of motion $m\ddot{q} = -m\omega^2 q_{\rm cl}$, and applying the boundary conditions we obtain the general solution

$$q_{\rm cl} = A\sin(\omega t) + B\cos(\omega t), \qquad B = q_I, \qquad A = \frac{q_F}{\sin(\omega\bar{t})} - q_I\cot(\omega\bar{t}).$$

Being Gaussian in the field q, the action separates as

$$S[q(t)] = S[q_{\rm cl}(t)] + S[\delta q(t)],$$

where

$$\begin{aligned} S[q_{\rm cl}] &= \frac{m}{2}\int_0^{\bar{t}} dt\,\left(\dot{q}_{\rm cl}^2 - \omega^2 q_{\rm cl}^2\right) \\ &= \frac{m\omega^2}{2}\left[(A^2-B^2)\frac{\sin(2\omega\bar{t})}{2\omega} + 2AB\frac{\cos(2\omega\bar{t})-1}{2\omega}\right] \\ &= \frac{m\omega}{2}\left[(q_I^2+q_F^2)\cot(\omega\bar{t}) - \frac{2q_Iq_F}{\sin(\omega\bar{t})}\right]. \end{aligned}$$

After treating the fluctuations (as described in the lecture notes) we obtain the result

$$\left\langle q_F|e^{-i\hat{H}\bar{t}/\hbar}|q_I\right\rangle = J(\bar{t})e^{iS[q_{\rm cl}]/\hbar}, \qquad J(\bar{t}) = \left(\frac{m\omega}{2\pi i\hbar\sin(\omega\bar{t})}\right)^{1/2},$$

periodic in $\bar{t}$ with frequency ω, and singular at $\bar{t} = n\pi/\omega$. In fact

$$\left\langle q_F|e^{-i\hat{H}\bar{t}/\hbar}|q_I\right\rangle \mapsto \begin{cases} \delta(q_F-q_I) & \bar{t} = 2\pi n/\omega, \\ \delta(q_F+q_I) & \bar{t} = \pi(2n+1)/\omega. \end{cases}$$

Physically, the reason for the singularity is clear: the harmonic oscillator is peculiar in having a spectrum with energies uniformly spaced in units of $\hbar\omega$. This means that when $\hbar\omega \times t/\hbar = 2\pi \times$ integer there is a coherent superposition of the states and the initial state is recovered.

(b) Given the initial condition $\psi(q, t=0)$, the time evolution of the wavepacket can be determined from the propagator as

$$\begin{aligned} \psi(q,t) &= \int_{-\infty}^{\infty} dq' \left\langle q|e^{-i\hat{H}t/\hbar}|q'\right\rangle \psi(q',0) \\ &= J(t)\int_{-\infty}^{\infty} dq' \frac{1}{(2\pi a)^{1/4}} e^{-q'^2/4a} e^{\frac{i}{\hbar}\frac{m\omega}{2}\left([q^2+q'^2]\cot(\omega t) - \frac{2qq'}{\sin(\omega t)}\right)} \end{aligned}$$

where $J(t)$ represents the time-dependent contribution arising from the fluctuations around the classical trajectory. Being Gaussian in q', the integral can be performed explicitly. Setting

$$\alpha = \frac{1}{2a} - \frac{i}{\hbar}m\omega\cot(\omega t), \qquad \beta = \frac{i}{\hbar}m\omega\frac{q}{\sin(\omega t)},$$

and performing the Gaussian integral over q', we obtain

$$\psi(q,t) = J(t)\frac{1}{(2\pi a)^{1/4}}\sqrt{\frac{2\pi}{\alpha}}e^{\beta^2/2\alpha}\exp\left[\frac{i}{2\hbar}m\omega q^2\cot(\omega t)\right]$$

Using the identity

$$\frac{\beta^2}{2\alpha} = -\frac{q^2}{4a(t)}\left(1 + i\kappa\cot(\omega t)\right)$$

where

$$a(t) = a\left[\cos^2(\omega t) + \kappa^{-2}\sin^2(\omega t)\right], \qquad \kappa = 2am\omega/\hbar,$$

we obtain

$$\psi(q,t) = \frac{1}{(2\pi a(t))^{1/4}}\exp\left[-\frac{q^2}{4a(t)}\right]e^{i\varphi(q,t)}$$

where $\varphi(q,t)$ represents a pure phase.[20] As required, under the action of the propagator, the normalisation of the wavepacket is preserved. Note that, if $a = \hbar/2m\omega$ (i.e. $\kappa = 1$), $a(t) = a$ for all times — i.e. it is a pure eigenstate.

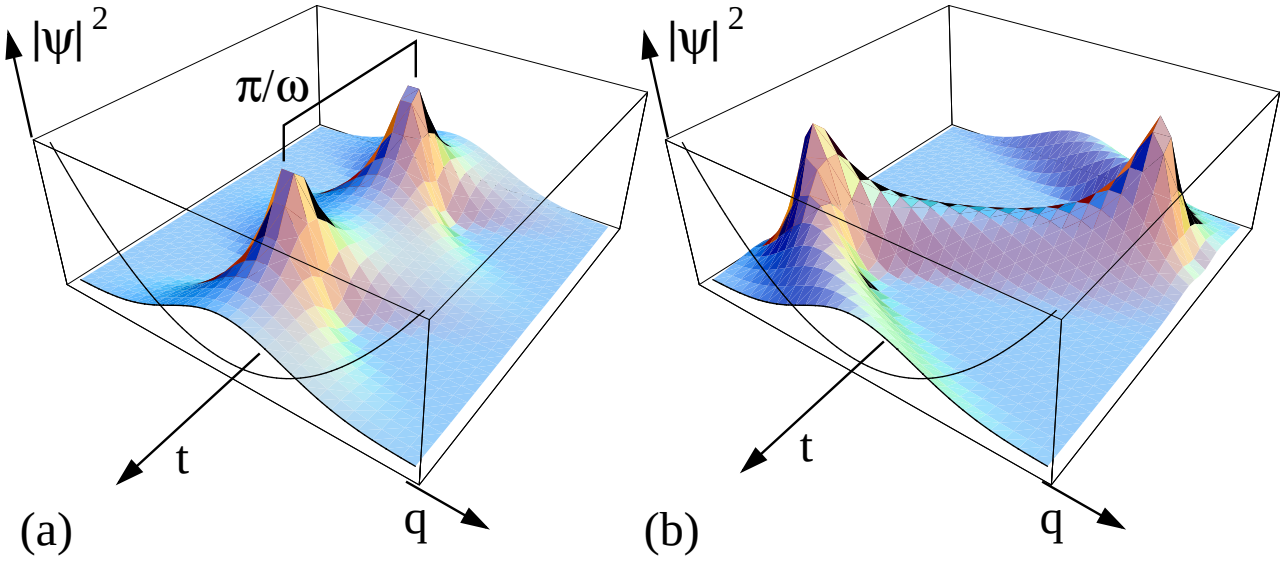

Figure 4.16: (a) Variation of a "stationary" Gaussian wavepacket in the harmonic oscillator taken from the solution, and (b) variation of the moving wavepacket.

(c) Still of a Gaussian form, the integration can again be performed explicitly for the new initial condition. In this case, we obtain an expression of the form above but with

$$\beta = \frac{i}{\hbar}\frac{m\omega}{\sin(\omega t)}\left(q - \frac{v}{\omega}\sin(\omega t)\right).$$

Reading off the coefficients, we find that the position and velocity of the wavepacket have the form

$$q_0(t) = \frac{v}{\omega}\sin(\omega t), \qquad v(t) = v\cos(\omega t).$$

coinciding with that of the classical dynamics. Note that, as above, the width $a(t)$ of the wavepacket oscillates at frequency ω.

[20] For completeness, we note that

$$\varphi(q,t) = -\frac{1}{2}\tan^{-1}\left(\frac{1}{\kappa}\cot(\omega t)\right) - \frac{\kappa q^2}{4a}\cot(\omega t)\left(\frac{a}{a(t)} - 1\right).$$

A3 The density matrix can be deduced from the general solution to problem 1:

$$\begin{aligned}\rho(q,q') &= \langle q|e^{-\beta H}|q'\rangle = \langle q|e^{-(i/\hbar)H(\hbar\beta/i)}|q'\rangle \\ &= \left(\frac{m\omega}{2\pi\hbar\sinh(\beta\hbar\omega)}\right)^{1/2}\exp\left[-\frac{m\omega}{2\hbar}\left((q^2+q'^2)\coth(\beta\hbar\omega)-\frac{2qq'}{\sinh(\beta\hbar\omega)}\right)\right].\end{aligned}$$

(i) In the low temperature limit $T \ll \hbar\omega$ ($\beta\hbar\omega \gg 1$), $\coth(\beta\hbar\omega)\to 1$, $\sinh(\beta\hbar\omega)\to e^{\beta\hbar\omega}/2$, and

$$\begin{aligned}\rho(q,q') &\to \left(\frac{m\omega}{\pi\hbar e^{\beta\hbar\omega}}\right)^{1/2}\exp\left[-\frac{m\omega}{2\hbar}(q^2+q'^2)\right] \\ &= \langle q|n=0\rangle\, e^{-\beta E_0}\,\langle n=0|q'\rangle\,.\end{aligned}$$

(ii) In the high temperature limit $T \gg \hbar\omega$, $\coth(\beta\hbar\omega)\to 1/\beta\hbar\omega - \beta\hbar\omega/3$, $1/\sinh(\beta\hbar\omega)\to 1/\beta\hbar\omega-\beta\hbar\omega/6$, and

$$\begin{aligned}\rho(q,q') &\to \left(\frac{m}{2\pi\beta\hbar^2}\right)^{1/2} e^{-m(q-q')^2/2\beta\hbar^2}\exp\left[-\frac{\hbar\beta m\omega^2}{6\hbar}(q^2+q'^2+qq')\right] \\ &\approx \delta(q-q')\exp\left[-\frac{\beta m\omega^2 q^2}{2}\right],\end{aligned}$$

the Maxwell-Boltzmann distribution!

A4 The aim of this problem is two-fold: the first is to further expose the correspondence between the quantum mechanical propagator and classical statistical mechanics. The second goal is to develop the notion of correlation functions from the path integral in the framework of a classical problem.

(a) Evaluating the second moment of the Gaussian distribution function, we find

$$\langle \mathbf{r}^2\rangle = \frac{3\hbar T}{m} \mapsto Ta.$$

(b) To sum over all field configurations of $\mathbf{r}$, we can extend the range of integration in the action to $\tau\in[-\infty,\infty]$ and sum over arbitrary configurations $\mathbf{r}(\tau)$. Setting

$$\mathbf{r}(\tau) = \int_{-\infty}^{\infty}\frac{d\omega}{2\pi}e^{i\omega\tau}\mathbf{r}(\omega),$$

we obtain

$$\left\langle(\mathbf{r}(T)-\mathbf{r}(0))^2\right\rangle = \int_{-\infty}^{\infty}\frac{d\omega}{2\pi}\int_{-\infty}^{\infty}\frac{d\omega'}{2\pi}\left(e^{i\omega T}-1\right)\left(e^{i\omega' T}-1\right)\langle\mathbf{r}(\omega)\cdot\mathbf{r}(\omega')\rangle_{\mathbf{r}(\omega)}$$

where, defining the normalisation (or partition function) $\mathcal{Z}$,

$$\langle\cdots\rangle_{\mathbf{r}(\omega)} = \frac{1}{\mathcal{Z}}\int D\mathbf{r}\cdots\exp\left[-\frac{1}{\hbar}\int_{-\infty}^{\infty}\frac{d\omega}{2\pi}\frac{1}{2}(m\omega^2+\kappa\omega^4)|\mathbf{r}(\omega)|^2\right].$$

Diagonal in the fields $\mathbf{r}(\omega)$, the integral over the Gaussian complex fields is easily performed and yields

$$\langle r_i(\omega) r_j(\omega') \rangle = \delta_{ij} 2\pi\delta(\omega - \omega') \frac{1}{\hbar(m\omega^2 + \kappa\omega^4)}$$

from which we obtain the expression sought in the question.

(c) Applying the integral identity, we obtain the final result

$$\left\langle (\mathbf{r}(T) - \mathbf{r}(0))^2 \right\rangle = \frac{3T}{\hbar m} \left[1 - \frac{1}{T}\sqrt{\frac{\kappa}{m}} \left(1 - e^{-T\sqrt{m/\kappa}} \right) \right],$$

from which we obtain the asymptotics

$$\left\langle (\mathbf{r}(T) - \mathbf{r}(0))^2 \right\rangle = \begin{cases} 3T/\hbar m & T\sqrt{m/\kappa} \gg 1, \\ 3T^2/2\hbar\sqrt{m\kappa} & T\sqrt{m/\kappa} \ll 1. \end{cases}$$

The physical interpretation of this result is clear: On chain length scales $T \gg \sqrt{\kappa/m}$ the chain rigidity has no effect, and the configurations coincide with the random walk. In the opposite limit, the rigidity of the chain dominates and the walk is directly, $r_{\rm rms} \sim Ta$. The length scale $a\sqrt{\kappa/m}$ therefore has the interpretation of a persistence length.

A5 This problem concerns the interaction of a discrete quantum particle with a fluctuating string. Our aim is to find the influence of the external fluctuations on the tunneling probability of the particle. Such problems fall under the category of macroscopic quantum tunneling.

(a) Expressed as a Euclidean time path integral, the transition probability is given by

$$\mathcal{Z} = \int Dq(\tau) e^{-S[q(\tau)]/\hbar}, \qquad S[q] = \int_0^\infty d\tau \left[\frac{m}{2}\dot{q}^2 + U(q) \right],$$

where the confining potential takes the form

$$U(q) = 2g \sin^2\left(\frac{\pi q}{q_0} \right).$$

The corresponding classical equation of motion is given by the **Sine-Gordon Equation**

$$m\ddot{q} - \frac{2\pi g}{q_0} \sin\left(\frac{2\pi q}{q_0} \right) = 0.$$

Applying the trial solution

$$\bar{q}(\tau) = \frac{2q_0}{\pi} \tan^{-1}\left(e^{\omega_0 \tau} \right),$$

we find the equation is satisfied if $\omega_0 = (2\pi/q_0)\sqrt{g/m}$.

From this result we obtain the "classical" action

$$\begin{aligned} S[\bar{q}] &= \int_0^\infty d\tau \left[\frac{m}{2}\dot{\bar{q}}^2 + U(\bar{q})\right] = \int_0^\infty d\tau m\dot{\bar{q}}^2 = m\int_0^{q_0} dq\dot{\bar{q}} \\ &= 2\frac{mq_0^2}{\pi^2}\omega_0. \end{aligned}$$

(b) In Fourier space, the action of the classical string takes the form

$$S_{\text{string}} = \int_{-\infty}^{\infty}\frac{d\omega}{2\pi}\int_{-\infty}^{\infty}\frac{dk}{2\pi}\frac{1}{2}(\rho\omega^2 + \sigma k^2)|u(\omega,k)|^2.$$

Representing the functional δ-function as the integral

$$\int Df \exp\left[i\int_{-\infty}^{\infty}\frac{d\omega}{2\pi}f(\omega)\left(q(-\omega) - \int_{-\infty}^{\infty}\frac{dk}{2\pi}u(-\omega,-k)\right)\right],$$

and performing the integral over the degrees of freedom of the string, we obtain

$$\int Due^{-S_{\text{string}}/\hbar - i\int d\tau f(\tau)u(\tau,0)} = \text{const.} \times \exp\left[-\int_{-\infty}^{\infty}\frac{d\omega}{2\pi}\int_{-\infty}^{\infty}\frac{dk}{2\pi}\frac{1}{2}\frac{\hbar}{(\rho\omega^2+\sigma k^2)}|f(\omega)|^2\right].$$

Applying the integral

$$\int_{-\infty}^{\infty}\frac{dk}{2\pi}\frac{1}{\rho\omega^2+\sigma k^2} = \frac{1}{|\omega|\eta},$$

where $\eta = \sqrt{\rho\sigma}$, and performing the Gaussian functional integral over the Lagrange multiplier $f(\omega)$, we obtain the effective action

$$S_{\text{eff}} = S_{\text{part.}} + \frac{\eta}{2}\int_{-\infty}^{\infty}\frac{d\omega}{2\pi}|\omega||q(\omega)|^2.$$

(c) Approximating the instanton/anti-instanton pair $q(\tau) = \bar{q}(\tau+\bar{\tau}) - \bar{q}(\tau-\bar{\tau})$ by a "top-hat" function we find

$$q(\omega) = \int_{-\bar{\tau}/2}^{\bar{\tau}/2} d\tau q_0 e^{i\omega\tau} = q_0\bar{\tau}\frac{\sin(\omega\bar{\tau}/2)}{(\omega\bar{\tau}/2)}.$$

Treating the dissipative term as a perturbation, we obtain the action

$$S_{\text{eff}} - S_{\text{part}} = \frac{\eta}{2}\int_0^{\omega_0}\frac{d\omega}{2\pi}|\omega|(q_0\bar{\tau})^2\frac{\sin^2(\omega\bar{\tau}/2)}{(\omega\bar{\tau}/2)^2},$$

where ω_0 serves as a high frequency cut-off. Taking $\omega\bar{\tau} \gg 1$ we obtain the approximate integral

$$2\times\frac{\eta}{4}\int_{1/\bar{\tau}}^{\omega_0}\frac{d\omega}{2\pi}q_0^2\frac{4}{\omega} = \frac{q_0^2}{\pi}\eta\ln(\omega_0\bar{\tau}).$$

Employing this result as a probability distribution, we find

$$\langle \bar{\tau} \rangle = \int d\bar{\tau} \bar{\tau} \exp\left[-\frac{q_0^2}{\pi\hbar} \eta \ln(\omega_0 \bar{\tau}) \right] \sim \text{const.} \times \int^{\infty} d\bar{\tau} \bar{\tau}^{1 - q_0^2 \eta / \pi\hbar}.$$

The divergence of the integral shows that for

$$\eta > \frac{2\pi\hbar}{q_0^2}$$

instanton/anti-instanton pairs are confined and particle tunnelling is prohibited.

A6 (a) Solving the Schrödinger equation, the wavefunctions obeying periodic boundary conditions take the form $\psi_m = e^{im\theta}$, m integer, and the eigenvalues are given by $E_m = m^2/2I$. Defining the quantum partition function as $\mathcal{Z} = \text{tr } e^{-\beta H}$ we obtain the formula in the text.

(b) Interpreted as a Feynman path integral, the quantum partition function takes the form of a propagator with

$$\mathcal{Z} = \int_0^{2\pi} d\theta \ \langle \theta | e^{-\beta \hat{H}} | \theta \rangle = \int_0^{2\pi} d\theta \int_{\theta(\beta)=\theta(0)=\theta} D\theta(\tau) \exp\left[-\int_0^{\beta} d\tau \mathcal{L} \right],$$

where the $\mathcal{L} = I\dot{\theta}^2/2$ denotes the Lagrangian. The trace implies that paths $\theta(\tau)$ must start and finish at the same point. However, to accommodate the invariance of the field configuration θ under translation by 2π we must must impose the boundary conditions shown in the question.

(c) Varying the action with respect to θ we obtain the classical equation $I\ddot{\theta} = 0$. Solving this equation subject to the boundary conditions, we obtain the solution given in the question. Evaluating the Euclidean action, one finds

$$\int_0^{\beta} (\partial_\tau \theta)^2 d\tau \ = \ \int_0^{\beta} \left[\frac{2\pi m}{\beta} + \partial_\tau \eta \right]^2 d\tau = \beta \left(\frac{2\pi m}{\beta} \right)^2 + \int_0^{\beta} (\partial_\tau \eta)^2 d\tau.$$

Thus, we obtain the partition function

$$\mathcal{Z} = \mathcal{Z}_0 \sum_{m=-\infty}^{\infty} \exp\left[-\frac{I}{2} \frac{(2\pi m)^2}{\beta} \right],$$

where

$$\mathcal{Z}_0 = \int D\eta(\tau) \exp\left[-\frac{I}{2} \int_0^{\beta} (\partial_\tau \eta)^2 d\tau \right] = \sqrt{\frac{I}{2\pi\beta}}.$$

denotes the free particle partition function. The latter can be obtained from direct evaluation of the free particle propagator (c.f. Problem 1).

(d) Applyly the Poisson summation formula with

$$h(x) = \exp\left[-\beta \frac{x^2}{2I} \right],$$

we find

$$\begin{aligned}\sum_{n=-\infty}^{\infty} \exp\left[-\beta\frac{x^2}{2I}\right] &= \sum_{n=-\infty}^{\infty}\int_{-\infty}^{\infty} d\phi \exp\left[-\beta\frac{\phi^2}{2I} + 2\pi i m\phi\right] \\ &= \sqrt{\frac{2\pi I}{\beta}}\sum_{m=-\infty}^{\infty}\exp\left[-\frac{I}{2}\frac{(2\pi m)^2}{\beta}\right].\end{aligned}$$

———————————————————————

Chapter 5

Functional Field Theory

In this short, relatively dry and absolutely essential chapter the concept of path integration is generalized to integration over quantum fields. I.e. we will develop an approach to quantum field theory that takes an integration over all configurations of a given field, weighted by an appropriate action, as its starting point. Methodologically, the formalism introduced in this chapter represents the backbone of the remainder of the book. This being so, conceptual aspects stand in the foreground and the discussion of applications is reduced to a minimum.

In this chapter, the concept of path integration will be extended from quantum mechanics to quantum field theory. Our starting point will be from a situation similar to the one outlined at the beginning of the previous chapter. Just as there are two different approaches to quantum mechanics, quantum field theory can also be formulated in two different ways: The formalism of canonically quantised field operators, and functional integration. As for the former, although much of the technology needed to efficiently implement this approach — essentially Feynman diagrams — originated in high energy physics, it was with the development of condensed matter physics through the 50's, 60's and 70's that this approach was driven to unprecedented sophistication. The reason is that, almost as a rule, the condensed matter problems investigated at that time necessitated perturbative summations to *infinite* order in the non-trivial content of the theory (typically interactions). This requirement led to the development of advanced techniques to sum up (subsets of) the perturbation series in many body interaction operators to infinite order.

In the 70's, however, essentially *non-perturbative* problems began to attract more and more attention — a still prevailing trend — and it turned out that the formalism of canonically quantised operators was not tailored to this type of physics. However, the alternative approach to many-body problems, functional integration, is ideally suited! The situation is similar to the one described in the last chapter where we saw that the Feynman path integral provided an entire spectrum of novel routes to approaching quantum mechanical problems (controlled semi-classical limits, analogies to classical mechanics, statistical mechanics, concepts of topology and geometry, etc.). Similarly, the introduction of functional

field integration into many-body physics spawned plenty of new theoretical developments, many of which were manifestly non-perturbative. Moreover, the advantages of the path integral approach in many-body physics is even more pronounced than in single particle quantum mechanics. Higher dimensionality introduces fields of a more complex internal structure allowing for non-trivial topology while, at the same time, the connections to classical statistical mechanics play a much more important role than in single particle quantum mechanics.

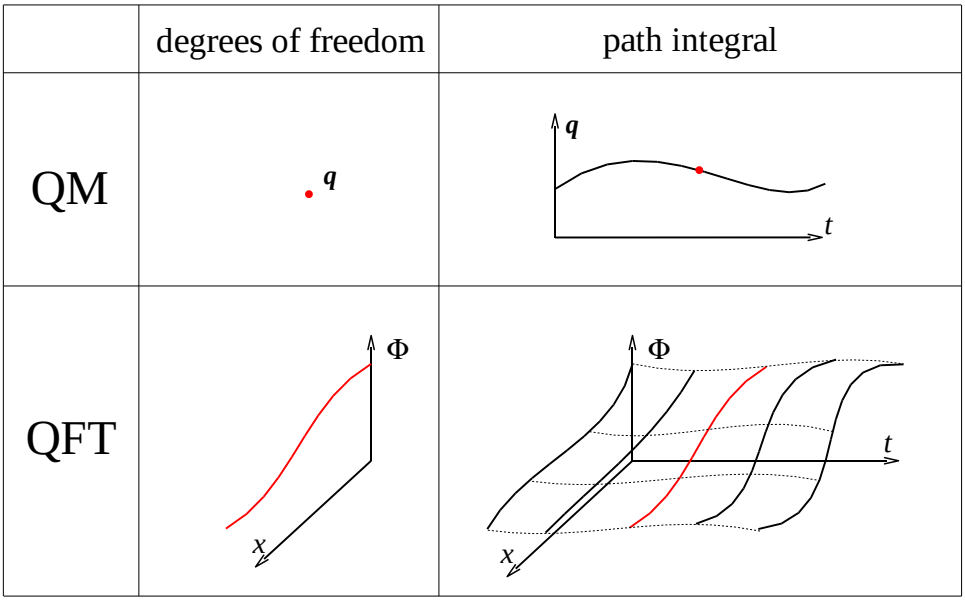

Figure 5.1: The concept of field integration. Upper panels: path integral of quantum mechanics. Integration over all time dependent configurations of a point degree of freedom leads to integrals over *curves*. Lower panels: field integral. Integration over time dependent configurations of d-dimensional continuum mappings (fields) leads to integrals over generalized $d+1$ *surfaces*

All these concepts will begin to play a role in subsequent chapters when applications of the field integral are discussed. However, the first issue we need address is how the new formalism actually looks like. Before embarking on the quantitative construction – the subject of the following sections – let us anticipate a little and discuss what kind of structures we shall have to expect. In quantum mechanics, we were starting from a single point degree of freedom, characterized by some coordinate $\mathbf{q}$ (or some other quantum numbers for that matter). Path integration then meant integration over all time dependent configurations $\mathbf{q}(t)$, i.e. a set of *curves* $t \mapsto \mathbf{q}(t)$ (see Fig. 5.1 upper panel.) In contrast, the degrees of freedom of field theory are continuous objects $\Phi(x)$ by themselves, where x parameterizes some d-dimensional base manifold and Φ takes values in some target manifold (Fig. 5.1, lower panel.) The natural generalization of a 'path' integral then implies integration over a single copy of these objects at each instance of time. I.e. we shall have to integrate over generalized *surfaces*, mappings from $(d+1)$-dimensional space-time into the field manifold, $(x,t) \mapsto \Phi(x,t)$. While this notion may sound worrysome, it is important to realize that, conceptually, nothing much changes in

comparison with the path integral. Only that instead of a 1-dimensional manifold – a curve – our object of integration will be a $(d+1)$-dimensional manifold.

We next proceed to formulate these ideas in quantitative terms.

▷ EXERCISE. If necessary, recapitulate the general construction scheme of path integrals (section **??**) and the connection between quantum fields and second quantized operators (page 53.)

5.1 Construction of the Many-Body Path Integral

The construction of a path integral for field operators follows the general scheme outlined at the end of section **??**. I.e. the basic idea will be to segment the time evolution of a quantum (many body) Hamiltonian into infinitesimal time slices and to absorb as much as is possible of the quantum dynamical phase accumulated during the short time propagation into a set of suitably chosen eigenstates. However, how would these operators look like? In the context of single particle quantum mechanics, the answer was clear, i.e. the basic structure of the Hamiltonian suggested to chose a representation in terms of coordinate and momentum eigenstates. Now, given that many particle Hamiltonians are conveniently expressed in terms of creation/annihilation operators, an obvious idea would be to search for eigenstates of *these* operators. Such states indeed exist and are called **coherent states**.

5.1.1 Coherent States (Bosons)

Our goal is therefore to find eigenstates of the Fock space operators $a^\dagger$ and a. Although the general form of these states will turn out to be the same for bosons and fermions, there are major differences regarding their algebraic structure. The point is that the anticommutation relations of fermions require that the eigenvalues of an annihilation operator themselves anticommute, i.e. they *cannot* be ordinary numbers. Postponing the introduction of the unfamiliar concept of anticommuting 'numbers' to the next section, we first concentrate on the bosonic case where problems of this kind do not arise.

So what form do the eigenstates $|\phi\rangle$ of the bosonic Fock space operators a, and $a^\dagger$ take? Being a state of the Fock space, an eigenstate $|\phi\rangle$ can be expanded as

$$|\phi\rangle = \sum_{n_1,n_2,\cdots} C_{n_1,n_2,\cdots}|n_1,n_2\cdots\rangle, \qquad |n_1,n_2\cdots\rangle = \frac{(a_1^\dagger)^{n_1}}{\sqrt{n_1}}\frac{(a_2^\dagger)^{n_2}}{\sqrt{n_2}}\cdots|0\rangle$$

where $a_i^\dagger$ creates a boson in state i, $C_{n_1,n_2,\cdots}$ represents a set of expansion coefficients, and $|0\rangle$ represents the vacuum. Here, for reasons of clarity, it is convenient to adopt this convention for the vacuum as opposed to the notation $|\Omega\rangle$ used previously. Furthermore, the many-body state $|n_1,n_2\cdots\rangle$ is indexed by a set of occupation numbers: n_1 in state $|1\rangle$, n_2 in state $|2\rangle$, and so on. Importantly, the state $|\phi\rangle$ can, in principle (and will in practice) contain a superposition of basis states which have different numbers of particles.

Now, if the minimum number of particles in state $|\phi\rangle$ is n_0, the minimum of $a_i^\dagger|\phi\rangle$ must be n_0+1. Clearly the *creation* operators $a_i^\dagger$ *cannot* possess eigenstates.

However, with annihilation operators this problem need not not arise. Indeed, the annihilation operators do possess eigenstates known as **bosonic coherent states**

$$\boxed{|\phi\rangle \equiv \exp\Big[\sum_i \phi_i a_i^\dagger\Big]|0\rangle} \tag{5.1}$$

where the elements of $\phi = \{\phi_i\}$ represent a set of complex numbers. The states $|\phi\rangle$ are eigenstates in the sense that, for all i

$$\forall i: \quad \boxed{a_i|\phi\rangle = \phi_i|\phi\rangle} \tag{5.2}$$

i.e. they simultaneously diagonalise *all* annihilation operators. Noting that a_i and $a_j^\dagger$, with $j \neq i$, commute, Eq. (5.2) can be verified by showing that $a\exp(\phi a^\dagger)|0\rangle = \phi\exp(\phi a^\dagger)|0\rangle$. Using the result $[a,(a^\dagger)^n] = n(a^\dagger)^{n-1}$ (cf. Eq. 3.34) a Taylor expansion shows

$$\begin{aligned} a\exp(\phi a^\dagger)|0\rangle &= [a,\exp(\phi a^\dagger)]|0\rangle = \sum_{n=0}^{\infty}\frac{\phi^n}{n!}[a,(a^\dagger)^n]|0\rangle \\ &= \sum_{n=1}^{\infty}\frac{n\phi^n}{n!}(a^\dagger)^{n-1}|0\rangle = \phi\sum_{n=1}^{\infty}\frac{\phi^n}{(n-1)!}(a^\dagger)^{n-1}|0\rangle = \phi\exp(\phi a^\dagger)|0\rangle. \end{aligned}$$

Before utilise the coherent states for constructing a path integral, we need to discuss a few more of their properties:

▷ By taking the Hermitian conjugate of Eq. (5.2), we find that the 'bra' associated with the 'ket' $|\phi\rangle$ is a left eigenstate of the set of creation operators, i.e.

$$\forall i: \quad \boxed{\langle\phi|a_i^\dagger = \langle\phi|\bar{\phi}_i} \tag{5.3}$$

where $\bar{\phi}_i$ is the complex conjugate of ϕ_i, and $\langle\phi| = \langle 0|\exp[\sum_i \bar{\phi}_i a_i]$.

▷ It is a straightforward matter — e.g. by a Taylor expansion of Eq. (5.1) – to show that the action of a creation operator on a coherent state is given by

$$\forall i: \quad \boxed{a_i^\dagger|\phi\rangle = \partial_{\phi_i}|\phi\rangle} \tag{5.4}$$

Note that Eqs. (5.4) and (5.2) are consistent with the commutation relations $[a_i, a_j^\dagger] = \delta_{ij}$:

$$\begin{aligned} [a_i, a_j^\dagger]|\phi\rangle &= (a_i a_j^\dagger - a_j^\dagger a_i)|\phi\rangle \\ &= (\partial_{\phi_j}\phi_i - \phi_i\partial_{\phi_j})|\phi\rangle = |\phi\rangle. \end{aligned}$$

▷ The overlap between two coherent states is given by

$$\boxed{\langle\theta|\phi\rangle = \exp\Big[\sum_i \bar{\theta}_i\phi_i\Big]} \tag{5.5}$$

The proof of this identity proceeds as follows:

$$\langle\theta|\phi\rangle = \langle 0|e^{\sum_i \bar{\theta}_i a_i}|\phi\rangle = e^{\sum_i \bar{\theta}_i\phi_i}\langle 0|\phi\rangle = e^{\sum_i \bar{\theta}_i\phi_i},$$

where the third equality is due to (5.1).

▷ Evaluating (5.5) for $|\theta\rangle = |\phi\rangle$ gives the norm of a coherent state,

$$\boxed{\langle\phi|\phi\rangle = e^{\sum_i \bar{\phi}_i\phi_i}} \tag{5.6}$$

▷ Most importantly, the coherent states form a complete — in fact an overcomplete — set of states in Fock space:

$$\boxed{\int\prod_i \frac{d\bar{\phi}_i d\phi_i}{\pi} e^{-\sum_i \bar{\phi}_i\phi_i}|\phi\rangle\langle\phi| = 1_{\mathcal{F}}} \tag{5.7}$$

where $d\bar{\phi}_i d\phi_i = d\mathrm{Re}\,\phi_i d\mathrm{Im}\,\phi_i$, and $1_{\mathcal{F}}$ represents the unit operator or identity in the Fock space.

▷ INFO. The last result is most conveniently proven by means of **Schur's lemma**. In essence, Schur's lemma – which is proven in almost any textbook on group representation theory – states the following: Suppose we are given a linear irreducible representation of a group algebra $\{\hat{A}\}$. (In our case, the algebra will be given by the set of all operators $\{a_i, a_i^\dagger\}$. These operators act linearly in Fock space – a linear 'representation'. The representation is 'irreducible', i.e. all states can be reached by action of operators onto a single reference state (the vacuum).) Schur's lemma then states that an operator $\hat{X}$ that commutes with all generators of the algebra, $\forall\hat{A} : [\hat{A}, \hat{X}] = 0$, is proportional to the unit operator.

The proof that the operator on the left hand side of (5.7) commutes with the annihilation operators a_i proceeds as follows:

$$\begin{aligned} a_i \int d[\bar{\phi},\phi] e^{-\sum_i \bar{\phi}_i\phi_i}|\phi\rangle\langle\phi| &= \int d[\bar{\phi},\phi] e^{-\sum_i \bar{\phi}_i\phi_i}\phi_i|\phi\rangle\langle\phi| \\ &= -\int d[\bar{\phi},\phi]\left(\partial_{\bar{\phi}_i} e^{-\sum_i \bar{\phi}_i\phi_i}\right)|\phi\rangle\langle\phi| \overset{\text{by parts}}{=} \int d[\bar{\phi},\phi] e^{-\sum_i \bar{\phi}_i\phi_i}|\phi\rangle\left(\partial_{\bar{\phi}_i}\langle\phi|\right) \\ &= \int d[\bar{\phi},\phi] e^{-\sum_i \bar{\phi}_i\phi_i}|\phi\rangle\langle\phi|a_i, \end{aligned} \tag{5.8}$$

where, for brevity, we have set $d[\bar{\phi},\phi] \equiv \prod_i d\bar{\phi}_i d\phi_i/\pi$. Taking the adjoint of Eq. (5.8), we see that the left hand side of (5.7) also commutes with the creation operators, i.e. it must be proportional

to the unit operator. To fix the proportionality constant, we simply take the overlap with the vacuum:

$$\int d[\bar{\phi},\phi]e^{-\sum_i \bar{\phi}_i\phi_i}\langle 0|\phi\rangle\langle\phi|0\rangle = \int d[\bar{\phi},\phi]e^{-\sum_i \bar{\phi}_i\phi_i} = 1, \tag{5.9}$$

where the last equality follows from Eq. (4.40). Eqs. (5.8) and (5.9) prove (5.7). Note that the coherent states are overcomplete in the sense that they are not mutually orthogonal (see Eq. (5.5)). The exponential weight $e^{-\sum_i \bar{\phi}_i\phi_i}$ appearing in the resolution of the identity compensates for the overcounting achieved by integrating over the whole set of coherent states.

With these definitions we have all we need to construct the many-body path integral for the bosonic system. However, before we do so, we will first introduce the fermionic version of the coherent state. This will allow us to construct the path integrals for bosons and fermions simultaneously, thereby emphasising the similarity of their structure.

5.1.2 Coherent States (Fermions)

Surprisingly, much of the formalism above generalises to the fermionic case: Creation operators cannot have eigenstates and, due to their mutual anticommutativity, it would seem that the set of annihilation operators can not be diagonalised simultaneously. To see the latter, suppose we had found a fermionic version of a coherent state such that, for all i,

$$\boxed{a_i|\eta\rangle = \eta_i|\eta\rangle} \tag{5.10}$$

where η_i is the eigenvalue. Although the structure of this equation appears to be equivalent to its bosonic counterpart (5.2) it has one frustrating feature: Anticommutativity of the fermionic operators, $[a_i, a_j]_+ = 0$, where $i \neq j$, implies that the *eigenvalues* η_i also have to anticommute,

$$\boxed{\eta_i\eta_j = -\eta_j\eta_i.} \tag{5.11}$$

Clearly, these objects cannot be ordinary numbers. In order to define a fermionic version of coherent states, we somehow have to generalize the concept of 'numbers' so as to allow for behaviour like (5.11). "*In mathematics you don't understand things. You just get used to them!*" — Johann von Neumann, (1903-1957) . For clarity, and to remove any mystery from the definitions (5.10) and (5.11), let us outline a constructive procedure whereby objects $\{\eta_i\}$ with the desired properties can be defined in a mathematically clean way.

There is a mathematical structure ideally suited to generalize the concept of ordinary number(fields), namely **algebras**. We recapitulate the that an algebra $\mathcal{A}$ is a vector space endowed with a multiplication rule $\mathcal{A} \times \mathcal{A} \to \mathcal{A}$. So, let us *construct* an algebra $\mathcal{A}$ by starting out from a set of elements, or generators, $\eta_i \in \mathcal{A}, i = 1, \ldots N$, and imposing the rules

i) The elements η_i can be added and multiplied with complex numbers, i.e.

$$c_0 + c_i\eta_i + c_j\eta_j, \in \mathcal{A} \quad c_0, c_i, c_j \in \mathcal{C}, \tag{5.12}$$

i.e. $\mathcal{A}$ will be a vectorspace over the *complex* numbers.

ii) The product,

$$\begin{aligned} \mathcal{A} \times \mathcal{A} &\to \mathcal{A}, \\ (\eta_i, \eta_j) &\mapsto \eta_i \eta_j \end{aligned}$$

is associative and anticommutative, i.e. obeys the anti-commutation relation (5.11). Because of the associativity of this operation, there is no ambiguity when it comes to forming products of higher order, i.e. $(\eta_i\eta_j)\eta_k = \eta_i(\eta_j\eta_k) \equiv \eta_i\eta_j\eta_k$. The definition entails that products of odd order in in the number of generators anti-commute, while (even,even) and (even,odd) combinations commute (exercise).

By virtue of (i) and (ii), the set $\mathcal{A}$ of all linear combinations

$$c_0 + \sum_{n=1}^{\infty} \sum_{i_1,\cdots i_n=1}^{N} c_{i_1,\ldots,i_n} \eta_{i_1} \ldots \eta_{i_n},$$

$c_0, c_{i_1,\ldots,i_n} \in \mathcal{C}$ spans a finite dimensional associative algebra $\mathcal{A}$,[1], known as the **Grassmann algebra**[2] (sometimes also **exterior algebra**).

▷ INFO. Grassmann algebras find a number of realizations in mathematics, the most basic being exterior multiplication in linear algabra: Given an N-dimensional vector space V, let V^* be the dual space, i.e. the space of all linear mappings, or 'forms' $\Lambda : V \to \mathbb{C}, v \mapsto \Lambda(v)$, where $v \in V$. (Like V, V^* is a vector space of dimension N.) Next, define exterior multiplication through, $(\Lambda, \Lambda') \to \Lambda \wedge \Lambda'$, where $\Lambda \wedge \Lambda'$ is the mapping

$$\begin{aligned} \Lambda \wedge \Lambda' : V \times V &\to \mathbb{C} \\ (v, v') &\mapsto \Lambda(v)\Lambda'(v') - \Lambda(v')\Lambda'(v). \end{aligned}$$

This operation is manifestly anti-commutative: $\Lambda \wedge \Lambda' = -\Lambda \wedge \Lambda'$. Identifying the N linearly basis forms $\Lambda_i \leftrightarrow \eta_i$ with generators and $\wedge$ with the product, we see that the space of exterior forms of a vector space forms a Grassmann algebra.

Apart from their anomalous commutation properties, the generators $\{\eta_i\}$, and their product generalization $\{\eta_i\eta_j, \eta_i\eta_j\eta_k, \ldots\}$ resemble ordinary, albeit anti-commutative numbers. (In practice, the algebraic structure underlying their definition can safely be ignored. All we will need to work with these objects is the basic rule (5.11) and the property (5.12).) We repeat that $\mathcal{A}$ not only contains anticommuting but also commuting elements, i.e. linear combinations of an *even* number of η_i's are overall commutative. (This mimics the behaviour of the Fock space algebra: products of an even number of annihilation operators $a_ia_j \ldots$ commute with all other linear combinations of a_i's. In spite of this similarity,

[1] whose dimension can be shown to be 2^N (exercise!)

Hermann Günter Grassmann 1809-1877, credited for inventing what is now called Exterior Algebra.

[2]

the η_i's must not be confused with the Fock space operators. There is nothing the η_i's act upon.)

To make practical use of the new concept, we need to go beyond the level of pure arithmetics. Specifically, we need to introduce functions of anti-commuting numbers, and elements of calculus. Remarkably, most of the concepts of calculus not only naturally generalize to anti-commuting number fields: Contrary to what one might expect, the anti-commutative generalization of differentiation, integration, etc. turns out to be much *simpler* than in ordinary calculus.

▷ Functions of Grassmann numbers are defined via their Taylor expansion:

$$\xi_1, \ldots, \xi_k \in \mathcal{A}: \qquad f(\xi_1, \ldots, \xi_k) = \sum_{n=0}^{\infty} \sum_{i_1, \cdots i_n = 1}^{k} \frac{1}{n!} \frac{\partial^n f}{\partial \xi_{i_1} \cdots \partial \xi_{i_n}}\Big|_{\xi=0} \xi_{i_n} \cdots \xi_{i_1} \tag{5.13}$$

where f is an (analytic) function. Note that the anticommutation properties of the algebra implies that the series terminates after a *finite* number of terms. E.g. in the simple case where η is first order in the generators of the algebra, $N = 1$, and

$$f(\eta) = f(0) + f'(0)\eta$$

(due to the fact that $\eta^2 = 0$).

▷ Differentiation with respect to Grassmann numbers is defined by

$$\boxed{\partial_{\eta_i} \eta_j = \delta_{ij}} \tag{5.14}$$

Note that in order to be consistent with the commutation relations, the differential operator ∂_{η_i} must itself be anti-commutative. E.g.

$$\partial_{\eta_i} \eta_j \eta_i \overset{i \neq j}{=} -\eta_j .$$

▷ The integral over Grassmann variables is defined by

$$\boxed{\int d\eta_i = 0, \qquad \int d\eta_i \eta_i = 1} \tag{5.15}$$

Note that the definitions (5.13), (5.14) and (5.15) imply that *Grassmann differentiation and integration are identical*:

$$\int d\eta f(\eta) = \int d\eta (f(0) + f'(0)\eta) = f'(0) = \partial_\eta f(\eta).$$

Let us now proceed and apply the Grassmann algebra to the construction of fermion coherent states. To this end we need to enlarge the algebra even further, so as to allow

for a multiplication of Grassmann numbers and Fermion operators. In order to be consistent with the anticommutation relations, we need to require that *Fermion operators and Grassmann generators anticommute*,

$$[\eta_i, a_j]_+ = 0. \tag{5.16}$$

It then becomes a straightforward matter to demonstrate that the **fermionic coherent states** are given by

$$\boxed{|\eta\rangle = \exp\Big[-\sum_i \eta_i a_i^\dagger\Big]|0\rangle} \tag{5.17}$$

i.e. by a structure perfectly analogous to the bosonic states (5.1). To prove that the states (5.17) indeed fulfil the defining relation (5.10) we note that

$$\begin{aligned} a_i \exp(-\eta_i a_i^\dagger)|0\rangle &\overset{(5.13)}{=} a_i(1-\eta_i a_i^\dagger)|0\rangle \overset{(5.16)}{=} \eta_i a_i a_i^\dagger|0\rangle \\ &= \eta_i|0\rangle = \eta_i(1-\eta_i a_i^\dagger)|0\rangle = \eta_i \exp(-\eta_i a_i^\dagger)|0\rangle. \end{aligned}$$

This, in combination with the fact that a_i and $\eta_j a_j^\dagger$ $(i \neq j)$ commute proves (5.10). Note that the proof has actually been simpler than in the bosonic case; the fermionic Taylor series terminated after the first contribution. This observation is representative of a general rule: Grassmann calculus is simpler than standard calculus, all series are finite, integrals always converge, etc.

It is a straightforward matter — and also a good exercise — to demonstrate that the properties (5.3), (5.4), (5.5), (5.6) and, most importantly (5.7) carry over to the fermionic case. One merely has to identify a_i with a fermionic operator and replace the complex variables ϕ_i by $\eta_i \in \mathcal{A}$. Apart from a few sign changes and the $\mathcal{A}$-valued arguments, the fermionic coherent states differ only in two respects from their bosonic counterpart: firstly, the Grassmann variables $\bar{\eta}_i$ appearing in the adjoint of a fermion coherent state,

$$\langle\eta| = \langle 0|\exp\left[-\sum_i a_i\bar{\eta}_i\right] = \langle 0|\exp\left[\sum_i \bar{\eta}_i a_i\right],$$

are *not* related to the η_i's of the state $|\eta\rangle$ via some kind of complex conjugation. Rather η_i and $\bar{\eta}_i$ are strictly independent variables.[3] Secondly, the Grassmann version of a Gaussian integral (exercise: prove it!)

$$\int d\bar{\eta}d\eta e^{-\bar{\eta}\eta} = 1.$$

[3] In the literature, complex conjugation of Grassmann variables is sometimes defined. This concept, although appealing from an aesthetic point of view — symmetry between bosons and fermions — is problematic. The difficulties become apparent, when supersymmetric theories are considered, i.e. theories where operator algebras containing both bosons and fermions are considered (so-called super-algebras). It is not possible to introduce a complex conjugation that leads to compatibility with the commutation relations of a super-algebra. It thus seems to be better to abandon the concept of Grassmann complex conjugation altogether. Note that although in the bosonic case, complex conjugation is inevitable (in order to define convergent Gaussian integrals, say), no such need arises in the fermionic case

Definition	$\|\psi\rangle = \exp\Big[-\zeta\sum_i \psi_i a_i^\dagger\Big]\|0\rangle,$ Bosons : $(\zeta=-1)$ $\psi_i \in \mathcal{C}$ Fermions : $(\zeta=+1)$ $\psi_i \in \mathcal{A}$
Action of a_i	$a_i\|\psi\rangle = \psi_i\|\psi\rangle$ $\langle\psi\|a_i = \partial_{\bar\psi_i}\langle\psi\|$
Action of $a_i^\dagger$	$a_i^\dagger\|\psi\rangle = -\zeta\partial_{\psi_i}\|\psi\rangle$ $\langle\psi\|a_i^\dagger = \langle\psi\|\bar\psi_i$
Overlap	$\langle\psi'\|\psi\rangle = e^{\sum_i \bar\psi_i'\psi_i}$
Completeness	$\int\prod_i \frac{d\bar\psi_i d\psi_i}{\pi^{(1-\zeta)/2}} e^{-\sum_i \bar\psi_i\psi_i}\|\psi\rangle\langle\psi\| = 1_{\mathcal{F}}$

Table 5.1: Basic Properties of Coherent States

does not contain the π's characteristic of standard Gaussian integrals. (For a more comprehensive discussion of Gaussian Grassmann integrals see Appendix 5.4.) Thus, the measure term of the fermionic analogue of (5.7) does not contain the π-denominator.

For the sake of future reference, the most important properties of Fock-space coherent states are summarised in table 5.1.

5.2 Field Integral for the Quantum Partition Function

Having introduced coherent states, we will see that the construction of path integrals for many-body systems no longer presents substantial difficulties. However, what does the phrase 'path-integral *for many body systems*' actually mean? In the next chapter we will see that much of the information on quantum many particle systems is stored in expectation values of products of creation/anihilation operators, i.e. expressions of the structure $\langle a^\dagger a \ldots\rangle$. By an analogy to be explained then, objects of this type are generally called **Green functions**. More important for our present discussion, at any finite temperature, the averaging $\langle\ldots\rangle$ entering the definition of Green functions is over

the quantum Gibbs distribution $\hat{\rho} \equiv \mathcal{Z}^{-1} e^{-\beta(\hat{H}-\mu\hat{N})}$, where, as usual,

$$\mathcal{Z} = \text{tr } e^{-\beta(\hat{H}-\mu\hat{N})} = \sum_n \langle n|e^{-\beta(\hat{H}-\mu\hat{N})}|n\rangle, \tag{5.18}$$

is the quantum partition function, $\beta \equiv 1/k_B T$, μ denotes the chemical potential, and the sum extends over a complete set of Fock space states $|n = \{n\}\rangle$. (For the time being we neither specify the statistics of the system – bosonic or fermionic – nor the structure of the Hamiltonian.)

Ultimately, we will want to construct and evaluate path integral representations of many body Green functions. Later we will see that all these representations, can be derived by a few straightforward manipulations form a prototypical path integral, namely that for $\mathcal{Z}$. Further, the (path integral of the) partition function is of importance in its own right: it contains much of the information needed to characterise the *thermodynamic* properties of a many-body quantum system.[4] We thus begin our journey into many body field theory with a construction of the path integral for $\mathcal{Z}$.

To prepare the representation of (5.18) in terms of coherent states, we insert the resolution of unity

$$\mathcal{Z} = \int d[\bar{\psi}, \psi] e^{-\sum_i \bar{\psi}_i \psi_i} \sum_n \langle n|\psi\rangle\langle\psi|e^{-\beta(\hat{H}-\mu\hat{N})}|n\rangle. \tag{5.19}$$

We next wish to get rid of the – now redundant – Fock space summation over $|n\rangle$ (another resolution of unity). To bring the summation into the form $\sum_n |n\rangle\langle n| = 1_{\mathcal{F}}$, we commute the factor $\langle n|\psi\rangle$ to the right hand side. However, in performing this seemingly innocuous operation, we must be careful not to miss a sign change who's presence will have a important consequences for the structure of the *fermionic* path integral: Whilst for bosons, $\langle n|\psi\rangle\langle\psi|n\rangle = \langle\psi|n\rangle\langle n|\psi\rangle$, the fermionic coherent states change sign upon permutation, $\langle n|\psi\rangle\langle\psi|n\rangle = \langle -\psi|n\rangle\langle n|\psi\rangle$ (i.e. $\langle -\psi| = \exp[-\sum_i \bar{\psi}_i a_i]$). The presence of the sign is a direct consequence of the anti-commutation relations between Grassmann variables and Fock space operators (exercise). Note that, as both $\hat{H}$ and $\hat{N}$ contain operators in even numbers, the sign is insensitive to the presence of the Boltzmann factor in (5.19). Making use of the sign factor ζ defined in section 3, the result of the interchange can be formulated as

$$\mathcal{Z} = \int d[\bar{\psi}, \psi] e^{-\sum_i \bar{\psi}_i \psi_i} \sum_n \langle -\zeta\psi|e^{-\beta(\hat{H}-\mu\hat{N})}|n\rangle\langle n|\psi\rangle$$

[4] In fact, the statement above is not entirely correct. Strictly speaking thermodynamic properties involve the **thermodynamic potential**

$$\Omega = -k_B T \ln \mathcal{Z}$$

rather than the partition function itself. At first sight it seems that the difference between the two is artificial — one might first calculate $\mathcal{Z}$ and then take the logarithm. However, typically, one is unable to determine $\mathcal{Z}$ in closed form, but rather one has to perform a perturbative expansion, i.e. the result of a calculation of $\mathcal{Z}$ will take the form of a series in some small parameter ϵ. Now a problem arises when the logarithm of the series is taken. In particular, the Taylor series expansion of $\mathcal{Z}$ to a given order in ϵ does *not* automatically determine the expansion of Ω to the same order. Fortunately, the situation is not all that bad. It turns out that the logarithm essentially rearranges the combinatorial structure of the perturbation series in an order known as a **cumulant expansion**.

$$= \int d[\bar{\psi},\psi] e^{-\sum_i \bar{\psi}_i \psi_i} \langle -\zeta|\psi| e^{-\beta(\hat{H}-\mu\hat{N})}|\psi\rangle, \tag{5.20}$$

where the equality is based on $\sum_n |n\rangle\langle n| = 1_{\mathcal{F}}$. Eq. (5.20) can now be directly subjected to the general construction scheme of the path integral.

To be concrete, let us assume that the Hamiltonian is limited to a maximum of two-body interactions (c.f. Eqs. (3.8) and (3.13)),

$$\hat{H}(a^\dagger, a) = \sum_{ij} h_{ij} a_i^\dagger a_j + \sum_{ijkl} V_{ijkl} a_i^\dagger a_j^\dagger a_k a_l. \tag{5.21}$$

Note that all annihilation operators stand to the right of the creation operators. Fock space operators of this structure are said to be **normal ordered**.[5] The reason for emphasising normal ordering is that such an operator can be readily diagonalised by means of coherent states: Dividing the 'time interval' β into N segments and inserting coherent state resolutions of unity (steps 1, 2 and 3 of the general scheme), Eq. (5.20) takes the form

$$\mathcal{Z} = \int_{\substack{\bar{\psi}^0 = -\zeta\bar{\psi}^N \\ \psi^0 = -\zeta\psi^N}} \prod_{n=0}^{N} d[\bar{\psi}^n, \psi^n] e^{-\delta \sum_{n=0}^{N-1} \left[\delta^{-1}(\bar{\psi}^n - \bar{\psi}^{n+1})\cdot\psi^n + H(\bar{\psi}^{n+1},\psi^n) - \mu N(\bar{\psi}^{n+1},\psi^n)\right]}, \tag{5.22}$$

where $\delta = \beta/N$ and

$$\frac{\langle\psi|\hat{H}(a^\dagger,a)|\psi'\rangle}{\langle\psi|\psi'\rangle} = \sum_{ij} h_{ij}\bar{\psi}_i\psi'_j + \sum_{ijkl} V_{ijkl}\bar{\psi}_i\bar{\psi}_j\psi'_k\psi'_l \equiv H(\bar{\psi},\psi'),$$

(similarly $N(\bar{\psi},\psi')$), and in writing Eq. (5.22) we have used the shorthand $\psi^n = \{\psi_i^n\}$ etc.

Finally, sending $N \to \infty$ and taking limits analogous to those leading from (4.7) to (4.8) we obtain the continuum version of the path integral,[6]

$$\boxed{\mathcal{Z} = \int D(\bar{\psi},\psi) e^{-S[\bar{\psi},\psi]}, \qquad S = \int_0^\beta d\tau \left[\bar{\psi}\partial_\tau\psi + H(\bar{\psi},\psi) - \mu N(\bar{\psi},\psi)\right],} \tag{5.23}$$

where

$$D(\bar{\psi},\psi) = \lim_{N\to\infty} \prod_{n=1}^{N} d[\bar{\psi}^n, \psi^n]$$

[5] More generally, an operator is defined to be 'normal ordered' with respect to a given vacuum state $|0\rangle$, if and only if it annihilates $|0\rangle$. Note that the vacuum need not necessarily be defined as a zero particle state. If the vacuum contains particles, normal ordering need not lead to a representation where all annihilators stand to the right. If, for whatever reason, one is given a Hamiltonian whose structure differs from (5.21), one can always affect a normal ordered form at the expense of introducing commutator terms. E.g. normal ordering the quartic term leads to the appearance of a quadratic contribution which can be absorbed into $h_{\alpha\beta}$.

[6] Whereas the bosonic continuum limit is indeed perfectly equivalent to the one taken in constructing the quantum mechanical path integral ($\lim_{\delta\to 0}\delta^{-1}(\bar{\psi}^{n+1} - \bar{\psi}^n) = \partial_\tau|_{\tau=n\delta}$ gives an ordinary derivative etc.), a novelty arises in the fermionic case. The notion of replacing differences by derivatives is purely symbolic for Grassmann variables. There is no sense in which $\bar{\psi}^{n+1} - \bar{\psi}^n$ is small. The symbol $\partial_\tau\bar{\psi}$ rather denotes the formal (and well defined expression) $\lim_{\delta\to 0}\delta^{-1}(\bar{\psi}^{n+1} - \bar{\psi}^n)$.

and the fields satisfy the boundary condition

$$\bar{\psi}(0) = -\zeta\bar{\psi}(\beta), \quad \psi(0) = -\zeta\psi(\beta). \tag{5.24}$$

Notice that the structure of the action nicely fits into the general scheme discused in the previous chapter. By analogy, one would expect that the exponent of the many body path integral carries the significance of an Hamiltonian action, $S \sim \int(p\dot{q} - H)$, where (q, p) symbolically stands for a set of generalized coordinates and momenta. In the present case, the natural pair of canonically conjugate *operators* is $(a, a^\dagger)$. One would then interpret the eigenvalues $(\psi, \bar{\psi})$ as 'coordinates' (very much like (q, p) are the eigenvalues of the operators $(\hat{q}, \hat{p})$.) Adopting this interpretation, we see that the exponent of the path integral indeed has the canonical form of an Hamiltonian action and, therefore, is easy to memorize.

In a more explicit way of writing, the action associated to the general pair-interaction Hamiltonian (5.21) is given by

$$S = \int_0^\beta d\tau \left[\sum_{ij} \bar{\psi}_i(\tau) \left[(\partial_\tau - \mu)\delta_{ij} + h_{ij} \right] \psi_j(\tau) + \sum_{ijkl} V_{ijkl} \bar{\psi}_i(\tau)\bar{\psi}_j(\tau)\psi_k(\tau)\psi_l(\tau) \right]. \tag{5.25}$$

Eqs (5.23) and (5.25) define the **functional integral in the time representation** (in the sense that the fields are functions of a time variable). In practice we shall mostly find it useful to represent the action in an alternative, Fourier conjugate representation. To this end, note that, due to the boundary conditions (5.24), the functions $\psi(\tau)$ can be interpreted as functions on the entire time axis which are periodic/antiperiodic on the interval $[0, \beta]$. As such they can be represented in terms of a Fourier series,

$$\psi(\tau) = \frac{1}{\sqrt{\beta}} \sum_{\omega_n} \psi_n e^{-i\omega_n \tau}, \qquad \psi_n = \frac{1}{\sqrt{\beta}} \int_0^\beta d\tau \psi(\tau) e^{i\omega_n \tau},$$

where

$$\omega_n = \begin{cases} 2n\pi T, & \text{bosons}, \\ (2n+1)\pi T, & \text{fermions} \end{cases}, \quad n \in \mathcal{Z} \tag{5.26}$$

are known as **Matsubara frequencies**. Substituting this representation into (5.23) and (5.25), we obtain

$$\mathcal{Z} = \int D(\bar{\psi}, \psi) e^{-S[\bar{\psi}, \psi]}, \tag{5.27}$$

where $D(\bar{\psi}, \psi) = \prod_n d[\bar{\psi}_n, \psi_n]$ defines the measure (for each Matsubara index n we have an integration over a coherent state basis $\{|\psi_n\rangle\}$), and the action takes the form

$$\begin{aligned} S[\bar{\psi}, \psi] = &\sum_{ij} \sum_n \bar{\psi}_{in} \left[(-i\omega_n - \mu)\, \delta_{ij} + h_{ij} \right] \psi_{jn} + \\ &+ \frac{1}{\beta} \sum_{ijkl} \sum_{n_1 n_2 n_3 n_4} V_{ijkl} \bar{\psi}_{in_1} \bar{\psi}_{jn_2} \psi_{kn_3} \psi_{ln_4} \delta_{n_1+n_2, n_3+n_4}. \end{aligned} \tag{5.28}$$

Here we have used the identity $(1/\beta)\int_0^\tau d\tau e^{-i(\omega_{n_1}+\omega_{n_2}-\omega_{n_3}-\omega_{n_4})\tau} = \delta_{\omega_{n_1}+\omega_{n_2},\omega_{n_3}+\omega_{n_4}}$. Eqs. (5.27) and (5.28) define the **frequency representation of the field integral**.[7]

▷ INFO. In performing calculations in the Matsubara representation one sometimes run into convergence problems (which will manifest themselves in the form of ill-convergent Matsubara frequency summations). In such cases it will be important to remember that Eq. (5.28) does not actually represent the *precise* form of the action. What is missing is a convergence generating factor whose presence follows from the way in which the integral was constructed, and which will save us in cases of non-convergent sums (except, of course, cases where divergences have a physical origin). More precisely, since the fields $\bar{\psi}$ are evaluated infinitesimally later than the operators ψ (c.f. Eq. (5.22)), the h and μ-dependent contributions to the action acquire a factor $\exp[-i\omega_n\delta]$, δ infinitesimal. Similarly, the V contribution picks up a factor $\exp[-i(\omega_{n_1}+\omega_{n2})\delta]$. In cases where the convergence is not critical, we will omit these contributions. However, once in a while it is necessary to remember their presence.

5.2.1 Partition Function of Non-Interacting Gas

As a first exercise, let us consider the partition function of the non-interacting gas, $\mathcal{Z}_0$. (Later, this object will prove to be a 'reference' in the development of weakly interacting theories.) In some sense, the field integral formulation of the non-interacting partition function has a status similar to that of the path integral for the quantum harmonic osciallator: The direct quantum mechanical solution of the problem is straightforward (exercise: recapitulate how it is done) and application of the full artillery of the field integral seems to be a bit ludicrous. From a pedagogical point of view, however, the free partition function is a good problem; it provides us with the welcome opportunity to introduce a number of practical concepts of field integration within a comparatively simple setting.

Consider, then the partition function (5.23) for $H(\bar{\psi},\psi) = H_0(\bar{\psi},\psi) = \sum_{ij}\bar{\psi}_i H_{0ij}\psi_j$. Diagonalising H_0 by a unitary transformation U, $H_0 = UDU^\dagger$ and transforming integration variables $U^\dagger\psi \equiv \phi$, the action assumes the form,

$$S = \sum_a \sum_{\omega_n} \bar{\phi}_{an}(-i\omega_n + \xi_a)\phi_{an},$$

where $\xi_a \equiv \epsilon_a - \mu$ and ϵ_a are the single particle eigenvalues. Remembering that the fields $\phi_a(\tau)$ are independent integration variables (exercise: why does the transformation $\psi \to \phi$

[7] As for the signs of the Matsubara indices appearing in (5.28), note that the Fourier representation of $\bar{\psi}$ is defined as

$$\bar{\psi}(\tau) = \frac{1}{\sqrt{\beta}}\sum_n \bar{\psi}_n e^{+i\omega_n\tau}, \qquad \bar{\psi}_n = \frac{1}{\sqrt{\beta}}\int_0^\beta d\tau\bar{\psi}(\tau)e^{-i\omega_n\tau}.$$

In the bosonic case, this sign convention is motivated by $\bar{\psi}$ being the complex conjugate of ψ. For reasons of notational symmetry, this convention is adopted in the fermionic case, too.

has Jacobian unity?), we find that the partition function decouples, $Z = \prod_a Z_a$, where

$$Z_a = \int D(\bar{\phi}_a, \phi_a) e^{-\sum_n \bar{\phi}_{an}(-i\omega_n + \xi_a)\phi_{an}} = \prod_n (-i\omega_n + \xi_a)^\zeta, \tag{5.29}$$

and the last equality follows from the fact that the integrals over ϕ_{an} are one-dimensional complex or Grassmann Gaussian integrals. At this stage, we have left all aspects of field integration behind us and reduced the problem to one of computing an infinite product over factors $i\omega_n - \xi_a$. Since products are usually more difficult to get under control then sums, we take the logarithm of $\mathcal{Z}$ to obtain the free energy

$$F = -T \ln \mathcal{Z} = -T \ln \prod_{a,n} (-i\omega_n + \xi_a)^\zeta = -T\zeta \sum_{an} \ln(-i\omega_n + \xi_a). \tag{5.30}$$

▷ INFO. Before proceeding with this expression, let us take a second look at the intermediate identity (5.29). Our calcuation showed

$$\mathcal{Z} = \prod_{an} (-i\omega_n + \xi_a)^\zeta$$

to be the product over all eigenvalues of the operator $-i\hat{\omega} + \hat{H} - \mu\hat{N}$ defining the action of the non-interacting system. (Here, $\hat{\omega} = \{\omega_n \delta_{nn'}\}$.) But that is nothing just the determinant:

$$\boxed{\mathcal{Z} = \det\left[-i\hat{\omega} + \hat{H} - \mu\hat{N}\right]^\zeta}. \tag{5.31}$$

We derived that result by first converting to an eigenvalue integration and then doing the one-dimensional integrals over 'eigencomponents' ϕ_{an}. While technically straightforward, that – explicitly representation-dependent – procedure is not well suited to generalization to more complex problems. (Keep in mind that later on we will want to embed the free action of the non-interacting problem into the more general framework of an interacting theory.)

Indeed, it is not at all *necessary* to refer to an eigenbasis: In the *bosonic* case, Eq. (4.46) tells us that Gaussian integration over a bilinear $\sim \bar{\phi}\hat{X}\phi$ generates the inverse determinant of $\hat{X}$. But what about the Grassmann case? The answer is that all Gaussian integration formulae summarized in section 4.5 have Grassmann-analogs. The only difference is that in the Grassmann case determinants appear in the *numerator* rather than in the denominator (as exemplified by (5.31).) (As a matter of fact, (5.29) is already proof of that relation.) The Grassmann side of Gaussian integration is reviewed in full in Appendix 5.4.

We now have to face up to a technical problem: How do we compute sums of the $\sum_n \ln(i\omega_n - x)$? In fact, it takes little anticipation to foresee that sums of the type

$$\sum_{n_1,n_2,\ldots} X(\omega_{n_1}, \omega_{n_2}, \ldots),$$

where X symbolically stands for some function, will be a recurrent structure in the analysis of functional integrals. But how then, can sums of this type be computed? A good ansatz

would be to argue that for sufficiently low temperatures (temperatures smaller than any other characteristic energy scale in the problem), the sum can be traded for an integral: $T\sum_n \to \frac{1}{2\pi}\int d\omega$. However, this approximation is too crude to capture much of the characteristic temperature dependence one is usually interested in. Yet there exists an alternative, and much more accurate way of computing sums over Matsubara frequencies:

▷ INFO. Consider a single **Matsubara frequency summation**,

$$S \equiv \sum_n h(\omega_n), \tag{5.32}$$

where h is some function and ω_n may be either bosonic or fermionic (cf. Eq. (5.26).) The basic idea behind the standard scheme of evaluating sums of this type is to introduce a complex auxiliary function $g(z)$ that has simple poles at $z = i\omega_n$. The sum S then emerges as the sum of residues obtained by integrating the product gh along a suitably chosen path in the complex plane.

Typical choices of g include

$$g(z) = \begin{cases} \dfrac{\beta}{\exp(\beta z)-1}, & \text{bosons} \\ \dfrac{\beta}{\exp(\beta z)+1}, & \text{fermions} \end{cases}, \text{ and } \quad g(z) = \begin{cases} \dfrac{\beta}{2}\coth(\beta z/2), & \text{bosons} \\ \dfrac{\beta}{2}\tanh(\beta z/2), & \text{fermions,} \end{cases} \tag{5.33}$$

where in much of this section we will employ the functions of the first column. (Notice the similarity between these functions and the familiar Fermi and Bose distribution functions.) In practice, the choice of the counting function is mostly a matter of taste, safe for some cases where one of the two options is dictated by convergence criteria.

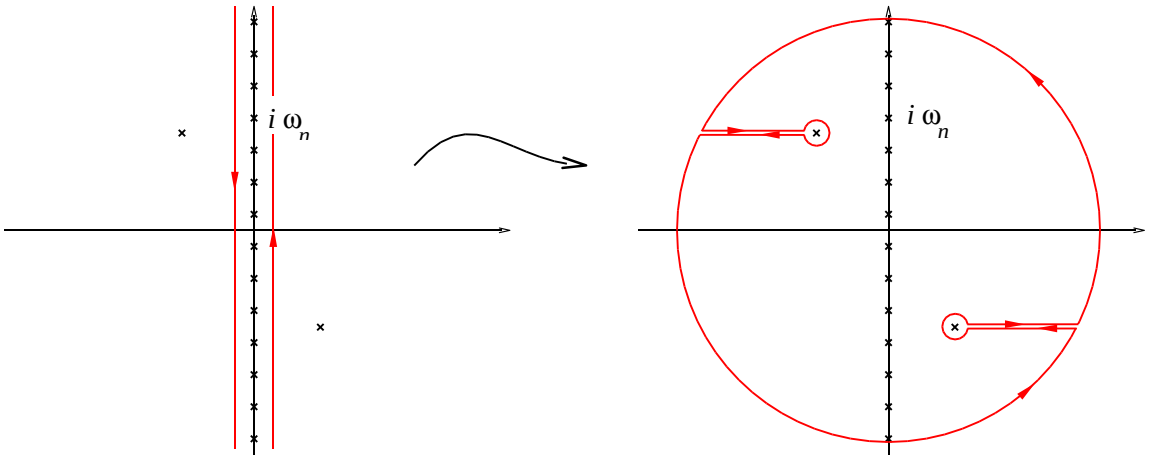

Figure 5.2: Left: integration contour employed in calculating the sum (5.32). Right: Deformed integration contour

Integration over the path shown in the left part of Fig. 5.2 then produces

$$\frac{1}{2\pi i}\oint dz g(z)h(-iz) = \sum_n \text{Res}\,(g(z)h(-iz)|_{z=i\omega_n} = -\zeta\sum_n h(\omega_n) = -\zeta S,$$

where in the third identity we have used that the 'counting functions' g are chosen so as to have residue $-\zeta$ and it is assumed that the integration contour closes at $z \to \pm i\infty$. (The difference between using the first and the second column of (5.33) lies in the value of the residue. In the latter case it equals unity rather than ζ.) Now, the integral along a contour in the immediate vicinity of the poles of g is usually not doable. However, as long as we are careful not to cross any singularities of g or the function $h(-iz)$ (the latter symbolically indicated by isolated crosses in the figure[8]), we are free to distort the integration path, ideally to a contour along which the integral *can* be done. Finding a suitable contour is not always straightforward. If the product hg decays sufficiently fast at $|z| \to \infty$ (i.e. faster than z^{-1}), one will ususally try to 'inflate' the original contour to an infinitely large circle (Fig. 5.2, right.)[9] The integral along the outer perimeter of the contour then vanishes and one is left with the integral around the singularities of the function h. In the simple case where $h(-iz)$ posesses a number of isolated singularities at $\{z_k\}$ (i.e. the situation indicated in the figure) we thus obtains[10]

$$S = \zeta \frac{1}{2\pi i} \oint h(-iz)g(z) = \zeta \sum_k \operatorname{Res} h(-iz)g(z)|_{z=z_k},$$

i.e. the task of computing the infinite sum S has been reduced to that of evaluating a number of residues (always possible!)

To illustrate the procedure on a simple example, let us consider the function

$$h(\omega_n) = \frac{\zeta T}{i\omega_n e^{-i\omega_n \delta} - \xi},$$

where δ is positive infinitesimal. This choice of h is not actually not as artificial as it may seem:

▷ EXERCISE. The expectation value of the **number of particles** in the grand canonical ensemble is defined through

$$N \equiv -\frac{\partial F}{\partial \mu},$$

where F is the free energy. In the non-interacting case, the latter is given by Eq. (5.30), and, remembering that $\xi_a = \epsilon_a - \mu$, one obtains

$$N \approx \zeta T \sum_{an} \frac{1}{i\omega_n - \xi_a}.$$

Why did we write '$\approx$' instead of '$=$'? The reason is that the right hand side, obtained by naive differentiation of (5.30), is ill-convergent. (The sum $\sum_{n=-\infty}^{\infty} \frac{1}{n+x}$, x arbitrary, does not exist!) At this point we have to remember the remark made in the on p. 172. I.e., had we carefully treated the discretization of the field integral, both the logarithm of the free energy and $\partial_\mu F$

[8] Remeber that a function that is analytic in the entire complex plane is either constant or zero.

[9] Notice that the condition $|fg| \overset{|z|\to\infty}{<} z^{-1}$ is not as restrictive as it may seem. The reason is that the function f will mostly be related to physical observables that approach some limit, or vanish, for large excitation energies. This implies vanishing in at least portions of the complex plane. The convergence properties of g depend on the concrete choice of the counting function. (Exercise: explore the convergence properties of the functions shown in Eq. (??).)

[10] If you are confused about signs, note that the contour encircles the singularities of h in clockwise direction.

would pick up infinitesimal phases $\exp(-i\omega_n\delta)$. Exercise: keep track of the discretization of the field integral from its definition to (5.30) to show that the accurate expression for N reads as

$$N = \zeta T \sum_{an} \frac{1}{i\omega_n e^{-i\omega_n\delta} - \xi_a} = \sum_a \sum_n h(\omega_n)|_{\xi=\xi_a},$$

where h is the function introduced above. (Note that the necessity to keep track of the life-buoy $e^{-i\delta\omega_n}$ does not arise too often. Most Matsubra sums of physical interest relate to functions f that decay faster than z^{-1}.)

To evaluate the sum $S = \sum_n h(\omega_n)$, we first observe that the product $h(-iz)g(z)$ has benign convergence properties. Further, the function $h(-iz)$ has a simple pole that, in the limit $\delta \to 0$, lies on the real axis at $z = \xi$. This leads to

$$\sum_n h(\omega_n) = -\zeta \operatorname{Res} g(z)h(-iz)|_{z=\xi} = -\frac{1}{e^{\beta\xi} + \zeta}.$$

We have thus arrived at the important identity

$$\boxed{-\zeta T \sum_n \frac{1}{i\omega_n - \xi_a} = \begin{cases} f_{\rm b}(\epsilon_a), & \text{bosons,} \\ f_{\rm f}(\epsilon_a), & \text{fermions} \end{cases}} \tag{5.34}$$

where the first equality has to be understood in a qualified sense and

$$f_{\substack{\rm f \\ \rm b}}(\epsilon) = \frac{1}{\pm 1 + \exp(\epsilon - \mu)} \tag{5.35}$$

is the Fermi/Bose distribution function. As a corrloary we note that the expectation value for the number of particles in a non-interacting quantum gas assumes the familiar form

$$N = \sum_a f_{\rm f/b}(\epsilon_a).$$

Before turning back to our discussion of the partition function, let us note that life is not allways as simple as with the example above. E.g. more often than not, the function f not only contains isolated singularities but also cuts or worse singularities. Under such circumstances, a good choice of the integration contour can be far from straightforward!

We turn back to our problem of computing the sum (5.30). Considering for a moment a fixed eigenvalue $\xi_a \equiv a$, we need to evaluate the sum

$$S \equiv \sum_n h(i\omega_n),$$

where $h(\omega_n) \equiv -\zeta T \ln(-i\omega_n + \xi) = -\zeta T \ln(i\omega_n - \xi) + C$ and C is an inessential constant. As discussed before, we represent the sum as

$$S = \frac{\zeta}{2\pi i} \oint g(z)h(-iz),$$

where $g(z) = \beta(e^{\beta z} + \zeta)^{-1}$ is (β times) the distribution function and the contour encircles the poles of g as in Fig. 5.2, left. Now, there is an essential difference to our previously discussed example, viz. the function $h(-iz) = -\zeta T \ln(z-\xi)+C$ has a branch *cut* along the real axis, $z \in (-\infty, \xi)$. To avoid contact with this singularity, we distort the integration contour as shown in Fig. 5.3. Noticing that the (suitably regularized, cf. our previous discussion of the particle number N) integral along the perimeter vanishes, we conclude that

$$S = \frac{T}{2\pi i} \int_{-\infty}^{\infty} d\epsilon g(\epsilon) \left(\ln(\epsilon^+ - \xi) - \ln(\epsilon^- - \xi) \right) ,$$

where $\epsilon^{\pm} = \epsilon \pm i\eta$, $\eta > 0$ is infinitesimal and we have used that $g(\epsilon^{\pm}) \simeq g(\epsilon)$ is continuous across the cut. (Also, without changing the value of the integral (why?), we have enlarged the integration interval from $(-\infty, \xi]$ to $(-\infty, \infty)$.) To evaluate the integral, we observe that

$$g(\epsilon) = \zeta \partial_\epsilon \ln \left(1 + \zeta e^{-\beta\epsilon}\right)$$

and integrate by parts:

$$S = \frac{\zeta T}{2\pi i} \int d\epsilon \ln \left(1 + \zeta e^{-\beta\epsilon}\right) \left(\frac{1}{\epsilon^+ - \xi} - \frac{1}{\epsilon^- - \xi} \right) \overset{(4.35)}{=} -\zeta T \ln \left(1 + \zeta e^{-\beta\xi}\right) .$$

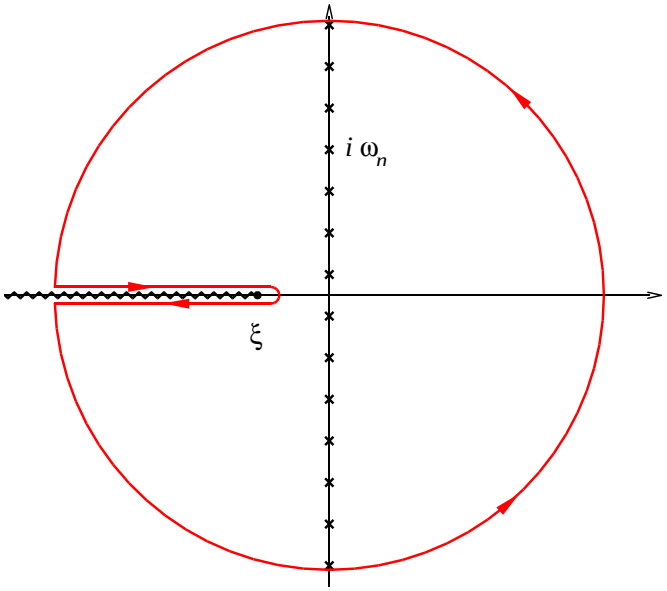

Figure 5.3: Integration contour employed in calculating the free energy.

Insertion of this result into (5.30) finally obtains the familiar expression

$$F = -\zeta T \sum_a \ln \left(1 + \zeta e^{-\beta(\epsilon_a - \mu)}\right) \tag{5.36}$$

for the free energy of the non-interacting Fermi/Bose gas. While this result could have been obtained much more straightforwardly by the methods of quantum statistical mechanics, we will shortly see how powerful a tool the methods discussed in this section are when it comes to the analysis of less elementary problems!

5.3 Summary and Outlook

This concludes our preliminary introduction to the field integral. We have learned how to represent the partition function of a quantum many body system in terms of a generalized path integral. We also saw that, irrespective of the structure of the Hamiltonian, the evaluation of the field integral leads to summations over a discrete set of frequencies. A method has been introduced whereby such sums can be done.

The field integral representation of the partition function will be the basic platform on which the rest of the book is based. However, the critical reader will object that beyond the construction of this formal representation, the present chapter did not add much to our understanding of concrete physical problems, i.e. there has been virtually no discussion of *applications* of the formalism. The reason is, of course, that none of the 'non-trivial' field integrals one might be interested in can be done in closed form. (This reflecting the fact that safe for a few exotic exceptions, interacting many body problems do not have closed solutions.) I.e. before emplyoing the field integral to solve serious problems we need to develop a spectrum of approximation strategies, perturbation theory, linear response theory, mean field methods, instanton techniques and the like. The construction and application of such methods will be the subject of the following chapters.

5.4 Appendix: Grassmann Gaussian Integration

The prototype of all Grassmann Gaussian integration formulae is

$$\boxed{\int d\bar{\eta}d\eta e^{-\bar{\eta}a\eta} = a,} \tag{5.37}$$

where $a \in \mathbb{C}$ takes arbitrary values. Eq. (5.37) is derived by a first order Taylor expansion of the exponential and application of Eq. (5.15). The multi-dimensional generalization of (5.37) is given by

$$\int d(\bar{\boldsymbol{\phi}}, \boldsymbol{\phi}) e^{-\bar{\boldsymbol{\phi}}^T \mathbf{A} \boldsymbol{\phi}} = \det \mathbf{A}, \tag{5.38}$$

where $\bar{\boldsymbol{\phi}}$ and $\boldsymbol{\phi}$ are N-component vectors of Grassmann variables, the measure $d(\bar{\boldsymbol{\phi}}, \boldsymbol{\phi}) \equiv \prod_{i=1}^{N} d\bar{\boldsymbol{\phi}}_i d\boldsymbol{\phi}_i$ and $\mathbf{A}$ may be an arbitrary complex matrix. For matrices that are unitarily diagonalisable, $\mathbf{A} = \mathbf{U}^\dagger \mathbf{D} \mathbf{U}$, with $\mathbf{U}$ unitary, and $\mathbf{D}$ diagonal, Eq. (5.38) is proven in the same way as its complex counterpart (4.46): One changes variables $\boldsymbol{\phi} \to \mathbf{U}^\dagger \boldsymbol{\phi}$, $\bar{\boldsymbol{\phi}} \to \mathbf{U}^T \bar{\boldsymbol{\phi}}$. Since $\det \mathbf{U} = 1$, the transform leaves the measure invariant (see below) and leaves us with N decoupled integrals of the type (5.37). The resulting product of N eigenvalues is just the determinant of $\mathbf{A}$. (That route was taken in the text.) For general (non-diagonalisable) $\mathbf{A}$, the identity is proven by straightforward expansion of the exponent. The expansion terminates at N'th order and by commuting through integration variables it can be shown that the resulting N'th order polynomial of matrix elements of $\mathbf{A}$ is the determinant. (Exercise: carry out this procedure for $N = 2$).[11]

[11] As with ordinary integrals, Grassmann integrals can also be subjected to **variable transforms**. Suppose we are given an integral

$$\int d(\bar{\boldsymbol{\phi}}, \boldsymbol{\phi}) f(\bar{\boldsymbol{\phi}}, \boldsymbol{\phi})$$

and wish to change variables according to

$$\bar{\nu} = \mathbf{M} \bar{\boldsymbol{\phi}}, \quad \nu = \mathbf{M}' \boldsymbol{\phi}, \tag{5.39}$$

where, for simplicity, $\mathbf{M}$ and $\mathbf{M}'$ are complex matrices (i.e. we here restrict ourselves to linear transforms). One can show that

$$\begin{aligned} \bar{\nu}_1 \dots \bar{\nu}_N &= \det M \bar{\eta}_1 \dots \bar{\eta}_N, \\ \nu_1 \dots \nu_N &= \det M' \eta_1 \dots \eta_N. \end{aligned} \tag{5.40}$$

(There are different ways to prove this identity. The most straightforward one is by explicitly writing out (5.39) in components and commuting all Grassmann variables to the right. A more elegant way is to argue that the coefficient relating the right and the left hand sides of (5.40) must be an Nth order polynomial of matrix elements of $\mathbf{M}$. In order to be consistent with the anti-commutation behaviour of Grasmann variables, the polynomial must obey commutation relations which uniquely characterise a determinant. Excercise: Check the relation for $N = 2$). On the other hand, the integral of the new variables must obey the defining relation,

$$\int d\bar{\nu} \bar{\nu}_1 \dots \bar{\nu}_N = \int d\nu \nu_1 \dots \nu_N = (-)^{N+1},$$

The Grassmann version of (4.47) reads

$$\boxed{\int d(\bar{\boldsymbol{\phi}}, \boldsymbol{\phi}) e^{-\bar{\boldsymbol{\phi}}^T \mathbf{A} \boldsymbol{\phi} + \bar{\nu}^T \cdot \boldsymbol{\phi} + \bar{\boldsymbol{\phi}}^T \cdot \nu} = \det \mathbf{A} e^{\bar{\nu} \mathbf{A}^{-1} \nu}} \tag{5.41}$$

To prove that relation, notice that $\int d\eta f(\eta) = \int d\eta f(\eta + \nu)$, i.e. in Grassmann integrals one can shift variables as in the ordinary case. The proof of the Gaussian relation above thus proceeds in complete analogy to the complex case. As with (4.47), Eq. (5.41) can also be employed to generate further integration formulae. Defining

$$\langle \cdots \rangle \equiv \det \mathbf{A}^{-1} \int d(\bar{\boldsymbol{\phi}}, \boldsymbol{\phi}) e^{-\bar{\boldsymbol{\phi}}^T \mathbf{A} \boldsymbol{\phi}} (\cdots)$$

and expanding both the left and the right hand side of (5.41) to leading order in the 'monomial' $\bar{\nu}_j \nu_i$, we obtain

$$\langle \eta_j \bar{\eta}_i \rangle = A^{-1}_{ji}.$$

The N-fold iteration of this procedure finally gives

$$\boxed{\langle \eta_{j_1} \eta_{j_2} \ldots \eta_{j_n} \bar{\eta}_{i_1} \bar{\eta}_{i_2} \ldots \bar{\eta}_{i_n} \rangle = \sum_P \text{sgn } P A^{-1}_{j_1 i_{P1}} \ldots A^{-1}_{j_n i_{Pn}}}$$

where the signum of the permutation accounts for the sign changes accompanying the interchange of Grassmann variables.

---

where $d\bar{\nu} = \prod_{i=1}^N d\bar{\nu}_i$ and the sign on the right hand side is due to the fact that $\int d\nu_1 d\nu_2 \nu_1 \nu_2 = -\int d\nu_1 \nu_1 \int d\nu_2 \nu_2 = -1$. Eqs. (5.40) and (5.39) enforce the identity

$$d\bar{\nu} = \det \mathbf{M} d\bar{\boldsymbol{\phi}}, \qquad d\nu = \det \mathbf{M}' d\boldsymbol{\phi},$$

which combines to give

$$\int d(\bar{\boldsymbol{\phi}}, \boldsymbol{\phi}) f(\bar{\boldsymbol{\phi}}, \boldsymbol{\phi}) = \det(\mathbf{M}\mathbf{M}') \int d(\bar{\nu}, \nu') f(\bar{\boldsymbol{\phi}}(\bar{\nu}), \eta(\nu)).$$

5.5 Problem Set

Q1 Explore normalization, overlap, completeness properties of Grassmann coherent sates. Spin coherent states ...

Q2 Real time field integral.

Q3 **Field integral vs. path integral:** Consider the simplest bosonic many body Hamiltonian:

$$\hat{H} = \left(a^\dagger a + \frac{1}{2} \right) \hbar\omega. \tag{5.42}$$

where $a^\dagger$ creates 'structureless' particles (states defined in a one-dimensional Hilbert space.) In section 2.1.1 we had seen that $\hat{H}$ can be interpreted as the Hamiltonian of a single osciallator degree of freedom. Show that, indeed, the *field*integral for the partition function $\mathrm{tr}\,(\exp(-\beta\hat{H}))$ can be mapped onto the (imaginary time) *path*integral of an harmonic oscillator by a suitable variable transformation. Hint: Let yourself be guided by the fact that the conjugate operator pair $(a, a^\dagger)$ is related to the momentum and coordinate operator $(\hat{p}, \hat{q})$ through a canonical transformation.

Q4 Compute the coherent state path integral of the Hamiltonian (5.42). (However, there is no need to be precise about the global normalization of the integral.) Then apply the formula (4.22) to evaluate the resulting infinite product over Matsubara frequencies. Fix the normalization of the result by demanding that in the zero temperature limit, $\beta \to \infty$, the oscillator must be in its ground state. Finally, compute the partition function by elementary means and check your result.

Additional exercise: repeat the same steps for the 'fermionic oscillator', $\hat{H} = (c^\dagger c + 1/2)\hbar\omega$, where $[c, c^\dagger]_+ = 1$ are fermion operators. (You need the auxiliary formula $\prod_n \left(1 - \left(\frac{x}{\pi(2n+1)} \right)^2 \right) = \cos\left(\frac{x}{2}\right)$.

Q5 Field representation of the one-dimensional free fermion. Comparison with free bose theory.

Q6 Some frequency summations.

Q7 partition function from coherent state representation.

Q8 partition function from discrete determinant representation.

Q9 persistent current problem

5.5.1 Answers

A1 Solution, coherent states ...

A2 In the coherent state representation, the quantum partition function of the oscillator Hamiltonian is expressed in terms of the path integral

$$\mathcal{Z} = \int D[\bar{\phi}, \phi] \exp\left[- \int_0^\beta d\tau \left(\bar{\phi} \partial_\tau \phi + \hbar\omega \bar{\phi} \phi \right) \right], \tag{5.43}$$

where $\phi(\tau)$ denotes a complex scalar field, the constant factor $e^{-\beta\hbar\omega/2}$ has been absorbed into the measure of the functional integral $D[\bar{\phi}, \phi]$, and we have set the chemical potential $\mu = 0$. The connection between the coherent state and Feynman integral is established by the change of field variables,

$$\phi(\tau) = \left(\frac{m\omega}{2\hbar} \right)^{1/2} \left[q(\tau) + \frac{ip(\tau)}{m\omega} \right]$$

where $p(\tau)$ and $q(\tau)$ represent real fields. Substituting, and rearranging some terms by integrating by parts, the connection is established,

$$\mathcal{Z} = \int D(p,q) \exp\left[- \int_0^\beta d\tau \left(\frac{p^2}{2m} + \frac{1}{2} m\omega^2 q^2 - \frac{i}{\hbar} p\dot{q} \right) \right].$$

A3 Dealing first with the bosonic oscillator, and making use of the Gaussian functional integral for complex fields (see Eq. (5.43)), we obtain

$$\begin{aligned} \mathcal{Z}_B &= \int D[\bar{\phi}, \phi] \exp\left[- \int_0^\beta d\tau \bar{\phi} \left(\partial_\tau + \hbar\omega \right) \phi \right] \sim \det(\partial_\tau + \hbar\omega)^{-1} \sim \prod_{\omega_n} \left[i\omega_n + \hbar\omega \right]^{-1} \\ &\sim \prod_{n=1}^{\infty} \left[(\hbar\omega)^2 + \left(\frac{2n\pi}{\beta} \right)^2 \right]^{-1} \sim \prod_{n=1}^{\infty} \left[1 + \left(\frac{\hbar\omega\beta}{2\pi n} \right)^2 \right]^{-1} \sim \frac{1}{\sinh(\hbar\omega\beta/2)}. \end{aligned}$$

Now, in the limit of small temperatures, the partition function is dominated by the ground state, $\lim_{\beta\to\infty} \mathcal{Z}_B = e^{-\beta\hbar\omega/2}$, which fixes the constant of proportionality,

$$\mathcal{Z}_B = \frac{1}{2\sinh(\hbar\beta\omega/2)}.$$

Similarly one can perform the Gaussian integration in the fermionic case. In this case, the product over the eigenvalues stands in the numerator, and

$$\begin{aligned} \mathcal{Z}_F &\sim \prod_{\omega_n} \left[i\omega_n + \hbar\omega \right] \sim \prod_{n=1}^{\infty} \left[(\hbar\omega)^2 + \left(\frac{(2n+1)\pi}{\beta} \right)^2 \right] \\ &\sim \prod_{n=1}^{\infty} \left[1 + \left(\frac{\hbar\omega\beta}{(2n+1)\pi} \right)^2 \right] \sim \cosh(\hbar\omega\beta/2). \end{aligned}$$

Fixing the normalization as before in the bosonic case, we find

$$\mathcal{Z}_F = 2e^{-\beta\hbar\omega} \cosh(\hbar\beta\omega/2).$$

Altogether, these results are easily confirmed by direct computation, viz

$$\begin{aligned}
\mathcal{Z}_B &= e^{-\beta\hbar\omega/2}\sum_{n=0}^{\infty} e^{-n\beta\hbar\omega} = \frac{e^{-\beta\hbar\omega/2}}{1-e^{-\beta\hbar\omega}} = \frac{1}{2\sinh(\beta\hbar\omega/2)} \\
\mathcal{Z}_F &= e^{-\beta\hbar\omega/2}\sum_{n=0}^{1} e^{-n\beta\hbar\omega} = e^{-\beta\hbar\omega/2}(1+e^{-\beta\hbar\omega}) = 2e^{-\beta\hbar\omega}\cosh(\hbar\beta\omega/2).
\end{aligned}$$

Chapter 6

Perturbation Theory

Analytical machinery to approximately solve many body problems is introduced. Employing the so-called ϕ^4-theory as an example, we learn how to describe systems that are not too far from a known reference state by perturbative methods. Diagrammatic methods are introduced as a tool to efficiently implement perturbation theory at large orders. The new concepts are then applied to an analysis of various properties of the weakly interacting electron gas.

In previous chapters we have stated time and again that the majority of many particle problems cannot be solved in closed form. So we have to begin to think about approximate strategies. One promising ansatz is that when approaching the low temperature physics of a many particle system we often have some idea, however vague, of its preferred states and/or its low energy excitations. One may then set out to explore the system by using these prospected ground state configurations as a working platform. E.g. one might expand the Hamiltonian in the vicinity of the reference state and check that, indeed, the residual 'perturbations' acting in the low energy sector of the Hilbert space are weak and can be dealt with by some kind of approximate expansion. Consider, e.g., the Heisenberg magnet. An exact solution of this system is out of question. However, we know (or, more conservatively, 'expect') that at zero temperature the spins will be frozen out to configurations aligned along some (domainwise) constant magnetization axes. Residual fluctuations around these configurations, described by the Holstein-Primakoff boson excitations, or spinwaves, discussed before can be described in terms of a controlled expansion scheme. Similar programs work for countless other physical systems.

These considerations dictate much of our further strategy. We will need to construct methods to identify and describe the lowest energy configurations of many particle systems – often called 'mean fields' – and learn how to do perturbation theory around them. In essence, the first part of that program amounts to solving a variational problem, a relatively straightforward task. However, the formulation of perturbation strategies requires some preparation and, equally important, a good deal of critical caution (this because many systems notoriously defy perturbative assaults, a fact easily misjudged!) We thus turn the logical sequence of the two steps upside down and devote *this* chapter to an

introduction to many body perturbation theory. This will include a number of applications, i.e. problems where the mean field is trivial an perturbation theory alone suffices to produce meaningful results. Perturbation theory superimposed on non-trivial mean-fields will then be the subject of the next chapter.

6.1 Perturbation Theory I: General Structures and Low-Order Expansions

As with any other perturbative approach, many body perturbation theory amounts to an expansion of observables in powers of some parameter, typically, the coupling strength of an interaction operator. However, before discussing how this program is implemented in practice, it is imperative to develop some understanding of the mathematical status of such 'series expansions'. (To motivate the point: it may, and often *does* happen that the infinite order expansion in the 'small parameter' of the problem does not exist in a mathematical sense!) This can be achieved by considering

6.1.1 An Instructive Integral

Consider the integral

$$I(g) = \int \frac{dx}{\sqrt{2\pi}} e^{-\frac{1}{2}x^2 - gx^4}. \tag{6.1}$$

It can be regarded as a miniscule caricature of a particle subject to some harmonic potential (x^2) plus 'interaction' (x^4). For small $g \ll 1$, it is natural to treat the interaction perturbatively, i.e. to expand

$$I(g) \approx \sum_n g^n I_n, \tag{6.2}$$

where

$$g^n I_n = \frac{(-g)^n}{n!} \int \frac{dx}{\sqrt{2\pi}} e^{-\frac{1}{2}x^2} x^{4n} = (-g)^n \frac{(4n-1)!!}{n!} \overset{n\gg 1}{\sim} \left(\frac{gn}{e}\right)^n.$$

and the last proportionality is based on the Stirling formula $n! \overset{n\gg 1}{\sim} n^n e^{-n}$.

This estimate should alert us. It states that, strictly speaking, a series expansion in the 'small parameter' g does not exist. No matter how small g, at $\sim (1/g)$th in the perturbative expansion, the series begins to diverge. In fact, it is easy to predict this breakdown on qualitative grounds: For $g > 0$ ($g < 0$), the integral (6.1) is convergent (divergent). This implies that the series expansion of the function $I(g)$ around $g = 0$ must have zero radius of convergence. However, there is also a more 'physical' way of understanding the phenomenon. Consider a one-dimensional version of (4.45), where the 'Gaussian average' is given by (4.44):

$$\int \frac{dx}{\sqrt{2\pi}} e^{-\frac{1}{2}x^2} x^{4n} = \sum_{\substack{\text{all possible} \\ \text{pairings of } 4n \text{ objects}}} 1 = (4n-1)!!.$$

The factor $(4n-1)!!$ measures the combinatorial freedom to pair up $4n$ objects. This suggests to interpret the breakdown of the perturbative expansion as the result of a

competition between the smallness of the expansion parameter g and the combinatorial proliferation of equivalent contributions, or 'pairings', contributing to the Gaussian integral. Physically, the combinatorial factor can be interpreted as the number of different 'partial amplitudes' contributing to the net result at any given order of perturbation theory. Eventually, the exponential growth of this figure overpowers the smallness of the expansion parameter which is when perturbation theory breaks down. (Oddly the existence of this, rather general mechanism is usually not mentioned in textbook treatments of quantum perturbation theory!)

Does the ill-convergence of the series imply that perturbative approaches to problems of the structure (6.1) are doomed to fail? Fortunately, this is not so. While the *infinite* series $\sum_{n=0}^{\infty} g^n I_n$ is divergent, a *partial* resummation $\sum_{n=0}^{n_{\max}} g^n I_n$ can yield excellent approximations to the exact result $I(g)$. To see this, let us use that $|e^{-gx^4} - \sum_{n=0}^{n_{\max}} \frac{(gx^4)^n}{n!}| \leq \frac{(-gx^4)^{n_{\max}+1}}{(n_{\max}+1)!}$ to estimate the error

$$\left| I(g) - \sum_{n=0}^{n_{\max}} g^n I_n \right| \leq g^{n_{\max}+1} I_{n_{\max}+1} \overset{n_{\max}\gg 1}{\sim} \left(\frac{g n_{\max}}{e}\right)^{n_{\max}}$$

Variation wrt $n_{\max}$ shows that the error reaches its minimum when $n_{\max} \sim g$ where it scales like $e^{-1/g}$. Notice the exponential dependence of the error on the coupling g. E.g. for a small coupling $g \approx 0.01$, 100th order perturbation theory would lead to an approximation of astronomic absolute precision e^{-100}. In contrast, for $g \approx 0.3$, perturbation theory becomes bad already after 3rd order!

Summarizing, the moral to be taken home from the analysis of the integral (6.1) (and which generalizes to theories of more complex structure) is that perturbative expansions should not be confused with rigorous Taylor expansions. They rather represent **asymptotic expansions**, in the sense that for weaker and weaker coupling a *partial* resummation of the perturbation series leads to an ever more precise approximation to the exact result. For weak enough coupling the distinction between Taylor expansion and asymptotic expansion becomes academic (at least for physicists). However, for intermediate or strong coupling theories, the asymptotic character of perturbation theory must be kept in mind.

6.1.2 ϕ^4-Theory

While the integral discussed in the previous section told us something about the general status of perturbation theory, we need to proceed to the level of *functional* integrals to learn more about the practical implementation of perturbative methods. The simplest interacting field theory displaying all relevant structures is defined through

$$Z \equiv \int \mathcal{D}\phi e^{-S[\phi]}, \qquad S[\phi] \equiv \int d^d x \left(\frac{1}{2}\partial\phi\partial\phi + \frac{r}{2}\phi^2 + g\phi^4\right), \tag{6.3}$$

where ϕ is a scalar bosonic field. Owing to the structure of its interaction term, this model is often referred to as **ϕ^4-theory**. The ϕ^4-model not only provides a prototypical environment in which features of interacting field theories can be explored, it also appears in numerous applications. E.g. close to its critical point, the d-dimensional Ising model

is described by the ϕ^4-action (see the info-block below.) More generally, it can be shown that the long range behaviour of classical statistical systems with a single order parameter (e.g. the density of a fluid, uni-axial magnetisation etc.) is described by the ϕ^4-action[1]. Within the context of statistical mechanics, $S[\phi]$ is known as the **Ginzburg-Landau free energy functional** (less frequently also as the **Landau-Wilson model**.)

▷ INFO. The d-dimensional **Ising model** describes the classical magnetism of a lattice of magnetic moments $S_i \in \{1, -1\}$ that can take only two values ± 1. It is defined through the Hamiltonian

$$H = \sum_{ij} S_i C_{ij} S_j - \sum_i H_i S_i, \tag{6.4}$$

where $C_{ij} = C(|i-j|)$ is a correlation matrix describing the mutual interaction of the spins, H an external magnetic field and the sums run over the sites of a d-dimensional lattice (assumed hypercubical for simplicity.)

The Ising model is the simplest model describing classical magnetism. In low dimensions $d = 1, 2$, it can be solved exactly, i.e. the partition function and all observables depending on it can be computed rigorously (see our discussion in chapter XX.) However, for generic dimensions no closed solutions exist and one has to resort to approximation strategies. Below we will show that the long range physics of the system is described by ϕ^4-theory. Notice that (safe for the exceptional case $d = 1$ discussed in chapter XX) the system is expected to display a magnetic *phase transition*. As a corrolary this implies that the ϕ^4-model must exhibit much more interesting behaviour than its innocent apperence suggests!

Consider the partition function

$$Z = \sum_{\{S_i\}} e^{\sum_{ij} S_i K_{ij} S_j + \sum_i h_i S_i}, \tag{6.5}$$

where $K \equiv -\beta C$ and $h \equiv \beta h$. The feature that prevents us from rigorously computing the configurational sum is, of course, the correlation between the spins. We can remove that correlation at, however, a price: Let us consider the 'fat unity',

$$1 = \mathcal{N} \int \mathcal{D}\psi \, e^{-\frac{1}{4}\sum_{ij} \psi_i (K^{-1})_{ij} \psi_j},$$

where $\mathcal{D}\psi \equiv \prod_i d\psi_i$, K^{-1} is the inverse of the correlation matrix and $\mathcal{N} = \sqrt{\det(4\pi K^{-1})}$ a factor normalizing the integral to unity. A shift of the integration variables, $\psi_i \to \psi_i - 2(K\mathbf{S})_i$, brings the integral into the form (Here $(K\mathbf{S})_i$ is the ith component of the vector obtained by multiplying the matrix K to the vector $\mathbf{S} = \{S_i\}$.)

$$1 = \mathcal{N} \int \mathcal{D}\psi \, e^{-\frac{1}{4}\sum_{ij} \psi_i (K^{-1})_{ij} \psi_j + \sum_i S_i \psi_i - \sum_{ij} S_i K_{ij} S_j}.$$

We now multiply this representation of unity to the partition function and obtain

$$Z = \mathcal{N} \int \mathcal{D}\psi \sum_{\{S_i\}} e^{-\frac{1}{4}\sum_{ij} \psi_i (C^{-1})_{ij} \psi_j + \sum_i S_i (\psi_i + h_i)} \tag{6.6}$$

[1] Heuristically, this is explained by the fact that $S[\phi]$ is the simplest interacting (i.e. non-Gaussian) model action invariant under inversion $\phi \leftrightarrow -\phi$. (The action of an uniaxial magnet should depend on the value of the local magnetization, but not on its sign.) A purely Gaussian theory might describe wave-like fluctuations of the magnetization, but not the 'critical' phenomenon of a magnetic transition. One thus needs, at least, a ϕ^4-interaction term. Later on we will see that more complex monomials of ϕ, such as ϕ^6 or $(\partial\phi)^4$, are inessential in the long range limit.

We have, thus, removed the correlation between the spin variables at the expense of the introduction of a new continuous field $\{\psi_i\}$. Why do this? Because a multi-dimensional integral $\int \mathcal{D}\psi$ is usually easier to deal with than a multi-dimensional sum $\sum_{\{S_i\}}$ over discrete objects. The transformation leading from (6.5) to (6.6) is our first example of a so-called **Hubbard-Stratonovich transformation**. One field is decoupled on the expense of the introduction of another. Notice that in spite of the somewhat high-minding denotation, the transformation is tantamount to a simple shift of a Gaussian integration variable, a feature shared by all Hubbard-Stratonovich transformations!

The summation $\sum_{\{S_i\}} = \prod_i \sum_{S_i}$ can now be trivially done:

$$\begin{aligned} Z &= \mathcal{N} \int \mathcal{D}\psi \, e^{-\frac{1}{4}\sum_{ij} \psi_i (K^{-1})_{ij} \psi_j} \prod_i (2\cosh(\psi_i + h_i) = \\ &= \mathcal{N} \int \mathcal{D}\psi \, e^{-\frac{1}{4}\sum_{ij} \psi_i (K^{-1})_{ij} \psi_j + \sum_i \ln\cosh(\psi_i + h_i)} \\ &= \mathcal{N} \int \mathcal{D}\psi \, e^{-\frac{1}{4}\sum_{ij} (\psi_i - h_i)(K^{-1})_{ij} (\psi_j - h_j) + \sum_i \ln\cosh(\psi_i)}, \end{aligned}$$

where we have absorbed the inessential factor $\prod_i 2$ in the normalization $\mathcal{N}$. We finally change integration variables from ψ_i to $\phi_i \equiv \frac{1}{2}(K^{-1}\boldsymbol{\psi})_i$ and arrive at the intermediate result

$$Z = \mathcal{N} \int \mathcal{D}\phi \, e^{-\sum_{ij} \phi_i K_{ij} \phi_j + \sum_i \phi_i h_i + \sum_i \ln\cosh(2(K\phi)_i)}.$$

This representation of the problem still does not look very inviting. To bring it into a form amenable to further analytical evaluation, we need to make the simplifying assumption that we are working at low temperatures such that the exponential weight $K_{ij} = \beta C(|i-j|)$ inhibits strong flucutations of the field ϕ. More precisely, we assume that $|\phi_i| \ll 1$ and that the spatial profile of the field is smooth. To make use of these conditions, we switch to a Fourier representation,

$$\begin{aligned} \phi_i &= \frac{1}{\sqrt{N}} \sum_{\mathbf{k}} e^{-i\mathbf{k}\cdot\mathbf{r}_i} \phi(\mathbf{k}), \\ K_{ij} &= \frac{1}{N} \sum_{\mathbf{k}} e^{-i\mathbf{k}\cdot(\mathbf{r}_i - \mathbf{r}_j)} K(\mathbf{k}) \end{aligned}$$

and expand $\ln\cosh(x) = \frac{1}{2}x^2 - \frac{1}{12}x^4 + \ldots$. Noting that $(K\phi)(\mathbf{k}) = K(\mathbf{k})\phi(\mathbf{k}) = K(0)\phi(\mathbf{k}) + \frac{1}{2}\mathbf{k}^2 K''(0)\phi(\mathbf{k}) + \mathcal{O}(\mathbf{k}^4)$, we conclude that the low temperature expansion of the action has the general structure

$$S[\phi] = \sum_{\mathbf{k}} [\phi_{\mathbf{k}}(c_1 + c_2 \mathbf{k}\cdot\mathbf{k})\phi_{-\mathbf{k}} + c_3 \phi_{\mathbf{k}} h_{-\mathbf{k}}] + \frac{c_4}{N} \sum_{\mathbf{k}_1,\ldots,\mathbf{k}_4} \phi_{\mathbf{k}_1}\phi_{\mathbf{k}_2}\phi_{\mathbf{k}_3}\phi_{\mathbf{k}_4}\delta_{\mathbf{k}_1+\mathbf{k}_2+\mathbf{k}_3+\mathbf{k}_4} + \mathcal{O}(\mathbf{k}^4, h^2, \phi^6)$$

▷ EXERCISE. Show that the coefficients c_i are given by

$$\begin{aligned} c_1 &= K(0)(1 - 2K(0)), \\ c_2 &= \frac{1}{2}K''(0)(1 - 4K(0)), \\ c_3 &= 1, \\ c_4 &= \frac{4K(0)}{3}. \end{aligned}$$

Switching back to a real space representation and taking a continuum limit, the $S[\phi]$ assumes the form of a prototypical ϕ^4-action

$$S[\phi] = \int d^d r \left(c_1 \partial\phi\partial\phi + c_2\phi\phi + c_3\phi h + N c_4 \phi^4 \right).$$

A rescaling of variables $\phi \to \frac{1}{\sqrt{c_{12}}}\phi$ finally brings the action into the form (6.3) with coefficients $r = c_2/c_1$ and $g = c_4/(2c_1)$.[2]

We have thus succeeded in describing the low temperature phase of the Ising model in terms of a ϕ^4-model. While the structure of the action could have been guessed on symmetry grounds, the 'microscopic' derivation has the advantage that it yields explicit expressions for the coupling constants. There is actually one interesting aspect about the dependence of these constants on the parameters of the microscopic model. Consider the constant c_2 controlling the **k**-independent contribution to the Gaussian action: $c_2 \propto K''(0)(1 - 4K(0)) \propto (1 - 4\beta C(0))$. Since $C(0)$ must be positive to ensure the overall stability of the model (why?) the constant c_2 will change sign at a certain 'critcal temperature' β^*. For temperatures lower than β^*, the Gaussian action is unstable (i.e. fluctuations with low wavevector become unbound) and the anharmonic term ϕ^4 alone controls the stability of the model. Clearly, the behaviour of the system will change drastically at this point. Indeed, the critical temperature $c_2(\beta^*) = 0$ marks the position of the magnetic phase transition, a point to be discussed in more detail below.

Let us begin our primer of perturbation theory by introducing some nomenclature[3]. To save writing, we define the notation

$$\langle \ldots \rangle \equiv \frac{\int \mathcal{D}\phi\, e^{-S[\phi]}(\ldots)}{\int \mathcal{D}\phi\, e^{-S[\phi]}}, \tag{6.7}$$

for the functional integral, weighted by the action S, of a any expression $(\ldots)$. Due to the structural similarity to the thermal averages of statistical mechanics, $\langle \ldots \rangle$ is sometimes called a **functional average** or **functional expectation value**. Similarly, we define

$$\langle \ldots \rangle_0 \equiv \frac{\int \mathcal{D}\phi\, e^{-S_0[\phi]}(\ldots)}{\int \mathcal{D}\phi\, e^{-S_0[\phi]}} \tag{6.8}$$

for the functional average over the Gaussian action $S_0 \equiv S|_{g=0}$. The average over a product of field variables,

$$C_n(\mathbf{x}_1, \mathbf{x}_2, \ldots, \mathbf{x}_n) \equiv \langle \phi(\mathbf{x}_1)\phi(\mathbf{x}_2)\ldots\phi(\mathbf{x}_n) \rangle \tag{6.9}$$

is called an **(n-point) correlation function**, sometimes also just **n-point function** for brevity[4].

---

[2] The only difference is that the magnetic ϕ^4-action contains a term linear in ϕ and h. The reason is that in the presence of a finite magnetic field the action is no longer invariant under inversion $\phi \to -\phi$.

[3] Neeless to say, that the jargon introduced below is not restricted to the ϕ^4-example!

[4] Notice that, depending on the context and/or scientific community, the phrase 'n-point function' sometimes refers C_{2n} instead of C_n.

The 1-point function $C_1(\mathbf{x}) = \langle\phi(\mathbf{x})\rangle$ simply measures the expectation value of the field amplitude. For the particular case of the ϕ^4-problem above the phase transition and, more generally, the majority of field theories with an action even in the field amplitudes, $C_1 = 0$ and the first non-vanishing correlation function is the 2-point function

$$G(\mathbf{x}_1 - \mathbf{x}_2) \equiv C_2(\mathbf{x}_1, \mathbf{x}_2). \tag{6.10}$$

(Why does C_2 depend only on the *difference* of its arguments?) The 2-point function is sometimes also called the **propagator** of the theory, the **Green function**, or, especially in the more formal literature, the **resolvent operator**. The existence of different names suggests that we have met with an important object. Indeed, we will shortly see that the Green function not only represents a central building block of the theory but also carries profound physical significance.

▷ INFO. To develop some understanding of the meaning of this object, let us recall that the average of a linear field amplitude, $\langle\phi(\mathbf{0})\rangle$, vanishes. (See the figure, where a cartoon of a few 'typical' field configurations is sketched as a function of coordinate.) However, the average of the *squared* amplitude $(\phi(\mathbf{0}))^2$ is certainly non-vanishing, simply because we are integrating over a positive object. Now, what happens if we split our single observation point into two, $\langle(\phi(\mathbf{0}))^2\rangle_0 \to \langle\phi(\mathbf{0})\phi(\mathbf{x})\rangle_0 = G(\mathbf{x})$. For asymptotically large $\mathbf{x}$ it is likely that the two amplitudes do not know of each other, i.e. $G(\mathbf{x}) \stackrel{|\mathbf{x}|\to\infty}{\longrightarrow} 0$. However, this vanishing will not happen instantly. The reason is that the field amplitudes are *correlated* over a certain range in space. E.g. if $\phi(\mathbf{0}) > 0$, the field amplitude will, on average, stay positive in an entire neighbourhood of $\mathbf{0}$ just because rapid fluctuations of the field are energetically costly (the gradient term in the action!). The spatial correlation profile of the field is described by the function $G(\mathbf{x})$.

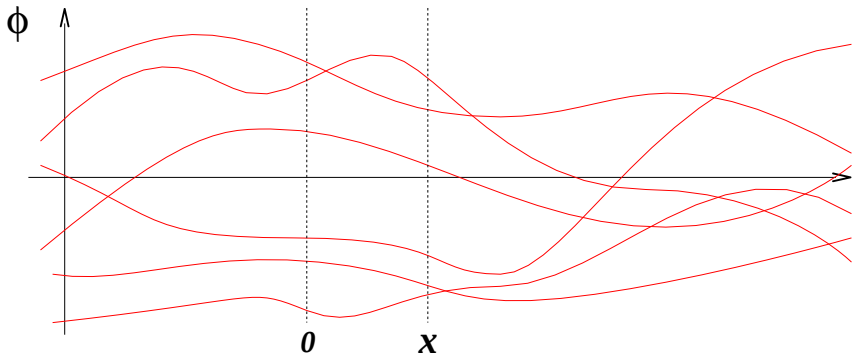

Figure 6.1: Cartoon of a few 'typical' field amplitudes. Positive and negative amplitudes enter with equal weight, hence the vanishing of $\langle\phi(\mathbf{0})\rangle$. However, the correlation function G is non-vanishing.

How does the correlation behaviour of the field relate to the basic parameters of the action. A quick answer can be given by **dimensional analysis**. The action of the theory must be dimensionless (because it appears as the argument of an exponential.) Denoting the dimension of any quantity X by $[X]$, and using that $\left[\int d^d r\right] = L^d$, $[\partial] = L^{-1}$, inspection of (6.3) obtains the set of relations,

$$L^{d-2}\,[\phi]^2 = 1,$$

$$L^d\,[r]\,[\phi]^2 = 1,$$
$$L^d\,[g]\,[\phi]^4 = 1,$$

from where follow $[\phi] = L^{(d-2)/2}$, $[r] = L^{-2}$, $[g] = L^{d-4}$. In general, both system parameters, g and r carry a non-zero length-dimension. However, temporarily concentrating on the non-interacting sector, $g = 0$, the only parameter of the theory, r, has dimensionality L^{-2}. Arguing in reverse, we conclude that any intrinsic length scale produced by the theory, (e.g. the range over which the fields are correlated), must scale as $\sim r^{-1/2}$.

A more quantitative description can be obtained by considering the **free propagator** of the theory,

$$G_0(\mathbf{x}) \equiv \langle \phi(\mathbf{0})\phi(\mathbf{x})\rangle_0, \tag{6.11}$$

Since the momentum representation of the Gaussian action is simply given by

$$S_0[\phi] = \frac{1}{2}\sum_{\mathbf{p}} \phi_{\mathbf{p}}(p^2 + r)\phi_{-\mathbf{p}},$$

it is convenient to first compute G_0 in momentum space:

$$G_0(\mathbf{p}) \equiv \int d^d x\, e^{i\mathbf{p}\cdot\mathbf{x}} G_0(\mathbf{x}) = \sum_{\mathbf{p}'} \langle \phi_{\mathbf{p}}\phi_{\mathbf{p}'}\rangle_0.$$

Using the Gaussian contraction rule (4.43) the free functional average evaluates to $\langle \phi_{\mathbf{p}}\phi_{\mathbf{p}'}\rangle_0 = \delta_{\mathbf{p}+\mathbf{p}'}(p^2 + r)^{-1}$, i.e.[5]

$$G_0(\mathbf{p}) = \langle \phi_{\mathbf{p}}\phi_{-\mathbf{p}}\rangle_0 = \frac{1}{p^2 + r}. \tag{6.12}$$

To obtain $G(\mathbf{x})$, we need to compute the inverse transform

$$G_0(\mathbf{x}) = \frac{1}{L^d}\sum_{\mathbf{p}} e^{-i\mathbf{p}\cdot\mathbf{x}} G_0(\mathbf{p}) \approx \int \frac{d^d k}{(2\pi)^d}\frac{e^{-i\mathbf{p}\cdot\mathbf{x}}}{p^2 + r}, \tag{6.13}$$

where we have assumed that the system is large, i.e. the sum over momenta can be exchanged for an integral.

For simplicity, let us compute the integral for a one-dimensional system. (For the two- and three-dimensional case see the problem set.) Writing $p^2 + r = (k + ir^{1/2})(k - ir^{1/2})$, we see that the (complex extension of the) k integral has simple poles at $\pm ir^{1/2}$. For x smaller (larger) than zero, the integrand is analytic in the upper (lower) complex k-plane and closure of the integration contour to a semicircle of infinite radius obtains

$$G_0(x) = \int \frac{dk}{2\pi}\frac{e^{-i\mathbf{p}\cdot\mathbf{x}}}{(k + ir^{1/2})(k - ir^{1/2})} = \frac{e^{-r^{1/2}|x|}}{2r^{1/2}}. \tag{6.14}$$

This result teaches us something interesting. Typically, correlations decay exponentially, at a rate set by the **correlation length** $\xi \equiv r^{-1/2}$. However, as r approaches 0, the system becomes *long range correlated*. The origin of this phenomenon can be understood by inspecting the structure of the Gaussian contribution to the action (6.3). For $r \to 0$ (and still neglecting the ϕ^4-contribution) nothing prevents the constant field mode $\phi(\mathbf{x}) = \phi_0 = \text{const.}$ from becoming

[5] The result $G_0(\mathbf{p}) = (p^2+r)^{-1}$ clarifies why G is referred to as a 'Green function'. Indeed, $G_0(\mathbf{p})$ is (the momentum representation of the) Green function of the differential equation $(-\partial_{\mathbf{r}}^2 + r)G(\mathbf{r}, \mathbf{r}') = \delta(\mathbf{r} - \mathbf{r}')$.

infinitely large, i.e. the fluctuating contribution to the field becomes relatively less important than the constant offset. The increasing 'stiffness' of the field in turn manifests itself in a growth of spatial correlations (cf. Fig. 6.1.) Notice that this fits in nicely with our previous statement that $r = 0$ marks the position of a phase transition. Indeed, the buildup of infinitely long range spatial correlations is known to a be a hallmark of second order phase transitions.

6.1.3 Perturbation Theory at Low Orders

Having discussed the general structure of the theory and of its free propagator, let us turn our attention to the role of the interaction contribution to the action,

$$S_{\text{int}}[\phi] \equiv g \int d^d x\, \phi^4.$$

Within the jargon of fieldtheory, an integrated monomial of a field variable (like ϕ^4) is commonly called an **(interaction) operator** or a **vertex (operator)**. Keeping the words of caution made in section 6.1.1 in mind, we wish to explore perturbatively how the interaction vertex affects the functional expectation value of any given field observable, i.e. we wish to analyse expansions of the type

$$\langle X[\phi] \rangle \approx \frac{\sum_{n=0}^{\cdots} \frac{(-g)^n}{n!} \left\langle X[\phi] \left(\int d^d x\, \phi^4 \right)^n \right\rangle_0}{\sum_{n=0}^{\cdots} \frac{-(g)^n}{n!} \left\langle \left(\int d^d x\, \phi^4 \right)^n \right\rangle_0} \approx \sum_{n=0}^{n_{\max}} X^{(n)}, \tag{6.15}$$

where X may be any observable and $X^{(n)}$ denotes the contribution of nth order to the expansion in g. The summation limits in numerator and denominator are symbolic because, as explained above, we will need to terminate the total perturbative expansion at a certain finite order $n_{\max}$.

▷ EXERCISE. Recapitulate section 4.5.4 on continuum Gaussian integration.

To keep the discussion concrete, let us focus on the perturbative expansion of the propagator. (A physical application relating to this expansion will be discussed in section XX below.) The zeroth order contribution $G^{(0)} = G_0$ has been discussed before, so the first non-trivial term we have to explore is $G^{(1)}$:

$$G^{(1)}(\mathbf{x}, \mathbf{x}') = -g \left(\left\langle \phi(\mathbf{x}) \int d^d y\, \phi(\mathbf{y})^4 \phi(\mathbf{x}') \right\rangle_0 - \left\langle \phi(\mathbf{x}) \phi(\mathbf{x}') \right\rangle_0 \left\langle \int d^d y \phi(\mathbf{y})^4 \right\rangle_0 \right). \tag{6.16}$$

Since the functional average is now over a *Gaussian* action, this expression can be evaluated by Wick's theorem, Eq. (4.50). E.g. the functional average of the first of the two terms leads to (integral signs and constants stripped off for clarity)

$$\left\langle \phi(\mathbf{x}) \phi(\mathbf{y})^4 \phi(\mathbf{x}') \right\rangle_0 =$$

$$= 3\langle\phi(\mathbf{x})\phi(\mathbf{x}')\rangle_0 \left[\langle\phi(\mathbf{y})\phi(\mathbf{y})\rangle_0\right]^2 + 12\langle\phi(\mathbf{x})\phi(\mathbf{y})\rangle_0 \langle\phi(\mathbf{y})\phi(\mathbf{y})\rangle_0 \langle\phi(\mathbf{y})\phi(\mathbf{x}')\rangle_0 =$$
$$= 3G_0(\mathbf{x}-\mathbf{x}')G_0(\mathbf{0})^2 + 12G_0(\mathbf{x}-\mathbf{y})G_0(\mathbf{0})G_0(\mathbf{y}-\mathbf{x}'), \tag{6.17}$$

where we have used that the operator inverse of the Gaussian action is, by definition, the free Green function (cf. Eq. (6.11).) Also notice that the total number of terms appearing on the right hand side equals $15 = (5-1)!!$ which is just the number of distinct pairings of 6 objects. (Cf. with Eq. (4.50) and with our discussion of section 6.1.1.) Similarly, the second contribution to $G^{(1)}$ leads to

$$\langle\phi(\mathbf{x})\phi(\mathbf{x}')\rangle_0\langle\phi(\mathbf{y})^4\rangle_0 = 3\langle\phi(\mathbf{x})\phi(\mathbf{x}')\rangle_0[\langle\phi(\mathbf{y})^2\rangle_0] = 3G_0(\mathbf{x}-\mathbf{x}')G_0(\mathbf{0})^2.$$

Before analysing these structures in any more detail, let us make some general observations. The first order expansion of G contains a number of factors $G(\mathbf{0})$, the free Green function evaluated at coinciding points. This bears disturbing consequences. To see this, consider $G(\mathbf{0})$ evaluated in momentum space:

$$G(\mathbf{0}) = \int \frac{d^d\mathbf{p}}{(2\pi)^d}\frac{1}{p^2+r}. \tag{6.18}$$

For dimensions $d > 1$, dhe integral is divergent at large momenta or short wavelengths; we have met with an **ultraviolett (UV) divergence**. Physically, the divergence implies that already at first order our expansion runs into a difficulty which is obviously related to the short distance structure of the system. How can this problem be overcome? One way out is to remember that field theories like the ϕ^4-model represent effective low temperature, or *long* wavelength, approximations to more microscopic models. The range of applicability of the action must be limited to wavelengths $> a$, or momenta $k < a^{-1}$, where a is some microscopic cutoff parameter. It seems that once that cutoff has been built in, the convergence problem is solved. However, there is something unsatisfactory to this option: All our perturbative corrections, and therefore the final result of the analysis, exhibit strong sensitivity on the microscopic cutoff parameter. But this is not what we expect of a sensible low energy theory (cf. the discussion of chapter **??**)! The UV problem signals that something more interesting is going on than a naive cutoff regularization could remove. We will discuss this point extensively in chapter XX.

However, even if we temporarily close our eyes on the UV-phenomenon, there is another problem. For dimensions $d \leq 2$, and in the limit $r \to 0$, $G(\mathbf{0})$ diverges also at **small momenta**, an **infrared (IR) divergence**. Being related to structures at *large wavelengths*, this type of singularity should attract our attention even more than the UV-divergence mentioned above. Indeed, it is intimately related to the buildup of longranged correlations in the limit $r \to 0$ (cf. the structure of the integral (6.13).) We will come back to the discussion of the IR-singularities, and their connection to the UV-phenomenon in chapter XX.

The considerations above show that the perturbative analysis of functional integrals will come with all sorts of divergences. On top of that, there is another, less fundamental, but also important point: Looking at Eq. (6.17), we have to concede that the expression does not look particularly inviting. To make the point we wish to score more plastic, let us consider the core contribution to the expansion at *second* order in g:

▷ EXERCISE. Show that the 10-th order contraction leads to the 945 terms

$$\begin{aligned}
&\langle\phi(\mathbf{x})\phi(\mathbf{y})^4\phi(\mathbf{y}')^4\phi(\mathbf{x}')\rangle_0 = \\
&= 9G_0(\mathbf{x}-\mathbf{x}')G_0(\mathbf{0})^4 + 72G_0(\mathbf{x}-\mathbf{x}')G_0(\mathbf{y}-\mathbf{y}')^2G_0(\mathbf{0})^2 + 24G_0(\mathbf{x}-\mathbf{x}')G_0(\mathbf{y}-\mathbf{y}')^4 + \\
&+\Big[36G_0(\mathbf{x}-\mathbf{y})G_0(\mathbf{x}'-\mathbf{y})G_0(\mathbf{0})^3 + 144G_0(\mathbf{x}-\mathbf{y})G_0(\mathbf{x}'-\mathbf{y})G_0(\mathbf{y}-\mathbf{y}')^2G_0(\mathbf{0}) + \\
&+144G_0(\mathbf{x}-\mathbf{y})G_0(\mathbf{x}'-\mathbf{y}')G_0(\mathbf{0})^2G_0(\mathbf{y}-\mathbf{y}') + 96G_0(\mathbf{x}-\mathbf{y})G_0(\mathbf{x}'-\mathbf{y}')G_0(\mathbf{y}'-\mathbf{y})^3 + \\
&\quad +(\mathbf{y}\leftrightarrow\mathbf{y}')\Big]
\end{aligned}$$

Note: Our further discussion will not rely on this result. It only serves illustrative purposes.

Clearly, Eq. (6.19) is highly in-transparent. There are seven groups of different terms, but it is not obvious how to attribute any meaning to these contributions. Further, would we consider the full second order Green function $G^{(2)}$, i.e. account for the expansion of both numerator *and* denominator in (6.2), we would find that some contributions cancel out (exercise {for energetic readers}: show it!). Clearly, the situation will not improve at third and higher order in g!

We thus see that to efficiently apply perturbative concepts beyond lowest orders a more efficient formulation of the expansion is needed. The key to the construction of a better language lies in the observation that our previous notation is full of redundancy. I.e. before the full contraction of a perturbative contribution, we represent our fields by $\phi(\mathbf{x})$. A more compact way of keeping track of the presence of that field is shown in the upper portion of the figure: Draw a point (with an optional '$\mathbf{x}$' labeling its position) and attach a little leg to it. The leg indicates that the fields are sociable objects, i.e. they need to find a partner to pair with. After the contraction, a pair $\langle\phi(\mathbf{x})\phi(\mathbf{y})\rangle \to G_0(\mathbf{x}-\mathbf{y})$ becomes a free Green function. Graphically, this information can be represented by pairwise connecting the legs of the field symbols to lines, where each line is identified with a Green function connecting the two terminating points. The full contraction of a free correlation function $\langle\phi(\mathbf{x}_1)\phi(\mathbf{x}_2)\ldots\phi(\mathbf{x}_{2n})\rangle_0$ is represented by the set of all distinct diagrams formed by pairwise connection of the field vertices.

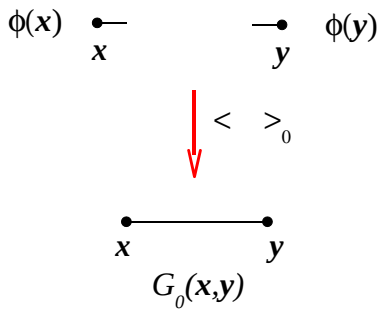

Fig. 6.2 shows the graphical representation of the contraction of Eq. (6.17). (The cross appearing on the lhs represents four field operators sitting at the same point $\mathbf{y}$. According to our rule formulated above, each of the two diagrams on the rhs represents the product of three Green functions, taken between the specified coordinates. Further, each contribution is weighted by a combinatorial factor, i.e. the number of *identical* diagrams of that structure. Consider, e.g., the second contribution on the rhs. It is formed by connecting the 'external' field vertex at $\mathbf{x}$ to *any* of the legs of the internal

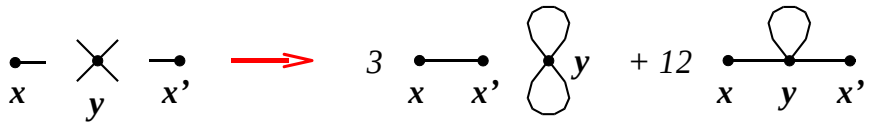

Figure 6.2: Graphical representation of a first order in g contraction contributing expansion of the Green function.

vertex at $\mathbf{y}$: 4 possibilities. Next, the vertex at $\mathbf{x}'$ is connected with one of the remaining three unsaturated vertices at $\mathbf{y}$: 3 possibilities. The last contraction $\mathbf{y} \leftrightarrow \mathbf{y}$ is fixed, i.e. we obtain altogether $3 \times 4 = 12$ equivalent diagrams. ('Equivalent' that each of these represents the same configuration of Green functions.)

▷ EXERCISE. Verify that the graphical representation of the second order contraction (6.19) is as shown in Fig. 6.3[6]. Associate diagrams to individual contributions appearing in (6.19) and try to reproduce the combinatorial factors.

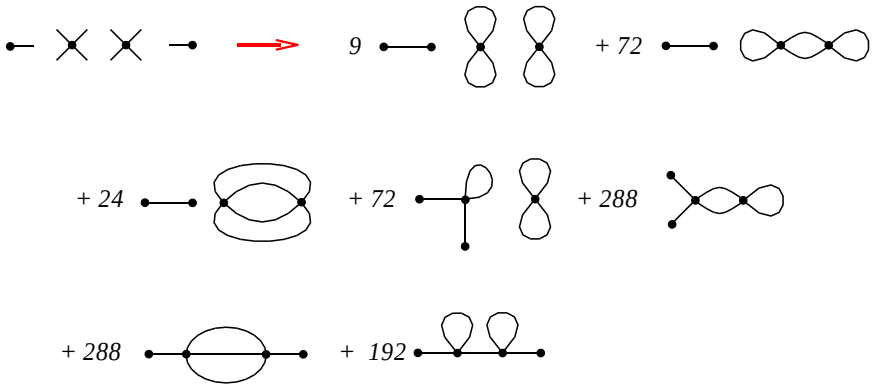

Figure 6.3: Graphical representation of the second order correction to the Green function.

The graphic representation of the contractions shown in Figs. 6.2 and 6.3, provides us with sufficient background to list some general aspects of the diagrammatic approach:

▷ First a trivial, point: Diagrammatic methods help to efficiently *represent* the perturabative expansion. However, we are still left with the problem (see the discussion above) of *computing* the analytical expressions corresponding to individual diagrams. To go back from an nth order graph to its analytical representation one (i) attaches coordinates to all field vertices, (ii) identifes lines between points with Green functions, (iii) multiplies the graph with the overall constant $\frac{g^n}{n!}$, and (iv) integrates over all coordinates of the internal coordinates. When one encounters expressions like $G^{(n)}$ = 'sum of graphs', the operations (i)-(iv) are implicit.

[6] In the figure, the coordinates carried by the field vertices have been dropped for notational simplicity. To restore the full information carried by any of these 'naked' graphs one attaches coordinates $\mathbf{x}$ and $\mathbf{x}'$ to the external field vertices and integration-coordinates $\mathbf{y}_i$ to each of the i nodes that do not connect to an external field vertex. Since no information is lost, diagrams are often represented without explicit reference to coordinates.

- ▷ As should be clear from the clear from the formulation of our basic rules, there is no fixed rule as to how to represent a diagram. I.e. as long as no lines are cut any kind of reshaping, twisiting, rotatiting, etc. of the diagram leaves its content invariant. (At large orders of perturbation theory, it often takes a second look to identify two differently drawn diagrams as equivalent.)

- ▷ From the assembly of diagrams contributing to any given order, a number of internal structures immanent to the series expansion become apparent. E.g. looking at the diagrams shown in Fig. 6.2, we notice that some are simply connected, some are not. Among the set of **connected diagrams** (no's. 5,6,7) there are some whose 'core portion', i.e. the content of the diagram after the legs connecting to the external vertices has been removed, can be cut into two pieces just by cutting one more line (no. 7). Others (no's. 5,6) show a higher degree of internal entanglement. One can also attach a **loop order** to a diagram, i.e. the number of inequivalent loops formed by segments of Green functions (for Fig. 6.3: 4,3,3,3,2,2,2, in that order.) One (correctly) expects that these structures, which are difficult to discern from the equivalent analytical representation, will reflect themseleves in the mathematics of the perturbative expansion. We will come back to discussing this point below.

- ▷ Then there is the issue of **combinatorics**. The diagrammatic representation eases to determine the combinatorial factors appearing in the expansion. However, the problem of getting the combinatorics right remains non-trivial. (If you are not impressed with the factors entering the second order expansion, consider the 93.555 terms contributing at third order!) In some sub-disciplines of theoretical physics, the art of identifying the full set of combinatorial coefficients at large orders of perturbation theory has been developed to great sophistication. Indeed, one can set up refined sets of diagrammatic construction rules which to considerable extend automatize the combinatorics. Pedagogical discussions of these rules can be found, e.g. in the textbooks [**?**, **?**]. However, as we will see shortly, the need to explicitly carry out a large order expansion, with account for all diagrammatic sub-processes, rarely arises in modern condensed matter physics; mostly one is interested in *subclasses* of diagrams, for which the combinatorics is less problematic. For this reason, the present text does not contain a state of the art exposition of all diagrammatic tools and interested readers are referred to the literature.

- ▷ Finally, and perhaps most importantly, the diagrammatic representation of a given contribution to the perturbative expansion often suggests a **physical interpretation** of the corresponding physical process. (After all, any term contributing to the expansion of a physical observable must correspond to some 'real' physical process.) Unfortunately, the ϕ^4-theory is not well suited to illustrate this aspect, i.e. void of any dynamical content, it is a little bit *too* simple. However, the possibility to 'read' individual diagrams will becom evident in the next section when we discuss an an application to the interacting electron gas.

Above we have introduced the diagrammatic approach on the example of field expectation values $\langle\phi(\mathbf{x})(\phi(\mathbf{y})^4)^n\phi(\mathbf{x}')\rangle_0$. However, to obtain the Green function to any given order in

perturbation theory, we need to add to these expressions contributions emanating from the expansion of the denominator of the functional average (cf. Eqs. (6.15) and (6.16).) While, at first sight, the need to keep track of even more terms seems to complicate matters, we will see that the opposite is true! The combined expansion of numerator and denominator leads to a miraculous 'cancellation mechanism' which greatly *simplifies* the analysis.

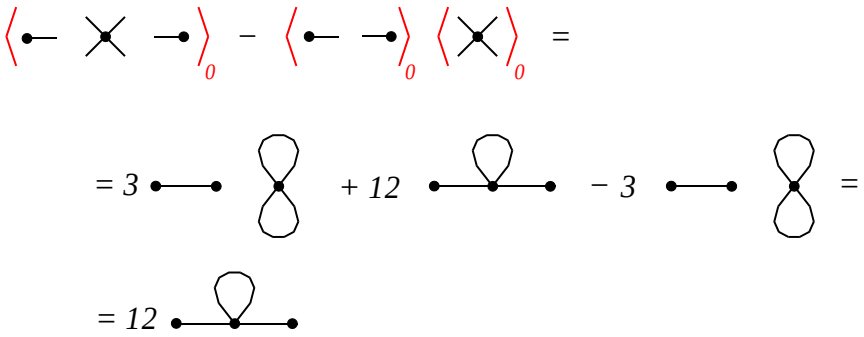

Figure 6.4: Graphical representation of the first order correction to the Green function: Vaccuum graphs cancel out.

Let us exemplify the functioning of that mechanism on $G^{(1)}$. The three diagrams corresponding to the contractions of Eq. (6.16) are shown in Fig. 6.4, where integral signs and coordinates are dropped to simplify. On the l.h.s. of the equation brackets $\langle \ldots \rangle_0$ indicate that the second contribution comes from the expansion of the denominator. The point to be noticed is that the graph produced by the contraction of that term cancels against a contribution coming from the numerator. One further observes that the cancelled graph is of special type: It contains an interaction vertex that does not connect to any of the external vertices. Diagrams with that property are commonly denoted **vacuum graphs**[7].

▷ EXERCISE. Construct the diagram representation of $G^{(2)}$ and verify that the expansion of the nominator eliminates all vacuum graphs of the numerator. I.e. verify that $G^{(2)}$ is given by the sum of connected diagrams shown in Fig. 6.5.

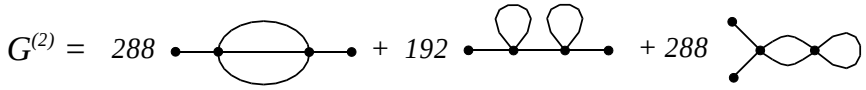

Figure 6.5: Graphical representation of the second order contribution to the Green function.

The cancellation of vaccuum graphs pertains to higher order correlation functions *and* to all orders of the expansion:

[7] The denotation 'vacuum graph' has historical reasons. Diagrammatic methods where invented in the 50's, in the context of particle theory. Instead of thermal averages $\langle \ldots \rangle_0$, one considered matrix elements $\langle \Omega | \ldots | \Omega \rangle$ taken in the ground state of 'vacuum' of the field theory. That motivated to dub matrix elements $\langle \Omega | (S_{\rm int}[\phi])^n | \Omega \rangle$ not containing an external field vertex 'vacuum graphs'.

The contribution to a correlation function $C^{(2n)}(\mathbf{x}_1, \ldots, \mathbf{x}_{2n})$ at lth order of perturbation theory is given by the sum of all graphs, *excluding* vacuum graphs.

E.g. the first order expansion of the 4-point function $C^{(4)}(\mathbf{x}_1, \ldots \mathbf{x}_4)$ is shown in the figure, where coordinates $\mathbf{x}_i \leftrightarrow i$ are abbreviated by indices and '+ pert.' stands for 6 permutations obtained by interchanging arguments. In the literature, the statement of vacuum graph cancellation is sometimes referred to as the **linked cluster theorem**. Notice that by the linked cluster feature, two flies are clasped by one stroke: First we are relieved of the burden of a double expansion of numerator and denominator, second only non-vacuum contributions to the expansion of the former need to be kept.

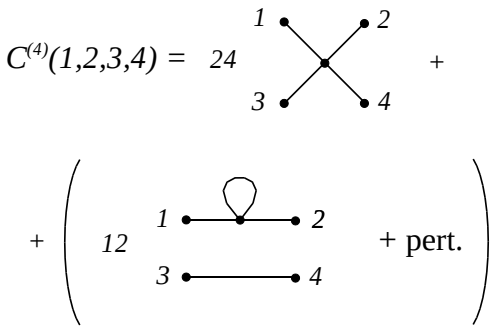

▷ INFO. The **proof of the linked cluster theorem** is not difficult. Consider a contribution of nth order to the expansion of the numerator of (6.15): $\frac{(-g)^n}{n!} \langle X[\phi] (\int \phi^4)^n \rangle_0$. The contraction of that expression will lead to a sum of vacuum graphs of pth order and non-vacuum graphs of $(n-p)$th order, where p runs from 0 to n. The pth order contribution is given by

$$\frac{1}{n!}\binom{n}{p} \left\langle X[\phi] \left(\int \phi^4\right)^{n-p} \right\rangle_{0,\text{n.v.}} \left\langle \left(\int \phi^4\right)^{p} \right\rangle_0 ,$$

where the subscript $\langle \ldots \rangle_{0,\text{n.v.}}$ indicates that the contraction excludes vacuum graphs and the combinatorial coefficient counts the number of possibilities to pick p vertices ϕ^4 of a total of n vertices to form a vacuum graph. Summing over p, we find that the expansion of the numerator, split into vacuum and non-vacuum contributions, reads as,

$$\sum_{n=0}^{\infty} \sum_{p=0}^{n} \frac{(-g)^n}{(n-p)!p!} \left\langle X[\phi] \left(\int \phi^4\right)^{n-p} \right\rangle_{0,\text{n.v.}} \left\langle \left(\int \phi^4\right)^{p} \right\rangle_0 .$$

By a straightforward rearrangement of the summations, this can be rewritten as

$$\sum_{n=0}^{\infty} \frac{(-g)^n}{n!} \left\langle X[\phi] \left(\int \phi^4\right)^{n} \right\rangle_{0,\text{n.v.}} \sum_{p=0}^{\infty} \frac{(-g)^p}{p!} \left\langle \left(\int \phi^4\right)^{p} \right\rangle_0 .$$

The p-summation exactly equals the expansion of the denominator, so we are left with the sum over all non-vacuum contractions □.

Before concluding this section, let us discuss one last technical point. The translational invariance of the ϕ^4-action suggests to represent the theory in momentum space. Indeed, the **momentum space representation** of the propagator (6.12) is much simpler than the real space form, and the subsequent analytical evaluation of diagrams will be formulated in momentum space anyway (cf. the prototypical expression (6.18).)

The diagrammatic formulation of the theory in momentum space is straightforward. All we need to do to is slightly adjust the graphical code. Inspection of Eqs. (6.12) shows that the elementary contraction should now be formulated as indicated in the figure. Only fields with opposite momentum can be contracted; the line carries this momentum as a label. Notice that the momentum representation of the field vertex $(\phi(\mathbf{x}))^4$ is **not** given by $(\phi_{\mathbf{p}})^4$. Fourier transformation of the vertex rather leads to the three-fold convolution

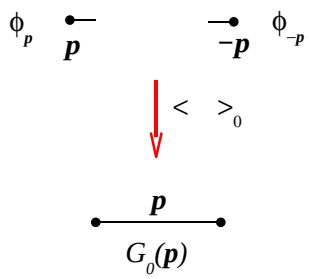

$$\int d^d x \phi(\mathbf{x})^4 \to \frac{1}{L^d} \sum_{\mathbf{p}_1,\ldots,\mathbf{p}_4} \phi_{\mathbf{p}_1}\phi_{\mathbf{p}_2}\phi_{\mathbf{p}_3}\phi_{\mathbf{p}_4}\delta_{\mathbf{p}_1+\mathbf{p}_2+\mathbf{p}_3+\mathbf{p}_4}\,.$$

The graphical representation of the first order correction to the Green function (i.e. the momentum space analog of Fig. 6.4) is shown in Fig. 6.6. It is useful to think about the vertices of the momentum-space diagrammatic language in the spirit of 'Kirchhoff laws': The addition of all momenta flowing into a vertex equals zero. Consequently (think about it!) the *total* sum of all momenta 'flowing' into a diagram from external field vertices must equal zero, too: $\langle \phi_{\mathbf{p}_1}\phi_{\mathbf{p}_2}\ldots\phi_{\mathbf{p}_n}(\ldots)\rangle_0 \to \delta_{\sum_{i=1}^n \mathbf{p}_i}(\ldots)$. This fact expresses the conservation of the total momentum characteristic for theories with global momentum conservation.

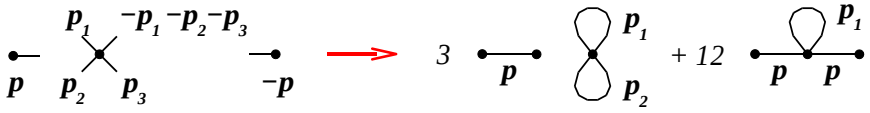

Figure 6.6: Momentum space representation of a first order contribution to the Green function. Internal momenta $\mathbf{p}_i$ are integrated over.

▷ EXERCISE. Represent the diagrams of the second order contraction 6.3 in momentum space. Convince yourself that that the 'Kirchhoff law' suffices to fix the result. Observe that the number of summation over internal momenta equals the number of loops.

This concludes the first part of our introduction to the formal elements of perturbation theory. Critical readers will object that while we undertook some efforts to efficiently *represent* the perturbative expansion we have not in the least answered the question of how interactions will actually modify the results of the free theory. Indeed, we are not yet in a position to quantitatively address this problem, the reason being that we first need to better understand origin and remedy of the UV/IR-divergences observed above.

However, temporarily ignoring the presence of this roadblock, let us try to outline what kind of information can be extracted from perturbative analyses, *in principle*. One important point to be noted is that in condensed matter physics[8] low order perturbation theory

[8] There are subdisciplines of physics, where the situation is different. E.g. consider the high precision scattering experiments of atomic and sub-atomic phyiscs. In these areas, the power of a theory to quantitatively predict the dependence of scattering rates on the strength of the projectile/target interaction (the 'perturbation') is a measure of its quality. Such tests involve large order expansions in the physical coupling parameters.

is usually not enough to obtain *quantitative* results. The fact that the 'perturbation' couples to a macroscopic number of degrees of freedom[9] usually necessitates summation of infinite (sub)series of a perturbative expansion or even the application of non-perturbative methods. This, however, does not in the least mean that the tools developed above are useless: Given a system subject to unfamiliar interactions, low order perturbation theory will usually be applied as a first sonde to qualitatively explore the situation. E.g. a malign divergence of the expansion in the interaction operator may signal the presence of an instability towards the formation of a different phase. Or, it may turn out that certain contributions to the expansion are 'physically more relevant' than others. Technically, such contributions usually crrespond to diagrams of a regular graphical structure. If so, a summation over all 'relevant processes' may be in reach. In either case, low order expansions provide vital hints as to the appropriate strategy of further analysis. In the next subsections we will discuss two examples which may help to make these remarks more transparent.

6.2 Ground State Energy of the Interacting Electron Gas

In section 3.2.1 we began to consider the physics of highly mobile electron compounds. We argued that the system can be described in terms of the free particle Hamiltonian (3.16) plus the interaction operator (3.2.1). While we have reviewed the physics of the non-interacting system, nothing had been said about role of electron-electron interactions. Yet by now we have developed enough analytical machinery to address this problem. Below we will apply concepts of perturbation theory to estimate the contribution of electronic correlations to the ground state energy of a Fermi system. However, before plunging into the technicalities of that analysis, it is worthwhile to discuss some qualitative aspects of the problem.

[9] In contrast, low order expansions in *external* perturbation (e.g. experimentally applied electric or magnetic fields etc.) usually work fine, see chapter XX.

6.2.1 Qualitative Aspects

A principal question we will need to address is under which physical conditions interaction are 'weak' (in comparison to the kinetic energy), i.e. when does a perturbative approach to the interacting electron system make sense at all. To estimate the relative magnitude of the two contributions to the energy, let us assume that each electron occupies an average volume r_0^3. According to the uncertainty relation, the minimum kinetic energy per particle will be of $\mathcal{O}(\hbar^2/mr_0^2)$. On the other hand, assuming that each particle interacts predominantly with its nearest neighbours, the Coulomb energy is of $\mathcal{O}(e^2/r_0)$. The ratio of the two energy scales defines the **dimensionless density parameter**

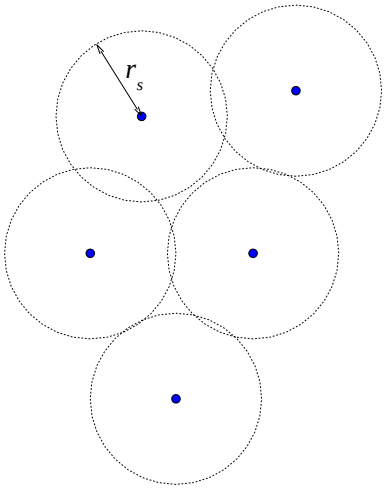

$$\frac{e^2}{r_0}\frac{mr_0^2}{\hbar^2} = \frac{r_0}{a_0} \equiv r_s,$$

where $a_0 = \hbar^2/e^2m$ denotes the Bohr radius[10]. Physically, r_s is the radius of the spherical volume containing one electron on average; the denser the electron gas, the smaller r_s. We have thus identified the electron density as the relevant parameter controlling the relative strength of electron-electron interactions.

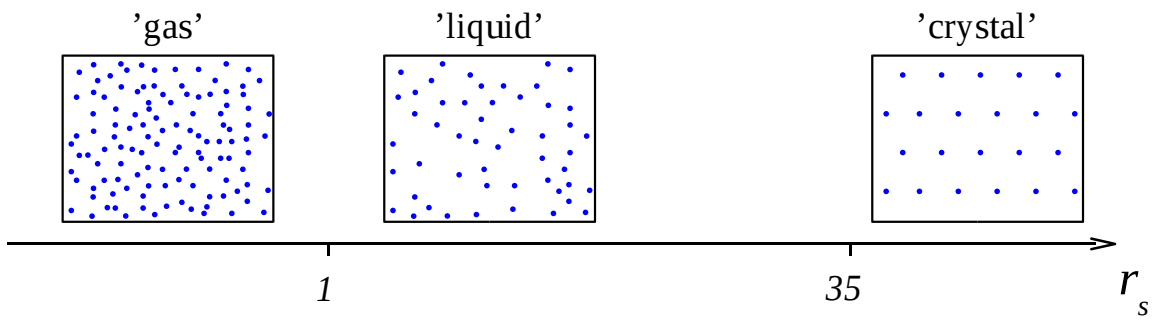

Figure 6.7: Cartoon of configurations of the electron system for different densities. At large densities, the system is in a gaesous, weakly correlated phase. For densities $r_s > 36$ one expects a crystalline configuration. At intermediate densities, the system is governed by strong electronic correlations, a 'liquid'.

Below, we will be concerned with the regime of high density $r_s \ll 1$ or weak Coulomb interaction. In the opposite limit, $r_s \gg 1$, properties become increasingly dominated by electronic correlations. Ultimately, for sufficiently large r_s (or low density) it is believed that the electron gas undergoes a (first order) phase transition to a condensed or 'solid'

[10] Notice that our estimate of the relative magnitude of energy scales mimics Bohr's famous qualitative discussion of the average size of hydrogen atoms.

phase known as a **Wigner crystal**[11]. Although Wigner crystals have never unambiguously been observed, several experiments performed on low density electron gases[12] are consistent with a Wigner crystal ground state. Monte-Carlo simulation suggests that Wigner crystallisation may occur for densities $r_s > 37$. (Note that this scenario relies crucially on being at low temperatures, and the long-range nature of the Coulomb interaction. In particular, if the Coulomb interaction is screened $V(r) \sim e^{-r/\lambda}$, $r_s \sim (r_0/a_0)e^{-r_0/\lambda}$ and the influence of Coulomb interaction at low densities becomes diminished.)

Metal	r_s	Metal	r_s
Li	3.2	Be	1.9
Na	3.9	Al	2.1
K	4.9	Sn	2.2
Cu	2.7	Pb	2.3

Table 6.1: Density parameters of a number of metals.

For $r_s \sim O(1)$, the potential and kinetic energies are comparable. This regime of intermediate coupling is notoriously difficult to describe quantitatively. Yet most metals lie in a regime of intermediate coupling $2 < r_s < 6$. Fortunately, there is overwhelming evidence to suggest that a *weak coupling* description holds even well outside the regime over which microscopic theory can be justified. The phenomenology of the intermediate coupling regime is the realm of Landau's[13] **Fermi Liquid Theory**[14].

The fundamental principle underlying the Fermi liquid theory is one of "adiabatic continuity" [?]: In the absence of an electronic phase transition (such as Wigner crystallisation), a non-interacting ground state evolves smoothly or adiabatically into the interacting ground state as the strength of interaction is increased[15]. An elementary

[11] Eugene P. Wigner 1902-1995; 1963 Nobel Laureate in Physics for his contributions to the theory of the atomic nucleus and the elementary particles, particularly through the discovery and application of fundamental symmetry principles.

[12] E. M. Goldys *et al.*, Phys. Rev. B **46**, 7957 (1992); R. G. Clark *et al.*, Physica B**201**, 301 (1994).

[13] Lev D. Landau 1908-1968, 1962 Nobel Laureate in Physics for his pioneering theories for condensed matter, especially liquid helium.

[14] L. D. Landau, Sov. Phys. JETP **3**, 920 (1956); *ibid.* **5**, 101 (1957).

[15] As a simple non-interacting example, consider the adiabatic evolution of the bound states of a quantum particle as the confining potential is changed from a box to a harmonic potential well. While the wavefunctions and energies evolve, the topological characteristics of the wavefunctions, i.e. the number of the nodes, and therefore the assignment of the corresponding quantum numbers remains unchanged.

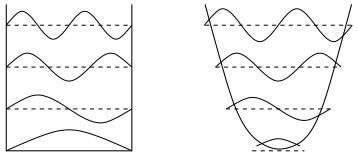

excitation of the non-interacting system represents an "approximate excitation" of the interacting system (i.e. the 'lifetime' of an elementary excitation is long). Excitations are quasi-particles (and quasi-holes) above a sharply defined Fermi surface.

The starting point of Fermi liquid theory are a few phenonomenological assumptions, all rooted in the adiabacity principle. E.g. it is postulated that the density of quasi-particles can be described in terms of a momentum dependent density distribution $n(\mathbf{p})$ which, in the limit of zero interaction, evolves into the familiar Fermi distribution. Outgoing from this one, and a few more postulates a broad spectrum of observables can be analysed without further 'microscopic' calculation. Its remarkable success (as well as the few notorious failures) have made Landau Fermi liquid theory the subject an important area of modern condensed matter physics but one which we are not goint to explore any further. (Interested readers are referred to one of several excellent reviews, e.g. xxx.) Instead, motivated in part by the phenomenological success of 'adiabatic continuity', we will continue with developing a microscopic theory of the weakly interacting three-dimensional electron gas, $r_s \ll 1$.

6.2.2 Perturbative Approach

Starting point of the perturbative analysis is the functional representation of the free energy $F = -T \ln \mathcal{Z}$, (cf. Eq. (5.28))

$$\mathcal{Z} = \int D(\bar{\psi}, \psi) e^{-S[\bar{\psi},\psi]} \tag{6.19}$$

$$S[\psi, \bar{\psi}] = \sum_p \bar{\psi}_{p\sigma} \left(-i\omega_n - \mu + \frac{\mathbf{p}^2}{2m} \right) \psi_{p\sigma} + \frac{T}{2L^3} \sum_{pp'q} \bar{\psi}_{p+q\sigma} \psi_{p\sigma} V(\mathbf{q}) \bar{\psi}_{p'-q\sigma'} \psi_{p'\sigma'}.$$

Here we have introduced the **four momentum** $p \equiv (\mathbf{p}, \omega_n)$ comprising frequency and vectorial momentum[16].

Similarly to the Green function discussed in the previous section, the free energy can be expanded in terms of an interaction parameter. To fix a reference scale against which to compare the correlation energies, let us begin by computing the free energy (5.36) of the non-interacting electron gas:

$$F^{(0)} = -T \sum_{\mathbf{p}\sigma} \ln \left(1 + e^{-\beta(p^2/(2m)-\mu)} \right) \stackrel{T\to 0}{\longrightarrow} \sum_{p^2/(2m)<\mu,\sigma} \frac{p^2}{2m} \simeq \frac{3}{5} N\mu, \tag{6.20}$$

where $\mu \equiv p_F^2/(2m)$, $N = (\sqrt{2}/\pi^2) m^{3/2} L^3 \mu^{1/2}$ is the number of particles and the last estimate is obtained by replacing the sum over momenta by an integral. According to Eq. (6.20), the average kinetic energy per particle equals (3/5)th of the Fermi energy. To relate this scale to our previously introduced density parameter r_s, we chose to measure all energies in units of the Rydberg energy (alias the ionization energy of hydrogen),

$$E_{\mathrm{Ry}} = me^4/2 = 13.6\mathrm{eV}.$$

[16] Notice that 'four momentum' p and the modulus of the 'three momentum' $p = |\mathbf{p}|$ are denoted by the same symbol (standard notation!). Howver, usually this should not cause confusion.

One then verifies that

$$\frac{F^{(0)}}{E_{\rm Ry}} \sim N r_s^{-2}. \tag{6.21}$$

We next turn to the discussion of interactions. Formal expansion of F to first order in the interaction strength $\sim V$ obtains

$$F^{(1)} = \frac{T^2}{2L^3} \left\langle \sum_{pp'q} \bar{\psi}_{p+q\sigma} \psi_{p\sigma} V(\mathbf{q}) \bar{\psi}_{p'-q\sigma'} \psi_{p'\sigma'} \right\rangle_0 , \tag{6.22}$$

where $\langle \ldots \rangle_0$ is the functional average w.r.t. the non-interacting action.

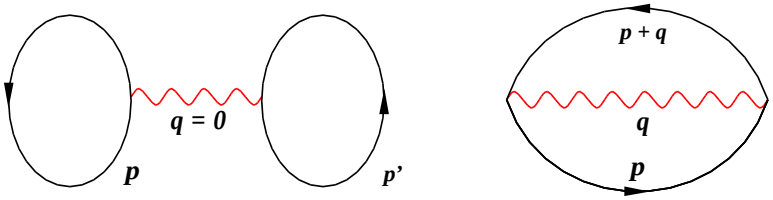

Figure 6.8: First order contribution to the free energy of the interacting electron Gas. Wavy line: Coulomb interaction, solid line: free electronic Green function.

The two[17] diagrams contributing to this expression are shown in Fig. 6.8. To account for the specifics of the electron gas, we are using a diagrammatic code slightly different from that of the previous section:

- ▷ The Coulomb interaction is represented by a wavy line labeled by the momentum argument $\mathbf{q}$.
- ▷ A contraction $\langle \bar{\psi}_{p\sigma} \psi_{p\sigma} \rangle_0$ is indicated by a solid arrow representing the **free Green function of the electron gas**,

$$G_p \equiv \frac{1}{i\omega_n + \mu - \frac{\mathbf{p}^2}{2m}}, \tag{6.23}$$

  i.e. the inverse of the free action. Labeling the contraction by an arrow (instead of an unidirectional line as in ϕ^4-theory) is motivated by two points. First, the mnemonic purpose of indicating that a contraction $\langle \psi_\mu \bar{\psi}_\lambda \rangle_0$ describes the *creation* of an electron with quantum numbers λ followed by the *annihilation* of an electron at μ, a directed process. Second, there are situations (e.g. when a magnetic field is present) where $\langle \psi_{n\sigma}(\mathbf{r}) \bar{\psi}_{n\sigma}(\mathbf{r}') \rangle_0 \neq \langle \psi_{n\sigma}(\mathbf{r}') \bar{\psi}_{n\sigma}(\mathbf{r}) \rangle_0$.
- ▷ The sum of all *four*-momenta emanating from an interaction vertex formed by a wavy line and two electron field lines equals zero (think about it!) – the 'Kirchhoff law'.

[17] Remember that in a theory with complex or Grassmann fields, only contractions $\sim \langle \bar{\psi}\psi \rangle_0$ exist. I.e. there is a total of $n!$ distinct contributions to a contraction $\langle \bar{\psi}\psi \ldots \psi \rangle_0$ of $2n$ field operators.

▷ Finally, we have to be careful about **sign factors** arising when Grassmann variables are interchanged. However, the anti-commutativity of the fields merely leads to an overall factor $(-)^{N_l}$, where N_l is the number of loops of a diagram. (To verify that claim, one notices that a loop is formed by 'ringwise contraction' $\langle\bar\psi_1\psi_2\bar\psi_3\ldots\psi_N\rangle_0$, $(2\to 3)(4\to 5)\ldots((N-2)\to(N-1))(N\to 1)$. The last contraction introduces the minus sign.)

Turning to the discussion of the specific diagrams shown in Fig. 6.8, we notice that the first one, generally known as a **Hartree contribution** *vanishes*. Technically, this is a consequence of the fact that the interaction line connecting the two loops carries zero momentum. However, as discussed in section 3.2.1, $V(\mathbf{q}=0)=0$. Physically, the vanishing of the Hartree contribution is a consequence of charge neutrality. Indeed, the two Green function loops $\sum_p G(p)$ measure the local particle density of the electron gas (cf. with our discussion on page 175 p.) Global charge neutrality requires that that the electronic density cancels against the density of the ionic background. However, notice that this cancellation mechanism relies on our assumption of overall spatial homogeneity. Only in a spatially uniform system, the density of the electron gas *locally* compensates against the positive counter-density. In realistic metals, the inevitable presence of impurities breaks translational invariance and there is no reason for the Hartree contribution to vanish. Indeed, the analysis of Hartree type contributions to the correlation energy in disordered electronic media is a subject of ongoing research.

While the Hartree term describes the classical interaction of charge densities through the Coulomb potential, the second diagram in Fig. 6.8, known as a **Fock contribution** is quantum. Translating back from the diagrammatic level to Green functions, we obtain

$$F^{\mathrm{F},(1)} = -\frac{T^2}{L^3}\sum_{p,p'} G_p G_{p'} V(\mathbf{p}-\mathbf{p}') = -\frac{T^2}{L^3}\sum_{\mathbf{p},n} G_{\mathbf{p},n}\sum_{\mathbf{q},m} G_{\mathbf{p}+\mathbf{q},m} V(\mathbf{q}) = \tag{6.24}$$

$$= -\frac{1}{L^3}\sum_{\mathbf{p},\mathbf{p}'} f_{\mathrm{f}}(\epsilon_{\mathbf{p}}) f_{\mathrm{f}}(\epsilon'_{\mathbf{p}})\frac{e^2}{|\mathbf{p}-\mathbf{p}'|^2} \overset{T\to 0}{=} -\frac{1}{L^3}\sum_{\epsilon_{\mathbf{p}},\epsilon_{\mathbf{p}'}<\mu}\frac{e^2}{|\mathbf{p}-\mathbf{p}'|^2} = -\frac{e^2 L^3 p_F^4}{(2\pi)^4}.$$

Here, the sign factor in the first equality is due the odd number of Fermion loops, the third equality is based on (**??**), and the evaluation of the last sum can be found, e.g., in the textbook**??**. (Up to numerical factors, the result follows from dimensional considerations. We are integrating the inverse square of the distance in momentum space ([momentum]$^{-2}$) over two Fermi spheres ([momentum]^6). Since the integral is convergent at low momenta, it must scale as the fourth power of the upper cutoff $\sim p_F^4$.) Division through the Rydberg energy leads to

$$\frac{F^{(1)}}{E_{\mathrm{Ry}}} = \text{const.}\cdot\frac{N}{r_s}, \tag{6.25}$$

where the constant is of order unity.

This result conforms with our previous heuristic estimates of the density dependence of correlation energies. However, a closer analysis shows that other predictions following from (6.24) are less sensible. To understand what goes wrong, let us rewrite the sum of

$F^{(0)}$ and $F^{(1)}$ as

$$F^{(0)} + F^{(1)} = \sum_{|\mathbf{p}|<p_F} \left(\frac{|\mathbf{p}|^2}{2m} - \frac{1}{L^3} \sum_{\epsilon_{\mathbf{p}'}<\mu} \frac{e^2}{|\mathbf{p}-\mathbf{p}'|^2} \right).$$

This way of writing suggests that the interaction of an electron with momentum $\mathbf{p}$ with all partner electrons of momentum $\mathbf{p}'$ leads to a reduction of the single particle energy by an amount $2e^2L^{-3}\sum_{\epsilon_{\mathbf{p}'}<\mu}|\mathbf{p}-\mathbf{p}'|^{-2}$.[18]

Evaluation of the sum (exercise) leads to

$$F^{(0)} + F^{(1)} = \sum_{|\mathbf{p}|<p_F} \left(\frac{|\mathbf{p}|^2}{2m} - \frac{e^2 p_F}{2\pi} G(|\mathbf{p}|/p_F) \right),$$

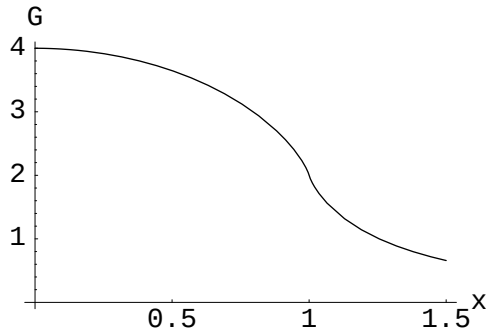

where the function

$$G(x) = 2 + \frac{1-x^2}{x} \ln \left| \frac{1+x}{1-x} \right|.$$

is shown in the figure.

The most important characteristic of the scaling function G is a logarithmically diverging derivative at $x = 1$ (check it!) To appreciate the consequences of this feature, let us consider the single particle **densitiy of states** (DoS)

$$\rho(\epsilon) = \sum_{\mathbf{p}\sigma} \delta(\epsilon - \epsilon_p),$$

where

$$\epsilon_p = \frac{p^2}{2m} - \frac{e^2 p_F}{2\pi} G(p/p_F),$$

is the first oder Fock single particle energy. Approximating the sum by an integral, we obtain

$$\rho(\epsilon) = \frac{L^3}{\pi^2} \int_0^\infty p^2 dp\, \delta(\epsilon - \epsilon_p) = \frac{L^3 p(\epsilon)^2}{\pi^2} \left(\frac{d\epsilon_p}{dp} \right)^{-1},$$

where p_ϵ is defined through $\epsilon_{p_\epsilon} = \epsilon$. The singularity of the derivative of $G(p/p_F)$ at $p = p_F$ implies that the density of states is predicted to *vanish* as ϵ approaches the Fermi energy, clearly a non-sensical result[19].

The origin of this pathological divergence can be traced back to the longranged $|\mathbf{r}|^{-1} \to |\mathbf{q}|^{-2}$ decay of the Coulomb potential (cf. Eq. (6.22)). Yet we know that in systems with mobile charge carriers electrostatic forces are *screened*, i.e. decay exponentially. Microscopically, screening is due to the polarization of a medium in response to

[18] Why reduction?: Charge neutrality implies that the classical correlation energy vanishes. However, being fermionic particles, electrons tend to avoid each other even more than classical particles would do. I.e. quantum statistics leads to a *lowering* of the correlation energy below the classical value 0.

[19] The majority of transport observables in metals is proportional to the DoS at the Fermi energy, i.e. $\rho(\mu) = 0$ would entail vanishing of almost all transport coefficients.

an applied electric field. This by itself is an interaction effect, albeit one of 'higher order' in the Coulomb interaction. I.e. if we ever want to observe signatures of the screening mechanism, we need to advance to higher orders in the expansion in V.

Let us then consider the second order contribution

$$F^{(2)} = -\left(\frac{T^2}{2L^3}\right)^2 \left\langle \left(\sum_{pp'q} \bar{\psi}_{p+q\sigma}\psi_{p\sigma} V(\mathbf{q}) \bar{\psi}_{p'-q\sigma'}\psi_{p'\sigma'} \right)^2 \right\rangle_{0,c},$$

where the subscript indicates that only connected diagrams contribute.

▷ EXERCISE. Show that two-fold expansion of $F = -T \ln \left(\int \mathcal{D}(\bar{\psi},\psi) \exp(-S[\bar{\psi},\psi]) \right)$ in the interaction operator S_{int} leads to $F^{(2)} = T\left[\langle (S_{\text{int}})^2\rangle_0 - [\langle S_{\text{int}}\rangle_0]^2\right]$. Convince yourself that the second term cancels disconnected diagrams. Apply arguments similar to those involved in the proof of the linked cluster theorem to verify that the cancellation of disconnected graphs pertains to all orders in the expansion of F. I.e. the free energy can be obtained by expanding the partition function $\mathcal{Z}$ (not its logarithm) and keeping only connected diagrams; dropping disconnected contributions is equivalent to taking the logarithm.

Connected contraction of the eight field operators leads to four distinct types of diagrams (exercise) of which two are of Hartree type (i.e. contain a zero momentum interaction line $v(\mathbf{q}=\mathbf{0})$.) The non-vanishing diagrams $F^{(2),1}$ and $F^{(2),2}$ are shown in the figure. Translating these diagrams to momentum summations over Green functions, we obtain (exercise)

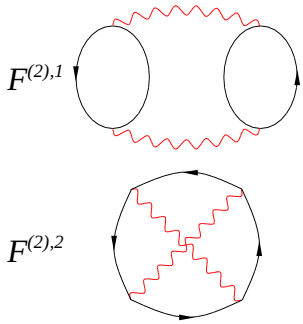

$$F^{(2),1} = -\frac{2T^3}{L^6} \sum_{p_1,p_2,q} G_{p_1} G_{p_1+q} G_{p_2} G_{p_2+q} V(\mathbf{q})^2, \qquad (6.26)$$

$$F^{(2),2} = -\frac{T^3}{L^6} \sum_{p,q_1,q_2} G_p G_{p-q_1} G_{p-q_1-q_2} G_{p-q_2} V(\mathbf{q}_1) V(\mathbf{q}_2).$$

While at first sight these expressions do not look very illuminating, closer inspection reveals some structures: Reflecting the fact that electronic transport in solids is carried by excitations at the Fermi energy, the electron Green function (6.23) assumes large values for momenta $\mathbf{p} \simeq p_F$. This implies that only configurations where all momentum arguments carried by the Green function are close to the Fermi surface significantly contribute to the sums (6.26). Considering the first sum, we see that for small $|\mathbf{q}|$ and $|\mathbf{p}_i| \simeq p_F$, this condition is met, i.e. there are two unbound summations over momentum shells around the Fermi surface. However, with the second sum, the situation is less favourable. For fixed $|\mathbf{p}_1| \simeq p_F$ fine-tuning of *both* $\mathbf{q}_1$ and $\mathbf{q}_2$ is necessary to bring all momenta close to p_F, i.e. effectively one momentum summation is frozen out. There is no need to enter detailed calculations to predict that due to the relatively larger 'phase volume' $F^{(2),1}/F^{(2),2} \gg 1$, where the ratio will be proportional to the area of the Fermi surface which, in turn, is proportional to the density of the elctron gas: For large densities, the second Fock diagram can be neglected in comparison with the first.

Of course, there must be a 'more physical' way of understanding this observation. The Green function lines in the diagrams $F^{(2),i}$ describe the propagation of quasi-particles and

-holes[20] on the background of the interacting medium. Now, the diagram $F^{(2)}$ contains a simply connected propagator line: A single particle-hole excitation undergoes a second order interaction process with itself (see Fig. 6.9 left.) In contrast, the first diagram $F^{(2),1}$ involves two independent electron hole excitations, as shown in Fig. 6.9, right. Since in a dense electron gas a second order interaction process will more likely involve different rather than just a single particle, this type of interaction processes is more important. Also notice that the process shown in Fig. 6.9 right can be interpreted as a 'polarization' of the medium due to the excitation of electron-hole pairs.

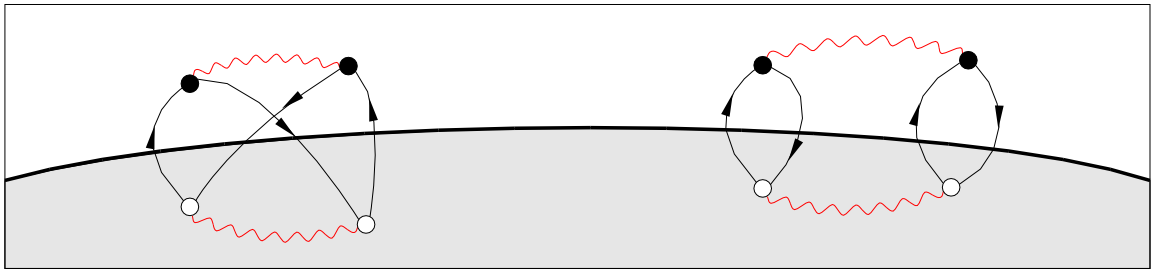

Figure 6.9: Cartoon of second order Fock contributions to the free energy of the electron gas. Left: Interaction process involving a single electron-hole pair. An electron is virtually exited above the Fermi energy, recombines with a hole state left behind by a second electron which then jumps into the hole created by the initial excitation. Right: Virtual excitation of independent electron-hole pairs.

The above picture readily generalizes to interaction processes of higher order. In the high density limit, dominant contributions to the free energy should contain one free integration over the Fermi momentum per interaction process. A moment's thought shows that only diagrams of 'ring graph' structure (see the figure) meet this condition. Expanding the free energy functional to nth order in the interaction operator and retaining only diagrams of that structure, we obtain

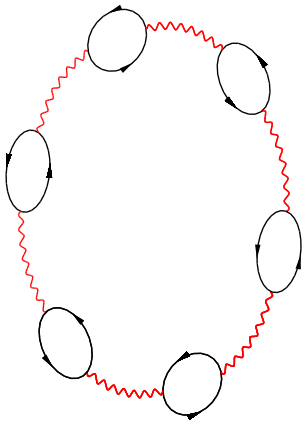

$$F^{(n)}_{\mathrm{RPA}} = -\frac{T}{2n}\sum_q \left(\frac{2T}{L^3}V(\mathbf{q})\sum_p G_p G_{p+q}\right)^n . \qquad (6.27)$$

(To understand the multiplicative factor $1/n$, notice that $F^{(n)}$ results from the connected contraction of an operator $\sim (n!)^{-1}\langle (S_{\mathrm{int}}[\bar\psi,\psi])^n\rangle_{0,c}$. There are $(n-1)!$ different ways of arranging the interaction operators S_{int} to a ring shaped structure, i.e. the diagram carries a global factor $(n-1)!/n! = 1/n$.)

[20] In principle, the system consists of physical electrons immersed onto a globally positve background. However (cf. the discussion of section 3.2.1), keeping in mind that at low temperatures dynamical processes take place in the immediate vicintiy of the Fermi surface, a more problem oriented way of thinking about states is in terms of quasi-particles and quasi-holes, i.e. electronic states immediately above and below the Fermi surface.

In (6.27) the subscript 'RPA' stands for **random phase approximation**[21]. However, more important than the denotation is the fact that we have (a) managed to identify a particularly relevant subclass of diagrams contributing to the plethora of interaction processes, that (b) there is a physical parameter controlling the dominance of these diagrams and (c) that we are apparently able to sum up the entire series of nth order RPA-interaction contributions. Indeed, summation over n leads to the simple result

$$F_{\rm RPA} = \frac{T}{2}\sum_q \ln\left(1 - V(\mathbf{q})\Pi_q\right), \tag{6.28}$$

where we have introduced the **polarization operator**[22],

$$\Pi_q \equiv \frac{2T}{L^3}\sum_p G_p G_{p+q}. \tag{6.30}$$

Eq. (6.28) represents our first example of an infinite order expansion. However, before turning to the discussion of further aspects of infinite order perturbation theory, let us stay for a moment with the RPA free energy. Specifically, we should like to investigate whether the RPA repairs the pathology in the Fermi surface density of states observed above.

The last unknown we need to compute before turning to the discussion of the RPA free energy is the polarization operator. In a more explicit way of writing,

$$\Pi_{\mathbf{q},\omega_m} = \frac{2}{L^3}\sum_{\mathbf{p}} T\sum_{\omega_n} \frac{1}{i\omega_n - \xi_{\mathbf{p}}}\frac{1}{i\omega_{n+m} - \xi_{\mathbf{p}+\mathbf{q}}}.$$

The frequency sum has been computed in the problem set of the previous chapter:

$$\Pi_{\mathbf{q},\omega_m} = \frac{2}{L^3}\sum_{\mathbf{p}} \frac{f_F(\epsilon_{\mathbf{p}+\mathbf{q}}) - f_F(\epsilon_{\mathbf{p}})}{i\omega_m + \xi_{\mathbf{p}+\mathbf{q}} - \xi_{\mathbf{p}}}. \tag{6.31}$$

The evaluation of the momentum sum is straightforward if a bit tedious. As a result of a calculation outlined in the following info box we obtain

$$\Pi_{q,\omega_m} = -\nu_0\left[1 - \frac{i\omega_m}{v_F q}\ln\left(\frac{i\omega_m + v_F q}{i\omega_m - v_F q}\right)\right], \tag{6.32}$$

[21] The attribute 'random phase' seems to allude to the fact that the quantum mechanical phase carried by the particle-holes excitations stirred up by interactions goes lost after each elementary polarization process. Contrary to more generic contributions to F where quantum phases may survive more complex interaction processes. Also notice that more than one approximation scheme in stasistical physics has been dubbed 'random phase'.

[22] The definition (6.30) applies to the specific case of a three-dimensional translationally invariant system. More generally, the polarization operator is defined as the frequency/momentum Fourier transform of the connected average

$$\langle\bar\psi(\mathbf{x},\tau)\psi(\mathbf{x},\tau)\bar\psi(\mathbf{x}',\tau')\psi(\mathbf{x}',\tau')\rangle_c. \tag{6.29}$$

Notice that, in general, the behaviour of the polarization operator will be affected by electronic interactions (neglected in the RPA.)

where

$$\nu_0 \equiv \sum_{\mathbf{p},\sigma} \delta(\mu - \epsilon_p) = 2 \int \frac{d^3p}{(2\pi)^3} \delta(\epsilon_p - \mu) = \frac{m p_F}{\pi^2} \tag{6.33}$$

is the DoS per volume of non-interacting electrons at the Fermi surface.

▷ INFO. For an isotropic three-dimensional system at zero temperature, the polarization operator (6.31) becomes a function of $|\mathbf{q}|$ and ω_n, known as the **Lindhard function**. The evaluation of the momentum sum is greatly simplified by noting that, due to the difference of the Fermi functions, only momenta with $|\mathbf{p}| \simeq p_F$ significantly contribute. Assuming that $|\mathbf{q}| \ll p_F$, we may thus linearize

$$\xi_{\mathbf{p}+\mathbf{q}} - \xi_{\mathbf{p}} = \frac{1}{m} \mathbf{p} \cdot \mathbf{q} + \mathcal{O}(q^2),$$

where the term of $\mathcal{O}(q^2)$ is negligibly small. Similarly,

$$f_F(\epsilon_{\mathbf{p}+\mathbf{q}}) - f_F(\epsilon_{\mathbf{p}}) \simeq \partial_{\epsilon_p} f_F(\epsilon_p) \frac{1}{m} \mathbf{p} \cdot \mathbf{q} \simeq -\delta(\epsilon_p - \mu) \frac{1}{m} \mathbf{p} \cdot \mathbf{q},$$

where in the zero temperature limit the last equality becomes exact. Converting the momentum sum into an integral, we thus obtain

$$\Pi_{\mathbf{q},\omega_m} = 2 \int \frac{d^3p}{(2\pi)^3} \delta(\epsilon_p - \mu) \frac{\frac{1}{m} \mathbf{p} \cdot \mathbf{q}}{i\omega_m + \frac{1}{m} \mathbf{p} \cdot \mathbf{q}}.$$

Writing $\frac{1}{(2\pi)^3} \int d^3p = \frac{1}{(2\pi)^3} \int p^2 dp \int d\Omega$, where $\int d\Omega$ is the integral over the three-dimensional unit sphere, and $\mathbf{p} = p\mathbf{n}$, with $|\mathbf{n}| = 1$, the integral can be evaluated to

$$\begin{aligned}
\Pi_{\mathbf{q},\omega_m} &= -\frac{2}{(2\pi)^3} \int p^2 dp \int d\Omega\, \delta(\epsilon_p - \mu) \frac{v_F \mathbf{n} \cdot \mathbf{q}}{i\omega_m + v_F \mathbf{n} \cdot \mathbf{q}} = \\
&= -\underbrace{\frac{2}{(2\pi)^3} \int p^2 dp \int d\Omega\, \delta(\epsilon_p - \mu)}_{\nu_0} \frac{1}{\int d\Omega\, 1} \int d\Omega \frac{v_F \mathbf{n} \cdot \mathbf{q}}{i\omega_m + v_F \mathbf{n} \cdot \mathbf{q}} = \\
&= -\frac{\nu_0}{2} \int_{-1}^{1} dx \frac{v_F x q}{i\omega_m + v_F x q} = -\nu_0 \left[1 - \frac{i\omega_m}{v_F q} \ln \left(\frac{i\omega_m + v_F q}{i\omega_m - v_F q} \right) \right].
\end{aligned}$$

To obtain the free energy, we need to substitute the Lindhard function into (6.28) and sum over $q = \{\mathbf{q}, \omega_m\}$. Yet due to the complicated dependence of the function Π_{q,ω_m} on its arguments, this final part of the calculation is far from trivial. An asymptotic expression for the high density expansion of the RPA approximation to F was was first obtained in a famous study of Gell-Mann and Brueckner[23][24]. The free energy per particle, measured

[23] M. Gell-Mann and K. Brueckner, Phys. Rev. **106**, 364 (1957).

Murray Gell-Mann: Born 1929. 1969 Nobel Laureate in Physics for his contributions and discoveries concerning the classification of elementary particles and their interactions.

[24]

in atomic units, they found

$$\frac{F_{\rm RPA}}{E_{\rm Ry}N} = -0.142 + 0.0622\ln(r_s). \tag{6.34}$$

For a derivation of this result we refer the interested reader to the literature. (In the late 50th, motivated largely by applications to the physics of heavy nuclei, the perturbative calculation of ground state energies had become an industry. A comprehensive discussion of the subject, and details of the asymptotic r_s-expansion of $F_{\rm RPA}$ can be found, e.g., in [?].) When added to the kinetic energy (6.21) and the first order correlation energy (6.25), the structure of the density expansion of the free energy becomes clear: The sum over all RPA diagrams yields the coefficient of $\mathcal{O}(1)$ of the expansion in r_s.[25].

More important for our present discussion is the conceptual meaning of the RPA, notably the connection to screening. To understand this point, let us temporarily consider the expectation value of the particle number $N = \partial_\mu F$, rather than the free energy itself. Specifically, we with to compare the first order correction to the non-interacting result $N^{(1)} = -\partial_\mu F^{(1)}$ with the RPA, $N_{\rm RPA} = -\partial_\mu F_{\rm RPA}$. Noting that

$$\partial_\mu G_p = -(G_p)^2,$$

we readily find (cf. Eq. (6.24))

$$N^{(1)} = -\frac{2T^2}{L^3}\sum_{p,q}(G_p)^2 G_{p+q}V(\mathbf{q}).$$

After a second differentiation, $\rho^{(1)} = \partial_\mu N^{(1)}$, this expression would lead to the pathological DoS, a consequence of the un-screened interaction line. The diagrammatic visualitation of $N^{(1)}$ is shown in Fig. 6.10 a).

Now, consider the μ-derivative of $F_{\rm RPA}$, Eq. (6.28):

$$\begin{aligned} N_{\rm RPA} = -\partial_\mu F_{\rm RPA} &= \frac{T}{2}\sum_q \frac{V(\mathbf{q})\partial_\mu \Pi(q)}{1 - V(\mathbf{q})\Pi_q} = \\ &= -\frac{T^2}{L^3}\sum_q \frac{V(\mathbf{q})}{1 - V(\mathbf{q})\Pi_q}\left[\sum_p G_{p+q}(G_p)^2 + (q \leftrightarrow -q)\right] = \\ &= -\frac{2T^2}{L^3}\sum_q \frac{V(\mathbf{q})}{1 - V(\mathbf{q})\Pi_q}\sum_p G_{p+q}(G_p)^2 = \\ &= -\frac{2T^2}{L^3}\sum_q V_{\rm eff}(q)\sum_p G_{p+q}(G_p)^2, \end{aligned} \tag{6.35}$$

where we have defined the 'effective' interaction

$$V_{\rm eff}(q) \equiv \frac{1}{V(\mathbf{q})^{-1} - \Pi_q} \equiv \frac{V(\mathbf{q})}{\epsilon(q)} \tag{6.36}$$

[25] Here we follow a convention (used mostly in the older literature) where the RPA starts from the *second* order ring diagram $F^{(2),1}$. However, henceforth we will refer to the 'RPA' as the sum over all ring diagrams, including the first one $F^{F,(1)}$.

with the generalized **dielectric function**

$$\epsilon(q) \equiv 1 - V(\mathbf{q})\Pi_q. \tag{6.37}$$

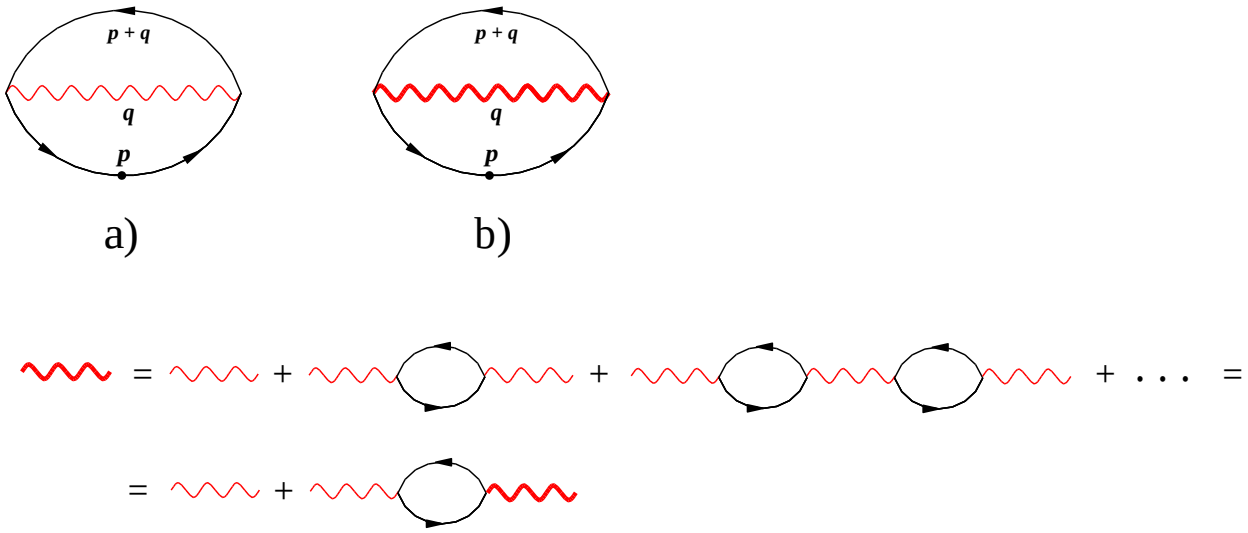

Figure 6.10: Diagrammatic visualization of expectation value of the particle number. a) First order Fock correction. b) RPA approximation where the definition of the RPA interaction line is shown in the bottom part of the figure.

Structurally, N_{RPA} resembles the first order expression $N^{(1)}$, only that the 'bare' Coulomb interaction has been replaced by the effective interaction V_{eff}. From its definition, is clear that V_{eff} represents a geometric series over polarization bubbles, augmented by bare interaction lines. This is vizualized in Fig. 6.10 b), where the fat line is defined in the bottom part of the figure. In fact, we do not need to stare at the analytical expression (6.35) to understand the origin of this expression: The μ-differentiation acting on F^{RPA} may pick any of the n rings contributing to $F^{(n)}_{\mathrm{RPA}}$ in (6.27). The 'differentiated ring' becomes the bubble in Fig. 6.10, while all other rings conspire to form the $(n-1)$th order contribution to the effective interaction line.

At this stage, the connection between RPA and the collective electromagnetic response of the charged system becomes discernible. We remember that the electric field $\mathbf{E}$ in a medium is related to the vacuum field $\mathbf{D}$ through $\mathbf{D}(\mathbf{q},\omega) = \epsilon(\mathbf{q},\omega)\mathbf{E}(\mathbf{q},\omega)$, where the dielectric function $\epsilon(\mathbf{q},\omega) = 1 + 4\pi\chi(\mathbf{q},\omega)$ is determined by the **electromagnetic susceptibility**, i.e. a function that measures the tendency of the medium to 'respond' or adjust to an external electromagnetic perturbation. Identifying $\mathbf{E}$ ($\mathbf{D}$) with the gradient of the 'dressed' potential V_{eff} (the 'bare' potential V), we conclude that on the level of the microscopic theory, $4\pi\chi(\mathbf{q},\omega) = V(\mathbf{q})\Pi(\mathbf{q},\omega)$, i.e. the susceptibility is proportional to the polarization operator Π_q. These connections motivate the introduction of the dielectric function as in Eq. (6.37) above.

The full complexity of the polarization of the dense homogeneous electron gas is encoded by the Lindhard function (6.32). However, there are some interesting limiting cases, where the situation simplifies: Inspection of (6.32) shows that the Lindhard function depends on the dimensionless ratio between two characteristic length scales: the

'wavelength' q^{-1}, and the distance v_F/ω an excitation propagating with Fermi velocity traverses during the time ω^{-1}. For small frequencies, $v_F/\omega \gg q^{-1}$, the electron gas has enough time to optimally adjust to the spatial variation $\sim q^{-1}$ of the potential, i.e. to screen out electro-neutrality violating potential fluctuations. In this **static limit**, we may expand

$$\Pi_{\mathbf{q},\omega_m} \overset{\omega \ll qv_F}{=} -\nu_0 + \mathcal{O}(\omega/v_F q).$$

The electron gas interacts through the effective potential,

$$V_{\text{eff}}(q) \overset{\omega \ll qv_F}{=} \frac{1}{V(\mathbf{q})^{-1} + \nu_0} = \frac{4\pi e^2}{q^2 + \frac{e^2}{4\pi}\nu_0}.$$

The constant

$$\lambda \equiv \left(\frac{4\pi}{\nu_0 e^2}\right)^{1/2} \tag{6.38}$$

is known as the **Thomas-Fermi screening** length. Indeed, it is straightforward to verify that the inverse Fourier transform

$$V_{\text{eff}}(\mathbf{r}) = e^2 \frac{e^{-|\mathbf{r}|/\lambda}}{|\mathbf{r}|}, \tag{6.39}$$

i.e. the potential is exponentially supressed, or screened, on length scales $|\mathbf{r}| > \lambda$.

▷ EXERCISE. To verify Eq. (6.39), introduce polar coordinates $\mathbf{q}(q, \theta, \phi)$ in $\mathbf{q}$-space and first do the elementary integrations over ϕ and θ. It is then straightforward to do the remaining q-integration over the radial coordinate in analogy to the contour integral (6.14).

We also note that Thomas-Fermi screening repairs our problem with the density of states. The pathology discussed on p 206 found its origin in the $1/q^2$-singularity of the unscreened potential. This IR singularity is now cut off at momenta $q \sim \lambda^{-1}$ implying benign behaviour of the DoS. Using that the density parameter r_s scales with the Fermi energy as (exercise) $r_s \sim \mu^{-1/2}$, and differentiating $\rho = \partial_\mu^2 F$, it is indeed straightforward to verify that the RPA-expansion of F no longer leads to singular behaviour of ρ at the Fermi energy.

It is also intereting to consider the limit $v_F/\omega \ll q^{-1}$ of essentially **dynamic polarization**. Expansion of $\Pi_{\mathbf{q},\omega_m}$ to first order in $v_F q/\omega \ll 1$ leads to

$$\Pi_{\mathbf{q},\omega_m} \overset{\omega \gg qv_F}{=} -\frac{\nu_0}{3}\left(\frac{v_F q}{\omega_m}\right)^2 + \mathcal{O}((v_F q/\omega)^4),$$

and

$$V_{\text{eff}}(\mathbf{q}, \omega_m) = \frac{4\pi e^2}{q^2} \frac{1}{1 + \frac{4\pi\nu_0 e^2 v_F^2}{3\omega^2}}.$$

Using that (exercise) the particle density $n \equiv N/L^3 = k_F^3/(6\pi^2)$, this can be rewritten as

$$V_{\text{eff}}(\mathbf{q}, \omega_m) = \frac{4\pi e^2}{q^2} \frac{1}{1 + \frac{\omega_p^2}{\omega_m^2}},$$

where the **plasma frequency** is defined as

$$\omega_p \equiv \left(\frac{4\pi n e^2}{m}\right)^{1/2}.$$

The form of the numerator of this expression actually hints at a collective instability of the electron gas at frequencies $\sim \omega_p$. Referring for a more rigorous discussion to the next chapter, we can understand the origin of the instability by an heuristic argument. What we need to remember is that the current formalism is developed for imaginary times τ. Eventually we will be interested in real-time dynamics, i.e. we need to analytically continue back to $t \sim i\tau$. In the language of frequencies, this amounts to a continuation process $i\omega_m \to \omega$ from Matsubara frequencies to real frequencies. Sloppily substituting a real frequency into the potential, we obtain

$$V_{\text{eff}}(\mathbf{q}, \omega_m \to i\omega) = \frac{4\pi e^2}{q^2} \frac{1}{1 - \frac{\omega_p^2}{\omega^2}},$$

i.e. the system seems to respond singularly to excitations with frequency $\omega \sim \omega_p$. The cause of this instability is the well known plasmon mode of the electron gas.

▷ INFO. The physics of the **plasmon mode** can be heuristically understood as follows. Imagine the electron gas uniformly displaced by a distance x against the postively charged backgroud. This will lead to the formation of oppositely charged surface charge layers at both ends of the system. The surface charge densities $\rho_\pm = \pm exn$ lead to an electric field $E = 4\pi enx$ directed opposite to the displacement vector. Mobile charge carriers inside the system are thus subject to a force $-4\pi e^2 nx$. The solution of the equation of motion $m d_t^2 x = -4\pi e^2 nx$ oscillates at a frequency $\omega_p = (4\pi e^2 n/m)^{1/2}$, the plasma frequency. Since the motion of the charge carriers is in turn responsible for the buildup of the charged surface layers, we conclude that the system performs a collective oscillatory motion, known as the plasmon excitation.

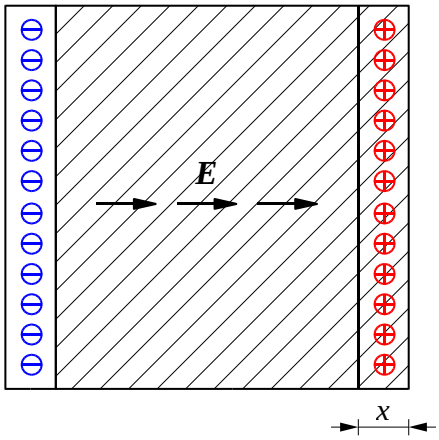

At this point we conclude our preliminary discussion of the electron gas. We have seen that large order perturabation theory can be applied to successfully explain various features of the interacting system: energetic lowering due to quantum correlation, screening, and even collective instabilities.

The interacting electron gas is but an example of many other application theatres of diagrammatic perturbation theory. After the full potential of the approach had become evident – in the late 50ties and early 60ies – diagrammatic techniques of great sophistication where developed, and applied to a plethora of many body problems. Indeed, more than two decades passed before large order perturbation theory eventaully ceased to be

the undisputedly most important tool of theoretical condensed matter physics. Reflecting the great practical relevance of the approach, there is a huge body of textbook literature concentrating on perturbatice methods (see e.g. Refs.[?, ?, ?, ?]). Although it would make little sense to again expose the field in its full development, a few generally important concepts of diagrammatic perturbation theory are summarized in the next section for reference purposes. (The section can be skipped at first reading.)

6.3 Perturbation theory II: Infinite Order Expansions

Turning back to the prototypical ϕ^4-model, it is the purpose of the present section to introduce a number of general concepts of infinite order perturbative summations. As should be clear from the discussion above, a meaningful summation over an infinite set of diagrams neccessitates the existence of a class of perturbative corrections that is 'more important' than others. In practice, what we need is small parameter that discriminates between diagrams of different structure. In our example above, this parameter was the density r_s of the eletron gas. However, in other settings, the control parameter N may be defined quite differently: large values of a spin, S, the number of colours, N_c, in QCD, the number of spatial dimensions, d, the number of modes of an optical wave guide, etc. Unfortunately, in real life environments, these parameters are typically far from large, $S = 1/2$, $d = N_c = 3$, etc. So, we have to resort to a poor mans strategy where we develop a controlled and self consistent theory in the limit of asymptotically large of the control parameter and *hope* that some fragments of truth survive the limit down to more mundane values of N. Perhaps unexpectedly, this strategy often works astonishingly well down to values $N = \mathcal{O}(1)$.

So let us, then, begin by introducing a large control parameter into a ϕ^4 type theory. This can be done by promoting ϕ from a scalar to an N-component vector field $\boldsymbol{\phi} = \{\phi^a\}$, $a = 1, \ldots, N$. The self-interaction of the field is modeled as $g \int dx \phi^a \phi^a \phi^b \phi^b$, i.e. an expression that is 'rotationally' invariant in $\boldsymbol{\phi}$-space. The action of our modified theory is thus given by

$$S[\boldsymbol{\phi}] \equiv \int d^d x \left(\frac{1}{2} \partial \boldsymbol{\phi}^T \partial \boldsymbol{\phi} + \frac{r}{2} \boldsymbol{\phi}^T \boldsymbol{\phi} + \frac{g}{N} (\boldsymbol{\phi}^T \boldsymbol{\phi})^2 \right), \tag{6.40}$$

where the factor $1/N$ in front of the interaction constant has been introduced for later convenience.

As before we shall concentrate on the Green function

$$G^{ab}(\mathbf{x}-\mathbf{y}) = \langle \phi^a(\mathbf{x})\phi^b(\mathbf{y})\rangle$$

as a 'test observable'. Denoting the Green function by a bold line, the free Green function $G_0 \equiv \langle \phi^a(\mathbf{x})\phi^b(\mathbf{y})\rangle_0 \propto \delta^{ab}$ by a thin line, and the interaction operator by a wavy line (Since the four fields vertices entering the interaction are no longer indiscriminate, the interaction 'point' representation of section 6.1.3 is no longer suitable.) the structure of the first and second order expansion of the Green function is shown in the upper portion of Fig. 6.11. For simplicity, the combinatorial factors weighting individual diagrams have been omitted.

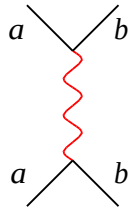

6.3.1 Self Energy Operator

Even without resorting to the large N structure of the theory, it is possible to bring some order in the spaghetti of diagrams contributing to the expansion. Indeed, there are two distinct subclasses of diagrams: diagrams that can be cut into two halfes just by cutting a single *internal* Green function line (no's $4, 6, 8, \ldots$) and those that cannot (no's $1, 2, 3, 5, 7, 9, 10, 11, \ldots$). This observation motivates to lump all subportions of the exansion that cannot be simply cut – they are called **one-particle irreducible diagrams** – into a structural subunit. In Fig. 6.11 this entitiy, which is commonly called the **self energy operator** sometimes also the **effective mass operator**, is denoted by a hatched circle. The first and second order expansion of the self energy is shown in the bottom part of the figure.

With that definition, the Green function becomes a 'chain' of self energy operators, separated by free Green function lines, as shown in the second equality of the figure. A convenient representation of that expansion is shown in the third equality. An insertion of the full Green function after the first self energy correction recursively generates the full series.

Let us translate these statements into the language of formulae. Denoting the set of all self energy diagrams by $\hat{\Sigma} = \{\Sigma^{ab}(\mathbf{x}-\mathbf{y})\}$[26], the expansion of the Green function assumes the form

$$\begin{aligned}\hat{G} &= \hat{G}_0 + \hat{G}_0\hat{\Sigma}\hat{G}_0 + \hat{G}_0\hat{\Sigma}\hat{G}_0\hat{\Sigma}\hat{G}_0 + \ldots = \\ &= \hat{G}_0 + \hat{G}_0\hat{\Sigma}\hat{G}. \end{aligned} \tag{6.41}$$

Here, the operator products involve summation over coordinates and internal indices, i.e $(\hat{A}\hat{B})^{ab}(\mathbf{x}-\mathbf{y}) = \int d^d z A^{ac}(\mathbf{x}-\mathbf{z})B^{cb}(\mathbf{z}-\mathbf{y})$. Recursion relations of this type are commonly referred to as **Dyson equations**. The Dyson equation states that the problem of calculating $\hat{G}$ is essentially tantamount to that of analysing the self energy. To make this point more explicit, let us reformulate the Dyson equation in momentum space:

$$\hat{G}(\mathbf{p}) = \hat{G}_0(\mathbf{p}) + \hat{G}_0(\mathbf{p})\hat{\Sigma}(\mathbf{p})\hat{G}(\mathbf{p}) \Leftrightarrow [\mathbf{1} - \hat{G}_0(\mathbf{p})\hat{\Sigma}(\mathbf{p})]\hat{G}(\mathbf{p}) = \hat{G}_0(\mathbf{p}).$$

[26] The conservation of global momentum of the theory implies (think about it!) that, like the Green function, the self energy depends only on the *difference* of its coordinate arguments.

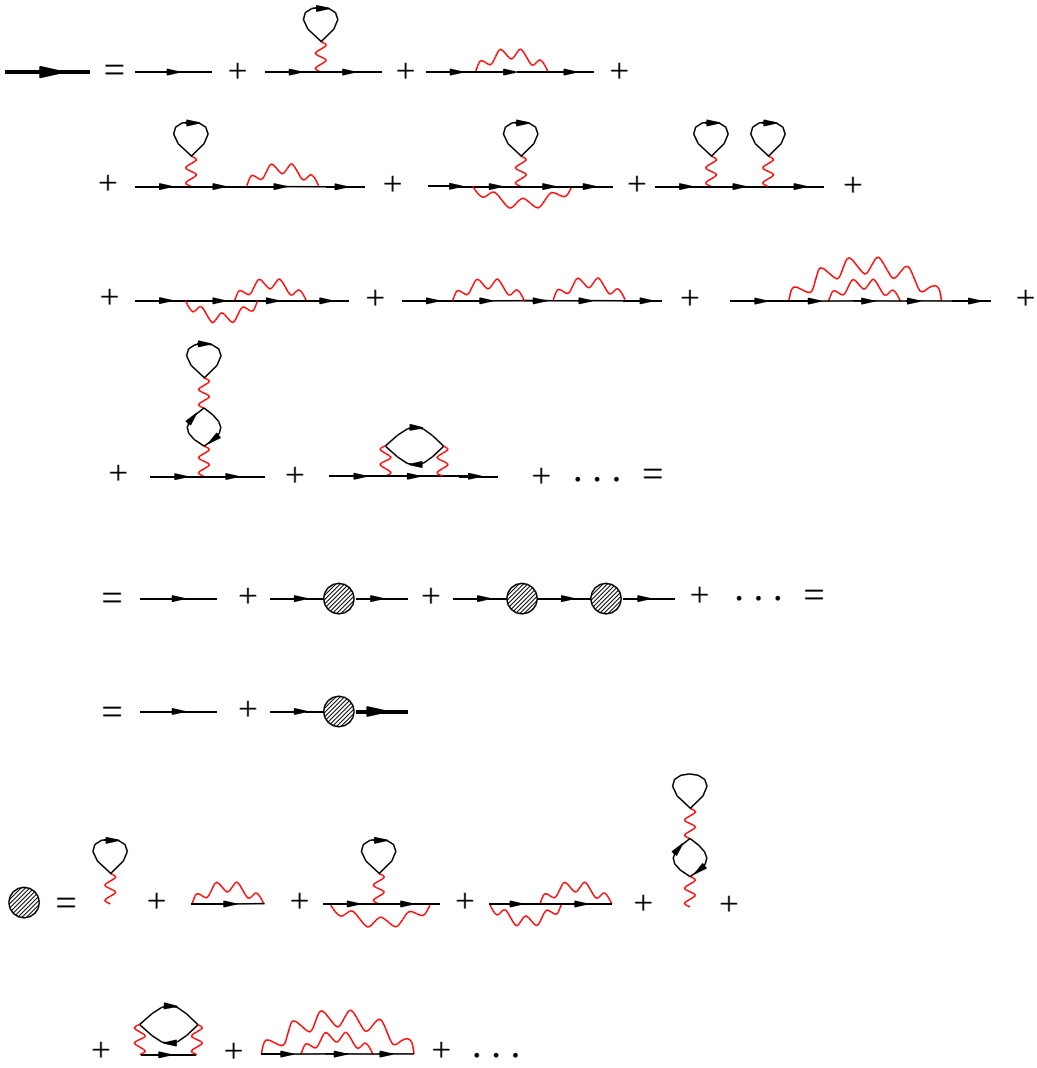

Figure 6.11: Expansion of the Green function of ϕ^4-theory. Bottom: Expansion of the self energy operator

where we have used the convolution theorem, or, more physically, the fact that all scattering processes lumped into the self energy separately conserve momentum. (Matrix)multiplication of this identity from the right with $[\mathbf{1} - \hat{G}_0(\mathbf{p})\hat{\Sigma}(\mathbf{p})]^{-1}$ leads to

$$\hat{G}(\mathbf{p}) = [\mathbf{1} - \hat{G}_0(\mathbf{p})\hat{\Sigma}(\mathbf{p})]^{-1}\hat{G}_0(\mathbf{p}) = \left[(\hat{G}_0(\mathbf{p}))^{-1} - \hat{\Sigma}(\mathbf{p})\right]^{-1}.$$

Finally, using that $\hat{G}_0(\mathbf{p})^{-1} = \{(p^2 + r)\delta^{ab}\}$, we arrive at the formal solution

$$\boxed{G^{ab}(p) = \left(\left[p^2 + r^2 - \hat{\Sigma}(p)\right]^{-1}\right)^{ab}.} \tag{6.42}$$

This equation teaches us two things. First, the full information on the Green function is indeed stored in the self energy, second the self energy somehow 'adds' to the arguments p^2 and r entering the quadratic action, a point to be discussed in more detail below.

But how then do we compute the self energy operator? In fact, the construction recipe follows from what has been said above. By definition, the n-th order contributions to the self energy operator is generated by connected and one-particle irreducible contraction of n interaction operators (weighted with the appropriate combinatorial factor $1/n!$.) Two field vertices stay un-contracted as connectors to the free Green function lines contacting the self energy. E.g., the first order contribution is given by (exercise)

$$\Sigma^{(1)ab}(\mathbf{p}) = \delta^{ab}\frac{2g}{L^d}\left(\frac{1}{N}\sum_{\mathbf{p}'}G_0(\mathbf{p}') + \sum_{\mathbf{p}'}G_0(\mathbf{p}-\mathbf{p}')\right),$$

where the first (second) contribution correspond to the first (second) diagram in the self energy expansion of Fig. 6.11.

▷ EXERCISE. Reprensent the second order contribution $\Sigma^{(2)}$ in terms of Green functions.

Once the self energy has been computed to any desired order, the result is substituted into (6.42) and one obtains the Green function.

▷ INFO. The critical reader will note that there are some problems with the line of arguments above. First, we have tacitly ignored the issue of combinatorics. (How do we know that once we have plugged the expansion of the self energy into the Dyson equation we get the same result a brute force direct expansion of the Green function would have obtained?) To understand that the two-step program 'first compute self energy, then substitute into Dyson series' indeed produces correct results, let us consider the nth order contribution to the expansion of the Green function with it's overall combinatorial factor $1/n!$. Now imagine that we want to distribute those diagrams that contain, say, one free internal Green function over two self energy operators according to $G_0\Sigma G_0\Sigma G_0$. Assuming that the first self energy operator is of order $m < n$ and the second one of order $n-m$, we notice that there are $\binom{n}{m}$ possibilities to distribute the interaction vertices over the two self energies. That means that we obtain an overall combinatorial factor $\frac{1}{n!}\binom{n}{m} = \frac{1}{m!(n-m)!}$. But $1/m!$ and $1/(n-m)!$ are precisely the combinatorial factors that appear in the definition of an m and and $(n-m)$th order self energy operator, respectively. Arguing in reverse, we conclude that the prescription above indeed produces the correct combinatorics.

A second objection concerns the consistency of the expansion. I.e. nth order expansion of the self energy is, of course, by no means equivalent to nth order expansion of the Green function, nor to any specific order of the expansion. Indeed, when working with the concept of a self energy, structuring the expansion according its order in the interaction operator does not make much sense. We should rather focus on the summation of specific *infinite* order diagram classes as exemplified in the previous section and discussed in more general terms below.

6.3.2 Large N Expansion

So far we have not yet made reference to the N-component structure of the theory. However, let us now assume that N is very large, i.e. that we may be content with an expansion of the Green function to leading order in $1/N$. This condition can be made

explicit by sending $N \to \infty$ and declaring

$$\lim_{N\to\infty} G^{aa}(\mathbf{p})$$

to our observable of interest.

The limit of large N entails a drastic simplification of the diagrammatic expansion. Each interaction vertex comes with an overall $1/N$ which must be compensated by a summation over field-components to produce a contribution that survives the limit $N \to \infty$. This condition removes numerous diagrams contributing to the diagrams contributing to the series. I.e. in the Green function expansion of Fig. 6.11 only the first, third and eigth diagram survive the limit. In all other contributions, interaction and Green function lines are interwoven in a way that does not leave room for one field-index summation per interaction vertex.

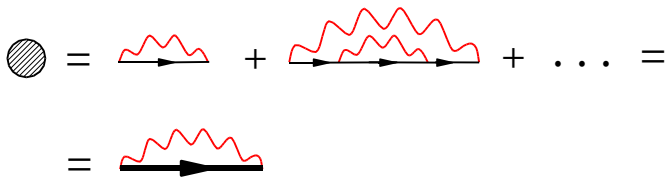

Figure 6.12: Non-crossing approximation of the self energy. Notice that in the last diagram the propagator line represents the *full* Green function.

Inspection of the series shows that only diagrams of the structure shown in Fig. 6.12 survive the limit of large N: interaction lines that do not terminate in Green function bubbles and do not cross. The approximation – in the limit of infinite N it becomes exact – that retains only these contributions is commonly called the **non-crossing approximation (NCA)**. More poetically, the diagrams contributing to the reduced expansion are sometimes called 'rainbow diagrams'. Importantly, the NCA self energy can be computed in closed form. All one has to realize is that the summation over all rainbow diagrams amounts to substitution of the *full* NCA Green function under a single interaction line (think about it!). Using that in the NCA the self energy is proportional to unitiy in the field-index space, we can express this fact through the formula

$$\hat{\Sigma}(\mathbf{p}) \overset{\text{NCA}}{=} gL^{-d}\sum_{\mathbf{p}} G(\mathbf{p}) = gL^{-d}\sum_{\mathbf{p}} \left(p^2 + r^2 - \Sigma(\mathbf{p})\right)^{-1}. \tag{6.43}$$

In the literature, this equation goes under the name **self consistent Born approximation**. It is a 'Born approximation', because, formally, it looks like a first order perturbative correction (the overall factor g^1)[27]. The approximation is 'self consistent', because the self energy recursively appears on the rhs of the equation again, i.e. the equation is in fact not of first but of infinite order.

▷ INFO. Although the objective of the present section is general structures, let us briefly review the **solution of a how a Born equation**. To keep things simple, let us assume that

[27] In the chapter XX we will see how the self energy operator relates to Born scattering theory.

we are dealing with the low energy approximation to some microscopic model, i.e. that the momentum summations must be cut off at some upper limit Λ. We further make the (self consistently to be checked) assumption that the solution for the self energy operator will come out momentum independent $\Sigma(\mathbf{p}) = \Sigma$. This leads to

$$\Sigma \approx -g \int^{\Lambda} \frac{d^d p}{(2\pi)^d} \frac{1}{p^2 + r^2 - \Sigma}$$

The evaluation of the integral depends on the dimensionality and on the analytical structure of the energy denominator. E.g. assuming that $d = 2$ and that the parameter r^2 will be much smaller than the self energy induced by scattering – an assumption to be checked self consistently later on –, we obtain

$$\Sigma \approx -\frac{g}{4\pi} \int_0^{\Lambda^2} d(p^2) \frac{1}{p^2 - \Sigma} \simeq -\frac{g}{4\pi} \ln\left(-\frac{\Lambda}{\Sigma}\right).$$

A solution $\Sigma(g, \Lambda)$ can now be sought by approximate analytical methods, or graphically. (One plots the both sides of the equation as a function of Σ and seeks for a crossing point.)

However, for our present discussion, more important than the detailed dependence of Σ on the input parameters g and Λ is the principal meaning of the self energy: Apparently, Σ adds to the parameter r^2 of the naked Green function. (Notice that the solution of the equation determining Σ will be negative.) Remembering that $r \sim \xi^{-1}$, one concludes that the interaction operator lowers the spatial correlation of the system. That is indeed what one should expect intuitively: Scattering due to interactions acts as a source of 'disorder' inside the system.

At this stage, it is worthwhile to step back and to see what we have got. We have managed to compute the Green function to *infinite* order in an expansion in the set of 'relevant' diagrams. How does that together with what has been said in section 6.1.1 about the 'asymptotic' nature of perturbative series? The reason is that the exponential proliferation of the number of diagrams, i.e. the mechanism that led to the eventual breakdown of the perturbative expansion, is blocked by the limit $N \to \infty$. Only subclasses of diagrams, with far fewer members, contribute and the series remains summable.

The large N principle is actually not limited to the expansion of the Green function. To illustrate the point, let us briefly consider the expansion of the **four point correlation function**

$$C^{(4)}(\mathbf{q}) = \frac{1}{N} \sum_{ab} \frac{1}{L^{2d}} \sum_{\mathbf{p},\mathbf{p}'} \langle \phi^a(\mathbf{p}) \phi^a(\mathbf{p}+\mathbf{q}) \phi^b(\mathbf{p}') \phi^b(\mathbf{p}'+\mathbf{q}) \rangle.$$

In the next chapter we will see that objects of that architecture represent the most important information carriers of the theory. Unlike the previously discussed Green function, they directly relate to observable quantities. In the many-body literature, the *four* point function is dentoed as a **two particle propagator**, indicating that it describes the joint propagation of two states. Referring for a more substantial discussion of the meaning of this object to the next chapter we here concentrate on the formal aspects of its perturbative expansion.

The structure of the expansion of the four point function is shown in Fig. 6.13 where, for simplicity, momentum/component-indices are indicated only once. The simplest diagram contributing to the expansion consists of just two Green functions. It encapsulates

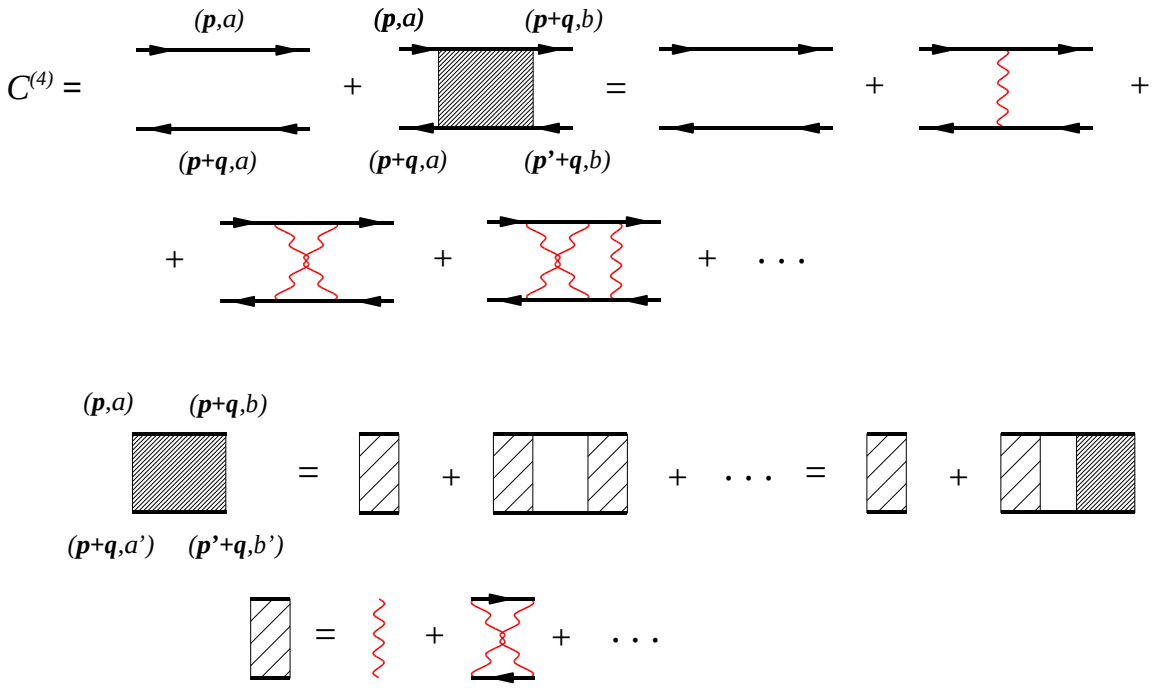

Figure 6.13: Expansion of the four point function. Notice that the arrows represent the full Green function, i.e. all diagrams 'renormalizing' the two-particle subunits of the diagram are automatically included.

all disconnected contractions, $\sim \langle \phi^a(\mathbf{p})\phi^b(\mathbf{p}')\rangle\langle \phi^a(\mathbf{p}+\mathbf{q})\phi^b(\mathbf{p}'+\mathbf{q})\rangle \sim \delta^{ab}\delta_{\mathbf{p}\mathbf{p}'}$ contributing to $C^{(4)}$. All other contractions simulatenously involve all four field operators, i.e. they contain interaction lines between the Green functions. The sum of all these contributions is represented by the diagram containing the hatched surface. A few low order contributions to the expansion are explicitly shown in the first and second line. Notice that all arrows appearing in these diagrams are fat ones. This means that diagrams 'dressing' the two-particle sub-units of the expansion are automatically included. E.g. the second contribution containing just a single interaction line between the two-particle propagators in fact represents an entire series of diagrams obtained by substituting the expansion of Fig. 6.11 for the full Green function. (In an analytical calculation, one will account for these contributions simply by substitution of the self-energy renormalized Green function for each arrow.)

▷ EXERCISE. Write down the analytical expressions contributing to the low order diagrams shown in the first and second line of the figure.

All diagrams involving interactions between the two Green functions have in common that they contain four external 'legs', i.e. the Green function connectors to the external field operators. If you imagine these legs removed, you end up with a 'core contribution' often called the **vertex**. (The denotation is motivated by the fact that the first contribution to the vertex is, indeed, the contracted interaction vertex of the action, see diagram no. 2.) In the figure, the vertex is denoted by a tightly hatched area. Our problem with

the two-particle propagator is to analyse this object.

Similarly to the situtation with the Green function, the expansion of the vertex can given some structure. To this end, notice that some of the diagrams contributing to the vertex (e.g. the second diagram in the second line with external legs removed) can be cut into two just by cutting two internal Green function lines. Vertex diagrams of this type are called **two-particle reducible**, in analogy to the 'one-particle reducible' contributions to the expansion of the Green function. As with the expansion of the Green function, we lump all *irreducible* contributions to vertex (e.g. the last diagram in the first line, or the first diagram in the second line, external legs removed) into a structural subunit called the **irreducible vertex**. In the figure, that unit is denoted by a lightly hatched area. The first few diagrams contributing to the irreducible vertex are shown in the fourth line of the figure. Apparently, the irreducible vertex plays a role similar to the self energy of the Green function. Expressed in terms of the irreducible vertex, the expansion assumes the regular form shown in the third line.

To represent these graphical relations in analytical form, we denote the full vertex by the symbol $\hat{\Gamma} = \{\Gamma^{aa',bb'}(\mathbf{p},\mathbf{p}',\mathbf{q})\}$ and the irreducible vertex by $\hat{\Gamma}_0 = \{\Gamma_0^{aa',bb'}(\mathbf{p},\mathbf{p}',\mathbf{q})\}$. Here, the indices a, a', b, b' keep track of the index labels carried by the four Green functions entering the vertex. (Although we have *defined* our correlation function such that $a = a', b = b'$ a generalisation to a four-fold index label is neccessary to formulate the recursion (6.44).) The three momentum arguments represent the momenta of the Green functions connecting to the vertex operators, as indicated explicitly in the the first line of the figure. (Remember that the theory has overall momentum conservation, i.e. three momentum arguments suffice to unambiguosly fix the momentum dependence of Γ and $C^{(4)}$.) The content of the third line of the figure can then be expressed in terms of a closed recursion relation:

$$\Gamma^{aa',bb'}(\mathbf{p},\mathbf{p}',\mathbf{q}) = \Gamma_0^{aa',bb'}(\mathbf{q},\mathbf{p}',\mathbf{p}) + \sum_{cc'} \frac{1}{L^d} \sum_{\mathbf{p}''} \Gamma_0^{aa',cc'}(\mathbf{q},\mathbf{p}'',\mathbf{p}) G(\mathbf{p}'') G(\mathbf{p}''+\mathbf{q}) \Gamma^{cc',bb'}(\mathbf{p}'',\mathbf{p}',\mathbf{q}), \quad (6.44)$$

Equations of this type are (often) called **Bethe-Salpter equations**. Comparison with (6.41) shows that this equation appears to be conceptually similar to the Dyson equation for the one-particle Green function[28]. Indeed, the principle behind most recursion relations of perturbation theory is a structure like

$$\boxed{\hat{X} = \hat{X}_0 + \hat{X}_0 * \hat{Z} * \hat{X},} \quad (6.45)$$

where $\hat{X}$ is our object of interest (e.g. $\hat{\Gamma}$), $\hat{X}_0$ its 'free' version, $\hat{Z}$ a subunit that is, in some sense, 'irreducible' ($\hat{\Sigma}$ or $\hat{\Gamma}_0 GG$) and $*$ some generalized matrix convolution.

Owing to the importance of the two-particle propagator the solution of Bethe-Salpeter type equations is a center issue in many areas of many body physics. In most cases only

[28] We can make the analogy perfect, by defining a 'one-particle vertex' $\hat{\Gamma}^{(1)} = \hat{G}^{(0)-1}[\hat{G} - \hat{G}^{(0)}]\hat{G}^{(0)-1}$. Inspection of the second equality of Fig. 6.11 shows that the expansion of $\Gamma^{(1)}$ starts and ends with a self energy operator, i.e. the first free Green function line G_0 is removed, and so are the two external G_0's connecting to the self energy operator. In manifest analogy to (6.44), the analytical formula for $\Gamma^{(1)}$ then

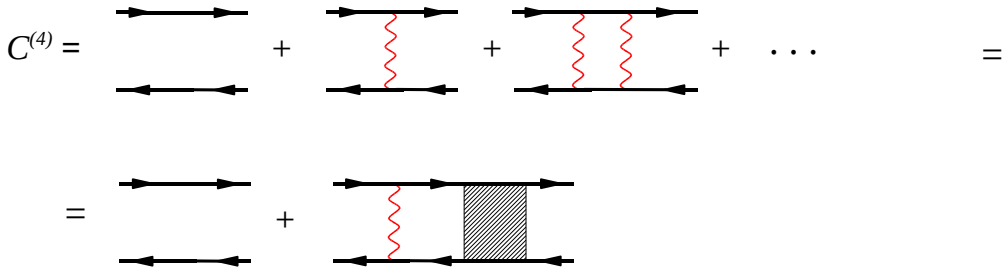

Figure 6.14: Large N expansion of the two particle correlation function into a 'ladder structure'.

approximate solutions can be obtained. With our present example, 'approximate' means that we send N to large values and seek for a solution to leading order in N^{-1}. In that limit, the only surviving contribution to the irreducible vertex is the first one, i.e. a plain interaction line. As with the self energy operator discussed in the previous section, all diagrams with 'entangled' interaction lines are frustrated in the sense that we do not have as many index summations as interaction constants $\sim g/N$. Such contributions vanish in the limit of large N. We thus conclude that the Bethe Salpeter equation assumes the simple form

$$\Gamma^{a,b}(\mathbf{p},\mathbf{p}',\mathbf{q}) = -\frac{g}{NL^d} - \frac{g}{N}\sum_c \frac{1}{L^d}\sum_{\mathbf{p}''} G(\mathbf{p})G(\mathbf{p}+\mathbf{q})\Gamma^{c,b}(\mathbf{p}'',\mathbf{p}',\mathbf{q}),$$

where $\Gamma^{ab} \equiv \Gamma^{aa',bb'}\delta^{aa'}\delta^{bb'}$[29]. This equation can be simplified even further by making the ansatz $\Gamma^{ab}(\mathbf{p},\mathbf{p}',\mathbf{q}) = \Gamma(\mathbf{q})$, where Γ is independent of discrete indices and input momenta $\mathbf{p}$ and $\mathbf{p}'$. (When solving a perturbative recursion relation, it is always a good idea to try an ansatz of maximal simplicity, i.e. an ansatz that is no more complex than the constituting elements of the equation.) Then,

$$\Gamma(\mathbf{q}) = \frac{g}{NL^d} + gP(\mathbf{q})\Gamma(\mathbf{q}) \Rightarrow \Gamma(\mathbf{q}) = \frac{g}{NL^d}\frac{1}{1-gP(\mathbf{q})}, \tag{6.46}$$

where we have introduced the abbreviation $P(\mathbf{q}) = \frac{1}{L^d}\sum_{\mathbf{p}} G(\mathbf{p})G(\mathbf{p}+\mathbf{q})$. In principle, one may now proceed by substituting the large N expansion of the Green function (6.42) and computing the function $P(\mathbf{q})$ by integration over $\mathbf{p}$. This would produce a closed exression for Γ and, by virtue of (please check!)

$$C^{(4)}(\mathbf{q}) = P(\mathbf{q})\left[\frac{1}{L^d} + N\Gamma(\mathbf{q})P(\mathbf{q})\right],$$

---

reads as

$$\hat{\Gamma}^{(1)} = \Sigma + \Sigma G_0 \hat{\Gamma}^{(1)}.$$

[29] We here use that the large-N approximation of the irreducible vertex forces the two input indices a, a' to be equal (the same of the output indices.) A word of caution: striktly speaking, our large N-approximation of the irreducible vertex explicitly *uses* that the input/output indices entering our *definition* of the vertex are equal. I.e. would we compute a correlation function where the two input/output indices are different (but that will seldomly occur in realistic applications.) the large N approximaiton of the four point functions would no longer assume the simple form of a regular ladder.

our correlation function. Since the emphasis in this section is on conceptual aspects of perturbation theory, we will not push the analysis to it's very end. (For an analysis of the Bethe-Salpeter equation in a context more interesting than ϕ^4-theory, see the problem set.) Yet there is one aspect about the expression for $\Gamma(\mathbf{q})$ worth noticing: Imagine $P(\mathbf{q})$ expanded in a Taylor series in $\mathbf{q}$ and consider the zeroth order contribution, $P(0)$. From the definition of the Green function (6.42) we have

$$P(0) = \frac{1}{L^d}\sum_{\mathbf{p}} G(\mathbf{p})^2 = \partial_\Sigma \frac{1}{L^d}\sum_{\mathbf{p}} G(\mathbf{p}) \stackrel{(6.43)}{=} g^{-1}\partial_\Sigma \Sigma = g^{-1}. \tag{6.47}$$

Substitution into the formula for Γ shows that for small momenta the expansion of the numerator of the vertex starts with a power of $\mathbf{q}$. (By symmetry, the first non-vanishing contribution will be of $\mathcal{O}(q^2)$. That means that both the vertex and the four point correlatio function are *long ranged* objects. I.e. unlike the Green function, they do not decay exponentially, but power law like. The long-rangedness of the four point function has observable consequences, as will be discussed in the next chapter.

Summarizing, our discussion of the two- and four-point function, and of the RPA theory of the interacting electron gas has shown that if a large parameter is present, (a) relevant subclasses of perturbative contributions can be identified and (b) summed to infinite order. As a matter of fact, there are not too many of these summable diagram classes. Ring-diagrams, rainbow-diagrams and ladder-diagrams nearly exhaust the set of 'friendly' corrections, amenable to analytical summation. Notice that, so far, we have largely restricted ourselfes to the discussion of abstract summation schemes, i.e. we still need to learn more about how intermediate results like (6.42) or (6.46) can be translated into concrete physical information. These aspects will be discussed – on applications more rewarding that plain ϕ^4 theory – a little bit later. However, at this point we leave the discussion of formal perturbation theory. While a state of the art exposition of the subject would require much more space – for pedagogical and condensed matter oriented texts on perturbative methods, see [**?**, **?**] – the material introduced in this section suffices for nearly all purposes of the present text. (Readers motivated to practice diagrammatic summation techniques on a number of interesting problems are invited to look at the problem set.)

Turning back to our prototypical problem of the interacting electron gas, we next aim to extend the purely diagrammatic methods discussed above to a more powerful hybrid approach comprising of perturbative concepts in combination with functional methods.

6.4 Summary and Outlook

This concludes our prelminary introduction into the concepts of perturbation theory. We have seen that general perturbative expansions mostly have the status of 'asymptotic' rather than convergent series. We learned how to efficiently encode perturbative series by graphical methods and how to asses the 'importance' of individual contributions. Further we saw how the presence of a large parameter can be utilized to firmly establish infinite order expansions. A number of recursive techniques were introduced to sum up diagram sequences of infinite order.

However, a second look at the discussion of the previous sections shows that our center tool, the functional integral actually played not much of a role. All it did was provide the combinatorial framework of the perturbative expansion of correlation functions. However, for that we hardly need the full feathered machinery of functional integration. Indeed, the fundamentals of the perturbative approach were laid in the 50th, way before people even began to think about the conventional path integral. (For a pure operator construction of the perturbative expansion, see the problem set.)

More importantly, the so far analysis has a serious methodological weakage: All subclasses of relevant diagrams shared the common feature that they contained certain 'subunits', more structured than the elementary propagator or the interaction line. E.g. the RPA diagrams were orgainized in terms of polarization bubbles, the NCA diagrams had their rainbows, and the ladder diagrams their rungs. Within the diagrammatic approach, in each diagram these units are reconstructed 'from scratch', i.e. in terms of elementary propagators and interaction lines. However, taking the general philosphy on information reduction declared in the beginning of the text seriously, we should strive to make the 'important' structural elements of an expansion to our *elementary* degrees of freedom. This program is hardly realizable within purely diagrammatic theory. However, the functional integral is ideally suited to introducing degrees of freedom hierarchically, i.e. trading microscopic objects for entities of higher complexity. The combination of functional integral techniques with perturbation theory to a fairly powerful theoretical machniery will be the subject of the next chapter.

6.5 Problem Set

Q1 Equivalence QM pert. theory., functional pert. theory.

Q2 Diagrammatics of the disordered electron gas.

Q3 Coulomb blockade

Q4 Attractive electron-electron interaction through phonons.

Q5 Cooper vertex for finite magnetic field.

Q6 Wick theorem without functional integrals.

Q7 Electron Green function with magnetic field (persistent currents).

Chapter 7

Mean Field Theory

Field integral oriented approaches to address interacting problems are introduced. We learn how elements of the perturbative approach developed in the previous chapter can be formulated more efficiently. Methods for detecting and exploring non-trivial reference states – 'mean fields' - are introduced. A fusion of perturbative and mean field methods will provide us with analytical machinery powerful enough to address a spectrum of interesting applications: superfluidiy, superconductivity and a number of manifestation of interactions in normal metals.

As mentioned in the beginning of the last chapter, the perturbative machinery developed in the previous sections is but a part of a larger framework. In fact, the diagrammatic expansion itself already contained hints indicating that a straightforward expansion of a theory in the interaction operator might not always be an optimal strategy: All previous examples that contained a large parameter N – and usually it is only problems of this type that are amenable to analytical analysis – had in common that the diagrammatic analysis bore out structures of 'higher complexity'. (E.g. series of polarization operators rather than series of the elementary Green functions, etc.) This phenomenon suggests that large N problems should qualify for a more efficient, or physical formulation.

While these remarks appear to be largely methodological, the rational behind searching for an improved theoretical formulation is in fact much deeper. Our previous examples had in common that the perturbative expansion was benign. However, we already saw some glimpses indicating that more drastic things may happen. E.g. for frequencies approaching the plasma frequency, the polarization operator of the weakly interacting electron gas developed an instability. The appearance of such instabilities usually indicates that one is formulating a theory around the 'wrong' reference state (in that case, the uniformly filled Fermi sphere of the non-interacting electron gas.) Thus, what we should like to develop is a theoretical framework that is capable of (a) detecting the 'right' reference states, or 'mean fields' of a problem, (b) enables us to efficiently apply perturbative methods around these states and all that (c) in a language using the 'physical' rather than the plain microscopic degrees of freedom as fundamental units.

The subject of the next sections will be the construction of a functional integral based

approach that meets these criteria. Unlike in previous chapters the discussion will be decidedly application-oriented. After the formulation of the general strategy of field integral based mean field methods, the next section will address a problem we have treated before, viz. the weakly interacting electron gas. The exemplification of the new concepts on a known problem will enable us to better understand the tight connection between the mean-field approach and straightforward perturbation theory. In the next sections we will then turn to the discussion of problems which lie decidedly outside the range of direct perturbative summation, viz. superfluidity and superconductivity.

7.1 Mean Field Theory

Roughly speaking, the functional approach to problems with a large parameter proceeds according to the following program:

1. Identify what you believe are relevant structural units. (That part of the program *can* efficiently be carried out by the straightforward methods discussed above.)

2. Introduce a new field-degree of freedom ϕ that represents the new hierarchy of degrees of freedom.

3. Trade the integration over 'microscopic fields' for an integration over ϕ, a step often effected by the so-called Hubbard-Stratonovich transformation.

4. Subject the action $S[\phi]$ to a stationary phase analysis. (The justification for applying stationary phase methods is provided by the existence of a large parameter $N \gg 1$.) Often, at this stage instabilities in the theory show up – an indicator of a physically interesting problem!

5. Expand the functional integral around the solution of the stationary phase equations, the so-called 'mean field' and compute physical observables.

In the next subsection, we illustrates how that program works on an example studied diagrammatically before, the plasma theory of the electron gas.

7.1.1 Functional Approach to the Weakly Interacting Electron Gas

Let us go back to the functional of the interacting electron gas (6.19). What prevents us from computing the ψ-integral along the lines of the free-fermion integrals discussed in the previous section is the interaction term with its quartic ψ dependence. However, it is actually a straightforward matter to reduce, or 'decouple' that operator down to a quadratic expression. To do so, we multiply the functional integral by the 'fat unity'

$$1 = \mathcal{N} \int \mathcal{D}\phi e^{-\frac{1}{8\pi TL^3}\sum_q \phi_q \mathbf{q}^2 \phi_{-q}},$$

where ϕ is a *bosonic* field variable and $\mathcal{N}$ is defined so as to normalize the integral to unity. Notice that the summation is over a four-momentum $q = (\mathbf{q}, \omega_m)$ comprising a vectorial momentum and a Bosonic Matsubara frequency. We next shift ϕ_q as

$$\phi_q \to \phi_q + 4ieTV(\mathbf{q})\rho_q,$$

where $\rho_q \equiv \sum_p \bar{\psi}_{p+q\sigma}\psi_{p\sigma}$. This produces the expression

$$1 = \mathcal{N}\int \mathcal{D}\phi e^{-\frac{1}{8\pi TL^3}\sum_q \phi_q \mathbf{q}^2\phi_{-q} + \frac{ie}{L^3}\sum_q \rho_q\phi_{-q} + \frac{T}{L^3}\sum_q \rho_q \frac{2\pi e^2}{\mathbf{q}^2}\rho_{-q}} =$$
$$= \mathcal{N}\int \mathcal{D}\phi e^{-\frac{1}{8\pi TL^3}\sum_q \phi_q \mathbf{q}^2\phi_{-q} + \frac{ie}{L^3}\sum_{q,p} \bar{\psi}_{p+q}\phi_{-q}\psi_{\mathbf{p}\sigma} + \frac{T}{L^3}\sum_q \rho_q \frac{2\pi e^2}{\mathbf{q}^2}\rho_{-q}}$$

The rational behind performing this seemingly unmotivated exercise can be seen in the last contribution to the exponent. Noticing that $2\pi e^2/\mathbf{q}^2 = V(\mathbf{q})/2$, we realize that this term exactly equals the quartic interaction contribution to the fermionic path integral, albeit with opposite sign. Multiplication of our unity with $\mathcal{Z}$ thus leads to

$$\mathcal{Z} = \int \mathcal{D}\phi \int \mathcal{D}(\bar{\psi}, \psi) e^{-S[\phi,\bar{\psi},\psi]}, \tag{7.1}$$
$$S[\phi, \bar{\psi}, \psi] = \frac{1}{8\pi TL^3}\sum_q \phi_q \mathbf{q}^2 \phi_{-q} + \sum_{pp'} \bar{\psi}_p \left[\left(-i\omega_n - \mu + \frac{\mathbf{p}^2}{2m}\right)\delta_{pp'} + \frac{ie}{L^3}\phi(\mathbf{p}' - \mathbf{p})\right]\psi_{p'},$$

i.e. an expression that is free of quartic interactions. Before proceeding, let us briefly rewrite the action in real space. With $\phi_q = T\int_0^\beta d\tau \int d^3r e^{iqr + i\omega\tau}\phi(\mathbf{r}, \tau)$,

$$S[\phi, \bar{\psi}, \psi] = \int d^3r \int_0^\beta d\tau \left\{\frac{1}{8\pi}\partial\phi\partial\phi + \bar{\psi}\left[\partial_\tau - \mu - \frac{\Delta}{2m} + ie\phi\right]\psi\right\}.$$

This notation reveals a physical interpretation of the field ϕ. Apparently, ϕ couples to the action of the fermions like a space/time dependent imaginiary *voltage*. The first term of the action, too conforms with that interpretation; it is proportional to the integral over $\partial\phi\partial\phi = \mathbf{E}^2$, where $\mathbf{E}$ is the electric field correspoding to the voltage ϕ, i.e. the Lagrangian energy density associated to the electric component of an electromagnetic field. Before proceeding with the discussion with the less intuitively accessible but technically more convenient momentum space representation of the action, let us take a step back and discuss the general philosophy of the manipulations that led from the original partition function to the two-field representation (6.19).

▷ INFO. The chain of manipulation exemplified above, i.e. the 'decoupling' of a quartic interaction through an auxiliary field is called the **Hubbard-Stratonovich transformation**. While that denotation may sound impressive, the essence of the Hubbard-Stratonovich transformation is a straightforward manipulation of a Gaussian integral. To make this point more transparent, let us reformulate the Hubbard-Stratonovich transformation in a notation that is not burdened by the presence of model-specific constants. Consider, then, an interaction operator of the architecture

$$S_{\text{int}} = V_{\alpha\beta\gamma\delta}\bar{\psi}_\alpha\psi_\beta\bar{\psi}_\gamma\psi_\delta,$$

where $\bar{\psi}$ and ψ may be either bosonic or fermionic field variables, the indices $\alpha, \beta, \ldots$ refer to an unspecified set of quantum numbers, Matsubra frequencies, etc., and $V_{\alpha\beta\gamma\delta}$ is an interaction matrix element. Now, introduce composite operators, $\hat{\rho}_{\alpha\beta} \equiv \bar{\psi}_\alpha \psi_\beta$ to rewrite the interaction as

$$S_{\rm int} = V_{\alpha\beta\gamma\delta} \hat{\rho}_{\alpha\beta} \hat{\rho}_{\gamma\delta}.$$

We can compactify the notation even further by introducing a composite indices $m \equiv (\alpha\beta)$, $n \equiv (\gamma\delta)$, whereupon

$$S_{\rm int} = \hat{\rho}_m V_{mn} \hat{\rho}_n$$

acquires the structure of a generalized bilinear form. To reduce the action to a form quadratic in the ψ's, multiply the exponentiated action by unity:

$$e^{-\hat{\rho}_m V_{mn} \hat{\rho}_n} = \mathcal{N} \int \mathcal{D}\phi \, e^{-\frac{1}{4}\phi_m V^{-1}_{mn} \phi_n} e^{-\hat{\rho}_m V_{mn} \hat{\rho}_n},$$

where ϕ is bosonic and $\mathcal{N}$ ensures unit-normalization of the ϕ-integral. Notice that V^{-1}_{mn} stands for the inverse of the matrix V_{mn} (i.e. not for the inverse $(V_{mn})^{-1}$ of individual matrix elements.) One next shifts the variable ϕ_m according to

$$\phi_m \to \phi_m + 2i(V\hat{\rho})_m,$$

where the notation $(V\hat{\rho})$ is shorthand for $V_{mn}\hat{\rho}_n$. As a result,

$$e^{-\hat{\rho}_m V_{mn} \hat{\rho}_n} = \mathcal{N} \int \mathcal{D}\phi \, e^{-\frac{1}{4}\phi_m V^{-1}_{mn} \phi_n - i\phi_m \hat{\rho}_n},$$

i.e. the term quadratic in $\hat{\rho}$ gets cancelled out[1]. This completes the Hubbard-Stratonovich transformation. We have traded the interaction operator for (a) the integration over an auxiliary field, coupled (b) to a ψ-bilinear (the operator $\phi_m \hat{\rho}_m$.)

A few suppementary comments:

- ▷ In essence, the Hubbard-Stratonovich transformation is tantamount to formula (4.42), read in reverse. An exponentiated square is *removed* in exchange for a linear coupling. (In (4.42) we showed how temrs linear in the integration variable can be removed.)

- ▷ To make the skeleton outlined above a well defined prescription, one has to be more specific about the meaning of the Gaussian integration over the kernel $\phi_m V^{-1}_{mn} \phi_n$. I.e. the integration variables can be real (in which case the matrix V better be positive), or complex. (In the latter case, V must have suitable Hermiticity properties.)

- ▷ There is some freedom as to the choice of the integration variable. E.g. the factor of 1/4 in front of the Gaussan weight $\phi_m V^{-1}_{mn} \phi_n$ was introduced for mere convenience (viz. to generate a coupling $\phi_m \hat{\rho}_m$ free of numerical factors.) If one does not like to invert the matrix kernel V_{mn}, one can scale as $\phi_m \to (V\phi)_m$, whereupon the key formula reads as

$$e^{-\hat{\rho}_m V_{mn} \hat{\rho}_n} = \mathcal{N} \int \mathcal{D}\phi \, e^{-\frac{1}{4}\phi_m V_{mn} \phi_n - i\phi_m V_{mn} \hat{\rho}_n},$$

[1]Here we have assumed that the matrix V is symmetric. If it is not, we can apply the relation $\hat{\rho}_m V_{mn} \hat{\rho}_n \equiv \rho^T V \rho = \frac{1}{2}\left[\hat{\rho}^T (V + V^T)\hat{\rho}\right]$ to symmetrize the interaction.

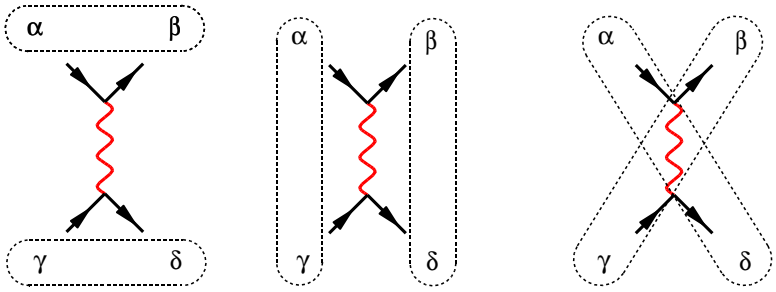

Figure 7.1: On the different options to Hubbard-Stratonovich decouple an interaction operator. Left: decoupling in the 'density' channel. Middle: decoupling in the 'pairing' or 'Cooper' channel. Right: Decoupling in the 'exchange' channel.

The Hubbard-Stratonovich transformation as such is exact. However, to make it a meaningful operation, it must be motivated by some physical considerations. In our discussion above we split the interaction by chosing $\hat{\rho}_{\alpha\beta}$ as a composite operator. However, there clearly is some arbitrariness whith this choice. E.g. why not pair the fermion-bilinears according to $(\bar{\psi}_\alpha\psi_\delta)(\bar{\psi}_\gamma\psi_\delta)$, or otherwise? The three inequivalent choices of pairing up operators are shown in Fig. 7.1 where, as ususal, the wavy line with attached field vertices represents the interaction, and the dashed ovals indicate how the field operators are paired.

The version of the transformation discussed above corresponds to the left diagram of the figure. That type of pairing is sometimes referred to as decoupling in the **direct channel**. The denotation becomes more transparent if we consider the example of the electron-electron interaction,

$$S_{\rm int} = \frac{1}{2}\int d\tau \int d^dr d^dr'\, \bar{\psi}_\sigma(\mathbf{r},\tau)\psi_\sigma(\mathbf{r},\tau)V(\mathbf{r}-\mathbf{r}')\bar{\psi}_{\sigma'}(\mathbf{r}',\tau)\psi_{\sigma'}(\mathbf{r}',\tau),$$

i.e. $\alpha=\beta=(\mathbf{r},\tau,\sigma)$, $\gamma=\delta=(\mathbf{r}',\tau,\sigma')$, $V_{\alpha\beta\gamma\delta}=V(\mathbf{r}-\mathbf{r}')$. The 'direct' decoupling proceeds via the most obvious choice, i.e. the density operator $\hat{\rho}(\mathbf{r},\tau)=\bar{\psi}_\sigma(\mathbf{r},\tau)\psi_\sigma(\mathbf{r},\tau)$. One speeks about decoupling in a 'channel' because, as will be explicated below, the propagator of the decoupling field can be interpreted in terms of two Green function lines tied together by multiple interactions, a composite object reminiscent of a 'channel'.

However, more important than the terminology is the fact that there are other choices for ρ. Decoupling in the **exchange channel** is generated by the choice $\rho_{\alpha\gamma}\sim\bar{\psi}_\alpha\psi_\delta$. 'Exchange' because, in the context of the coulomb interaction, the reversed pairing of field operators is reminiscent of the exchange contraction generating Fock-type contributions. Finally, one may decouple in the **Cooper channel**, $\hat{\rho}=\bar{\psi}_\alpha\bar{\psi}_\gamma$, $\rho_{\beta\gamma}=\rho^\dagger_{\gamma\beta}$. Here, the pairing field is conjugate to two creation operators. Below we will see that this type of decoupling is tailor made to problems of superconductivity.

The remarks above may may convey the impression of a certain arbitrariness inherent to the Hubbard-Stratonovich philosophy. Indeed, the 'right' choice of the decoupling field can only be motivated by physical reasoning, not by plain mathematics. This is to say that the transformation as such is exact, no matter what channel we chose. However, later on we will want to proceed to derive an effective low energy theory based on the decoupling field. In cases where one has accidentally decoupled in an 'unphysical' channel, it will be difficult, if not impossible to destill a meaningful low energy theory for the field ϕ conjugate to ρ; although the intital model still contains the full microscopic information (by virtue of the exactness of the transformation) it is not amenable to furhter approximate manipulations.

In fact, one is frequently confronted with situations where more than one Hubbard-Stratonovich field is needed to capture the full physics of the problem. To appreciate this point, consider the Coulomb interaction in momentum space.

$$S_{\rm int} = \frac{1}{2}\sum_{p_1,\ldots,p_4} \bar\psi_\sigma(p_1)\psi_\sigma(p_2)V(\mathbf{p}_1-\mathbf{p}_2)\bar\psi_{\sigma'}(p_3)\psi_{\sigma'}(p_4)\delta_{p_1-p_2+p_3-p_4}. \tag{7.2}$$

In principle, we can decouple this interaction by any of the three options discussed above. However, 'interesting' physics is usually generated by processes where one of the three unbound momenta entering the interaction vertex is small. Only these interaction processes have a chance to accumulate to an overall collective excitation of low energy (cf. our previous discussion of the RPA, the interacting electron gas, and many of the examples to follow.) It may be instructive to imagine the situation geometrically: In the three dimensional cartesian space of free momentum coordinates (p_1, p_2, p_3) entering the vertex, there are three thin layers, where one of the momenta is small, (q, p_2, p_3), (p_1, q, p_3), (p_1, p_2, q), $|q| \ll |p_i|$. (Why not make *all* momenta small? Because that would be in conflict with the condition that the Green functions connecting to the vertex be close to the Fermi surface.) One will thus often chose to break down the full momentum summation to a restricted summation over the small-momentum sublayers:

$$\begin{aligned} S_{\rm int} \simeq \frac{1}{2}\sum_{p,p',q} \Big(& \bar\psi_\sigma(p)\psi_\sigma(p+q)V(\mathbf{q})\bar\psi_{\sigma'}(p')\psi_{\sigma'}(p'-q) - \\ & \bar\psi_\sigma(p)\psi_{\sigma'}(p+q)V(\mathbf{p}'-\mathbf{p})\bar\psi_{\sigma'}(p'+q)\psi_\sigma(p') - \\ & \bar\psi_\sigma(p)\bar\psi_{\sigma'}(-p+q)V(\mathbf{p}'-\mathbf{p})\psi_\sigma(p')\psi_{\sigma'}(-p'+q)\Big) \end{aligned}$$

Now, each of these three contributions has its own predestinated choice of a slow decoupling field. The first term should be decoupled in the direct channel $\hat\rho_{\rm d}(q) \sim \sum_p \bar\psi_\sigma(p)\psi_\sigma(p+q)$, the second in the exchange channel $(\hat\rho_{\rm x})_{\sigma\sigma'} \sim \sum_p \bar\psi_\sigma(p)\psi_{\sigma'}(p+q)$, and the third in the Cooper channel $(\hat\rho_{\rm c})_{\sigma\sigma'}(p) \sim \sum_p \bar\psi_\sigma(p)\bar\psi_{\sigma'}(-p+q)$. One thus winds up with an effective theory that contains three independent slow Hubbard-Stratonovich fields. (Notice that the decoupling fields in the exchange and in the Cooper channel carry a spin-structure.)

Notice that in our discussion above of the high-density electron gas we decoupled in the direct channel. That choice is made because we already know *in advance* (viz. from our previous discussion) that relevant contributions to the free energy of the system are generated by RPA-type contraction of operators $\hat\rho_{\rm d}(q) \sim \sum_p \bar\psi_\sigma(p)\psi_\sigma(p+q)$, where q is small. If we *hadn't known*, a more careful three-fold Hubbard-Stratonovich decoupling, followed (see below) by a careful analysis of the decoupled action would have identified the density channel as relevant.

After this digression on the principles of the transformation, we turn back to the discussion of the electron gas.

The Hubbard-Stratonovich transformation leaves us with a situation where the fermion action has become quadratic – on the price of the introduction of a second field. At any rate, we have come reached a position where the fermion integration in (7.1) can be done:

$$\mathcal{Z} = \int \mathcal{D}\phi\, e^{-\frac{1}{8\pi TL^3}\sum_q \phi_q \mathbf{q}^2 \phi_{-q}} \det\left[-i\hat\omega - \mu + \frac{\hat{\mathbf{p}}^2}{2m} + \frac{ie}{L^3}\hat\phi\right], \tag{7.3}$$

where the Gaussian identity (5.38) has been used. As usual, the carets appearing under the argument of the determinant indicate that symbols have to be interpreted as operators (acting in the space of Matsubara and Hilbert space components.)

The standard procedure to deal with the determinants generated at intermediate stages of the manipulation of a field integral is to re-exponentiate them. This is done by virtue of the formula

$$\boxed{\ln\det\hat{A} = \text{ tr }\ln\hat{A},} \tag{7.4}$$

valid for arbitrary (non-singular) operators $\hat{A}$. Eq. (7.4) is readily proven by switching to an eigenbasis:

$$\ln\det\hat{A} = \sum_a \ln(\epsilon_a) = \text{ tr }\ln\hat{A},$$

where ϵ_a are $\hat{A}$'s eigenvalues and we have used that the eigenvalues of $\ln\hat{A}$ are $\ln\epsilon_a$. Thus,

$$\begin{aligned}\mathcal{Z} &= \int \mathcal{D}\phi\, e^{-S[\phi]},\\ S[\phi] &= \frac{1}{8\pi T L^3}\sum_q \phi_q \mathbf{q}^2 \phi_{-q} - \text{tr }\ln\left[-i\hat{\omega} - \mu + \frac{\hat{\mathbf{p}}^2}{2m} + \frac{ie}{L^3}\hat{\phi}\right],\end{aligned} \tag{7.5}$$

This is as far as exact manipulations carry us. We have managed to trade the integration over the interacting Grassmann field for an integration over an auxiliary field ϕ. A field, that is, of which we believe that it encapsulates the relevant degrees of freedom of the model. This completes steps 1., 2., and 3. of the general synopsis outlined above.

The next step is to subject the action to a stationary phase analysis, i.e. we seek for solutions to the set of saddle point equations,

$$\forall q = (\mathbf{q}\neq 0,\omega): \qquad \frac{\delta S[\phi]}{\delta\phi_q} \stackrel{!}{=} 0.$$

The function $\phi(\mathbf{x},t) \leftrightarrow \phi_q$ obtained by Fourier transformation of the solutions to these equations is commonly called the **mean field**. The denotation can be understood by inspection of the argument of the 'tr ln' above. The structure $\mu - \hat{\mathbf{p}}^2/2m + ie/L^3\phi$, where ϕ is a *fixed* configuration (to be determined by solving the saddle point equations) looks like the Hamilton operator of particles subject to some kind of background, or 'mean' field. The notation on the left hand side of the saddle point equations indicates that our original interaction $V(\mathbf{q})$ and, therefore, the decoupling field ϕ do not possess a zero momentum mode (charge neutrality.)

The concrete evaluation of the functional derivative $\delta S/\delta\phi$ leads us to the question as to how one differentiates the trace of the logarithm of the operator

$$\hat{G}^{-1}[\phi] = -i\hat{\omega} - \mu + \frac{\hat{\mathbf{p}}^2}{2m} + \frac{ie}{L^3}\hat{\phi}$$

with respect to its argument? (The denotation $\hat{G}^{-1}$ is motivated by the structural similarity to an inverse Green function.) Owing to the presence of the trace, the differentiation can be carried out as if G where a function:

$$\frac{\delta}{\delta\phi_q}\,\text{tr}\ln\left(\hat{G}^{-1}[\phi]\right) = \text{ tr }\left(\frac{\delta}{\delta\phi_q}\ln\left(\hat{G}^{-1}[\phi]\right)\right) = \text{ tr }\left(\hat{G}[\phi]\frac{\delta}{\delta\phi_q}\hat{G}^{-1}[\phi]\right),$$

where in the first equality we have used that the taking the trace and differentiation are commutative operations. The second equality essentially relies on the presence of the trace, i.e. in general the non-commutativity of $\hat{G}^{-1}$ and $\delta_\phi \hat{G}^{-1}$ implies $\delta_\phi f(\hat{G}^{-1}) \neq f'(\hat{G}^{-1})\delta_\phi \hat{G}^{-1}$.)

We next explicate this operation on the operator appearing in the action. (For tutorial reasons, and paying the price that the notation is somewhat messy, all index dependences are spelled out explicitly

$$\begin{aligned}
\frac{\partial}{\partial \phi_q} S[\phi] &= \frac{1}{4\pi T L^3} V(\mathbf{q})\phi_{-q} - \text{ tr } \left[\hat{G}[\phi]\frac{\delta}{\delta \phi_q}\hat{G}^{-1}[\phi]\right] = \\
&= \frac{1}{4\pi T L^3} V(\mathbf{q})\phi_{-q} - 2\sum_{q_1 q_2} \left(\hat{G}[\phi]\right)_{q_1 q_2} \left(\frac{\delta}{\delta \phi_q}\hat{G}^{-1}[\phi]\right)_{q_2 q_1} = \\
&= \frac{1}{4\pi T L^3} V(\mathbf{q})\phi_{-q} - \frac{2ie}{L^3}\sum_{q_1 q_2} (\hat{G}[\phi])_{q_1 q_2}\delta_{q_1 - q_2, q} = \\
&= \frac{1}{4\pi T L^3} V(\mathbf{q})\phi_{-q} - \frac{2ie}{L^3}\sum_{q_1} (\hat{G}[\phi])_{q_1, q_1 - q} \stackrel{!}{=} 0. \qquad (7.6)
\end{aligned}$$

Here, the factor of two appearing in front of the double summation in the second line counts the electron spin. In the essential third equality we have used that $\hat{G}^{-1}$ is linear in its argument ϕ and that $(\frac{\delta}{\delta \phi_q}\hat{\phi})_{q_1 q_2} = \delta_{q_1 - q_2, q}$. That last relation follows from the rules of functional differentatiation. In fact (owing to the discreteness of the momentum) we are not even differentiating functionals: $\hat{\phi}$ is a matrix in momentum space. It's matrix elements are are given by components ϕ_q: $(\hat{\phi})_{q_1, q_2} = \phi_{q_1 - q_2}$. Differentiation of that matrix wrt ϕ_q then produces another matrix with matrix elements 1 for $q_1 - q_2 = q$ and zero otherwise. (Admittedly, it takes some time to get used to differentiation formulae of that type.)

Equations of that type are not solved from scratch but by making a physically motivated ansatz, i.e. *guessing* a solution. Naturally, the first try will be a homogeneous solution, $\phi(\mathbf{x}, t) \equiv \bar{\phi} = \text{const.}$, i.e. one relies on the picture that a spatially and temporaly varying field configuration is energetically more costly than a constant one, and, therefore, cannot determine a stable extremum.

▷ INFO. But be aware, there exist translationally invariant problems with inhomogeneous mean fields or, more tricky, a homogeneous solution exists but is energetically inferior to a structured one. There may be sets of degenerate solutions, etc. Often, when new theories describing unknown territory have been developed, the search for the 'right' mean field turned out to be a matter of long, and sometimes controversial research.

In the present context, spatial and temporal homogeneeity translates to $\phi_{\mathbf{q},\omega} = 0$ if either ω or $\mathbf{q}$ are non-zero. That, indeed, solves the mean field equation: Assuming that all fluctuating components of ϕ are switched off, the Green function operator becomes diagonal in momentum space, $(\hat{G}[\phi])_{q_1, q_2} \propto \delta_{q_1, q_2}$. We thus see that for non-vanishing q both terms in the equation vanish. But then, the zero-momentum component $\phi_{q=0}$ does

not exist anyway (again, charge neutrality), whence $\hat{\phi} = 0$ is the sought for solution of our mean field problem. That settles step 4. of the general program.

We next proceed to expand the functional in fluctuations around $\phi = 0$. Since the mean field vanishes, it does not make sense to introduce new notation, i.e. we will denote the fluctuations again by the symbol ϕ. As regards the first term in the action (7.5), it is already quadratic and there is nothing to do. The logarithmic contribution can be expanded as if we were dealing with a function (again, a consequence of the trace), i.e.

$$\begin{aligned}\text{tr ln}\left[-i\hat{\omega} - \mu + \frac{\hat{\mathbf{p}}^2}{2m} + \frac{ie}{L^3}\hat{\phi}\right] &= \text{tr ln}(\hat{G}_0^{-1}) + \\ &+\frac{ie}{L^3}\text{tr ln}(\hat{G}_0\hat{\phi}) + \frac{1}{2}\left(\frac{e}{L^3}\right)^2 \text{tr ln}(\hat{G}_0\hat{\phi}\hat{G}_0\hat{\phi}) + \ldots,\end{aligned}$$

where

$$\hat{G}_0^{-1} \equiv -i\hat{\omega} - \mu + \frac{\hat{\mathbf{p}}^2}{2m}$$

is the momentum and frequency diagonal operator whose matrix elements give the free Green function of the electron gas. Now, let us discuss the terms appearing on the right hand side in turn. Being ϕ-independent, the first term gives just an overall constant multiplying the functional integral, viz. a constant that must describe the non-interacting content of the theory. Indeed,

$$e^{\text{tr ln}(\hat{G}_0^{-1})} = e^{-\text{tr ln}(\hat{G}_0)} = \det(\hat{G}_0)^{-1} \equiv \mathcal{Z}_0$$

is just the partition function of the non-interacting electron gas. The second term of the expansion, linear in $\hat{\phi}$ vanishes on account of our mean field analysis. (We are expanding around an extremum! exercise: Write out the momentum representation of the first order contiribution to re-confirm its vanishing.) The third term is the interesting one. Remembering that $\hat{\phi}$ couples to the theory like a voltage, this term describes how voltage flucutations are affected by the presence of the electron gas. That must have something to do with screening!

To understand this connection let us make the momentum dependence of the second-order term explicit (exercise):

$$\begin{aligned}\frac{1}{2}\left(\frac{e}{L^3}\right)^2 \text{tr}\,(\hat{G}_0\hat{\phi}\hat{G}_0\hat{\phi}) &= \left(\frac{e}{L^3}\right)^2 \sum_p \sum_q G_{0,p}\phi_q G_{0,p-q}\phi_{-q} = \\ &= \frac{e^2}{2TL^3}\sum_q \Pi_q\phi_q\phi_{-q},\end{aligned}$$

where in the last line we meet again with the polarization operator (6.30). Combination with the first term in the action finally leads to

$$S_{\text{eff}}[\phi] = \frac{1}{2TL^3}\sum_q \phi_q\left(\frac{\mathbf{q}^2}{4\pi} - e^2\Pi_q\right)\phi_{-q} + \mathcal{O}(\phi^4), \tag{7.7}$$

where we noted that odd powers of ϕ vanish by the symmetry of the problem (exercise.)

Eq. (7.7) is a very suggestive result. Ignoring the coupling to the electron gas, ϕ represents a field with bare 'propagator' $\sim \mathbf{q}^{-2}$, i.e. the long range correlation mediated by the electric field in vacuum. Coupling the field to a medium leads to the appearence of a 'self energy' $\sim \Pi_q$. As we saw above, that self energy converts the long ranged power law correlation into something exponential – screening. The form of the screened propagator exactly coinicides with the effective RPA interaction (6.36) derived diagrammatically above. In passing we note that the structures emerging in the functional integral analysis support a unified way of 'reading' the theory; There appear 'propagators', 'self-energies', etc. irrespective of the concrete context, i.e. irrespective of whether we are dealing with a fermionic field (ψ) or a bosonic one (ϕ).

From here it is a one-line calculation to reproduce the result for the RPA free energy of the electron gas discussed above. Gaussian integration over the field ϕ (step 5. of the program) leads to

$$\mathcal{Z}_{\mathrm{RPA}} = \mathcal{Z}_0 \prod_q \left(1 - \frac{4\pi e^2}{\mathbf{q}^2}\Pi_q\right)^{-1/2},$$

where we have noted that the ϕ-integration was unit-normalized, i.e. for $\Pi = 0$, the integral collapses to unity. Taking the logarithm, we obtain

$$F_{\mathrm{RPA}} = -T(\ln(\mathcal{Z}) - \ln(\mathcal{Z}_0)) = \frac{T}{2}\sum_q \ln\left(1 - \frac{4\pi e^2}{\mathbf{q}^2}\Pi_q\right),$$

in agreement (6.28).

At this point, it may be worthwhile to halt and to compare our two approaches to the problem, diagrammatics and field integration. We first note that the functional integral formulation indeed leads to the 'reduced' description we wanted to obtain: The minimal degree of freedom (ϕ) directly couples to the physically relevant entities of the theory (Π_q). The downside is that to formulate the approach, we had to go through some preparatory work, notably work that required anticipatory physical insight into the problem (i.e. the correct choice of the Hubbard-Stratonovich transformation.) However, that turned out to be a well invested effort. After the identification of ϕ as the 'good' field, the further construction of the theory proceeded along the lines of a largely 'automatized program' (seeking saddle points, expanding etc.). E.g. there was no need to battle with combinatorial problems. Further, in functional integral approaches the risk to miss relevant contributions, or diagrams, to the expansion of a theory is far less pronounced than in direct diagrammatic expansions. But undoubtedly the most important advantage of the functional integral route is its extensibilty. E.g. an expansion of the theory to higher orders in ϕ would have generated an interacting theory of voltage flucutations. Correlations on the level of that theory correspond to diagrams beyond the RPA level, i.e. diagrams whose direct and error-free summation would require much higher developed skills. However, the construction developing a theory of these 'interacting plasmon modes' is beyond the scope of the present text.

The mean field optimizing the problem above was particularly simple, $\phi = 0$. More intereseting situations arise if one is met with non-vanishing mean field configurations, i.e. the perturbation theory has to be organized around a state different from the trivial

vacuum state of the theory. In the next section we discuss superfluidity as an example that nicely illustrates the richness of the phenomena that may arise under such circumstances.

7.2 Bose-Einstein Condensation and Superfluidity

We consider a bosonic theory defined through

$$\mathcal{Z} = \int \mathcal{D}(\bar{\psi},\psi)\, e^{-S[\bar{\psi},\psi]}, \tag{7.8}$$
$$S[\bar{\psi},\psi] = \int_0^\beta d\tau \int d^d r \left[\bar{\psi}(\mathbf{r},\tau)\left(\partial_\tau + \hat{H}_0 - \mu\right)\psi(\mathbf{r},\tau) + \frac{1}{2}g(\bar{\psi}(\mathbf{r},\tau)\psi(\mathbf{r},\tau))^2\right],$$

where ψ is a complex field subject to the standard boundary condition $\psi(\,.\,,\beta) = \psi(\,.\,,0)$. The functional integral $\mathcal{Z}$ describes the physics of a system of bosonic particles in d-dimensions subject to a contact interaction of strength g. For the moment the specific structure of the one-body operator $\hat{H}_0$ need not be specified.

The most remarkable phenomena displayed by systems of the type (7.8) are Bose-Einstein condensation and superfluidity. However, contrary to a widespread prejudice, these two effects do not mutually depend on each other: superfluidity can arise without condensation and vice versa. We begin our discussion with the more elementary of the two,

7.2.1 Bose-Einstein Condensation

As most readers will remember from elementary courses on statistical mechanics, **Bose-Einstein condensation** is called the effect that a macroscopic fraction of the number of particles of the system populate a single state. To see how this phenomenon is born out of the functional integral formalism, let us temporarily switch off the interaction and assume that the one-particle Hamiltonian has been diagonalized:

$$\mathcal{Z}_0 \equiv \mathcal{Z}\Big|_{g=0} = \int \mathcal{D}(\bar{\psi},\psi)\, \exp\left[-\int_0^\beta d\tau \sum_a \bar{\psi}_a(\tau)\left(\partial_\tau + \epsilon_a - \mu\right)\psi_a(\tau)\right] =$$
$$= \int \mathcal{D}(\bar{\psi},\psi)\, \exp\left[-\sum_{an} \bar{\psi}_{an}\left(-i\omega_n + \epsilon_a - \mu\right)\psi_{an}\right],$$

where in the last line we have switched to a frequency representation. Without loss of generality, we may assume that the eigenvalues $\epsilon_a \geq 0$ are positive with a ground state $\epsilon_0 = 0$ [2]. (I.e. unlike in the previoulsy discussed fermion problems, we should not carry the picture of *low* energy excitations superimposed on *high* energy microscopic degrees of freedom in mind; Here, everything will take place in the vicinity of the ground state of the *microscopic* single particle Hamiltonian.) Also notice that, by stability, the chemical potential determining the number of particles in the system must be negative. Otherwise

[2] The chemical potential μ can always be adjusted so as to meet this condition.

the Gaussain weight corresponding to the low lying states $\epsilon_a < -\mu$ would change sign resulting in an ill-defined theory.

From our discussion of section 5.2.1 we remember that the number of particles in the system,

$$N(\mu) = T \sum_{na} \frac{1}{i\omega_n - \epsilon_a + \mu} = \sum_a f_{\rm b}(\epsilon_a),$$

where

$$f_{\rm b}(\epsilon) = \frac{1}{e^{\beta(\epsilon-\mu)} - 1}$$

is the Bose distribution. For a given number of particles, this equation determines the temperature dependence of the chemical potential, $\mu(T)$. How does the chemical potential scale with the temperature? Mainly for illustrative purposes, a plot of the Bose distribution function is shown in the figure. As the temperature is reduced, the distribution function controlling the population of individual states decreases. Since the number of particles must be kept constant, this scaling must be counteracted by increasing the the chemical potential.

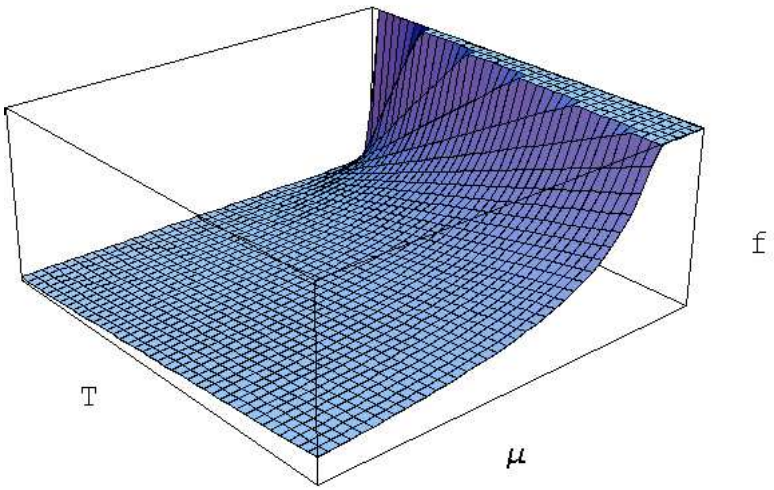

Figure 7.2: Schematic plot of the ground state Bose distribution function $f_{\rm b}(0)$ as a function of temperature and chemical potential (both measured in arbitrary units.) The plot mainly serves illustrative purposeses. In fact, $f_{\rm b}(0)$ depends only on the ratio μ/T and a one-dimensional graph would suffice to store the information shown as a surface graph above.

Below a certain critical temperature T_c, even the maximum value of the chemical potential, $\mu = 0$, will not suffice to keep the distribution function $f(\epsilon_{a\neq 0})$ large enough to accomodate all particles in the states of non-vanishing energy, i.e.

$$\sum_{a>0} f(\epsilon_a)\Big|_{\mu=0} \overset{T\leq T_c}{\equiv} N_1 < N.$$

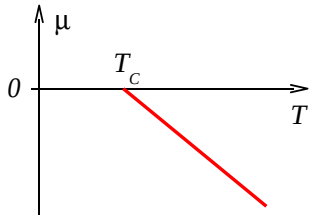

I.e. below that critical temperature the chemical potential stays constant at 0 (see the figure). However a macroscopic number of particles $N - N_1$ gathers in the ground state: Bose-condensation

▷ INFO. Since its prediction in the early twenties by Bose and Einstein the phenomenon of Bose condensation has been a standard textbook subject. However, it took seven decades before the condensation of Bosonic particles was for the first time directly[3] observed in **experiment**. The reason for this delay is that the critical temperature for the condensation of particles that are comfortably accessible to experiment – that is, atoms – is absurdly low.

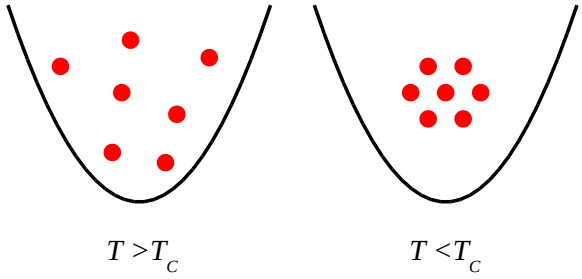

Figure 7.3: Cartoon of atoms caught in a magnetic trap. Below a critical temperature, T_c the atoms condense into a lump occupying a single zero energy state.

However, in 1995 the group of E. Cornell and C. Wieman at Colorado University managed to cool down a system of rubidium atoms down to temperatures of 20 billionths (!) of a Kelvin[4]. To reach these temperatures, a gas of rubidium atoms was caught in a magnetic trap, i.e. a configuration of magnetic field gradients that couple to the magnetic moments of the atoms so as to keep the system spatially localized. (See the theorists cartoon in Fig. 7.3.)

The gas of atoms was then brought to a temperature of $\mathcal{O}(10^{-5})K$ – still way too hot to condense – by laser cooling. (The one-line explanation of that cooling mechanism is that atoms confronted with a suitably adjusted ray of monochromatic light may transmit more of their kinetic energy to the photons than they get back; they cool down.) To lower the temperature still further, the principle of 'evaporative cooling' was applied: By lowering the potential well of the trap, a fraction of the atoms, namely those with large kinetic energy, was allowed to escape. The remaining portion of atoms had low kinetic energy, i.e. low temperature. What

[3] By 'direct' we mean a controlled preparation of a state of condensed massive bosonic particles. There are numerous 'indirect' manifestations of condensed states, e.g. the anomalous properties of the Helium liquids at low temperatures or of Cooper-pair condensates in superconductors.

[4] M. H. Anderson, J.R. Ensher, M.R. Matthews, C.E. Wieman, and E. A. Cornell, Science **269**, 198 (1995).

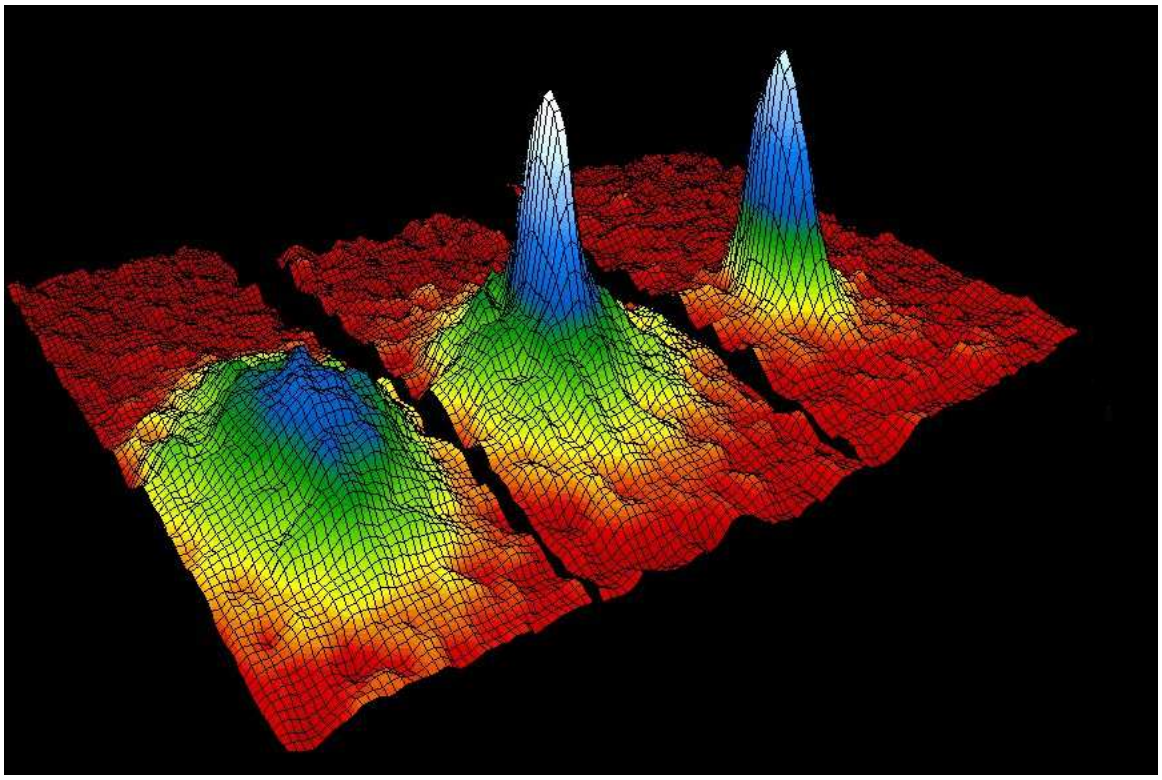

Figure 7.4: Spectroscopic images of a gas of atoms at 400nK (left), 200nK (middle), and 50nK (right). The peak in the density distribution signals the onset of condensation.

sounds like a simple recipe actually represents a most delicate experimental procedure. (E.g. if the trap potential is lowered to strongly, all atoms decide to go away and there is nothing left to condense. If the trapping is too strikt, the atoms remain too hot, etc.) However, after a more than a decade of intensive experimental preparation, the required temperatures had been reached.

Spectroscopic images of the Bose condensatation process are shown in Fig. 7.4 for three different values of the temperature. Lowering the temperature is accompanied by the formation of a peak in the density distribution, an unambiguous indication of the transition to a condensed state. The preparation of a Bose condensed state of matter was awarded the 2001 Nobel prize in physics. Since 1995 the research on atomic condensates has made tremendous progress. By now, it is possible to prepare complex states of Bose condensed matter such as atomic vortices, condensates in different dimensionalities, or even an artificial crystalline state of matter (see Fig. **??**). However, a detailed discussion of these interesting developments would be beyond the scope of the present text.

We next ask how the phenomenon of Bose condensation can be implemented into our functional integral representation. Evidently, the characteristics of the condensate will be described by the zero field component $\psi_0(\tau)$. The problem with this zero mode is that below the condensation transition its action apears to be unbound: Both the chemical potential and the eigenvalue are zero. That means that the action of the zero-Matsubara

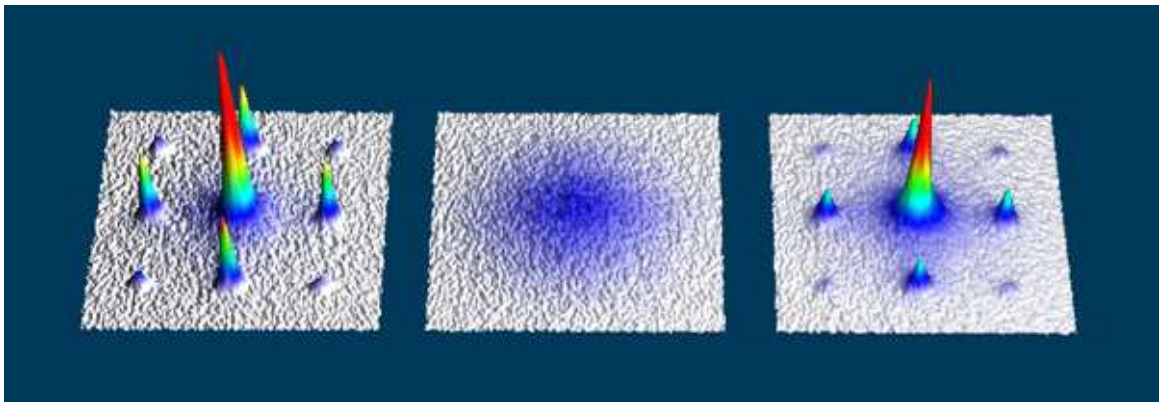

Figure 7.5: The creation of an artificial mono-atomic crystal from a bose condensate. A system of bosons in a condensed state – the latter signalled by the prononounced coherent intensity peaks in the left portion of the figure – is exposed to a 'grid' formed by two crossing fields of intense laser radiation. For strong enough field amplitudes, the electromagnetic radiation interferes to a periodic lattice of deep potential minima. These minima become occupied by one atom each. The result is an artificial mono-atomic crystal, characterized by the absence of coherent superposition of atomic wave function amplitudes, i.e. an equilibrated density profile (middle). If the laser intesity is lowered, the atoms re-arrange to the characteristic density distribution of the condensate (right).

component $\psi_{0,0}$ vanishes. We will deal with this difficulty in a pragmatic way. That is, we will not treat $\psi_0(\tau)$ as an integration variable but rather as a *time independent* Lagrange multiplier to be used to fix the number of particles below the transition. I.e. we introduce an reduced action as

$$S_0|_{\mu=-0} = -\bar{\psi}_0 \beta\mu\psi_0 + \sum_{a\neq 0,n} \bar{\psi}_{an} \left(i\omega_n + \epsilon_a - \mu\right) \psi_{an},$$

where the subscript $\mu = -0$ indicates that the action describes the system at infinitesimal negative μ. (In order to be able to use μ as a differentiation variable, we do not yet set $\mu = 0$.) To understand the rational behind this simplification note that

$$N = -\partial_\mu \mathcal{F}_0 = \partial_\mu T \ln \mathcal{Z}_0 = \bar{\psi}_0\psi_0 + T \sum_{a\neq 0,n} \frac{1}{i\omega_n - \epsilon_a} = \bar{\psi}_0\psi_0 + N_1 \tag{7.9}$$

determines the number of particles. According to this expression, $\bar{\psi}_0\psi_0 = N_0$ sets the number of particles in the condensate. Now, what enables us to regard ψ_0 as a time independent field? Remebering the construction of the path integral, we note that introduction of time dependent fields, or 'time slicing' was necessitated by the fact that the operators appearing in the Hamiltonian of a quantum theory do not, in general, commute. (Otherwise we could have decoupled

$$\mathrm{tr}\, \left(e^{-\beta(\hat{H}-\mu\hat{N})(a^\dagger,a)}\right) \simeq \int d(\bar{\psi},\psi) e^{-\beta(\hat{H}-\mu\hat{N})(\bar{\psi},\psi)}$$

in terms of a *single* coherent state resolution, i.e. a 'static' configuration.) Reading this obseravation in reverse, we conclude that the dynamic content of the field integral repre-

sents the quantum character of a theory. (Alluding to this fact, the temporal fluctuations of field variables are often referred to as **quantum fluctuations**.) Conversely,

> A static approximation in a field integral $\psi(\tau) = \psi_0 = \text{const.}$ amounts to replacing a quantum degree of freedom by its classical approximation.

(In order to distinguish them from quantum fluctuations, fluctuations in the 'classical' static sector of the theory are called **thermal fluctuations**.) To justify the approximation of $a_0 \leftrightarrow \psi_0$ by a classical object, notice that upon condensation,

$$N_0 = \langle a_0^\dagger a_0 \rangle$$

will assume 'macroscopically large' values. On the other hand the commutator $[a_0, a_0^\dagger] = 1$, continues to be of $\mathcal{O}(1)$. It thus seems to be legitimate to neglect all commutators of the zero operator a_0 in comparison with its expectation value – a classical approximation[5]. Unfortunately, however, the actual state of affairs with the classical treatment of the condensate state is more complex than the simple argument above suggests. (For a good discussion, see [?].) However the net result of a more thorough analysis[6] still is that treating ψ_0 as classical is a legitimate approximation.

Now, we are still left with the problem that the ψ_0-integration appears to be undefined. The way out is to remember that the partition function should extend over those states only that contain an (average) number of N particles. That is, Eq. (7.9) has to be interpreted as an relation that *fixes* the modulus $\bar{\psi}_0\psi_0$ so as to adjust the appropriate value of N. (For a clean discussion of the choice of the thermodynamic variables in the present context, see again Ref.[?].)

7.2.2 The Interacting Bose Gas

Now, let us relax the condition of zero interaction and study the system for small but finite g. To keep the discussion concrete, we specialize to the case of a clean ballistic single particle system,

$$\hat{H}_0 = \frac{\hat{p}^2}{2m}.$$

(Notice that the ground state wave function of this system a spatially constant zero momentum wave function.) By adiabatic continuity we expect that much of the picture developed above will survive generalization to a finite interaction. In particular the ground state, which in the case under consideration corresponds to a temporal *and* spatially constant mode ψ_0, will continue to be macroscopically occupied. Under these circumstances, surely the dominant contribution to the action will come from the classical ψ_0 sector:

$$S[\bar{\psi}_0, \psi_0] = \beta \left(-\mu \bar{\psi}_0 \psi_0 + \frac{g}{2L^d} (\bar{\psi}_0 \psi_0)^2 \right). \tag{7.10}$$

[5] Notice the similarity of that reasoning to the arguments employed in connection with the semiclassical treatment of spin systems in the limit of large S (section 3.2.3.)

[6] In principle, the temporally fluctuating contributions to the zero mode, $\psi_{0,n\neq 0}$ can be treated as ordinary integration variables. However, the integration over these modes does not essentially affect the properties of the model.

(Notice the similarity of that action to the integrand of the toy problem discussed in section 6.1.1.) Importantly, the stability of the action is now guaranteed by the interaction vertex, no matter how small $g > 0$ (see the schematic plot of the action in Fig. 7.6.) Accordingly, we will no longer treat ψ_0 as a fixed parameter but rather as an ordinary intergration variable. Integration over all field components will produce a partition function $\mathcal{Z}(\mu)$ that depends parameterically on the chemical potential. As usual in statistial physics, the latter can then be employed to fix the particle number. (Notice that vis-a-vis thermodynamic aspects the interacting system appears to behave more 'naturally' then its ideal, non-interacting approximation. This reflects a general feature of bosonic systems; interactions 'regularize' a number of peculiar features of the ideal gas.)

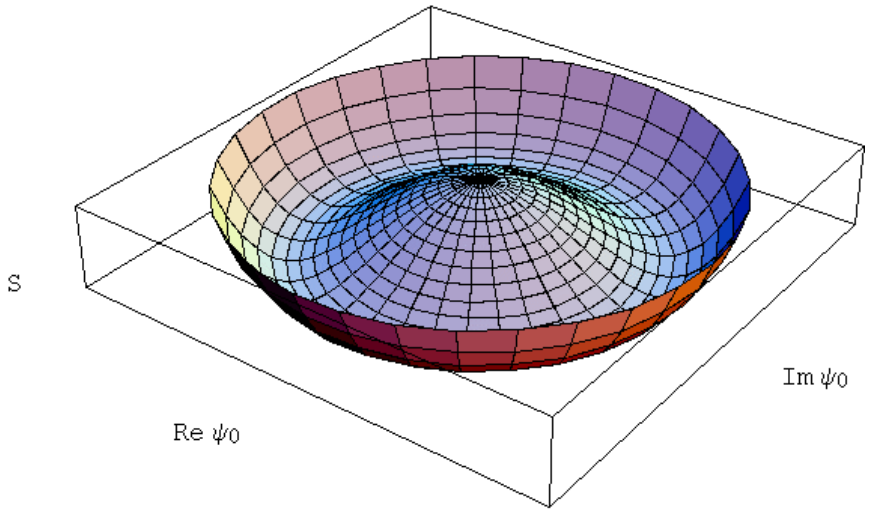

Figure 7.6: The action $S[\bar{\psi}_0, \psi_0]$ as a function of real and imaginary part of the condensate field. The most important features of the action are (a) the existence of a degenerate minimum determined by the set of solutions of the equation $\partial_{|\psi_0|} S = 0$ and (b) the large amplitude asymptotics $\sim \beta g |\psi_0|^4$ stabilizing the ψ_0-integration.

Coming back to the ψ_0-integration, we observe that for low enough temperature, the problem is an ideal candidate for a saddle point analysis. Variation of the action w.r.t. ψ_0 generates the equation

$$\psi_0 \left(-\mu + \frac{g}{L^d} \bar{\psi}_0 \psi_0 \right) = 0.$$

This equation is solved by any configuration $\psi_{0,\mathrm{mf}}$ with modulus $|\psi_{0,\mathrm{mf}}| = \sqrt{\mu L^d / g} \equiv \gamma$. In spite of its innocent appearance, this observation reveals a lot of 'deep' information on the system:

- ▷ For $\mu < 0$, i.e. above the condensation threashold of the non-interacting system, the equation has only the trivial solution $\psi = 0$. Which means that no stable condensate amplitude exists.
- ▷ Below condensation, the squared modulus $|\psi_{0,\mathrm{mf}}| \propto L^d$, reflecting the macroscopic population of the ground state.

▷ The equation couples only to the *modulus* of ψ_0. I.e. the present situation is different from our previously encountered examples in that the solution to the stationary phase equation is continuously degenerate; dach configuration $\psi_{0,\mathrm{mf}} = \gamma \exp(i\phi), \phi \in [0, 2\pi]$ is a solution.

For our present discussion, the last of the three aspects mentioned above is the most important. It raises the question which of the configurations $\psi_{0,\mathrm{mf}} = \gamma \exp(i\phi)$ is the 'right' one?

Without loss of generality, we may chose $\psi_{0,\mathrm{mf}} = \gamma$, i.e. a real solution, as a reference configuration for our theory. That choice amounts to picking a particular minimum lying in the 'mexican hat' structure of Fig. 7.6. However, it is clear that an expansion of the action around that minimum will be singular: fluctuations $\psi_{0,\mathrm{mf}} \to \psi_{0,\mathrm{mf}} + \delta\psi$ that do not leave the azimuthally symmetric well of degenerate minima do not change that action and, therefore, have vanishing expansion coefficients. This entails that in the present situation we will not get away with a simple scheme 'saddle point plus quadratic fluctuations.' (There is nothing that constrains the deviations $\delta\psi$ to be small.) The integral over fluctuations around mean field configurations has to be done in a more careful way.

▷ INFO. What we are encountering here is a mechanicsm called **spontaneous symmetry breaking**. The phenomenon is very general, and, whenever it arises, the consequences tend to be grave. To understand the general principle, consider an action $S[\psi]$ with a *global continuous* symmetry under some transformation g. By which we mean that the action remains invariant, $S[\psi] = S[g\psi]$ under a transformation of all fields simultaneously, $\forall i \in M : \psi_i \to g\psi_i$, where M is the base manifold. The transformation is 'continuous' in the sense that the g's ought to take values in some manifold, typically a group G.

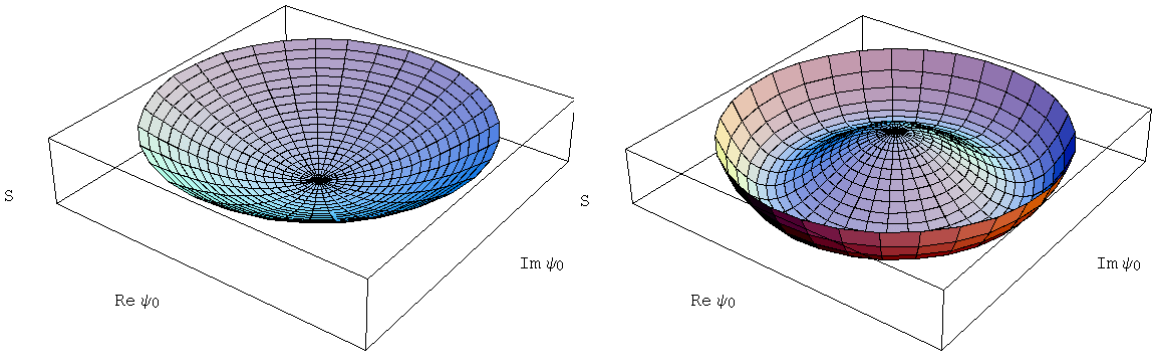

Figure 7.7: Zero mode action of the weakly interacting bose gas for $\mu > 0$ (left) and $\mu < 0$ (right).

Some examples: The action of a Heisenberg ferromagnet is invariant under **rotation** of all spins simultaneously by the same amount, $\mathbf{S}_i \to g\mathbf{S}_i$. In this case, $g \in G = \mathrm{O}(3)$, the three dimensional rotation group. The action of the displacement fields $\boldsymbol{\phi}$ describing elastic deformations of a solid (phonons) is invariant under simultaneous **translation** of all displacements $\boldsymbol{\phi}_i \to \boldsymbol{\phi}_i + \mathbf{a}$, i.e. the symmetry manifold is the the d-dimensional translation group $G \simeq \mathbb{R}^d$. In the example above, we had a U(1) symmetry under phase multiplication $\psi_0 \to e^{i\phi}\psi_0$. This phase

freedom expresses the **global gauge symmetry** of quantum mechanics under transformation by a phase, a point we will discuss in more detail below.

Now, given a theory with globally G invariant action, two scenarios are conceivable. Either the ground states share the invariance properties of the action or they do not. The two alternatives are illustrated in Fig. 7.7 for the example of the bose system. For $\mu > 0$, the action $S[\bar{\psi}_0, \psi_0]$ has a single ground state at $\psi_{0,\mathrm{mf}} = 0$. This state is trivially symmetric under the action of $G = \mathrm{U}(1)$. However, for negative μ, i.e. in the situation discussed above, there is a degenerate *manifold* of ground states, defined through $|\psi_{0,\mathrm{mf}}| = \gamma$. These ground states transform into each other under the action of the gauge group, however, none of them individually is invariant.

With the other examples mentioned above, the situation is similar. Only that for symmetry groups more complex than the one-dimensional manifold U(1), the ground states will, in general, be invariant under transformation by the elements of a certain subgroup $\{\mathbf{1}\} \subseteq H \subseteq G$. (That includes the two extremes $H = \{\mathbf{1}\}$ and $H = G$.) E.g. below the transition temperature, the ground state of the Heisenberg magnet will be given by (domainwise) aligned configurations of spins. Assuming that the spins point in z-direction, the ground state is invariant under the abelian subgroup $H \subset \mathrm{O}(3)$ containing all rotations around the z-axis. However, invariance under the full rotation group is manifestly broken. Solids represent states where the translation symmetry is fully broken, i.e. all atoms collectively occupy a fixed pattern of spatial positions in space, $H = \{\mathbf{1}\}$, etc.

In spite of the un-deniable existence of solids, magnets, and Bose condensates of definite phase, the notion of a ground state that does not share the full symmetry of the theory may appear paradoxical, or at least 'un-natural'. E.g. even if any particular ground state of the potential of Fig. 7.7, right 'breaks' the rotational symmetry, shouldn't all these states enter the partition sum with equal statistical weight, such that the net outcome of the theory is again fully symmetric?

To understand why symmetry breaking is a 'natural' and observable phenomenon, it is instructive to perform a little gedanken experiment: Imagine the partition function of a classical[7] ferromagnet,

$$\mathcal{Z} = \mathrm{tr}\left(e^{-\beta(F - \mathbf{H}\cdot\sum_i \mathbf{S}_i)}\right),$$

where F is the rotationally invariant part of the energy functional and $\mathbf{H}$ represents a weak external field. (Alternatively, we can think of $\mathbf{H}$ as an *internal* field, caused by an ever so slight structural imperfection of the system.) In the limit of vanishing field strength, the theory becomes manifestly symmetric. Symbolically,

$$\lim_{N\to\infty}\lim_{H\to 0} \mathcal{Z} \longrightarrow \text{rot. sym.},$$

where the limit $N \to \infty$ serves as a mnemonic indicating that we consider systems of macroscopic size. However, keeping in mind that the model ought to describe a real life magnet, the order of limits taken above appears questionable. Since the external perturbation couples to a macroscopic number of spins, a more natural description of an 'almost' symmetric situation would be

$$\lim_{H\to 0}\lim_{N\to\infty} \mathcal{Z} \longrightarrow ?$$

The whole point now is that the two orders of limits lead to different results. In the latter case, for any $\mathbf{H}$, the $N \to \infty$ system is described by an *explicitly* symmetry broken action. No matter

[7] The same argument can be formulated for the quantum magnet.

how small the magnetic field, the energetic cost to rotate $N \to \infty$ spins against the field is too high, i.e. ground state $|\mathbf{S}\rangle$ below the transition temperature will be uniquely aligned, $\mathbf{S}_i \parallel \mathbf{H}$. When we then send $\mathbf{H} \to 0$ in an after step that particular state will remain the observable reference state of the system. Although, formally, a spontaneous thermal fluctuation rotating all spins by the same amount $|\mathbf{S}\rangle \to |g\mathbf{S}\rangle$ would not cost energy, that flucutation can be excluded by entropic reasoning[8]. (Similarly to the fact that one rarely observes water kettles crashing into the kichen wall as a consequence of a concerted thermal fluctuation of the water molecules.)

However, the appearance of non-trivial ground states is just one effect of spontaneous symmetry breakdown. Equally important, residual fluctuations around the ground state lead to the formation of so-called **soft modes** (sometimes also **massless modes**, i.e. field configurations ϕ_q whose action $S[\phi]$ vanishes in the limit of long wavelengths $q \to 0$. Specifically, the soft modes forming on top of a symmetry broken ground state are called **Goldstone modes**. As a rule, the presence of soft modes in a continuum theory has important phenomenological consequences. To understand this point, notice that the general structure of a soft mode action is given by

$$S[\phi] = \sum_{q,i} \phi_q \left[c_1^i |q_i| + c_2^i q_i^2\right] \phi_{-q} + \mathcal{O}(\phi^4, q^3), \tag{7.11}$$

where $c_{1,2}^i$ are coefficients. As exemplified in section 6.1.2, the absence of a constant contribution to the action (i.e. a contribution that does not vanish in the limit $q \to 0$) signals the existence of long-ranged power-law correlations in the system. As we will see shortly, the vanishing of the action in the long wave lengths limit $q \to 0$ further implies that soft modes dominantly contribute to practically all observable system properties.

▷ EXERCISE. Explore the structure of the propagator $F(q) \equiv \langle \phi_q \phi_{-q} \rangle$ of $S[\phi]$ to convince yourself that the arguments then formulated for the specific case of the ϕ^4 theory are of general validity. To this end, notice that for small q,

$$F(q) \sim |q|^{-n},$$

where n is the index of the first non-vanishing coefficient $c_1, c_2, \ldots$. I.e. the propagator is dominated by the smallest q-power appearing in the acition. The power law behaviour of the correlation function implies a homogeneity relation $F(q/\lambda) = \lambda^i F(q)$. Show that this scaling relation entails that the Fourier transform $F(r \equiv |\mathbf{r}|) = \langle \phi(\mathbf{r})\phi(0) \rangle$ obeys the 'scaling law'

$$F(\lambda r) = \lambda^{-d+n} F(r).$$

This in turn implies that the real space correlation function also decays like a power law

$$F(r) \sim r^{-d+n},$$

i.e. in a 'long ranged' manner. Explore the breakdown of the argument for an action with a finite massterm. Convince yourself that in that case, the decay would be exponential, i.e. 'short ranged'.

But what, then, are origin and nature of the soft Goldstone modes caused by the spontaneous breakdown of a symmetry? To understand this point let us consider the action the action of a symmetry group element g on a (symmetry broken) ground state ψ_0 (cf. Fig. 7.8 middle.) By

[8] In chapter XX, we will show that that (overly) simple picture breaks down in dimensions $d \leq 2$.

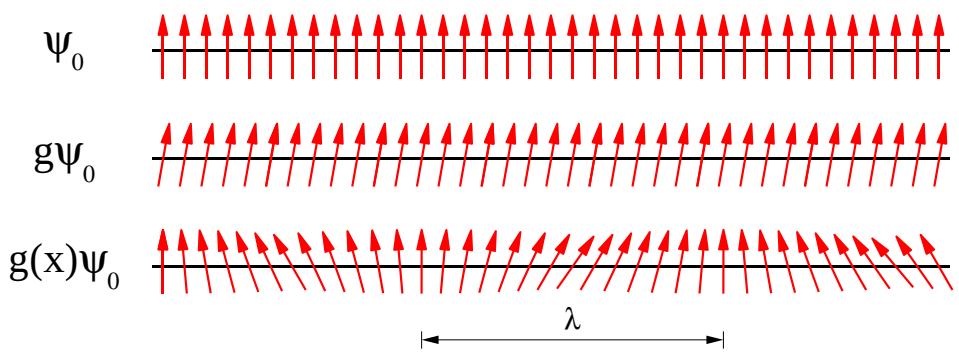

Figure 7.8: The princple beyond Goldstone mode formation. Up: a ground state. Middle: A *globally* transformed state (also a ground state). Bottom: A *locally* transformed state whose action depends on the fluctuation rate.

definition, $S[g\psi_0] = S[\psi_0] =$ extr. still assumes its extremal value. Assuming that g is close to the group identity, we write $g = \exp\left(\sum_a \phi_a T_a\right)$, where the $\{T_a\}$ are generators living in the Lie algebra of the group and ϕ_a are some expansion coefficients[9]. Expressing fluctuations around ψ_0 in terms of the 'coordinates' ϕ_a, we conclude that the action $S[\phi] = 0$. However, if we promote the global transformation to a transformation with a weakly fluctuating spatial profile, $g \to g(x)$, $\psi_0 \to g(x)\psi_0$ (cf. Fig. 7.8 bottom) a price will have to be paid. That is, for a spatially fluctuating coordinate profile $\{\phi_a(x)\}$, $S[\phi] \neq 0$, where the energy cost depends inversely on the fluctuation rate λ of the field ϕ. The expansion of S in terms of gradients of ϕ is thus bound to lead to a soft mode action of the type (7.11).

In view of their physical importance, an important question to ask is how many independent of these soft modes exist. The answer can be straightforwardly given on the basis of the geometric picture developed above: Suppose our symmetry group G has dimension r, i.e. its Lie algebra is spanned by r linearly independent generators $T_a, a = 1, \ldots, r$. If the subgroup $H \subset G$ has dimension $s < r$, s of these generators can be chosen so as to leave the ground state invariant. On the other hand, the remaining $p \equiv r - s$ generators inevitably create Goldstone modes. In the language of group theory, these generators span the coset space G/H. E.g. for the ferromagnet, $H = \mathrm{O}(2)$ is the one-dimensional subgroup of rotations around the quantization axis (e.g. the z-axis). Since the rotation group has dimension 3, there must be two independent Goldstone modes. These can be generated by the action of the rotation, or angular momentum generators $J_{x,y}$ acting on the z-aligned ground state. The coset space $\mathrm{O}(3)/\mathrm{O}(2)$ can be shown to be isomorphic to the two-sphere, i.e. the sphere traced out by the spins as they fluctuate around the ground state.

One may ask why we bothered to formulate these things in the abstract language of Lie groups and generators, etc. The reason is that the connection between the coordinates parameterizing the Goldstone modes $\phi_i, i = 1, \ldots, p$, residual 'massive modes' $\kappa_j, j = 1, \ldots, n - p$, and the original coordinates $\psi_i, i = 1, \ldots, n$ of the problem, respectively, is usually nonlinear and sometimes not even very transparent. With problems more complex then the three prototypical examples mentioned above, it is usually well invested time to first develop a good understanding of the geometry of the problem before specific coordinate systems are introduced.

After these general considerations it is time to get back to the Bose system and to explore

[9]Here we have used that, for any reasonable model, G will be a Lie-group, i.e. a group with the structure of a differentiable manifold.

the physical consequences of Goldstone mode formation on a concrete example!

7.2.3 Superfluidity[10]

Turning back to the action of the Bose clean bose gas below condensation ($\mu > 0$),

$$S[\bar{\psi},\psi] = \int_0^\beta d\tau \int d^d r \left[\bar{\psi}(\mathbf{r},\tau)\left(\partial_\tau - \frac{\partial^2}{2m} - \mu\right)\psi(\mathbf{r},\tau) + \frac{g}{2}(\bar{\psi}(\mathbf{r},\tau)\psi(\mathbf{r},\tau))^2\right],$$

we chose to expand the theory around the particular ground state $\bar{\psi}_{0,\mathrm{mf}} = \psi_{0,\mathrm{mf}} = (\mu L^d/g)^{1/2} = \gamma$. (Of course, any other state lying in the mexican hat minimum of the action would do just as good.) Notice that the quantum ground state corresponding to the configuration $\psi_{0,\mathrm{mf}}$ is unconventional in the sense that it cannot have a definite particle number. The reason is that according to the correspondence $\psi \leftrightarrow a$ between coherent states and operators, respectively, a non-vanishing *functional* expectation value of ψ_0 is equivalent to a non-vanishing *quantum* expectation value $\langle a_0\rangle$. Assuming that at low temperatures, the thermal average $\langle\ldots\rangle$ will project onto the ground state $|\Omega\rangle$, we conclude that $\langle\Omega|a_0|\Omega\rangle \neq 0$, i.e. $|\Omega\rangle$ cannot be a state with a definite number of particles[11].

The symmetry group U(1) acts on this state by multiplication, $\psi_{0,\mathrm{mf}} \to e^{i\phi}\psi_{0,\mathrm{mf}}$ and $\bar{\psi}_{0,\mathrm{mf}} \to e^{-i\phi}\bar{\psi}_{0,\mathrm{mf}}$. Knowing that the action of a weakly modulated fielf $\phi(\mathbf{r},\tau)$ will be massless, we introduce coordinates

$$\psi(\mathbf{r},\tau) = [\rho_0 + \delta\rho(\mathbf{r},\tau)]^{1/2} e^{i\phi(\mathbf{r},\tau)},$$
$$\bar{\psi}(\mathbf{r},\tau) = [\rho_0 + \delta\rho(\mathbf{r},\tau)]^{1/2} e^{-i\phi(\mathbf{r},\tau)},$$

where $\rho_0 \equiv \gamma^2 = \bar{\psi}_{0,\mathrm{mf}}\psi_{0,\mathrm{mf}}$ is the condensate density. Evidently, the variable $\delta\rho$ parameterizes deviations of the field $\psi(\mathbf{r},\tau)$ off the extremum. These excursions are energetically costly, i.e. $\delta\rho$ will turn out to be a massive mode. Also notice that the transformation of coordinates $(\bar{\psi},\psi) \to (\delta\rho,\phi)$, viewed as a change of integration variables, has Jacobian unity.

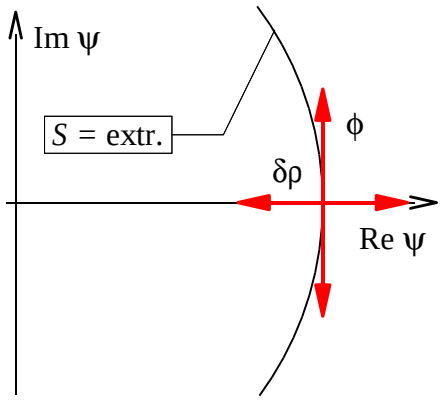

▷ INFO. As we are dealing with a (functional) integral, there is a lot of freedom as to the choice of integration parameters. (I.e. unlike in the operator formulation, there is no a priori constraint for a transform to be 'canonical'.) However, physically meaningful changes of representation will usually be **canonical transformations**, in the sense that the corresponding

[10] The theory of the weakly interacting superfluid to be discussed below was originally devised by Bogoliubov, then in the language of second quantisation (see N. N. Bogoliubov, Izv. Akad. Nauk SSSR, Ser. Fiz. **11**, 77 (1947).)

[11] However, as usual with *grand* canonical descriptions, in the thermodynamic limit, the *relative* uncertainty in the number of particles, $(\langle\hat{N}\rangle^2 - \langle\hat{N}^2\rangle)/\langle\hat{N}\rangle^2$ will become vanishingly small.

transformations of operators would conserve the commutation relations. Indeed, the transformation above meets this condition, as can be seen by inspection of the *operator* transform

$$a(\mathbf{x}) \equiv \hat{\rho}(\mathbf{x})^{1/2}\, e^{i\hat{\phi}(\mathbf{x})},$$
$$a^\dagger(\mathbf{x}) \equiv e^{-i\hat{\phi}(\mathbf{x})}\, \hat{\rho}(\mathbf{x})^{1/2},$$

where the rhs defines the operator pair $(\hat{\rho}, \hat{\phi})$. To verify the canoticity of this transformation, let us presume canonical relations

$$[\hat{\rho}(\mathbf{x}), \hat{\phi}(\mathbf{x}')] = i\delta(x - x'),$$
$$[\hat{\rho}(\mathbf{x}), \hat{\rho}(\mathbf{x}')] = [\hat{\phi}(\mathbf{x}), \hat{\phi}(\mathbf{x}')] = 0,$$

and check the consistency of that assumption. Since for $x \neq x'$ all operators trivially commute, we may drop the position index and verify that

$$[a, a^\dagger] = \left[\hat{\rho}^{1/2}\, e^{i\hat{\phi}}, e^{-i\hat{\phi}}\, \hat{\rho}^{1/2}\right] = \hat{\rho} - e^{-i\hat{\phi}}\hat{\rho}e^{i\hat{\phi}} =$$
$$= \hat{\rho} - e^{-i[\hat{\phi}, \cdot\,]}\hat{\rho} = \hat{\rho} - \hat{\rho} + i[\hat{\phi}, \hat{\rho}] - \frac{1}{2}[\hat{\phi}, [\hat{\phi}, \hat{\rho}]] + \ldots = 1,$$

as required. (In the last line we have used the general operator identity $e^{\hat{A}}\hat{B}e^{-\hat{A}} = e^{[\hat{A}, \cdot\,]}\hat{B}$.)

We next substitute the density-phase relation into the action and expand to second order around the reference mean field. Ignoring gradients acting on the density field (in comparison with the 'potential' cost of these fluctuations), we obtain

$$S[\delta\rho, \phi] \approx \int_0^\beta d\tau \int d^d r \left[i\rho\partial_\tau\phi + \frac{\rho_0}{2m}(\partial\phi)^2 - \mu\rho\frac{g\rho_0^2}{2}\right]. \tag{7.12}$$

The first term of the action has the typical structure 'momentum $\times\, \partial_\tau$(coordinate)' indicative of a canonically conjugate pair of degrees of freedom. The second term measures the energy cost of spatially varying phase flucutations. However, notice that fluctuations with $\phi(\mathbf{r}, \tau) =$ const. do not cost energy – ϕ is a Goldstone mode. Finally, the third and fourth term describes the energy cost of massive fluctuations leaving the potential minimum.

Eq. (7.12) represents the Hamiltonian version of the action of the system, i.e. an action comprising coordinates ϕ and momenta $\delta\rho$. Gaussian integration over the field $\delta\rho$ leads us to the Lagrangian action (exercise):

$$S[\phi] \approx \frac{1}{2}\int_0^\beta d\tau \int d^d r \left[\frac{1}{g}(\partial_\tau\phi)^2 + \frac{\rho_0}{m}(\partial\phi)^2\right]. \tag{7.13}$$

Comparison with (1.4) identifies this action as old accquaintance, i.e. the d-dimensional oscillator action. Transcribing from our results of chapter 2 (see, e.g. Eq. (2.5)), we find that the energy $\omega_{\mathbf{k}}$ carried by elementary excitations of the system

$$\omega_{\mathbf{k}} = |\mathbf{k}|\frac{\rho_0}{mg} \tag{7.14}$$

scales linearly with momentum.

Let us now discuss the phenomenological implications of these results. The actions (7.12) and (7.13) describe the phenomenon of superfluidity. To make the connection between the fundamental degree of freedom of a superfluid system, the **supercurrent**, and the phase field explicit, let us consider the quantum mechanical current operator

$$\hat{\mathbf{j}}(\mathbf{x},\tau) = \frac{i}{2m}\left[\partial_{\mathbf{x}} a^\dagger(\mathbf{x},\tau) a(\mathbf{x},\tau) - a^\dagger(\mathbf{x},\tau)\partial_{\mathbf{x}} a(\mathbf{x},\tau)\right] \stackrel{\text{fun.int}}{\longrightarrow}$$
$$\longrightarrow \frac{i}{2m}\left[\partial_{\mathbf{x}} \bar{\psi}(\mathbf{x},\tau)\psi(\mathbf{x},\tau) - \bar{\psi}(\mathbf{x},\tau)\partial_{\mathbf{x}}\psi(\mathbf{x},\tau)\right] \approx \frac{\rho_0}{m}\partial_{\mathbf{x}}\phi(\mathbf{x},\tau), \quad (7.15)$$

where the the arrow indicates the functional integral correspondence of the operator description and we have neglected all contributions coming from spatial fluctuations of the density profile. (Indeed, these – massive – fluctuations describe the 'normal' contribution to the current flow.)

▷ INFO. **Superfluidity** is one of the most bizzare and fascinating phenomena displayed by condensed matter systems. Experimentally, the most straightforward access to superfluid states of matter is provided by the Helium liquids. Representative for many other effects displayed by superfluid states of Helium, we mention the capability of *He*-films to flow *up* the walls of a vessel (if the reward is that on the outer side of the container a low lying bassin can be reached) or to effortlessly propagate through porous media no normal fluid might possibly penetrate. Readers interested in learning more on the phenomenology of superfluid states of matter – a subject not for the present text to cover – are referred to, e.g. Ref. XX.

———————————————————————

So, the gradient of the phase variable is a measure of the current flow in the system. The behaviour of that degree of freedom can be understood by inspection of the stationary phase equations – alias, the Hamilton or Lagrange equations of motion – of Eq. (7.12) or (7.13). Going for the Hamiltonian option, we obtain (exercise)

$$\begin{aligned} i\partial_\tau \phi &= -g\delta\rho + \mu, \\ i\partial_\tau \delta\rho &= \frac{\rho_0}{m}\partial^2\phi = \boldsymbol{\partial}\cdot\mathbf{j}. \end{aligned}$$

The second of these equations represents (the imaginary time version) of a continuity equation. A current flow with non-vanishing divergence is accompanied by dynamical distortions in the density profile. The first equation tells us that the system adjusts to spatial fluctuations of the density by a dynamical phase fluctuation. The most remarkable feature of these equations is that they possess steady state solutions with non-vanishing current flow. Setting $\partial_\tau\phi = \partial_\tau\delta\rho = 0$, we obtain the conditions $\delta\rho = 0$ and $\boldsymbol{\partial}\cdot\mathbf{j} = 0$, i.e. below condensation, a configuration with uniform density profile can support a *steady state* divergenceless (super)current. Notice that a 'mass term' in the ϕ action would spoil this property, i.e. within our present approach, the phenomenon of supercurrent flow is intimately linked to the Goldstone mode character of the ϕ field.

▷ EXERCISE. Add a ficticious mass term to the ϕ-action and explore its consequences. How do the features discussed above present themselves in the Lagrange picture?

It is very instructive to interpret the phenomenology of supercurrent flow from a different, more microscopic perspective. What prevents steady state current flow in normal environments is the mechanism of **energy dissipation**. I.e. particles constituting the current flow scatter off imperfections inside the system thereby converting part of their energy into the creation of of elemenatary excitations. (Macroscopically, the conversion of kinetic energy into the creation of excitations manifests itself as heat production.) Apparently, this mechanism is incactivated in superfluid states of matter, i.e. the current flow is *dissipationless*.

How can the dissipative loss of energy be avoided. Trivially, no energy will be transmitted if there are no elementary excitations to create. Which, in reality means that the excitations of the system are energetically high-lying such that the kinetic energy stored in the current-carrying particles does not suffice to create them. But this is not the situtation we encouter in the superfluid! As we saw above, there is no energy gap separating the excitations of the system from the ground state. The dispersion $\omega(\mathbf{k})$ rather vanishes linearly as $\mathbf{k} \to 0$. However, there is an ingenuous little argument due to Landau showing that a linear excitation spectrum indeed suffices to stabilize dissipationless transport:

▷ INFO. Consider the flow of some fluid through a pipe (cf. Fig. 7.9 top left) . For definiteness, we assume that the flow occurs at uniform velocity $\mathbf{V}$. Assuming that the mass (of a certain portion of the fluid) equals M, the current carries a total kinetic energy $E_1 = M\mathbf{V}^2/2$. Now, suppose we view the situation from the point of view of the fluid, i.e. we perform a Galilei transformation into its own rest frame (top right.) From the point of view of the fluid, the walls of the pipe appear as moving with velocity $-\mathbf{V}$. Now, suppose that frictional forces between fluid an wall have left to the creation of an elementary excitation of momentum $\mathbf{p}$ and energy $\epsilon(\mathbf{p})$. I.e. the fluid is no longer at rest but carries kinetic energy. After a Galilei transformation back to the laboratory frame we find that the energy of the fluid after the creation of the excitation is given by (excercise)

$$E_2 = \frac{M\mathbf{V}^2}{2} + \mathbf{p}\cdot\mathbf{V} + \epsilon(\mathbf{p}).$$

Now, since the all energy needed to manufacture the excitation must have been provided by the liquid itself, energy conservation requires that $E_1 = E_2$, or $-\mathbf{p}\cdot\mathbf{V} = \epsilon(\mathbf{p})$. Since $\mathbf{p}\cdot\mathbf{V} > -|\mathbf{p}||\mathbf{V}|$, this condition can only be met if

$$|\mathbf{p}||\mathbf{V}| > \epsilon(\mathbf{p}). \tag{7.16}$$

System with a 'normal' gapless dispersion, $\epsilon(\mathbf{p}) \sim \mathbf{p}^2$ are categorically compatible with this energy-balance relation, i.e. no matter how small $|\mathbf{V}|$, quasi-particles of low momentum can always be excited. However, both, gapped dispersions $\epsilon(\mathbf{p}) \stackrel{\mathbf{p}\to 0}{\longrightarrow}$ const., *and* linear dispersions are incompatible with (7.16) if $\mathbf{V}$ becomes smaller than a certain **critical velocity** V_*. Specifically for a linear dispersion $\epsilon(\mathbf{p}) = v|\mathbf{p}|$, the critical velocity is given by $V_* = v$. For currents slower than that, the flow is dissipationless.

———————————————————————

Let us conclude our preliminary discussion of the Bose gas by a very important remark. Eqs. (7.12) and (7.13) suggest that we have managed to describe the long range behaviour of the condensed system in terms of a free Gaussian theory. That, however, is not quite so, a fact concealed by the notation used above. Indeed, we must not forget that ϕ is a phase field, defined only modulo 2π. (In Eqs. (7.12) and (7.13) this condition is

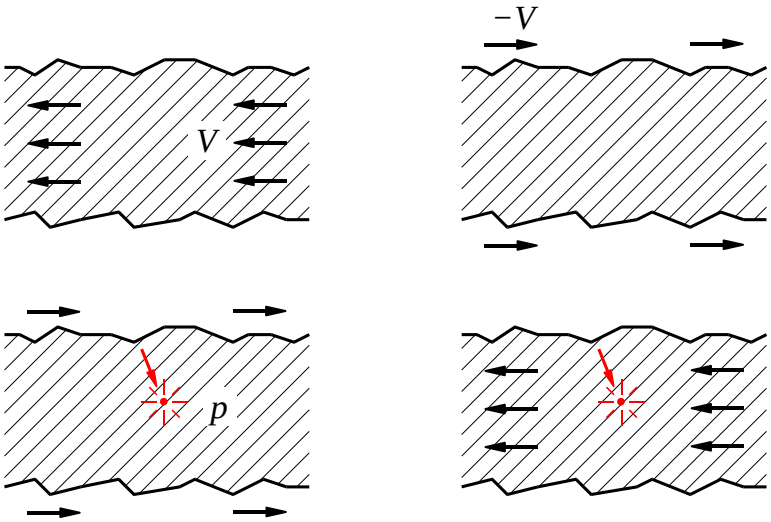

Figure 7.9: Up left: Flow of a fluid through a rough pipe. Up right: The same viewed from the rest frame of the fluid. Botom left: Dissipative creation of a (quasi-particle) excitation. Bottom right: The same viewed from the laboratory frame.

implicitly understood. At this point, it is perhaps worth to re-iterate that when dealing with Goldstone modes it is important to keep the underlying geometry in mind and not too tightly focus on a specific coordinate representation.) The fact that ϕ is defined only up to integer multiples of 2π manifests itself in the formation of the most interesting excitations of the superfluid: **vortices**, i.e. phase configurations $\phi(\mathbf{x}, \tau)$ that change by a multiple of 2π as one moves around a certain reference coordinate, the vortex center. Existing in parallel to the phonon-like excitations discussed above, these excitations lead to a wealth of observable phenomena, to be discussed in more detail in chapter XX. However, for the moment let us turn to the discussion of another prominent superfluid, the condensate of Cooper pairs, more generally known as the superconductor:

7.3 Superconductivity

The electrical resistivity of many metals and alloys drops suddenly to zero when the specimen is cooled to a sufficiently low temperature. This phenomenon, which goes by the name **superconductivity**, was first observed by Kammerlingh Onnes in Leiden in 1911, three years after he first liquefied Helium.[12] Equally striking, a superconductor cooled below its transition temperature in a magnetic field expels all magnetic flux from

[12] Kammerlingh Onnes 1853-1926 (left, photographed with van der Waals): 1913 Nobel Laureate in Physics for his investigations on the properties of matter at low temperatures which led, *inter alia* to the production of liquid helium.

its interior. This phenomenon of *perfect diamagnetism* is known as the **Meissner effect** and is characteristic of superconductivity.

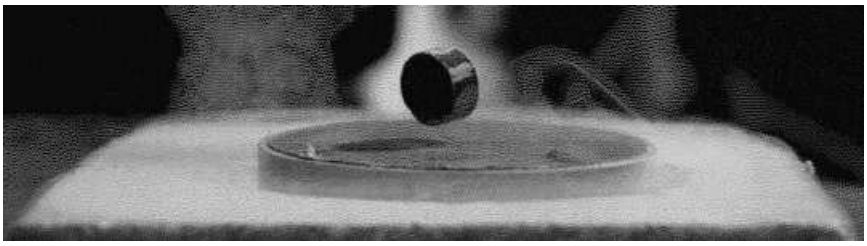

Figure 7.10: The levitation of a magnet above a (high temperature) superconductor due to the expulsion of magnetic flux.

Meissner effect and dissipationless transport are but two of a plethora of phenomena accompanying superconductivity. In fact, it is not even appropriate to speak about 'superconductivity' as a single term: Since the discvovery of the high-temperature cuprate superconductors in 1986 it has become evident that the physical mechanisms responsible for high-temperature and conventional superconductivity, respectively, must be strikingly different.

Along with the introduction of more advanced theoretical machinery, a variety of superconductor phenomena will be discussed in the remainder of this text. The present, introductory section is devoted to the formulation of the theoretical foundations of BCS superconductivity, all cast into the language of the field integral. Although the presentation should be reasonably self contained, the focus clearly is on the theoretical aspects of superconductivity, i.e. depending on temper and taste, some readers may find it useful to motivate the encounter with the formalism developed below by first (re)familiarizing themselves with the basic phenomenology of the BCS superconductor. (Representative for several pedagogical introductions, we mention the textbook[**?**].)

7.3.1 Basic Concepts of BCS Theory

This section is devoted to the introduction of basic elements of the theory of Bardeen-Cooper-Schrieffer- or BCS-superconductivity. We will not yet employ the field integral but rather try to develop some basic physical insight into the nature of the problem. Superconductivity is a complex phenomenon with many different aspects to it. Our approach will thus resemble that of the 'blind man's encounter with the elephant'[13] : Approaching the problem from varying perspectives, the next sections will highlight different aspects of superconductor physics. For readers meeting with these phenomena for the first time, the connection between the different fragments will perhaps remain somewhat opaque. However, eventually, when we employ the formalism of the field integral, all pieces will click into place and a more comprehensive pictuce of the superconductor will emerge.

[13] A famous parabola of Indiam mythology compares the search for ultimate truth to the encounter of a blind man and an elephant. In the beginning, randomly touching tail, ears, trunk, etc. the man will declare that he has met with an utterly incoherent phenomenon. However, persistent approach from varying perspectives will eventually show to him that this is not so.

The superconducting state is an ordered state of the conduction electrons of the metal, caused by the presence of a residual attractive interaction at the Fermi surface. The nature and origin of the ordering was explained by Bardeen, Cooper and Schrieffer[14]. At low temperatures, an attractive pairwise interaction can induce an instability of the electron gas towards the formation of bound pairs of time-reversed states $\mathbf{k}\uparrow$ and $-\mathbf{k}\downarrow$ in the vicinity of the Fermi surface.

▷ INFO. Where does an **attractive interaction** between equally charged particles come from? In conventional (BCS) superconductors, attractive correlations between electrons are due to the exchange of lattice vibrations, or phonons: The motion of an electron through a metal causes a dynamic local distortion of the ionic crystal (cf. Fig. 7.11.) Importantly, that process is governed by two totally different time scales: For an electron it takes a time $\sim E_F^{-1}$ to traverse the immediate vicinity of a lattice ion and to distort it out of its equilibrium position into a configuration that both particles find energetically beneficial. However, once the ion has been distorted it needs a time of $\mathcal{O}(\omega_D^{-1} \gg E_F^{-1})$ to relax back into its equilibrium position. Here, ω_D is the Debye frequency, i.e. the characteristic scale for phononic excitations. That means that long after elctron no. 1 is gone, a second electron may benefit from the distorted ion potential. The net effect of this retardation mechanism in an attractive interaction between the two electrons. Since the maximum energy scale of ionic excitations is given by the Debye frequency, the range of the interaction is limited to energies $\sim \omega_D$ around the Fermi surface. (For a quantitative formulation, see the problem set.) As regards the high temperature superconductors, the mechanism of pair formation is largely unknown.

Being made up of two fermions, the electron-electron bound states, known as **Cooper pairs** behave as bosons. At low temperatures, these bosonic degrees of freedom form a condensate which is responsible for the remarkable properties of superconductors such as perfect diamagnetism.

To understand the tendency to pair formation, consider the diagram shown in Fig. 7.12. The region of attractive correlation is indicated as a shaded ring of width $\sim 2\omega_D$. Now, condsider a two-electron state $|\mathbf{k}\uparrow, -\mathbf{k}\downarrow\rangle$ formed by two particles of (near) opposite momentum. Momentum conserving scattering of the constituting particle may lead to the formation of a new sate $|(\mathbf{k}+\mathbf{p})\uparrow, -(\mathbf{k}+\mathbf{p})\downarrow\rangle \equiv |\mathbf{k}'\uparrow, -\mathbf{k}'\downarrow\rangle$ of the same, opposite-momentum structure. Importantly, the momentum transfer $\mathbf{p}$ may trace out a large set of values of $\mathcal{O}(k_F^{d-1}\omega_D/v_F)$ without violating the condition that the final states be close to the Fermi momentum. (E.g. if the initial state hadn't been formed by opposite mo-

[14] J. Bardeen, L. N. Cooper and J. R. Schrieffer, Phys. Rev. **106**, 162 (1957); **108**, 1175 (1957).

John Bardeen 1908-1991 (left), Leon N. Cooper 1930- (centre), and J. Robert Schrieffer 1931- (right): 1972 Nobel Laureate in Physics for their jointly developed theory of superconductivity. (Bardeen was also recipient of the 1956 Nobel Laureate in Physics for his research on semiconductors and discovery of the transistor effect.)

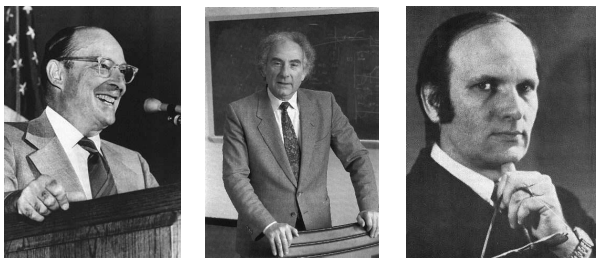

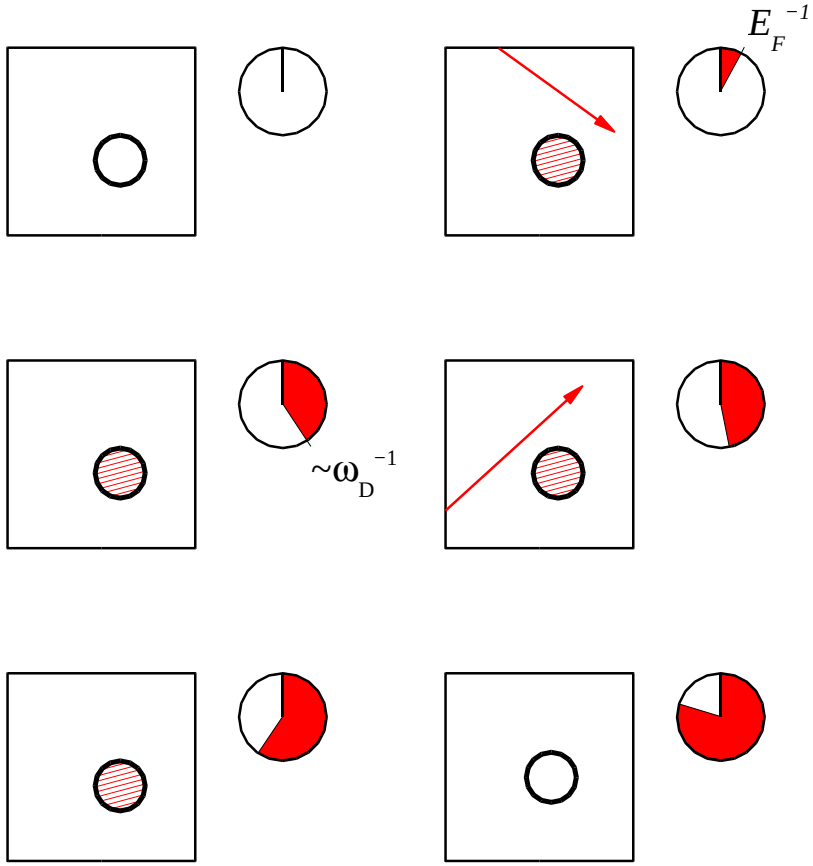

Figure 7.11: Cartoon on the origin of the attractive electron-phonon interaction. Top left: An ion in a solid. Top right: A passing-by electron needs a time of $\mathcal{O}(E_F^{-1})$ to traverse the vicinity of the ion. As a result of the electron-ion interaction, the latter gets excited into a state the two interaction partners find favourable. Middle left: Long ($\mathcal{O}(\omega_D)$) after the electron has left, the ion still resides in its non-equilibrium configuration. Middle right: A second conduction electron may benefit from this state, thereby being effectively *attracted* by the space-time trajectory of the original electron. Bottom left and right: Only after the ion has been left alone for a time $> \omega_D^{-1}$ it relaxes into its equilibrium state.

mentum particles, the phase space for scattering processes would be greatly diminished.) Remembering our previous discussion of the RPA approximation, we recognize a familiar mechanism: An a priori weak interaction may grade up its relevance by conspiring with a large phase space volume.

To explore this mechansism in quantitative terms, we we will adopt a simplified model defined by the Hamiltonian

$$\boxed{\hat{H} = \sum_{\mathbf{k}\sigma} \epsilon_{\mathbf{k}} \hat{n}_{\mathbf{k}\sigma} - \frac{g}{L^d} \sum_{kk'} c^\dagger_{\mathbf{k}+\mathbf{q}\uparrow} c^\dagger_{-\mathbf{k}\downarrow} c_{-\mathbf{k}'+\mathbf{q}\downarrow} c_{\mathbf{k}'\uparrow},} \tag{7.17}$$

where g is a positive constant. The Hamiltonian $\hat{H}$ should be interpreted as an effective model Hamiltonian describing the physics of a thin layer of width $\mathcal{O}(\omega_D)$ centered around

the Fermi surface (i.e. the region where a net attractive interaction prevails.) Although a more realistic model of attraction would involve a complicated momentum dependent interaction such as the one obtained from the consideration of the electron-phonon interaction, the simple constant pairing interaction captures the essential physics. More importantly, to simplify our discussion, we will take the electrons to be otherwise non-interacting. In fact, the presence of a repulsive Coulomb interaction of the electrons plays a crucial role in the controlling properties of the superconductor, a point to which we will return later. After the trio who first explored its phenomenology, the model Hamiltonian (7.17) is commonly referred to as the **BCS-Hamiltonian**.

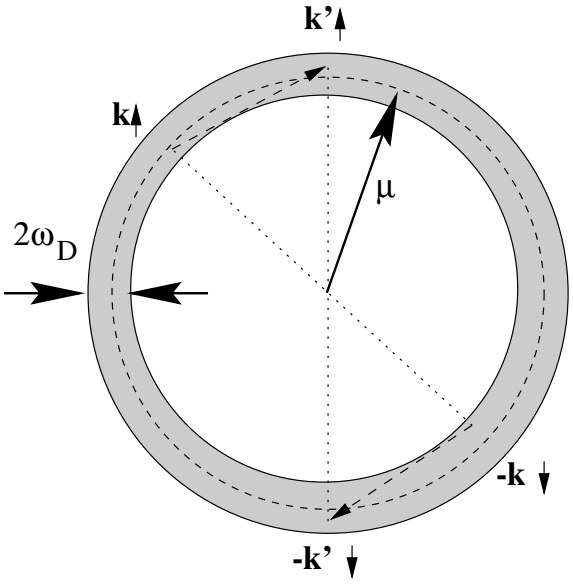

Figure 7.12: Schematic diagram showing the Fermi surface of the electron gas. The attractive interaction mediated by the exchange of phonons allows electrons within the Debye frequency ω_D of the Fermi surface to pair.

What the preliminary discussion above does not tell us is what is so special about an *attractive* interaction. Nor, what the phenomenological consequences of the Fermi surface pair scattering are. In the following we will address these latter questions from a number of different angles. The result will be a heuristic picture of the superconductor that will guide us in constructing the more rigorous field integral approach below. Mainly for illustrative purposes, we begin our discussion with a brief perturbative analysis of Cooper pair scattering. Proceeding in close analogy to the previous discussion of the RPA, we will discover the dramatic consequences of an *attractive* interaction on the ground state of the system. (However, this part of the discussion will be an optional (if instructive) element of the development of the theory. Readers who did not yet go through section 6.3 may skip this part of the discussion and proceed directly to section 7.3.3 where the mean field picture of the superconductor is developed.)

7.3.2 Cooper Instability

To explore the fate of a Cooper pair under multiple scattering, we consider the four point correlation function

$$C(\mathbf{q},\tau) = \frac{1}{L^{2d}} \sum_{\mathbf{k},\mathbf{k}'} \left\langle \bar{\psi}_{\mathbf{k}+\mathbf{q}\uparrow}(\tau)\bar{\psi}_{-\mathbf{k}\downarrow}(\tau)\ \psi_{\mathbf{k}'+\mathbf{q}\downarrow}(0)\psi_{-\mathbf{k}'\uparrow}(0)\right\rangle .$$

This correlation function describes the amplitude of Cooper pair propagation $|\mathbf{k}+\mathbf{q}\uparrow, -\mathbf{k}\downarrow\rangle \to |\mathbf{k}'+\mathbf{q}\uparrow, -\mathbf{k}'\downarrow\rangle$ in imaginary[15] time τ and averaged over all initial and final particle momenta[16]. As usual with problems whose solution can only depend on time *differences*, it is convenient to switch to a frequency representation. With

$$C(q) \equiv C(\mathbf{q},\omega_m) = T\int_0^\beta d\tau\, e^{-i\omega_m\tau} C(\mathbf{q},\tau),$$

where ω_m is bosonic, it is straightforward to verify that

$$C(q) = \frac{T^2}{L^{2d}} \sum_{k,k'} \left\langle \bar{\psi}_{k+q\uparrow}\bar{\psi}_{-k\downarrow}\ \psi_{k'+q\downarrow}\psi_{-k'\uparrow}\right\rangle .$$

To calculate the correlation function we employ the perturbative methods introduced in section 6.3. As with our previous analysis of the RPA, the density of the electron gas will play the role of a large parameter, i.e. what we need to do is expand the correlation function in pair interaction vertices g and keep only those terms to the expansion that come with one free momentum summation per interaction. Summation over these contributions leads to the ladder diagram series shown in Fig. 7.13 where the momentum labels of the Green functions are not explicated for clarity. According to the definition of the correlation function, the two Green function entering the ladder carry momentum $p+q$ and $-p$, respectively. Momentum conservation then implies, that the Green functions defining each consequtive rung of the ladder, too, carry near opposite momenta $p'+q$ and $-p'$, where p' is a summation variable.

▷ EXERCISE. Convince yourself that the ladder diagrams shown in the figure are the only diagrams that contain one free momentum summation per interaction vertex.

As in our previous discussion in section 6.3.2, the center part of the correlation function is described by a vertex Γ. The diagrammatic definition of that object is shown in the bottom line of the figure. Translating to formulae we obtain the Cooper version of a Bethe-Salpeter equation

$$\Gamma_q = g + \frac{gT}{L^d}\sum_p G_{p+q}G_{-p}\Gamma_q,$$

[15] As with our previously discussed applications of the path integral, information about the real time dynamics of the pair can be extracted from analytical continuation $\tau \to it$.

[16] Notice that the 'center of mass' momentum $\mathbf{q}$ of a pair $\frac{1}{L^d}\sum_{\mathbf{k}} |\mathbf{k}+\mathbf{q}\uparrow, -\mathbf{k}\downarrow\rangle$ can be interpreted as a variable Fourier conjugate to the position of the pair's center (exercise: show this by inverse Fourier transform). An equivalent interpretation of the correlation function C thus is that it describes the wandering of Cooper pair centers under the influence of scattering.

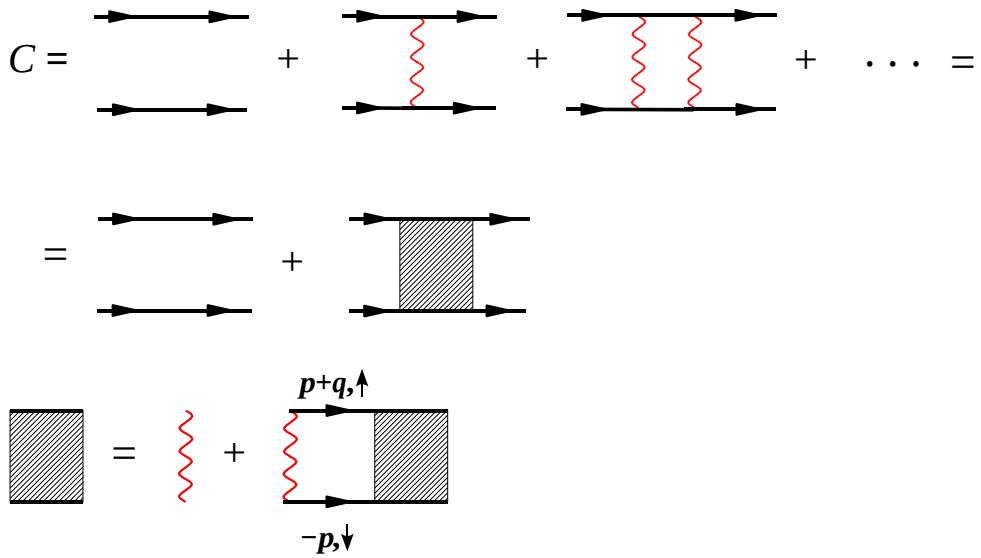

Figure 7.13: Two particle propagator in the presence of an (attractive) interaction. The two Green function lines defining each rung of the ladder carry momentum $p+q$ and $-p$, respectively, where p is a free summation variable. The vertex of the propagator is defined through the second line. It obeys the Bethe-Salpeter equation definied in the third line.

where we have anticipated that a solution independent of the intermediate momenta can be found. Solving this equation for Γ_q, we arrive at an equation structurally similar to (6.46):

$$\Gamma_q = \frac{g}{1 - \frac{gT}{L^d}\sum_p G_{p+q}G_{-p}}. \tag{7.18}$$

We next need to compute the sum over the running index $p = (\mathbf{p}, \omega_n)$. The frequency part of the summation has been done as example no. xx on page xx of the problem set of the previous chapter:

$$\begin{aligned}\frac{T}{L^d}\sum_p G_{p+q}G_{-p} &= \frac{1}{L^d}\sum_{\mathbf{p}} T\sum_n G_{\mathbf{p}+\mathbf{q},\omega_n+\omega_m}G_{-\mathbf{p},-\omega_n} = \\ &= \frac{1}{L^d}\sum_{\mathbf{p}} \frac{1 - f_{\rm f}(\xi_{\mathbf{p}+\mathbf{q}}) - f_{\rm f}(\xi_{-\mathbf{p}})}{i\omega_m + \xi_{\mathbf{p}+\mathbf{q}} + \xi_{-\mathbf{p}}} = \\ &= \frac{1}{L^d}\sum_{\mathbf{p}} \left(\frac{1}{2} - f_{\rm f}(\xi_{\mathbf{p}})\right)\left(\frac{1}{i\omega_m + \xi_{\mathbf{p}+\mathbf{q}} + \xi_{-\mathbf{p}}} + (\mathbf{q} \leftrightarrow -\mathbf{q})\right),\end{aligned}$$

where in the left line we have used the symmetry of the energy arguments, $\xi_{\mathbf{p}} = \xi_{-\mathbf{p}}$. Doing the summation for finite $\mathbf{q}$ is left as an instructive exercise in Fermi-surface integration (see the problem set.) However, for the sake of our present argument, it will be sufficient to perform the sum for zero external momentum $q = (0, 0)$ (i.e. we probe the fate of spatially homogeneous and static pair configurations.) Using the identity $\sum_{\mathbf{p}} F(\epsilon_{\mathbf{p}}) = \int d\epsilon \rho(\epsilon) F(\epsilon)$ to replace the momentum sum by an energy integral and remembering that the pairing

interaction is limited to a thin shell around the Fermi surface we then obtain

$$\frac{T}{L^d}\sum_p G_p G_{-p} = \int_{-\omega_D}^{\omega_D} d\epsilon\, \rho(\epsilon)\frac{1-2f_{\rm f}(\epsilon)}{2\epsilon} \simeq \rho\int_T^{\omega_D}\frac{d\epsilon}{\epsilon} = \rho\ln\left(\frac{\omega_D}{T}\right), \qquad (7.19)$$

where $\rho \equiv \rho(0)$ is the Fermi surface density of states and we have used that at energies $\epsilon \sim T$, the $1/\epsilon$ singularity of the integrand is cut off by the Fermi distribution function. Susbstitution of this result back into the expression for the vertex leads to

$$\Gamma_{0,0} \simeq \frac{g}{1-g\rho\ln\left(\frac{\omega_D}{T}\right)}.$$

From this result, we can read off essential elements of the transition to the superconducting state:

- ▷ We first note that the interaction constant appears in combination with the density of states. I.e. even an interaction of weak strength can lead to sizeable effects if only the density of states is large enough. From our previous qualitative discussion it should be clear that the scaling factor ρ simply measures the number of final states accessible to the scattering mechanism depicted in Fig. 7.12.

- ▷ The net strength of the Cooper pair correlation grows upon increasing the energetic range ω_D of the attractive force or, equivalently, lowering the temperature. Obviously, something drastic happens as $g\rho\ln\left(\frac{2\omega_D}{T}\right) = 1$ or

  $$T = T_c \equiv 2\omega_D \exp\left(-\frac{1}{g\rho}\right).$$

  At this **critical temperature**, the vertex develops a singularity. Since the vertex and the correlation function are related by multiplication by a number of (non-singular) Green functions, the same is true for the correlation function itself.

- ▷ As we will see momentarily, T_c marks the transition temperature to the superconducting state. At and below T_c a perturbative approach based on the Fermi sea of the non-interacting system as a reference state breaks down. The Cooper instability rather signals that we will have to look for an alternative ground state or 'mean field' viz. one that accounts for the strong binding of Cooper pairs.

In the next section, we will explore the nature of this state from a somewhat altered perspective.

7.3.3 Mean-Field Theory of Superconductivity

The discussion of the previous section suggests that at the transition temperature the system devlopes an instability towards pair binding, or 'condensation' . In the next section we will build on that observation to construct a quantitative approach, based on a Hubbard-Stratonovich decoupling in the Cooper channel. However, for the moment, let us stay on a less rigorous level and *assume* that the ground state $|\Omega\rangle$ of the theory is

characterized by the presence of a macroscopic number of Cooper pairs. More specifically, let us presume that the operator $\sum_{\mathbf{k}} c_{-\mathbf{k}\downarrow} c_{\mathbf{k}\uparrow}$ acquires a non-vanishing ground state expectation value,

$$\Delta = \frac{g}{L^d} \sum_{\mathbf{k}} \langle \Omega_s | c_{-\mathbf{k}\downarrow} c_{\mathbf{k}\uparrow} | \Omega_s \rangle, \qquad \Delta^* = \frac{g}{L^d} \sum_{\mathbf{k}} \langle \Omega_s | c^\dagger_{\mathbf{k}\uparrow} c^\dagger_{-\mathbf{k}\downarrow} | \Omega_s \rangle, \tag{7.20}$$

where we have included the coupling constant of the theory for later convenience. The assumption that Δ assumes a finite value (vanishes) below (above) the transition temperature T_c is tantamount to declaring Δ to the **order parameter of the superconductor transition**. However, at the present stage, this statement has the status of a mere presumption; we will have to explore its validity below.

At any rate, the non-vanishing expectation value of Δ looks strange. It clearly implies that the fermion many body state $|\Omega\rangle$ cannot have a definite number of particles. However, a better way to think about the problem is to remember the *bosonic* nature of the two-fermion pair state $|\psi_{\mathbf{k}\uparrow}, \psi_{-\mathbf{k}\downarrow}\rangle$. From this perspective, $c^\dagger_{\mathbf{k}\uparrow} c^\dagger_{-\mathbf{k}\downarrow}$ appears as the creator of a bosonic excitation. Non-vanishing of its expectation value implies a condensation phenomenon akin to the condensates discussed in section 7.2. Indeed, much of the remainder of this section will be devoted to the (semi-phenomenological) construction of a 'bosonic' mean field picture of the superconductor.

To develop that description, we substitute

$$g \sum_{\mathbf{k}} c_{-\mathbf{k}\downarrow} c_{\mathbf{k}\uparrow} = \Delta + \underbrace{\left(g \sum_{\mathbf{k}} c_{-\mathbf{k}\downarrow} c_{\mathbf{k}\uparrow} - \Delta \right)}_{\text{small}}$$

into the Hamiltonian and keep only terms which up to quadratic order in the electron operators. Adding the chemical potential, the 'mean-field' Hamiltonian takes the form

$$\hat{H} - \mu \hat{N} \simeq \sum_{\mathbf{k}} \left[c^\dagger_{\mathbf{k}\sigma} \xi_k c_{\mathbf{k}\sigma} - \left(\Delta^* c_{-\mathbf{k}\downarrow} c_{\mathbf{k}\uparrow} + \Delta c^\dagger_{\mathbf{k}\uparrow} c^\dagger_{-\mathbf{k}\downarrow} \right) \right] + \frac{L^d |\Delta|^2}{g}$$

known (in the Russian literature) as the **Bogoliubov** or **Gorkov** Hamiltonian (after its inventors, while the denotation **Bogoliubov-de Gennes Hamiltonian** more widespread in the anglosaxonian literature highlights the popularization of the mean field description by de Gennes.)

Indeed, the Gorkov Hamiltonian does not conserve the particle number. Instead, pairs of particles are born and annihilated out of the vacuum. To bring the mean-field Hamiltonian to a diagonal form, we proceed in analogy to our previous analysis of section 3.2.2 (where an Hamiltonian of similar structure $\sim a^\dagger a + aa + a^\dagger a^\dagger$ appeared.) That is, we recast the Fermion operators in a two component **Nambu spinor** representation

$$\Psi^\dagger_{\mathbf{k}} = \begin{pmatrix} c^\dagger_{\mathbf{k}\uparrow} & c_{-\mathbf{k}\downarrow} \end{pmatrix}, \qquad \Psi_{\mathbf{k}} = \begin{pmatrix} c_{\mathbf{k}\uparrow} \\ c^\dagger_{-\mathbf{k}\downarrow} \end{pmatrix}$$

comprising ↑-creators and ↓-annihilators into a single object. It is then a straightforward matter to show that the Hamiltonian assumes the bilinear form

$$\boxed{\hat{H} - \mu\hat{N} = \sum_{\mathbf{k}} \Psi^\dagger_{\mathbf{k}} \begin{pmatrix} \xi_{\mathbf{k}} & -\Delta \\ -\Delta^* & -\xi_{\mathbf{k}} \end{pmatrix} \Psi_{\mathbf{k}} + C,}$$

where the constant contribution $C = \sum_{\mathbf{k}} \xi_{\mathbf{k}} + \frac{L^d|\Delta|^2}{g}$. Now, being bilinear in the Nambu operators, the mean-field Hamiltonian can be brought to a diagonal form by employing the unitary transformation[17]

$$\chi_{\mathbf{k}} \equiv \begin{pmatrix} \alpha_{\mathbf{k}\uparrow} \\ \alpha^\dagger_{-\mathbf{k}\downarrow} \end{pmatrix} = \begin{pmatrix} \cos\theta_{\mathbf{k}} & \sin\theta_{\mathbf{k}} \\ \sin\theta_{\mathbf{k}} & -\cos\theta_{\mathbf{k}} \end{pmatrix} \begin{pmatrix} c_{\mathbf{k}\uparrow} \\ c^\dagger_{-\mathbf{k}\downarrow} \end{pmatrix} \equiv U_k \Psi_{\mathbf{k}}$$

(under which the anticommutation relations of the new electron operators $\alpha_{\mathbf{k}\sigma}$ are maintained — exercise). Note that the operators $\alpha^\dagger_{\mathbf{k}\uparrow}$ involve superpositions of $c^\dagger_{\mathbf{k}\uparrow}$ and $c_{-\mathbf{k}\downarrow}$, i.e. the *quasi*-particle states created by these operators contain linear combinations of particle and hole states; they certainly do not conserve the number of particles. Choosing Δ to be real[18] and setting $\tan(2\theta_{\mathbf{k}}) = -\Delta/\xi_{\mathbf{k}}$, i.e. $\cos(2\theta_{\mathbf{k}}) = \xi_{\mathbf{k}}/\lambda_{\mathbf{k}}$, $\sin(2\theta_{\mathbf{k}}) = -\Delta/\lambda_{\mathbf{k}}$, where

$$\lambda_{\mathbf{k}} = (\Delta^2 + \xi^2_{\mathbf{k}})^{1/2}. \tag{7.21}$$

the transformed Hamiltonian takes the form (exercise)

$$\begin{aligned} \hat{H} - \mu\hat{N} &= \sum_{\mathbf{k}} \lambda_{\mathbf{k}} \left(\alpha^\dagger_{\mathbf{k}\uparrow}\alpha_{\mathbf{k}\uparrow} - \alpha_{-\mathbf{k}\downarrow}\alpha^\dagger_{-\mathbf{k}\downarrow} \right) + C \\ &= \sum_{\mathbf{k}\sigma} \lambda_{\mathbf{k}} \alpha^\dagger_{\mathbf{k}\sigma}\alpha_{\mathbf{k}\sigma} + \sum_{\mathbf{k}} (\xi_{\mathbf{k}} - \lambda_{\mathbf{k}}) + \frac{|\Delta|^2 L^d}{g}, \end{aligned} \tag{7.22}$$

This result shows that the elementary excitations, the so-called **Bogoliubov quasi-particles**, created by $\alpha^\dagger_{\mathbf{k}\sigma}$, have a minimum energy Δ known as the energy gap.

To determine the ground state wavefunction one simply has to identify the state which is annihilated by all the quasi-particle annihilation operators $\alpha_{\mathbf{k}\sigma}$. This condition is met uniquely by the state

$$\boxed{|\Omega_s\rangle \equiv \prod_{\mathbf{k}} \alpha_{\mathbf{k}\uparrow}\alpha_{-\mathbf{k}\downarrow}|\Omega\rangle \sim \prod_{\mathbf{k}} \left(\cos\theta_{\mathbf{k}} - \sin\theta_{\mathbf{k}} c^\dagger_{\mathbf{k}\uparrow} c^\dagger_{-\mathbf{k}\downarrow} \right) |\Omega\rangle,}$$

where $|\Omega\rangle$ represents the vacuum state of the fermion operator algebra $\{c, c^\dagger\}$, and

$$\sin\theta_{\mathbf{k}} = \sqrt{\frac{1}{2}\left(1 - \frac{\xi_{\mathbf{k}}}{\lambda_{\mathbf{k}}}\right)^{1/2}}.$$

[17] It is instructive to compare with our previous analysis of section 3.2.2 where the bosonic nature of the problem enforced diagonalization by a non-compact *pseudo*unitary transformation.

[18] If Δ is not real, $\Delta = |\Delta|e^{i\phi}$, it can always be made so by the global gauge transformation $c_a \to e^{i\phi/2}c_a$, $c^\dagger_a \to e^{-i\phi}c^\dagger_a$. Notice the similarity to the gauge freedom that led to Goldstone mode formation in the previous section! Indeed, we will see momentarily that the gauge structure of the superconductor problem has equally farreaching consequences.

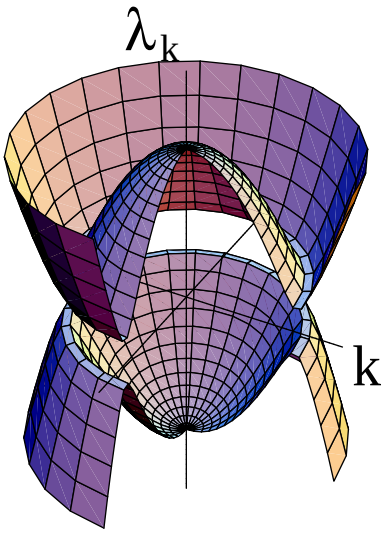

Figure 7.14: Quasi-particle energy spectrum $\lambda_{\mathbf{k}}$ as a function of $\mathbf{k}$. Notice that a gap develops at the Fermi energy separating the filled quasi-particle energy states from the empty.

To understand that $|\Omega_s\rangle$ is the ground state of the problem, notice that the lowest energy state of the oscillator Hamiltonian (7.22) is the vacuum of the algebra $\{\alpha, \alpha^\dagger\}$, i.e. the state anihilated by all $\alpha_{\mathbf{k},\uparrow/\downarrow}$. Clearly, all states $\prod_{\mathbf{k}} \alpha_{\mathbf{k},\uparrow}\alpha_{-\mathbf{k},\downarrow}|f\rangle$ constructed by application of the full set of anihilators onto a reference state $|f\rangle$ fulfill this condition *if* they are non-vanishing. It is straightforward to verify that for $|f\rangle = |\Omega\rangle$, this condition is met. Since the vacuum state of any algabra of canonically conjugate operators is unique, the state $|\Omega_s\rangle$ must, up to normalization, be *the* vacuum state. From the second representation given above, it is straightforward to verify that the normalization is unity.

We finally need to self consistently solve equations (7.20) for the input parameter Δ:

$$\Delta = \frac{g}{L^d}\sum_{\mathbf{k}}\langle\Omega_s|c_{-\mathbf{k}\downarrow}c_{\mathbf{k}\uparrow}|\Omega_s\rangle = \frac{g}{L^d}\sum_{\mathbf{k}}\sin\theta_{\mathbf{k}}\cos\theta_{\mathbf{k}} = \tag{7.23}$$

$$= \frac{g}{2L^d}\sum_{\mathbf{k}}\frac{\Delta}{(\Delta^2+\xi_{\mathbf{k}}^2)^{1/2}} \simeq \frac{g\Delta}{2}\int_{-\omega_D}^{\omega_D}\frac{\nu(\xi)d\xi}{(\Delta^2+\xi^2)^{1/2}} = g\Delta\nu_0\sinh^{-1}(\omega_D/\Delta) \tag{7.24}$$

where $\frac{1}{L^d}\sum_{\mathbf{k}} \to \int d\xi\ \nu(\xi)$, $\nu_0 \equiv \nu(\mu)$ denotes the density of states (per volume) at the Fermi surface and we have assumed that the pairing interaction g uniformly extends an energy scale ω_D. For pairing mechanisms which derive from the exchange of phonons, this energy scale is set by the corresponding Debye frequency. Solving this equation for

Δ, we obtain the important relation

$$\boxed{\Delta = \frac{\omega_D}{\sinh(1/g\nu(\mu))} \simeq 2\omega_D \exp\left[-\frac{1}{g\nu(\mu)}\right].} \tag{7.25}$$

Notice that this is the second time we encounter the combination of energy scales on the right hand side of the equation. Previously we had identified $T_c = 2\omega_D \exp(-(g\rho)^{-1})$ as the transition temperature at which the Cooper instability takes place. Our current discussion indicates that T_c equals the quasi-particle energy gap Δ. In fact, that identification might have been anticipated from our discussion above. At temperatures $T < \Delta$, thermal fluctuations are not capable of exciting quasi-particle states above the ground state. One thus expects that $T_c = \Delta$ separates a low temperature phase, characterized by the features of the anomalous pairing ground state, from a 'Fermi-liquid type' high-terperature phase where free quasi-particle excitations prevail.

The ground state $|\Omega_s\rangle$ and its quasi-particle excitations formally diagonalize the BCS-Hamiltonian. Before proceeding with the further development of the theory, let us pause to discuss a number of important properties of these objects.

Ground state: In the limit $\Delta \to 0$, $\sin^2\theta_{\mathbf{k}} \to \theta(\mu - \epsilon_{\mathbf{k}})$, and the ground state collapses to the filled Fermi sea with chemical potential μ. As Δ becomes non-zero, states in the vicinity of the Fermi surface rearrange themselves into a condensate of paired states. Remarkably, the collectively rearranged ground state involves single particle states with energy $\epsilon_{\mathbf{k}} > \mu$ in excess of the Fermi energy. (That follows simply from the energy dependence of the weight function $\sin\theta_{\mathbf{k}}$ entering the definition of the ground state, see Fig. 7.15.) However, the *total* energy of the ground state is lower than the energy $E_0 \equiv 2\sum_{|\mathbf{k}|<p_F} \xi_{\mathbf{k}}$ of the $g = 0$ Fermi sphere. To see this, one computes the expectation value

$$E_{|\Omega_s\rangle} \equiv \left\langle \Omega_s \left| \hat{H} - \mu\hat{N} \right| \Omega_s \right\rangle = \sum_{\mathbf{k}} (\xi_{\mathbf{k}} - \lambda_{\mathbf{k}}) + \frac{\Delta^2 L^d}{g}.$$

It is then straightforward to verify that for the mean field value of Δ given above, $E_{|\Omega_s\rangle} < E_0$, no matter how large g.

▷ EXERCISE. To show that $E_{|\Omega_s\rangle} < E_0$ it is convenient to represent the ground state energy of the Fermi see as $E_0 = \lim_{\Delta\to 0} E_{|\Omega_s\rangle}$. Use this representation (and the solution of the mean field equation) to verify that the superconductor ground state energy lies below that of the uncorrelated Fermi see.

It is also instructive to ask for the minimum value $E_{|\Omega_s\rangle}$ may assume upon *variation* of Δ for fixed g. Show that the solution of the variational equation $\partial_\Delta E_{|\Omega_s\rangle} = 0$ leads back to the mean field equation for Δ discussed above.

Excitations: Excitations above the ground state are described by the quasi-particle operators $\alpha^\dagger_{\mathbf{k}}$. According to Eq. (7.22), these states are gapped, i.e. it takes a minimum energy Δ to excite a quasi-particle state above the BCS ground state; the formerly ($g = 0$) continuous quasi-particle spectrum has acquired a gap. However, according to the adiabatic principle of quasi-particle formation, the states of the $g = 0$ system cannot

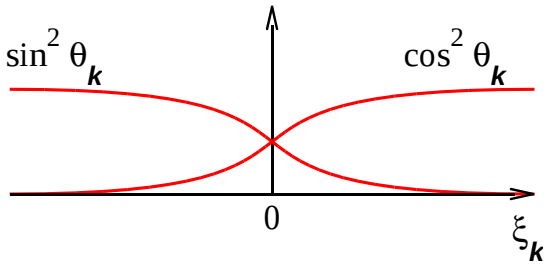

Figure 7.15: Schematic diagram showing the variation of the occupancy of the momemtum basis states in the ground state. $\sin\theta_k$ represents the occupancy of the $\mathbf{k}$ states. Note that the wavefunction of the ground state condensate involves the occupation of basis states with energies in excess of μ.

have simply disappeared. To understand where the states formerly populating the gap have gone, let us compute the quasi-particle DoS $\rho(\epsilon)$ in the vicinity of the Fermi surface, $\epsilon \approx \mu$:

$$\begin{aligned}\rho(\epsilon) &= \sum_{\mathbf{k}\sigma} \delta(\epsilon - \lambda_{\mathbf{k}}) = \\ &= \int d\xi \underbrace{\sum_{\mathbf{k}\sigma} \delta(\xi - \xi_{\mathbf{k}})}_{\rho_0(\xi)} \delta(\epsilon - \lambda(\xi)) \approx \rho_0 \sum_{s=\pm 1} \int_0^\infty d\xi \frac{\delta\left(\xi - s[\epsilon^2 - \Delta^2]^{1/2}\right)}{\left|\frac{\partial[\xi^2+\Delta^2]^{1/2}}{\partial\xi}\right|} = \\ &= 2\rho_0 \Theta(|\epsilon| - \Delta) \frac{|\epsilon|}{(\epsilon^2 - \Delta^2)^{1/2}},\end{aligned}$$

where in the third equality we have used that the DoS of the non-interacting system, ρ_0 is largely structureless across the Fermi surface and can be pulled out of the integral. A schematic plot of the BCS quasi-particle DoS is shown in the figure. Apparently, the spectral weight of the quasi-particles has been pushed from the Fermi surface to the interval $[\Delta, \infty]$. The divergence of the DoS at Δ signals that the majority of quasi-particle states populates the spectral region right above the gap.

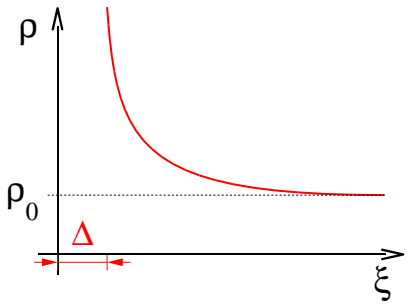

▷ EXERCISE. Integrate the result above to show that $\int_\Delta^E d\epsilon\, \rho(\epsilon) \overset{E\gg\Delta}{\longrightarrow} 2E\rho_0$, i.e. that no quasi-particle states have gone 'lost' upon swiching on superconductivity. That the number of states in the interval $[0, E]$ is twice as large as the number of positive energy states $\rho_0 E$ of the non-interacting system can be explained as follows: In the absence of superconductivity, states with $\xi < 0$ have negative energy, i.e. the creation of a hole below the Fermi energy *gains* energy. However, upon switching on superconductivity, the creation of a hole with $-\Delta < \xi < 0$ *costs* energy, namely the energy to break up a pair. The transferral of the $g = 0$ negative energy states to the positive energy continuum leads to a doubling of the $E > 0$ DoS.

The phenomenological analysis above explains important aspects of the physics of the BCS superconductor: the instability towards condensation, and the presence of a gap for quasi-particle excitations above the ground state. Indeed, it would be tempting to take the latter phenomenon as an explanation for the absence of electric resistivity below the transition temperature. I.e. if now low-lying quasi-particle excitations are available, shouldn't external current be able to flow through the system without dissipate loss of energy? Yet that picture neglects the most important excitation of the system, i.e. the collective phase mode. Above we had met the ad hoc agreement that the phase of the order parameter be set to zero. However, as with the superfluid, the phase represents a Goldstone mode and we must expect its presence to have important consequences. Indeed, it will turn out that the phase mode of the superconductor – in contradisctinction to its counterpart in the 'neutral' superfluid – holds responsible for much of the electromagnetic phenomena displayed by the superconductor.

From a modern point of view, a comprehensive picture of the superconductor, encompassing the consequences of Goldstone mode formation, and the BCS structures discussed above, is most efficiently developed within the field integral approach:

7.3.4 Superconductivity from the Field Integral

To investigate the BCS transition within the framework of the coherent state path integral, we start out from a coordinate representation of the BCS-Hamiltonian (7.17),

$$\hat{H}_{\rm BCS} = \int d^d r\, c^\dagger_\sigma(\mathbf{r}) \left[\frac{1}{2m}(-i\boldsymbol{\partial} - e\mathbf{A})^2 + ie\boldsymbol{\phi}\right] c_\sigma(\mathbf{r}) - g\int d\mathbf{r} c^\dagger_\uparrow c^\dagger_\downarrow c_\downarrow c_\uparrow.$$

Anticipating the emergence of non-trivial electromagnetic phenomena, we have coupled the single particle Hamiltonian to a vector potential $\mathbf{A} = \mathbf{A}(\mathbf{r},\tau)$ and a scalar potential $i\phi = i\phi(\mathbf{r},\tau)$[19]. Origin and physical consequences of these fields will be discussed somewhat later.

Expressed in the form of the coherent state path integral, the corresponding quantum partition function takes the form

$$\mathcal{Z} = \int D(\bar\psi,\psi) e^{-S[\bar\psi,\psi]},$$
$$S[\bar\psi,\psi] = \int_0^\beta d\tau \int d^d r \left[\bar\psi_\sigma \left(\partial_\tau + ie\boldsymbol{\phi} + \frac{1}{2m}(-i\boldsymbol{\partial} - e\mathbf{A})^2 - \mu\right)\psi_\sigma - g\bar\psi_\uparrow\bar\psi_\downarrow\psi_\downarrow\psi_\uparrow\right] \quad (7.26)$$

where $\psi(\mathbf{r},\tau)$ are Grassmann fields.

▷ INFO. In the field theoretical literature, the substitution

$$\partial_\tau \;\to\; \partial_\tau + ie\phi, \quad (7.27)$$
$$-i\boldsymbol{\partial} \;\to\; -i\boldsymbol{\partial} - e\mathbf{A} \quad (7.28)$$

[19] Notice that the Eucilidean character of the imaginary time theory suggests to couple the time-like scalar component of the potential through an additional 'i', i.e. our present ϕ is given by $(-i)\times$ the conventional scalar potential.

is sometimes called a **minimal coupling** of an electromagnetic field. It is 'minimal' in the sense that only orbital and potential coupling of the field are taken into account. (E.g. the field-spin interaction is neglected.) At the same time, the potential/vector-potential coupling is comlete enough to endow the theory with a **local gauge invariance** under U(1) transformations

$$\begin{aligned} \psi &\rightarrow e^{i\theta}\psi, && (7.29)\\ \bar{\psi} &\rightarrow e^{-i\theta}\bar{\psi}, && (7.30)\\ \phi &\rightarrow \phi + e^{-1}\partial_\tau\theta, && (7.31)\\ \mathbf{A} &\rightarrow \mathbf{A} + e^{-1}\boldsymbol{\partial}\theta, && (7.32) \end{aligned}$$

where $\theta = \theta(\mathbf{x}, \tau)$ is an arbitrary space-time dependent phase configuration.

The minimal coupling introduces the general quantum-electrodynamical gauge priniciple into the theory. This should be compared with the the discussion of the neutral superfluid where only invariance under *global* U(1) transformations was required.

As usual the quartic interaction of the fields prevents the partition function from being evaluated explicitly. Moreover, anticipating the existence of a transition of the electron gas to a condensed phase in which electrons in the vicinity of the Fermi surface are paired, we can expect that a perturbative expansion in the coupling constant g will be inadequate. Motivated by the mean-field theory discussed above, we will instead introduce a bosonic field Δ to decouple the interaction which will have the physical significance of the order parameter.

The decoupling is arranged using a Hubbard-Stratonovich transformation in the Cooper channel (cf. the discussion on page 231)

$$e^{g\int d\tau \int d\mathbf{r}\bar{\psi}_\uparrow\bar{\psi}_\downarrow\psi_\downarrow\psi_\uparrow} = \int \mathcal{D}(\Delta^*,\Delta)\exp\left\{-\int d\tau\int d\mathbf{r}\left[\frac{1}{g}|\Delta|^2 - \left(\Delta^*\psi_\downarrow\psi_\uparrow + \Delta\bar{\psi}_\uparrow\bar{\psi}_\downarrow\right)\right]\right\},$$

where $\Delta(\mathbf{r},\tau)$ represents a dynamically fluctuating complex field. Reflecting the behaviour of the bilinear $\psi_\downarrow\psi_\uparrow$, it obeys periodic temporal boundary conditions, $\Delta(0) = \Delta(\beta)$, i.e. Δ is a bosonic field variable. Would we take Δ to be homogeneous in space and time, the quantum Hamiltonian corresponding to the action would coincide with that of the mean-field Hamiltonian considered in the previous section. Following that analysis (but not making the a priori assumption $\Delta(\mathbf{r},\tau) = $ const.) we turn to the **Nambu spinor** representation

$$\bar{\Psi} = \begin{pmatrix} \bar{\psi}_\uparrow & \psi_\downarrow \end{pmatrix}, \qquad \Psi = \begin{pmatrix} \psi_\uparrow \\ \bar{\psi}_\downarrow \end{pmatrix}$$

comprising particle and hole degree of freedom in a single object. Expressed in terms of the Nambu spinor, the partition function takes the form

$$\mathcal{Z} = \int D(\bar{\psi},\psi)\int D(\Delta^*,\Delta)\exp\left\{-\int d\tau\int d\mathbf{r}\left[\frac{1}{g}|\Delta|^2 - \bar{\Psi}\hat{\mathcal{G}}^{-1}\Psi\right]\right\}$$

where

$$\hat{\mathcal{G}}^{-1} = \begin{pmatrix} [\hat{G}_0^{(\mathrm{p})}]^{-1} & \Delta \\ \bar{\Delta} & [\hat{G}_0^{(\mathrm{h})}]^{-1} \end{pmatrix},$$

$$[\hat{G}_0^{(\mathrm{p})}]^{-1} = -\partial_\tau - ie\phi - \frac{1}{2m}(-i\boldsymbol{\partial} - e\mathbf{A})^2 + \mu,$$
$$[\hat{G}_0^{(\mathrm{h})}]^{-1} = -\partial_\tau + ie\phi + \frac{1}{2m}(+i\boldsymbol{\partial} - e\mathbf{A})^2 - \mu \qquad (7.33)$$

is known as the **Gorkov Green function** and $G^{(\mathrm{p,h})}$ represent the non-interacting Green function of the particle and hole respectively.

▷ INFO. Computing the Ψ-representation of the action for a general single particle Hamiltonian $\hat{H}$, we find that

$$[\hat{G}_0^{(\mathrm{p})}]^{-1} = -\partial_\tau - \hat{H} \quad + \mu,$$
$$[\hat{G}_0^{(\mathrm{h})}]^{-1} = -\partial_\tau + \hat{H}^T - \mu.$$

(With $\boldsymbol{\partial}^T = -\boldsymbol{\partial}$, the expression above is identified as a special case of the more general form.) This representation is actually very suggestive. It tells us that the Green function of a hole is obtained from that of the electron by a sign change $\hat{H} \to -\hat{H}$ (the energy of a hole is the negative of the corresponding particle energy) followed by transposition $-\hat{H} \to -\hat{H}^T$, i.e. a quantum time reversal operation (a hole can be imagined as a particle propagating backwards in time.)

Using that $\hat{p}^T = -\hat{p}$ and $\hat{r}^T = \hat{r}$, the pair of Green functions can equivalently be represented through

$$[\hat{G}_0^{(\mathrm{p})}]^{-1} = -\partial_\tau - \hat{H}(\hat{r}, \hat{p}) + \mu,$$
$$[\hat{G}_0^{(\mathrm{h})}]^{-1} = -\partial_\tau + \hat{H}(\hat{r}, -\hat{p}) - \mu. \qquad (7.34)$$

The Gaussian integration over the Grassmann fields can now be performed straightforwardly, and yields the formal expression (cf. the analogous formula (7.5) for the normal electron system)

$$\mathcal{Z} = \int D(\Delta^*, \Delta) \exp\left[-\frac{1}{g}\int d\tau \int d\mathbf{r}\, |\Delta|^2 + \ln\det \hat{\mathcal{G}}^{-1}\right]. \qquad (7.35)$$

By introducing a Hubbard-Stratonovich decoupling of the local interaction, we have succeeded in expressing the quantum partition function as a path integral over an auxiliary bosonic field Δ. Further progress is possible only within some approximation.

Mean Field Equation

To identify a good 'platform' around which the 'tr ln' can be expanded perturbatively, we begin by seeking mean field configurations of Δ. A variation of the action wrt Δ generates the mean field equation (for the differentiation of the 'tr ln' with respect to Δ cf. the analogous calculation in Eq. (7.6))

$$\frac{1}{g}\bar{\Delta}(\mathbf{x}, \tau) + \mathrm{tr}\,\left(\hat{\mathcal{G}}(\mathbf{x}, \tau, \mathbf{x}, \tau) E_{12}^{\mathrm{ph}}\right) = 0,$$

where $E_{ij}^{\rm ph}$ is a 2×2-matrix in Nambu space that contains 0 everywhere safe for a 1 at position (i,j). Assuming that configurations extremizing the action will be spatially and temporally constant, i.e $\Delta(\mathbf{x},\tau)\equiv\Delta_0=$ const., and temporarily ignoring the dependence of the Green function on the field $(\phi,\mathbf{A})$, the equation simplifies to

$$\begin{aligned}\frac{1}{g}\bar{\Delta}_0 &= \mathrm{tr}\left[\begin{pmatrix} -\partial_\tau+\frac{\partial^2}{2m}+\mu & \Delta_0 \\ \bar{\Delta}_0 & -\partial_\tau-\frac{\partial^2}{2m}-\mu\end{pmatrix}^{-1}(\mathbf{x},\tau,\mathbf{x},\tau)\begin{pmatrix}1 & \\ & 0\end{pmatrix}\right]= \\ &= \frac{T}{L^d}\sum_{\mathbf{p},n}\begin{pmatrix} i\omega_n-\xi_p & \Delta_0 \\ \bar{\Delta}_0 & i\omega_n+\xi_p\end{pmatrix}_{21}=\frac{T}{L^d}\sum_{\mathbf{p},n}\frac{\bar{\Delta}_0}{\omega_n^2+\xi_p^2+|\Delta_0|^2},\end{aligned}$$

where in the second line we have switched to a frequency/momentum representation and, as usual, $\xi_p=p^2/(2m)-\mu$. Slightly rearranging the equation, we arrive at

$$\frac{1}{g}=\frac{T}{L^d}\sum_{\mathbf{p},n}\frac{1}{\omega_n^2+\lambda_p^2},$$

where $\lambda_p=(\xi_p^2+\Delta^2)^{1/2}>0$ as in Eq. (7.21) above. The summation over Matsubara frequencies on the rhs of this equation can straightforwardly be performed by means of the summation techniques discussed on pp **??** (also cf. the problem set of chapter 5):

$$\begin{aligned}\frac{1}{g} &= \frac{1}{L^d}\sum_{\mathbf{p}}\frac{1-2f_{\rm f}(\lambda_p)}{2\lambda_p}= \\ &= \int_{-\omega_D}^{\omega_D}d\xi\,\underbrace{\frac{1}{L^d}\sum_{\mathbf{p}}\delta(\xi-\xi_p)}_{\nu_0}\frac{1-2f_{\rm f}(\lambda(\xi))}{2\lambda(\xi)}\end{aligned}$$

where in the second line we have taken into account that the range of the attractive interaction is limited by ω_D. Noting that the integrand is even in ξ and using that $1-2f_{\rm f}(x)=\tanh(\beta x/2)$, we arrive at the celebrated **BCS gap equation**

$$\frac{1}{g\nu_0}=\int_0^{\omega_D}d\xi\,\frac{\tanh(\beta\lambda(\xi)/2)}{\lambda(\xi)}. \tag{7.36}$$

For small temperatures, $T\ll\Delta$, the tanh-function can be approximated as $\tanh(\beta\lambda(\xi)/2)=1$ and we arrive back to the $T=0$ gap equation (7.23) discussed above. However, presently we wish to be a bit more ambitious and explore the fate of the gap as the temperature is increased. Intuitively, one would expect that for large tempertures, thermal fluctuations will eventually wash out the gap above the ground state. On the other hand, we know empirically, that the onset of superconductivity has the status of a second order phase transition. Since the gap parameter Δ has the status of the order parameter of that transition – an identification to be substantiated shortly – we must expect that the vanishing of $\Delta(T)$ occurs in a singular manner (in analogy to, e.g., the magnetization of a ferromagnet at the Curie temperature.)

Indeed, it turns out that (for details, see the info-block below) the order parameter vanishes abruptly at the **critical temperature of the BCS transition**

$$T_c = \text{const.} \times \omega_D \exp\left(-\frac{1}{g\nu_0}\right), \tag{7.37}$$

where 'const.' is a numerical constant of $\mathcal{O}(1)$. Notice that this result is consistent with our perturbative analysis above. While we are presently approaching the problem from its low temperature phase, there we had perturbatively expanded around the non-interacting Fermi sphere, i.e. the phase of the high temtperature regime, not affected by superconductor correlations. We had found that at a scale that coincided up to numerical factors with T_c above, that phase became unstable towards condensation.

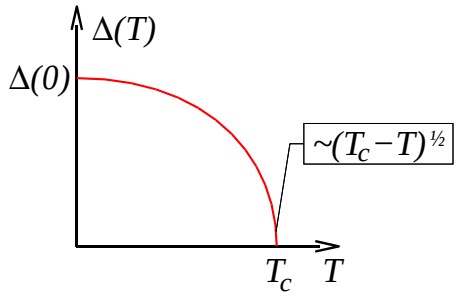

For temperatures slightly smaller than T_c,

$$\Delta = \text{const.} \times \sqrt{T_c(T_c - T)}, \tag{7.38}$$

i.e. the vanishing occurs with a diverging derivative, as is typical second order phase transitions. The interpolated temperature profile of the order parameter is shown in the figure. Notice that (again, up to numerical factors) the critical temperature T_c coinicides with the zero temperature value of the gap $\Delta(0)$. The square-root type profile of the gap function has been accurately confirmed by experiment (see. Fig. XX). In fact, that coincidence may be counted as an important source of evidence in favour of the microscopic validity of BCS theory.

▷ INFO. In spite of its inncocent appearance, the **finite temperature analysis of the gap equation** is not straightforward. Referring for a quantitative discussion to Ref. [**?**], we here restrict ourselves to exploring the gap profile in the vicinity of the transition temperature.

To determine the value of T_c, we proceed somewhat indirectly, i.e. we *assume* that a minimal temperture T_c determined through $\Delta(T_c) = 0$ exists and use that criterion to deterimine a condition for T_c. For $\Delta = 0$, $\lambda(\xi) = |\xi|$ and (7.36) assumes the form

$$\frac{1}{g\nu_0} = \int_0^{\omega_D/2T_c} dx \frac{\tanh(x)}{x},$$

where we have introduced $x \equiv \xi/2T_c$ as a dimensionless integration variable. Now, assuming the hierarchy of energy scales $\omega_D \gg T_c \sim \Delta$, the dominant contribution to the integral comes from the region $x \gg 1$, where $\tanh(x) \simeq 1$. This leads to the estimate

$$\frac{1}{g\nu_0} \simeq \int_1^{\omega_D/2T_c} \frac{dx}{x} = \ln(\omega_D/2T_c).$$

Solving for T_c, we arrive at (7.37).

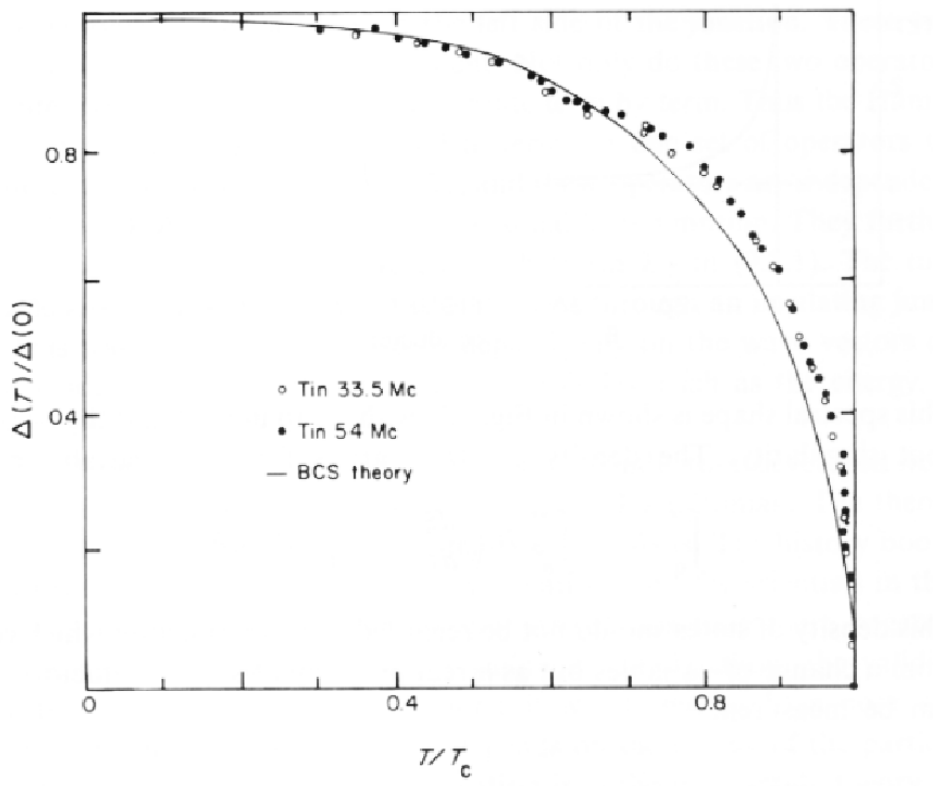

Figure 7.16: The points are ultrasonic attenuation data on the ratio $\Delta(T)/\Delta(0)$ (taken from R. W. Morse and H. V. Bohm, Phys. Rev. **108**, 1094 (1957.)). The solid line is the prediction of BCS theory.

Now, let us derive the approximate profile of the gap for temperatures T slightly smaller than T_c. Starting out from

$$\frac{1}{g\nu_0} = \int_0^{\omega_D/2T} dx \frac{\tanh[(x^2+\kappa^2]^{1/2})}{(x^2+\kappa^2)^{1/2}},$$

where $\kappa \equiv \Delta/2T \ll 1$, we add and subtract $\int dx \tanh(x)/x$:

$$\frac{1}{g\nu_0} = \int_0^{\omega_D/2T} dx \left[\frac{\tanh[(x^2+\kappa^2)^{1/2}]}{(x^2+\kappa^2)^{1/2}} - \frac{\tanh(x)}{x}\right] + \int_0^{\omega_D/2T} dx \frac{\tanh(x)}{x},$$

Arguing as above, the second integral estimates to

$$\int_0^{\omega_D/2T} dx \frac{\tanh(x)}{x} \approx \ln(\omega_D/2T) \approx \ln(\omega_D/2T_c) + \frac{\delta T}{T_c} = \frac{1}{g\nu_0} + \frac{\delta T}{T_c},$$

where we have introduced $\delta T \equiv T_c - T \ll T$ and expanded to linear order in δT. Thus,

$$-\frac{\delta T}{T_c} \approx \int_0^{\omega_D/2T} dx \left[\frac{\tanh[(x^2+\kappa^2)^{1/2}]}{(x^2+\kappa^2)^{1/2}} - \frac{\tanh(x)}{x}\right],$$

Now, the remaining integral can be split into a 'low energy region' $0 \leq x \leq 1$, and a 'high energy region' $1 < x < \omega_D/2T$. Using that for $x < 1$, $\tanh(x) \simeq x - x^3/3$, we find that the first region

gives a contribution $\sim \kappa^2$. With $\tanh(x) \overset{x>1}{\approx} 1$, the second region, too, contributes a term $\mathcal{O}(\kappa^2)$ which, however, is approximately independent of the large energy cutoff $\omega_D/2T$. Summarizing,

$$\frac{\delta T}{T_c} \approx \text{const.} \times \kappa^2 = \text{const.} \times \frac{\Delta^2}{T^2}.$$

Solving for Δ, we arrive at Eq. (7.38).

Having explored the large scale profile of the gap function, we next turn our attention to the vicintiy of the superconductor phase transition, i.e. to temperature regions, $\delta T = T_c - T \ll T$.

7.3.5 Ginzburg Landau Theory

In the vicinity of the phase transition, the gap parameter Δ is small (in comparision to the temperature.) That brings us in a position to perturbatively expand the action in (7.35) perturbatively in Δ. We will see that that expansion reveals a lot of information about the superconductor phase transition. Further, we will make the connection to the neutral superfluid (as well as important differences) explicit.

To keep the structure of the expansion as transparent as possible, we still ignore the coupling to the external field. Our task thus reduces to computing the expansion of $\operatorname{tr} \ln(\hat{\mathcal{G}}^{-1})$ in powers of Δ where

$$\hat{\mathcal{G}}^{-1} = \begin{pmatrix} -\partial_\tau + \frac{\partial^2}{2m} + \mu & \Delta \\ \bar{\Delta} & -\partial_\tau - \frac{\partial^2}{2m} - \mu \end{pmatrix}.$$

To facilitate that expansion, we formally define $\hat{\mathcal{G}}_0^{-1} \equiv \hat{\mathcal{G}}^{-1}\Big|_{\Delta=0}$ as well as

$$\hat{\Delta} \equiv \begin{pmatrix} & \Delta \\ \bar{\Delta} & \end{pmatrix}$$

to write

$$\begin{aligned} \operatorname{tr} \ln(\hat{\mathcal{G}}) &= \operatorname{tr} \ln(\hat{\mathcal{G}}_0^{-1} + \hat{\Delta}) = \\ &= \operatorname{tr} \ln\left(\hat{\mathcal{G}}_0^{-1}(1 + \hat{\mathcal{G}}_0\hat{\Delta})\right) = \operatorname{tr} \ln\left(\hat{\mathcal{G}}_0^{-1}\right) + \operatorname{tr} \ln\left(1 + \hat{\mathcal{G}}_0\hat{\Delta}\right) = \\ &= \text{const.} - \frac{1}{2}\sum_{n=0}^{\infty} \frac{1}{n} \operatorname{tr}\left((\hat{\mathcal{G}}_0\hat{\Delta})^{2n}\right). \end{aligned}$$

In the third equality we have used the relation $\operatorname{tr}\ln(\hat{A}\hat{B}) = \operatorname{tr}\ln(\hat{A}) + \operatorname{tr}\ln(\hat{B})$[20]. The third line contains the Taylor expansion of the lograrithm where we have used that (why?) odd contributions in $\hat{\Delta}$ vanish. We also noticed that $\operatorname{tr} \ln\left(\hat{\mathcal{G}}_0^{-1}\right)$, not containing any fluctuating field variables, gives an inessential constant contribution to the action.

[20] Noitice that for non-commutative matrices, in general $\ln(\hat{A}\hat{B}) \neq \ln\hat{A} + \ln\hat{B}$.

To give this formal expansion some meaning, let us consider the second order term in more detail. Substituting the explicit form of $\hat{\mathcal{G}}_0^{-1}$ it is straightforward to verify that

$$\begin{aligned}-\frac{1}{2}\,\mathrm{tr}\,\left((\hat{\mathcal{G}}_0\hat{\Delta})^2\right) &= -\,\mathrm{tr}\,\left(\hat{\mathcal{G}}_{0,11}\Delta\hat{\mathcal{G}}_{0,22}\bar{\Delta}\right) = \\ &= -\sum_q \frac{T}{L^d}\sum_p \hat{\mathcal{G}}_{0,11,p}\hat{\mathcal{G}}_{0,22,p-q}\Delta(q)\bar{\Delta}(q) = \\ &= \sum_q \frac{T}{L^d}\sum_{\mathbf{p},\omega_n} G_p G_{-p+q}\Delta(q)\bar{\Delta}(q),\end{aligned}$$

where in the last line we have used the representation of the composite Green function $\hat{\mathcal{G}}_0$ in terms of the particle Green function $G_p^{(\mathrm{p})} = G_p$ and the hole Green function $G_p^{(\mathrm{h})} = -G^{(\mathrm{p})}(-p) = -G_{-p}$ (cf. Eq. (7.34).) Combining this with the first term in the action of (7.35), we arrive at the quadratic action of the order parameter field,

$$S^{(2)}[\Delta,\bar{\Delta}] = \sum_q \left(\frac{1}{g} - \frac{T}{L^d}\sum_p G_p G_{-p+q}\right)\Delta(q)\bar{\Delta}(q).$$

This is the second time we meet with the characteristic combination $\Gamma_q^{-1} = \frac{1}{g} - \frac{T}{L^d}\sum_p G_p G_{-p+q}$: In our perturbative analysis of the Cooper channel (cf. Eq. (7.18)) we had identified the same expression as the (inverse) of the vertex Γ_q. To understand that connection, we should let the dust of our current technical operations settle and remember the general philosophy of the Hubbard-Stratonovich scheme. The field Δ was introduced to decouple an attractive interaction in the Cooper channel. In analogy to the field ϕ we used above to describe the RPA-approximation to the direct channel, the action of the field $\Delta \sim \bar{\psi}_\uparrow\bar{\psi}_\downarrow$ can be interpreted as the 'propagator' of the composite object $\bar{\psi}_\uparrow\bar{\psi}_\downarrow$. I.e. a quadratic contraction $\sim \langle\bar{\Delta}\Delta\rangle$ describes propagation in the Cooper channel $\sim \langle\bar{\psi}_\uparrow\bar{\psi}_\downarrow\psi_\downarrow\psi_\uparrow\rangle$, as described by a four point correlation function. That connection is made explicit by comparison of the quadratic action with the direct calculation of the Cooper four point function above.

However, unlike in section 7.3.2 where all we could do was to diagnose an instability as $\Gamma_{q=0}^{-1} \to 0$ we are now in a position to comprehensively explore the consequences of that phenonmenon. Indeed, $\Gamma_{q=0}^{-1} \to 0$ corresponds to a sign change of the quadratic action of the constant order parameter mode $\Delta(q=0)$. In the close vicinity of that point, the constant contribution to the action must scale as $\sim (T - T_c)$ such that we may conclude that the action assumes the form

$$S^{(2)}[\Delta,\bar{\Delta}] = \frac{1}{2}\int d\mathbf{x}\int_0^\beta d\tau\,\Delta\bar{\Delta}r(T) + \mathcal{O}(\boldsymbol{\partial}\Delta,\partial_\tau\Delta),$$

where $r(T) \sim T - T_c$ and $\mathcal{O}(\boldsymbol{\partial}\Delta,\partial_\tau\Delta)$ stands for temoral and spatial gradients whose role will be discussed shortly.

▷ Exercise. Use Eq. (7.19) and the expansion

$$f_{\mathrm{f}}(\epsilon,T) - f_{\mathrm{f}}(\epsilon,T_c) \simeq \partial_T|_{T=T_c} f_{\mathrm{f}}(\epsilon,T)(T-T_c) = -\partial_\epsilon f_{\mathrm{f}}(\epsilon,T_c)(T-T_c)\frac{\epsilon}{T}$$

to show that

$$r(T) = \rho \frac{T - T_c}{T_c}.$$

For temperatures below the transition, the quadratic action becomes unstable and – all in perfect analogy to our previous discussion of the superfluid condensate action – we have to seek rescue with the fourth order action $S^{(4)}$. At orders $n > 2$ of the expansion, spatial or temporal gradients can safely be neglected. (Due to the smallness of $\Delta \ll T$, they will certainly be smaller than the gradient contributions to $S^{(2)}$.) However, for $\Delta = \text{const.}$, it is straightforward to verify that

$$\begin{aligned} S^{(2n)} &= -\frac{1}{2n} \operatorname{tr} \left((\mathcal{G}_0 \hat{\Delta})^{2n} \right) = \\ &= -\frac{(-)^n}{2n} \sum_p \left(G_p G_{-p} \right)^n (\bar{\Delta}\Delta)^n = -\frac{(\bar{\Delta}\Delta)^n}{2n} \sum_{\mathbf{p},\omega_l} \left(\frac{1}{\omega_l^2 + \xi_p^2} \right)^n \simeq \\ &\simeq -\frac{\rho (\bar{\Delta}\Delta)^n}{2n} \sum_{\omega_l} \int_{-\omega_D}^{\omega_D} d\xi \left(\frac{1}{\omega_l^2 + \xi^2} \right)^n = \\ &= -\text{const.} \times \rho (\bar{\Delta}\Delta)^n \sum_{\omega_l} \frac{1}{\omega_l^{2n-1}} = \\ &= -\text{const.} \times \rho T \left(\frac{\bar{\Delta}\Delta}{T^2} \right)^{2n}, \end{aligned}$$

where 'const.' stands for numerical constants. In the second equality we have expressed the Gorkov Green function through the constituting particle and hole Green function, respectively, and in the essential fourth equality we noticed that for $\omega_D \gg T$, the integral over the energy variable is dominated by the infrared divergence at small ξ, i.e. $\int_0^{\omega_D} d\xi (\omega_l^2 + \xi^2)^n \simeq \int_{\omega_l}^{\infty} d\xi \xi^{-2n}$. This estimate tells us that the contributions of higher order to the expansion are (i) positive and (ii) small in the parameter $|\Delta|/T \ll 1$. This being so, it is sufficient to keep the fourth order term (and that one we indeed need to counterbalance the unstable second order term.) We thus arrive at

$$S[\Delta, \bar{\Delta}] = \int d\mathbf{x} \int_0^{\beta} d\tau \left(\frac{r(T)}{2} \Delta\bar{\Delta} + g(\Delta\bar{\Delta})^2 + \mathcal{O}(\boldsymbol{\partial}\Delta, \partial_\tau \Delta, |\Delta|^6) \right) \tag{7.39}$$

as an estimate for the effective action of the order parameter field. Here, $g \sim \rho T^{-3}$ shows only weak temperature dependence in the vicintiy of the transition. In Fig. 7.17, the action of a constant configuration $\Delta = \text{const}$ is shown as a function of $\operatorname{Re}\Delta$ and $\operatorname{Im}\Delta$ for a value $r(T > T_c) > 0$ and for a value $r(T < T_c) < 0$. Notice the analogy to the action of the condensate amplitude shown in Fig. 7.6.

▷ INFO. It is straightforward, to include finite spatial gradients into the derivation of the quadratic action $S^{(2)}$ (for details see, e.g. Ref. [?].) The resulting action for static but spatially fluctuating configurations $\Delta(\mathbf{r})$ reads as

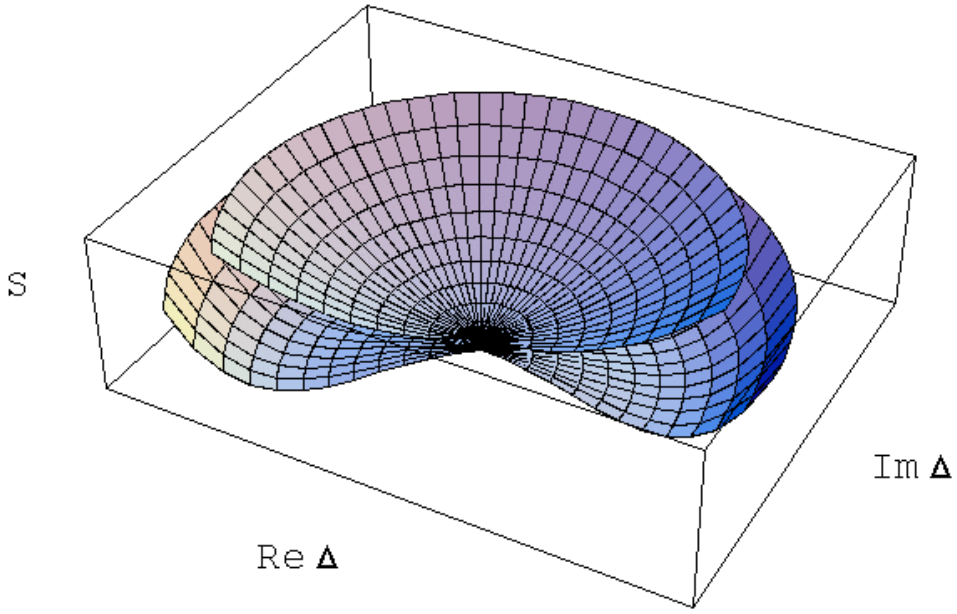

Figure 7.17: Action of a constant order parameter configuration Δ as a function of $\mathrm{Re}\,\Delta$ and $\mathrm{Im}\,\Delta$. The upper (lower) surface corresponds to a temperature $T > (<) T_c$

$$\boxed{S_{\mathrm{GL}}[\Delta,\bar{\Delta}] = \beta \int d\mathbf{x} \left[\frac{r}{2}\Delta\bar{\Delta} + \frac{c}{2}\boldsymbol{\partial}\Delta\boldsymbol{\partial}\bar{\Delta} + g(\Delta\bar{\Delta})^2 \right],} \tag{7.40}$$

where the constant $c \sim \rho_0 (v_F/T)^2$. This result is known as the **(classical) Ginzburg-Landau action** of the superconductor. It is called 'classical' because (cf. our remarks on page 244) temporal, or quantum fluctuations of Δ are ignored. Notice that the form of the action might have been anticipated on symmetry grounds alone. Indeed, (7.40) was proposed by Ginzburg and Landau as an effective action of superconductivtiy, way before the advent of the microscopic theory[21] – again a demonstration of the ingenuity of the phenomenological Landau school.

A generalization to finite temporal fluctutations leads to the **time dependent Ginzburg-Landau theory**, to be discussed below.

Eq. (7.39) makes the connection between the superconductor and the previously discussed superfluid explicit (cf. the condensate action (7.10). Above the transition temperature, $r > 0$, and the unique mean field configuration extremising the action (7.39) is given by $\Delta = 0$. However, below the critical temperature, $r < 0$ and a configuration with non-vanishing Cooper pair amplitude Δ_0 is energetically favourable:

$$\left.\frac{\delta S[\Delta,\bar{\Delta}]}{\delta\Delta}\right|_{\Delta=\Delta_0} = 0 \Rightarrow \bar{\Delta}_0 \left(r + 2g|\Delta_0|^2\right) = 0 \Rightarrow |\Delta_0| = \sqrt{\frac{-r}{-2g}} \sim \sqrt{T_c(T_c - T)},$$

[21] V. L. Ginzburg and L. D. Landau, *On the theory of superconductivity*, Zh. Eksp. Teor. Fiz. **20**, 1064 (1950).

in agreement with our previous estimate (7.38). Now, as with the superfluid, the mean field equation determines only the modulus of the order parameter while the phase remains unspecified. That observation suggests that we wind up with a picture essentially equivalent to that developed above for the superfluid: Below the transition, the symmetry of the action will be broken by the formation of a ground state with fixed global phase, e.g. $\Delta_0 \in \mathbb{R}$. That entails the formation of a phase-like Goldstone mode θ, where configurations $\Delta = e^{2i\theta}\Delta_0$ explore deviations off the reference groundstate[22]. Carrying on with drawing parallels to the superfluid, it would be tempting to conjecture that these phase fluctuations have a linear dispersion, i.e. that the system supports dissipationless supercurrents of *charged* particles: superconductivity.

However, at this point, we have over-streched the analogies to our previous discussion. What the argument above ignores is that the symmetry broken by the ground state of the superfluid was a *global* phase U(1). However, as explained on page267, the microscopic action of the superconductor possesses a more structured *local* gauge U(1) symmetry. As we will discuss momentarily, that difference entails drastic phenomenological consequences.

7.3.6 Action of the Goldstone Mode[23]

The consequences of the local gauge symmetry can only be explored in conjunction with the electromagnetic field $(\phi, \mathbf{A})$. We thus go back to our anchestor action (7.35) where, however, $\mathcal{G}$ is now meant to represent the full Gorkov Green function (7.33). For the moment, there is no need to specify the origin of the electromagnetic field, i.e. the field might represent an external probe applied by an experimentalist, or the background electromagnetic field controlled by the vacuum action $S_{\text{E.M.}} = \frac{1}{4}\int d\mathbf{x}d\tau F_{\mu\nu}F_{\mu\nu}$, where $F_{\mu\nu} = \partial_\mu A_\nu - \partial_\nu A_\mu$ is the electromagnetic field tensor[24]. However, in all what we are doing we will assume that the field is weak enough so as not to destroy the phenomenon of superconductivity, i.e. the mean modulus of the order parameter is still given by the value Δ_0, as described by the analysis of the previous section.

So, how then might an action describing the interplay of the phase degree of freedom and the electromagnetic field look like? Below we will derive that action by an explicit derivation, starting from the prototype (7.35). However, for the moment, let us stay on a less rigorous level and try to determine the structure of the action by *symmetry reasoning*. In doing so, we will be guided by a number of principles:

- ▷ The phase θ is a Goldstone mode, i.e. the action cannot contain terms that do not vanish in the limit $\theta \to$ const..
- ▷ We assume both gradients acting on the phase θ (but not neccessarily the phase itself) and the electromagnetic potentials to be small. That, is, we will be content with determining the structure of the action to lowest order in these quantities.

[22] The motivation for transforming by 2θ is that under a gauge transformation $\bar{\psi} \to e^{i\theta}\bar{\psi}$, the composite field $\Delta \sim \bar{\psi}\bar{\psi}$ should pick up *two* phase factors. However, the introduction of that muliplictiy factor is of course just a matter of convention; it can always be removed by rescaling of the field θ.

[23] To keep the notation simple, a unit charge convention $e = 1$ will be used throughout this section.

[24] Notice that we are working within the framework of imaginary time, or Eucilidean field theory, i.e. the definition of the field strength tensor does not involve a Minkovski metric (cf. the discussion on p ??.)

▷ By symmetry, the action must not contain terms with an odd number of derivatives. Nor for that matter mixed gradients of the type $\partial_\tau\theta\boldsymbol{\partial}\theta$. Reflecting a property of the microscopic model, the action must be rotational invariant.

▷ The action must be invariant under the local gauge transformation (7.29).

The first three criteria of that list would be satisfied by the trial action

$$S[\theta] = \int d\tau \int d^dx \, \left[c_1\partial_\tau\theta\partial_\tau\theta + c_2\boldsymbol{\partial}\theta\boldsymbol{\partial}\theta\right],$$

where c_1 and c_2 are constants. However, that action is clearly not invariant under a gauge shifting of the phase $\theta(\mathbf{x},\tau) \to \theta(\mathbf{x},\tau) + \varphi(\mathbf{x},\tau)$. It can, however, be endowed with that quality by minimal substitution of the electromagnetic potential:

$$S[\theta, A] = \int d\tau \int d^dx \, \left[c_1(\partial_\tau\theta - \phi)(\partial_\tau\theta - \phi) + c_2(\boldsymbol{\partial}\theta - \mathbf{A})(\boldsymbol{\partial}\theta - \mathbf{A})\right]. \tag{7.41}$$

Up to the order of two gradients, that action uniquely describes the energy cost associated to phase fluctuations. In combination with the action $S_{\text{E.M.}}$ controlling the fluctuation behaviour of the field $(\phi, \mathbf{A})$, it should provide us with a reasonably general description of the low energy electromagnetic properties of the superconductor. Notice, however, that the present line of arguments does not fix the coupling constants $c_{1,2}$. In particular, we cannot exclude that c_1 or c_2 vanish (as would be the case, e.g., for a non-superconducting system, cf. the problem set.) To determine the values of $c_{1,2}$ we need to either derive the action microscopically or to come up with more phenomenological input (see the two info blocks below). Either way one obtains

$$\begin{aligned} c_2 &= \frac{n_s}{2m} \\ c_1 &= \nu, \end{aligned} \tag{7.42}$$

where we have defined n_s as the density of the Cooper pair condensate. (For a precise definition, see below.)

▷ INFO. Beginning with c_2, let us briefly discuss the **phenomenological derivation** of the coupling constants. The starting point is the observation that the functional derivative

$$\left\langle \frac{\delta S}{\delta \mathbf{A}(\mathbf{x},\tau)} \right\rangle = \langle \mathbf{j}(\mathbf{x},\tau)\rangle$$

gives the expectation value of the current density operator. That relation follows on quite general grounds from the fact that a vector potential couples to the action of a system of charged particles $i = 1, \ldots, N$ through (cf. textbooks on classical mechanics)

$$S_{\mathbf{A}} \equiv \int d\tau \sum_i \dot{\mathbf{x}}_i \cdot \mathbf{A}(\mathbf{x}_i) = \int d\tau \int d^dx \sum_i \delta(\mathbf{x} - \mathbf{x}_i)\dot{\mathbf{x}}_i \cdot \mathbf{A}(\mathbf{x},\tau).$$

However, $\mathbf{j} = \frac{\delta S}{\delta A(\mathbf{x},\tau)} = \sum_i \delta(\mathbf{x} - \mathbf{x}_i(\tau))\dot{\mathbf{x}}_i(\tau)$ is just the definition of the total particle current density. Indeed, it is straightforward to verify that on the microscopic level (cf. e.g. Eq. (7.26))

$$\left\langle \frac{\delta S}{\delta \mathbf{A}} \right\rangle = \frac{1}{2m} \left\langle \bar{\psi}_\sigma(-i\boldsymbol{\partial} - \mathbf{A})\psi_\sigma + [(i\boldsymbol{\partial} - \mathbf{A})\bar{\psi}_\sigma]\psi_\sigma \right\rangle \equiv \langle \mathbf{j}\rangle,$$

where $\mathbf{j}$ is the quantum current density operator. Staying for a moment on the microscopic side of the theory, let us *assume* that a certain fraction of the formerly uncorrelated electronic states participates in the condensate. I.e. we write $\mathbf{j} = \mathbf{j}_{\rm n} + \mathbf{j}_{\rm s}$, where $\mathbf{j}_{\rm n}$, the current carried by the normal states of the system, will not be of further concern to us while $\mathbf{j}_{\rm s}$ is the 'supercurrent' carried by the condensate. Let us further assume that those states $\psi^{\rm s}$ participating in the condensate, carry a 'collective' phase θ with a non-vanishing average value, i.e. $\psi^{\rm s} = e^{i\theta}\tilde{\psi}^{\rm s}$, where the states $\psi^{\rm s}$ do not carry an structured phase information (i.e. the residual phase carried by the local amplitude $\tilde{\psi}^{\rm s}$ tends to average to zero.) Then, concentrating on the phase information carried by the condensate states and neglecting density fluctuations,

$$\left\langle \frac{\delta S}{\delta \mathbf{A}} \right\rangle \simeq \langle \hat{\mathbf{j}}^{\rm s} \rangle \simeq -\frac{n_s}{m} \langle \boldsymbol{\partial}\theta - \mathbf{A} \rangle$$

where $n_s \equiv \bar{\psi}^{\rm s}_\sigma \psi^{\rm s}$ is the density of the condensate.

Now, let us evaluate the fundamental relation $\langle \frac{\delta S}{\delta \mathbf{A}} \rangle = \langle \mathbf{j} \rangle$ on our trial action with its undetermined coupling constants:

$$\langle \mathbf{j} \rangle \stackrel{!}{=} \left\langle \frac{\delta S[\tilde{A}]}{\delta A} \right\rangle = -2c_2 \langle \boldsymbol{\partial}\theta - \mathbf{A} \rangle$$

Comparison with our phenomenological estimate for the expectation value of the (super)current operator above leads to the identification

$$c_2 = \frac{n_s}{2m}.$$

Turning to the coupling constant c_1, let us assume an electronic system has been subjected to a weak external potential modulation $\phi(\mathbf{x}, \tau)$. Assuming that the modulation fluctuates slowly enough to let the system adiabatically adjust to it (i.e. that it acts like a local modulation of the chemical potential) the particle density of the system would change as

$$\delta n(\mathbf{x}, \tau) = \delta n(\mu + \phi(\mathbf{x}, \tau)) \approx \frac{\partial n}{\partial \mu} \phi(\mathbf{x}, \tau) \approx \nu \phi(\mathbf{x}, \tau),$$

where we have approximately[25] identified $\partial_\mu n$ with the single particle density of states ν. The potential energy corresponding to the charge modulation is given by $\int d^d x\, \phi(\mathbf{x}, \tau) \delta n(\mathbf{x}, \tau) = \partial_\mu n \int d^d x\, \phi^2(\mathbf{x}, \tau)$. Comparing that expression with our trial action – which contains the time-integrated potential – we conclude that

$$c_1 = \partial_\mu n = \nu.$$

▷ INFO. For readers feeling ill at ease with the notoriously many 'assumes' of our previous discussion, we now derive the phase action by explicit **microscopic derivation**. The construction detailed below represents a typical, and our so-far most advanced, 'case study' of constructions of low energy quantum field theories in condensed matter physics. Although

[25] For systems with strong interparticle correlations, the **thermodynamic density of states** $\partial_\mu n = \frac{1}{L^2} \partial_\mu N$ may deviate significantly from the **single particle density of states** $\nu = \frac{1}{L^d} \sum_a \delta(\epsilon_a - \mu)$.

formulated for the specific example of the BCS superconductor, many of its structural sub-units appear in other applications in basically the same form. That 'universality' is our prime motivation for presenting the – admittedly lengthy – construction of the low-energy phase action of the superconductor in some detail.

Our starting point is the Gorkov Green function appearing under the 'tr ln' of the microscopic action (7.35)

$$\hat{\mathcal{G}}^{-1} = \begin{pmatrix} -\partial_\tau - i\phi - \frac{1}{2m}(-i\boldsymbol{\partial} - \mathbf{A})^2 + \mu & \Delta_0 e^{2i\theta} \\ \Delta_0 e^{-2i\theta} & -\partial_\tau + i\phi + \frac{1}{2m}(-i\boldsymbol{\partial} - \mathbf{A})^2 - \mu \end{pmatrix},$$

coupled to the full electromagnetic potential. To simplify the problem, we have set the modulus of the order parameter to Δ_0, i.e. concentrating on the Goldstone mode, we neglect massive flucutations $\Delta = \Delta_0 + \delta\Delta$ around the extremum of the free energy.

We next use the gauge freedom inherent to the theory to remove the phase dependence of the order paramter field. To do so, we introduce the unitary matrix

$$\hat{U} \equiv \begin{pmatrix} e^{-i\theta} & \\ & e^{i\theta} \end{pmatrix}$$

and transform the Green function as

$$\hat{\mathcal{G}}^{-1} \to \hat{U}\hat{\mathcal{G}}^{-1}\hat{U}^\dagger = \begin{pmatrix} -\partial_\tau - i\tilde{\phi} - \frac{1}{2m}(-i\boldsymbol{\partial} - \tilde{\mathbf{A}})^2 + \mu & \Delta_0 \\ \Delta_0 & -\partial_\tau + i\tilde{\phi} + \frac{1}{2m}(-i\boldsymbol{\partial} - \tilde{\mathbf{A}})^2 - \mu \end{pmatrix},$$

where the transformed electromagnetic potential is given by (exercise)

$$\tilde{\phi} = \phi + \partial_\tau\theta,$$
$$\tilde{\mathbf{A}} = \mathbf{A} - \boldsymbol{\partial}\theta.$$

(Reading the transformation in reverse we conclude that – an important physical fact that should be remembered – *the superconductor order parameter field is a gauge non-invariant quantity.* Under gauge trasformations it transforms as $\Delta \to e^{2i\theta}\Delta$, as suggested by the definition of $\Delta \sim \bar{\psi}\bar{\psi}$ as a pairing field. This fact entails, e.g., that the order parameter itself cannot be an experimentally accessible observable[26].) Due to unitary invariance of the trace, $\mathrm{tr}\ln(\hat{\mathcal{G}}^{-1}) = \mathrm{tr}\ln(\hat{U}\hat{\mathcal{G}}^{-1}\hat{U}^\dagger)$, the gauge transformed and the original Green function, respectively, equivalently represent the theory.

(Safe for the neglect of massive fluctuations $\delta\Delta$,) our so far treatment of the theory has been exact. However, to make further progress, we need to resort to approximations: Assuming that both the electromagnetic potential and spatio-temporal fluctuations of the phase mode are small, we will expand the action in powers of $(\tilde{\phi}, \tilde{\mathbf{A}})$. In the literature, expansions of this type are known as **gradient expansions**. I.e. we are performing an expansion were not the phase degree of freedom θ itself (due to its Goldstone character, θ can slide freely over the entire interval $[0, 2\pi]$) but rather its *gradients* $\partial_\tau\theta$, $\boldsymbol{\partial}\theta$ are assumed to be small.

To facilitate that expansion, it will be useful to represent the 2×2-matrix structure of the Green function through a Pauli matrix expansion:

$$\hat{\mathcal{G}}^{-1} = -\sigma_0\partial_\tau - \sigma_3\left(i\tilde{\phi} + \frac{1}{2m}(-i\boldsymbol{\partial} - \tilde{\mathbf{A}}\sigma_3)^2 - \mu\right) + \sigma_1\Delta_0 =$$
$$= \underbrace{-\sigma_0\partial_\tau - \sigma_3\left(-\frac{1}{2m}\partial^2 - \mu\right) + \sigma_1\Delta_0}_{\hat{\mathcal{G}}_0^{-1}} \underbrace{- i\sigma_3\tilde{\phi} + \frac{i}{2m}\sigma_0[\boldsymbol{\partial}, \tilde{\mathbf{A}}]_+}_{\hat{\chi}_1} \underbrace{- \sigma_3\frac{1}{2m}\tilde{\mathbf{A}}^2}_{\hat{\chi}_2},$$

[26] This follows from the fundamental doctrine of electrodynamics that gauge transformations must not cause observable effects.

where we have defined $\sigma_0 \equiv \mathbf{1}$. Expressed in terms of these quantities, the expansion of the action to first and second order in the field $\tilde{A}$ assumes the form

$$S[\tilde{A}] = -\mathrm{tr}\ln\left(\hat{\mathcal{G}}_0^{-1} - \hat{\mathcal{X}}_1 - \hat{\mathcal{X}}_2\right) = \text{const.} - \mathrm{tr}\ln\left(1 - \hat{\mathcal{G}}_0[\hat{\mathcal{X}}_1 + \hat{\mathcal{X}}_2]\right) =$$
$$= \text{const.} + \underbrace{\mathrm{tr}\left(\hat{\mathcal{G}}_0\hat{\mathcal{X}}_1\right)}_{S^{(1)}[\tilde{A}]} + \underbrace{\mathrm{tr}\left(\hat{\mathcal{G}}_0\hat{\mathcal{X}}_2 + \frac{1}{2}\hat{\mathcal{G}}_0\hat{\mathcal{X}}_1\mathcal{G}_0\hat{\mathcal{X}}_1\right)}_{S^{(2)}[\tilde{A}]} + \ldots, \tag{7.43}$$

where we used that $\hat{\mathcal{X}}_{1,2}$ are of fist and second order in the field, respectively. (Structures of this type appear frequently in the construction of low energy quantum field theories of many body systems. I.e. after the introduction of some auxiliary field ϕ through a suitably devised Hubbard-Stratonovich transformation, the microscopic bose/fermi degrees of freedom of the theory can be integrated out and one arrives at an action $\pm\,\mathrm{tr}\,\ln(\hat{\mathcal{G}}_0^{-1} + \hat{X}[\phi])$, where $\hat{\mathcal{G}}$ is the non-interacting Green function of the problem and $\hat{X}[\phi]$ an operator depending on the new field. An expansion of the logarithm to first and second order in $\hat{X}$ then leads to structures similar to those given above.)

In a more explicit way of writing, the first order action $S^{(1)}$ reads as (exercise)

$$S^{(1)}[\tilde{A}] = \frac{T}{L^d}\sum_p\ \mathrm{tr}\ \left[\hat{\mathcal{G}}_{0,p}\hat{\mathcal{X}}_1(p,p)\right] =$$
$$= \frac{T}{L^d}\sum_p\ \mathrm{tr}\ \left[\hat{\mathcal{G}}_{0,p}\left(i\sigma_3\tilde{\phi}_0 + \frac{i}{m}\sigma_0\mathbf{p}\cdot\tilde{\mathbf{A}}_0\right)\right],$$

where the subscripts 0 refer to the zero-momentum component of the fields $\tilde{\phi}$ and $\tilde{\mathbf{A}}$. Since the Green function $\hat{\mathcal{G}}_0$ is even in the momentum, the second contribution $\propto \mathbf{p}$ vanishes by symmetry. Further $(\partial_\tau\theta)_0 = 0\cdot\theta_0 = 0$, i.e. $\tilde{\phi}_0 = \phi_0$, i.e.

$$S^{(1)}[\tilde{A}] = \frac{iT}{L^d}\sum_p(\hat{\mathcal{G}}_{0,p,11} - \hat{\mathcal{G}}_{0,p,22})\phi_0,$$

where the indices refer to particle-hole space. To understand the meaning of that expression, notice that $\hat{\mathcal{G}}_{0,p,11} = \langle\bar{\psi}_{\uparrow,p}\psi_{\uparrow,p}\rangle_0$ gives the expectation value of the electronic spin-up density operator on the background of a fixed order parameter background. Similarly, $-\hat{\mathcal{G}}_{0,p,22} = -\langle\psi_{\downarrow,p}\bar{\psi}_{\downarrow,p}\rangle_0 = +\langle\bar{\psi}_{\downarrow,p}\psi_{\downarrow,p}\rangle_0$ gives the spin-down density. Summation of these sum of these expressions over frequencies and momenta produces the full electronic density: $\frac{T}{L^d}\sum_p(\hat{\mathcal{G}}_{0,p,11} - \hat{\mathcal{G}}_{0,p,22}) = \frac{N}{L^d}$, or

$$S^{(1)}[\tilde{A}] = iN\phi_0 = \frac{iN}{L^d}\int_0^\beta d\tau\int d^dx\,\phi(\mathbf{x},\tau).$$

Thus, the first contribution to our action simply describes the electrostatic coupling of the scalar potential to the total charge of the electron system. However, as with the Coulomb potential discussed above, the 'correct' interpretation of that expression is $S^{(1)} = 0$. That is, the total electrostatic interaction of the potential with the electron system must be – charge neutrality – compensated by an equally strong interaction with the positive counter charge of the ions (which is usually not indicated explicitly for notational convenience.)

We thus turn to the discussion of the second order action $S^{(2)}$. The term containing $\hat{\mathcal{X}}_2$, is built like the contribution $S^{(1)}$ discussed before. Thus, replacing $\hat{\mathcal{X}}_1$ by $\hat{\mathcal{X}}_2$,

$$\mathrm{tr}(\hat{\mathcal{G}}_0\hat{\mathcal{X}}_2) = \frac{n}{2m}\int_0^\beta\int d^dx\,\mathbf{A}(\mathbf{x},\tau)^2, \tag{7.44}$$

where we have introduced $n \equiv N/L^d$ as the total particle density. This contribution is known as the **diamagnetic term**. This is because it derives from the familiar diamagnetic contribution $\frac{1}{2m}\mathbf{A}^2$ to the electronic Hamiltonian. If it were for the diamagnetic term alone, an external field would lead to an *increase* of the energy. However, to obtain the complete picture, we need to include the magnetic field dependence of the operator $\hat{\mathcal{X}}_1$.

Substituting $\hat{\mathcal{X}}_1$ into our expression of interest, $\frac{1}{2}\mathrm{tr}\left(\hat{\mathcal{G}}_0\hat{\mathcal{X}}_1\hat{\mathcal{G}}_0\hat{\mathcal{X}}_1\right)$, and using that crossterms $\sim \tilde{\phi}\mathbf{p}\cdot\tilde{\mathbf{A}}$ vanish by the oddness of the momentum integration variable, we obtain

$$\frac{1}{2}\mathrm{tr}\left(\hat{\mathcal{G}}_0\hat{\mathcal{X}}_1\hat{\mathcal{G}}_0\hat{\mathcal{X}}_1\right) = \frac{T}{2L^d}\sum_{p,q}\mathrm{tr}\left(-\hat{\mathcal{G}}_{0,p}\,\sigma_3\tilde{\phi}_q\,\hat{\mathcal{G}}_{0,p}\,\sigma_3\tilde{\phi}_{-q} + \frac{1}{m^2}\hat{\mathcal{G}}_{0,p}\,\sigma_0\mathbf{p}\cdot\tilde{\mathbf{A}}_q\,\hat{\mathcal{G}}_{0,p}\,\sigma_0\mathbf{p}\cdot\tilde{A}_{-q}\right), \tag{7.45}$$

where, noting that we are already working at second order of the expansion, the residual dependence of the Green functions $\hat{\mathcal{G}}_0$ on the small momentum variable q has been neglected[27]. Alluding to its origin, viz. the paramagnetic operator $\sim \frac{1}{2m}[\mathbf{p},\tilde{\mathbf{A}}]_+$ of the electronic Hamiltonian, the magnetic contribution to this expression is called a **paramagnetic term**. Paramagnetic contributions to the action describe a *lowering* of the energy in response to external magnetic fields, i.e. the diagmagnetic and the paramagnetic term, respectively stand in competition.

To proceed, it is convenient to change from an explicit matrix representation of the Gorkov Green function to an expansion in terms of Pauli matrices[28]:

$$\begin{aligned}\hat{\mathcal{G}}_{0,p} &= \left[i\sigma_0\omega_n - \sigma_3\xi_{\mathbf{p}} + \sigma_1\Delta_0\right]^{-1} = \\ &= \frac{1}{\omega_n^2 + \xi_{\mathbf{p}}^2 + \Delta_0^2}\left[-i\sigma_0\omega_n - \sigma_3\xi_{\mathbf{p}} + \sigma_1\Delta_0\right].\end{aligned} \tag{7.46}$$

We next plug this representation into (7.45) and make use of relations like ($i,j = 1,2,3; \mu,\nu = 1,2,3,4$)

$$\begin{aligned}\sigma_i^2 = 1, \qquad & i \neq j: \ [\sigma_i,\sigma_j]_+ = 0, \\ \sigma_i\sigma_j = 2i\epsilon^{ijk}\sigma_k, \quad & \mathrm{tr}\,(\sigma_\mu) = 2\delta_{\mu 0},\end{aligned}$$

as well as (exercise)

$$\sum_{\mathbf{p}}(\mathbf{p}\cdot\mathbf{v})\,(\mathbf{p}\cdot\mathbf{v}')F(\mathbf{p}^2) = \frac{\mathbf{v}\cdot\mathbf{v}'}{d}\sum_{\mathbf{p}}\mathbf{p}^2F(\mathbf{p}^2)$$

for any rotationally invariant function $F(\mathbf{p}^2)$ to obtain

$$\begin{aligned}\frac{1}{2}\mathrm{tr}\left(\hat{\mathcal{G}}_0\hat{\mathcal{X}}_1\hat{\mathcal{G}}_0\hat{\mathcal{X}}_1\right) = \frac{T}{L^d}\sum_{p,q}\frac{1}{(\omega_n^2+\lambda_p^2)^2}\times \\ \times\left(\tilde{\phi}_q\tilde{\phi}_{-q}(-\omega_n^2+\lambda_p^2-2\Delta_0^2) - \frac{\mathbf{p}^2\tilde{\mathbf{A}}_q\cdot\tilde{\mathbf{A}}_{-q}}{3m^2}(-\omega_n^2+\lambda_p^2)\right),\end{aligned}$$

[27] i.e. we have set $\sum_{pq}(\hat{\mathcal{G}}_p\tilde{\phi}_q\hat{\mathcal{G}}_{p+q}\tilde{\phi}_{-q}) \approx \sum_{pq}(\hat{\mathcal{G}}_p\tilde{\phi}_q\hat{\mathcal{G}}_p\tilde{\phi}_{-q})$.

[28] A formula useful to remember is

$$\left[v_0\sigma_0 + \mathbf{v}\cdot\boldsymbol{\sigma}\right]^{-1} = \frac{1}{v_0^2-\mathbf{v}^2}\left[v_0\sigma_0 - \mathbf{v}\cdot\boldsymbol{\sigma}\right],$$

where $v = (v_0,\mathbf{v})$ is a four component vector of coefficients.

where, as before, $\lambda_p^2 = \xi_p^2 + \Delta_0^2$. We now substitute the sum of this result and the diamagnetic contribution (7.44) into the expansion (7.43), partially transform back to real space $\sum_q f_q f_{-q} = \int d\mathbf{x} d\tau f(\mathbf{x},\tau)^2$, and arrive at

$$S[\tilde{A}] = \int d^d x \int d\tau \Big[\underbrace{\frac{T}{L^d}\sum_p \frac{-\omega_n^2 + \lambda_p^2 - 2\Delta_0^2}{(\omega_n^2+\lambda_p^2)^2}}_{c_1} \tilde{\phi}(\mathbf{x},\tau)\tilde{\phi}(\mathbf{x},\tau) + \\ + \underbrace{\left(\frac{n}{2m} - \frac{1}{dm^2}\frac{T}{L^d}\sum_p \frac{\mathbf{p}^2(-\omega_n^2+\lambda_p^2)}{(\omega_n^2+\lambda_p^2)^2} \right)}_{c_2} \tilde{\mathbf{A}}(\mathbf{x},\tau)\tilde{\mathbf{A}}(\mathbf{x},\tau) \Big].$$

This intermediate result provides an indentification of our previously undetermined coupling constants $c_{1,2}$. The last step of the derivation, i.e. the sum over the 'fast' momentum p is now a relatively straightforward exercise. Beginning with the frequency summations, we note that the denominator has two isolated poles of second order at $\omega_n = \pm i\lambda_p$. Applying the standard summation rules it is then straightforward to verify that (exercise)

$$T\sum_n \frac{-\omega_n^2 + \lambda_p^2 - 2\Delta_0^2}{(\omega_n^2+\lambda_p^2)^2} = -\frac{1}{2\lambda_p}\left(f_{\rm f}(-\lambda_p)\left(\frac{\Delta}{\lambda_p}\right)^2 + f_{\rm f}'(-\lambda_p)\frac{\xi_p^2}{\lambda_p}\right) + (\lambda_p \leftrightarrow -\lambda_p) \approx -\frac{\Delta^2}{2\lambda_p^3}.$$

$$T\sum_n \frac{-\omega_n^2 + \lambda_p^2}{(\omega_n^2+\lambda_p^2)^2} = -\beta[f_{\rm f}(\lambda_p)(1-f_{\rm f}(\lambda_p)].$$

Thus, the coupling constant of the **potential contribution**,

$$c_1 = -\frac{1}{L^d}\sum_{\mathbf{p}} \frac{\Delta^2}{\lambda_p^3} = -\frac{\nu}{2}\int d\xi \frac{\Delta^2}{(\xi^2+\Delta^2)^{3/2}} = -\nu,$$

in agreement with our previous estimate. With the **magnetic contribution**, the situation is more interesting. Converting the momentum sum to an energy integral as usual, we obtain

$$c_2 = \frac{n}{2m} - \frac{\nu\mu}{dm}\int d\xi(-\beta)[f_{\rm f}(\lambda)(1-f_{\rm f}(\lambda)],$$

where we noted that the integrand is strongly peaked at the Fermi surface, i.e. that $\mathbf{p}^2 \approx 2m\mu$ can be pulled out of the integral.

This expression illustrates the competition of the diagmagnetic and the paramagnetic contribution in the magnetic response of the system. At for *small temperatures*, $T \ll \Delta$, the positivity of $\lambda_p = (\Delta^2 + \xi_p^2)^{1/2} \geq \Delta$ implies $f(\lambda_p) \approx 0$, i.e. approximate vanishing of the integral. Under these conditions,

$$c_2 \overset{T\ll\Delta}{\approx} \frac{n}{2m}$$

is weighted by the total density of the electron gas, and the response of the system is governed by the diagmagnetic term alone. Indeed, diamagnetic response is known to be a hallmark of superconductivity; the superconductor doesn't like magnetic fields, a phenomenon that culminates in the Meissner effect to be discussed shortly.

In contrast, for *large temperatures*, $T \gg \Delta$, the integral extends over energy domains much larger than Δ and we can approximate

$$\int d\xi(-\beta)[f_{\rm f}(\lambda)(1-f_{\rm f}(\lambda)] \approx \int_0^\infty d\xi(-\beta)[f_{\rm f}(\xi)(1-f_{\rm f}(\xi)] = -\int_0^\infty d\xi \partial_\xi f_{\rm f}(\xi) = f_{\rm f}(0) - f_{\rm f}(\infty) = 1,$$

to obtain[29]

$$c_2 \overset{T\gg\Delta}{\approx} \frac{n}{2m} - \frac{\nu\mu}{dm} = 0.$$

The near[30] cancellation of dia- and paramagnetic contributions is typicial for the response of normal conducting systems to external magnetic fields.

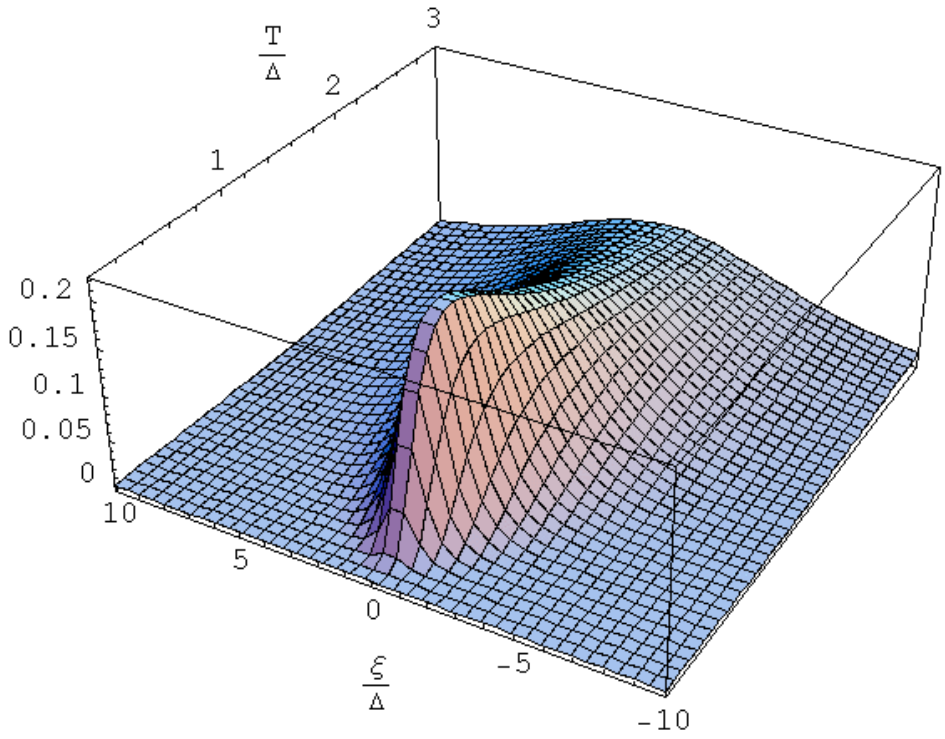

Figure 7.18: Plot of the function $\beta f_{\rm f}(\sqrt{\xi^2+\Delta^2})\left[1-f_{\rm f}(\sqrt{\xi^2+\Delta^2})\right]$ as a function of the dimensionless scales T/Δ and ξ/Δ. For $T/\Delta \to 0$, the function vanishes ($\to$ perfect diamagnetic respsonse). For $\frac{T}{\Delta} \gg 1$, the function traces out a peak of width $\propto T$ and total weight $\int f(1-f) = 1$ ($\to$ cancellation of dia- and paramagnetic response). At intermediate temperatures, $\int f(1-f) < 1$, resulting in a partial survival of diamagnetism.

At *intermediate* temperatures, the integral over the Fermi functions leads to a partial can-

[29] The last equality is straightforwardly verified by comparison of the two definitions

$$\left.\begin{matrix}\nu\\ n\end{matrix}\right\} = \frac{2}{L^d}\sum_{\mathbf{p}} \left\{\begin{matrix}\delta(\mu-\xi_p)\\ \Theta(\mu-\xi_p)\end{matrix}\right. = \frac{2}{(2\pi)^d}\int d^dp \left\{\begin{matrix}\delta(\mu-\xi)\\ \Theta(\mu-\xi)\end{matrix}\right. .$$

[30] Going beyond second lowest order perturbation theory in **A**, a careful analysis of the coupling of a (small) magnetic field to the orbital degrees of freedom of the Fermi gas shows that the cancellation of dia- and paramagnetic contributions is not perfect. The total response of the system is described by a weak diamagnetic contribution, $\chi_{\rm d}$, a phenomenon known as **Landau diamagnetism**. The diamagnetic orbital response is over-compensated by **Pauli paramagnetism**, i.e. the three times larger paramagnetic response of the Zeeman-coupled electron spin, $\chi_{\rm p} = -3\chi_{\rm d}$. For large magnetic fields, the situation changes totally, and more pronounced effects such as **Shubnikov de-Haas oscillations** or even the **quantum Hall effect** are observed.

cellation of the diamagnetic response. It is common to express that fact through the notation,

$$c_2 = \frac{n_s}{2m},$$

where the parameter

$$n_s \equiv n - \frac{2\nu\mu}{d}\int d\xi(-\beta)[f_{\rm f}(\lambda)(1-f_{\rm f}(\lambda)]$$

is known as the **superfluid density**. Historically, the concept of a 'superfluid density' was introduced at pre-BCS times, when a phenomenological model known as the **two fluid model** represented the state of the art of understanding superconductivity. (Remember that the experimental discovery of superconductivity preceeded its microscopic understanding by more than four decades!) The basic picture underlying that approach was that below the transition, a fraction of the electron system condenses into a dissipationless superfluid of density n_s, while the rest of the electrons remains in the state of a 'normal' Fermi liquid of density $n_n = n - n_s$. That simple model provided a phenonmenological explanation of a large number of superconductor phenomena, prior to the development of the first principle mircroscopic understanding in terms of BCS theory.

However, notwithstanding its success and its appealing simplicity, the two-fluid notion of a complete condensation $n_s(T \to 0) \to n$ at low temperatures cannot be maintained. Indeed, we have seen that BCS superconductivity is a Fermi surface phenomenon, i.e. the bulk of the electrons is oblivious to the existence of an attraction mechanism at energies $\mu \pm \omega_D$ and, therefore, will not enter a condensed state. Instead, our microscopic analysis produces a picture more subtle than the mere superposition of two fluids: As we saw above, the diamagnetic (paramagnetic) contribution to the response is provided by all quasi-particles (quasi-particles at the Fermi surface). In a normal metal, or, equivalently, a superconductor at $T \gg \Delta$, quasi-particle excitations at the Fermi surface conspire to cancel the diamagnetic contribution of all other quasi-particles. However, at $T \ll \Delta$ the existence of a Fermi surface quasi-particle *gap* blocks that compensation mechanism and a net diamagnetic signal remains. The farreaching phenomenological consequences of the sustained diamagnetic contribution will be discussed in the next section.

However, before leaving this section let us discuss one last technical point. Above we have – without much of a justification – expanded the phase action up to leading order in the gradients $\partial_\tau\theta$ and $\boldsymbol{\partial}\theta$. What is the **logics behind the gradient expansion**, i.e. why are we permitted to truncate the expansion at leading order? This question arises whenever low energy effective theories are derived from a microscopic parent theory by expanding in slow fluctuations, and it is worthwhile to address it in a general setting.

So, let us suppose we had performed some kind of Hubbard-Stratonovich transformation to describe a system of interest in terms of an action $S[\phi]$. We further assume that the action is invariant under a shift of the field by a constant, $\phi(\mathbf{x}) \to \phi(\mathbf{x}) + \phi_0$, i.e. that the action depends only on gradients $\partial\phi$. (To keep the notation simple, we do not explicitly distinguish between spatial and temporal gradients.) An expansion of the action in the field gradients then leads to a series of the formal momentum-space structure

$$S \sim N\sum_q \left[(l_0 q)^2\phi_q\phi_{-q} + (l_0 q)^4\phi_q\phi_{-q} + \ldots\right],$$

where N represents the large parameter of the theory[31], l_0 is some microscopic reference scale of [length] needed to make the action dimensionless, and the ellipses stand for terms of higher order

[31] In theories containing a large parameter N, that parameter mostly appears as a constant multiplying

in q and/or ϕ_q. Now, using that only field configurations with $S \sim 1$ significantly contribute to the field integral, we obtain the estimate

$$\phi_q \sim \frac{1}{\sqrt{N}} \frac{1}{l_0 q}$$

from the leading order term of the action. This means that terms of higher order in the field variable, $N(l_0 q \phi_q)^{n>2} \sim N^{1-n/2}$ are small in inverse powers of the large parameter of the theory and can be neglected. Similarly, terms like $N(l_0 q)^{n>2} \phi_q \phi_{-q} \sim (l_0 q)^{n-2}$. As long as we are interested in large scale fluctuations on scales $q^{-1} \gg l_0$, these terms, too, can be neglected.

Notice, that our justification to neglect terms of higher order relies on *two* independent parameters, large N and the smallness of the scaling factor $q l_0$. If $N = 1$ but still $q l_0 < 0$, terms involving two gradients but large powers of the field $\sim q^2 \phi_q^{n>2}$ are no longer negligible. Conversely, if $N \gg 1$ but one is interested in scales $q l_0 \simeq 1$, terms of second order in the field weighted by a large number of gradients $\sim q^{n>2} \phi_q^2$ must be taken into a account. An incorrect treatment of this point has been the source of numerous errors in the published literature!

7.3.7 Meissner Effect and Anderson-Higgs Mechanism

If you ask a person on the street to give a one-line definition of superconductivity, the answer will probably be that superconductors are metallic specimen showing no electrical resistance. However, to a physicist, that definition should have something unsatisfactory to it. It highlights only one of many remarkable features of superconductors and does not have any predicitive power. A better – if for most people incomprehensible – attempt of a definition would be to say that superconductivity arises when the quantum phases of a macroscopically large number of charged particles get locked to a collective degree of freedom. Indeed, that is exactly, what the action (7.41) tells us. Fluctuations of the phase of the condensate are penalized by a cost that scales with the (superfluid) density of the electron gas. This is to be contrasted to the situation in a normal metal where the action – the cancellation of the diamagnetic and the paramagnetic contribution! – usually does not contain the gradients of phase-like degrees of freedom.

Indeed, the macroscopic phase solidity of the BCS ground state wave function suffices to explain a large number of non-trivial phenomena related to superconductivity. To see this, let us consider a simplified version of the action (7.41). Viz., let us assume that (i) the temperature is high enough to exclude quantum fluctuations of the phase, $\partial_\tau \theta = 0$, and that there is no electric fields acting on our superconductor $\phi = 0, \partial_\tau \mathbf{A}(\tau) = 0$.

▷ INFO. Why do we relate the presence of **quantum fluctuations** to **temperature**? Let us re-iterate (cf. the remarks made on page 244) that a temporarily constant field variable acts like a classical degree of freedom. To understand why large temeperatures inhibit temporal fluctuations

all, or at least several operators of the action. E.g. in the fermionic problems discussed above, where N was proporitional to the density of states at the Fermi surface, the action contained a trace over all momentum states. The summation over these states then led to an overall factor N multiplying the action.

superimposed on the classical sector, let us take the phase action of the superconcutor as an example and write,

$$S[\theta] = \nu \int_0^\beta d\tau \int d^d x \, (\partial_\tau \theta)^2 + S_{\rm cl}[\theta],$$

where the first term determines the temporal fluctuation behaviour of the phase field, while $S_{\rm cl}$ is the 'classical' contribution to the action, i.e. the contribution independent of time derivatives. Switching to a frequency representation,

$$S[\theta] = \nu \sum_{m,\mathbf{q}} \omega_m^2 \theta_{m,\mathbf{q}} \theta_{-m,-\mathbf{q}} + S_{\rm cl}[\theta],$$

wherefrom we infer that quantum fluctuations, i.e. modes $\theta_{m\neq 0}$, become inessential at large temperatures. More specifically, modes with non-vanishing Matsubara frequency can be neglected when the quantum fluctuation energy (density) $\nu\omega_m^2 \propto T^2$ exceeds the characteristic energy scales appearing in $S_{\rm cl}[\theta]$.

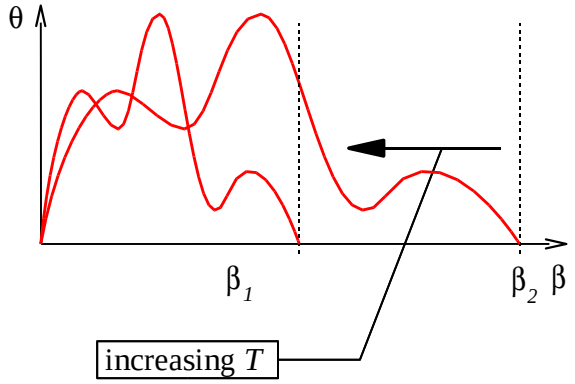

Figure 7.19: Qualitative picture behind the quadratic $\sim T^2$ energy increase of quantum fluctuations. As the temperature T is increased, the imaginary time interval $[0, \beta = T^{-1}]$ gets squeezed. The same happens to the temporal profiles of (quantum) fluctuating modes $\theta(\tau)$. Consequently, gradients $\partial_\tau \theta \propto T$ increase linearly with temperature, and the energy density $\sim (\partial_\tau\theta)^2 \propto T^2$ grows quadratically.

To heuristically understand the temperature scaling of the fluctuation energy, remember that the bose field $\theta(\tau)$ obeys periodic boundary conditions $\theta(0) = \theta(\beta)$. Inspection of Fig. 7.19 then shows that increasing the temperature, i.e. squeezing of the imaginary time interval $[0, \beta]$, leads to a linear increase of the gradients $\partial_\tau\theta \propto T$. Accordinly, the squared gradient appearing in the action increases quadratically with T. This mechanism confirms the intuitive expectation that quantum fluctuations – i.e. fundamentally a low energy phenomenon – should be damped out at increasing temperature.

Under these conditions, the action simplifies to

$$S[\mathbf{A}, \theta] = \beta \int d^d r \, \left[\frac{n_s}{2m} (\boldsymbol{\partial}\theta - \mathbf{A}) \cdot (\boldsymbol{\partial}\theta - \mathbf{A}) + \frac{1}{2} (\boldsymbol{\partial} \wedge \mathbf{A}) \cdot (\boldsymbol{\partial} \wedge \mathbf{A}) \right],$$

where we have explicitly included the action

$$\frac{1}{4} \int d\tau \int d^d x \, F_{\mu\nu} F_{\nu\mu} \overset{\phi=0, \mathbf{A}\,\text{static}}{=} \frac{\beta}{2} (\boldsymbol{\partial} \wedge \mathbf{A}) \cdot (\boldsymbol{\partial} \wedge \mathbf{A}) = \frac{\beta}{2} \int d^d r \, \mathbf{B} \cdot \mathbf{B}$$

due to fluctuations of the magnetic field and the notation

$$(\mathbf{v} \wedge \mathbf{w})_i \equiv (\mathbf{v} \times \mathbf{w})_i = \epsilon^{ijk} v_j w_k$$

is used. As pointed out above, the action is invariant under the gauge transformation $\mathbf{A} \to \mathbf{A} + \boldsymbol{\partial}\phi$, $\theta \to \theta + \phi$. One thus expects that integration over all realizations of θ – a doable task because the action is quadratic – will produce a purely $\mathbf{A}$-dependent, and gauge invariant action $S[\mathbf{A}]$. The integration over θ is most transparently formulated in momentum space where the action assumes the form

$$\begin{aligned} S[\mathbf{A},\theta] &= \beta \sum_{\mathbf{q}} \left(\frac{n_s}{2m} (i\mathbf{q}\theta_{\mathbf{q}} - \mathbf{A}_{\mathbf{q}}) \cdot (-i\mathbf{q}\theta_{-\mathbf{q}} - \mathbf{A}_{-\mathbf{q}}) + \frac{1}{2} (\mathbf{q} \wedge \mathbf{A}_{\mathbf{q}}) \cdot (\mathbf{q} \wedge \mathbf{A}_{-\mathbf{q}}) \right) = \\ &= \beta \sum_{\mathbf{q}} \left(\frac{n_s}{2m} [\theta_{\mathbf{q}} q^2 \theta_{-\mathbf{q}} - 2i\theta_{\mathbf{q}} \mathbf{q} \cdot \mathbf{A}_{-\mathbf{q}} + \mathbf{A}_{\mathbf{q}} \cdot \mathbf{A}_{-\mathbf{q}}] + \frac{1}{2} (\mathbf{q} \wedge \mathbf{A}_{\mathbf{q}}) \cdot (\mathbf{q} \wedge \mathbf{A}_{\mathbf{q}}) \right) \end{aligned}$$

The integration over the field components $\theta_{\mathbf{q}}$ is now straightforward and leads to an effective action for $\mathbf{A}$: $e^{-S[\mathbf{A}]} \equiv \int \Delta\theta e^{-S[\mathbf{A},\theta]}$, where

$$S[\mathbf{A}] = \beta \sum_{\mathbf{q}} \left(\frac{n_s}{2m} \left(\mathbf{A}_{\mathbf{q}} \cdot \mathbf{A}_{-\mathbf{q}} - \frac{(\mathbf{q} \cdot \mathbf{A}_{\mathbf{q}})(\mathbf{q} \cdot \mathbf{A}_{-\mathbf{q}})}{q^2} \right) + \frac{1}{2} (\mathbf{q} \wedge \mathbf{A}_{\mathbf{q}}) \cdot (\mathbf{q} \wedge \mathbf{A}_{\mathbf{q}}) \right).$$

To bring this result into a more suggestive form, let us split the vector potential into a **longitudinal and a transverse component**:

$$\mathbf{A}_{\mathbf{q}} = \underbrace{\mathbf{A}_{\mathbf{q}} - \frac{\mathbf{q}(\mathbf{q} \cdot \mathbf{A}_{\mathbf{q}})}{q^2}}_{\mathbf{A}^{\perp}_{\mathbf{q}}} + \underbrace{\frac{\mathbf{q}(\mathbf{q} \cdot \mathbf{A}_{\mathbf{q}})}{q^2}}_{\mathbf{A}^{\parallel}_{\mathbf{q}}}. \tag{7.47}$$

To motivate this decomposition, notice that

- ▷ the transverse component alone determines physical quantities, i.e. the magnetic field. (This follows from $\mathbf{B}_{\mathbf{q}} = i\mathbf{q} \wedge \mathbf{A}_{\mathbf{q}}$ and $\mathbf{q} \wedge \mathbf{q} = 0$.)
- ▷ The transverse component is gauge invariant. Under a gauge, $\mathbf{A}_{\mathbf{q}} \to \mathbf{A}_{\mathbf{q}} + i\mathbf{q}\phi_{\mathbf{q}}$. But $(\mathbf{q}\,\phi_{\mathbf{q}})^{\perp} = 0$. In the language of longitudinal/transverse components, the Coulomb gauge corresponds to a configuration where $\mathbf{A}^{\parallel} = 0$.
- ▷ the denotation 'longitudinal component' emphasizes that $\mathbf{F}^{\parallel}_{\mathbf{q}}$ is the projection of a vector field $\mathbf{F}_{\mathbf{q}}$ onto the argument vector $\mathbf{q}$. Correspondingly, the 'transverse component' is the orthogonal complement of the longitudinal component.

Applying some elementary rules of vector algebra, it is straightforward to verify that the effective action can be represented in the simple form

$$S[\mathbf{A}] = \frac{\beta}{2} \sum_{\mathbf{q}} \left(\frac{n_s}{m} + q^2 \right) \mathbf{A}^{\perp}_{\mathbf{q}} \cdot \mathbf{A}^{\perp}_{-\mathbf{q}}. \tag{7.48}$$

At this stage, it is worthwhile to stop and see what we have got: (i) Starting from a composite action containing the Goldstone mode θ and the gauge field $\mathbf{A}$, we have arrived at an action for the gauge field alone. In a way, the Goldstone mode has been absorbed into the (gauge degrees of freedom) of $\mathbf{A}$. However, (ii) the coupling to the Goldstone mode has not left the gauge field unaffected. Indeed, $S[\mathbf{A}]$ has picked up a **mass** term proportional to the superfluid density, i.e. unlike the vacuum, the action of long range field fluctuations $\mathbf{A}_{\mathbf{q}\to 0}$ no longer vanishes. That modification has serious phenomenological consequences to be discussed momentarily. (iii) The action is manifestly gauge invariant, as it must.

▷ INFO. The analysis above shows that the spontaneous breaking of a *global* U(1) symmetry and of a *local* gauge U(1) symmetry, respectively, lead to very different results. In the former case ($\to$ neutral superfluids), the soft action $S[\theta]$ of a phase-like Goldstone mode θ describes various long range phenomena, such as supercurrent formation, etc. In the latter case ($\to$ superconductors or, more generally, charged superfluids) the system is described by a composite action $S[\mathbf{A},\theta]$. The ubiquotus gauge symmetry can then be employed to absorb the Goldstone mode into the gauge field $S[\mathbf{A},\theta] \overset{\int \mathcal{D}\theta}{\to} S[\mathbf{A}]$. The most important effect of the coupling $\mathbf{A} \leftrightarrow \theta$ is that after the integration over the latter the former picks up a mass term. One sometimes says: 'The photon (vector potential) field has eaten up the Goldstone mode to become fat.' That principal mechanism was understood in 1964 by Higgs, wherefore it is called the **Higgs mechanism**, or crediting Andersons pioneering discussion of gauge symmetry breaking in the context of superconductivity, the **Anderson-Higgs mechanism**.

Mass generation due to spontaneous gauge symmetry breaking is a very general phenomenon, i.e. not limited to the relatively simple context of the collective phase of the superconductor. The Higgs mechanism found its so far most important application in 1967 when Weinberg and Salam embedded it into their unified theory of electromagnetic and weak interactions in particle physics. Although this is not a course about elementary particles, the role of the Higgs principle in the theory of electroweak interactions is of so fundametal importance to our understanding of the microscopic world that it is irresistible to briefly discuss its implications[32].

The **standard model of high energy physics** describes the microscopic world in terms of a few generations of leptonic (electrons, e, electron neutrino, ν_e, muon, μ, etc.) and hadronic (the quarks, u, d, s, c, t, b) elementary particles which interact through the quanta of certain gauge fields. In its original formulation, the model had one severe problem, viz. it did not know how to attribute *mass* to these particles. However, this stands in stark contrast to any kind of experimental observation. In particular, the quanta of the gauge fields of the weak and strong interaction are known to be extremely heavy, with rest masses of $\mathcal{O}(10^2 \mathrm{GeV}/c^2)$. In view of the *much* lighter masses of typical composite hadrons – the proton weighs $938\mathrm{MeV}/c^2$ – the mass of the gauge quanta can certainly not be explained in terms of some ficticious fine structure mechanisms superimposed on the core of the standard model, i.e. a principal modification was needed. It is now widely believed that the 'true' principle behind mass generation lies in a (Anderson)-Higgs-mechanism, i.e. the spontaneous breakdown of a gauge symmetry.

To sketch the principal idea of Weinberg and Salam, let us concentrate on a leptonic subsector of the theory, e.g. consider the two component object

$$\Psi \equiv \begin{pmatrix} \nu_e \\ e \end{pmatrix},$$

[32] For a pedagogical and *much* less superficial discussion, we refer to the textbook[?].

comprising an electron neutrino and a (left handed[33]) electron. Involving a charged particle, the Lagrangian controlling the dynamics of Ψ will surely posses a local U(1) gauge symmetry. However, on top of that, Weinberg and Salam proposed a much more farreaching symmetry structure. Without going into any detail we just mention that, building on principles proposed earlier (1954) by Yang and Mills, transformations

$$\Psi(x) \to U(x)\Psi(x), \qquad U(x) \in \mathrm{SU}(2), \qquad x \in \mathbb{R}^4,$$

locally mixing the two components ν_e and e of the 'isospinor' Ψ were introduced as a symmetry of the model. I.e. in analogy to the local U(1) gauge symmetry of quantum mechanics, it was postulated that the action $S[\Psi]$ possess a local gauge symmetry under the group of SU(2) transformations. In combination with the standard U(1), the theory had thus been endowed with a composite $\mathrm{U}(1) \times \mathrm{SU}(2)$-gauge structure. Physically, declaring a symmetry between the electron – interacting through electromagnetic forces – and the neutrino – weak interactions – was tantamount to a *fusion* of these types of interaction, i.e. the propsal of a theory of **electro-weak interactions**.

How can a theory defined through an action

$$S[\Psi] = \int d^d r\, \mathcal{L}(\Psi, \partial_\mu \Psi),$$

containing the isospinor Ψ and its derivatives be made invariant under non-abelian SU(2) gauge transformations? Referring for a more systematic discussion to chapter XX, let us briefly sketch the principal idea of **non-abelian gauge theory**: We first notice that a fermion bilinear $\sim \bar{\Psi}\partial_\mu \Psi$ is generally *not* gauge invariant. Under a mapping $\Psi \to U\Psi$ it transforms to $\Psi(\partial_\mu + U^{-1}\partial_\mu U)\Psi$. E.g. for $U = e^{i\phi} \in \mathrm{U}(1)$ a 'standard' gauge transformation, the extra term $U^{-1}\partial_\mu U = i\partial_\mu \phi \in i\mathbb{R}$ would be the ordinary 'derivative of a function', familiar from the gauge structure of quantum mechanics. More generally, for a non-abelian gauge transformation by an element $U \in \mathrm{G}$ of a general group (e.g. $\mathrm{G} = \mathrm{SU}(2)$), the gauge term $U^{-1}\partial_\mu U \in \mathrm{g}$ is an element of the Lie algebra g of the group[34], i.e. the action picks up a matrix-valued extra contribution.

To make the theory invariant, we have to introduce a gauge field. I.e. we generalize from ∂_μ to a covariant derivative $\partial_\mu + W_\mu$, where $W_\mu \in \mathrm{g}$. E.g. for $\mathrm{G} = \mathrm{U}(1)$, $W_\mu \equiv A_\mu \in \mathbb{R}$ is the ordinary gauge field of quantum mechanics. For $\mathrm{G} = \mathrm{SU}(2)$, $W_\mu = \sum_{a=1}^3 \alpha_a(s)\sigma_a \in \mathrm{su}(2)$, etc. Under a gauge transformation, the field W_μ transforms as

$$W_\mu \to U W_\mu U^{-1} - iU^{-1}\partial_\mu U,$$

I.e. in a way that makes the covariant bilinear, $\bar{\Psi}(\partial_\mu + W_\mu)\Psi$ invariant. For $\mathrm{G} = \mathrm{U}(1)$, $A_\mu \to UA_\mu U^{-1} - U\partial_\mu U^{-1} = A_\mu - i\partial_\mu \phi$ reduces to its familiar form. However, in the non-abelian case, the full structure on the rhs is needed to obtain invariance. The full action of the

[33] When viewed as a relativistic particle, the electron field has components of left and right chirality, but we shall not need to discuss that aspect any further.

[34] Pragmatically (for an abstract definition of Lie algebras we refer to textbooks of group theory), the Lie algebra of a group G whose elements $\mathrm{G} \ni g = \exp(T_a \alpha_a)$ can be represented by exponentiation of generators $\{T_a\}$, the Lie algebra $\mathrm{g} \ni T_a\alpha_a$ is the vector space spanned by the generators. E.g. the one-dimensional Lie algebra of $\mathrm{U}(1) \ni \exp(i\phi)$ is given by $\mathrm{u}(1) = \mathbb{R}$. (Indeed, we saw that the gauge su(2) term picked up by U(1) abelian gauging is real.) The Lie algebra su(2) of the group $\mathrm{SU}(2) \ni \exp \mathrm{su}(2) \left(i \sum_{a=1}^3 \alpha_a(x)\sigma_a\right)$ ($\{\sigma_i\}$ are the Pauli matrices) contains all linear combinations $\sum_{a=1}^3 \alpha_a \sigma_a$ of Pauli matrices. It is in fact straightforwared to convince oneself that for $U(x) = \exp\left(\sum_{a=1}^3 \alpha_a(x)\sigma_a\right)$, the derivative $U^{-1}\partial_\mu U \in \mathrm{su}(2)$.

gauge theory then reads as

$$S[\Psi, W] = \int d^d r \, \mathcal{L}(\Psi, (\partial_\mu - iW_\mu)\Psi) + S[W],$$

where the Lagrangian density contains the minimally coupled gauge field and the action $S[W]$ describes the fluctuation behaviour of W_μ[35].

Within a fully quantum mechanical setting, both the 'matter field' Ψ and the gauge field W_μ are quantized. The field quanta of the non-abelian gauge field are denoted as **vector bosons**, where the attribute 'vector' (somewhat misleadingly) refers to the higher dimensional geometry of the field and 'boson' emphasizes the generally bosonic statistic of a quantum gauge field.

We now have everything together to turn back to the particular context of the electro-weak interaction. Within the framework of the gauge theory, interactions between the particles e and ν_e are mediated by the gauge field W_μ (very much like in a U(1) theory, interactions between the electrons could be described in terms of a fluctuating U(1) vector potential, cf. section 7.1.1.) Experimental analysis of typical weak interaction processes, such as the elastic collision,

$$e + \nu_e \to e + \nu_e$$

indicates that the weak interaction forces are extraordinarily short ranged, with a decay profile $\sim \exp(-90\mathrm{GeV}r)$. However, according to the pure gauge theory, the propagator of W_μ should be long ranged $\sim r^{-1}$. This is the most severe manifestation of the mass problem of the electro-weak theory. In order to be consistent with experiment a mechanism is needed that makes the gauge field (very) massive.

Here is were the Higgs mechanism enters the stage. To solve the mass problem, Weinberg and Salam *postulated* the existence of a scalar (more precisely, a two component 'iso-sclar') bosonic particle, the **Higgs boson** ϕ. The action of the Higgs particle – again a postulate – is of generalized ϕ^4-type, i.e.

$$S[\phi, W_\mu] = \int d^d r \, \left[\frac{1}{2}(\partial_\mu - W_\mu)\phi^\dagger(\partial_\mu - W_\mu)\phi - \frac{m^2}{2}\phi^\dagger\phi + \frac{g}{2}(\phi^\dagger\phi)^2 \right],$$

where the minimal coupling to the gauge field provides the theory with local gauge invariance. The action of the Higgs has been deliberately designed so as to generate spontaneous symmetry breaking, i.e. the solution of the mean field equations is given by $|\phi| = \left(\frac{m^2}{g}\right)^{\frac{1}{2}}$, with undetermined phase. In perfect analogy to our discussion of the superconductor problem above, an integration over the phase degree of freedom (i.e. the Goldstone mode) then generates a mass term for the gauge fields. In summary, Weinberg and Salam proposed to explain the short-rangedness of the weak interaction through the presence of an extra particle, i.e. a particle that does not belong to the standard hadronic or leptonic generations of the standard model.

Since then, the hunt for the Higgs particle has been one of the big issues of particle physics. In 1983 vector bosons *of the predicted* mass have for the first time been observed in experiment (UA1 collaboration, Physics Letters **122 B**, 103 (1983)), i.e. the existence of a massive gauge structure is out of question. However, the detection of the Higgs – for many particle physicsts only a matter of time – turned out to be a more difficult task. In 2000 the ℵ-experiment installed at the LEP (Large Electron Positron collider) at CERN reported a 'shadowy' Higgs signal in the e^-e^+ scattering cross section at the predicted energy interval. However, at that time, the

[35] Typically, $S[W]$ will be given by generalization of the field strength tenssor $\int d^d r \, F_{\mu\nu}F_{\nu\mu}$ of the abelian theory, i.e. the *curvature* tensor on G.

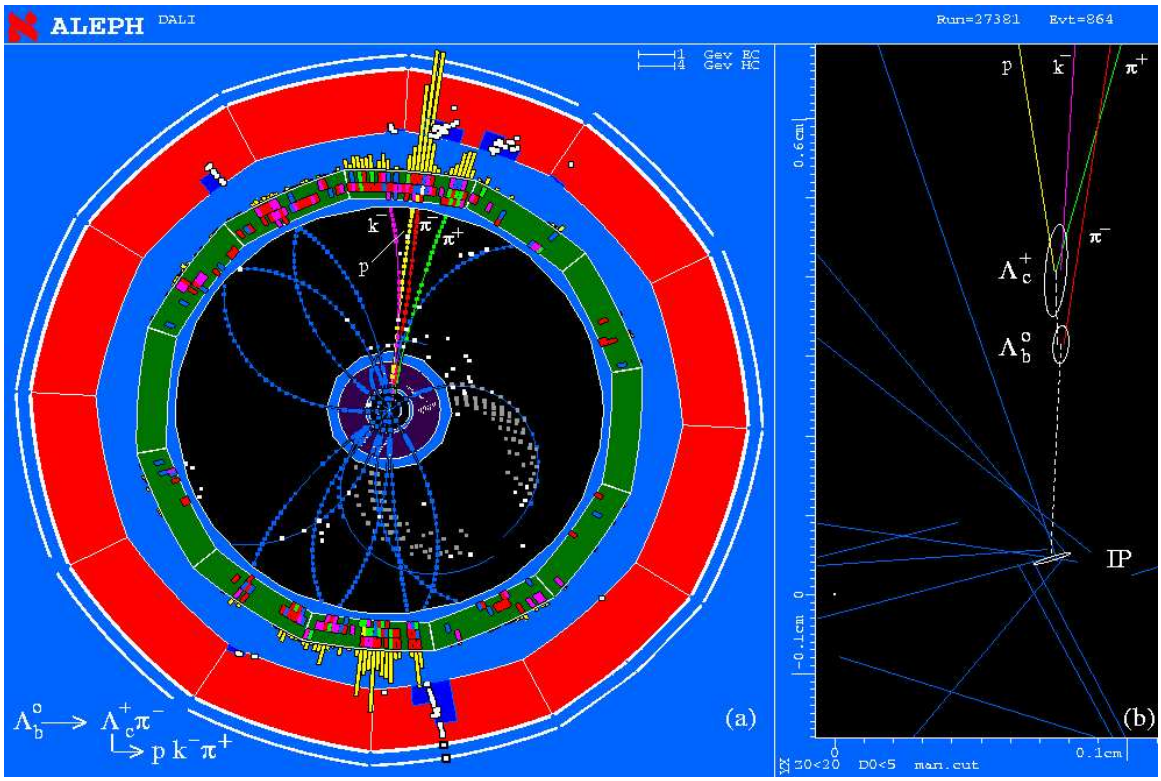

Figure 7.20: Computer generated vizualiztion of a scattering process recorded in the ℵ-experiment at CERN. Hidden somewhere in the 'jet' of particles generated as a result of the collision of the scattering particles should, hopefully, be the Higgs.

designated live time of LEP had already expired and one month after the detection of the first suspicious signals the machine was indeed shut down. Unfortunately, after the closedown of LEP only few accelarator projects offer the perspective to participate in the hunt for the Higgs. Presently, with the 'Superconducting SuperCollider' (SSC) disapproved by American congress, only the Stanford Linear Accellarator reaches the relevant energy scales. The situation may change when the Large Hadron Collider (LHC) at CERN commences its work in 2007.

In the meantime the collective data recorded at LEP over the past years has been subjected to critical review. Irritatingly, it turned out that the data reported in 2000 did not pass the test of a careful re-examination, i.e. presently (2001) there is *no* direct evidence for a Higgs particle. In view of the fact that the Higgs not only generates the mass of the vector bosons but of all particles known to the standard model, much indeed hinges on the question of its existence. (Some people even call the Higgs the 'god particle'.) If it did not exist, our understanding of the microscopic world would be turned upside down.

To conclude our discussion of BCS superconductivty, let us explore the phenomenological consequences of mass accumulation due to the Higgs mechanism. To this end, we vary the action (7.48) wrt $\mathbf{A}$ (keeping in mind the transversality condition $\mathbf{q}\cdot\mathbf{A}^{\perp}_{\mathbf{q}}=0$, we henceforth drop the superscript '$\perp$'), to obtain $(\frac{n_s}{m}+q^2)A_{\mathbf{q}}=0$, or

$$\left(\frac{n_s}{m}-\partial^2\right)A(\mathbf{r})=0. \tag{7.49}$$

Remembering that

$$\mathbf{B} = \boldsymbol{\partial} \wedge \mathbf{A},$$

multiplication of this equation by $\boldsymbol{\partial}\wedge$ produces the **first London equation**

$$\left(\frac{n_s}{m} - \partial^2\right) \mathbf{B}(\mathbf{r}) = 0. \tag{7.50}$$

For $n_s \neq 0$, this equation does not have a non-vanishing constant solution, i.e. we conclude that

A bulk superconductor cannot accomodate a magnetic field.

This phenomenon is known as the **Meissner effect**. To understand what happens at the interface between the vaccuum threaded by a constant magnetic field $\mathbf{B}_0$ and a superconductor, we solve the London equation to $\mathbf{B}(x) \sim \mathbf{B}_0 \exp(-x/\lambda)$, where

$$\lambda = \sqrt{\frac{2m}{n_s}}$$

is known as the **penetration depth** and x is the direction perpendicular to the interface. The physical mechanism behind the Meissner phenomenon is as follows: Above we saw that the magnetic response of a superconductor is fully diamagnetic. That is, in response to an external field, diamagnetic screening currents will be generated. The magnetic field generated by these currents counteracts the un-wanted external field. To see this explicitly, we obtain the current density induced by the field by differentiating the first term of the action[36] wrt $\mathbf{A}$:

$$\mathbf{j}(\mathbf{r}) = \frac{\delta}{\delta \mathbf{A}(\mathbf{r})} \int d^d r \, \frac{n_s}{2m} \mathbf{A} \cdot \mathbf{A} = \frac{n_s}{m} \mathbf{A}(\mathbf{r}), \tag{7.51}$$

i.e. the current density is directly proporitional to $\mathbf{A}$. This is the **second London equation**. Since the vector potential and the magnetic field, respectively, show the same decay profile (Eqs. (7.49) and (7.50)), the current density, too, decays exponentially inside the superconductor. However, along with doing so, it annihilates the external field.

▷ INFO. To heuristically understand the **incompability of magnetic fields and superconductive pairing** on a still more microscopic level, consider the real space representation of a Cooper pair state,

$$\langle \mathbf{r}, \mathbf{r} | \mathbf{k} \uparrow, -\mathbf{k} \downarrow \rangle \sim e^{-i\mathbf{k}\mathbf{r}} e^{+i\mathbf{k}\cdot\mathbf{r}} = \text{const.}.$$

The cancellation of the phases results from the fact that two electrons propagating with opposite momentum pick up opposite quantum phases. Thus, the pair state is a slowly fluctuating, and therefore stable object. However, in the presence of a magnetic field, the phase factors have to

[36] Generally, the electrical current density induced by a field is obtained (cf. the remarks made on page 278) by differentiating the field/matter part of the action $S[\mathbf{A}]$ wrt the vector potential. I.e. the purely field dependent part of the action does *not* contribute to the current density.

be generalized to (exercise: employ the WKB approximation to convince yourself of the validity of that statement.)

$$\langle \mathbf{r}, \mathbf{r} | \mathbf{k}\uparrow, -\mathbf{k}\downarrow \rangle \sim e^{-i\int(\mathbf{k}-eA)\cdot d\mathbf{r}} e^{-i\int(-\mathbf{k}-eA)\cdot d\mathbf{r}} \sim e^{2ie\mathbf{A}\cdot\mathbf{r}},$$

where we assumed that the vector potential varies only slowly accross our observation region of $\mathcal{O}(|\mathbf{r}|)$. I.e. the Cooper pair amplitude becomes an 'incoherent' phase dependent object. On the microscopic level, the lack of stability of the field dependent Cooper amplitude holds responsible for the aversion of the superconductor against magnetic fields.

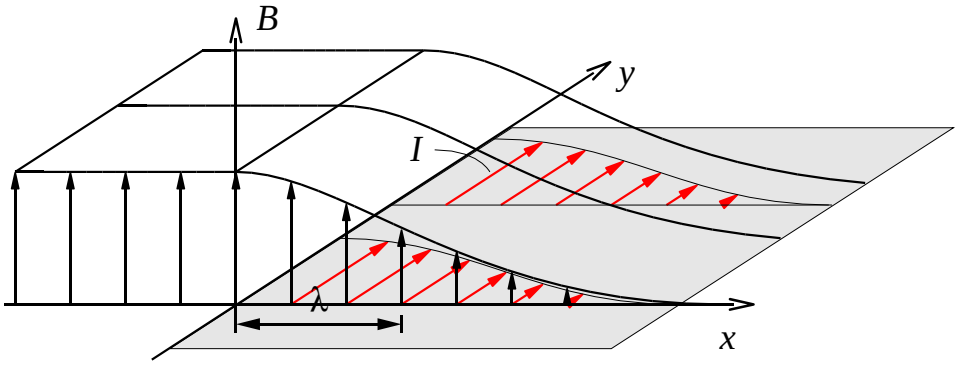

Figure 7.21: On the Meisser effect. Inside a superconductor (the shaded area), magnetic fields decay exponentially. Microscopically, an external field existing outside a superconductor vaccuum interface induces diamagnetic surface currents inside the superconductor. These currents generate a counter-field diminishing the external field.

▷ INFO. It is interesting to explore how a strong magnetic field eventually *does* make its way into the superconductor. To understand the **competition between superconductive ordering and magnetic field energy**, we need to go back to the Ginzburg-Landau action (7.40), i.e. to a description that involves both phase *and* amplitude of the order parameter (the latter detecting the presence or absence of a stable condensate.)

However, at the time when we derived that action, no attention had been paid to the electromagnetic properties of the system. Fortunately, after our general discussion of gauge invariance above, the minimal coupling of the system to the electromagnetic field is routine work. We simply have to remember that under a gauge transformation, $\Delta \to \Delta e^{2i\phi}$, i.e. $\boldsymbol{\partial}\Delta\boldsymbol{\partial}\bar{\Delta} \to (\boldsymbol{\partial} + 2i\boldsymbol{\partial}\phi)\Delta(\boldsymbol{\partial} - 2i\boldsymbol{\partial}\phi)\bar{\Delta}$. The gauge invariant extension of (7.40) thus reads as

$$S_{\mathrm{GL}}[\Delta, \bar{\Delta}] = \beta \int d\mathbf{x} \left[\frac{r}{2}\Delta\bar{\Delta} + \frac{c}{2}(\boldsymbol{\partial} - 2i\mathbf{A})\Delta(\boldsymbol{\partial} + 2i\mathbf{A})\bar{\Delta} + g(\Delta\bar{\Delta})^2 \right],$$

where, as usual, $\mathbf{A}$ gauges as $\mathbf{A} \to \mathbf{A} + \boldsymbol{\partial}\phi$. To monitor the fate of the order parameter as $|\mathbf{A}| \propto |\mathbf{B}|$ increases, consider the mean field equation (exercise)

$$\left[r + c(\boldsymbol{\partial} - 2iA)^2 + 4g|\Delta|^2 \right] \Delta = 0.$$

We assume that we are at temperatures below the zero-field superconductor transition, i.e. $r < 0$. Superconductive ordering exists, when the equation has a non-vanishing solution Δ.

Now, the third contribution on the lhs is positive, so a solution can exist only if the first two terms add to a net negative contribution. That in turn is requires that the eigenvalues of the minimally coupled operator

$$\mathrm{EV}\,(\boldsymbol{\partial} - 2i\mathbf{A})^2 \stackrel{!}{<} \frac{|r|}{c}.$$

Formally, $(\boldsymbol{\partial} - 2i\mathbf{A})^2$ is the kinetic energy operator of a particle of mass 1/2 in a uniform magnetic field. It's eigenvalues are the Landau levels,

$$\omega_c \left(n + \frac{1}{2} \right), \qquad n = 0, 1, \ldots$$

familiar from elementary quantum mechanics. Here, ω_c is the cyclotron frequency, $\omega_c = \frac{B}{m} = 2B$. Thus, a finite pairing amplitude can only be obtained if $|r|/c$ is larger than the energy of the lowest Landau level, or

$$B < B_{c1} \equiv \frac{|r|}{2c}.$$

For magnetic fields larger than that, the energy needed to expell the field is larger than the maximum gain of condensation energy $S[\Delta]$ and superconductivity breaks down. For so-called **superconductors of type I**, the energy balance condition is met for fields $B > B_{c1}$. However, there are superconductor materials – **superconductors of type II** – where the energy criterion opts for field penetration already for fields $B_{c2} < B < B_{c1}$ lower than the critical field B_{c1} specified by the mean field criterion above. For these systems, the superconductor and the field 'meet a compromise'. That is, **vortex tubes** of quantized flux penetrate the superconductor already for field strength smaller than B_{c1} but larger than the critical field strength B_{c2}, see Fig. 7.22 for a picture of a 'vortex lattice' penetrating a type II superconductor. Inside the cores of these vortices, the superconductor order parameter is suppressed, but outside it still exists. However, a detailed discussion of vortex formation and its conceptual relation to the *topology* of the order parameter field will be postponed until chapter XX.

To conclude this chapter late us discuss the most prominent superconductor phenomenon, **absence of electric resistivity.** Assume we had chosen a gauge, where an external electric field $\mathbf{E}$ is represented through $\mathbf{E} = -i\partial_\tau \mathbf{A}$ (i.e. the static component of the potential vanishes.) In this case, a time differentiation of the second London equation (7.51) obtains

$$-i\partial_\tau \mathbf{j} = -i\frac{n_s}{m}\partial_\tau \mathbf{A} = \frac{n_s}{m}\mathbf{E}.$$

Continuing back to real times we conclude

$$\partial_t \mathbf{j} = \frac{n_s}{m}\mathbf{E},$$

i.e. in the presence of an electric field the current increases linearly at a rate inversely proporitional to the carrier mass and proportional to the carrier density. The unbound increase of current is indicative of ballistic – i.e. dissipationless – motion of the condensate particles inside the superconductor. Now, an unboundedly increasing current is clearly unphysical, i.e. what the relation above really tells us is that a superconductor cannot maintain non-vanishing field gradients.

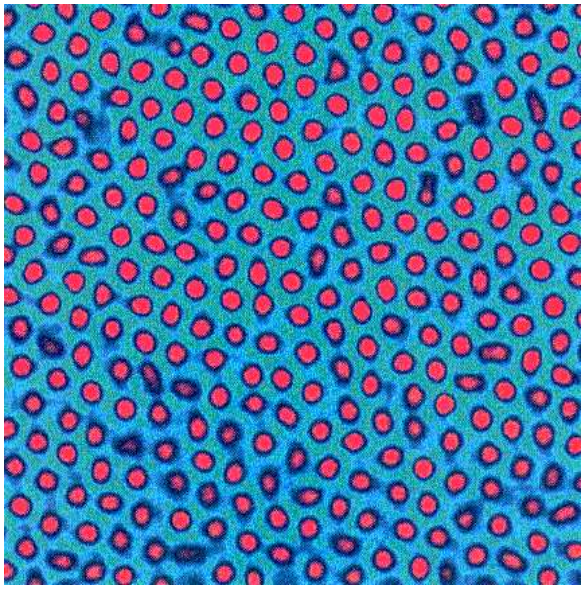

Figure 7.22: Bitter pattern of an Abrikosov vortex lattice. Each of the bright dots contains magnetic flux $\Phi = \frac{n}{h}$ where $1/h$ (or e/h in units where the electron charge is kept track of) is the magnetic flux quantum. Notice the approximately regular, hexagonal structure of the lattice.

▷ EXERCISE. Assuming that each particle is subject to Newton's equation of motion $m\ddot{\mathbf{x}} = \mathbf{E}$, obtain the current-field relation above. How would the relation between field and current change, if the equation of motion contained a friction term (modelling dissipation) $m\ddot{\mathbf{x}} = -\frac{m}{\tau}\dot{\mathbf{x}} + \mathbf{E}$.

7.4 Summary and Outlook

This concludes our preliminary discussion of functional mean field methods. We have learned how the integration over microscopic quantum fields can be traded for an integration over problem adjusted degrees of freedom. When then observed that the functional dependence of the action on the new coordinates is usually highly non-linear – the notorious 'trace logarithms' – and has to be dealt with by some kind of stationary phase analysis. While a first principle solution of the mean field equations is often not possible, all applications discussed in this chapters had in common that solutions could be found by 'educated guessing'. Importantly, we realized that these solutions did not always display the full symmetry of the action.

▷ INFO. However, it is important to realize that a number of **problem classes with complex mean field structure** have not been mentioned in this chapter. E.g. for certain lattice systems with discrete translational symmetry the optimal mean field solution shows **staggering**, i.e. changes sign under translation by one lattice spacing (see the problem set for examples.) Deceptively, these configurations usually exist in parallel to a solution that displays the full symmetry of the problem, but is of higher energy (and therefore unphyiscal.) I.e. the

'true solution' is camouflaged by the existence of an inferior but 'more symmetric' solutions[37].

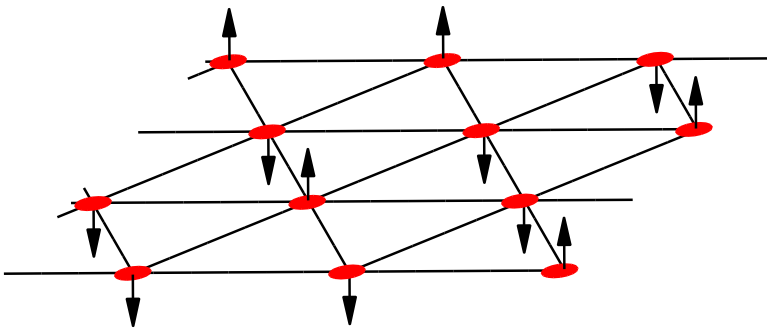

Figure 7.23: Triangular Ising lattice with antiferromagnetic exchange coupling. The system is frustrated in the sense that no configuration with alternating spin orientation exists.

Then, there are systems where the existence of meaningful stationary phase configurations is excluded by structural elements, such as **frustration**. As an example, consider the Ising antiferromagnet on a triangular lattice (cf. Fig. 7.23.) The system is frustrated in the sense that, by virtue of the antiferromagnetic coupling, it would like to occupy nearest neighbour sites by oppositely aligned spins. However, the topology of the lattice excludes the existence of such optimal configurations. As a consequence, the triangular Ising antiferromagnet abides in a 'disordered' state, i.e. a continuum of irregular and equally unattractive states enters the partition function with approximately equal weight. At any rate, no clearly defined stationary phase configuration exists.

Other systems, notably **glasses** (cf. the remarks on p 122), do posses an entire *continuum* of mean field configurations. I.e. there is a macroscopic number of (metastable) extremal configurations that are very close in energy space but may be very far from each other in configuration space. (E.g. two such configurations may differ by an restructuring of the atomic configuration of a glass at remote places.) The dynamics of such systems is governed by the process of **ageing**, i.e. transitions between different metastable extremal configurations on ultralarge timescales (observe the glass of your windows panes flowing down in the course of time!). It goes without saying that the 'mean field configurations' of glassy systems are irregular and not amenable to straightforward analytic calculation.

Finally, even systems possessing a spatially homogeneous mean field configuration may host *other* solutions of physical significance. Indeed, we have encountered a scenario of this type already in chapter 4 above. Exploring quantum double well tunneling, we observed that the imaginary time Euler-Lagrange equations of a particle in a doubly degenerate harmonic well ($\leftrightarrow$ the 'mean field equations') had a metastable constant solution ($\leftrightarrow$ the constant mean field). However, in addition to that, we had found **instantons**, i.e. temporally structured solutions of the mean field equations. Superficially, it looked like that, due to their non-vanishing action, instantons are irrelevant. However, for sufficiently long times the energetic inferiority of the single instanton was over-compensated by statistical aspects, i.e. the fact that a continuum of instantons entered the partition function with approximately equal weight. In the language of statistical mechanics: the large *entropy* associated to instanton configurations out-weighed the

[37] When dealing with problems whose lattice structure carries physical significance, it is therefore a good idea to try a number of different ansätze, i.e. trial solutions that transform differently under translation by a unit cell.

finite *energy* (or more precisely action) gap to be paid for a single instanton. Later, in chapter XX, we will see that entropy/energy competitions of this type are realized in many other other contexts of quantum and statistical field theory. E.g. the phase actions of the BCS superconductor or the superfluid possess (approximate) extremal configurations wherein the phase winds around an integer multiple of 2π as a fixed reference point in space is encircled (vortices). While the energy of an individual vortex solution may be high, the entropy corresponding to the choice its center eventually, for sufficiently large temperatures, dominates and leads to a proliferation of vortices in the system ($\leftrightarrow$ the analogue of the instanton gas). For a more qualified discussion of topologically non-trivial mean field configurations we refer to chapter XX.

We then expemplified on a number of different applications how low energy effective actions describing fluctuations on top of a reference mean field can be derived and evaluated. In cases where the mean field broke a continuous symmetry these actions were partially soft, i.e. contained Goldstone modes. We saw that the presence of a Goldstone mode has a dominant effect on the observable physical properties of a system.

As exemplified above, the theoretical machinery developed thus far enables us to tackle already highly non-trivial problems. However, to make the functional integral a unviversally applicable tool, two important gaps have yet to be filled in. First, we have so far mostly been content with discussing general *structures* of condensed matter theory (i.e. much of the discussion has been limited to general manipulations on the level of the effective action.) However, in applications one is typically interested in comparison with experimentally accessible data. I.e. we still need to provide links relating the field integral formalism to observables of experimental significance. Second, our so far discussion of the fluctuation behaviour of field theories has been quite limited. That is, we typically expanded an action to *second order* in what we believed was the 'physically relevant' degree of freedom and computed the corresponding determinants. However, we also saw that some problems contain anharmoticities of profound significance. E.g. the quartic term in ϕ^4-theory led to UV singularities whose nature remained largely obscure. We must, therefore, (i) develop criteria indicating under which circumstances a model can safely be limited to second order and (ii) in cases where it cannot, learn how to deal with its anharmonic content.

Beginning with the first one, these two topics, which are not quite as unrelated as one might believe, will be discussed in chapters XX and XX.

7.5 Problem Set

Q1 Coulomb blockade.

Q2 Cancellation diamagnetic/paramagnetic term for non-superconductors.

Q3 Stoner instability.

Q4 Antiferromagnetic instability.

Q5 Peierls instability

Q6 Change Lagrangian - Hamiltonian action in PI as a Hubbard-Stratonovich trafo.

Chapter 8

Correlation Functions

The chapter begins with a brief survey of concepts and techniques of experminental *condensed matter physics. We will argue that at an intermediate level experimental information is mostly encoded in objects known as 'correlation functions'. We will discuss in detail how correlation functions relate to experiment on the one hand and to the field integral formalism developed in previous chapters on the other hand. Specifically, we will explore how real time dynamical information can be obtained from an imaginary time formalism and derive a number of generally valid (and therefore extraordinarily useful) relations fulifilled by experimentally relevant correlation functions.*

In the last few chapters we have developed a number of key structural elements of theoretical condensed matter physics. Perhaps most importantly, we learned how to map the prototypical microscopic representations of many body problems onto effective low energy models, ideally models amenable to analytical evaluation. However, eventually we will want to go one step further and *test* the predictive power of these effective theories, i.e. compare to 'real' data obtained from experiment.

But what is actually meant by the phrase 'experiment'? Modern condensed matter physics knows of a plethora of sophisticated and highly differentiated techniques of experimental analysis: electric and thermal transport measurements, neutron, electron, Raman and x-ray scattering, calorimetric measurements, induction experiments, and many more (for a short glossary of prominent experimental techniques, see section 8.1.2 below.) While a comprehensive discussion of modern experimental condensed matter physics would be way beyond the scope of the present text, it is certainly well invested time to attempt an identification of some *structures* common to most experimental work in many body physics. Indeed, we will *need* a discussion of this type to meaningfully construct links between the theoretical body developed above and experiment.

8.1 A Crash Course in Modern Experimental Condensed Matter Physics

8.1.1 Basic Concepts

Broadly speaking, experimental condensed matter physics can be subdivided into three[1] large categories of analytical techniques:

- ▷ experiments probing thermodynamic coefficients,
- ▷ transport experiments,
- ▷ spectroscopy.

A summary of motivation, basic experimental setup, application areas, and concrete realization of these families will be given in the next section below. (Readers who are totally unfamiliar with the basic notions of experimental many body physics may find it illustrative to browse through this section before further reading.) The few occasional references to experimental data given in previous chapters were all to thermodynamic experiments. The reason for this restriction was that the link between theory and thermodynamic information is most straightforward. I.e. what one has to do is differentiate the partition function (alias the field integral) wrt a few *globally* defined coefficients (the temperature, a homogeneous magnetic field, etc.) This simplicity has both advantageous but also limiting aspects to it: On the one hand, thermodynamic data is highly universal[2] and, therefore, represents an important characteristic of a system. On the other hand, it neither contains information on spatial structures, nor on dynamical features. This means that the thermodynamics of a system often does not contain the full information needed to understand its basic physics, notably its excitations.

With the other two categories of experiments the situation is different. Transport and spectroscopic measurements can be used to probe both static *and* dynamical features of a system; further, fully angle/frequency resolved spectroscopic data contains detailed information on the spatio-temporal structure of the dominant excitations of a system, or, in other words, on their *dispersion relation*. It is for these reasons, that the focus in the present chapter will be on the last two of the experimental classes mentioned above.

In spite of the dazzling diversity of present day analytical and apparative techniques, there are a few common structures common to all experimental probes of condensed matter systems:

- ▷ First, the interaction of a solid with its environment is almost exclusively by electromagnetic forces. I.e. the basic setup of practically every experiment is that a condensed matter system is subjected to an external electromagnetic perturbation (a voltage drop, an influx of spin magnetic moments carried by a beam of neutrons,

[1] There are a few classes of experiments which do not fit comfortably into this three-fold scheme. This applies, e.g., to scanning tunneling microscopy, a technique to be discussed in more detail below.

[2] Remember that a few thermodynamic variables, i.e. *numbers*, suffice to unambigously characterize the state of a homogeneous system in equilibrium.

the local electric field forming at the tip of a scanning tunneling microscope, etc.) Formally, we can represent that perturbation by a (time dependent) contribution

$$\hat{H}_F = \int d^d r F_i(\mathbf{r}, t) \hat{X}_i(\mathbf{r}) \tag{8.1}$$

to the Hamiltonian of the system. Here, the coefficients F_i, sometimes referred to as generalized 'forces', represent a perturbation that couples to the system through some operators $\hat{X}$. E.g., $F_i(\mathbf{r}, t) = \phi(\mathbf{r}, t)$ could be a space and time dependent electric voltage coupling to density of the electronic charge carriers in the system $\hat{X}_i = \hat{\rho}$, etc.

- ▷ The use of the term 'perturbation' is appropriate, because the forces $\{F_i\}$ will in general be *much* weaker then the internal correlations of the system.

- ▷ The forces weakly perturbe the system out of its $F_i = 0$ reference state. The measurable effect of this intrusion will be that certain operators $\hat{X}'_i$ whose expectation values vanished in the unperturbed state begin to build up a non-vanishing expectation value $X'_i(\mathbf{r}, t) = \langle \hat{X}'_i(\mathbf{r}, t) \rangle$. (E.g. in response to an external voltage $F_i = \phi$ a current could begin to flow, $\hat{X}'_i = \hat{j}_i$, etc.) The ultimate goal of any theory will be to understand/predict the functional dependence of the measured values of X'_i on the forces F_j.

- ▷ In general, there is nothing we can say about that connection other than that $X'_i[F_j]$ will be *some* functional of the forces. However, for sufficiently weak forces the situation is simpler. In this case, we should expect that the functional relation between forces F_j and the expectation values X'_i is approximately *linear*, i.e. of the form

$$X'_i(\mathbf{r}, t) = \int d^d r' \int dt' \, \chi_{ij}(\mathbf{r}, \mathbf{r}'; t, t') F_j(\mathbf{r}', t') + \mathcal{O}(F^2).$$

While the quantities $\{F_j\}$ and $\{X'_i\}$ are externally adjustable/observable – either as experimental input/output, or as parameters in our theory – the integral kernel χ represents a purely *intrinsic* property of the system. It describes how the system 'responds' to the application of an external probe $\{F_i\}$ (wherefore it is commonly referred to as a **response function**.) This response is in turn governed by its dominant excitations, i.e. our prime objects of interest.

These considerations show that the response functions of a system play a principal role in the dialog between experiment and theory. Experimentally, they will be *measured* by relating the input $\{F_j\}$ to the response $\{X'_i\}$. Theory will attempt to *predict* the response behaviour, ideally in a way that conforms with experimental observation.

8.1.2 A List of Experimental Methods

To keep our discussion of the relation (experiment $\leftrightarrow$ theory) less abstract, we list a few prominent **experimental techniques of condensed matter physics**. Needless to say that the summary below cannot replace a real introduction to experimental solid state

physics. For an up to date exposition of this field we refer, e.g., to the (spectroscopy oriented) textbook[**?**]. Short and pedagogically written (if a bit outdated) introductions to a number of expermimental approaches can also be found in the textbook [**?**]. Also notice that this section mainly serves illustarative purposes, i.e. it is not indispensible for the understanding of the rest of the chapter. (Although readers bare of any background in experimental many body physics may welcome a bit of motivation before plunging into the formalism of correlation functions to be developed below.)

Thermodynamic Experiments

I.e. experiments that probe thermodynamic coefficients of a system. A prominent and important example is the **specific heat**, $c_v = \partial U/\partial T$, i.e. the rate of change of ineternal energy under changes of temperature. In magnetic systems, the **magnetic susceptibility** $\chi = \partial M/\partial H$ can be determined by measuring the magnetization building up in response to a (quasi)static magnetic field. The **(isothermal) compressibility**, $\kappa = -V^{-1}\partial V/\partial p$ measures volume changes in response to external pressure, etc.

The results produced by thermodynamic experiments are highly *universal*. (Remember that a few thermodynamic state variables suffice to unambiguosly characterize the state of a given system.) E.g., for given values of chemical potential, magnetic field, pressure, etc. a calorimetric exeriment will produce a one-dimensional *function* $c_v(T)$. The low temperature profile of that function generally contains important hints as to the nature of the low energy excitations of a system[3]. However, the universality of thermodynamic data also represents a limitation: Thermodynamic coefficients neither contain information on the *spatial* structure of a system nor on its *dynamics*.

Transport experiments

A sample is subjected to a gradient of a generalized 'voltage' U (see Fig. 8.1). The voltage U need not be electrical. Alternatively one can apply a temperature gradient $U = \Delta T$ or even attach the sample to two 'reservoirs' of different magnetization $\mathbf{U} = \Delta\mathbf{M}$. One then records the current flow induced by U. That current can be the electrical current I carried by the charge of mobile particles, or a 'spin current' I_s carried by their magnetic moments. Also notice, that the current need not neccessarily be parallel to the voltage gradient. E.g. in the presence of a perpendicular magnetic field, a voltage gradient will give rise to a transverse **Hall current** $I_\perp$.

The ratio of a current and a generalized voltage defines a **conductance**,

$$g = \frac{I}{U}.$$

A number of prominent conductance coefficients is summarized in table 8.1 below.

Conductance measurements represent the most common way to determine the transport behaviour of a metal or, in the thermal conduction properties of insulators. A

[3] E.g., the scpecific heat of the Fermi liquid $c_{v,\text{Fermi liquid}} \sim T$ is linear in temperature, that of phonons $c_{v,\text{phonon}} \sim T^3$ cubic, while the specific heat of a system without low-lying excitations vanishes exponentially (why?)

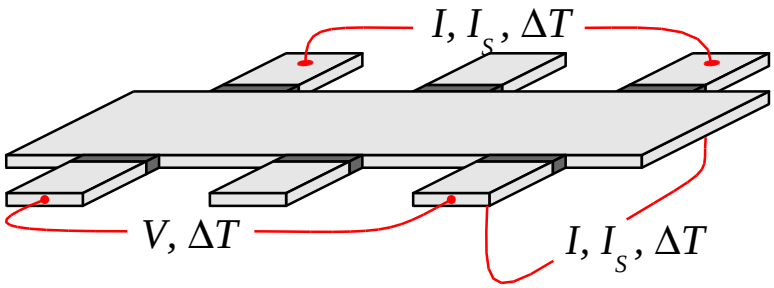

Figure 8.1: Basic setup of a transport experiment. The current flow in response to an applied voltage (or temperature) gradient is measured.

current	voltage	conductance
longitudinal electric I	V	(longitudinal) conductance, g
transverse electric $I_\perp$	V	Hall conductance, g_H
longitudinal spin I_s	V or $\Delta\mathbf{M}$	(longitudinal) spin conductance, g_s
transverse spin $I_{s,\perp}$	V or $\Delta\mathbf{M}$	spin Hall conductance, $g_{s,H}$
longitudinal electric I	ΔT	(longitudinal) thermal conductance, σ
transverse electric $I_\perp$	ΔT	thermal Hall conductance, σ_H

Table 8.1: A number of frequently analysed conductances.

disatvantage is that conductance measurements are invasive, i.e. the system has to be attached to contacts. There are situations where the local injection process of charge carriers at the contact (rather than the bulk transport behaviour one is interested in) determines the value of the conductance. (For a discussion of this point see the problem set.)

Spectroscopic Experiments

The general setup of a spectroscopic experiment is shown in Fig. 8.3. A beam of particles p – either massive particles (electrons, neutrons, muons, atoms, etc.) or the quanta of electromagnetic radiation – is generated in a source and then shot onto a sample. The essential kinematic information about the source beam is stored in a dispersion relation $(\mathbf{k}, \omega(\mathbf{k}))$[4]. The particles of the source beam then interact with constituents X of the sample to generate a secondary beam of scattered particles p'. Symbolically,

$$\begin{array}{ccccccc} p & + & X & \longrightarrow & p' & + & X' \\ \updownarrow & & \updownarrow & & \updownarrow & & \updownarrow \\ \mathbf{k}, \omega(\mathbf{k}) & & \mathbf{K}, \Omega(\mathbf{K}) & & \mathbf{k}', \omega(\mathbf{k}') & & \mathbf{K}', \Omega(\mathbf{K}'), \end{array}$$

where X' symbolically represents the final state of the process inside the sample. Notice that the particles p' leaving the sample need not be identical with those impingent onto the sample. (E.g. in photoemission spectroscopy, x-ray quanta kick electrons out off the

[4]For some sources, e.g. laser light, the preparation of a near-monochromatic source beam is (by now) standard. For others, e.g. neutrons, it requires enormous experimental skills (and a lot of money.)

core levels of solid state atoms, i.e. p are light quanta, p' electrons.) Further, the dominant scattering process may be elastic – e.g. x-rays scattering off the static lattice structure – or inelastic – e.g. neutrons scattering off phononic excitations. In either case, the accessible information about the scattering process is stored in the frequency momentum distribution $P(\mathbf{k}', \omega(\mathbf{k}'))$ of the scattered particles, as monitored by a detector.

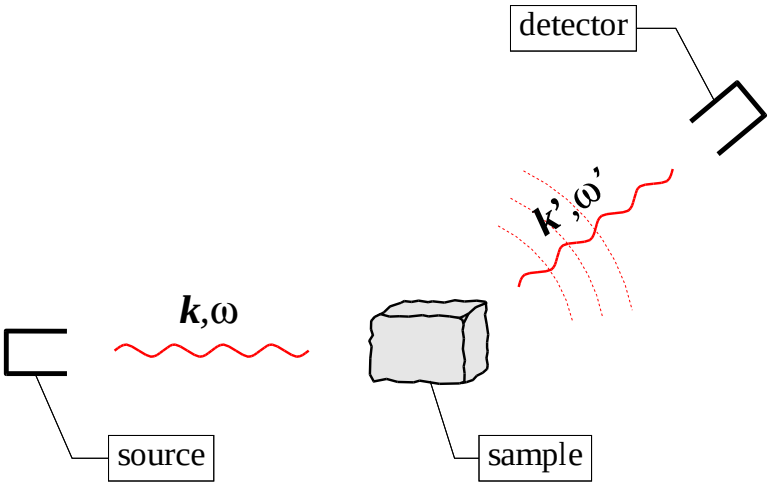

Figure 8.2: Basic setup of a spectroscopic experiment. A beam of electromagnetic radiation (or massive particles) of frequency/momentum $(\mathbf{k}, \omega(\mathbf{k}))$ is shot onto a target sample. The sample responds by emitting radition according to some distribution $P(\omega', \mathbf{k}')$ which is recorded by a detector. Notice that the emitted radiation can but need not contain the same type of particles as the source radiations. E.g. light quanta may lead to the emission of electrons (photo-emission spectroscopy.)

From this data one would like to relate back to the properties (i.e. the dispersion $(\mathbf{K}, \Omega(\mathbf{K}))$) of the states inside the solid, and here is where the detective work of spectroscopy begins. What we know is that the dispersion of the scattered particles and of the sample constitutents $(\mathbf{k}, \omega)$ and $(\mathbf{K}, \Omega)$, respectively, are related through an energy/momentum conservation law, i.e.

$$\begin{aligned} \mathbf{k} + \mathbf{K} &= \mathbf{k}' + \mathbf{K}', \\ \omega(\mathbf{k}) + \Omega(\mathbf{K}) &= \omega(\mathbf{k}') + \Omega(\mathbf{K}'). \end{aligned}$$

According to this relation, a 'resonant' peak in the recorded distribution $P(\mathbf{k}', \omega(\mathbf{k}'))$ signals the existence of an internal structure (an excitation, a lattice structure, etc.) of momentum $\Delta\mathbf{K} \equiv \mathbf{K}' - \mathbf{K} = \mathbf{k} - \mathbf{k}'$ and frequency $\Delta\Omega \equiv \Omega' - \Omega = \omega - \omega'$. However, what sounds like a straightforward recipe in principle, may be quite intricate in practice: Solid state components interact almost exclusively through electromagnetic forces. When charged particles are used as scattering probes, these interactions may actually turn out to be *too* strong. E.g., a beam of electrons may interact strongly with the surface states of a solid (rather than probing its bulk), or the scattering amplitude may be the result of a complicated process of large order in the interaction parameters, and therefore difficult to interpret. The obvious alternative – scattering of neutral particles– is met with problems

of other type (see below.) Notwithstanding these difficulties, spectroscopy is one of the most important sources of experimental information in condensed matter physics. A number of prominent 'sub-disciplines' of solid state spectroscopy are summarized below:

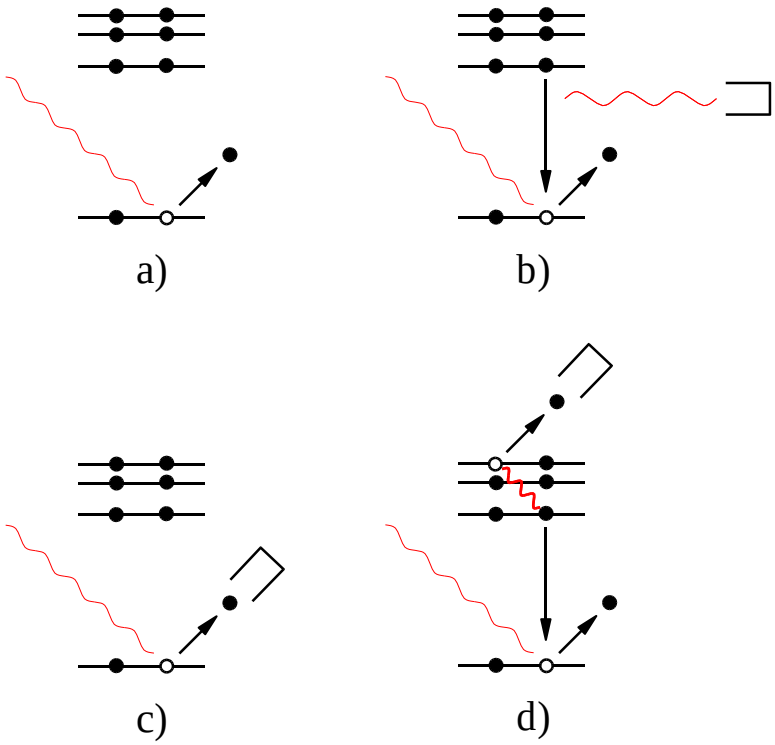

Figure 8.3: Different types of x-ray/electron spectroscopy: a) x-ray absorption. The loss of x-ray radiation due to the ionization of core levels is monitored. b) x-ray flourescence. The recombination of valence electrons with previously x-ray-emptied core levels leads to the emission of radiation, which also lies in the x-ray range. The spectral analysis of this radiation contains information on the level-structure of the system. c) photoemission spectroscopy (PES). The frequency-dependence of the electrons kicked out by x-ray core level ionization is monitored. d) Auger spectroscopy. The energy emitted by a valence electron recombining with a core level is transmitted to a second valence electron which leaves the solid as a high energy Auger electron.

- ▷ **Raman spectroscopy**: the inelastic scattering of visible light. Used to explore the dispersion of optical phonons (also magnons, plasmon modes or other electronic excitations.) Requires experimental skill because the 'Raman peak' is has to be separated from the much larger 'Raleigh peak' corresponding to the *elastic* scattering of light quanta.
- ▷ **Infrared spectroscopy**: scattering of light in the infrared range. Application areas include the analysis of vibrational modes in polycristalline solids and the study of band-gaps in semiconductors.
- ▷ **X-ray crystallography**: elastic scattering of x-rays off the lattice structure of a solid. (Notice that the typical wave length of x-rays $\sim 10^{-10}$m is of about the

size of typical inter-atomic spacings in solids.) From the angle resolved intensity profile (the so-called von Laue pattern), the structure of a crystalline substance can accurately be re-constructed. One of the 'classics' of solid state spectroscopy; in use since 1913.

- ▷ **X-ray/electron spectroscopy**: A number of spectroscopic techniques is based on the fact that the ionization energies of atomic core levels are comparable in magnitude to typical x-ray energies. In **x-ray absorption spectroscopy** the absorption of x-rays by a solid is measured as a function of the light frequency (cf. Fig. 8.3 a)). The absorption cross section rises in a quasi-discontinuous mannner whenever the energy of the x-rays becomes large enough to ionize an atomic core level of the solid state atoms. Due to interatomic correlations, these energies differ from the ionization energies of gazeous atoms, i.e. information about solid state binding energies is obtained. In **x-ray flourescence spectroscopy** the radiation emitted by valence electrons recombining with core holes created by incident x-ray radiation is measured (Fig. 8.3 b)). This type of spectroscopy is frequently used to chemically analyse a sample, or to detect the presence of impurity atoms. I.e. different elements have different core/valence excitation energies. Peaks in the flourescence spectrum at frequencies characteristic for individual atoms therefore identify the presence of these atoms in the target sample. In **photoemission spectroscopy (PES)** core electrons[5] knocked out by x-ray radiation are detected (Fig. 8.3 c).) The fully frequency/angle resolved measurement of the photo electron current, known as **angle resolved photo emission spectroscopy (ARPES)**, is one of the most important spectroscopic techniques in the experimental analysis of band structures. **Auger spectroscopy** is based on an interaction process of higher order (Fig. 8.3 d)): A core hole is created either by irradiation by x-rays (or high energy electrons). In a secondary process, part of the energy emitted by a recombining valence electron is transferred to another valence electron which leaves the atom and is detected.

- ▷ **Neutron scattering**: Thermal neutrons are scattered elastically or inelastically by a solid state target. Being a neutral particle, the neutron interacts only weakly with solid state constitutents (viz. magnetically, through its spin) and hence penentrates deeply into the sample. Due to its particular energy dispersion the neutron is tailor made to the analysis of low lying collective excitations (phonons, magnons, etc. E.g., the data shown in Fig. 3.13 was obtained by neutron spectroscopy.) Just as x-ray scattering, *elastic* neutron scattering can be employed to obtain cristallographic information. (E.g., the first experimental observation of the helical structure of DNA was by neutron scattering.) Unfortunately, the production of thermal neutrons requires a nuclear reactor, i.e. neutron scattering is an extremely *expensive*[6] exterimental technique.

- ▷ **Magnetic resonance**: A sample containing particles of non-vanishing moment is placed into a static (in practice, a slowly varying) magnetic field, strong enough to cause complete magnetic polarization. The sample is then exerted to an AC

[5] To access *valence* electrons, soft x-ray radiation or hard UV radiation can be employed.

[6] On the scale of the average cost of condensed matter experiments.

magnetic field perpendicular to the polarizing field. If the AC field frequency is in resonance with the Zeeman energy magnetic transitions are resonantly induced. The observable effect is a strongly enhanced radiation loss of the AC field.

In **nuclear magnetic resonance (NMR)** the nuclear spins of the sample are polarized. solid state physics, NMR is applied to obtain information about the magnetic properties of the *electronic states* of the solid: Due to the hyperfine interaction of the electron spin and the nuclear spin, the effective magnetic field seen by the nucleus partially depends on the sourrounding electron cloud. E.g., in metals, the Pauli paramagnetic response of the electrons causes a characteristic shifting of the spectral lines (as compared to the NMR spectra of nuclei in uncorrelated environmnents) known as the **Knight shift**. Analysis of this shift obtains information on the magnetic properties of the conduction band.

Resonance spectroscopy of transitions between spin polarized *electron* states, **electron spin resonance (ESR)**, is frequently used in chemical analysis and molecular physics.

▷ For the discussion of other spectroscopic techniques, e.g., **Mößbauer spectroscopy, positron-electron annihilation spectroscopy (PES), muon scattering, electron energy loss spectroscopy (EELS)**, etc. we refer to the literature.

▷ INFO. Representative for many other triumphs of spectroscopic experimental analysis in modern condensed matter physics, we briefly mention the **discovery of d-wave superconducting order in the cuprates.**

The crystallographic structure of high-temperature superconductors (HTSC) comprises two basic functional elements: (i) layered quasi-two dimensional CuO_2-lattice planes and (ii) inter-planar regions, mostly containing metallic spacer atoms in a certain concentration ratio (e.g. $La_{1-x}Sr_x$). The essential role of these spacer regions is to provide the CuO_2 planes with a suitable amount of mobile charge carriers. At a favourable charge carrier concentration, and for sufficiently low temperatures, the planes enter a superconducting state with highly unusual properties. The most striking of these is that, unlike in an ordinary BCS-superconductor, the order parameter is not constant but displays the momentum dependence of an $l = 2$, or d angular momentum eigenfunction.

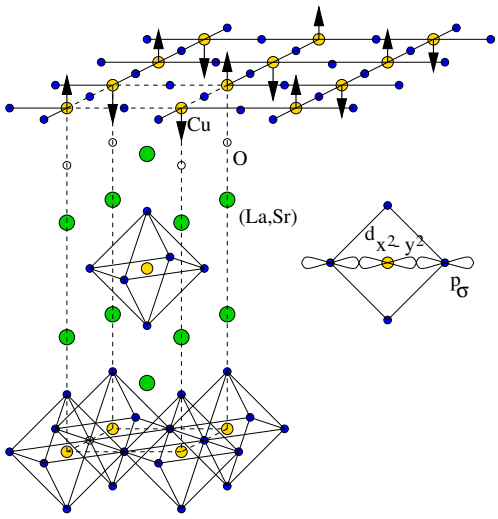

More precisely,

$$\Delta(\mathbf{p}) = \Delta_0(\cos(p_1) - \cos(p_2)),$$

where $p_{1,2} \in [-\pi, \pi]$ are the two components of the lattice momentum. The strong anisotropy of the order parameter holds responsible for most of the striking phenomenological differences between ordinary and high-temperature superconductors, respectively. To appreciate its importance, notice that along the two 'nodal lines' $|p_1| = |p_2|$ the order parameter actually vanishes.

Which means that at the four intersection points of these lines with the Fermi surface $|\mathbf{p}| = p_F$ no quasi-particle gap exists (cf. Fig. **??**.) (Exercise: Using that the normal part of the Hamiltonian $H_0(\mathbf{p}) = t(\cos(p_1) + \cos(p_2))$ displays the dispersion of an ordinary lattice hopping operator (cf. p **??**), employ the methods of section **??** to compute the quasi-particle energy spectrum.) I.e. unlike a BCS superconductor, the d-wave superconductor does accomodate energetically low-lying quasi-particle excitations. This feature implies strongly different phenomenological behaviour both with regard to transport and thermodynamics.

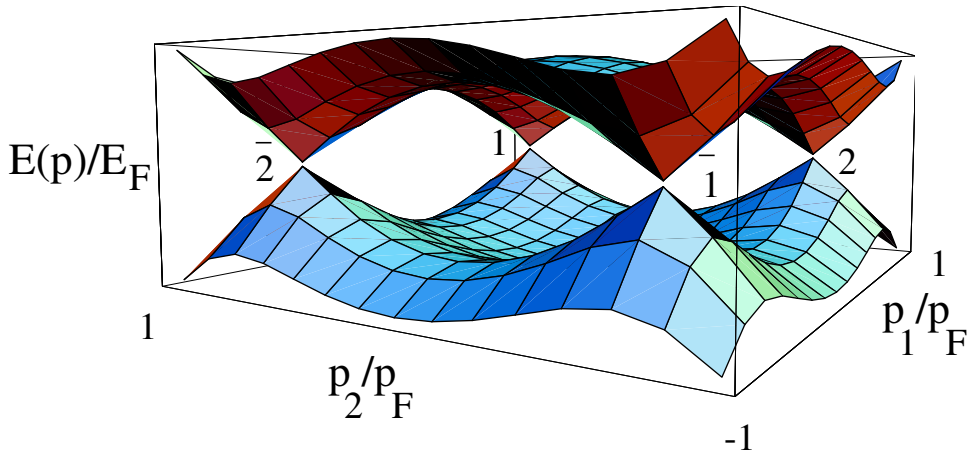

Figure 8.4: Plot of the quasi-particle dispersion relation of a d-wave superconductor. Notice the vanishing of the quasi-particle energy at four nodal points $1, \bar{1}, 2, \bar{2}$.

Irritatingly, there is so far no theoretical explanation of the basic mechanism of cuprate superconductivity, let alone the d-wave symmetry of the order parameter; this structural feature has been disclosed experimentally, viz. by high resolution ARPES spectroscopy. Fig. 8.5 shows ARPES data taken on the compound $Bi_2Sr_2CaCu_2O_{8+\delta}$. The experiment unambigously confirms the existence of quasi-particles at the intersection of the Fermi surface with the nodal lines $|p_1| = |p_2|$.

.

Other Experimental Techniques

There are a few experimental probes of condensed matter physics which do not fit comfortably into the threefold scheme 'transport / thermodynamics / spectroscopy' discussed above. This applies, e.g., to **Scanning Tunneling Microscopy (STM)**, a technique whose development by Binding and Rohrer in the eithies (Nobel prize, 1986) has led to a revolutionized the area of nano-technology.

The basic principle of STM is easily explained (see Fig. 8.6): A small tip, kept at positive eltrostatic potential, is brought in proximity to a surface. When the tip/surface separation becomes comparable to atomic scales, electrons begin to tunnel from the substrate onto the tip. The resulting tunnel-current is fed into a piezoelectric crystal which in turn levels the height of the tip. Through this mechanism, the surface/tip separation can be kept constant, with an accuracy of fractions of typical atomic scales. A horizontal

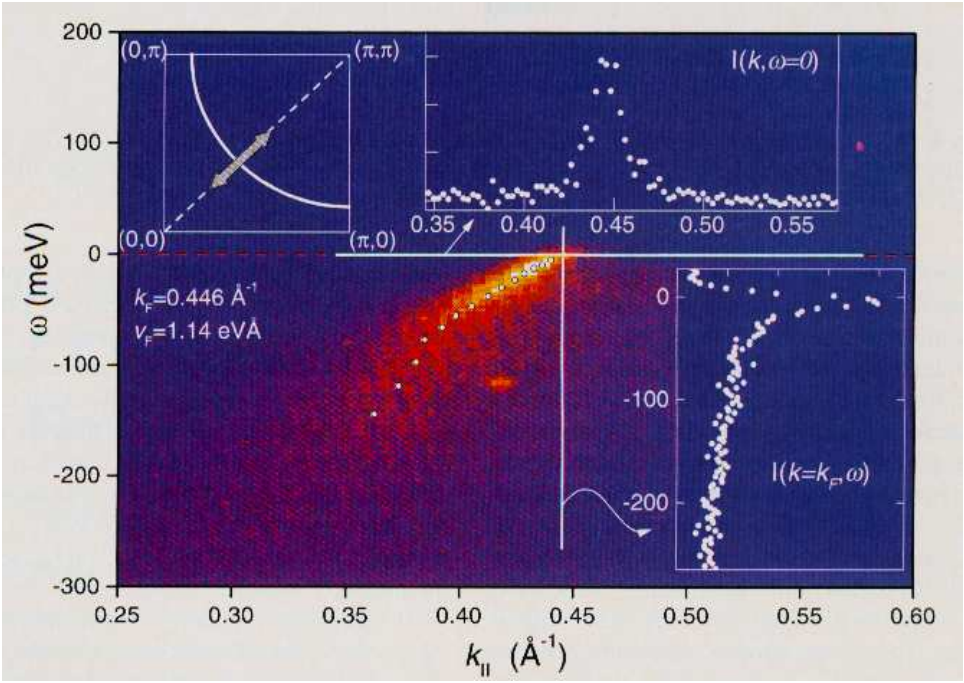

Figure 8.5: ARPES data taken on the high-temperature superconductor $Bi_2Sr_2CaCu_2O_{8+\delta}$. Clockwise from upper left: region of the Brillouin zone sampled in the experiment, cross section at constant $\omega = 0$, cross section at constant momentum. The colour code corresponds to measured intensities. Notice the intensity accumulation at the Fermi surface.

sweep of the tip then generates an accurate image of the surface profile. E.g., Fig. 8.7 shows an STM recording of a three dimensional copper surface. The STM principle can be reversed to artificially *move* atoms on the background of an extended mono-layer surface. E.g., the device shown in Fig. 4.12 was manufactured in this way.

8.2 Linear Response Theory

In the previous section we have argued that condensed matter experiments typically probe the (linear) response of a system to the application of weak electromagnetic perturbations $\{F_j\}$. The quantitative formulation of that statement read as

$$X_i(\mathbf{r},t) = \int d^d r' \int dt'\, \chi_{ij}(\mathbf{r},\mathbf{r}';t,t') F_j(\mathbf{r}',t') + \mathcal{O}(F^2), \tag{8.2}$$

where the functions $\{X_i\}$ were the expectation values of certain operators $\hat{X}_i'$ (currents, scattering intensities, etc.) building up in response to the perturbations $\{F_j\}$, and χ had been a 'response function' describing the functional connection between F_j's and R_i's.

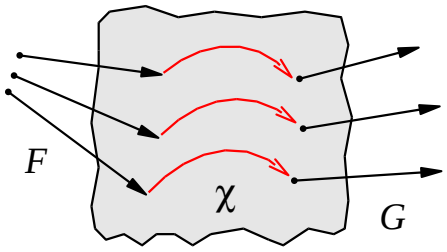

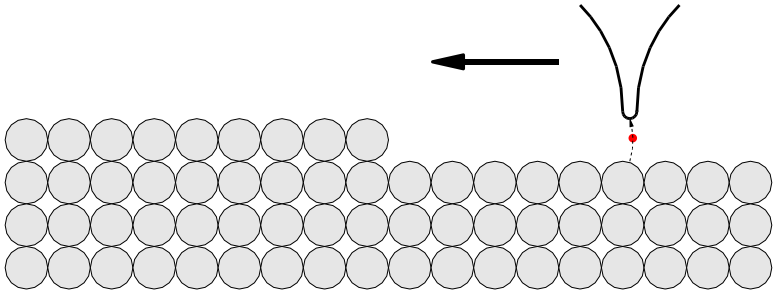

Figure 8.6: The principle of the STM microscope. A thin tip is moved is brought in close separation to a solid state surface. For sufficiently small separations electrons tunnel from the surface onto the tip, i.e. a tunneling current flows. That current is fed back into a piezoelectric crystal which levels the height of the tip. A horizontal scan (at fixed current) thus generates a three-dimensional image of the surface profile.

In the following we shall try to give the formal expression (8.2) a concrete meaning. Which means that we will relate the response function χ to microscopic elements of the theory familiar from previous chapters. However, before entering this discussion, let us list a few properties of χ that follow from common sense reasoning:

▷ The generalized forces $F_j(t')$ cannot cause an effect ($R_i(t)$) prior to their action, i.e.

$$\chi_{ij}(\mathbf{r}, \mathbf{r}'; t, t') = 0, \qquad t < t'.$$

This reflects the principle of **causality**. We say that the response is **retarded**.

▷ If the system Hamiltonian does not *explicitly* depend on time (which will usually be the case), the response depends only on the difference of the time coordinates, $\chi_{ij}(\mathbf{r}, \mathbf{r}'; t, t') = \chi_{ij}(\mathbf{r}, \mathbf{r}'; t - t')$. In this case it is convenient to Fourier transform the temporal convolution (8.2), i.e. to express the response relation in frequency space:

$$R_i(\mathbf{r}, \omega) = \int d^d r' \;\; \chi_{ij}(\mathbf{r}, \mathbf{r}'; \omega) F_j(\mathbf{r}', \omega) + \mathcal{O}(F^2). \tag{8.3}$$

The important statement made by Eq. (8.3) is that in the linear response regime, a (near) monochromatic perturbation acting at a certain frequency ω will cause a response of the *same* frequency. E.g., an AC voltage with frequecy ω will drive an AC current of the same frequency, etc. We can read this statement in reverse to say that *if* the system responds at frequencies $\neq \omega$ we have triggered a strong, *non-linear* response. Indeed, it is straightforward to verify (exercise) that an expansion of the general functional $R[F]$ to nth order in F generates a response with frequency $n\omega$[7].

According to Eq. (8.3) a peak in the response $R_i(\omega)$ at a certain frequency ω indicates a local maximum of the response function, i.e. the presence of an intrinsic excitation with characteristic frequency ω.

[7] While these 'side bands' are usually negligible, they may become sizeable in, e.g., laser-spectroscopic experiments. The field intensities reached by laser beams can easily so large as to generate frequency-doubled, or tripled response signals. However, these phenomena, which belong to the realm of **non-linear optics** are beyond the scope of the present text.

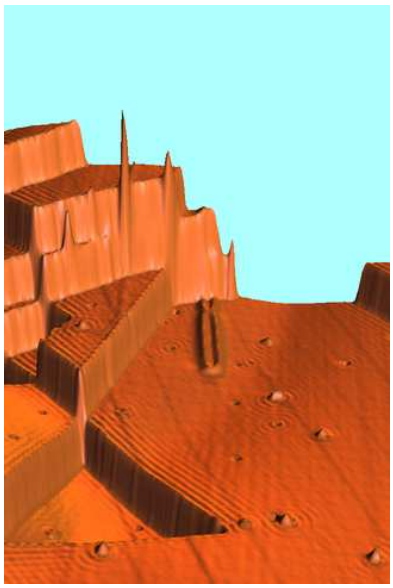

Figure 8.7: STM Image of a copper surface. The concentric ripples sourrounding the set of isolated imperfections are s-wave densitiy modulations of the atomic quantum wave functions!

▷ For systems that are translationally invariant, the response function depends only on differences between spatial coordinates, $\chi_{ij}(\mathbf{r},\mathbf{r}';t-t') = \chi_{ij}(\mathbf{r}-\mathbf{r}';t-t')$. Spatial Fourier transformation then leads to

$$R_i(\mathbf{q},\omega) = \chi_{ij}(\mathbf{q};\omega)F_j(\mathbf{q},\omega) + \mathcal{O}(F^2). \tag{8.4}$$

(In analogy to what was said above about the frequency response,) we conclude that a peak of the function $R_i(\mathbf{q},\omega)$ signals the presence of an exictation with frequency ω and momentum $\mathbf{q}$. We thus see that, at least in principle, linear response measurements are capable of exploring the full dispersion relation of the excitations of a system.

This is as much as we can say without going into more detail. In the following we will employ the field integral formalism to relate the response function to concrete microscopic system properties.

▷ EXERCISE. Consider a perturbation that couples foremostly to the atomic lattice centers of a solid (e.g., x-ray or neutron radiation.) Assume that the response function reflects this property in the sense that $\chi(\mathbf{r},\mathbf{r}')$ is non-vanishing only if both $\mathbf{r}$ and $\mathbf{r}'$ (approximately) coincide with a lattice point. Show that in this case the response of the system, G, is such that

$$\forall \mathbf{Q} \in \text{reciprocal lattice}: \qquad R(\mathbf{q},\omega) = R(\mathbf{q}+\mathbf{Q},\omega).$$

I.e. the angle resolved scattering pattern discplays the full periodicity structure of the reciprocal lattice and, therefore, of the original lattice as well. This is, in a nutshell, the main principle behind spectroscopic crystallography.

8.2.1 Microscopic Response Theory

We now set out to relate the response function to the microscopic elements of the theory. Above we had said that in quantum theory the response signal $X'(t)$ should be interpreted as the expectation value of some (single particle) operator[8]

$$\hat{X}' = c_a^\dagger X'_{aa'} c_{a'},$$

where c_a may be bosonic or fermionic operators. Within the formalism of the field integral the expectation value *at imaginary times* is thus given by

$$X'(\tau) = \left\langle \bar{\psi}_a(\tau) \hat{X}'_{aa'} \psi_{a'}(\tau) \right\rangle, \tag{8.5}$$

where, as usual, $\langle \ldots \rangle = \mathcal{Z}^{-1} \int d(\bar{\psi}, \psi) \exp(-S[F, \bar{\psi}, \psi])(\ldots)$ is the functional average over the action describing our system. The latter is given by

$$S[F, \bar{\psi}, \psi] = S_0[\bar{\psi}, \psi] + \delta S[F, \bar{\psi}, \psi],$$

where S_0 is the action of the unperturbed system and

$$\delta S[F, \bar{\psi}, \psi] = \int d\tau \hat{H}_F = \int d\tau F(\tau) \bar{\psi}_a(\tau) \hat{X}_{aa'} \psi_{a'}(\tau)$$

the perturbation introduced by the action of the generalized force (cf. Eq. (8.1).)

In practice, it is often convenient (for a better motivation, see the next section) to represent $X'(\tau)$ as a derivative of the functional free energy. To this end, let us formally couple our operator $\hat{X}'$ to a second 'generalized force' and define

$$\delta S'[F', \bar{\psi}, \psi] \equiv \int d\tau F'(\tau) \hat{X}'(\tau) = \int d\tau F'(\tau) \bar{\psi}_a(\tau) X'_{aa'} \psi_a(\tau)$$

as a new element of our action. With

$$S[F, F', \bar{\psi}, \psi] = S_0[\bar{\psi}, \psi] + \delta S[F, \bar{\psi}, \psi] + \delta S'[F', \bar{\psi}, \psi],$$

we then have

$$X(\tau) = \left. \frac{\delta}{\delta F'(\tau)} \right|_{F'=0} \ln \mathcal{Z}[F, F'],$$

where the notation

$$\mathcal{Z}[F, F'] = \int \mathcal{D}(\bar{\psi}, \psi) e^{-S[F, F', \bar{\psi}, \psi]}$$

indicates that the partition function $\mathcal{Z}$ functionally depends on the two generalized forces.

Now, if it were not for the presence of the driving force F, the expectation value R would vanish. On the other hand, we also assume that F is weak, in the sense that

[8] For notational clarity, the indices i and $\mathbf{r}$ labelling a multi-component set of local response quantities $X_i(\mathbf{r})$ will be dropped in this section. The same with $F_j(\mathbf{r}')$. Further, to avoid confusion with the expectation value X' both the operator $\hat{X}'$ itself and its matrix elements $\hat{X}_{aa'}$ will be designated by a caret throughout this section.

a linear approximation in F satisfactorily describes the measured value of X'. Noting that the formal first order expansion of a general functional $G[F]$ is given by $G[F] \simeq G[0] + \int d\tau' \left(\frac{\delta}{\delta G(\tau')} \Big|_{F=0} G[F] \right) F(\tau')$, we can write

$$X'(\tau) \simeq \int d\tau' \left(\frac{\delta^2}{\delta F'(\tau) F(\tau')} \Big|_{F=F'=0} \ln \mathcal{Z}[F, F'] \right) F(\tau').$$

Comparison with (8.2) then leads to the tentative identification

$$\chi(\tau, \tau') = \frac{\delta^2}{\delta F'(\tau) F(\tau')} \Big|_{F=F'=0} \ln \mathcal{Z}[F, F']$$

of the response kernel. Carrying out the derivatives, we find

$$\begin{aligned} \chi(\tau, \tau') = \frac{\delta^2}{\delta F'(\tau) F(\tau')} \Big|_{F=F'=0} \ln \mathcal{Z}[F, F'] = \\ = \mathcal{Z}^{-1} \frac{\delta^2}{\delta F'(\tau) F(\tau')} \Big|_{F=F'=0} \mathcal{Z}[F, F'] - \\ - \left(\mathcal{Z}^{-1} \frac{\delta}{\delta F'(\tau)} \Big|_{F'=0} \mathcal{Z}[0, F'] \right) \left(\mathcal{Z}^{-1} \frac{\delta}{\delta F(\tau')} \Big|_{F=0} \mathcal{Z}[F, 0] \right) \end{aligned}$$

Now, by construction the terms in parentheses are the functional expectation values $\langle \hat{X}'(\tau) \rangle$ and $\langle \hat{X}(\tau') \rangle$ taken over the unperturbed action. We had assumed that these averages vanish, so that our preliminary, and still very formal result for the response function is given by

$$\boxed{\chi(\tau, \tau') = \mathcal{Z}^{-1} \frac{\delta^2}{\delta F'(\tau) F(\tau')} \Big|_{F=F'=0} \mathcal{Z}[F, F'].} \tag{8.6}$$

Doing the two derivatives, we obtain a more concrete representation

$$\chi(\tau, \tau') = \left\langle \hat{X}(\tau') \hat{X}'(\tau) \right\rangle = \left\langle \bar{\psi}_a(\tau') X_{aa'} \psi_{a'}(\tau') \; \bar{\psi}_b(\tau) X'_{bb'} \psi_{b'}(\tau) \right\rangle \tag{8.7}$$

of the response function in terms of a four point correlation function.

▷ EXERCISE. Directly expand (8.5) to first order in the generalized force F to obtain this expression. As mentioned above, the usefulness of the derivative construction outlined above will become clear shortly.

▷ INFO. Eq. (8.7) indicates a connection between two seemingly very different physical mechanisms. To disclose this relation, let us consider the case where the observed and the driving operator, respectively, are equal $\hat{X} = \hat{X}'$. (In a moment we will see that the important application to the electromagnetic response of a system falls into this category.) Using the vanishing of the equilibrium expectation values, $\langle \hat{X}(\tau) \rangle = 0$, we can then rewrite (8.7) as

$$\chi(\tau, \tau') = \left\langle \left(\hat{X}(\tau') - \langle \hat{X}(\tau') \rangle \right) \left(\hat{X}(\tau) - \langle \hat{X}(\tau) \rangle \right) \right\rangle. \tag{8.8}$$

This relation is called the **fluctuation-dissipation theorem**. Indeed, the right hand side of the relation clearly describes the quantum-thermal fluctuation behaviour of the (physical observable represented through) the operator $\hat{X}$. In contrast, the left hand side is of dissipative nature. E.g. for the case $\hat{X} = \mathbf{j}$ (see below), χ describes the conduction behaviour of the system, i.e. the way in which the kinetic energy of a charge carrier beam is dissipated among the intrinsic excitations of the system.

We might now proceed to evaluate this function by means of the machinery introduced in the previous chapters and that is, indeed, how the response function will be computed in practice. However, before doing so, we must face up to one more *conceptual* problem. What we are after is the *real time* response $X(t)$ to a *real time* dynamical perturbation $F(t)$. However, our functional integral formalism produces, naturally, an imaginary time response $\chi(\tau, \tau')$. In fact, real/imaginary time mismatches of this kind arose frequently in the problems we studied earlier in this text; we are generally interested in real time dynamical processes while the formalism produces imaginary time answers. In previous chapters we sneeked around that discrepancy by remembering that the imaginary time setup could be obtained by analytical continuation $t \to i\tau$ of the integration contour of a real time functional integral. Reverting this 'Wick rotation' we argued that a real time answer $X(t)$ can be extracted from an imaginary time result $X(\tau)$ by *substitution* $\tau \to it$.

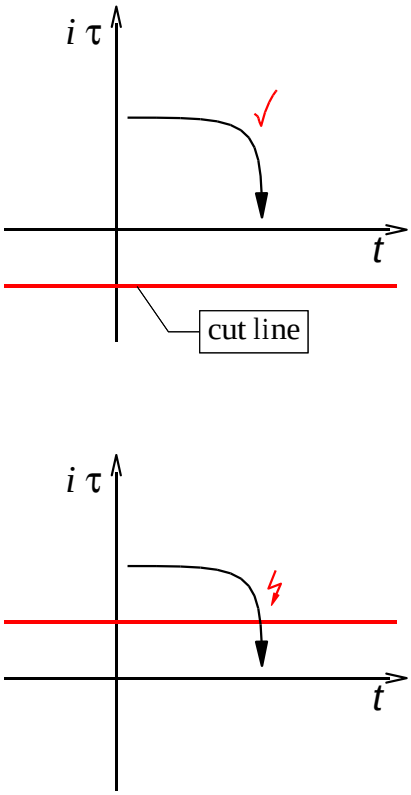

In the majority of cases, this procedure indeed leads to correct results. However, sometimes one has to be more careful and that applies, in particular, to our present linear response calculus. Indeed, the simple substitution $F(\tau) \to F(t) = F(\tau \to it)$ is a crude shortcut of what mathematically should be a decent analytical continuation. Problems with this prescription arise when the answer $F(\tau)$ generated by the functional integral contains singularities in the complex τ-plane[9]. If a ficticious contour interpolating between the limiting points τ and it inevitably crosses these singularities, the simple subsitution prescription is met with a problem (see the cartoon above.)

The upshot of these considerations is that before proceeding with the construction of the linear response formalism, we need to develop a better understanding of the

[9] What is meant by this statement is that the quantity $F(\tau)$ produced by evaluating the functional integral can formally be interpreted as a function on the imaginary axis of a complex time. Analytical continuation then leads to a generalization $F(z)$, where z may take values in a two-dimensional submanifold of the complex plane. What we imply when we substitute $F(\tau) \to F(\tau \to it)$ is that the analyticity domain includes the real axis, *and* that analytical continuation amounts to a simple re-substitution of the argument. Both assumptions may happen to be violated.

8.3 Analytic Structure of Correlation Functions

It is the purpose of this section to clarify – at last – the connection between imaginary and real time correlation functions. Throughout much of the section section we will be back to the traditional operator representation, i.e. expressions with carets, $\hat{X}$, represent canonically quantized operators and $\langle \ldots \rangle = \mathcal{Z}^{-1} \,\mathrm{tr}\,(\exp(-\beta(\hat{H} - \mu\hat{N}))(\ldots))$ is the quantum thermal expectation value.

Restricting ourselves to correlation functions of operators taken at two different times[10], the general definition of the **imaginary time correlation function** reads as

$$\boxed{C^{\tau}_{X_1X_2}(\tau_1 - \tau_2) \equiv -\left\langle T_\tau \hat{X}_1(\tau_1)\hat{X}_2(\tau_2)\right\rangle \equiv -\begin{cases} \langle \hat{X}_1(\tau_1)\hat{X}_2(\tau_2)\rangle, & \tau_1 \geq \tau_2, \\ -\zeta_{\hat{X}}\langle \hat{X}_2(\tau_2)\hat{X}_1(\tau_1)\rangle, & \tau_2 > \tau_1, \end{cases}} \tag{8.9}$$

where $\hat{X}_1(c, c^\dagger)$ are arbitrary operators represented in terms of either boson or fermion operators $\{c, c^\dagger\}$. The time dependence of these operators is defined through the **imaginary time Heisenberg representation**,

$$\hat{X}(\tau) \equiv e^{\tau(\hat{H}-\mu\hat{N})}\hat{X}e^{-\tau(\hat{H}-\mu\hat{N})}, \tag{8.10}$$

i.e. the imaginary time analog of the real time Heisenberg representation familiar from quantum mechanics[11]. The role of the **time ordering operator** T_τ, whose action is defined through the second equality[12], is to chronologically order the two operators $\hat{X}_1(\tau_1)$ and $\hat{X}_2(\tau_2)$.

Notice that for $\hat{X}_i = c^\dagger_\alpha X_{i\alpha\beta}c_\beta$, the second quantised representation of one body operators X_i, the definition above describes the response functions discussed in the previous section. For $\hat{X}_1 = c_\alpha, \hat{X}_2 = c^\dagger_\beta$, (8.9) coincides with the one-body imaginary time correlation functions ('Green functions') discussed earlier in this text. I.e. (8.9) and its real time descendants to be discussed momentarily cover most of the correlation functions of relevance in many body physics.

▷ INFO. Although we shall postpone the discussion of the connection to the field integral formalism for a while, it is instructive to compare the definition (8.9) to the field integral correlation function (8.7) defined above. Indeed, *if* the quantities $\hat{X}_i(\tau_i)$ in (8.9) were to be interpreted as the functional representation of second quantized operators, $\hat{X}(a^\dagger, a) \to \hat{X}(\bar{\psi}, \psi)$, the two correlation functions would coincide. The reason is that the time ordering operation acting on the functional representation of an operator pair is redundant, $T_\tau \hat{X}_1(\bar{\psi}(\tau_1), \psi(\tau_1))\hat{X}_2(\bar{\psi}(\tau_2), \psi(\tau_2)) = \hat{X}_1(\bar{\psi}(\tau_1), \psi(\tau_1))\hat{X}_2(\bar{\psi}(\tau_2), \psi(\tau_2))$ (why?). In other words, the correlation function (8.9) reduces to (8.7), when the operators are represented within the field integral formalism. (The reason

[10] According to our discussion above, correlation functions of this type suffice to explore the linear response of a system. Although the situation with non-linear response signals is more complicated, much of what we are going to say below has general validity.

[11] Within imaginary time theory it is customary to absorb the chemical potential into the dynamical evolution of an operator.

[12] The sign factor $\zeta_{\hat{X}} = \pm 1$ depends on the statistics of $\hat{X}_i$. (I.e. $\zeta_{\hat{X}} = -1$ if $\hat{X}_i$ are bosonic. ($\hat{X}_i$ is bosonic if $\{c, c^\dagger\}$ are Bose operators *or* if it is of even order in a fermion algebra.) or $\zeta_{\hat{X}} = 1$ if they are fermionic.)

why T_τ is *not* redundant for canonically quantized operators is that these have a non-vanishing commutator/anticommutator at equal times.)

In a mannner that is difficult to motivate in advance, we next introduce not one but *three* different response functions of a real time argument.

Substituting in (8.9) real time arguments for imaginary times, $\tau \to it$, we obtain the **real time response function**

$$\boxed{C^T_{X_1X_2}(t_1 - t_2) = -i \left\langle T_t \hat{X}_1(t_1)\hat{X}_2(t_2) \right\rangle ,} \tag{8.11}$$

where the factor of i has been introduced for later convenience, T_t chronologically orders real times, and

$$\hat{X}(t) \equiv e^{it(\hat{H}-\mu\hat{N})}\hat{X}e^{-it(\hat{H}-\mu\hat{N})},$$

are real time Heisenberg operators. While this expression appears to be the 'natural' generalization of (8.9), it is *not* our prime object of interest. Much more physical significance carries the **retarded response function**

$$\boxed{C^+_{X_1X_2}(t_1 - t_2) = -i\Theta(t_1 - t_2) \left\langle [\hat{X}_1(t_1), \hat{X}_2(t_2)]_{\zeta_{\hat{X}}} \right\rangle ,} \tag{8.12}$$

i.e. an object that exists only for times $t_1 > t_2$ (hence the attribute 'retarded'). The complementary time domain, $t_1 < t_2$ is described by the **advanced response function**

$$\boxed{C^-_{X_1X_2}(t_1 - t_2) = +i\Theta(t_2 - t_1) \left\langle [\hat{X}_1(t_1), \hat{X}_2(t_2)]_{\zeta_{\hat{X}}} \right\rangle .} \tag{8.13}$$

▷ INFO. What is the **physical meaning of the real time retarded response function?** To understand this point we need to reformulate the linear response arguments given above in the language of the canonical operator formalism. What we would like to compute is the expectation value

$$X'(t) = \left\langle \hat{X}' F(t) \right\rangle , \tag{8.14}$$

building up in response to the presence of a weak perturbation $F(t)\hat{X}$ in the system Hamiltonian $\hat{H} = \hat{H}_0 + F(t)\hat{X}$. In (8.14), the superscript 'F' indicates that the time evolution of $\hat{X}'$ follows the full Hamiltonian (including the perturbation $F(t)\hat{X}$.) In contrast, the angular brackets represent a thermal average $\langle \ldots \rangle = \mathcal{Z}^{-1} \operatorname{tr} (\exp(-\beta\hat{H}_0)(\ldots))$ that does *not* include the perturbation[13]. The philosophy behind that convention is that somewhere in the distant past, $t \to -\infty$, the system has been prepared in a thermal equilibrium distribution of the unperturbed Hamiltonian $\hat{H}_0$. As time evolved a perturbation $\propto F(t)$ was gradually switched on until it began to affect the expectation value of the dynamically evolved operator $\hat{X}'$. (One need not be irritated by the somewhat artificial definition of that **switching on procedure**; all it tells us is that $\hat{X}$ acts on a system in thermal equilibrium, an assumption that is unproblematic if the perturbation is sufficiently weak.) To compute the expectation value, it is convenient to switch

[13] To simplify the notation, the chemical potential has been absorbed into the definition of $\hat{H}$.

to a representation, wherein the evolutionary changes due to the action of the perturbation are separated:

$$X'(t) = \left\langle \hat{U}^{F\,-1}(t)\hat{X}'(t)\hat{U}^F(t) \right\rangle \tag{8.15}$$

where $\hat{U}^F(t) = \hat{U}_0^{-1}(t)\hat{U}(t)$, the evolution of $\hat{X}'$ follows the standard Heiseberg dynamics $\hat{X}'(t) = \hat{U}_0(t)\hat{X}'\hat{U}_0^{-1}(t)$, and $\hat{U}(\hat{U}_0)$ generates the time evolution of the full (unperturbed) Hamiltonian. Using the defining equations of these evolution operators, it is straightforward to verify that $\hat{U}^F$ obeys the differential equation,

$$d_t\hat{U}^F(t) = -iF(t)\hat{X}(t)\hat{U}^F(t),$$

i.e. the time evolution of $\hat{U}^F$ is controlled by the (Heisenberg representation) of the perturbation $\hat{X}$. According to conventional time dependent quantum mechanical perturbation theory, the solution of this differential equation (with boundary condition $\hat{U}^F(t \to -\infty) \to \mathbf{1}$) is given by

$$\hat{U}^F(t) = T_t \exp\left(-i\int_{-\infty}^{t} dt' F(t')\hat{X}(t')\right) \simeq \mathbf{1} - i\int_{-\infty}^{t} dt' F(t')\hat{X}(t') + \ldots.$$

Substituting this result into (8.15) we obtain

$$X'(t) = -i\int dt'\theta(t-t')F(t')\left\langle [\hat{X}'(t), \hat{X}(t')] \right\rangle = \int dt'\, C^+_{X'X}(t-t')F(t'),$$

i.e. the retarded response function turns out to generate the linear response of $\hat{X}_1$ to the presence of the perturbation. In other words, the function C^+ is our prime object of interest, while all other correlation functions defined above play the (potentialy important) role of supernumeraries.

We next set out to explore the connection between the different correlation functions definied above. In doing so, the principal question that should be at the back of our minds is 'how do we obtain the retarded real time function C^+ provided we know the imaginary time correlation function C^τ?' The key to the answer to this question lies in a highly formal representation of the correlation functions $C^{t,\tau,+,-}$, known as the **Lehmann representation**. This representation is obtained by representing the correlation functions in terms of an exact eigenbasis $\{|\Psi_\alpha\rangle\}$ of the system: representing the trace entering the thermal expectation values as $\mathrm{tr}(\ldots) = \sum_\alpha \langle\Psi_\alpha|\ldots|\Psi_\alpha\rangle$, and inserting a resolution of unity $\mathbf{1} = |\Psi_\beta\rangle\langle\Psi_\beta|$ between the two operators appearing in the definition of the correlation function it is straightforward to show that, e.g.,

$$C^T(t) = -i\mathcal{Z}^{-1}X_{1\alpha\beta}X_{2\beta\alpha}e^{it\Xi_{\alpha\beta}}\left(\Theta(t)e^{-\beta\Xi_\alpha} - \zeta_X\Theta(-t)e^{-\beta\Xi_\beta}\right). \tag{8.16}$$

Here, E_α is the eigenvalue corresponding to a state Ψ_α and we have introduced the shorthand notations

$$\begin{aligned} \Xi_\alpha &\equiv E_\alpha - \mu N_\alpha, \\ \Xi_{\alpha\beta} &\equiv \Xi_\alpha - \Xi_\beta, \\ X_{\alpha\beta} &\equiv \langle\Psi_\alpha|\hat{X}|\Psi_\beta\rangle. \end{aligned}$$

We next Fourier transform C^T to[14]

$$C^T(\omega) = \int_{-\infty}^{\infty} dt\, C^T(t) e^{i\omega t - \eta|t|} = \tag{8.17}$$
$$= \mathcal{Z}^{-1} X_{1\alpha\beta} X_{2\beta\alpha} \left[\frac{e^{-\beta\Xi_\alpha}}{\omega + \Xi_{\alpha\beta} + i\eta} + \zeta_{\hat{X}} \frac{e^{-\beta\Xi_\beta}}{\omega + \Xi_{\alpha\beta} - i\eta} \right],$$

where the convergence generating factor η – which will play an important role throughout! – has been introduced to make the Fourier representation well defined[15].

Eq. (8.17) is the Lehmann representation of the real time correlation function. What is the use of this representation? Clearly, Eq. (8.17) will be of little help for any practical purposes; the equation makes explicit reference to the exact eigenfunctions/states of the system but if we had access to *these* objects, we had solved the full problem anyway. The principal purpose of spectral resolutions such as (8.17) rather is to disclose exact connections between different types of correlation functions, and the analytical structure of these objects in general. To do so, we first need to compute the Lehmann representation of the other correlation functions. Proceeding as with the real time function above, it is straightforward to show that

$$\left\{ \begin{array}{c} C^T \\ C^+ \\ C^- \end{array} \right\} (\omega) = \mathcal{Z}^{-1} X_{1\alpha\beta} X_{2\beta\alpha} \left[\begin{array}{cc} \dfrac{e^{-\beta\Xi_\alpha}}{\omega + \Xi_{\alpha\beta} \left\{ \begin{array}{c} + \\ + \\ - \end{array} \right\} i\eta} & + \zeta_{\hat{X}} \dfrac{e^{-\beta\Xi_\beta}}{\omega + \Xi_{\alpha\beta} \left\{ \begin{array}{c} - \\ + \\ - \end{array} \right\} i\eta} \end{array} \right]. \tag{8.18}$$

From this result, a number of important features of the correlation functions can readily be read off. Anticipating the analytical structures alluded to above, we should think of $C^{T,+,-}(z)$ as functions of a *complex* variable z. (The representations above display the restriction $C^{T,+,-}(z = \omega)$ to the real axis.) This, extended interpretation allows us to look at $C^{T,+,-}$ as complex functions with singularities in the immediate vicinity of the real axis. More specifically,

- ▷ The retarded correlation function C^+ has singularities for $z = -\Xi_{\alpha\beta} - i\eta$ slightly below the real axis. It is, however, analytic in the entire upper complex half plane $\mathrm{Im}\,(z) \geq 0$. Conversely,
- ▷ the advanced correlation function G^- has singularities above the real axis. It is analytic in the lower half plane $\mathrm{Im}\,(z) \leq 0$. Notice that C^+ and C^- are connected through complex conjugation,

$$C^+(\omega) = \left[C^-(\omega) \right]^* . \tag{8.19}$$

[14] Whereever no confusion may arise, we omit the operator subscript $C_{XX'}$ carried by the correlation functions.

[15] Indeed, we can attach physical significance to this factor. The switching-on procedure outlined above can be implemented by attaching a small damping term $\exp(-|t|\eta)$ to an otherwise purely oscillatory force . If we absorb this factor into the definition of all Fourier integrals, $\int dt\, (F(t) e^{-t|\eta|}) e^{i\omega t} (\ldots) \to \int dt\, F(t)\, (e^{-t|\eta|} e^{i\omega t})\, (\ldots)$, we arrive at the Fourier regularization mentioned above.

▷ The time ordered correlation function has singularities on either side of the real axis (which makes it harder to analyse.)

▷ The spacing of the singularities in the vicinity of the real axis contains important information about the fundamental excitations of the system (cf. Fig. 8.8). E.g. consider the case where $\hat{X}_1 = c_a^\dagger$ and $\hat{X}_2 = c_b$ are one-particle creation and annihilation operators (no matter whether bosonic or fermionic.) In this case, $N_\alpha - N_\beta \equiv \Delta N = 1$ (independent of the state indices α, β) and $E_\alpha - E_\beta$ is of the order of the *single particle* energies of the system. (For a non-interacting system, $E_\alpha - E_\beta$ *strictly* coinicides with the single particle energies, why?) I.e. the singularities of $C^{T,+,-}$ map out the single particle spectrum of the system. This can be understood intuitvely by remembering the meaning of the one particle correlation function as the amplitude for creation of a state $|a\rangle$ followed by the anihilation of a state $|b\rangle$ at some later time. It is clear that the time Fourier transform of the amplitude $|a\rangle \stackrel{t}{\to} |b\rangle$ becomes 'large' when the phase $\sim \omega t$ of the Fourier argument is in resonance with an eigenphase $\sim (E_\alpha - E_\beta)t$ supported by the system. (If you don't find this statement plausible, explore the simple example of, e.g., a plane wave Hamiltonian.) Similarly, for a two particle correlation function, $\hat{X}_1 \sim c_a^\dagger c_b$, the energies $E_\alpha - E_\beta$ describe the spectrum (the 'energy cost') of two particle excitations, etc.

Also notice that the single particle spectrum can be continuous (in which case the functions $C^{T,+,-}$ have *cuts* parallel to the real axis), or discrete (isolated poles.)

▷ Once one of the correlation functions is known, all others follow straightforwardly from a simple dictionary: using the familiar Dirac identity,

$$\lim_{\eta \searrow 0} \frac{1}{x + i\eta} = -i\pi\delta(x) + \mathcal{P}\frac{1}{x}, \tag{8.20}$$

where $\mathcal{P}$ is the prinicpal part, it is a straightforward matter to show that (exercise!)

$$\boxed{\text{Re}\, C^T(\omega) = \text{Re}\, C^+(\omega) = \text{Re}\, C^-(\omega)} \tag{8.21}$$

and

$$\boxed{\text{Im}\, C^T(\omega) = \pm\, \text{Im}\, C^\pm(\omega) \begin{cases} \coth\left(\frac{\beta}{2}(\omega - \mu\Delta N)\right), & \text{bosons} \\ \tanh\left(\frac{\beta}{2}(\omega - \mu\Delta N)\right), & \text{fermions.} \end{cases}} \tag{8.22}$$

i.e. the information stored in the three different functions is essentially equivalent.

After our so-far discussion of the real time correlation functions, the analysis of the imaginary time function C^τ is straightforward. The imaginary time analog of (8.16) reads as

$$C^\tau(\tau) = -\mathcal{Z}^{-1} X_{1\alpha\beta} X_{2\beta\alpha} e^{\Xi_{\alpha\beta}\tau} \left(\Theta(\tau) e^{-\beta\Xi_\alpha} + \zeta_{\hat{X}} \Theta(-\tau) e^{-\beta\Xi_\beta}\right). \tag{8.23}$$

Inspection of this representation for positive and negative times, respectively, shows that C^τ shares its periodicity properties with the operators $\hat{X}_{1,2}$:

$$C^\tau(\tau) = \zeta_{\hat{X}} C^\tau(\tau + \beta), \qquad \tau < 0. \tag{8.24}$$

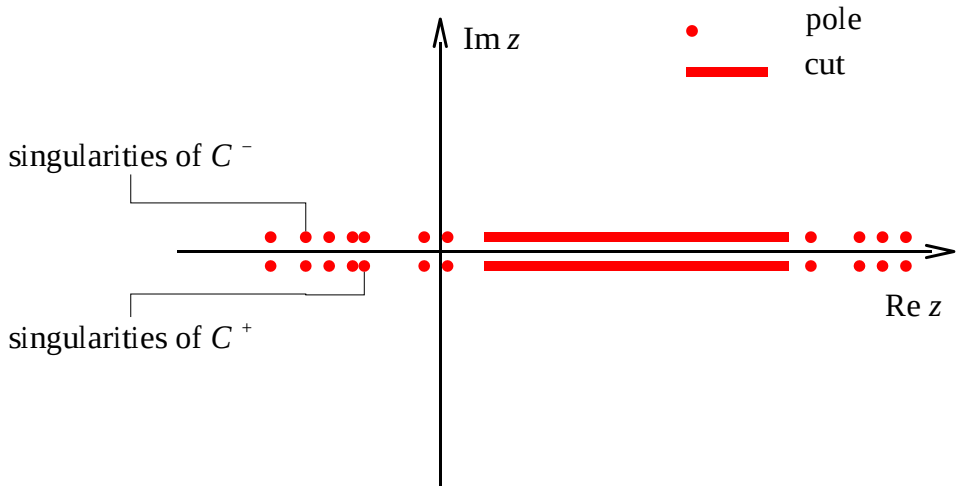

Figure 8.8: Diagram illustrating the singularities of advanced and retarded correlation functions in the complex plane.

Consequently, C^τ can be expanded in a Matsubara Fourier representation, just like a conventional operator,

$$C^\tau(i\omega_n) = \int_0^\beta C^\tau(\tau) e^{i\omega_n \tau},$$

where, depending on the nature of the operators $\hat{X}_{1,2}$, ω_n may be a bosonic or a fermionic Matsubara frequency. Applying this transformation to the Lehmann representation (8.23), we obtain

$$C^\tau(i\omega_n) = \mathcal{Z}^{-1} \frac{X_{1\alpha\beta} X_{2\beta\alpha}}{i\omega_n + \Xi_{\alpha\beta}} \left[e^{-\beta\Xi_\alpha} + \zeta_X e^{-\beta\Xi_\beta} \right]. \tag{8.25}$$

Our final task is to relate the four correlation functions defined through (8.18) and (8.25) to each other. To this end, we define the 'master function'

$$C(z) = \mathcal{Z}^{-1} \frac{X_{1\alpha\beta} X_{2\beta\alpha}}{z + \Xi_{\alpha\beta}} \left[e^{-\beta\Xi_\alpha} + \zeta_X e^{-\beta\Xi_\beta} \right]. \tag{8.26}$$

depending on a complex argument z. When evaluated for $z = \omega^+, \omega^-, i\omega_n$, respectively, the function $C(z)$ coincides with C^+, C^-, C^τ. Further, $C(z)$ is analytic everywhere except for the real axis. This knowledge suffices to construct the sought for relation between different correlation functions: Suppose we had succeeded in computing $C^\tau(i\omega_n) = C(z = i\omega_n)$ for *all* positive Matsubara frequencies[16] . Further, assume we had managed to find an analytic extension of $C(z = i\omega_n) \to C(z)$ into the entire upper complex plane $\mathrm{Im}\, z > 0$. The evaluation of that extension on the infinitesimally shifted real axis $z = \omega + i0$ then coincides with the retarded Green function $C^+(\omega)$. In other words,

[16] Keep in mind that in practical computations of this type we will not proceed through the Lehmann representation.

To find $C^+(\omega)$ we need to (i) compute $C^\tau(i\omega_n)$ for all positive Matsubara frequencies (e.g. by means of the thermal field integral) and then (ii) continue the result down to the real axis, $i\omega_n \to \omega + i0$.

The advanced Green function C^- is obtained analogously, by analytic extension from the thermal correlation function $C^\tau(\omega_n < 0)$ to frequencies with a negative offset, $\omega - i0$.

These statements follow from a theorem of complex function theory stating that two analytic functions $F_1(z)$ and $F_2(z)$ coincide *iff* $F_1(z_n) = F_2(z_n)$ on a sequence $\{z_i\}$ with a limit point in the domain of analyticity. (In our case $i\omega_n \to i\infty$ is the limit point.) From inspection of (8.26) we already know that $F_1(i\omega_n) \equiv C^+(\omega \to i\omega_n)$ coincides with $F_2(i\omega_n) = C^\tau(i\omega_n)$. Thus any analytic extension of C^τ must coincide with C^+ everywhere in the upper complex plane, including the infinitesimally shifted real axis.

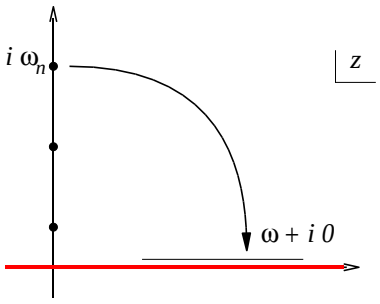

▷ EXERCISE. Writing $z = \omega \pm i\eta$ transform the spectral representation (8.26) back to time space:

$$C(t) = \frac{1}{2\pi} \int d\omega \; e^{-i\omega t} C(\omega \pm i\eta).$$

Convince yourself that for $\mathrm{Im}(z)$ positive (negative), the temporal correlation function $C(t)$ contains a Θ-function $\Theta(t)$ ($\Theta(-t)$). (Hint: Cauchies theorem.) Importantly, the presence of this constraint does not hinge on η being infinitesimal. It even survives generalization to a frequency dependent *function* $\eta(\omega) > 0$. (For the physical relevance of this statment, see below.) All what matters is that for $\eta > 0$ the function $C(\omega \pm i\eta)$ is analytic in the upper (lower) complex half plane. This observation implies a very important **connection between analyticity and causality**: Temporal correlation functions whose frequency representation is analytic in the upper (lower) complex half plane are causal (anticausal). (A time dependent function is called '(anti)causal' if it vanishes for (postive) negative times.)

How is continutation process required to find the retarded correlation function carried out in practice? Basically, the answer follows from what was said above: If we know the correlation function $C^\tau(\omega_n)$ for all positiive Matsubara frequencies, and if that function remains analytic upon substitution $C^\tau(\omega_n \to -iz)$ of a general element of the full complex half plane, the answer is simple. We merely have to *substitute* $\omega_n \to -i\omega + 0$ into our result to obtain the retarded correlation function. Sometimes, however, we simply do not know $C^\tau(i\omega_n)$ for all positive frequencies. (E.g., because we were working within an effective low energy theory whose regime of validity is restricted to frequencies $\omega_n < \omega^*$ smaller than some cutoff frequency.) In this case, we are in serious trouble. Everything then hinges on finding a 'meaningful' model function which can be extended to infinity and whose evaluation for small frequencies $\omega_n < \omega^*$ coincides with our result; there are no generally applicable recipes how to deal with such situations.

▷ INFO. As a special case of great practical importance, let us briefly explore the **non-**

interacting single particle Green function, i.e. the single-particle correlation function $\hat{X}_1 = c_a$, $\hat{X}_2 = c_a^\dagger$ for a non-interacting system. (We assume that $\{|a\rangle\}$ is an eigenbasis of the one-particle Hamiltonian.) Expectedly, these correlation functions assume a particularly simple form.

In the non-interacting case, the eigenstates $|\alpha\rangle = |a_1, a_2, \ldots\rangle$ are Slater determinants of single particle eigensates $|a_i\rangle$. Their energy is $E_\alpha = \epsilon_{a_1} + \epsilon_{a_2} + \ldots$, were ϵ_a are the single particle energies. Using that $E_\beta = E_\alpha + \epsilon_a$ (why?) one then verifies that the correlation function acquires the simple form

$$C(z)\Big|_{\substack{\hat{X}_1 = c_a \\ \hat{X}_2 = c_a^\dagger}} \equiv G_a(z) = \frac{1}{z - \xi_a},$$

i.e. the partition function entering the definition of the general correlation function cancels against the thermally weighted summation over $|\alpha\rangle$ (please check!) Notice that the thermal version of this Green function, $G_a(i\omega_n) = (i\omega_n - \xi_a)^{-1}$ appeared previously as the fundamental building block of perturbation theory. This is, of course, no coincidence: within the formalism of the field integral, the Green function appeared as the functional expectation value $\langle \bar{\psi}_{a,n} \psi_{a,n} \rangle_0$ taken with respect to the Gaussian non-interacting action. But this object is just the functional representation of the operator correlation function considered above.

Building on this representation, it is customary to introduce a **Green function operator** through

$$\hat{G}(z) \equiv \frac{1}{z + \mu - \hat{H}}.$$

By design, the eigenvalues of this operator – which are still functions of z – are given by the correlation function $G_a(z)$ above. Numerous physical observables can compactly represented in terms of the operator Green function. E.g., using (8.20) it is straightforward to verify that the single particle DoS obtains as

$$\boxed{\rho(\epsilon) = -\frac{1}{\pi} \text{Im tr } \hat{G}^+(\epsilon),} \tag{8.27}$$

by taking the trace of the retarded Green function (operator.)

To illustrate the procedure of analytic continuation, let us consider a few elementary examples (for a more elaborate problem, see section XX):

1. For the single particle Green function ($\hat{X}_1 = c_a, \hat{X}_2 = c_a^\dagger$)

   $$G_a(\omega_n) = \frac{1}{i\omega_n - \xi_a}$$

   of an elementary excitation with energy ϵ_a, the continuation amounts to a mere substitution,

   $$G_a^+(\omega) = \frac{1}{\omega + i0 - \xi_a}$$

2. We saw that quasi-particle interactions lead to the appearance of a – generally complex – self energy $\Sigma(z)$:

   $$G_a(\omega_n) \to \frac{1}{i\omega_n - \xi_a - \Sigma(i\omega_n)},$$

where we have simplified the notation by suppressing the potential dependence of the self energy on the Hilbert space index a. Extension down to the real axis leads to

$$G_a^+(\omega) = \frac{1}{\omega^+ - \xi_a - \Sigma(\omega^+)}, \tag{8.28}$$

where $\omega^+ \equiv \omega + i0$ and $\Sigma(\omega^+)$ is the analytic continuation of the function $\Sigma(z)$ to the real axis. Although the specific structure of the self energy depends on the problem under consideration, a few statement can be made in general. Specifically, decomposing the self energy into real and imaginary part,

$$\begin{aligned} \mathrm{Re}\Sigma(\omega^+) &= +\mathrm{Re}\Sigma(\omega^-) \\ \mathrm{Im}\Sigma(\omega^+) &= -\mathrm{Im}\Sigma(\omega^-) > 0. \end{aligned} \tag{8.29}$$

In words: the self energy function has a cut on the real axis. Upon crossing the cut, its imaginary part changes sign. This important feature of the self energy can be understood from different perspectives. Formally, it follows from Eq. (8.19) relating retarded and advanced Green function through complex conjugation. More intuitively, the sign dependence of the imaginary part can be understood as follows: suppose we start from a non-interacting imaginary time formalism and gradually switch on interactions. The (Landau) principle of adiabatic continuity implies that nowhere in this process must the Green function – alias the propagator of the theory – become singular. This implies, in particular, that the combination $i\omega_n + \mathrm{Im}\Sigma_{i\omega_n}$ must not become zero, lest the dangerous real axis of the energy denominator be touched. The safeguard preventing the vanishing of the imaginary part of the energy denominator is that $\mathrm{Im}\Sigma$ and ω_n have the same sign. Of course, this feature can be checked order by order in perturbation theory.

Decomposing the self energy according to $\Sigma = \Sigma' + i\Sigma''$ into real and imaginary part, (8.28) implies the interpretation of $\mathrm{Im}\,\Sigma = \Sigma''$ as (one half of the) **effective lifetime** of a particle. To see this, let us transform $G^+(\omega)$ back to time space:

$$G^+(t) = \frac{1}{2\pi}\int d\omega\; e^{-i\omega t} G^+(\omega) \approx e^{it(\xi_a + \Sigma') - t\Sigma''}\Theta(t),$$

where we have made the (over)simplifying assumption that the dependence of the self energy operator on ω is negligible: $\Sigma(\omega) \approx \Sigma$. (exercise: check the second equality above.) Interpreting $G^+(t)$ as the amplitude for propagation in the state $|a\rangle$ during a time interval t, and $|G^+|^2$ as the associated *probability*, we observe that the probability to stay in state $|a\rangle$ decays exponentially,

$$|G^+|^2 \propto e^{-2t\Sigma''},$$

i.e. $2\Sigma'' \equiv \frac{1}{\tau}$ can be identified as the inverse of the 'lifetime' τ of state $|a\rangle$. The appearence of a finite life time expresses the fact that in the presence of interactions, *single particle* states no longer represent stable objects but rather tend to decay into the continuum of correlated many body states. This picture will be substantiated in section 8.3.1 below.

3. Let us apply Eq. (8.27) to compute the BCS quasi-particle DoS of a superconductor.

   In section 7.3.3 we saw that the thermal Gorkov Green function of a superconductor with spatially constant real order parameter is given by

$$\hat{G}(i\omega_n) = \Big[i\omega_n - (\hat{H} - \mu)\sigma_3 - \Delta\sigma_1 \Big]^{-1}.$$

   switching to an eigen-representation and using Eq. (**??**) to invert the Pauli matrix structure we obtain

$$-\frac{1}{\pi}\mathrm{tr}\,\hat{G}(i\omega_n) = -\frac{1}{\pi}\sum_a \mathrm{tr}\,\left[\frac{-i\omega_n + \xi_a\sigma_3 + \Delta\sigma_1}{\omega_n^2 + \xi_a^2 + \Delta^2}\right] = \frac{2i\omega_n}{\pi}\sum_a \frac{1}{\omega_n^2 + \xi_a^2 + \Delta^2}$$

   Next, performing our standard change from a summation over eigenenergies to an integral, we arrive at

$$-\frac{1}{\pi}\mathrm{tr}\,\hat{G}(i\omega_n) \simeq \frac{2i\omega_n}{\pi}\rho_0 \int d\xi \frac{1}{\omega_n^2 + \xi^2 + \Delta^2} = \frac{2i\omega_n\rho_0}{\sqrt{\omega_n^2 + \Delta^2}}.$$

   This is the quantity we need to continue to real frequencies. To this end we adopt the standard convention whereby the cut of the $\sqrt{}$-function is on the negative real axis, that is,

$$\sqrt{-r + i0} = -\sqrt{-r - i0} = i\sqrt{|r|}$$

   for r negative real. Then,

$$-\frac{1}{\pi}\mathrm{tr}\,\hat{G}(i\omega_n \to \epsilon^+) = \frac{2\epsilon^+\rho_0}{\sqrt{-\epsilon^{+2} + \Delta^2}} \simeq \frac{2\epsilon\rho_0}{\sqrt{-\epsilon^2 - i0\,\mathrm{sgn}\,(\epsilon) + \Delta^2}},$$

   where we anticipate that the infinitesimal offset of ϵ in the numerator is irrelevant (trace its fate!) and use that for ϵ approaching the real axis only the *sign* of the imaginary offset matters: $(\epsilon + i0)^2 \simeq \epsilon^2 + 2i0\epsilon \simeq \epsilon^2 + 2i0\,\mathrm{sgn}\,\epsilon$. Finally, taking the imaginary part of that expression, we arrive at the standard BCS form

$$\rho(\epsilon) = \mathrm{Im}\,\frac{2\epsilon\rho_0}{\sqrt{-\epsilon^2 - i0\,\mathrm{sgn}\,(\epsilon) + \Delta^2}} = \begin{cases} 0 & |\epsilon| < \Delta \\ \frac{2|\epsilon|\rho_0}{\sqrt{\epsilon^2 - \Delta^2}} & |\epsilon| > \Delta \end{cases},$$

   computed in Eq. (**??**) in a slightly different manner.

8.3.1 Sum Rules and Other Exact Identities

In the next section we will apply the analytical structures discussed above to construct a powerful theory of real time linear response. However, before doing so, let us stay for a moment with the formal Lehmann representation to disclose a number of exact identities, or 'sum rules' obeyed by the correlation functions introduced in the previous section. Admittedly, this addition to our discussion above does not directly relate to the formalism of linear response, and readers wishing to proceed in a more streamline manner are invited to skip this section at first reading.

In fact, the formulae we are going to collect are not specific to *any* particular context and that is precisely their merit: Identities based on the analytical structure of the Lehmann representation are exact and enjoy general applicability. They can be used to (a) obtain full knowledge of a correlation function from fragmented information – e.g. we saw in Eqs. (8.21) and (8.22) how all three real time correlation functions can be obtained once only one of them is known –, and, equally important, (b) to gauge the validity of approximate calculations. The violation of an exact identity within an approximate analysis is usually an herold of serious trouble, i.e. such deviations mostly lead to physically meaningless results.

The Spectral (Density) Function

We begin by considering an object that carries profound physically significance in its own right, especially in the area of strongly correlated fermion physics, viz. (-2 times) the imaginary part of the retarded correlation function,

$$\boxed{A(\omega) \equiv -2\,\mathrm{Im}\, C^{+}(\omega).} \tag{8.30}$$

Eq. (8.30) defines the so-called **spectral function** or **spectral density function**. Using Eq. (8.20) and the Lehmann representation (8.18) it is straightforward to verify that it has the spectral decomposition

$$A(\omega) = 2\pi \mathcal{Z}^{-1} X_{1\alpha\beta} X_{2\beta\alpha} \left[e^{-\beta \Xi_\alpha} + \zeta_{\hat{X}} e^{-\beta \Xi_\beta} \right] \delta(\omega + \Xi_{\alpha\beta}). \tag{8.31}$$

▷ INFO. To understand the **physical meaning of the spectral function** let us consider the case where $\hat{X}_{1,2}$ are single particle creation/anihilation operators, $\hat{X}_1 = c_a$, $\hat{X}_2 = c_a^\dagger$. (We assume that the non-interacting part of the system Hamiltonian, $\hat{H}_0 + \hat{V}$ is diagonalized by a basis $\{|a\rangle\}$.) For a non-interacting problem, $\hat{V} = 0$, it is then straightforward to show that

$$A_a(\omega) = 2\pi\delta(\omega - \xi_a),$$

i.e. the spectral function is singularly peaked at the single particle energy (measured from the chemical potential) of the state $|a\rangle$. Here, the subscript 'a' indicates that we are dealing with a spectral function defined for a pair of one-body operators $c_a, c_a^\dagger$.

Heuristically, the singular structure of $A_a(\omega)$ can be understood by observing that in the non-interacting case the state $|\alpha\rangle + |a\rangle$ obtained by adding a single particle $|a\rangle$ to the Slater determinant $|\alpha\rangle$ is, again, an eigenstate of the system. In particular, it is orthogonal to all states but itself whence the eigenstate summation over $|\beta\rangle$ contains only a single non-vanishing term. We say that the 'spectral weight' carried by the (unit-normalized) state $|\alpha\rangle + |a\rangle$ is concentrated on a single eigenstate of the system.

What happens to this picture if interactions are switched on? In this case, the addition $|\alpha\rangle + |a\rangle$ of a single particle state to a many body eigenstate will, in general, no longer be an eigenstate of the system. In particular, there is no reason to believe that this state is orthogonal to all but one $N+1$ particle states $|\beta\rangle$. We have to expect that the spectral weight carried by the (still unit-normalized) state $|\alpha\rangle + |a\rangle$ gets distributed over many, potentially, a continuum of states $|\beta\rangle$.

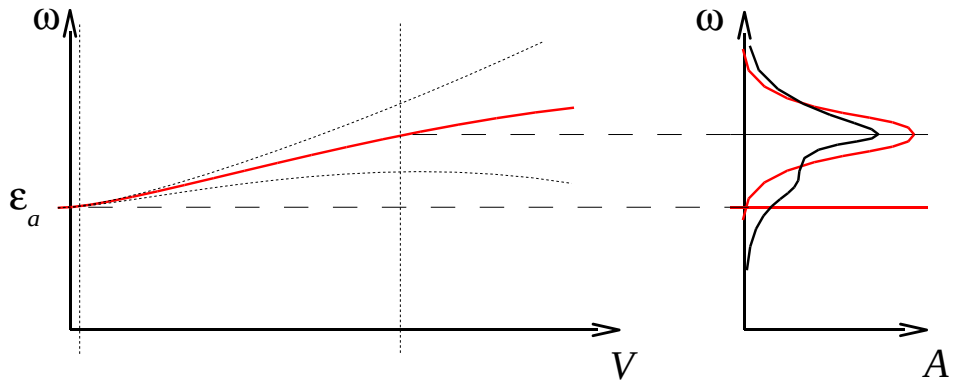

Figure 8.9: Diagram illustrating the meaning of the spectral function. For zero interaction, $V = 0$, the spectral weight is singularly concentrated on the single particle energies of the system. As interactions are switched on, the spectral weight is distributed amond a continuum of states concentrated around a shifted center point. The width of the distribution increases with growing interaction strength. Black solid curve: (schematic) shape of the spectral function if the self energy carries pronounced ω-dependence.

It is instructve to explore the consequences of this phenomenon in the representation (8.28) where the effect of interactions has been lumped into a self energy operator Σ. Taking the imaginary part of this expression we find

$$A_a(\omega) = 2\pi \frac{\Sigma''(\omega)}{(\omega - \xi_a - \Sigma'(\omega))^2 + (\Sigma''(\omega))^2},$$

where Σ' and Σ'' denote real and imaginary part of the self energy, respectively, and we have neglected the infinitesimal imaginary offset of ω^+ in comparison with the finite imaginary contribution $i\Sigma''$. The result above suggests that the net effect of interactions is

- ▷ an effective shift of the single particle energy $\epsilon_a \to \epsilon_a + \Sigma(\omega)$ by the real part of the self energy operator: interactions lead to a distortion of the single particle energy spectrum, an effect that follows, e.g., from straightforward perturbative reasoning. More importantly,

- ▷ The δ-function obtained in the non-interacting case gets smeared to a Lorentzian (see Fig. 8.9). In a way, the spectral weight carried by the many body states $|\alpha\rangle + |a\rangle$ is distributed over a continuum of neighbouring states wherefore the spectral function loses its singular character. The width of the smearing interval is proportional to the imaginary part of the self energy and, therefore, to inverese of the lifetime τ discussed in the previous section.

Notice that the smeared spectral function still obeys the normalization condition unity, $\int \frac{d\omega}{2\pi} A_a(\omega) = 1$, as in the non-interacting case[17]. This suggests an interpretation of A as a probability measure describing in which way the spectral weight carried by the state $c_a^\dagger|\alpha\rangle$ is spread out over the continuum of many body states $|\beta\rangle$. To put that interpretation onto a firm basis, not bound to the self energy representation above, we consider the spectral decomposition (8.31). The positivity of all terms contributing to the rhs of the equation implies $A_a(\omega) > 0$, a condition neccessarily

[17] Strictly speaking, we can only integrate A if the variance of $\Sigma(\omega)$ over the intervall $[\xi_a + \Sigma' - \Sigma'', \xi_a + \Sigma' - \Sigma'']$ in which the Lorentzian is peaked is negligible. But see below.

obeyed by any probability measure. To verify the general validity of the unit-normalization condition we integrate Eq. (8.31) over ω:

$$\begin{aligned}\int \frac{d\omega}{2\pi} A_a(\omega) &= \mathcal{Z}^{-1} c_{a\alpha\beta} c^\dagger_{a\beta\alpha} \left[e^{-\beta\Xi_\alpha} + \zeta_c e^{-\beta\Xi_\beta} \right] = \\ &= \mathcal{Z}^{-1} \left(\langle\alpha| c_a c_a^\dagger |\alpha\rangle \sum_\alpha e^{-\beta\Xi_\alpha} + \zeta_c \langle\beta| c_a^\dagger c_a |\beta\rangle \sum_\beta e^{-\beta\Xi_\beta} \right) = \\ &= \mathcal{Z}^{-1} \sum_\alpha e^{-\beta\Xi_\alpha} \langle\alpha| \underbrace{c_a c_a^\dagger + \zeta_{\hat{X}} c_a^\dagger c_a}_{[c_a, c_a^\dagger]_{\zeta_c} = 1} |\alpha\rangle = \underbrace{\mathcal{Z}^{-1} \sum_\alpha e^{-\beta\Xi_\alpha}}_{1} = 1.\end{aligned}$$

Positivity and unit-normalization of $A_a(\omega)$ indeed suggest that this function measures the distribution of spectral weight over the many-body continuum.

To further substantiate that interpretation, consider the integral of the spectral function weighted by the Fermi- or Bose-distribution function:

$$\begin{aligned}\int \frac{d\omega}{2\pi} f_{\mathrm{f/b}}(\omega) A_a(\omega) &= \mathcal{Z}^{-1} c_{\alpha\beta} c^\dagger_{\beta\alpha} \left[e^{-\beta\Xi_\alpha} + \zeta e^{-\beta\Xi_\beta} \right] \int d\omega\, \delta(\omega + \Xi_{\alpha\beta}) \frac{1}{e^{\beta\omega} + \zeta} = \\ &= \mathcal{Z}^{-1} c_{\alpha\beta} c^\dagger_{\beta\alpha} \left[e^{-\beta\Xi_\alpha} + \zeta e^{-\beta\Xi_\beta} \right] \frac{1}{e^{\beta\Xi_{\beta\alpha}} + \zeta} = \\ &= \mathcal{Z}^{-1} c_{\alpha\beta} c^\dagger_{\beta\alpha} e^{-\beta\Xi_\beta} \left[e^{\beta\Xi_{\beta\alpha}} + \zeta \right] \frac{1}{e^{\beta\Xi_{\beta\alpha}} + \zeta} = \\ &= \mathcal{Z}^{-1} \sum_\beta e^{-\beta\Xi_\beta} \langle\beta| c_a^\dagger c_a |\beta\rangle = \langle \hat{n}_a \rangle,\end{aligned}$$

which tells us that if we weigh the spectral density function of a single particle state $|a\rangle$ with the thermal distribution function and integrate over all frequencies, we obtain the total occupation of that state. The relation

$$\boxed{\int \frac{d\omega}{2\pi} f_{\mathrm{f/b}}(\omega) A_a(\omega) = \langle \hat{n}_a \rangle} \tag{8.32}$$

indeed states that A_a is a distribution function describing in which way the spectral weight of the state $c_a^\dagger |\alpha\rangle$ spreads over the continuum of exact eigenstates.

A number of exact identities involving correlation functions are formulated in terms of the spectral function. We begin by showing that the spectral function carries the same information as the correlation function itself. (In view of the fact that A obtains by removing the real part of C, this result might come as a surprise.) Indeed,

$$\boxed{C(z) = \int_{-\infty}^{\infty} d\omega\, \frac{A(\omega)}{z - \omega}.} \tag{8.33}$$

To verify this identiy, we start out from $A(\omega) = -\frac{1}{2\pi i}(C^+(\omega) - C^-(\omega))$. Next, note that the first (second) term contributing to the rhs of the definition is (a) analytic in the upper (lower) half of the complex ω-plane and (b) decays as $\sim \omega^{-1}$ for $|\omega| \to \infty$. For $\mathrm{Im}\, z > 0$, the theorem of residues then implies that the C^--term does not contribute to the integral.

(Without enclosing singularities, the integration contour can be closed in the lower half plane.) As for the C^+-contribution, we integrate over an infinite semi-circle γ closing in the upper half plane to obtain

$$\int_{-\infty}^{\infty} d\omega \frac{A(\omega)}{z-\omega} \overset{\mathrm{Im}\, z>0}{=} -\frac{1}{2\pi i}\int_{\gamma} d\omega \frac{C^+(\omega)}{z-\omega} = C(z), \tag{8.34}$$

where the second identity relies on the analyticity of C^+ in the upper half plane. The case $\mathrm{Im}\, z < 0$ is treated analogously.

We thus find that knowledge of the imaginary part suffices to reconstruct the full correlation function. (Notice however, that the identity (8.33) is heavily 'non-local'. I.e. we need to know the spectral function for it *all* ω, including $\omega \to \pm\infty$, to re-obtain the correlation function at a given value of z.)

Considering the second equality in (8.34) and setting $z = \omega^+$, we obtain

$$C^+(\omega) = -\frac{1}{2\pi i}\int d\omega \frac{C^+(\omega')}{\omega - \omega' + i0}.$$

Representing the denominator under the integral in terms of the Dirac identity (8.20) and collecting terms the identity assumes the form

$$C^+(\omega) = \frac{1}{\pi i}\int d\omega\, C^+(\omega')\mathcal{P}\frac{1}{\omega' - \omega}.$$

It is customary to consider real and imaginary part of this relation separately whence one arrives at the celebrated **Kramers-Kronig-relations** or **dispersion relations**

$$\boxed{\begin{aligned} \mathrm{Re}\, C^+(\omega) &= \frac{1}{\pi}\int d\omega'\, \mathrm{Im}\, C^+(\omega')\mathcal{P}\frac{1}{\omega'-\omega}, \\ \mathrm{Im}\, C^+(\omega) &= -\frac{1}{\pi}\int d\omega'\, \mathrm{Re}\, C^+(\omega')\mathcal{P}\frac{1}{\omega'-\omega}, \end{aligned}} \tag{8.35}$$

▷ INFO. To get an idea of the **physical significance of the Kramers-Kronig relation** let us anticipate a little and note that the scattering amplitude of particles sent onto a medium at energy ω is proportional to the retarded Green function $C^+(\omega)$. Taking the scattering of electromagnetic radiation off a solid state sample as an example, the Kramers-Kronig relation then tells us that the real part of the scattering amplitude – the index of refraction – is proportional to the imaginary part – the index of absorption – integrated over all energies. I.e. the Kramers-Kronig relation establishes a connection between the to seemingly unrelated physical mechanisms of absorption and refraction. Other areas of application of dispersion relations include high energy physics, optics (both classical and quantum) and many more.

———————————————————

In the next section we discuss a concrete example of applications of the Kramers-Kronig relations in many body physics.

A Case Study: The Dielectric Function

Eq. (8.35) represents a 'master identity' from which numerous other exact relations can be obtained. As an example for the derivation and usefulness of these identities, let us consider the frequency and momentum dependent **dielectric function** $\epsilon(q,\omega)$, i.e. *the* object describing the polarization properties of a medium in the presence of an electromagnetic field. In section 6.2 we have explored the dielectric function within the framework of the RPA approximation. However, as we are about to discuss exact reations we should now be a bit more ambitious than that, i.e. we should base our on a more generally valid representation of the dielectric function.

Indeed, it is a straightforward exercise (see the problem set) in linear response theory to show that

$$\epsilon(\mathbf{q},\omega) = \left[1 - \frac{V_0(\mathbf{q})}{L^d}\int d\tau e^{i\omega_m\tau}\langle\hat{n}(\mathbf{q},\tau)\hat{n}(-\mathbf{q},0)\rangle_c\Big|_{i\omega_m\to\omega^+}\right]^{-1}, \tag{8.36}$$

where $V_0(\mathbf{q}) = 4\pi e^2/q^2$ is the bare Coulomb potential, $\langle\hat{n}\hat{n}\rangle_c$ denotes the connected thermal average of two density operators $\hat{n}(\mathbf{q},\tau) = c^\dagger_{\mathbf{q}}(\tau)c_{\mathbf{q}}(\tau)$, and the symbol $\omega_m \to \omega^+$ symbolically indicates the analytical continuation to real frequencies. Heuristically, Eq. (8.36) can be understood by noting that $1/\epsilon = V_{\text{eff}}/V_0$ measures the ratio between the effective potential felt by a test charge in a medium and the vacuum potential. The difference between these two quantities is due to the polarizability of the medium which, in turn, is a measure of its inclination to build up charge distortions $\delta\langle\hat{n}\rangle$ in response to the action of the potential operator $\sim \int V_0\hat{n}$. In linear response theory[18] theory, $\delta\langle\hat{n}\rangle$ is given by the kernel $\int\langle\hat{n}\hat{n}\rangle V_0$, i.e. the second term in (8.36).

We thus observe that the (inverse of the) dielectric function is determined by the retarded correlation function $C^+(\mathbf{q},\omega)$ with $\hat{X}_1 = \hat{X}_2 = \hat{n}(\mathbf{q})$. (For obvious reasons, this function is called the retarded **density-density response function**. It appears as an important building block in many areas of many body physics.) We next show how analyticity arguments and the two limit relations (**??**) and (**??**) can be employed to derive a number of strong test criteria for the dielectric function.

Building on the relation

$$\epsilon(\mathbf{q},\omega)^{-1} = 1 - \frac{V_0(\mathbf{q})}{L^d}C^+(\mathbf{q},\omega), \tag{8.37}$$

we next show how analyticity arguments and certain limit relations can be employed to derive strong strong test criteria for the dielectric functions. We first apply the Kramers-Kronig relation to $\epsilon^{-1} - 1 \propto C^+$ to obtain

$$\mathrm{Re}\,\epsilon(\mathbf{q},\omega)^{-1} - 1 = \frac{1}{\pi}\int_{-\infty}^{\infty} d\omega'\,\mathrm{Im}\,\epsilon(\mathbf{q},\omega')^{-1}\mathcal{P}\frac{1}{\omega'-\omega}.$$

Using that $\mathrm{Im}\,\epsilon(\mathbf{q},\omega')^{-1} = -\mathrm{Im}\,\epsilon(-\mathbf{q},-\omega')^{-1} = -\mathrm{Im}\,\epsilon(\mathbf{q},-\omega')^{-1}$, where the first identity holds for the Fourier transform of arbitrary functions and the second follows from real

[18] The linear response approximation is quite appropriate here because the standard definition of the dielectric function $\epsilon = \lim_{V_0\to 0} V_0/V_{\text{eff}}$ implies an infinitesimally weak external perturbation.

space symmetry, the integral can be compactified to

$$\mathrm{Re}\,\epsilon(\mathbf{q},\omega)^{-1} = 1 + \frac{2}{\pi}\int_0^\infty d\omega'\,\mathrm{Im}\,\epsilon(\mathbf{q},\omega')^{-1}\mathcal{P}\frac{\omega'}{\omega'^2-\omega^2}. \tag{8.38}$$

We next consider this relation for the special case $\omega = 0$ and $|\mathbf{q}| \to 0$. Probing this limit is motivated by the fact that the behaviour of the static dielectric function $\epsilon(\mathbf{q}, \omega = 0)$ is infinitely more simple to analyse than that of the generic function $\epsilon(\mathbf{q},\omega)$. The reason is, of course, that a static external field does not prompt any dynamical response of the system. Indeed, one can show on general grounds (see the info block below and Eq. (**??**) above) that in the static limit,

$$\epsilon^{-1}(\mathbf{q},0) = (1+\nu|\mathbf{q}|^{-2})^{-1} \overset{|\mathbf{q}|\to 0}{\longrightarrow} 0. \tag{8.39}$$

Substitution of this result into (8.38) then leads to result

$$\boxed{\lim_{\mathbf{q}\to 0}\int_0^\infty d\omega\,\frac{\mathrm{Im}\,\epsilon(\mathbf{q},\omega)^{-1}}{\omega} = -\frac{\pi}{2}} \tag{8.40}$$

Eq. (8.40) is a typical example of a **sum rule**. For the derivation of a few more sum rules to be obeyed by the dielectric function, see Ref. [**?**].

▷ INFO. To understand the behaviour of the **dielectric function in the static limit**, imagine a system of charged particles subject to a potential $V_0(\mathbf{r})$. Since V_0 is static, it does not drive the system out of equilibrium. In particular, all fermionic quasi-particle states[19] are filled up to a *uniform* chemical potential μ. This, however, necessitates a re-distribution of charge. The reason is that the potential shifts the energies ϵ_a of quasi-paricle states $|a\rangle$ according to $\epsilon_a \to \epsilon_a - V_{\mathrm{eff}}$, where V_{eff} is the effective potential seen by the particles. For low temperatures, states will be filled up to an energy $\mu - V_{\mathrm{eff}}$ (see Fig. 8.10). We can make this argument quantitative by introducing a distribution function $f_{\mathrm{eff}}(\epsilon) \equiv f_{\mathrm{f}}(\epsilon - V_{\mathrm{eff}})$ locally controlling the occupation of quasi-particle states. In a linear approximation, the induced charge density *screening* the external potential is then given by

$$\begin{aligned}\rho_{\mathrm{ind}}(\mathbf{r}) &= -\frac{1}{L^d}\sum_a (f_{\mathrm{eff}}(\epsilon_a) - f_{\mathrm{f}}(\epsilon_a)) = -\nu\int_{-\infty}^\infty d\epsilon (f_{\mathrm{eff}}(\epsilon) - f_{\mathrm{f}}(\epsilon)) \\ &= -\nu\int_{-\infty}^\infty d\epsilon (f_{\mathrm{f}}(\epsilon - V_{\mathrm{eff}}(\mathbf{r})) - f_{\mathrm{f}}(\epsilon)) \approx \nu\int_{-\infty}^\infty d\epsilon\,\partial_\epsilon f_{\mathrm{f}}(\epsilon) V_{\mathrm{eff}}(\mathbf{r}) = -\nu V_{\mathrm{eff}}(\mathbf{r}).\end{aligned}$$

To compute the difference between the external and the effective potential, respectively, we assume that the former had been generated through some charge density ρ: $-\partial^2 V_0 = 4\pi\rho_0$, or $V_0(\mathbf{q}) = 4\pi\mathbf{q}^{-2}\rho_0(\mathbf{q})$. In contrast, the full potential V_{eff} will be generated by a charge distribution ρ_{eff} comprising the external charge and the screening charge,

$$V_{\mathrm{eff}}(\mathbf{q}) = 4\pi\mathbf{q}^{-2}(\rho_0(\mathbf{q}) + \rho_{\mathrm{ind}}(\mathbf{q})) = V_0(\mathbf{q}) - 4\pi\nu\mathbf{q}^{-2}V_{\mathrm{eff}}(\mathbf{q}).$$

[19] We assume that we are dealing with a Fermi liquid, i.e. that we can think of the constituents of the system as fermionic quasi-particles, in the spirit of the Landau's theory.

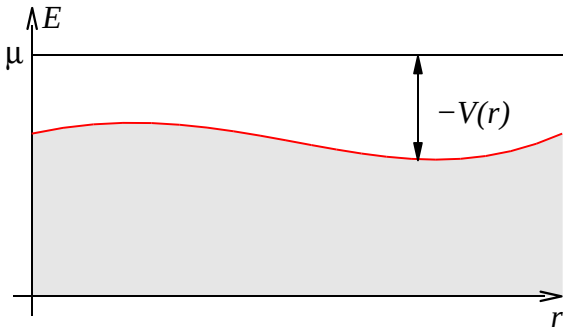

Figure 8.10: On the idea of Thomas-Fermi screening. A long range modulated static potential shifts the quasi-particle energies according to $\epsilon_a \to \epsilon_a + V_{\rm eff}(\mathbf{r})$. (In order for this relation to make sense, the typical spatial extent of a quasi-particle must, of course, be smaller than the modulation range of $V(\mathbf{r})$.) Quasi-particle states are occupied up to energies $\epsilon_{\rm max}(\mathbf{r})$ (indicated by a solid line) where $\epsilon_{\rm max}(\mathbf{r}) + V_{\rm eff}(\mathbf{r}) = \mu$ and μ is the global chemical potential controlling the total particle number in equilibrium.

We thus find that

$$\epsilon(\mathbf{q},0) = \frac{V_0(\mathbf{q})}{V_{\rm eff}(\mathbf{q})} = 1 + 4\pi\nu|\mathbf{q}|^{-2},$$

as stated above. Indeed, we had obtained this result, generally known as **Thomas-Fermi screening**, long before within the more microscopic framework of the RPA. In contrast, the merit of the present argument is that it not based on any specific approximation scheme[20].

While Eq. (8.40) was for the specific example of the dielectric function, the general construction recipe finds much more general applicability: one (a) represents a quantity of physical interest (here, the dielectric function) in terms of a retarded response function which then, (b), is plugged into a Kramers-Kronig type relation. This produces a frequency non-local connection between the response function at a given frequency to an integral ('sum') over all other frequencies. The latter, (c), is evaluated for a reference frequency for which our reference quantity is generally known (here, $\omega \to 0$.) This produces an integral relation which should hold under very general conditions. As mentioned in the beginning of the section, sum rules play an important role as test criteria for physical approximation schemes. The application of such relations is exemplified in the problem set on a concrete model dielectric function of the weakly disordered electron gas.

Experimental Access to the Spectral Density function

Above we have seen that the spectral density function contains highly resolved microscopic information on a many body system. But how do we access this information other than by theoretical model calculation? Interestingly, it turns out that the spectral function is not only central to theoretical analysis but also directly related to a key experimental observable, the **inelastic scattering cross section.**

[20] although the argument is a bit phenomenological and does rely on the Fermi liquid doctrine.

To understand this connection, consider again the prototypical setup of a scattering experiment shown in Fig. 8.3. The frequency and angle resolved scattering cross section is a measure of the rate of transitions $(\epsilon, \mathbf{k}) \to (\epsilon', \mathbf{k}')$ from the incoming state $(\epsilon, \mathbf{k})$ into an outgoing state $(\epsilon', \mathbf{k}')$. To give the problem a quantum mechanical formulation, we first note that that the full Hilbert space $\mathcal{H}$ of the system is the direct product of the Fock space, $\mathcal{F}$, of the target system and the single particle space, $\mathcal{H}_1$ of the incoming particle species,

$$\mathcal{H} = \mathcal{F} \otimes \mathcal{H}_1.$$

We assume that the interaction between the incoming particle and the constituent particles of the system is governed by an interaction Hamiltonian whose conventional (first quanitzed) real space representation reads,

$$\hat{H}_{\rm int} = \sum_i V(\hat{\mathbf{r}}_i - \hat{\mathbf{r}}).$$

Here, $\hat{\mathbf{r}}_i$ are the positions of the system's particles and $\hat{\mathbf{r}}$ is the position of the incoming particle. For simplicity we assume that the interaction is pointlike, $V(\hat{\mathbf{r}} - \hat{\mathbf{r}}') = C\delta(\hat{\mathbf{r}} - \hat{\mathbf{r}}')$, where C is some constant. (The generalization to more general interaction potentials (excercise!) is straightforward.) The second quantized representation of the interaction operator then reads,

$$\hat{H}_{\rm int} = C \int d\mathbf{r}\, \delta(\hat{\mathbf{r}} - \mathbf{r}) c^\dagger(\mathbf{r}) c(\mathbf{r}), \tag{8.41}$$

where $\hat{\mathbf{r}}$ keeps its significance as a single particle operator acting in the space $\mathcal{H}_1$. An alternative, and for all what follows more convenient representation is given by

$$\hat{H}_{\rm int} = \frac{C}{(2\pi)^3} \int d\mathbf{r} d\mathbf{q}\, e^{i\mathbf{q}(\hat{\mathbf{r}} - \mathbf{r})} c^\dagger(\mathbf{r}) c(\mathbf{r}) = C \int d\mathbf{q}\, e^{i\mathbf{q}\hat{\mathbf{r}}} \hat{\rho}_{\mathbf{q}},$$

where we have made use of a plane wave representation of the δ-distribution, $\delta(\mathbf{r}) = (2\pi)^{-3} \int d\mathbf{q} \exp(i\mathbf{q}\mathbf{r})$ and

$$\hat{\rho}_{\mathbf{q}} \equiv \frac{1}{(2\pi)^3} \int d\mathbf{r}\, e^{-i\mathbf{q}\mathbf{r}} c^\dagger(\mathbf{r}) c(\mathbf{r})$$

describes density modulations in the target system of characteristic momentum $\mathbf{q}$. Assuming for simplicity, that the sample is kept at zero temperature (is in its ground state), a scattering process of *first order* in the interaction Hamiltonian described by the transition amplitude

$$\mathcal{A}_{\mathbf{q}} = \langle \beta, \mathbf{k} - \mathbf{q} | \hat{H}_{\rm int} | 0, \mathbf{k} \rangle,$$

where 0 represents the ground state of the system and $|\beta\rangle$ may be any exact eigenstate of the target system[21]. Substitution of the representation of the interaction Hamiltonian above brings the transition amplitude into the form

$$\mathcal{A}_{\mathbf{q}} = \langle \beta, \mathbf{k} - \mathbf{q} | \hat{H}_{\rm int} | 0, \mathbf{k} \rangle \propto \langle \beta | \hat{\rho}_{\mathbf{q}} | 0 \rangle. \tag{8.42}$$

[21] Using the nomenclature of Fig. 8.3 we might identify $|0\rangle$ with a ground state of zero collective momentum $\mathbf{K} = 0$ and $|\beta\rangle = |\mathbf{K}' = \mathbf{q}\rangle$ with a state that has absorbed the momentum of the scattered particle. The present discussion is more general in that it does not assume that the target eigenstates carry definite momentum.

A first conclusion to be drawn from (8.42) is that the scattering amplitude probes *density modulations* in the bulk system. According to **Fermi's golden rule** (please recapitulate) the transition rate associated to the scattering amplitude $\mathcal{A}_{\mathbf{q}}$ is given by

$$\mathcal{P}_q = 2\pi \sum_\beta |\langle\beta|\hat{\rho}(\mathbf{q})|0\rangle|^2 \delta(\omega - \Xi_{\beta 0}), \tag{8.43}$$

where $\Xi_{\beta 0} = E_\beta - E_0 > 0$ is the excitation energy of $|\beta\rangle$ above the ground state and the δ-distribution enforces the conservation of energy. The summation over β reflects the fact that only the beam of scattered particle is observed while the final state of the target remains unspecified.

It is instructive to reformulate Eq. (8.43) in a number of different ways. Representing the δ-distribution as a temporal integral $\delta(\omega) = \frac{1}{2\pi}\int dt\, \exp(-i\omega t)$, we obtain

$$\begin{aligned}
\mathcal{P}_q &= \int dt \sum_\beta |\langle\beta|\hat{\rho}_{\mathbf{q}}|0\rangle|^2 e^{-it(\omega-\Xi_\beta)} = \\
&= \int dt e^{-i\omega t} \sum_\beta \langle 0|e^{i(\hat{H}-\mu\hat{N})t}\hat{\rho}_{-\mathbf{q}} e^{-i(\hat{H}-\mu\hat{N})t}|\beta\rangle\langle\beta|\hat{\rho}_{\mathbf{q}}|0\rangle = \\
&= \int dt e^{-i\omega t}\langle 0|e^{i(\hat{H}-\hat{\mu}N)t}\hat{\rho}_{-\mathbf{q}} e^{-i(\hat{H}-\mu\hat{N})t}\hat{\rho}_{\mathbf{q}}|0\rangle = \\
&= \int dt e^{-i\omega t}\langle 0|\hat{\rho}_{-\mathbf{q}}(t)\hat{\rho}_{\mathbf{q}}(0)|0\rangle.
\end{aligned}$$

This formulation clearly illustrates the connection between the observable scattering rate and microscopic system characteristics, i.e. the rate $\mathcal{P}_{\omega,\mathbf{q}}$ is a measure for the dynamical propagation of density modulations of wavelength $\mathbf{q}$ at time scales $\sim \omega^{-1}$.

To establish the connection to the previously developed apparatus of response functions, we introduce the abbreviation $\hat{\rho}_{\mathbf{q},\alpha\beta} = \langle\alpha|\hat{\rho}_{\mathbf{q}}|\beta\rangle$ and reformulate (8.43) as

$$\begin{aligned}
\mathcal{P}_q &= -2\,\mathrm{Im} \sum_\beta \rho_{\mathbf{q},\beta 0}\rho_{-\mathbf{q},0\beta}\frac{1}{\omega^+ + \Xi_{0\beta}} = \\
&= -2\lim_{T\to 0}\,\mathrm{Im}\,\mathcal{Z}^{-1}\sum_{\alpha\beta}\rho_{\mathbf{q},\beta\alpha}\rho_{-\mathbf{q},\alpha\beta}\frac{e^{-\beta\Xi_\alpha}}{\omega^+ + \Xi_{\alpha\beta}} \\
&= -2\lim_{T\to 0}\,\mathrm{Im}\,\mathcal{Z}^{-1}\sum_{\alpha\beta}\rho_{\mathbf{q},\beta\alpha}\rho_{-\mathbf{q},\alpha\beta}\frac{e^{-\beta\Xi_\alpha} - e^{-\beta\Xi_\beta}}{\omega^+ + \Xi_{\alpha\beta}} = \qquad (8.44) \\
&= -2\lim_{T\to 0}\,\mathrm{Im}\,C^+_{\mathbf{q},\mathbf{q}}(\omega) = A(\mathbf{q},\omega), \qquad (8.45)
\end{aligned}$$

where $A(\mathbf{q},\omega)$ is the spectral density function evaluated for the density operators $\hat{X}_1 = \rho_{\mathbf{q}}$, $\hat{X}_2 = \rho_{-\mathbf{p}}$. In the second line we used that for $T \to 0$, the Boltzmann weight $\exp(-\beta\Xi_\alpha)$ projects onto the ground state. Similarly, for $\omega > 0$, the the added contribution $\exp(-\beta\Xi_\beta)$ does not give a non-vanishing contribution (why?).

We thus observe that information about scattering cross sections, too, is carried by retarded real time response functions. Specifically,

The inelastic scattering cross section for momentum transfer $\mathbf{q}$ and energy exchange ω is a direct probe of the spectral density function $A(\mathbf{q}, \omega)$.

Although the derivation above did not exactly follow the linear response scheme, it had the same weak coupling perturbative flavour. (The golden rule is a first order perturbative apporoximation!) While we derived our formula for the particular case of a short range density coupling, it is clear that more general beam-target coupling mechanism would lead to an expression of the same architecture, i.e. a suitably defined retarded response function.

8.4 Electromagnetic Linear Response

In the last two sections we have put everything together needed to compute the response of physical systems to moderately weak perturbations. We learned how to linearize the response signal in the strength of its cause and to extract real time dynamical information from imaginary time data. In this section we illustrate the functioning of this formalism on its undoubtedly most important application, the response to the general electromagnetic field.

The general setup of the problem is easily formulated: suppose a system of charged particles has been subjected to an electromagnetic signal represented through a scalar potential $\phi(\mathbf{x}, t)$ and/or a vector potential $\mathbf{A}(\mathbf{x}, t)$. To simplify the notation, we represent the perturbation through a $(d+1)$-dimensional[22] potential $A(x) = (\phi(x), \mathbf{A}(x))$, where $x \equiv (t, \mathbf{x})$ is a $(1+d)$-dimensional space-time argument vector. The system will respond to this perturbation by a redistribution of charges, $\rho(x) \equiv \langle \hat{\rho}(x) \rangle$, and/or the onet of current flow $\mathbf{j}(x) \equiv \langle \hat{j}(x) \rangle$. Comprising charge and vectorial current into a $(d+1)$-dimensional generalized current vector $j = (\rho, \mathbf{j})$, our task is to identify the linear functional

$$j = K[A] + \mathcal{O}(A^2)$$

relating the current to its driving potential. In a somewhat more explicit way of writing,

$$j_\mu(x) = \int_{t'<t} d^{d+1}x' \, K_{\mu\nu}(x, x') A^\nu(x'), \tag{8.46}$$

where the condition $t' < t$ indicates that the response is retarded – a current cannot be induced prior to the action of the potential. The positioning of the indices on the rhs of the equation indicates the use of a Minkowski metric, i.e.

$$v_\mu w^\nu \equiv -v_0 w_0 + \sum_{i=1}^{3} v_i w_i.$$

[22] To not unneccessarily exclude important applications of the formalism to effectively two- or one-dimensional problems, the dimensionality of space is left open.

This convention is motivated by the Minkowskian space-time structure of electrodynamics[23]. To compute the elements of the response tensor, we proceed according to the general recipe constructed in the preceeding sections: we first employ the general formalism to derive the imaginary time response $K(\mathbf{x}, \mathbf{x}'; \omega_n)$, and then continue to real frequencies $i\omega_n \to \omega + i0$.

However, before formulating this program in detail, let us derive two fundamental constraints to be fulfilled by the kernel K. First, a gauge potential $A_\mu = \partial_\mu f$ (f is a function) cannot drive a physical current. Substituting this condition into Eq. (8.46) we find

$$0 \stackrel{!}{=} \int_{t'<t} d^{d+1}x'\, K_{\mu\nu}(x,x')\partial^\nu f(x') = -\int_{t'<t} d^{d+1}x'\, \partial^\nu_{x'} K_{\mu\nu}(x,x') f(x').$$

Since f is arbitrary we conclude $0 = K_{\mu\nu}\overleftarrow{\partial^\nu}$ where the arrow indicates that the derivative acts from the right. Second, current conservation demands $\partial^\mu j_\mu = 0$, or, transscribed to Eq. (8.46),

$$0 \stackrel{!}{=} \int_{t'<t} dx'^{d+1}\, \partial^\mu_x K_{\mu\nu}(x,x') A^\nu(x').$$

Due to arbitrariness of A_μ this condition can only be generally valid if $\overrightarrow{\partial^\mu}\ K_{\mu\nu} = 0$. Summarizing,

> Gauge invariance and particle number conservation demand that
>
> $$\overrightarrow{\partial^\mu}\, K_{\mu\nu} = K_{\mu\nu}\, \overleftarrow{\partial^\nu} = 0. \tag{8.47}$$

We next turn to the derivation of the linear response kernel. Our starting point is an observation made already in chapter 1 (and several times thereafter), viz. the fact that (cf. Eq. (**??**)) the coupling of matter to the classical electromagnetic is described by a bilinear contribution

$$S_c = \int d^4x\, \hat{j}_\mu A_\mu \tag{8.48}$$

to the *imaginary* time action. In this expression we are back to an Euklidean metric

$$v_\mu w_\nu \equiv v_0 w_0 + \sum_{i=1}^{3} v_i w_i,$$

on account of the definition, $j_0 \equiv i\rho$, $A_0 \equiv i\phi$ of imaginary time current and vector potential, respectively. The additional i appearing in this convention mirrors the i of the temporal component of the imaginary time vector $(t, \mathbf{x}) \to (i\tau, \mathbf{x})$. Notice, however, that we are merely changing *conventions*, i.e. both imaginary and real time action contain the invariant contribution $-\rho\phi + \mathbf{j}\cdot\mathbf{A}$. To keep the notation simple, we will not indicate

[23] In a more mundane way of speaking: this convention absorbs the minus signs that would otherwise appear in formulae expressing gauge invariance and/or current conservation of the theory.

the difference between imaginary time and real time vectors explicitly; the appropriate convention is determined by the context in which we are operating.

This appealingly simple structure (8.48) is all we need to write down a general expression for the linear response kernel: comparison with section 8.2.1 shows that $F = F' = A_\mu$, i.e. the generalized force, F, and the auxiliary 'force' F' used to generate the expectation value of $\hat{j}$ by differentiation are both given by A_μ. Eq. (8.7) then tells us that

$$\boxed{K_{\mu\nu}(x,x') = \mathcal{Z}^{-1}\,\frac{\delta^2}{\delta A_\mu(x) A_\nu(x')}\mathcal{Z}[A]\bigg|_{A=0}\,,} \tag{8.49}$$

which is one of the most important relations of microscopic response theory. Notice that due to the interchangeability of the two derivatives, $K_{\mu\nu}(x,x') = K_{\nu\mu}(x',x)$. This symmetry in turn implies that – an observation repeatedly made before – gauge invariance, $K_{\mu\nu}\overleftarrow{\partial_\nu} = 0$, and particle number conservation, $\overrightarrow{\partial_\mu}\,K_{\mu\nu} = 0$, represent different sides of the same coin.

Eq. (8.49) is a very general, but also very formal result. To give it some meaning, it is instructive to evaluate the two derivatives for a few specific functionals $\mathcal{Z}[A]$:

Electromagnetic Response of the Microscopic Theory

As a particularly important example, we consider the microscopic action of a Fermi or Bose system in the presence of an electromagnetic field. Ignoring the coupling of the field to the spin degrees of freedom

$$S[\bar\psi,\psi,A] = \int_0^\beta d\tau \int d^dr\;\bar\psi_\sigma\left(\partial_\tau + \boldsymbol{\phi} - \frac{1}{2m}(i\boldsymbol{\partial} + \mathbf{A})^2 - \mu + V_0\right)\psi_\sigma + S_{\rm int}[\bar\psi,\psi],$$

where V_0 denotes a (field independent) potential. With $A_0 = i\phi$, $A_i = (\mathbf{A})_i$ and

$$\begin{aligned}\hat{j}_0 &= i\hat\rho = i\bar\psi_\sigma\psi_\sigma,\\ \hat{j}_i = (\hat{\mathbf{j}})_i &= \frac{1}{2m}\bar\psi_\sigma(i\overleftrightarrow{\partial_i} + A_i)\psi_\sigma,\end{aligned} \tag{8.50}$$

where $f\overleftrightarrow{\partial_i}\,g \equiv f\partial_i g - (\partial_i f)g$, we bring the action into the canonical form

$$S[\bar\psi,\psi,A] = \int d\tau d^dr\; j^A_\mu A_\mu + S_0[\bar\psi,\psi],$$

where S_0 is field independent and the notation j^A hints to the important fact that the current itself depends on the vector potential. Application of Eq. (8.49) then obtains

$$\begin{aligned}K_{\mu\nu}(x,x') &= \mathcal{Z}^{-1}\,\frac{\delta^2}{\delta A_\mu(x)A_\nu(x')}\bigg|_{A=0}\int \mathcal{D}(\bar\psi,\psi)e^{-S[\bar\psi,\psi,A]} =\\ &= \mathcal{Z}^{-1}\,\frac{\delta}{A_\nu(x')}\bigg|_{A=0}\int \mathcal{D}(\bar\psi,\psi)\left(\hat{j}^A_\mu + A_\mu\partial_A\hat{j}^A_\mu\right)(x)\,e^{-S[\bar\psi,\psi,A]} =\\ &= \left\langle \delta(x-x')\delta_{\mu\nu}\,2\partial_A\hat{j}^A_\mu(x) + \left(\hat{j}^A_\mu + A_\mu\partial_A\hat{j}^A_\mu\right)(x)\left(\hat{j}^A_\nu + A_\nu\partial_A\hat{j}^A_\nu\right)(x')\right\rangle\bigg|_{A=0},\end{aligned}$$

where the angular brackets stand for functional averaging. Setting $A = 0$, we obtain

$$\boxed{K_{\mu\nu}(x,x') = \frac{1}{2m}\delta(x-x')\delta_{\mu\nu}(1-\delta_{\mu 0})\,\langle\hat{\rho}(x)\rangle + \langle\hat{j}^p_\mu(x)\hat{j}^p_\nu(x')\rangle.} \tag{8.51}$$

The first term contributing to the response kernel is known as the **diamagnetic term**. Indeed, following its trace back through the derivation we find that this term originates from the diamagnetic contribution $\sim A^2$ to the Hamiltonian. Conversely,

$$\hat{j}^p \equiv \hat{j}\Big|_{A=0}$$

is called the paramagnetic contribution to the current operator. The functional expectation value $\sim \langle\hat{j}^p\hat{j}^p\rangle$ defines the so-called **paramagnetic term**.

Notwithstanding its not very appealing structure, Eq. (8.51) represents a strong result which encompasses virtually all aspects of electromagnetic linear response[24]. E.g. the diagonal vectorial components $K_{ii}, i = 1,2,3$ of the response tensor describe the **longitudinal conductivity** of the system (see the next section.) In cases where a magnetic field is present, the off-diagonal components $K_{i\neq j}$ measure the **Hall-conductivity**. The temporal components K_{00} describe the **density response** of the system, a feature that is of importance for, e.g., the analysis of scattering data (see the problem set), etc.

Electromagnetic Response of Effective Theories

In cases where we are operating on a level beyond the microscopic description, i.e. within the framework of an effective low energy theory, the structure of the response tensor may differ from (8.51). To identify the 'effective' response tensor, we need to carry out a canonical two-step program: (i) identify the coupling of the electromagnetic potential to the relevant degrees of freedom. (In cases where one hasn't kept track of the field dependence from the very beginning, it usually suffices to *minimally couple* the field, i.e. to introduce the components A_μ so as to make the action gauge invariant.) (ii) Do the two-fold derivative (8.49).

We illustrate the procedure on a familiar example, viz. the action of the collective phase θ of the BCS superconductor. In section **??** we had seen that

$$S[\theta] = \int d\tau d^dx\,\left[\nu(\partial_\tau\theta)^2 + \frac{n_s}{2m}(\boldsymbol{\partial}\theta)^2\right].$$

Under a gauge transformation induced by some funciton $f(x)$, $\partial_\mu\theta \to \partial_\mu\theta + \partial_\mu f$, i.e. the gauge invariant extension of the action reads as (cf. Eq. (7.41))

$$S[\theta,A] = \int d\tau \int d^dx\,\left[\nu(\partial_\tau\theta-\phi)(\partial_\tau\theta-\phi) + \frac{n_s}{2m}(\boldsymbol{\partial}\theta-\mathbf{A})(\boldsymbol{\partial}\theta-\mathbf{A})\right].$$

Differentiating this result with respect to the components $\mathbf{A}_i$ we obtain

$$K_{ii'}(x,x') = -\frac{n_s}{m}\left[1 - \frac{n_s}{m}\langle\partial_i\theta(x)\partial_j\theta(x')\rangle\right] \tag{8.52}$$

[24] Except for spin-related phenomena.

for the vectorial components of the response tensor. It is left as an (instructive) exercise to show that the final evaluation of this expression leads to the Meissner effect and a diverging longitudinal conductivity, as obtained in a different manner in section 7.3.7 (see the problem set.)

8.4.1 Longitudinal Conductivity of the Disordered Electron Gas

Eq's (8.51) and (8.52) exemplify the structure of the response tensor after the master formula (8.49) has been applied. What remains to obtain a concrete result for the conductivity, say, is to evaluate the two- ($\langle\hat{\rho}\rangle$) or four- ($\langle\hat{j}\hat{j}\rangle$) point correlation functions appearing in these expressions. Of course, the details of this last step of the program sensitively depends on the microscopic structure of the theory under consideration, i.e. no universally applicable computational recipe can be formulated. Notwithstanding these differences in details, a number of large scale structural elelements are recurrent in the mathematical analysis of the current-current correlation functions of microscopic response theory.

To illustrate these common structures we consider an example which is of considerable importance in its own right, viz. the **longitudinal AC conductivity of the electron gas**.

The AC conductivity is defined through

$$\mathbf{j}(\omega) = \sigma(\omega)\mathbf{E}(\omega), \tag{8.53}$$

i.e. as the coefficient relating the current density to a homogeneous external field oscillating with frequency ω. In the absence of symmetry breaking perturbations such as a strong *magnetic* field or system-intrinsic anisotropies, the current flow will be in-line with the field gradient. This justifies the scalar, rather than a more complex tensorial ansatz for the conductivity in Eq. (8.53) (For a more complex situation, see the problem set.)

▷ INFO. Before entering the details of the linear response calculation, it instructive to recapitulate how the **conductivity can be obtained from common sense reasoning.** To this end, let us look at the world from the persective of an individual conduction electron. In the presence of an electric field, the electron will be subject to two different forces: the force of the field, $e\mathbf{E}$, and a dissipative friction force $-\frac{m}{\tau}\dot{\mathbf{r}}$ inhibiting its free accelaration. The time rate of this damping process is essentially set by the scattering rate off static impurities, m/τ. To a first approximation, the dynamics of the electron is thus described by the equation of motion

$$m\ddot{\mathbf{r}} = e\mathbf{E}(t) - \frac{m}{\tau}\dot{\mathbf{r}},$$

or, in Fourier representation,

$$-im\omega\mathbf{v}(\omega) = e\mathbf{E}(\omega) - \frac{m}{\tau}\mathbf{v}(\omega).$$

Solving for $\mathbf{v}$ we find that the current density $\mathbf{j} = n\mathbf{v}$ (n is the particle density) is given by $\mathbf{j}(\omega) = \sigma(\omega)\mathbf{E}(\omega)$ with

$$\boxed{\sigma(\omega) = \frac{ne}{m}\frac{1}{\frac{1}{\tau} - i\omega}.} \tag{8.54}$$

In the limit $\omega \gg \tau^{-1}$, $\sigma(\omega) \simeq i\frac{ne}{m}\omega^{-1}$, i.e. the electronic current is determined by the ballistic motion of the electrons in the electric force field. Conversely, in the DC limit $\omega \to 0$, $\sigma = \frac{ne\tau}{m}$, the field drives a steady current density whose value is limited by the amount of momentum relaxation.

Below we will compute the conductivity under the simplifying assumption that Coulomb or other types of many body interactions are negligible[25]. In contrast, the discussion of the info block above shows that any meaningful analysis of the conductivity *must* account for the presence of static disorder; without disorder, the field would make the electrons freely accelerate, i.e. there would be no such thing like steady current flow in metals. Thus, what we should have in mind when we think about the conductivity is, $\langle\sigma\rangle$, i.e. the conductivity averaged over all realizations of a microscopic disorder potential[26]. To obtain the conductance, we compute the current flow in the system in response to a vector potential $\mathbf{A}$ where $\partial_t \mathbf{A} = \mathbf{E}$ generates the electric field. Anticipating that after averaging over impurities the system will be effectively translationally invariant, the analysis is most economically carried out in momentum space, i.e. we compute the expectation value $\mathbf{j}(\mathbf{q} \to 0, \omega)$ in response to a potential $\mathbf{A}(\mathbf{q} \to 0, \omega)$, where the limit $\mathbf{q} \to 0$ indicates that we are interested in a spatially homogeneous external field. Fourier transforming Eq. (8.51) in the difference $x - x'$ of coordinates (cf. the remarks made in connection with Eq. (8.4)), one verifies that the appropriate response kernel is given by

$$K(q) = \frac{1}{m}\langle\langle\hat{\rho}\rangle\rangle + \frac{1}{L^d}\langle\langle\hat{j}^p_{i,q}\hat{j}^p_{i,-q}\rangle\rangle, \tag{8.55}$$

where the vectorial index i is arbitrary and the double brackets indicate the two-fold average over the quantum thermal distribution and the disorder potential, respectively. Also notice that the connection $\omega_m \mathbf{A}(q) = \mathbf{E}(q)$ implies

$$\sigma(\omega) = \lim_{\mathbf{q}\to 0} \frac{1}{\omega_m} K(q)\Big|_{i\omega_m \to \omega + i0}. \tag{8.56}$$

To process this expression, we substitute the Fourier transform of Eq. (8.50) (exercise)

$$\hat{\rho} = \sum_p \bar{\psi}_{\sigma,p}\psi_{\sigma,p}$$
$$\hat{j}^p_{i,q} = \frac{1}{2m}\sum_p (2\mathbf{p} + \mathbf{q})_i \bar{\psi}_{\sigma,p}\psi_{\sigma,p+q}$$

[25] Nonetheless, the calculation will still be fairly technical. If you find the Drude conductivity of the electron gas too elementary an observable to justify these efforts, please keep in mind that our prime motivation is methodological; technical operations very similar to those detailed here appear in practically every quantum response analysis.

[26] A good question to ask is whether the conductivity of any particular realization of a disordered metal will differ from the averaged conductivity, i.e. whether the conductivity is a 'self-averaging' quantitiy. This leads one to the intereting problem of **conductance fluctuations** which is, however, beyond the scope of the present text (see the problem set, though.)

into (8.55) and apply Wick's theorem (cf. section **??**) to compute the thermal expectation value. This leads to

$$K(q) = \frac{T}{m}\sum_{n,\mathbf{p}}\langle G_{n;\mathbf{p},\mathbf{p}}\rangle + \frac{2T}{L^d(2m)^2}\sum_{n;\mathbf{p},\mathbf{p}'}(2\mathbf{p}+\mathbf{q})_i(2\mathbf{p}'+\mathbf{q})_i\langle G_{n+m;\mathbf{p}+\mathbf{q},\mathbf{p}'+\mathbf{q}}G_{n;\mathbf{p},\mathbf{p}'}\rangle, \quad (8.57)$$

where the factor of 2 accounts for the spin summation (for simplicity we assume that the Hamiltonian in spin-independent), $G_{n;\mathbf{p},\mathbf{p}'} \equiv \langle\bar{\psi}_{n,\mathbf{p}}\psi_{n,\mathbf{p}'}\rangle$ is the thermal electron Green function for a particular realization of the disordered background, and the remaining bracket stands for the disorder average. (Notice that before disorder averaging, the system lacks translational invariance, i.e. the single particle Green function is not diagonal in momentum space.) A diagrammatic representation of the paramagnetic response kernel in terms of Green functions is shown in the upper part of the figure, where the wavy lines stand for the current operator and the dashed lines symbolically represent the scattering off the static impurity potential.

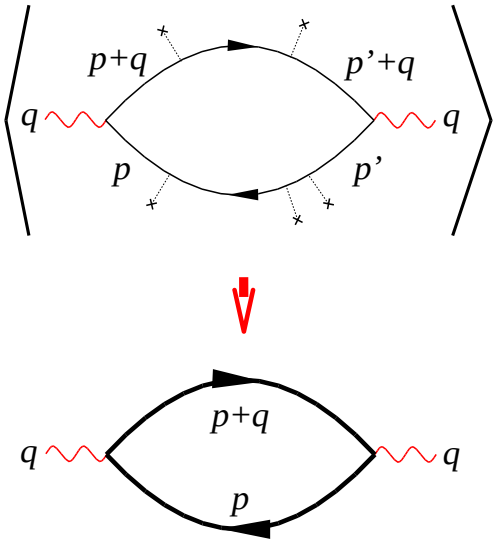

To make further progress with this expression, we shall adopt an approximation that critical readers may find fairly questionable: we will replace the average of the two-Green function correlator by an impurity average of the individual Green functions, $\langle GG\rangle \to \langle G\rangle\langle G\rangle$[27]. This is illustrated in the bottom part of the figure, where the thick lines represent Green functions averaged over the microscopic potential. In the problem set of chapter 6 it has been shown that these averaged Green functions are given by

$$\langle G_{n;\mathbf{p},\mathbf{p}'}\rangle = \delta_{\mathbf{p},\mathbf{p}'}G_p \equiv \frac{\delta_{\mathbf{p},\mathbf{p}'}}{i\omega_n - \xi_{\mathbf{p}} + \frac{i}{2\tau}\mathrm{sgn}\,\omega_n},$$

where τ defines the mean impurity scattering time. (Remember what has been said above about the meaning of the imaginary part of the Green function denominator as an effective lifetime. In the present context, τ measures the time after which a particle with initial momentum $\mathbf{p}$ gets scattered into states of different momentum.) Substituting this result into (8.57), we obtain

$$K(q) = \frac{T}{m}\sum_p G_p + \frac{2T}{L^d(2m)^2}\sum_p(2\mathbf{p}+\mathbf{q})_i(2\mathbf{p}+\mathbf{q})_i\, G_{p+q}G_p, \quad (8.58)$$

i.e. the problem to that of computing a frequency/momentum sum over the running index p. Looking at the structure of (8.57), one might be tempted to perform the frequency

[27] Readers who have made their way through the disorder related questions of the problem sets of previous chapters are invited to critically assess the validity of this approximation (see the problem set of this chapter.) The result of this analysis is that for hard impurity scattering potentials, i.e. impurtity potentials $\langle\mathbf{p}|V|\mathbf{p}'\rangle = \text{const.}$ that scatter isotropically over the entire momentum shell the approximation above becomes justifiable in the limit $\mathbf{q} \to 0$.

summation by one of our standard summation formulae. However, a moments thought shows that this strategy won't work. The reason is that in the present case, the extension of the Green function to the complex plane

$$G_p = G_{\mathbf{p}}(z) = \frac{1}{z - \xi_{\mathbf{p}} + \frac{i}{2\tau}\mathrm{sgn}\,\mathrm{Im}\,z}$$

has a *cut* along the real axis. Which means that the product $G_{\mathbf{p}+\mathbf{q}}(z+i\omega_m)G_{\mathbf{p}}(z)$ has cuts at $\mathrm{Re}(z) = 0$ and $\mathrm{Re}(z + i\omega_m) = 0$ (see Fig. 8.11.) To get around this difficulty, we need to integrate over a contour that (a) encompasses all Matsubara frequencies an (b) avoids the cut lines. While there is no simply contour that does the job, a joint integration over the three contours $\gamma_{1,2,3}$ shown in Fig. 8.11 faithfully represents the Matsubara sum:

$$\sum_m G_p G_{p+q} = \frac{\beta}{2\pi i} \oint_{\gamma_1 \cup \gamma_2 \cup \gamma_3} dz f_{\mathrm{f}}(z) G_{\mathbf{p}}(z) G_{\mathbf{p}+\mathbf{q}}(z + i\omega_m).$$

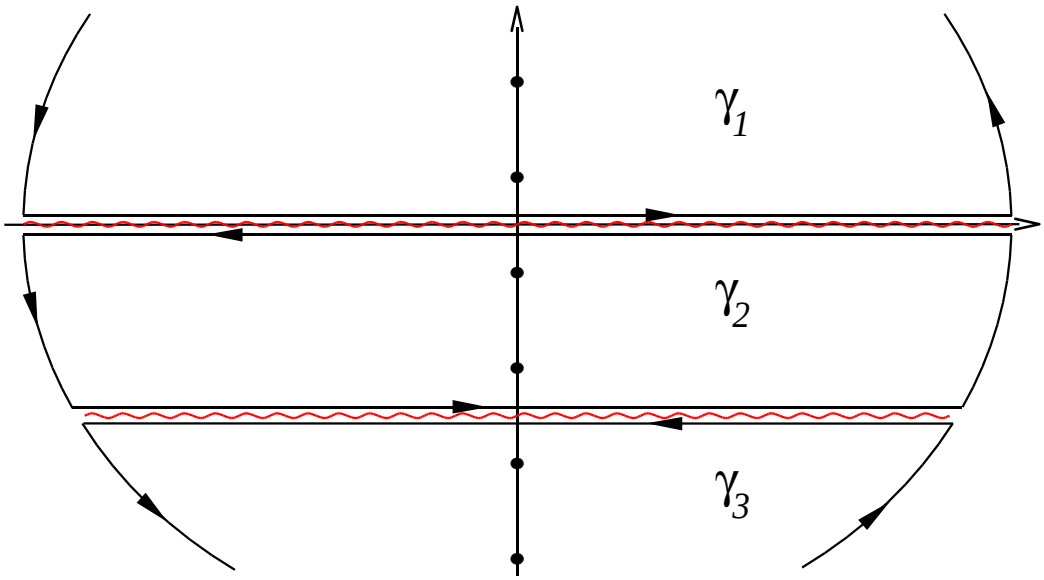

Figure 8.11: Analytical structure of the frequency summation in Eq. (8.57). The wavy lines indicate the cuts of the Green functions. Integration over the contours $\gamma_{1,2,3}$ gives the frequency sum.

The three integrals contributing to the sum lead to very different results: as shown in the problem set, the two integrals over the contours γ_1 and γ_3 cancel against the diamagnetic contribution to the response tensor, i.e. the first term in Eq. (8.58).

▷ INFO. To heuristically understand that the contribution from the contours γ_1 and γ_3 is unphysical, notice that, e.g.,

$$\frac{\beta}{2\pi i} \oint_{\gamma_1} dz f_{\mathrm{f}}(z) G_{\mathbf{p}}(z) G_{\mathbf{p}+\mathbf{q}}(z + i\omega_m) =$$

$$= \frac{\beta}{2\pi i}\int_{-\infty}^{\infty} d\epsilon f_{\rm f}(\epsilon) G_{\mathbf{p}}(\epsilon + i0) G_{\mathbf{p}+\mathbf{q}}(\epsilon + i\omega_m) \overset{i\omega_m\to\omega+i0}{\longrightarrow}$$
$$= \frac{\beta}{2\pi i}\int_{-\infty}^{\infty} d\epsilon f_{\rm f}(e) G_{\mathbf{p}}(\epsilon + i0) G_{\mathbf{p}+\mathbf{q}}(\epsilon + \omega + i0).$$

I.e. the integral extends over a product of two retarded single particle Green functions. Now, remember that in the end of the day, we want to compute the conductance, i.e. a quantity that bears reminiscence to a transition *probability* (viz. the probability for electrons propagating under the influence of an applied electric field.) In quantum mechanics, probabilities $\sigma \sim GG^*$ appear as products of *amplitudes*, G. Indeed, we had seen before, that the retarded Green function can be interpreted as a transition amplitude of quantum mechanical particles. We also saw, that its complex conjugate, G^*, is an advanced Green function. I.e. our admittedly very handwaving argument indicates that the quantum dynamics of conduction should be described in terms of products of advanced and retarded Green functions. However, a product of two retarded (or two advanced) Green functions lacks an obvious physical interpretation. Indeed, these contributions cancel against the diamagnetic term.

We thus focus on the integral over γ_2:

$$\frac{\beta}{2\pi i}\oint_{\gamma_2} dz f_{\rm f}(z) G_{\mathbf{p}}(z) G_{\mathbf{p}+\mathbf{q}}(z + i\omega_m) =$$
$$= \frac{\beta}{2\pi i}\int_{-\infty}^{\infty} d\epsilon f_{\rm f}(\epsilon)\left[G_{\mathbf{p}}(\epsilon - i0) G_{\mathbf{p}+\mathbf{q}}(\epsilon + i\omega_m) - G_{\mathbf{p}}(\epsilon - i\omega_m) G_{\mathbf{p}+\mathbf{q}}(\epsilon + i0)\right] \overset{i\omega_m\to\omega+i0}{\longrightarrow}$$
$$\overset{i\omega_m\to\omega+i0}{\longrightarrow} \frac{\beta}{2\pi i}\int_{-\infty}^{\infty} d\epsilon\, f_{\rm f}(\epsilon)\left[G_{\mathbf{p}}(\epsilon^-) G_{\mathbf{p}+\mathbf{q}}(\epsilon^+ + \omega) - G_{\mathbf{p}}(\epsilon^- - \omega) G_{\mathbf{p}+\mathbf{q}}(\epsilon^+)\right] =$$
$$= \frac{\beta}{2\pi i}\int_{-\infty}^{\infty} d\epsilon\,[f_{\rm f}(\epsilon) - f_{\rm f}(\epsilon + \omega)] G_{\mathbf{p}}(\epsilon^-) G_{\mathbf{p}+\mathbf{q}}(\epsilon^+ + \omega),$$

where in the first equality we have used the symmetry $f_{\rm f}(\epsilon + i\omega_m) = f_{\rm f}(\epsilon)$ of the distribution function under translation by bosonic frequencies. Substituting this result into (8.58) and (8.56) we arrive at the intermediate result

$$\sigma(\omega) = \frac{1}{2\pi}\int_{-\infty}^{\infty} d\epsilon\, \frac{f_{\rm f}(\epsilon) - f_{\rm f}(\epsilon + \omega)}{\omega} \frac{2}{L^d m^2} \sum_{\mathbf{p}} \mathbf{p}_i^2 G_{\mathbf{p}}^-(\epsilon) G_{\mathbf{p}}^+(\epsilon + \omega), \tag{8.59}$$

where $G_{\mathbf{p}}^{\pm}(\epsilon) = (\epsilon - \xi \pm \frac{i}{2\tau})^{-1}$.

The analytical structure of this result actually discloses a number of important elements of the electronic conduction process: an AC field of frequency ω creates electron hole pairs of excitation energy ω. The phase volume accessible to these processes is measured by the ϵ-integral, weighted by the difference of two Fermi functions, i.e. Fermi statistics demands that the energy of the to-be-excited electron lies within a shell $[\mu-\omega,\mu]$ at the Fermi surface (see the figure.) The dynamics of the excited electron is described by a retarded Green function of energy $\epsilon+\omega$.

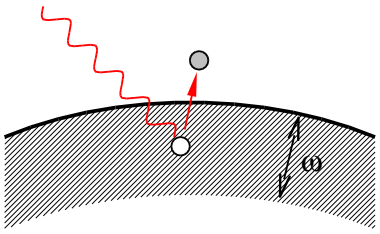

Conversely, the dynamics of the hole is described by the *advanced* Green function. Heuristically, this can be understood by noting that the advanced Green function describes the (ficticious) propagation of an electron *backwards* in time. However, an electron propagating in chrnologically reversed direction can be interpreted as an hole moving *forward* in time. (Think about it!) Thus, the advanced electronic Green function effectively represents a descriptor of hole dynamics. That the product of two Green functions is weighted by two operators $\mathbf{p}_i/m$ reflects the fact that current transport essentially depends on the velocity of the electrons.

To do the sum over $\mathbf{p}$ we note that for a radially symmetric function $F(\xi_{\mathbf{p}})$,

$$\int d^dp\,\mathbf{p}_i^2F(\xi_{\mathbf{p}})=\frac{1}{d}\int d^dp\,p^2F(\xi_{\mathbf{p}})=\frac{2m}{d}\int d\xi\,(\xi+\mu)\nu(\xi)F(\xi).$$

Identifying the function F with the product of our two Green functions, we obtain

$$\begin{aligned}\frac{2}{L^d}\sum_{\mathbf{p}}\mathbf{p}_i^2G_{\mathbf{p}}(\epsilon^-)G_{\mathbf{p}}(\epsilon^++\omega)&=m\int_{-\mu}^{\infty}d\xi\,(\xi+\mu)\nu(\xi)G^+(\epsilon)G^-(\epsilon+\omega)\simeq\\&\simeq m\mu\nu\int_{-\infty}^{\infty}d\xi\,G^+(\epsilon)G^-(\epsilon+\omega)=\frac{2\pi m\mu\nu}{\frac{1}{\tau}-i\omega},\end{aligned}$$

where in the third equality we have used that the Green functions are strongly peaked on scales $\tau^{-1}\ll\mu$ around $\xi=0$ implying that to a very good approximation the ξ-integration can be extended to the entire real axis and the energy variation of the density of states $\nu(\xi)$ on the effective interval of integration is negligible. The last integral can be done by elementary means or, more elegantly, by closing the ξ-integration contour in the upper or lower half plane and using the analytic structure of the Green functions. Substituting the result into our formula for $\sigma(\omega)$ and using that $\int d\epsilon(f_{\rm f}(\epsilon)-f_{\rm f}(\epsilon+\omega))\omega^{-1}\simeq 1$ we arrive at the final result (8.56).

At this point it is rewarding to pause for a moment to look back at a number of large scale structures of the analysis:

- ▷ on the microscopic level, the *two* point function $\langle\hat{j}\hat{j}\rangle$ of current operators is represented in terms of a *four* point function $\sim\langle\bar{\psi}\psi\bar{\psi}\psi\rangle$ of field operators. A moment's thought shows that **four point correlation functions** generically appear as microscopic descriptors of the response functions of quantum single particle operators

(simply because in second quantization, a single particle operator maps onto a bilinear of field operators), and, therefore, the vast majority of response functions in total.

▷ This observation implies a **hierarchy of correlation functions**: E.g. in our non-interacting example, the retarded response correlation functions was described in terms of a product of an advanced and a retarded microscopic single particle correlation function[28]. This almost trivial observation is of some importance becaues it entails

▷ A **separation of energy scales.** The argument $(\omega, \mathbf{q})$ of the response function is a measure of the frequency/momentum scale of the external perturbation. These parameters are to be distinguished from the argument $(\epsilon, \mathbf{p})$ of the single particle propagators microscopically describing the response process. In many cases, the two sets of scales are parametrically different. E.g. in the problem discussed above, $(\omega, \mathbf{q})$ is set by the resolution of an external electronic apparatus and, therefore, much slower than the frequency/momentum scale $(\omega, \mathbf{p})$ of electronic charge carriers at the Fermi surface. Under these circumstances, the ratios ω/ϵ and $|\mathbf{q}|/|\mathbf{p}|$, respectively, define small expansion parameters which can be used in the approximate evaluation of the response kernel. (In other cases, e.g. spectroscopic analysis of microscopic single particle excitations, it is essential that $(\omega, \mathbf{q})$ and $(\epsilon, \mathbf{p})$ are of the same order.)

8.5 Summary and Outlook

This completes our preliminary survey of theory and application of correlation functions in many body physics. We have seen that correlation functions, notably real time retarded response functions, represent a principal interface between experiment and theory. The connection between these objects and experimental data – the latter represented through expectation values of certain operators – was established by a formalism known as linear response: assuming an experimentally imposed perturbation of a many body system to be weak, its repsonse could be analysed within a controlled expansion scheme whose leading order term identified as a retarded correlation function.

A number of general properties of the response function – e.g. causality – could be identified from common sense reasoning. However, to develop a full understanding of this object, notably the connection between the imaginary time response function (the quantity produced by evaluation of the field integral) and its retarded real time counterpart (the quantity we are interested in) we had to go beyond that level. Indeed, we saw that the relation between various types of correlation functions could be disclosed by means of an amazingly strong spectral representation that was simple, exact, and

[28] For interacting problems, the response functions non longer neatly splits into a product of two single particle Green functions. Instead, the four field operators describing the response functions can be connected by an arbitrarily complicated network of interaction vertices. However, ulitimately the propagators connecting this network are again the single particle Green functions of the problem.

not dependent on any particular physical context (while not being particularly useful for practical computational purposes.)

The structural elements developed in the first parts of the chapter were finally bundeled into a powerful theory of electromagnetic linear response. We illustrated the application of this machinery on the example of the longitudinal conductivity of the electron gas and tried to point out a number of computational elements common to most concrete microscopic linear response calculations.

In the next chapter we will be back to the intrinsic development of the theory. We will get acquainted with the renormalization group, a powerful analytical tool designed to analyse correlation functions (and other objects of physical interest) within the vast space left open between straightforward perturbation theory on the one end and the few available exact evaluation schemes on the other end.

8.6 Problem Set

Q1 Orthogonality catastrophy

Q2 definition of the dielectric function

Q3 density-density response function of the disordered electron gas.

Q4 tunnel Hamiltonian

Q5 dielectric function from linear response formalism

Q6 model dielectric function

Q7 scattering linear response

Q8 electromagnetic response tensor of complex scalar field theory, sigma model.

Q9 conductivity, Meissner effect from response tensor

Q10 Hall conductivity in classical approximation

Q11 cancellation diamagnetic RR/AA

Chapter 9

The Renormalization Group

A first introduction into the framework of the so-called 'renormalization group' (RG). Starting out from the discussion of two introductory examples, we will get to know the RG as a concept – as opposed to a rigourously defined method – whereby non-linear theories can be analysed beyond the level of plain perturbation theory. We then proceed to discuss idea and functioning of RG methods in more general terms. Concepts such as scaling, dimensional analysis, the connection to the general theory of critical phenomena, and a number of concrete implementations of the RG program will be introduced and exemplified on a number of applications.

In chapter 6 we introduced the ϕ^4-model as an arch-prototype of interacting continuum theories. We saw that the non-linearities inherent to the model had to be taken seriously and introduced means to treat them perturbatively: Wick-contractions and their diagrammatic implementation. However, a critical review of that discussion shows that we actually left the state of a affairs in a rather miserable shape. First, we could not even build on any firm justification of the ϕ^4-action as such. I.e. the ϕ^4 continuum description was obtained by a gradient expansion of, in that particular application, a d-dimensional Ising model. But what what was the justification of terminating that expansion at second order in the number of gradients or, for that matter,excluding terms of order $\mathcal{O}(\phi^{(n>4)})$. In fact, questions of this type can be asked regarding any of the many continuum approximations we have performed throughout the first chapters of this course. Second, after we had identified a number of terms contributing to the perturbative expansion of the model (i.e. reprensented them in terms of momentum integrals over the non-interacting Green function) we realized that these were badly misbehaved. Those terms we constructed explicitly (cf., e.g., Eq. (6.18) and the equation before) contained divergences at large momenta. We also saw that in the transition region between the ferro- and the paramagnetic phase, respectively, these integrals were prone to build up infrared divergences. But what is worst, we had to concede that we had no clue as to how to overcome these problems! Needless to say that difficulties similar to those exemplified on the ϕ^4-model will show up in many other contexts as well.

To better understand origin and remedy of the problems above, we certainly need to

develop some new ideas. To this end, let us re-iterate that the central driving force of all our efforts is the devlopment of a better understanding of *long range* system characteristics. On the other hand, models such as ϕ^4 exhibit fluctuations on all lengthscales, including the shortest, and it was precisely these short-wavelength fluctuations that held responsible for most of our difficulties. But in principle, we already know how deal with situations of this kind. What we should aim for is integrating over all short-range fluctuations thereby generating an *effective* action for the long range degrees of freedom. We exemplified this program on numerous examples before where some slow field was coupled to rapidly fluctuating microscopic fields which were subsequently integrated out.

The only problem with our current application is that ϕ^4-theory does not know of any clear cut separation into 'fast' and 'slow' degrees of freedom. Rather, all fluctuations ranging from the shortest scales (of the order of some microscopic cutoff a limiting the applicability of the theory) to the longest scales (of the order of, say, the system size L) are treated on the same footing. However, to nonetheless implement the scheme of integrating-over-fast-modes-to-generate-an-effective-action-of-the-slow-modes we may artificially *declare* a certain length scale $a^{(1)} \equiv b > a$, as the scale separating 'short wavelength fluctuations' on scales $[a, a^{(1)}]$ from 'long wavelength fluctuations' on scales $[a^{(1)}, L^{-1}]$. Having done so, we may proceed to integrate out the short range fluctuations thereby changing the action of the long ranged degrees of freedom. Since the short range action is by no means simpler than the action of the long range degrees of freedom (both in fact equal to the ϕ^4-action) this step will involve approximations. Indeed, the integration procedure may lead to a number of conceivable scenarios. E.g., it may corrupt the algebraic structure of the long-wavelength action, leaving us with a theory fundamentally different from the one we began with. Alternatively, it may turn out that the effective action of the slow degrees of freedom is structurally similar to the original one, in which case the entire effect of integrating over the fast fluctuations amounts to a changed set of coupling constants.

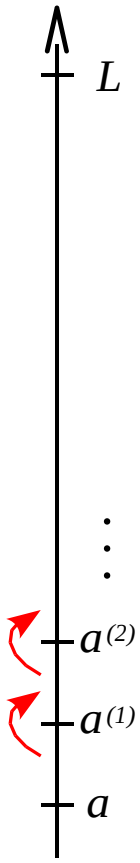

In that latter case, we are in good shape. We have arrived at a theory identical the old one except for (a) a different, or **renormalized** set of coupling constants and (b) an increased short distance cutoff $a \to a^{(1)} = ba$. The obvious further course of action will then be to *iterate* the procedure. We will declare a new cutoff $a^{(2)} = ba^{(1)} = b^2 a$, integrate out fluctuations on scales $[a^{(2)}, a^{(1)}]$, etc. Along with recursively integrating out more and more layers of fluctuations, the coupling constants of the theory change, or 'flow', until the cutoff $a^{(n)} \sim L^{-1}$ has become comparable to the length scales we are interested in. (In a way to be substantiated below,) the renormalized set of coupling constants then encodes much of the information on the long range behaviour of the model we are interested in.

The line of thoughts above summarizes the essential idea of the renormalization group program. Of course, the approach would be utterly useless had we to perform each recursion step $a^{(n-1)} \to a^{(n)}$ explicitly. However, a moments thought shows that this is

not so. Indeed, the whole idea relies on the recursive reproduction of the model in each step. That is, each step contains the full information on the further evolution of the action and, therefore, the model as such.

Admittedly, at first reading the idea of a flow of coupling constants on account of a recursive integration procedure must sound abstract. Therefore, before developing the general framework of the renormalization scheme any further, we shall illustrate its functioning on two concrete examples.

▷ INFO. The **advent of renormalization group ideas** in the late sixties and early seventies marks the transition between two different epoches. While research had previously focussed on the development and application of ever more sophisticated perturbative techniques, the seventies arguably stood under the spell of the renormalization program.

In the second half of the sixties ideas to recursively generate flows of coupling constants came up – apparently in independent developments – both in condensed matter and in particle physics. However, it took the insight of K. Wilson (see K. Wilson, Rev. Mod. Phys. **47**, 773 (1975), still one of the best introductions to the approach!) to realize the full potential of that approach and to develop it to a widely applicable tool. It is probably fair to say that Wilsons original formulation of the approach, and its later extension by others led to revolutionary progress condensed matter physics, particle physics and general statistical mechanics. Perhaps not less importantly, the RG concept turned out to be one of the major driving forces behind the partial unification of these fields.

In fact, the (highly unfortunate) **denotation 'renormalization group'** discloses much of the historical origin of the approach. A widespread doctrine of late sixties' particle physics had been that on a fundamental level our world could be understood in terms of symmetries and their implementation through groups – the eightfold way. In an attempt to absorb the newly developed RG approach into this general framework of thinking, it got dubbed renormalization *group*. Of course, a linkage between group structures and renormalization methods would not have been drawn had it been utterly unjustified. Indeed, one may argue that the sequence of RG transformations outlined above defines the structure of a *semi*group[1]. However, the connection between RG transformation and group algebraic structures is not only highly formal but also counterproductive. (It suggests a conceptual bond that simply isnt't there.) Besides, the group interpretation of the RG transformation is completely useless with regard to practical aspects.

———————————————————————

[1]To this end, one should interpret an individual RG transformation as an abstract mapping between two actions: $S \stackrel{R}{\to} S'$, where S is the original action, S' the action with increased short distance cutoff, and R the mapping between them. We next notice that these transformations can be iterated, or 'multiplied', $R \circ R'$. A moment's thought shows that the composition law obeys the defining conditions of a semigroup: there is a unit-transformation (nothing is integrated out) and the iteration is associative. (We are dealing with a *semi*group because the RG transformation is irreversible, it does not have an inverse.)

9.1 Example I: The One-Dimensional Ising Model

To illustrate the implementation of the RG program on a simple example (in fact *the* simplest example) we consider the $1d$ Ising model (cf. pp 188) defined through

$$\hat{H} = -J \sum_{ij} S_i S_j - H \sum_i S_i,$$

where the index i runs through a $1d$ sequence of sites, $S_i = \pm 1$ is the (uni-axial) magnetization of site i and H an external field. Throughout this section we will stick to the discrete spin representation of the model, i.e. unlike in section 6.1.2 we do not map it onto a continuum model. However, this does not hamper our the discussion of the RG program: Simply regard $-\beta\hat{H}[S]$ as a 'functional' of the discrete 'field' $\{S_i\}$, and all steps outlined above can be carried out without substantial modification.

9.1.1 Exact Solution

The $1d$ Ising model is exactly solvable, i.e. all its macroscopically observable properties can be computed in closed form. (This is, indeed, a welcome feature as it will provide us with a reference with which the results obtained by the RG program can be compared.) Both, the exact solution of the model and its RG formulation rely on a particular representation known as a **transfer matrix representation**. To understand the idea of this representation, notice that the Boltzmann weight of the problem factorizes according to

$$e^{-\beta\hat{H}} = e^{-\sum_{i=1}^{N}(-KS_iS_{i+1}-hS_i)} = \prod_{i=1}^{N} T(S_i, S_{i+1}),$$

where we have introduced the dimensionless parameters $K \equiv \beta J < 0$ and $h = \beta J$, and the weight T is defined through

$$T(S, S') = \exp\left(KSS' + \frac{h}{2}(S + S')\right).$$

We further assume that our system has N sites and obeys periodic boundary conditions $S_{N+1} = S_1$. Defining a two-component matrix T through

$$T_{11} = T(1,1), \qquad T_{12} = T(1,-1), \qquad T_{21} = T(-1,1), \qquad T_{22} = T(-1,-1),$$

we then observe that the partition function of the system is given by

$$Z = \sum_{\{S_i\}} e^{-\beta\hat{H}} = \sum_{\{S_i\}} \prod_{i=1}^{N} T(S_i, S_{i+1}) = \sum_{\{n_i\}} \prod_{i=1}^{N} T_{n_i n_{i+1}} = \mathrm{tr}\left(T^N\right).$$

We have thus managed to represent the partition function of the problem as a trace over the Nth power of the two dimensional 'transfer' matrix T[2]. By this representation, we

[2]The denotation 'transfer matrix' originates in an interpretation of the Ising model as a ficticious dynamical process in which a state S_i is 'transferred' to a state S_{i+1}, where the transition amplitude is given by $S(i_i, i_{i+1})$.

have almost solved the problem. Indeed, we can write

$$Z = \mathrm{tr}\left(T^N\right) = \lambda_+^N + \lambda_-^N,$$

where $\lambda_\pm$ are the two eigenvalues of the matrix

$$T = \begin{bmatrix} e^{K+h} & e^{-K} \\ e^{-K} & e^{K-h} \end{bmatrix}.$$

It is a straightforward exercise to verify that these eigenvalues are given by

$$\lambda_\pm = e^K \left[\cosh(h) \pm \sqrt{\sinh^2(h) + e^{4K}}\right].$$

Notice that $\lambda_+ > \lambda_-$. This implies that in the thermodynamic limit $N \to \infty$ the contribution of the latter may be neglected so that $Z \overset{N\to\infty}{\longrightarrow} \lambda_+^N$. Taking the logarithm of this expression and re-inserting the original system parameters we find that in the thermodynamic limit the free energy is given by

$$F = -N\left(J + T\ln\left[\cosh(\beta H) + \sqrt{\sinh^2(\beta H) + e^{-4\beta J}}\right]\right). \tag{9.1}$$

From here, we can straightforwardly compute the magnetization M of the system by differentiation wrt the magnetic field. The result is that the magnetization per spin, m, is given by

$$m \equiv \frac{M}{N} = \frac{\sinh(\beta H)}{\sqrt{\sinh^2(\beta H) + e^{-4\beta J}}}. \tag{9.2}$$

For illustration, two magnetization curves are shown in the figure, where the profile with the steep gradient corresponds to the lower temperature. Notice that the system does not magnetize in the absence of an external field, i.e. unlike its higher-dimensional cousins, the $1d$ model does not display sponataneous symmetry breaking.

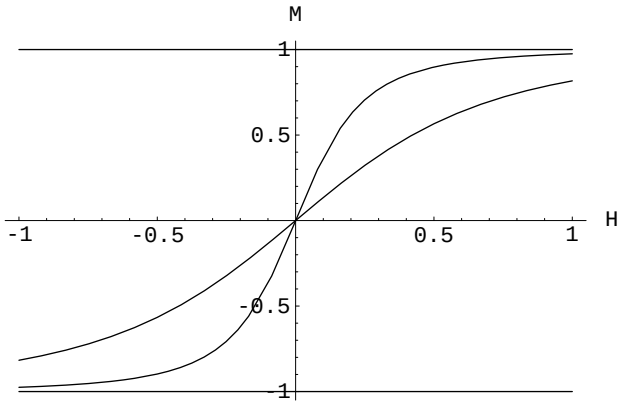

▷ INFO. It is actually not difficult to understand the reasons for the **absence of spontaneous symmetry breaking** in the $1d$ Ising model: suppose the system *had* a critical temperature T_c below which all spins order either to $S_i = 1$ or $S_i = -1$ (Fig. **??** top.) Now, imagine a segment of M consequtive spins, say, tentatively decided to flip. For doing so, they would have to pay a price of $\mathcal{O}(2J)$, viz. the energy assoiciated to the unfavourable spin alignment at the two ends of the anomalous region. However, on the other hand, there are N different choices for putting the sector of M flipped spins, i.e. the energy loss is counteracted by an entropic factor

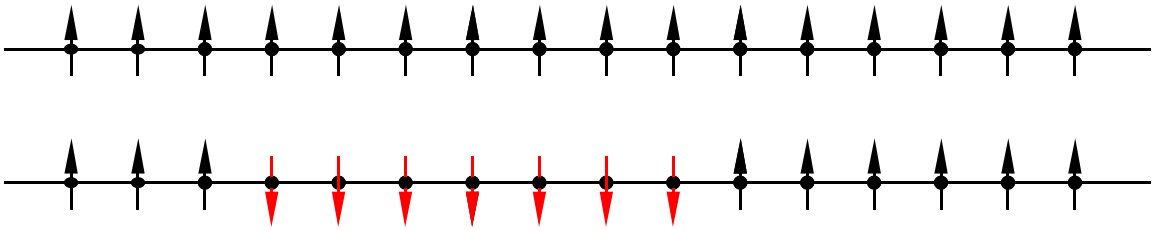

Figure 9.1: On the absence of spontaneous symmetry breaking in the $1d$ Ising model. No matter how low the temperature, the energy cost associated to the freation of a segment of flipped spins is outweighed by the entropy gain.

$T \ln(N)$. Thus, no matter how small T, for large enough systems, the *free* energy balance for flipping spin regions is positive, implying that the system will be in a disordered phase.

To wich extend do these arguments carry over to Ising systems of higer dimensionality? Consider, e.g., a two-dimensional variant of the model. Here the formation of a large connected region of M mismatched spins costs an energy price of at least $U \sim MJ^{1/2}$. To see this, notice that the energy is proportional to the one-dimensional boundary between the two different spin sectors. For a close to circulare geometry of the anomalous region, the boundary assumes its minimum length $\sim M^{1/2}$, leading to the above estimate for U.

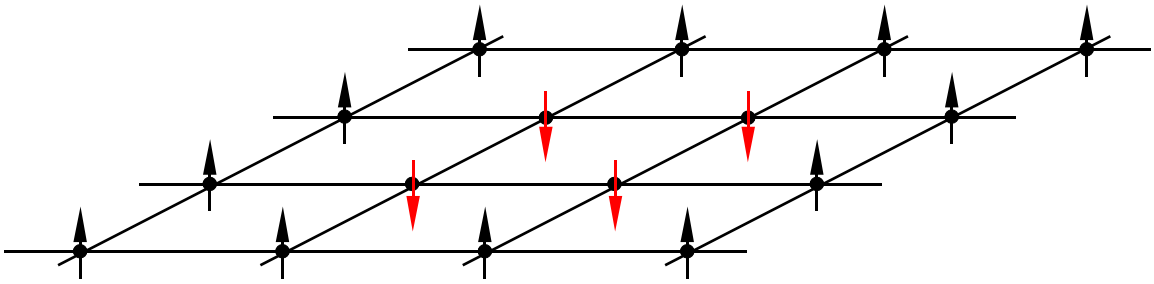

Figure 9.2: On the phenomenon of spontaneous symmetry breaking in Ising models of higher dimensionality. Entropic factors no longer have the capacity to overpower the extensive grow of energy associated to the formation of mismatched regions.

However, we still have by and large $\ln N$ different choices of putting the rebellious region. (Allowing for geometries other than circular, the energy/entropy balance becomes more complicated. However, we do not expect it to change qualitatively.) Thus, for $2d$, $F \sim JM^{1/2} - T \ln N$. No matter how small T, it therefore is energetically impossible to flip a thermodynamic $M \sim N^{x>0}$ sector of spins. We conclude that the $(d > 2)$-dimensional Ising model *does* exhibit a phase transition into an ordered low temperature phase.

This observation illustrates that

> The phenomenon of spontaneous symmetry breaking occurs only in systems of sufficiently large dimensionality. The threshold dimension below which entropic mechanism exclude spontaneous symmetry breaking is called the **lower critical dimension.**

Our argument above indicates that the lower critical dimension of the Ising model, or more generally,

> The lower critical dimension of systems with discrete broken symmetries is $d = 1$.

Having said so, an obvious question to ask is what is the lower critical dimension for systems with *continuous* symmetries (e.g., the U(1) symmetry of the superfluid, the O(3)-symmetry of the Heisenberg ferromagnet, etc.). To answer this question, we may proceed in analogy to the Ising case. I.e. we assume that a critical temperature exists below which the system is ordered. Using, for concreteness, the language of magnetic phenomena, we might say that the system is magnetized into a uniform state $\mathbf{S}(\mathbf{r}) = S\mathbf{e}_d$, where $\mathbf{e}_d$ is the unit vector in d-direction. Expanding the action $S[\mathbf{S}]$ around that configuration, one obtains, to lowest order,

$$S[\mathbf{S}] = \beta c \int d^d r \, \partial\theta\partial\theta,$$

where $\theta(\mathbf{r})$ is a generalized polar angle measuring fluctuations around the ordered state and c a coupling constant. We next ask for the thermal (or, if appropriate, quantum-thermal) expectation value $\langle\langle \mathbf{S}_d(\mathbf{r})\rangle\rangle$ of the d-component of the spin variable anywhere in the system. Assuming that we are close to the ordered state, an expansion in θ obtains

$$\mathbf{S}_d(\mathbf{r}) = S\cos(\theta) = S\left(1 - \frac{1}{2}\theta^2 + \ldots\right).$$

We now proceed to *check* whether the close-to-ordered assumption was actually legitimate. For this, we have to verify that in

$$\langle \mathbf{S}_d(\mathbf{r})\rangle = S - \frac{S}{2}\langle\theta(\mathbf{r})\theta(\mathbf{r})\rangle + \ldots$$

the fluctuation term is much smaller than the leading order constant contribution. Doing the Wick contraction with respect to the quadratic action, and switching to momentum space, we obtain

$$\langle \mathbf{S}_d(\mathbf{r})\rangle \approx S - \frac{ST}{2c}\sum_{\mathbf{q}}\frac{1}{q^2} \approx S - \frac{ST}{2c}\left(\frac{L}{2\pi}\right)^d \int \frac{d^d q}{q^2}.$$

The crucial observation now is that in dimensions $d \leq 2$, the integral is actually divergent. In the marginal case $d = 2$,

$$\int_{L^{-1}}^{a^{-1}} \frac{d^2 q}{q^2} = \pi \ln(L/a),$$

where we used that the momentum integral should be limited by a short (long) wavelength cutoff of the order of the inverse lattice spacing (the system size). In the thermodynamic limit, the integral grows without bounds implying that the assumption of an ordered state was ill-founded no matter how small temperature. The system is in an disordered state and, noting that nowhere did we rely on specifics of the spin system, we conclude

> The lower critical dimension of systems with broken continuous symmetries is $d = 2$ (**Mermin-Wagner theorem.**)

Obvioulsy, the divergence of the fluctuation integral is due to the fact that for large wavelength and in low dimensions, the integration volume (alias the entropy) of fluctuations $\sim q^d$ scales slower to zero than the energy cost $\sim q^2$. I.e. as in the Ising case, the Mermin-Wagner theorem can be understood as the statement of a competition of energy and entropy.

For completeness, we mention that the proof of the theorem (of which we gave a fairly abridged version here) in a subtle way relies on the fact that the symmetry in question is compact. For the (rare) class of sysmtems with non-compact, e.g. hyperbolic, symmetries, the statement does not hold.

9.1.2 Elements of Scaling Theory

Eq. (9.2) represents the full solution of the problem. We have explicitly obtained the magnetization as function of the magnetic field and the microscopic coupling constant of the model. Other thermodynamic characteristics, such as the magnetic susceptibility $\chi = -\partial_H^2 F$, can be generated by further differentiation wrt to H and/or T. However, in the vast majority of physically interesting problems we will *not* be in posession of a closed analytical solution. Which means that before comparing the exact solution with the outcome of the RG program we should reformulate the former in an univeraslly applicable *language*. I.e. a code that can be used to characterize the behaviour of a model irrespective of the particular method by which this behaviour has been analysed.

This objective leads us right away back to the notion of **correlation functions**. All models we might possibly be interested in display non-trivial fluctuation behaviour on large length scales. Indeed, in the vicinity of critical points marking the position of phase transitions, we expect the onset of critical fluctuations, i.e. the buildup of fluctuations on *all* length scales. (For a precise formulation of the phase transition related terminology used here, see below.) One of the central working hypotheses of the theory of these 'critical phenomena' is that in the vicinity of a transition point there is only one length scale of physical relevance, viz. the **correlation length** ξ. Within the context of the Ising model (cf. our previous discussion on p **??**) the latter is defined as the decay constant of the correlation function

$$C(r_1 - r_2) \equiv \langle S(r_1)S(r_2)\rangle - \langle S(r_1)\rangle\langle S(r_2)\rangle \sim \exp(-|r_1 - r_2|/\xi),$$

where we have switched to a continuum notation $S_i \to S(r)$, to emphasize the large-distance character of the present line of thought. To relate this quantity to the thermodynamic system characteristics we already have in our hands, we note that the magnetic susceptibility is given by

$$\chi = -\partial_H^2 F\Big|_{H=0} = \partial_H^2 T \ln Z\Big|_{H=0} = \beta \int dr dr' \left(\langle S(r)S(r')\rangle - \langle S(r)\rangle\langle S(r')\rangle\right) = \quad (9.3)$$

$$= \beta L \int dr\, C(r). \quad (9.4)$$

In words, the susceptibility obtains as the integral over the correlation function measuring the fluctuation behaviour of the spins.

▷ INFO. In fact, this is yet another manifestation of the **fluctuation dissipation theorem** discussed in the previous chapter. A dissipative quantity (presently, the susceptibility) is determined by the fluctuation behaviour of the system.

Comparison with the definition of the correlation function above obtains

$$\chi \sim \xi,$$

i.e. the susceptibility is directly proportional to the length scale determining the decay of correlations in the system. So far, we have not yet made use of the specific results obtained for the Ising models above. However, to actually work out the correlation length for our present example, all we have to do is differentiate (9.2) again wrt H, to obtain

$$\xi \sim \chi \sim \partial_H \Big|_{H=0} m \sim e^{2K}, \tag{9.5}$$

i.e. the correlation length exponentially increases in the limit $T \to 0$ on a scale set by the microscopic 'stiffness constant' J. This result should not be too surprising. Unlike in $d > 1$, the $1d$ Ising magnet does not display a finite temperature phase transition between a ferro- and a paramagnetic phase, respectively. It takes a limit $T \to 0$ to 'order' the system an make in long range correlated.

In the vicinity of a critical point, the correlation length is believed to be the only relevant length scale in the problem. Specifically, all observables X of dimensionality $[\text{length}]^{D_X}$ should obey the **scaling form**

$$X \sim \xi^{D_X} g_X,$$

where g_X is a dimensionless function. Let us explore this concept on our present example. The 'reduced free energy',

$$f(T) \equiv \frac{F}{TL}, \tag{9.6}$$

has dimension L^{-1}. Noting that $N \sim L$, a straightforward low temperature expansion of (9.1) indeed obtains

$$f(T) - f(0) = \xi^{-1} \left(-1 - \frac{1}{2} \xi^2 h^2 \right) \equiv \xi^{-1} g(\xi h), \tag{9.7}$$

where we have subtracted the infinite but inessential constant $f(0)$ and assumed that $1 \gg \xi^{-1} \gg h$. (The scaling form above actually suggests that the magnetic field has dimension L^{-1}, a prediction to be substantiated below.)

We have thus found that the correlation length of the $1d$ Ising system diverges according to (9.5) upon approaching zero temperature and that the free energy obeys the scaling law (9.7). Of course, this is only a fraction of the full information stored in the exact solution. However, the reduced set of data has the striking advantage that it is of general relevance. Indeed, we saw above that the correlation length is directly related to measurable system properties such as the magnetic susceptibility. Similarly, the output of experiments on systems with long range correlations is commonly encoded in the language of scaling relations. In other words, we have extracted that part of the information of the exact solution that carries universal relevance and can be compared to the output of other approaches.

9.1.3 Renormalization

We next explore what the renormalization group approach has to say about the problem. According to the general scheme outlined in the beginning of the chapter, we should aim to devise an algorithm to recursively trace out parts of the slow scale fluctuations of the model, on account of a modification of the action of the remaining degrees of freedom. An obvious strategy whereby this renormalization step may be effected is to subdivide our spin chains into regular clusters of b neighbouring spins (see Fig. 9.3). We may then proceed to sum over the 2^b sub-configurations of each cluster, thereby generating an effective functional describing the inter-cluster energy balance. While it is clear that this energy functional exists, a far less obvious question to ask is whether it will again have the form of an effective Ising spin system. Remarkably, the answer is positive so that we can say that the Ising model is 'renormalizable'. The structural reproduction of the model implies that we can think of each cluster as some kind of meta-Ising spin, or **block spin**. More importantly, it guarantees that the renormalization step qualifies for iteration: in a second RG step, b block spins are grouped to a new cluster (now comprising b^2 of the microscopic spins) which are then traced out, etc. We next discuss how this algorithm works in concrete terms.

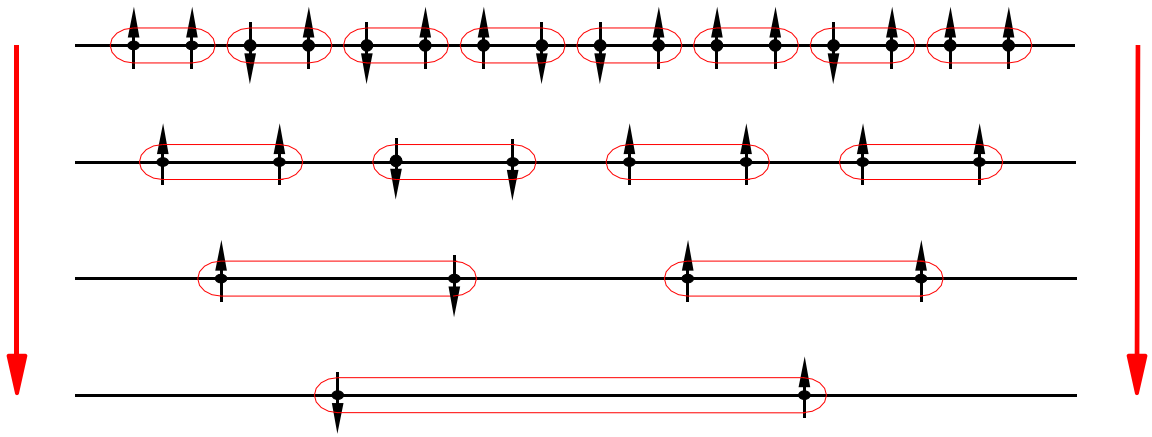

Figure 9.3: RG or blockspin transformation of the Ising model illustrated for clusters of size $b = 2$. An r-fold iteration of the procedure reduces the degrees of freedom by a factor 2^r.

Within the transfer matrix approach to the problem, a cluster of b spins is represented through n transfer matrices T. Taking the partial trace over its degrees of freedom amounts to passing from these n matrices to the product $T' = T^b$. (By construction of the approach, the internal index summation involved in taking the product amounts to tracing out the degrees of freedom of the cluster.) The transition from the original partition function $\mathcal{Z}$ to the new partition function $\mathcal{Z}'$ is defined through

$$\mathcal{Z}_N(K,h) = \mathrm{tr}\,(T^N) = \mathrm{tr}\,((T^b)^{N/b}) = \mathrm{tr}\,(T')^{N/b} = \mathcal{Z}_{N/b}(K',h'), \tag{9.8}$$

where the notation makes the parametric dependence of the partition function on the size of the system, N, and on the coupling constants K, h explicit. Notice that the line above makes the highly non-obvious prediction that the reduced trace, $\mathrm{tr}\,(T')^{N/b}$ can again be

expressed as an Ising partition function, or, equivalently, that the effective transfer matrix T' has the same algebraic structure as the elementary matrices T.

To verify this statement, we explore the structure of the product matrices T' for the simplest case of $b = 2$ block spins. Introducing the abbreviations

$$u \equiv e^{-K}, \qquad v \equiv e^{-h},$$

we have

$$T = \begin{bmatrix} e^{K+h} & e^{-K} \\ e^{-K} & e^{K-h} \end{bmatrix} = \begin{bmatrix} u^{-1}v^{-1} & u \\ u & u^{-1}v \end{bmatrix},$$

while the product takes the form

$$T' \equiv T^2 = \begin{bmatrix} u^2 + u^{-2}v^{-2} & v + v^{-1} \\ v + v^{-1} & u^2 + u^{-2}v^2 \end{bmatrix} \stackrel{!}{=} C \begin{bmatrix} u'^{-1}v'^{-1} & u' \\ u' & u'^{-1}v' \end{bmatrix}.$$

In the last equality we demand that the new transfer matrix be of the same structure as the original one. However, noting that this requirement will introduce three conditions (for the three independent entries of the symmetric matrices T and T',) we are willing to accept the appearance an overall multiplicative constant C[3]. Having introduced this new parameter, we have enough freedom to solve the three equations

$$Cu' = v + v^{-1}, \qquad Cu'^{-1}v'^{-1} = u^2 + u^{-2}v^{-2}, \qquad Cu'^{-1}v' = u^2 + u^{-2}v^2$$

to the not so appealingly looking result

$$u' = \frac{\sqrt{v + v^{-1}}}{(u^4 + u^{-4} + v^2 + v^{-2})^{1/4}}, \qquad v' = \frac{\sqrt{u^4 + v^2}}{\sqrt{u^4 + v^{-2}}}, \tag{9.9}$$

and $C = \sqrt{v + v^{-1}}(u^4 + u^{-4} + v^2 + v^{-2})^{1/4}$. As a corrolary we remark that the possibility to rerepresent the new transfer matrix in the same algebraic structure as the old one implies that the transformed model again describes an Ising spin system (viz. the spin system whose transfer matrix would be given by T'.) However, the action of the new, block-spin system,

- ▷ sits at a diferent temperature, magnetic field and exchange constant (as described by the new values of the coupling constants (u', v'), and
- ▷ describes fluctuations on length scales that are twice as large as in the original system. In particular, the short distance cutoff has been doubled.

To make further progress, we focus on the two relevant parameters u' and v' and observe that the result of the block spin transformation can be represented as a discrete map

$$\begin{bmatrix} u' \\ v' \end{bmatrix} = \begin{bmatrix} f_1(u, v) \\ f_2(u, v) \end{bmatrix},$$

where the functions $f_{1,2}$ are defined through (9.9). In Fig. 9.4 sequences of points generated by iterative application of the map f are shown for different values of 'initial conditions' (u_0, v_0).

[3] Taking the product of the new transfer matrices, we see that this constant appears appears in the partition function as $\mathcal{Z}' \sim C^{N/b}$. I.e. the free energy picks up an overall additive constant $F' \sim -\frac{NT}{b} \ln C$ which will be of no further significance.

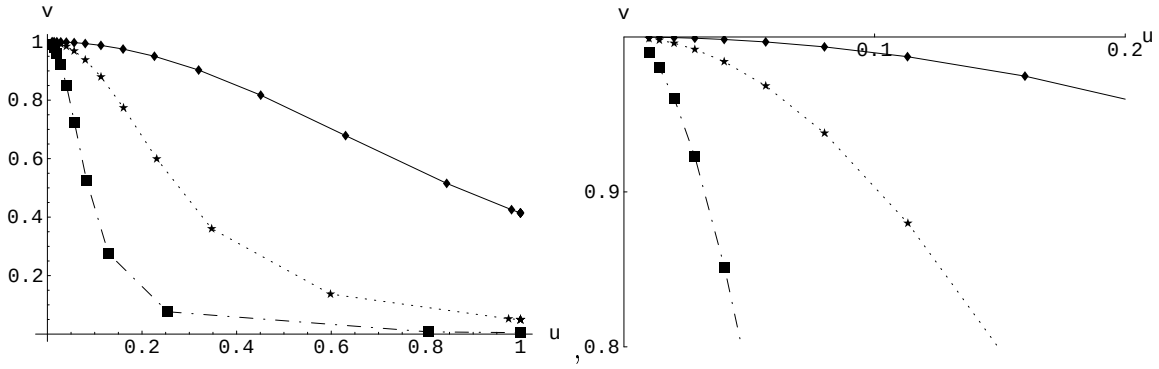

Figure 9.4: The flow of coupling constants of the $1d$ Ising model generated by iteration of the RG transformation. The three lines shown are for starting values $(u, v) = (0.01, 0.9999)$ (diamonds), $(0.01, 0.999)$ (stars), and $(0.01, 0.99)$ (boxes). Right: magnification of the zero temperature fixed point region.

The morphology of these **RG trajectories** essentially determines our further course of action. Evidently, the map f possesses two disjoint sets of **fixed points**, i.e. points (u^*, v^*) that stay invariant under application of the map f:

$$\begin{bmatrix} u^* \\ v^* \end{bmatrix} = \begin{bmatrix} f_1(u^*, v^*) \\ f_2(u^*, v^*) \end{bmatrix},$$

Inspection of (9.9) shows that this is the case for (a) the point $(u^*, v^*) = (0, 1)$, and (b) the line $(u^*, v^*) = (1, v)$.

Fixed point sets represent the the most important structural characteristic of an RG analysis. They organize the space of 'flowing' coupling constants into sectors of qualitatively different behaviour. To illustrate this phenomenon on our current example, notice that at a fixed point all characteristics of the model, including its correlation length ξ remain invariant. On the other hand, we noticed above that an RG step is tantamount to doubling the fundamental length scale of the system. These two features only go together if either $\xi = 0$ or $\xi = \infty$. (Please think about this statement.) Indeed, the line of fixed points identified above has $u = \exp(-\beta J) = 1$ meaning that $\beta = 0$. This is the limit of infintely large temperatures at which we expect the model to be in a state of maximal thermal disorder, $\xi = 0$. Besides the high-temperature fixed line, there is a zero-temperatue fixed point $(u, v) = (\exp(-\beta J), \exp(-\beta h)) = (0, 1)$ implying $T \to 0$ and $h = 0$. Upon approaching zero temperature, the system is expected to order and to build up long range correlations, $\xi \to \infty$.

Notice, however, an important difference between the high- and the low-temperature fixed point set. While the former is an **attractive fixed point** in the sense that the RG trajectories approach it asymptotically, the latter is a **repulsive fixed point**. I.e. no matter at what low temperature we start, the RG flow will drive us into a regime of effectively higher temperature or lower ordering. (Of course, the *physical* temperature does not change under renormalization. All we are saying is that the block-spin model appears like an Ising model at a higher temperature than the original system.)

To explore the low temperature phase of the system quantitatively, we may *linearize* the RG map in the vicinity of the $T = 0$ fixed point. That is, comprising the fixed

point data into a two component vector, $\mathbf{x}^* \equiv (u^*, v^*)^T = (1,0)^T$ and assuming that $\Delta\mathbf{x}$ parameterizes a a small deviation from the fixed point, we write

$$\mathbf{x}^* + \Delta\mathbf{x}' = \mathbf{f}(\mathbf{x}^* + \Delta\mathbf{x}) \approx \mathbf{f}(\mathbf{x}^*) + \partial_{\mathbf{x}}\mathbf{f} \cdot \Delta\mathbf{x} + \mathcal{O}(\Delta\mathbf{x}^2).$$

Now, on account of the fixed point property $\mathbf{f}(\mathbf{x}^*) = \mathbf{x}^*$, we obtain the linearized map

$$\Delta\mathbf{x}' = \partial_{\mathbf{x}}\mathbf{f} \cdot \Delta\mathbf{x} + \mathcal{O}(\Delta\mathbf{x}^2).$$

To explore the linearized mapping in more detail, it is convenient to introduce yet another pair of variables, viz.

$$r \equiv u^4, \qquad s \equiv v^2,$$

where upon the RG transformation becomes rational,

$$r' = \frac{2 + s + s^{-1}}{r + r^{-1} + s + s^{-1}}, \qquad s' = \frac{r + s}{r + s^{-1}}.$$

Differentiating this map at $(r,s) = (1,0)$, it is straightforward to show that

$$\begin{bmatrix} \Delta r' \\ \Delta s' \end{bmatrix} = \begin{bmatrix} 4 & \\ & 2 \end{bmatrix} \begin{bmatrix} \Delta r \\ \Delta s \end{bmatrix}.$$

We finally note that this result was obtained for the particular case of a block spin transformation with $b = 2$, i.e. we can formally write

$$\begin{bmatrix} \Delta r' \\ \Delta s' \end{bmatrix} = \begin{bmatrix} b^2 & \\ & b \end{bmatrix} \begin{bmatrix} \Delta r \\ \Delta s \end{bmatrix}. \tag{9.10}$$

Of course, this re-formulation would be non-sensical if it would not generalize to $b \neq 2$. However, this is the case, as can be seen by noting that a transformation with $b = 4$, say, is equivalent to a two-fold application of a $b = 2$ transformation. (Indeed, $(2^2)^2 = 4^2$ and $2^2 = 4$.)

To make use of Eq. (9.10), we again consider the reduced free energy (9.6): $f(\Delta r, \Delta s) \equiv -N^{-1} \ln \mathcal{Z}_N(K(\Delta r), h(\Delta s)) \equiv -N^{-1} \ln \mathcal{Z}_N(\Delta r, \Delta s)$ and reformulate Eq. (9.8) according to

$$f(\Delta r, \Delta s) = -\frac{1}{N} \ln \mathcal{Z}_N(\Delta r, \Delta s) = -\frac{1}{N'b} \ln \mathcal{Z}_{N'}(\Delta r', \Delta s') = \frac{1}{b} f(b^2 \Delta r, b \Delta s).$$

This equation describes the 'scaling' of the free energy density under block spin transformations (all in the linearizable low temperature regime.) or, equivalently, changes of the fundamental length scale at which we consider our model. E.g., for $b = 8$ the rhs of the equation describes how the model would look like from a 'fuzzy' point of view where all degrees of freedom on scales $< b$ have been comprised into a single structural unit.

Importantly, b is a free parameter without intrinsic significance; it can be set to any desired value. E.g. we may find it convenient to look at our model at scales where $b^2 \Delta r = 1$. With this choice we obtain

$$f(\Delta r, \Delta s) = \Delta r^{1/2} f(1, \Delta s / \Delta r^{1/2}) \equiv \Delta r^{1/2} g(\Delta s / \Delta r^{1/2}),$$

where the dimensionless *one-parameter* function g is defined through the second equality. We finally relate back to the physical system parameters characterizing our model:

$$\Delta r = r - 0 = r = u^4 = e^{-4K},$$
$$\Delta s = s - 1 = v^2 - 1 = e^{-2h} - 1 \simeq -2h,$$

which brings us to

$$f = e^{-2K} g(e^{2K} h). \tag{9.11}$$

This is the scaling form predicted by the RG analysis. Notice that a non-trivial statement is made. The a priori dependence of the free energy on two independent system parameters K, h has been reduced to a one parameter function, times an overall prefactor. Indeed, we expect on general grounds that (see the discussion of the previous section) the reduced free energy should scale with the inverse of the correlation length ξ which in turn diverges upon approaching the zero temperature fixed point. Comparison with (9.11), and noting that there are no reasons for the rescaled free energy $g(x) = f(1, x)$ to diverge by itself, we conclude that the divergence of ξ is driven by the prefactor, i.e.

$$\xi \sim e^{2K},$$

in agreement with the result of the exact analysis. With this identification we obtain

$$f = \xi^{-1} g(\xi h),$$

i.e. the magnetic field appears in conjunction with the correlation length and we have reproduced the exact asymptotic (9.7).

Notice that there is no reason to be too irritated about the excessive appearance of vague proportionalities '$\sim$'. As fixed points are approached, physical systems tend to build up all sorts of singular scales. The most fundamental of these is the correlation length, but the divergence of ξ usually entails singular behvaiour of other physical quantities. These singularities characterize much of the observable behaviour of a system both theoretically and, in fact, experimentally. In the immediate vicinity of a fixed or transition point all but the strongest driving forces of singular scaling are of secondary importance. That is why we could, e.g., conclude from (9.11) that $\xi \sim \exp(2K) \sim \exp(2\beta J)$. We know on general grounds that $f \sim \xi^{-1}$. On the other hand, (9.11) implies that the leading (i.e. exponential) driving force behind the divergence of that scaling factor must sit in $\exp(2\beta J)$. This leads to the idnetification $\xi \sim \exp(2\beta J)$, where all other factors of proportionality are of secondary importance.

In section XX below we will discuss these scaling arguments from a more general perspective. However, before doing so, let us exemplify an RG analysis on a second case study.

9.2 Example II: Disordered Quantum Wires

In section 3.2.2 we discussed the physics of interacting fermions in one dimension. We saw that unlike in a Fermi liquid, the fundamental excitations of the system are charge

(and spin) density waves – collective excitations describing the wave like propagation of spin and charge degrees of freedom, respectively. Going beyond the level of an idealized translationally invariant environment, the question we wish to address below is to what extend the propagation of these modes will be hampered by the presence of imperfections, or impurities in the wire.

This problem is of considerable practical relevance. All candidates for real life realizations of one-dimensional conductive systems – semiconductor quantum wires, conducting polymers, carbon nanotubes, quantum Hall edges, etc. – will in general contain imperfections. Further, and unlike in systems of higher dimensionality, a spin/charge degree of freedom propagating down a one-dimensional channel will inevitably hit any impurity blocking its way. We thus expect that impurtity scattering has a relatively stronger impact on the transport behaviour of the system than in higher dimensions.

However, there is a second, more subtle, reason as to why we should expect disorder to have a drastic effect on the conduction behaviour of $1d$ quantum wires: Imagine a wave package of characteristic momentum k_F impingent from the left onto an impurity at position $x = 0$. The total wave amplitude to the left of the impurity, $\psi(x) \sim \exp(ik_F x) + r\exp(-ik_F x)$ will be a linear superposition of the incoming amplitude $\sim \exp(ik_F x)$ and the reflected outgoing amplitude $\sim r\exp(-ik_F x)$, where r is the reflection coefficient. Thus, the electronic density profile,

$$\rho(x) = |\psi(x)|^2 \sim 1 + |r|^2 + 2\,\mathrm{Re}\,\left(re^{-2ik_F x}\right),$$

contains a $2k_F$ oscillatory contribution known as a **Friedel oscillation**. What is more, a closer analysis (see the problem set) shows that in one dimension, the amplitude of these oscillations decays rather slowly[4], namely as $\sim x^{-2}$. The key point now is that in the presence of electron-electron interactions other particles approaching the impurity will notice the charged density pattern of the Friedel oscillation as a source of scattering. The additional scattering potential then creates a secondary Friedel oscillation, etc. We thus expect that even a weak imperfection in a Luttinger liquid acts as a 'catalyst' for the recursive buildup of a *strong* potential.

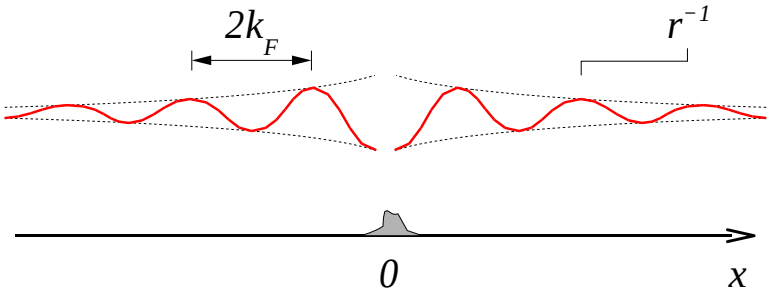

Figure 9.5: Cartoon on the buildup of $2k_F$-periodic Friedel oscillations in the vicinity of an impurity.

Below we will quantitatively confirm this conjecture by RG methods. However, before

[4] Of course, the argument above, relying on an oversimplified plane wave modeling of the incoming electron state is too crude to predict the spatial profile of the Friedel pattern.

doing so, we must first identify a model describing the scattering of charge density wave[5] off impurities. Starting from the boson representations of the interacting quantum wire developed in section (3.2.2), this is a non-trivial (and interesting) exercise in operator algebra. However, readers wishing to proceed in a more streamlined manner, i.e. not be distracted from the further development of the RG program, are invited to directly proceed to the next section where the effective low energy model derived in section 9.2.1 will be subjected to an RG analysis.

9.2.1 Tomonaga-Luttinger Model with an Impurity

▷ EXERCISE. Re-familiarize yourself with the the phyiscs of the $1d$ electron gas (section 3.2.2).

To prepare the extension to the presence of disorder let us recapitulate that the dynamics of the unperturbed system could be described in terms of two density operators $\hat{\rho}_{sq}$ measuring the presence of left- or right-moving ($s = L, R$) density modulations of characteristic wavelength $\sim q^{-1}$. More specifically, we employed a set of bosonic operators $\{b_q, b_q^\dagger\}$, related to operators $\{\hat{\rho}_{sq}\}$ by a trivial scale transformation, as basic degrees of freedom in which to represent the model.

In contrast, a local impurity sitting in the wire at position $x = 0$, say, might be described through

$$\hat{H}_{\text{imp}} \equiv V_0 a^\dagger(0) a(0), \tag{9.12}$$

where V_0 measures the impurity strength and $a(0), a^\dagger(0)$ are *fermion* operators. Since there is little reason to sacrifice the powerful representation of the bulk theory outlined above, the first problem we need to address is how to represent the fermionic operator algebra in terms of collective mode operators.

Boson Representation of Fermion Operators (Heuristic)

We begin by defining yet another operator pair through

$$\partial_x \Phi_s(x) \equiv -2\pi\sigma_s \hat{\rho}_s(x), \tag{9.13}$$

where $\sigma_s = (+/-)$ for $s = L/R$ as before. The newly defined operators $\hat{\Phi}_s$ are related to the charge densitiy operators $\hat{\rho}_s$ through integration, i.e. apparently, they have something to do with the total amount of left/right moving charge in the system. (For the utility of such objects, see below.) However as it stands, the differential equation (9.13) defines the $\hat{\Phi}_s$'s only up to a 'constant', i.e. the addition of an x-independent operator to a solution of the differental equation $\hat{\Phi}_s(x)$ is again a solution. To uniquely specify a set of solutions, we demand fulfillment of the commutation relation relations

$$[\hat{\Phi}_s(x), \hat{\Phi}_{s'}(x')] = -i\pi\delta_{ss'}\sigma_s \,\text{sgn}\,(x - x'), \tag{9.14}$$

known as the **Kac-Moody commutator algebra**.

[5] To keep the analysis simple, we neglect the dynamics of the spins throughout.

▷ EXERCISE. Use (3.35) to verify that the differential equation (9.13) is consistent with these relations. Show that the explicit solution fulfilling the Kac-Moody commutator algebra is given by

$$\hat{\Phi}_s = \pi\sigma_s \int_{-\infty}^{\infty} dx'\, \hat{\rho}_s(x')\,\mathrm{sgn}(x'-x) = -2\pi\sigma_s \left(\int_{-\infty}^{x} dx'\, \hat{\rho}_s(x') - \frac{\hat{N}_s}{2} \right), \tag{9.15}$$

where $\hat{N}_s = \int_{-\infty}^{\infty} \hat{\rho}_s$ is the total amount of s-moving charge.

We next employ the operators $\hat{\Phi}$ to identify a generalized Bose representation of the fermion field. As is symptomatic for our present analysis, we we shall not try to construct this representation explicitly, but rather rely on commutatation relations. Using the same notation as in section 3.2.2 we begin by decomposing the operator $a(x)$ into a left- and a right-moving contribution:

$$\begin{aligned} a(x) = \frac{1}{L^{1/2}} \sum_p e^{ipx} a_p \approx \frac{1}{L^{1/2}} \tilde{\sum_q} \left(e^{ik_F x} e^{iqx} a_{Rq} + e^{-ik_F x} e^{iqx} a_{Lq} \right) \equiv \\ \equiv e^{ik_F x} a_L(x) + e^{-ik_F x} a_R(x). \end{aligned}$$

It is then straightforward to verify the commutation relations

$$[a_s(x), \hat{\rho}_{s'}(x')] = a_s(x)\delta_{ss'}\delta(x-x'),$$

which entail

$$[a_s(x), \hat{\Phi}_{s'}(x')] = -\delta_{ss'}\sigma_s \pi\, \mathrm{sgn}(x'-x) a_s(x).$$

We now claim that these relations are *consistent* with the boson representation

$$\boxed{a(x) = \eta^{-1/2} \left(e^{ik_F x} e^{i\hat{\Phi}_R(x)} + e^{-ik_F x} e^{i\hat{\Phi}_L(x)} \right),} \tag{9.16}$$

or $a_s(x) = \eta^{-1/2} e^{i\hat{\Phi}_s(x)}$. Here η is an infinitesimal scaling factor with $[\eta] =$ length. While the presence of a prefactor of this dimensionality is required by $[a_s(x)] =$ length, its parametric value will not be of much concern in the following[6].

To verify the boson representation above, it is convenient to use the general relation,

$$[F(\hat{A}), \hat{B}] = F'(\hat{A})[\hat{A}, \hat{B}],$$

valid for general operators $\hat{A}, \hat{B}$ and functions F, provided the commutator $[\hat{A}, \hat{B}]$ is a c-number. Since the commutator of two $\hat{\Phi}$'s taken at different points in space is a number, we can employ this relation to obtain

$$\begin{aligned} [a_s(x), \hat{\Phi}_{s'}(x')] = \eta^{-1/2} [e^{i\hat{\Phi}_s(x)}, \hat{\Phi}_{s'}(x')] = \eta^{-1/2} e^{i\hat{\Phi}_s(x)} [i\hat{\Phi}_s(x), \hat{\Phi}_{s'}(x')] = \\ = e^{i\hat{\Phi}_s(x)} \pi\delta_{ss'}\sigma_s\, \mathrm{sgn}\,(x-x') = -\pi\delta_{ss'}\sigma_s\, \mathrm{sgn}\,(x'-x) a_s(x), \end{aligned}$$

[6] In fact, one can show that η is infinitesimal, viz. it plays the role of the effective discretization spacing of the 'Riemann sums' underlying our integral definitions: Remembering that all integrals appearing in the present context arise as continuum approximations to discrete sums, we set $\int dx \equiv \eta \sum_i$, where $\{i\}$ defines a discretization of the integration support into segments of length η. To verify this statement, one needs to explore the singularity of the anti-commutator $[a_s(x), a_s(x')]_+ = \delta(x-x')$. This in turn necessitates a careful regularization of the short distance singularities arising when $x \to x'$. For a detailed discussion of this point we refer to ...

in agreement with the commutator relation identified above.

▷ EXERCISE. Verify the auxiliary identity above by Taylor expansion of $F(\hat{A})$. Employ the Baker-Campbell-Hausdorff formula

$$e^{\hat{A}}e^{\hat{B}} = e^{\hat{A}+\hat{B}+\frac{1}{2}[\hat{A},\hat{B}]}$$

(valid if $[\hat{A},\hat{B}]$ is a c-number) to verify that the boson representation of the fermion operators is anti-commutative, $[a_s(x), a_{s'}(x')]_+ = [a_s^\dagger(x), a_{s'}(x')]_+ = 0$ for $x \neq x'$.

Referring for a more rigorous construction to the problem set, we identify (9.16) as a tentative representation of the fermion operator in terms of the collective mode fields $\hat{\Phi}$. Readers wishing to understand the structure of this representation in intuitive terms are also advised to consult the problem set.

▷ INFO. For the sake of completeness, let us go through a simple argument showing that (9.16) *cannot* be a completely faithful representation of the fermion operator. The reason is that the collective fields $\hat{\Phi}_s$ obtain through integration of charge density operatos $\hat{\rho}_s \sim a_s^\dagger a_s$, i.e. of operators that conserve the particle numbers. Consequently, the rhs of (9.16), too, conserves the number of particles, in blatant contradiction to the lhs. To remedy this defect, one multiplies the prototypical representation by a unitary operator $\hat{F}_s$, $e^{i\hat{\Phi}_s(x)} \to \hat{F}_s e^{i\hat{\Phi}_s(x)}$, known as a **Klein factor**. Roughly speaking, the role of the Klein factors is to correctify the previously incorrect overall particle number balance. Notice, however, that the introduction of Klein factors does not lead to a 'significant' complication of the theory, the reason being the there is just *one* such operator per particle species $s = L/R$. (The $\hat{F}$'s do not depend on position.) Further, in most cases, only particle number conserving bilinears, $a_s^\dagger(x)a_s(x)$ finally survive the functional average, in which case the Klein factors drop out.

More generally, the bosonic representation of fermion operators involves a number of subtleties, most of which we are tacidly sweeping under the carpet. For a pedagogical and carefully written discussion of the subject, we refer to the paper J. von Delft and H. Schoeller, Ann. Phys. **4**, 225 (1998). (Or to the problem set, where the effective low energy model we are interested in will be derived in adequate rigour.)

We now have everything together to represent the perturbation $H_{\rm imp}$ in terms of the fields $\hat{\Phi}$. Substitution of (9.16) into (9.12) leads to

$$\hat{H}_{\rm imp} = \frac{V_0}{\eta}\left[e^{-i\hat{\Phi}_R(0)} + e^{-i\hat{\Phi}_L(0)}\right]\left[e^{i\hat{\Phi}_R(0)} + e^{i\hat{\Phi}_L(0)}\right].$$

Naively, it would seem that the purely right/left-moving contributions to this product drop out, $e^{-i\hat{\Phi}_s(0)}e^{i\hat{\Phi}_s(0)} \stackrel{?}{=} 1$. However, owing the the non-trivial commutation relations of $\hat{\Phi}_s$ with itself, some care must be exercised in evaluating these products. Rather than evaluating the two factors at coinciding points, we apply a **point splitting procedure**, i.e we interpret the product according to

$$e^{-i\hat{\Phi}_s(x)}e^{i\hat{\Phi}_s(x)} \equiv e^{-i\hat{\Phi}_s(x+\eta)}e^{i\hat{\Phi}_s(x-\eta)} = e^{-i(\hat{\Phi}_s(x+\eta)-\hat{\Phi}_s(x-\eta))+\frac{1}{2}[\hat{\Phi}_s(x+\eta),\hat{\Phi}_s(x-\eta)]} = \approx (-i)^{\sigma_s}e^{-2i\eta\partial\hat{\Phi}_s(x)}, \tag{9.17}$$

where η is the infinitesimal offset introduced above and the first equality is based on the Baker-Campbell-Hausdorff formula. Substitution of this result into the boson representation of $\hat{H}_{\rm imp}$ leads to

$$\hat{H}_{\rm imp} = c_1 \partial\hat{\phi}(0) + c_2 \cos(\theta(0)),$$

where the coupling constants $c_1 = 2V_0$, $c_2 = 2V_0\eta^{-1}$ and we have defined 'center of mass coordinates' through

$$\hat{\phi} = \frac{1}{2}(\hat{\Phi}_L + \hat{\Phi}_R),$$
$$\hat{\theta} = \frac{1}{2}(\hat{\Phi}_L - \hat{\Phi}_R).$$

Notice that the transformation $(\hat{\Phi}_L, \hat{\Phi}_R) \to (\hat{\phi}, \hat{\theta})$ is 'canonical' in the sense that the new fields, too, obey a Kac-Moody type commutator relation

$$[\hat{\phi}(x), \hat{\theta}(x')] = \frac{i\pi}{2}\,\mathrm{sgn}\,(x - x'). \tag{9.18}$$

To complete the derivation of the model we need to express the bulk part of the Hamiltonian in terms of the fields $(\hat{\phi}, \hat{\theta})$. In section 3.2.2 we had seen that the Hamiltonian of the quantum wire could be represented as

$$\begin{aligned}\hat{H} &= \frac{\pi v_F}{L}\sum_q (\hat{\rho}_{Lq}, \hat{\rho}_{Rq}) \begin{pmatrix} 1+\frac{g_4}{2\pi} & \frac{g_2}{2\pi} \\ \frac{g_2}{2\pi} & 1+\frac{g_4}{2\pi}\end{pmatrix} \begin{pmatrix}\hat{\rho}_{L-q}\\ \hat{\rho}_{R-q}\end{pmatrix} = \\ &= \pi v_F \int dx\,(\hat{\rho}_L(x), \hat{\rho}_R(x)) \begin{pmatrix} 1+\frac{g_4}{2\pi} & \frac{g_2}{2\pi} \\ \frac{g_2}{2\pi} & 1+\frac{g_4}{2\pi}\end{pmatrix} \begin{pmatrix}\hat{\rho}_L(x)\\ \hat{\rho}_R(x)\end{pmatrix}\end{aligned}$$

in terms of density modes. Now, remembering that $\hat{\rho}_s = -\frac{1}{2\pi}\partial_x\hat{\Phi}_s$ as well as

$$\begin{pmatrix}\hat{\Phi}_L\\ \hat{\Phi}_R\end{pmatrix} = \begin{pmatrix}1 & -1\\ 1 & 1\end{pmatrix}\begin{pmatrix}\hat{\theta}\\ \hat{\phi}\end{pmatrix},$$

one verifies that

$$\hat{H} = \frac{v}{2\pi}\int dx (g(\partial\hat{\phi})^2 + g^{-1}(\partial\hat{\theta})^2),$$

with the two coupling constants

$$\begin{aligned} v &\equiv v_F\left[\left(1+\frac{g_4}{2\pi}\right)^2 - \left(\frac{g_2}{2\pi}\right)^2\right]^2 \\ g &\equiv \left[\frac{1+\frac{g_2}{2\pi}-\frac{g_4}{2\pi}}{1+\frac{g_2}{2\pi}+\frac{g_4}{2\pi}}\right]^{1/2}. \end{aligned} \tag{9.19}$$

Collecting terms, we obtain

$$\hat{H} = \frac{v}{2\pi}\int dx\left[g(\partial\hat{\phi})^2 + g^{-1}(\partial\hat{\theta})^2\right] + c_1\partial\hat{\phi}(0) + c_2\cos(2\hat{\theta}(0)) \tag{9.20}$$

for the Hamiltonian of the Luttinger liquid with an impurity at $x = 0$.

The structure of the perturbation at $x = 0$ can be simplified somewhat by noting that the first term, $\partial\hat{\phi}(0)$, was obtained by bosonization of the sum of two local density operators $\sim a_L^\dagger(0)a_L(0) + a_R^\dagger(0)a_R(0)$. But can these operators cause any nontrivial physical effects? Particles propagating in the L-strand, say, are obliged to propagate to the left and that with fixed velocity v_F. Thus, a local perturbation $\sim a_L^\dagger(0)a_L(0)$ blocking their way cannot effectively change the dynamics. (For that, it would take an operator $\sim (a_L^\dagger(0)a_R(0) + \text{h.c.})$ coupling the left and the right moving sector, respectively.) All the perturbation can do is multiply the outgoing electron field to the left of the impurity by an inessential scattering phase. Indeed, it is a straightforward exercise (do it!) to verify that an operator $V(a_L^\dagger(0)a_L(0) + a_R^\dagger(0)a_R(0))$ can be removed from the fermion Hamiltonian by a gauge transformation $a_s(x) \to e^{i\sigma_s v_F^{-1} V_0 \Theta(x)} a_s(x)$. Noting that the field ϕ has much in common with a phase, we observe that the shift $\hat{\phi}(x) \to \hat{\phi}(x) + \frac{\pi c_1}{vg}\Theta(x)$ removes the operator $c_1\partial\hat{\phi}(0)$ from the bosonized Hamiltonian above[7]. We will thus ignore this operator and take

$$\boxed{\hat{H} = \frac{v}{2\pi}\int dx \left[g(\partial\hat{\phi})^2 + g^{-1}(\partial\hat{\theta})^2\right] + c\cos(2\hat{\theta}(0))} \tag{9.21}$$

as our effective Hamiltonian where we have re-labeled the scattering strength according to $c_2 \to c$.

Transition to the Field Integral Picture

Owing to the transcendental dependence on $\hat{\phi}(0)$, the model above is no longer amenable to exact solution. Nor, for reasons to become clear momentarily, is there a sensible perturbative solution to the problem. However, in the next section we will show how the role of the impurity can be explored by RG methods. To prepare this analysis, we should pass on from a Hamiltonian operator description of the problem to one in terms of a field integral[8]. Irritatingly, however, it is not at all clear at all how that functional integral might be obtained! Our previous constructions of field integrals for many body systems essentially relied on the availability of coherent state partitions of unity adjusted to properly normal ordered Hamiltonians. However, from our present discussion it is not evident how to normal order the Hamiltonian above[9], let alone how to find a suitable Fock space resolutions of unity.

In the problem set we will deal with this difficulty by constructing a (ϕ, θ)-formulation of the field integral 'from scratch', i.e. starting from the microscopic fermion action. However, for the moment, let us proceed pragmatically and simply *postulate* that a field

[7] Notice, however, that this transformation changes the boundary conditions of $\hat{\phi}$. In cases where the boundaries are of importance, e.g., for systems with the topology of a ring, the gauge transformation above is no longer innocuous, reflecting the fact that for these systems a local density perturbation causes a shift in the spectrum (exercise.)

[8] Which is not to say that Hamilton operators categorically disqualify as starting points for RG analyses.

[9] For that, we should first represent the fields $(\hat{\theta}, \hat{\phi})$ in terms of a boson algebra (along the lines of section 3.2.2 and than normal order the latter. (For details, see the aforementioned literature.)

integral exsitst of the standard form $\int \exp(-\text{action})$ exists. But what is the action of current system? According to general principles, the imaginary time action of a system with conjugate coordinates and momenta (q,p) is given by

$$S[q,p] = \int d\tau (p\partial_\tau q + H(p,q)).$$

Further, Eq. (9.18) tells us that the operators $\hat{\theta}$ and $\hat{\Pi} \equiv -\frac{i}{\pi}\partial\hat{\phi}$ are canonically conjugate, $[\hat{\Pi}(x), \hat{\theta}(x')] = \delta(x-x')$. We thus declare

$$S[\theta,\Pi] \equiv \int d^2x \left[\Pi\partial_\tau\theta + v\left(\frac{1}{2\pi g}(\partial_x\theta)^2 - \frac{\pi g}{2}\Pi^2\right) + c\cos(2\theta)\delta(x)\right]$$

to be the Hamiltonian action of the problem, where $\int d^2x \equiv \int dx \int d\tau$ is the integration over two-dimensional Euclidean space time. Now, the dependence of S on the momentum Π is quadratic which suggests to integrate over this field. Doing so, we arrive at the Lagrangian representation of the partition function,

$$\boxed{\begin{aligned} \mathcal{Z} &= \int \mathcal{D}\theta\, \exp(-S[\theta]), \\ S[\theta] &= \int d^2x \left[\frac{1}{2\pi g}\left(v(\partial_x\theta)^2 + \frac{1}{v}(\partial_\tau\theta)^2\right) + c\cos(2\theta)\delta(x)\right]. \end{aligned}} \tag{9.22}$$

What prevents us from solving the problem rigorously is the transcendental dependence of the action on $\phi(x=0,\tau)$. For all other values of x, the action is quadratic which suggests to integrate over all field amplitudes $\phi(x\neq 0,\tau)$ prior to addressing the $x=0$ action.

Integration Over the Modes $\theta(x\neq 0,\tau)$

Defining $\theta(0,\tau)\equiv\tilde{\theta}(\tau)$, the partition partition function can be written as

$$\mathcal{Z} = \int \mathcal{D}\tilde{\theta}\, \exp(-S[\tilde{\theta}]),$$

where

$$\exp(-S[\tilde{\theta}]) = \int \mathcal{D}\theta \left(\prod_\tau \delta(\tilde{\theta} - \theta(0,\tau))\right) \exp(-S[\theta])$$

is the action integrated over all field amplitudes save for $\theta(0,\tau)$ and $\prod_\tau \delta(\tilde{\theta}-\theta(0,\tau))$ is a product of δ-functions (one for each time slice) imposing the constraints $\theta(0,\tau)=\tilde{\theta}(\tau)$. We next represent each of these delta functions as $\delta(\tilde{\theta}-\theta(0,\tau)) = \frac{1}{2\pi}\int dk(\tau)\exp(ik(t)\tilde{\theta} - \theta(0,\tau))$ to obtain

$$\begin{aligned} \exp(-S[\tilde{\theta}]) &= \mathcal{N}\int \mathcal{D}\theta\mathcal{D}k \exp\left[-S[\theta] + i\int d\tau k(\tau)(\tilde{\theta}(\tau)-\theta(0,\tau))\right] = \\ &= \mathcal{N}\int \mathcal{D}\theta\mathcal{D}k \times \\ &\times \exp\left[-\int d^2x \left(\frac{1}{2\pi g}\left[v(\partial_x\theta)^2 + v^{-1}(\partial_\tau\theta)^2\right] + (c\cos(2\tilde{\theta}) + ik(\tilde{\theta}-\theta))\delta(x)\right)\right]. \end{aligned}$$

The advantage gained by this representation is that we can set $\cos(2\theta(0,\tau)) \to \cos(2\tilde{\theta}(\tau))$ whereupon the θ-dependence of the action becomes purely quadratic. To proceed, we switch to momentum space,

$$\exp(-S[\tilde{\theta}]) = \mathcal{N}\int \mathcal{D}\theta\mathcal{D}k \times$$
$$\times \exp\left[-\frac{T}{L}\sum_{q,\omega_n}\left[\frac{1}{2\pi g}\left(vq^2 + v^{-1}\omega_n^2\right)|\theta_{q,n}|^2 + ik_n\theta_{q,-n}\right] - ik_n\tilde{\theta}_{-n} + S_{\rm imp}[\tilde{\theta}]\right],$$

where $S_{\rm imp}[\tilde{\theta},k]$ impurity sector of the action, and integrate over θ:

$$\exp(-S[\tilde{\theta}]) = \mathcal{N}\int \mathcal{D}k \exp\left[-\frac{\pi g T}{2L}\sum_{q,\omega_n} k_n (vq^2 + v^{-1}\omega_n^2)^{-1} k_{-n} - ik_n\tilde{\theta}_{-n} + S_{\rm imp}[\tilde{\theta}]\right] =$$
$$= \mathcal{N}\int \mathcal{D}k \exp\left[-\frac{\pi T g}{4}\sum_{\omega_n} k_n|\omega_n|^{-1}k_{-n} - ik_n\tilde{\theta}_{-n} + S_{\rm imp}[\tilde{\theta}]\right] =$$
$$= \exp\left[-\frac{1}{\pi T g}\sum_n \tilde{\theta}_n|\omega_n|\tilde{\theta}_{-n} + S_{\rm imp}[\tilde{\theta}]\right].$$

Substitution of the explicit form of the impurity action leads to the final form of the now $(0+1)$-dimensional partition function

$$\boxed{\begin{aligned}\mathcal{Z} &= \int \mathcal{D}\tilde{\theta}\ \exp(-S[\tilde{\theta}]),\\ S[\tilde{\theta}] &= \frac{1}{\pi T g}\sum_n \tilde{\theta}_n|\omega_n|\tilde{\theta}_{-n} + c\int d\tau \cos(2\tilde{\theta}(\tau))\end{aligned}} \tag{9.23}$$

The entire effect of the bulk of the electron gas at $x \neq 0$ went into the first term. Owing to its non-analytic dependence on the frequency argument, the time representation of this operator is unpleasant and better be avoided.

▷ EXERCISE. Show that the Fourier transform of $|\omega_n|$ is given by

$$|\omega_n| \xrightarrow{\text{F.T.}} \frac{\pi T}{\sin^2(\pi T\tau)}.$$

Use this result to show that the time representation of the last operator in the effective action is given by the non-local expression

$$\frac{\pi T^2}{g}\int d\tau d\tau' \frac{\tilde{\theta}(\tau)\tilde{\theta}(\tau')}{\sin^2(\pi T(\tau-\tau'))}.$$

▷ INFO. However, the physical interpretation of this operator is straightforward enough. In the absence of the impurity, the system is described by a set of harmonic oscillators. We

can thus think of the degree of freedom $\theta(0,\tau)$ as the coordinate of a 'bead' embedded into an infinitely extended harmonic chain. From the point of view of this bead, the nighbouring degrees of freedom hamper its free kinetmatic motion, i.e. to move, the bead has to drag an entire 'string' of oscillators behind. In other words, a local excitation of the $x = 0$ oscillator will lead to **dissipation** of kinetic energy into the continuum of neighbouring oscillators. Clearly, the rate of dissipation will increase with both, the stiffness of the oscillator chain (g^{-1}) and the frequency of the excitation (ω_n), as described by the last operator in (9.23).

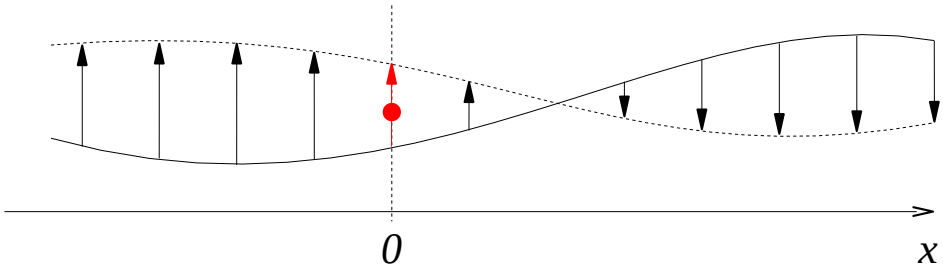

Figure 9.6: On the dissipative interpretation of the $|\omega_n|$-operator. Explanation, see text.

9.2.2 Renormalization Group Analysis

We now proceed to explore the physical behaviour of the system described by the effective action (9.23). To do so, we might decide on a physical observable of interest which would then be calculated by taking appropriate functional averages with respect to the effective action $S[\tilde{\theta}]$. However, presently, we shall proceed in a somewhat more indirect manner: what we are foremostly interested in is the influence of the impurity operator, as described by the second contribution to the effective action, on the long range behaviour of the model. Above we had speculated that a conspiracy of Friedel oscillations and interactions will lead to an effective enhancement of the scattering strength. If so, a recursive integration over short wavelength degrees of freedom should produce an effective or renormalized action for the longer ranged fluctuations with an enhanced impurity strength. A suspected mechanism of this type is tailor made for renormalization group analysis.

Following the general philosophy outlined in the beginning of the chapter, we begin by *arbitraily* subdividing the set of all fields $\{\theta\}$ into short and long wavelength degrees of freedom, respectively. E.g., assuming that the maximum frequency up to which the effective bosonic theory of the problem applies is given by Λ, we might say that fluctuations on scales $\Lambda/b < |\omega_n| < \Lambda$ are 'fast' ($b > 1$) while those with $|\omega_n| < \Lambda/b$ are 'slow'.

▷ INFO. Notice that this way to subdivide the integration degrees of freedom differs from what we did before. In the previous example, we carried out an RG transformation by integrating out field fluctuations on short scales in it real space, i.e. we performed some kind of **real space renormalization**. Here, we chose to integrate over a high-lying sector in frequency space. Alluding to the status of frequency as the $(d+1)$th component of a generalized momentum,

this way to implement the RG transformation is called **momentum shell renormalization**. While the previously discussed real space renormalization may be better accessible in intuitive terms, it is usually less convenient to carry out analytically[10]. It goes without saying that the net outcome of any RG strategy must not depend on the specific choice of the integration procedure.

Our first objective now is to explore how the effective action of the slow degrees of freedom looks like after the fast fluctuations have been integrated out. To prepare this integration, we exclicitly decompose a general field amplitude $\theta(\tau)$ according to

$$\begin{aligned}\theta(\tau) &\equiv \theta_s(\tau) + \theta_f(\tau),\\ \theta_s(\tau) &\equiv \sum_{n,s} e^{i\omega_n\tau}\theta_n \equiv \int_s d\omega\, e^{i\omega\tau}\theta(\omega),\\ \theta_f(\tau) &\equiv \sum_{n,f} e^{i\omega_n\tau}\theta_n \equiv \int_f d\omega\, e^{i\omega\tau}\theta(\omega),\end{aligned} \tag{9.24}$$

into a slow contribution $\theta_s(\tau)$ and its fast complementary $\theta_f(\tau)$ part. Here we have introduced the abbreviation $\sum_{n,s} \equiv \sum_{|\omega_n|<\Lambda/b}$ and $\sum_{n,f} \equiv \sum_{\Lambda_b\leq|\omega_n|<\Lambda}$. In the second part of the definition, anticipating that we shall be working at very low temperatures $T \ll \Lambda$, we represented the discrete frequency summations by integrals $\int_s d\omega \equiv \int_{|\omega|<\Lambda/b} d\omega$ and $\int_f d\omega \equiv \int_{\Lambda_b\leq|\omega|<\Lambda}$. (It is a good exercise to convince oneself of the legitimacy of this simplification at every step of the construction below.)

Substituting this decomposition into the continuum representation

$$S[\theta] = 2g\int_{|\omega|<\Lambda} d\omega\,\theta(\omega)|\omega|\theta(-\omega) + c\int d\tau\cos(2\theta(\tau)) \tag{9.25}$$

of the effective action (9.23), we obtain

$$\begin{aligned}S[\theta_s,\theta_f] &= S_s[\theta_s] + S_f[\theta_f] + S_{\rm imp}[\theta_s,\theta_f],\\ S_s[\theta_s] &= \frac{2}{g}\int_s d\omega\,\theta(\omega)|\omega|\theta(-\omega)\\ S_f[\theta_f] &= \frac{2}{g}\int_f d\omega\,\theta(\omega)|\omega|\theta(-\omega)\\ S_{\rm imp}[\theta_s,\theta_f] &= c\int d\tau\cos(2\theta_s(\tau)+2\theta_f(\tau)),\end{aligned}$$

i.e. an action that is just as complex as the original one. To proceed with this expression, we will resort to an approximation that is difficult to justify in advance. Defining

$$e^{-S_{\rm eff}[\theta_s]} \equiv e^{-S_s[\theta_s]}\int \mathcal{D}\theta_f\, e^{-S_f[\theta_s]-S_{\rm imp}[\theta_s,\theta_f]},$$

as well as $\langle\ldots\rangle_f \equiv \int\mathcal{D}\theta_f\, e^{-S_f[\theta_f]}(\ldots)$ and assuming that the coupling constant c is small, we approximate

$$e^{-S_{\rm eff}[\theta_s]} = e^{-S_s[\theta_s]}\left\langle e^{-S_{\rm imp}[\theta_s,\theta_f]}\right\rangle_f =$$

[10] As regards numerical renormalization procedures, the situation can be different.

$$= e^{-S_s[\theta_s]} \langle 1 - S_{\rm imp}[\theta_s, \theta_f] + \ldots \rangle_f \approx e^{-S_s[\theta_s]} e^{-\langle S_{\rm imp}[\theta_s,\theta_f]\rangle_f}. \qquad (9.26)$$

That is, assuming that the coupling constant c is in some sense small, we expand in c – which appears to be similar to our previous perturbative approaches – only to re-exponentiate it in the next step – a manipulation very different from plain perturbation theory. Evidently, the validity of this step is bound to small values of the coupling constant. However, before attempting a more qualified justification, let us tentatively accept the approximation above and explore its consequences.

We first compute the average

$$\begin{aligned}
\langle S_{\rm imp}[\theta_s,\theta_f]\rangle_f &= c \int \mathcal{D}\theta_f \, e^{-S_f[\theta_f]} \int d\tau \cos(2\theta_f(\tau) + 2\theta_s(\tau)) \\
&= \frac{c}{2} \int d\tau \, e^{2i\theta_s(\tau)} \int \mathcal{D}\theta_f \, e^{-\frac{2}{g}\int_f d\omega\, \theta(\omega)|\omega|\theta(-\omega)} e^{2i\int_f d\omega\, e^{i\omega\tau}\theta(\omega)} + \text{c.c.} = \\
&= \frac{c}{2} \int d\tau \, e^{2i\theta_s(\tau)} e^{-\frac{g}{2}\int_f d\omega\, |\omega|^{-1}} + \text{c.c.} = \\
&= c \int d\tau \, \cos(2\theta_s) e^{-g\int_{\Lambda/b}^{\Lambda} \frac{d\omega}{\omega}} = \\
&= c \int d\tau \, \cos(2\theta_s) e^{-g\ln(b)} = c b^{-g} \int d\tau \, \cos(2\theta_s).
\end{aligned}$$

We thus arrive at the remarkable conclusion that the effective action for the slow field

$$S_{\rm eff}[\theta_s] = \frac{2}{g} \int_s d\omega\, \theta(\omega)|\omega|\theta(-\omega) + c b^{-g} \int d\tau \, \cos(2\theta_s)$$

is structurally identical to the action we started out from; in other words, we have seen that the action is *renormalizable*. Nonetheless, the $S_{\rm eff}$ differs in two important points from the initial action S above: first, the integration over the fast fields led to a change of the coupling constant of the perturbation, second, the new action takes values on field configurations that fluctuate on scales $|\omega_n| < \Lambda/b$, only.

The next step of the RG program should be to *compare* the status of the model before and after the integration over the fast fields. However, two model actions taking values on different sets of field configurations cannot be sensibly compared. What we should rather do is *rescale* the fundamental unit of time/frequency such that after rescaling $(\tau, \omega) \to (\tau', \omega')$, the transformed field $\theta_s(\omega) \to \theta'(\omega')$, too, fluctuates on all scales $|\omega'| < \Lambda$. (Please think about this point!) We thus introduce a rescaled frequency variable according to

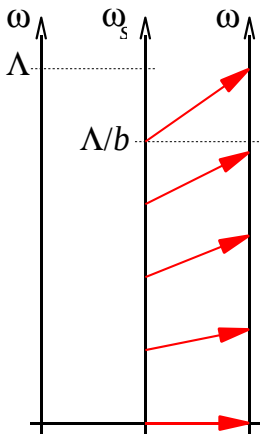

$$\omega' \equiv b\omega.$$

This change of variables entails a number of secondary transformations. In order to keep the dimensionless combination $\omega\tau$ relating time to frequency invariant, we set

$$\tau' \equiv b^{-1}\tau.$$

As for the transformation of the field variable θ, there is some freedom (because θ is an integration variable which can be transformed arbitrarily.) However, the Fourier representation Eq. (9.24) implies that after the transformation of $\theta(\tau)$, say, has been fixed, the transformation of $\theta(\omega)$ follows from our previous rescaling of frequency/time. In order to keep the algebraic structure of the cos-operator invariant, we chose to define $\theta'(\tau') \equiv \theta_s(\tau)$. Eq. (9.24) then enforces

$$\theta'(\omega') = b^{-1}\theta(\omega).$$

Substitution of the new variables $\omega', \tau', \theta'(\tau'), \theta'(\omega')$ into the effective action then obtains

$$S_{\rm eff}[\theta_s] = S'[\theta'] \equiv \frac{2}{g}\int_{|\omega'|<\Lambda} d\omega'\, \theta'(\omega')|\omega'|\theta(-\omega') + cb^{1-g}\int d\tau' \cos(2\theta'(\tau')),$$

Notice that the first contribution to the action remained invariant, save for the fact that the integration now extends over the full interval $|\omega'| < \Lambda$, as before the RG step.

▷ INFO. Notice that, without any calculation, the transformation of the action under the rescaling of variables could have been anticipatied from **dimensional analysis**: the definition $\omega' = b\omega$ implies that all contributions to the action of dimension [frequency]^d change by a factor b^{-d}. Since $\theta(\tau)$ is a dimensionless phase, we have $[\theta(\tau)] = 1$ while $[\theta(\omega)] = [\text{frequency}]^{-1}$. Thus, the first term of the action has dimension 1 and remains invariant. The second operator carries the dimension $[d\tau] = [\text{frequency}]^{-1}$ and, therefore, changes by a factor b.

———————————————————————

We are now in a position to compare the effective actions $S[\theta]$ and $S'[\theta']$ before and after the integration over the fast modes, respectively. Obviously, the principal effect of the integration over fast modes is that the coupling constant of the impurity operator changed according to

$$c \to c(b) \equiv cb^{1-g}. \tag{9.27}$$

(Do not forget, however, a point that is implicit in the notation: the new action describes fluctuations on slower frequency scales or larger temporal scales. That this difference is not manifest in the notation is due to the fact that we chose to measure the 'new' frequency continuum in rescaled variables $\omega' = b\omega$.)

This finding contains a preliminary answer to the question formulated above. To recapitulate, we asked how the presence of the impurity manifests itself in large scale transport properties of the system. What we have found is that an integration over short fluctuations of the collective field θ alters the effective strength of the impurity. This change is a manifestation of the mechanism sketched qualitatively above, viz. the mutual influence of the Friedel scattering pattern and interactions in the electron gas. Indeed, we observe that in the non-interacting case, i.e. for $g = 1$, (cf. Eq. (9.19)), the coupling constant does not change. For repulsive (attractive) interactions $g < 1$ ($g > 1$) the coupling increases (decreases) in accord with the qualitiative picture formulated above.

However, our so far result merely indicates how the coupling constant changes after one RG step, and this is clearly not the information we should be content with. Notably, Eq. (9.27) depends in a nonuniversal manner on how we chose to disect the frequency spectrum (the parameter b). However, ideally, we would like to know the value of the

coupling constant after all degrees of freedom down to a certain infrared cutoff scale $\omega_{\rm min}$ have been integrated out. (E.g., the role of $\omega_{\rm min}$ might be taken by temperature, the oscillation frequency of an external perturbation, etc.) The general route towards obtaining this information is to iterate the RG step, i.e. setting $c \equiv c^{(0)}$ and $c' \equiv c^{(1)}$, we explore the sequence of coupling constants $c^{(0)} \to c^{(1)} \to c^{(2)} \to \ldots$. For all what follows, it will be convenient to think of this sequence as some kind of dynamical system. In each discrete 'time step', the variable c changes according to $c \to c' = cb^{1-1/g} = ce^{\ln b(1-1/g)}$. Assuming that $b = 1 + \epsilon$ is very close to unity (which means that in each step only an asymptotically thin layer in frequency space is 'shaven off'), we can encapsulate this information in the differential equation

$$\frac{c' - c}{\epsilon} \approx \frac{dc}{d\epsilon} \approx \frac{dc}{d\ln b} = c(1-g).$$

In RG theory, the evolution equation describing the flow of the coupling constant under an infinitesimal change of the control parameter,

$$\boxed{\frac{dc}{d\ln b} \equiv \beta(c) = c(1-1/g)} \tag{9.28}$$

is known as a **Gell-Mann-Low equation**. For historical reasons, the right hand side of the equation is called the ***β*-function**.

Eq. (9.28) makes the interpretation of the RG generated change of the coupling constant as a dynamical system manifest. Thinking of the parameter $t \equiv \ln b$ as some 'time coordinate', we can integrate the evolution equation to obtain[11]

$$c(t) = c(0)e^{(1-g)t},$$

where $c(t=0) = c(b=1)$ has the status of the bare coupling constant of the theory. (Remember that for $b = 1$, $\Lambda_{\rm eff} = \Lambda/b = \Lambda$, which is the level of the unrenormalized theory.)

However, at which time $t_{\rm max}$ should we stop the renormalization flow? Or, what is the 'real' value of the coupling constant? The answer to these questions is somewhat application-specific. E.g., imagine we had coupled the system to an external perturbation of characteristic frequency ω_m. In that case, we might want to integrate out all degrees of freedom with frequency $\omega_{n>m}$ to then explore the effective low energy theory at scales $\sim \omega_m$. I.e., we would set $\Lambda_{\rm eff} = \omega_m$, or $t = \ln(\Lambda/\omega_m)$. The effective theory would then look structurally identical to the microscopic one with, however, a renormalized coupling constant $c = c(0)(\Lambda/\omega_m)^{1-g} \propto \omega_m^{g-1}$. (Notice that both the bare constant $c(0)$ and the cutoff Λ depend in a non-universal manner on microscopic elements of the model. The use of the proportionality sign indicates that we are not, in general, interested in these

[11] Critical readers will notice that this result coincides with the change of the coupling constant obtained after the first RG step. This coincidence, however, is a consequence of the simple structure of the β-function in the present example. In more complicated cases, the change of the coupling constant after an infinitesimal RG step will structurally different from the result obtained after following the RG flow all the way down to the IR cutoff. The concept of a β-function and its integration are therefore indispensable elements of the theory.

details but rather focus on the dependence of the coupling constant on the low energy scale ω_m.) Alternatively, we might want to integrate out all degrees of freedom down to the lowest frequency allowed by Matsubara frequency quantization, $\Lambda_{\rm eff} = 2\pi T$. In this case $c \propto T^{g-1}$. For a system of finite extent L, we might argue that the spectrum of the modes $\theta(k)$ is quantized with $\omega_{\rm min} = \pi v/L$. In this case, the effective value of the coupling at the lowest frequencies would be $c \propto L^{1-g}$. Summarizing, the RG flow should be terminated at a low energy scale determined by the specific problem under consideration.

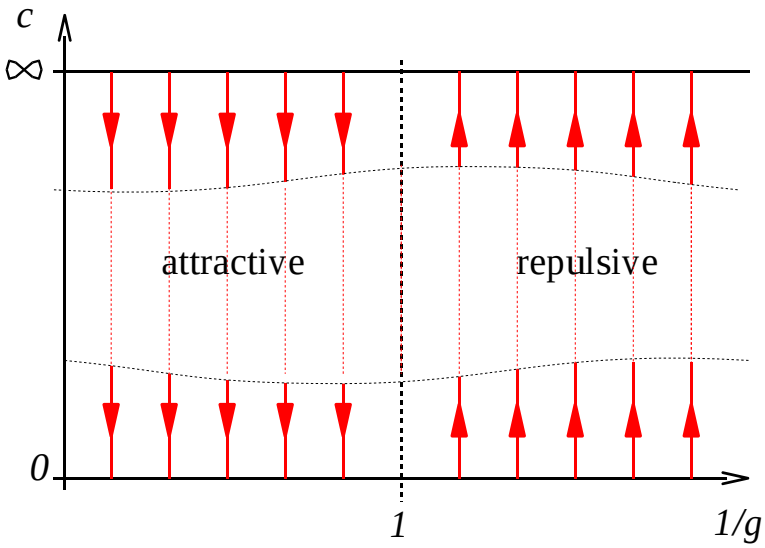

Figure 9.7: Flow of the coupling strength c of an impurity embedded into a quantum wire as a function of the interaction strength. The region of intermediate impurity strength is terra incognita as it is neither amenable to weak nor to strong coupling expansion schemes. The line $(g = 1, c)$ is a 'fixed line' where, due to the absence of interactions, the coupling strength does not change.

Our so far results on the behaviour of the coupling constant are summarized in the bottom part of Fig. 9.7. We found that for interaction parameters $g > 1$ ($g < 1$), the coupling strength decreases (increases). The noninteracting case $g = 1$ defines a fixed line where the coupling strength does not change. However, at this stage, at last, we must remember that the analysis was based on a spurious expansion of the action to first order in the impurity operator. This implies that in the repulsive case, even if the inital value of the coupling constant was small, it will soon flow into a region where the perturbative RG analysis loses its meaning (indicated by a wavy line in the figure.) How do we know what happens after the coupling constant has disappeared into the forbidden zone? Remarkably, it turns out that for the model (Luttinger liquid + impurity) not only the regime of weak impurity strength but also the complementary case of asymptotically large perturbations (the upper part of the figure) is amenable to analytical analysis. As a result of a strong coupling perturbative expansion (see the problem set) one finds that the coupling constant flows to (away from) infinite coupling for repulsive (attractive) interactions. It is thus tempting to conjecture a globaly increasing/decreasing flow continuously interpolating between the two asymptotic regimes. (Application of the machinery of conformal field

theory to the problem has indeed shown this conjecture to be true.)

▷ INFO. However, notwithstanding the limitation to small values of the coupling, we still have to discuss the **consistency of the fast field integration**, i.e. to show that the re-exponentiation of the impurity operator after the averaging over fast fluctuations (see Eq. (9.26)) underlying the previous analysis is legitimate; clearly, this step is not equivalent to a straightforward perturbative expansion. What we are effectively saying in Eq. (9.26) is that $\langle \exp(-S_{\rm imp})\rangle \approx \exp(-\langle S_{\rm imp}\rangle)$, i.e. that the functional average of the exponeniated action can effectively be replaced for the exponential of the averaged action. To explore the legitimacy of this claim, let us explore the relevance of a typical correction to this approximation. E.g. an expansion of the exponent to second order in the impurity operator would lead to expressions of the type

$$\left\langle c^2 \int d\tau d\tau' \, \cos(2\theta_s(\tau) + 2\theta_f(\tau)) \cos(2\theta_s(\tau') + 2\theta_f(\tau')) \right\rangle_c ,$$

where we use a connected average $\langle \hat{A}\hat{B}\rangle_c \equiv \langle \hat{A}\hat{B}\rangle - \langle \hat{A}\rangle\langle \hat{B}\rangle$ because the square of the averaged action $\sim \left(\langle c \int \cos(2\theta)\rangle\right)^2$ is already included in our previous scheme. At first sight, this expression looks worrysome. When averaged over the fast field θ_f we are bound to generate a composite operator that depends in a non-local manner on two time arguments τ and τ'. Re-exponentiation of *these* objects would lead to an action much more complicated than the original one.

However, before losing hope, let us have a closer look on the fast field average of the expression above. Representing the cos-functions as sum of exponentials, we are led to consider expressions of the type

$$\begin{aligned}
&\left\langle \exp\left[\pm 2i(\theta_s(\tau) + \theta_f(\tau))\right] \exp\left[\pm 2i(\theta_s(\tau') + \theta_f(\tau'))\right] \right\rangle_c \propto \\
&\quad \propto \left\langle \exp\left[2i \int_f d\omega \, \left(\pm e^{i\omega\tau} \pm e^{i\omega\tau'} \right) \theta(\omega) \right] \right\rangle - \left(\left\langle \exp\left[\pm 2i \int_f d\omega \, e^{i\omega\tau} \theta(\omega) \right] \right\rangle \right)^2 = \\
&\quad = \exp\left[-g \int_f d\omega \, |\omega|^{-1} \left(1 \pm \cos(\omega(\tau - \tau')) \right) \right] - \left(\exp\left[-\frac{g}{2} \int_f d\omega \, |\omega|^{-1} \right] \right)^2 = \\
&\quad = b^{-2g} \left(\exp\left[\mp g \int_{\Lambda/b}^{\Lambda} \frac{d\omega}{\omega} \cos(\omega(\tau - \tau')) \right] - 1 \right) \approx 0.
\end{aligned}$$

Here, the $\pm$-signs in the first line indicate the four different possible occurrences of signs, in the third equality we used our previous results on the integrals over the high lying frequency shell, and in the crucial fourth equality noticed we used that typically, $(\tau - \tau') > b/\Lambda, 1/\Lambda$, such that the oscillatory term integrates to something close to zero. can be neglected in comparison with the constant.

The estimate above is limited to time arguments $|\tau - \tau'|\Lambda/b > 1$ outside a narrow strip $|\tau - \tau'| \sim b/\Lambda$. To show that the contribution of composite operators from these domains, too, is negligible, we employ an argument that is symptomatic for RG analyses: consider the connected average

$$\begin{aligned}
&\left\langle c^2 \int_{|\tau-\tau'|<b/\Lambda} d\tau d\tau' \, \cos(2\theta_s(\tau) + 2\theta_f(\tau)) \cos(2\theta_s(\tau') + 2\theta_f(\tau')) \right\rangle_c \propto \\
&\qquad \propto b \int d\tau \;\; \left\langle \cos^2(2\theta_s(\tau)) + 2\theta_f(\tau)) \right\rangle_c =
\end{aligned}$$

$$\propto b^{-4g+1} \int d\tau \, \cos^2(2\theta_s(\tau)) + \text{const.}$$

where the notation highlights that the integration area is proportional to b and we used that for those narrow time windows, the field integration will be oblivious to the difference between $\theta(\tau)$ and $\theta(\tau')$. The third line is obtained by averaging the integrand along the lines of our previous calculations.

After the rescaling of time/and frequency to restore the old cutoff, the operator gets multiplied by another factor of b, i.e. the overall scaling factor is given by $b^{2(1-2g)}$. This factor tells us that the composite operator generated by higher order cumulative expansion of the action is of lesser **operator relevance** than the contributions we are keeping. For values of the interaction $g \approx 1$ not too distant from unity, the relative value of the coupling constants of the anomalous operator $\propto b^{2(1-2g)}$ and of the standard $\cos(2\theta)$ contribution, $\propto b^{1-g}$ respectively, will scale to 0 as b is increased. A classification of operators according to their relative relevance under the RG transformation indeed forms the general basis for the limitation of low energy actions to few contributions. Viz. those contributions that promise to be of strongest scaling relevance as larger and larger field fluctuations are probed. We will discuss this point more systematically in the next section.

Before leaving this section, let us make a few general observations on the renormalization procedure. We first notice that it would have been futile to attack the problem by the 'plain' perturbation theory developed in chapter 6. The reason is that the propagator of the $(0+1)$-dimensional effective theory, $|\omega|^{-1}$, leads to logarithmic divergences when integrated over unbound frequency intervals. I.e. the present theory is again plagued by the UV/IR divergences observed above in different other contexts. In section 6.1 we had argued that, in principle, a way to overcome these problems was to introduce an UV- and, if needed, an IR-cutoff into the theory. However, we soon dismissed this option because it seemed evident that it would lead to spurious non-universal cutoff dependences of physical results.

How do these observations relate to what we are doing presently. Obviosuly, the present[12] version of the RG proceedure, too, relies on the introduction of a cutoff regularizing the logarithmic UV divergences mentioned above; apparently, the RG procedure shares a lot of common structures with the perturbative approach. But somehow, we managed to extract the information we were interested in – the dependence of the impurity strength on long range system parameters – in a cutoff invariant manner[13]. The key to obtaining this information was to introduce not one, but an entire hierarchy of cutoffs and to integrate over each of these domains recursively.

[12] Below we will get acquainted with UV regurlarization proceedures which are not based on the introduction of a cutoff.

[13] One may object that the solutions of the β-functions given above actually *do* contain the bare cutoff through an initial condition; they also depend on the bare coupling strength, and, possibly, other 'non-universal' system parameters. However, that need not worry us: in most applications (both experimentally and theoretically) one is not so much interested in the 'absolute value' of physical observables (as these usually depend on unknown material parameters anyway) but rather in the way these observably *change* as a relevant control parameter is varied. The important feature found above is that the rate at which the effective impurity strength varies with temperature, say, is largely universal and cutoff independent.

Now, a subtle and important point is that this procedure does *not* imply that the cutoff or, more generally, short scale fluctuations of the model have silently made their way out of the theory. After all, the UV divergences mentioned before are manifestations of a large 'phase volume' of field fluctuations which are likely to somehow affect the system's behaviour. To understand the 'implicit' way through which these fluctuations enter our results, let us get back to a remark made on p 374. There, we had said that upon scaling time/frequency, each operator changes according to its physical dimension. I.e. an operator carrying the dimension $(\text{time})^d$ would pick up a scaling factor b^d. The scaling dimension of an operator predicted by its 'physical' dimension is called the **naive scaling dimension**, the **canonical scaling dimension**, or, for obscure reasons, the **engineering dimension**.

The denotations indicate, however, that these dimensions are not the last word on the actual scaling behaviour of an operator. Indeed, the net result of the RG analysis was that our operator of interest, $\int d\tau \cos(\phi)$, an object of engeneering dimension 1 changes according to b^{1-g}. The correction to the naive scaling dimension (presently, g) is called the **anomalous dimension** of an operator. It's origin lies in the (cutoff-dependent) phase volume of fluctuations co-determining the change of an operator during each RG step. Put differently, we can say that the cutoff Λ, by itself a quantity of dimension $(\text{time})^{-1}$ acts like a 'grey eminence' implicitly affecting the scaling behaviour of an operator. The anomalous scaling dimensions of the theory effectively determine its long range observable behaviour and, therefore, represent quantities of prime interest.

9.3 Renormalization Group: General Theory

Having discussed two extended examples, we are in a position to attempt a reasonably general outline of the RG strategy. Suppose then, we are given a field theory defined through the action

$$S[\phi] \equiv \sum_{a=1}^{N} g_a \mathcal{O}_a[\phi],$$

where ϕ is some (in general multi-component) field, g_a are coupling constants and $\mathcal{O}_a[\phi]$ certain operators. For concreteness, we may hink of these operators as

$$\mathcal{O}_a = \int d^d x (\partial\phi)^n \phi^m,$$

i.e. as space-time local operators involving powers of field and of its derivatives, although more general structures are conceivable[14] By 'renormalization of the theory', we refer to a scheme to derive a set of equations, so-called **Gell-Mann-Low equations**, describing the change of the coupling constants $\{g_a\}$ as flucutations of the theory are successively integrated out.

[14] E.g. in our previous example of the Luttinger liquid an operator $\int d\omega \theta(\omega)\theta(-\omega)|\omega|$ appeared. When represented in time space, this operator is highly non-local.

9.3.1 Gell-Mann-Low Equations

There are a number of methodological different procedures whereby the aforementioned set of flow equations can be obtained from the microscopic theory. We here formulate this step in a language adjusted to applications in statistical field theory (as opposed to particle physics, say.) While there is considerable freedom in the actual implementation of the RG procedure, all methods have in common that they proeceed in a sequence of three more or less canonical steps:

I: Subdivision of the Field Manifold

In a first step, we decompose the integration manifold $\{\phi\}$ into a sector to be integrated out, $\{\phi_f\}$, and a complementary set, $\{\phi_s\}$. E.g., we may

- ▷ proceed according to a generalized **block spin scheme** and integrate over all degrees of freedom located within a certain structural unit in the base manifold $\{\mathbf{x}\}$. (This scheme is adjusted to lattice problems where $\{\mathbf{x}\} = \{\mathbf{x}_i\}$ is a discrete set of points. However, as pointed out above, even then it is difficult to implement analytically. Alternatively, and more frequently,

- ▷ one decides to integrate over a certain sector in momentum space. When this sector is defined to be a shell $\Lambda/b \leq |\mathbf{p}| < \Lambda$, one speeks of a **momentum shell integration**. Naturally, within this scheme the theory will be explicitly cutoff dependent at intermediate stages. Alternatively,

- ▷ one may decide to integrate over *all* high-lying degrees of freedom $\lambda^{-1} \leq |\mathbf{p}|$. In this case, we will, of course, encounter divergent integrals. An elegant way to handle these divergences is to apply **dimensional regularization**. Referring for an introduction to this method to section XX below, we here merely mention that the idea is to formally generalize from integer dimensions d to generlized fractional dimensions $d \pm \epsilon$. One motivation for doing so (for another, see below) is that, miraculously, the formal extension of the characteristic integrals appearing during the RG step to non-integer dimensions are *finite*. As long as one stays clear of the dangerous values $d =$ integer one can then safely monitor the dependence of the integrals on the IR cutoff λ^{-1}.

- ▷ For a discussion of alternative schemes, such as the introduction of short distance *real space* cutoffs underlying the so-called **operator product expansion** we refer to the literature (see, e.g., the (excellent!) textbook [**?**].)

II: RG Step

The second, and central part of the program is to actually integrate over short range fluctuations. As exemplified above, this step usually involves approximations. In most cases, one will proceed by a so-called **loop expansion**, i.e. one organizes the integration over the fast field ϕ_f according to the number of independent momentum integrals – loops – that occur after the appropriate contractions (for the definition of loops, see 6.1. Of

course, this strategy makes sense only if we can guarantee that the contribution of loops of higher orders is in some sense small, a precondition that is, alas, often difficult to meet. At any rate, to qualifiedly explore the functioning loop numbers as an expansion parameter, we first need to understand the key role played by space-dimensionality in the present context. We will get back to this point in section 9.4.)

As a result of the integration one obtains an action

$$S'[\phi_s] \equiv \sum_a g'_a \mathcal{O}'_a[\phi_s],$$

with altered coupling constants, depending on the slow sector of the field. Notice that the integration over fast field fluctuations may actually lead to the generation of 'new' operators, i.e. operators that have not been present in the bare action. In such cases one has to investigate whether the newly generated operators are 'relevant' (see below) in their scaling behaviour. If so, the appropriate way to proceeed is to include these operators into the action from the very beginning (with an a priori undetermined coupling constant.) One then verifies whether the augmented action represents a complete system, i.e. one that does not lead to the generation of operators beyond those that are already present. If neccessary, one has to repeat this step until a closed system is obtained.

III: Rescaling

One next rescales frequency/momentum so that the rescaled field amplitude ϕ' fluctuates on the same scales as the originial field ϕ, i.e. one sets

$$q \to bq,$$
$$\omega \to b^z \omega.$$

Here, the **frequency renormalization exponent** z may be unity or equal to two, or for that matter to a non-integer value, depending on the effective dispersion relating frequency and momentum. We finally notice that the field ϕ itself is an integration variable which may be rescaled arbitrarily. Using this freedom, we select a term in the action which be believe governs the behaviour of the 'free' theory – in a theory with elastic coupling this might, e.g, be the leading order gradient operator $\sim \int d^d r \partial\phi\partial\phi$ – and require that it be *strictly* invariant under the RG step. To this end we designate a dimension L^{d_ϕ} to the field, chosen so as to compensate the factor b^x arising after the renormalization of the operator. The resaling

$$\phi \to b^{d_\phi}\phi,$$

is known as **field renormalization**. It renders the 'leading' operator in the action scale invariant.

As a result of all these manipulations, we obtain a renormalized action

$$S[\phi] = \sum_a g'_a \mathcal{O}_a[\phi]$$

which is entirely described by the set of changed coupling constants, i.e. the effect of the RG step is fully encapsulated in the mapping

$$\mathbf{g}' = \tilde{R}(\mathbf{g})$$

relating the old value of the vector of coupling constants $\mathbf{g} = \{g_a\}$ to the renormlized one $\mathbf{g}' = \{g_a'\}$. By letting the control parameter, $l \equiv \ln b$, of the RG step assume infinitesimal values, one can make the difference beween bare and renormalized coupling constants, respectively, arbitrarily small. It is then natural to express the difference $\mathbf{g}' - \mathbf{g} = \tilde{R}(\mathbf{g}) - \mathbf{g}$ in the form of a **generalized β-function** or **Gell-Mann-Low equation**

$$\boxed{\frac{d\mathbf{g}}{dl} = R(\mathbf{g}),} \tag{9.29}$$

where the rhs is defined through $R(\mathbf{g}) = \lim_{l\to 0} l^{-1}(\tilde{R}(\mathbf{g}) - \mathbf{g})$.

▷ INFO. As mentioned in the beginning of the section, the formulation of the RG step above is actually not the only one possible. For instance, in high energy physics, **other renormalization schemes** appear to be more natural. In this area of physics, there is actually no reason to believe in the existence of a well defined 'bare' action with finite coupling constants. (Contrary to the situation in condensed matter physics, the bare action of quantum electrodynamics, say, is principally inaccessible.) What we are legitimate to require, though, is that after an integration over UV divergent fluctuations, the 'renormalized' coupling constants of the theory (which in turn determine observables such as the physical electron mass.) are finite. One may then just the same *postulate* that the bare coupling constants of the theory are actually infinite. The value of these infinities is fine tuned so to combine with the fluctuation induced 'infinities' to finite renormalized coupling constants. Alternatively, one may deliberately add extra operators, so-called **counter terms**, to the action which are designed so as to cancel divergences due to fluctuations. However, the net result of all these RG schemes (which, as one can show, are by and large equivalent) is a mapping describing the flow of the coupling constants upon variation of a controll parameter.

9.3.2 Analysis of the Gell-Mann-Low Equations

The Gell-Mann-Low equation (9.29) represents the prinipal result of an RG analysis. Thinking of the control parameter l as some kind of 'time variable', we identify this equation as the descriptor of a generalized dynamical system, viz. the system describing the evolution of the effective coupling constants of a model upon chaning length or time scales. As with any other dynamical system, the prime structural characteristic of the set of equations (9.29) is the system of its **fixed points**, i.e. the submanifold $\{\mathbf{g}^*\}$ of points in coupling constant space which are stationary under the flow:

$$R(\mathbf{g}^*) = 0.$$

Once the coupling constants are fine tuned to a fixed point, the system no longer changes under subsequent RG transformations. In particular it remains invariant under the change of space/time scale associated to the transformation. Alluding to the fact that they look the same no matter how large a magnifying glass is used, systems with this property are referred to as **self similar**. (E.g. **fractals** such as the Julia set shown in Fig 9.8 are

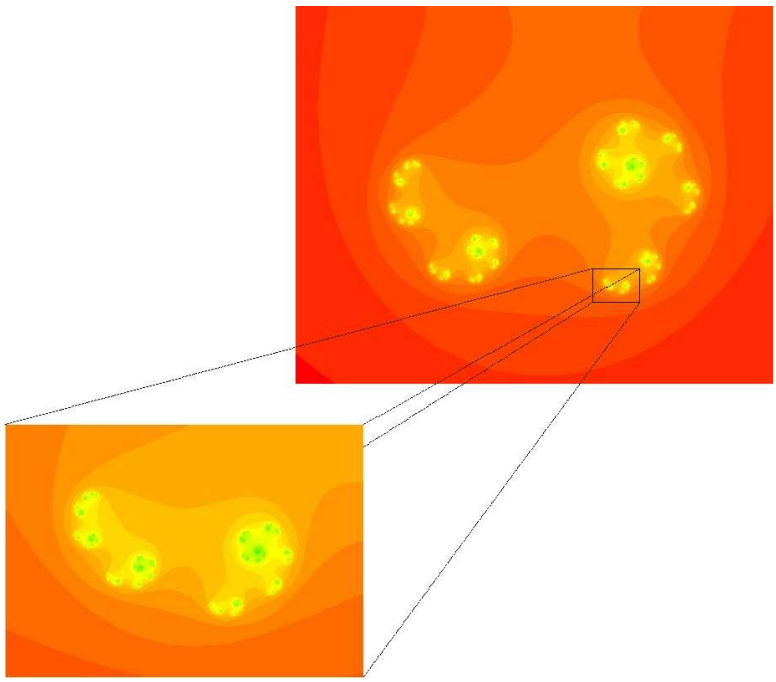

Figure 9.8: The fractal Julia set. The set is self similar in the sense that any of its sub-regions caontains the full information of the original set.

paradigmatic examples of self similar systems; the magnification of any sub-region of the fractal looks identical to the full system.) -

Now, to each system we can attribute at least one *intrinsic* length scale, viz. the length ξ determining the exponential decay of field correlations. However, the existence of a finite, and pre-determined intrinsic length scale clearly does not go together with invariance under scale transformations. We thus conclude that at a fixed point, either $\xi = 0$ (not so interesting), *or* $\xi = \infty$. However, a diverging correlation length $\xi \to \infty$ is a hallmark of a second order phase transition. We thus tentatively identify fixed points of the RG flow as candidates for transition points of the physical system. (For a more comprehensive review of phase transitions and the critcial phenomena accompanying them, see section XX below.)

This being so, it is natural to pay special attention to the behaviour of the flow in the immediate vicinity of the fixed point manifolds. If the set of coupling constants, $\mathbf{g}$, is sufficiently close to a fixed point, $\mathbf{g}^*$, it will be sufficient to consider the linearized mapping

$$R(\mathbf{g}) = R((\mathbf{g} - \mathbf{g}^*) + \mathbf{g}^*) \approx W(\mathbf{g} - \mathbf{g}^*),$$

where the matrix W is defined through

$$W_{ab} = \left.\frac{\partial R_a}{\partial g_b}\right|_{\mathbf{g}=\mathbf{g}^*}$$

To explore the properties of flow, we assume that we had managed to diagonalize the matrix W. Denoting the eigenvalues by $\lambda_\alpha, \alpha = 1, \ldots, N$, and the *left*-eigenvectors[15] by

[15] Since there is no reason for W being symmetric, the left- and right-eigenvectors may be different.

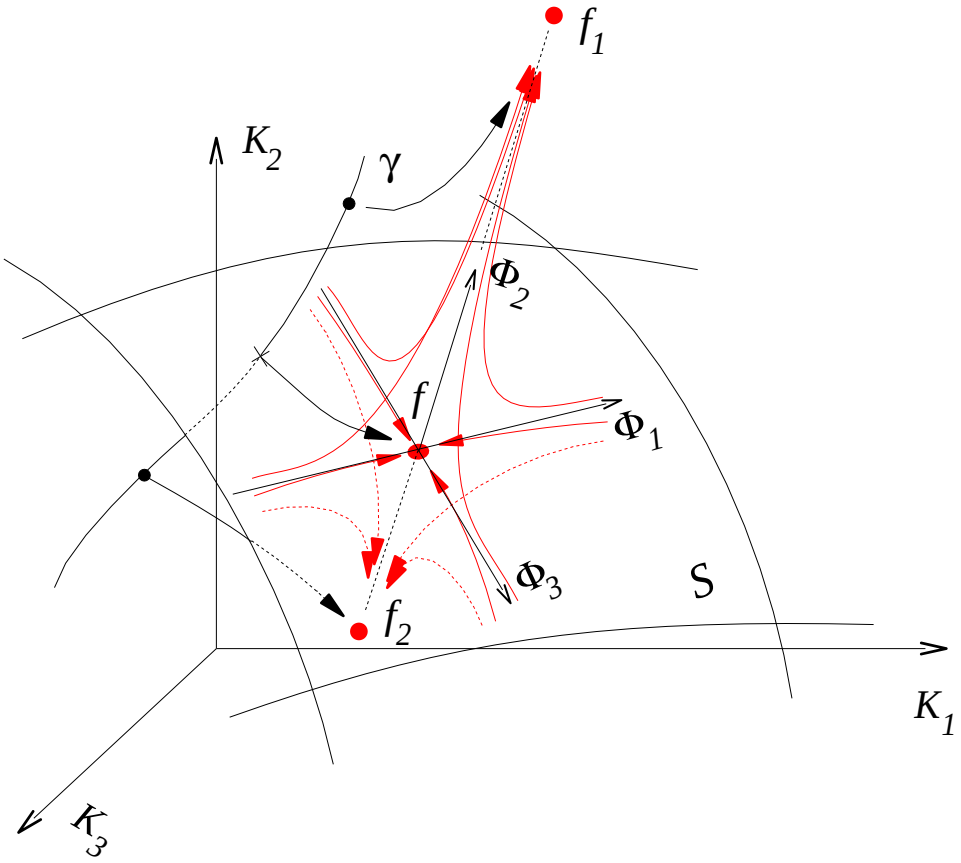

Figure 9.9: Qualitative visualization of the RG flow in the vicinity of a fixed point with two irrelevant (Φ_1, Φ_3) and one relevant (Φ_2) scaling fields. The manifold S defined through the vanishing of the relevant field, $\Phi_2 = 0$, is called a critical surface. On this submanifold, the RG flow is directed towards the fixed point f. Deviations off criticality make the system approach one of the stable fixed points f_1 or f_2.

$\boldsymbol{\phi}_\alpha$, we then have

$$\boldsymbol{\phi}_\alpha^T W = \lambda_\alpha \boldsymbol{\phi}_\alpha^T.$$

The advantage of proceeding via the unconventional set of left-eigenvectors is that it allows us to conveniently express the flow of the physical coupling constants under renormalization. To this end, let v_α be the αth component of the vector $\mathbf{g} - \mathbf{g}^*$ when represented in the basis $\{\boldsymbol{\phi}_\alpha\}$:

$$v_\alpha = \boldsymbol{\phi}_\alpha^T (\mathbf{g} - \mathbf{g}^*).$$

These components display a particularly simple behaviour under renormalization:

$$d_l v_\alpha = \boldsymbol{\phi}_\alpha^T \, d_l(\mathbf{g} - \mathbf{g}^*) = \boldsymbol{\phi}_\alpha^T \, W(\mathbf{g} - \mathbf{g}^*) = \lambda_\alpha \boldsymbol{\phi}_\alpha^T \, (\mathbf{g} - \mathbf{g}^*) = \lambda_\alpha v_\alpha.$$

Under renormalization, the coefficients v_α change by a mere scaling factor λ_α, wherefore they are called **scaling fields** (which is somewhat unfortunate nomenclature. The coefficients v_α actually aren't fields but simply a set of l-dependent *coefficients*. Namely the

coefficients of the vector of coupling constants when expressed in the basis of eigenvectors $\boldsymbol{\phi}_\alpha$.) These equations are trivially integrated to

$$\boxed{v_\alpha(l) \sim \exp(l\lambda_\alpha).} \tag{9.30}$$

This result suggests to discriminate between at least three different types of scaling fields:

- ▷ For $\lambda_\alpha > 0$ the flow is directed away from the critical point. The associated scaling field is said to be **relevant** (in the sense that it forcefully drives the system away from the critical region.) In Fig. 9.9, v_2 is a relevant scaling field.
- ▷ In the complementary case, $\lambda_\alpha < 0$, the flow is attracted by the fixed point. Scaling fields with this property (v_1, v_3) are said to be **irrelevant**.
- ▷ Finally, scaling fields which are invariant under the flow, $\lambda_\alpha = 0$, are called **marginal**[16].

The distinction of relevant/irrelevant/marginal scaling fields in turn implies a classification of different types of fixed points:

- ▷ For one thing, there are **stable fixed points**, i.e. fixed points whose scaling fields are all irrelevant or, at worst, marginal. These points define what we might call 'stable phases of matter': when you release a system somewhere in the parameter space sourrounding any of these attractors, it will scale towards the fixed point and eventually sit there. Or, expressed in more physical terms, looking at the problem at larger and larger scales will make it more and more resemble the infinitely correlated self-similar fixed point configuration. (Remember, e.g., the example of the high temperature fixed (line) of the $1d$-Ising model met previously.) By construction the fixed point is inert against moderate variations in the microscopic morphology of the system, i.e. it genuinely represents what one might call a 'state of matter'. Often, but not always, stable fixed points correspond to the phase of asymptotically low ($\xi \to \infty$, the system is in an ordered state) or high ($\xi \to 0$, the system is maxmially disordered) temperature. (Arguably, heating or cooling a system indefinitely, introduces a certain element of stability, towards formation of either an ordered or an entropic configuration.)
- ▷ Complementary to stable fixed points, there are **unstable fixed points**. All scaling fields are relevant. (Cf. the $T = 0$ fixed point of the $1d$ Ising model.) These fixed points represent the concept of a Platonic ideal: you can never get there and even if you managed to approach it closely, the harsh conditions of reality will make you to flow away from it. Although unstable fixed points do not correspond to realizable form of matter they are of importance in as much as they 'orient' the global RG flow of the system.

[16] A marginal scaling field corresponds to a direction in coupling constant space with vanishing partial derivative, $\partial_{\phi_\alpha} R\big|_{\mathbf{g}^*=0} = 0$. In this case, to obtain a refined picture, one sometimes considers the second order derivative, $\partial^2_{\phi_\alpha} R\big|_{\mathbf{g}^*=0} \equiv 2x$. In the vicinity of the fixed point, the scaling field then behaves as $d_l v_\alpha = x v_\alpha^2$. For $x > 0$ ($x < 0$) the field has the status of a **marginially relevant (irrelevant)** scaling field. It relevant (irrelevant) on account of the non-vanishing direction of the flow. However, it is also 'marginal' because the speed of the flow decreases upon approaching the critical regime.

▷ Finally, there is the **generic class of fixed points** with both relevant and irrelevant scaling fields. These point are of particular interest in as much as they can be associated to **phase transitions.** To understand this point, we first note that the r, $0 < r < N$ eigenvectors Φ_α associated to irrelevant scaling fields span the tangent space of an $N - r$ dimensional manifold known as the **critical surface** (or **critical line** if $r = 1$. For an illustration for the case $r = 2$, see Fig. 9.9.) This critical manifold forms the bassin of attraction of the fixed point. I.e whenever a set of physical coupling constants $\mathbf{g}$ is fine tuned so that $\mathbf{g} \in S$, the expansion in terms of scaling fields *only* contains irrelevant contributions and the system will feel attracted to the fixed point as if it were a stable one.

However, an ever so slight deviation away from the critical surface introduces a relevant component driving the system exponentially away from the fixed point. A sketch of the resulting flow is shown in Fig. 9.9 for the case of just one relevant scaling field. E.g. for the case of the ferromagnetic phase transition – to be discussed in more detail in the next section – deviations from the critical temperature T_c are relevant. If we consider a system only slightly above or below T_c, it may initially (on intermediate length scales) appear to be critical. However upon further increasing the scale, the relevant deviation will become virulent and drive the system away from criticality, either towards the stable high temperature fixed point of the paramagnetic phase ($T > T_c$) or towards the ferromagnetic low temperature phase ($T < T_c$).

This picture actually suggests that systems with generic fixed points typically possess complementary stable fixed points, i.e. fixed points towards which the flow directs after it has left the critical region. We also notice that a scaling direction that is relevant at one fixed point (e.g. Φ_2 at the critical fixed point) may be irrelevant at others (Φ_2 at the high and low temperature fixed point.)

▷ INFO. The discussion above suggests that the concept of renormalization is intimately linked to the **theory of phase transitions and critical phenomena.** Indeed, the majority of textbooks on the subject – of which there are by now quite a few[**?**, **?**] – mostly carry titles as 'Phase transitions and the renormalization group', or the like. Which correctly indicates that these two concepts are related like siamese twins. Now, in view of the fundus of available excellent literature (and of the fact that we are approaching the field from a more operational, perspective) we shall not attempt yet another 'introduction to critical phenomena' here. Rather, we will summarize in a concise, but hopefully self contained manner those few facts of the theory of criticality that are absolutely necessary to put the concept of renormalization into a larger physical context:

The most fundamental[17] descriptor of a transition between is its **order parameter**, M, i.e. a quantity whose value unambiguosly identifies in which phase we are in. Classical examples include the magnetization for the ferromagnetic-paramagnetic transition, the density for the liquid-vapour transition, the order parameter amplitude for the BCS transition, etc. (However, to keep the nomenclature definite, we shall mostly use the language of the ferromagnetic transition in the following.)

[17] But notice, that there are transitions whose order parameter is actually *unknown*. A famous example is the **quantum Hall transition**, to be discussed in more detail in chapter XX

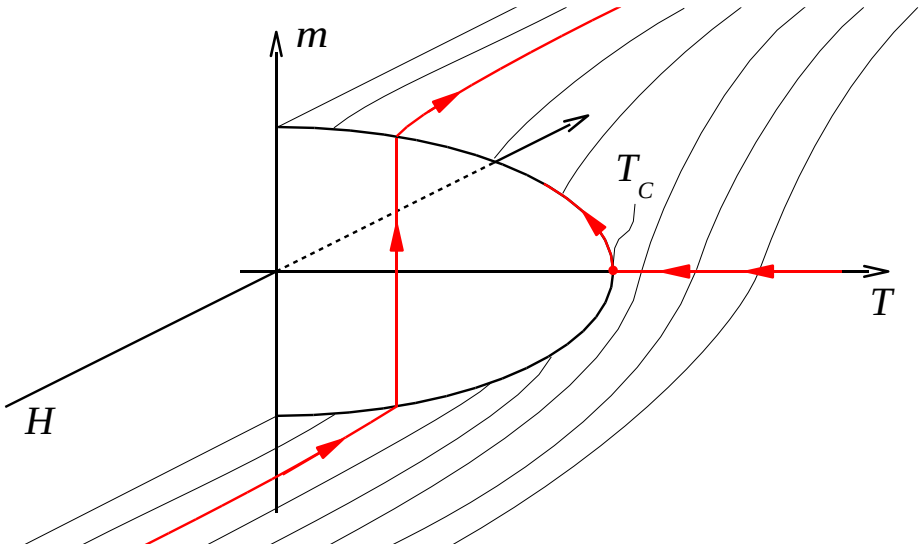

Figure 9.10: Phase diagram of the ferromagnetic transition. Tuning a magnetic field at fixed temperature $T < T_c$ below the magnetization temperature, T_c, through zero causes the magnetization to jump: $[0, T_c]$ is a line of *first* order transitions. This line terminates in the unique second order transition point of the system, $(T = T_c, H = 0)$: lowering temperature at $H = 0$ from large values down to T_c causes a non-analyitic but continuous onset of a finite magnetization.

Now, let us recapitulate[18] that transitions between different phases of matter fall into two large categories: **first order phase transitions**, defined by the fact that the order parameter exhibits a discontinuous jump across the transition line, and the complementary class of **second order transitions**, where the order parameter changes in a non-analytic but continuous manner. (The two cases are exemplified in Fig. 9.10 for the case of a ferromagnetic substance.)

The physics of second order transitions is generally more interesting that that of first order transitions. To substantiate this claim, we note that, as a thermodynamic state variable, the order parameter is coupled to a **conjugate field**, H: $M = -\partial_H F$, where F is the free energy. At a second order transition, M changes non-analytically which means that the second order derivative, a **thermodynamic susceptibility**, $\chi = -\partial_H^2 F$ develops a singularity. We now recapitulate that – the flucutation dissipation theorem – the susceptibility is intimately linked to the field flucutation behaviour of the system. More precisely, χ is proporitional to the integral over the correlation function C determining the fluctuation behaviour of the fields (cf. Eq. (9.3).) A divergence of the susceptibility implies the buildup of infinitely long ranged field fluctuations – interesting physics.

The divergence of the susceptibility goes along with non-analytic and/or singular behaviour of all sorts of other physical quantities. In fact, an even stronger statement can be made. We have seen that right at the transition/fixed point the system is self similar. This implies that the behaviour of its various characteristics must be described by *power laws*. Referring for a more substantial discussion to section 9.3.3 below, we here merely support this statement by a heuristic argument. Consider a function $f(t)$, where f is representative for an observable of interest and t for a control parameter (a scaling field) determining the distance to the transition

[18] Readers abosulutely unfamiliar with the thermodynamics of phase transitions may wish to consult the corresponding section of a textbook on statistical mechanics.

point. In the immediate vicinity of the transition point, f is expected to *scale*, i.e. under a change of the length scale $x \to x/b$, $t \to tb^{D_t}$, the function f must, at most, change by a factor reflecting its own scaling dimension. $f(t) = b^{D_f} f(tb^{D_t})$. (A more serious, structural change of the function would be at conflict with asymptotic self similarity.) Mathematically, speaking, this equation amounts to *homogeneity* of the function f, equivalently expressed by $f \sim t^{-D_f/D_t}$.

The set of different exponents characterizing the relevant powerlaws occuring in the vicinity of the transition are known as **critical exponents**. For at least four different reasons, the set of critical exponents reprensents *the* most important structural fingerprint of a transition:

1. They carry universal significance, i.e. we do not have to invent a set of critical exponents for each transition anew. (E.g. the divergence of the correlation length, $\xi \sim |t|^{-\nu}$ is characterized by a critical exponent commonly, and irrespective of the particular transition under consideration denoted by ν.)

2. The set of critical exponents carries the same information as the set of exponents of the scaling fields, i.e. knowledge of the critical exponents is equivalent ot the knowledge of the linear dynamical system characterizing the flow in the transition region. (In fact, the set of critical exponents *over*determines the scaling field exponents, i.e. it contains redundancy. E.g., of the six critical exponents characterizing the magnetic transition only two are independent. The others are inter-related by so-called[19] **scaling laws** to be discussed below.

3. Critical exponents are fully universal; they are numbers.

4. Perhaps most importantly, the critical exponents represent quantities that can be measured. In fact, their universality and structural importance makes them quantities of prime experimental interest.

In the following we briefly go through the list of the most relevant exponents, $\alpha, \beta, \gamma, \delta, \eta, \nu, \eta, z$[20]. Although we shall again use the language of the magnetic transition it is clear that, and how, the definition of most exponents readily generalizes to other systems.

α : In the vicinity of the critical temperature, the **specific heat**

$$C = -T^2 \partial_T^2 F$$

scales as $C \sim |t|^{\alpha}$, where t measures the distance to the critical point. Note that by virtue of this definition a non-trivial statement is made: although the phases above and below the transition are essentially different, the scaling exponents controlling the behaviour of C are identical. The same applies to all other exponents listed below.

β : Approaching the transition temperature from below, the **magnetisation** vanishes as $M \equiv -\partial_H F|_{H \searrow 0} \sim (-t)^{\beta}$.

γ : The **magnetic susceptibility** behaves as $\chi \equiv \partial_h M|_{h \searrow 0} \sim |t|^{\gamma}$.

[19] Unfortunately, the language used in the field of critical phenomena makes over-excessive use of the prefix 'scaling-'.

[20] Historically, and in complete lack of imagination, the exponents have been designated by a bunch of six early letters of the greek alphabet. The exceptional designation of the last exponent, z, indicates that it is of newer date.

δ : At the critical temperature, $t = 0$, the **field dependence of the magnetisation** is given by $M \sim |h|^{1/\delta}$.

ν : Upon approaching the transition point, the **correlation length** diverges as $\xi \sim |t|^{-\nu}$,

η : which implies that the correlation function

$$C(r) \sim r^{-(d-2+\eta)} \exp(-r/\xi)$$

crosses over to power law scaling. To understand the definition of the power law, notice that $C \sim \langle\phi\phi\rangle$ carries twice the dimension of the field ϕ. The engeneering dimension of the latter follows from the requirement that the gradient operator $\sim \int d^d r \partial\phi\partial\phi$ be dimensionless: $[\phi] = L^{(2-d)/2}$, according to which $C(r)$ has canonical dimension L^{2-d}. The exponent η, commonly called the **anonmalous dimension** of the correlation function measures the mismatch between the observed and the canononical dimension, respectively.

z : A quantum theory can be looked at as some kind of classical theory in $d+1$ dimensions. The theory is 'quantum critical' if the effective classical theory contains a critical point. In the vicinty of that point large fluctuations are observed in both the d spatial directions and the temporal 'direction'. However, the different physical origin of these dimensions manifests itself in the scaling being anisotropic. Denoting the correlation length in temporal direction by τ, we define $\tau \sim \xi^z$, where deviations $z \neq 1$ in the **dynamical exponent** measure the degree of anisotropy.

Now, a moments thought shows that of the six classical exponents only a few can be really independent: above we had said that, modulo irrelevant perturbations, the flow in the vicinity of a transition point is controlled by the relevant scaling fields. Referring for a more quantitative discussion to section XX below, we anticipate that for the magnetic transition, the magnetic field will certainly represent a relevant perturbation (a fact readily expressed by he positivity of the exponent δ.) Also, deviations from the critical temperature, $t \neq 0$, are relevant[21]. However, that's it; in the asymptotic vicinity of the transition, the flow is controlled by a 2-dimensional dynamical system. Which suggests that four constraining equations should reduce the set of six classical exponents to only two independent exponents. Historically, these equations, the aforementioned **scaling laws**, were discovered one-by-one (at a time when the underlying connections to the system of 'scaling fields' had not yet been known.) For the sake of reference, these constraint equations (along with the name of the people who discovered them) are listed below. In section 9.3.3 below we will then exemplify how the scaling laws can be transparently derived from the intrinsic structure of the theory.

Fisher	$\nu(2-\eta) = \gamma$
Rushbrooke	$\alpha + 2\beta + \gamma = 2$
Widom	$\beta(1-\delta) = \gamma$
Josephson	$2 - \alpha = \nu d$

The practical importance of this table lies in the fact that we need to compute/measure only two exponents – no matter which – to completely nail down the scaling structure of the theory.

---

[21] If you find it difficult to think of temperature as a 'coupling constant', remember that in our derivation of the ϕ^4-model as the relevant theory of the magnetic transition the coupling constant of the 'mass operator' $r \int d^d r\, \phi^2$ turned out to be proportional to $t = |T - T_c|/T_c$.

In the next section we will see that the dynamical system of the scaling fields encapsulates practically all information on the 'critical' fluctuation phenomena accompanying a phase transition. However, for the moment we shall restrict ourselves to the discussion of one more aspect of conceptual importance, viz. **universality**. The point is that there are actually not so many fundamentally different **universality classes** of different critical systems. (I.e. different dynamical systems of scaling fields.) Roughly speaking, and leaving more esotheric classes of phase transitions appart, $\mathcal{O}(10^1)$ fundamentally different types of flows reccurantly appear in practical applicatations. This has to be compared to the $\mathcal{O}(10^?)$ different physical systems that display second order phase transitions. The important statement made here is that the plethora of all these transitions can be grouped into a very limited set of different universality classes. Remarkably, the origin of this universality can readily be understood from the concept of critical surfaces:

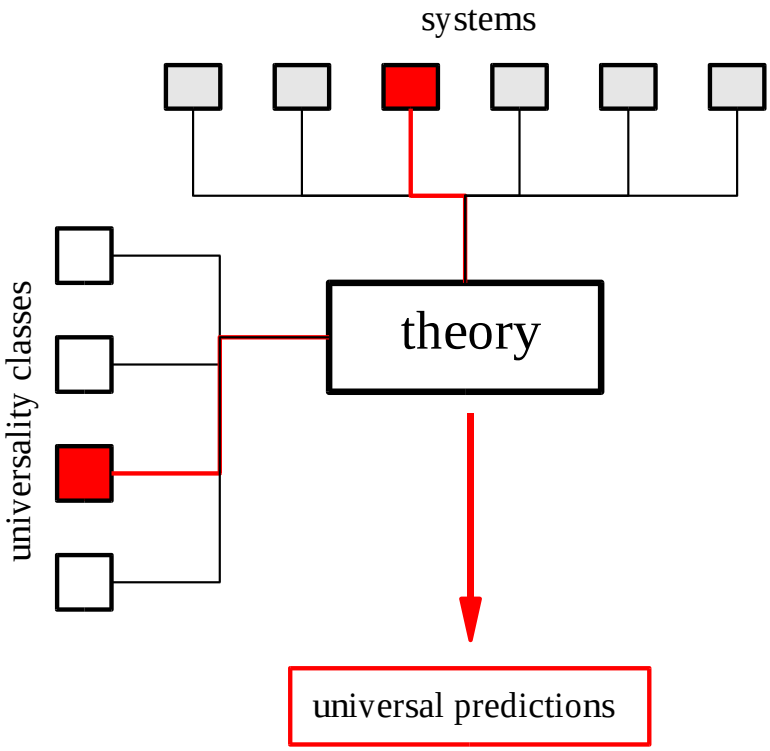

Figure 9.11: On the universality of phase transition behaviour. To each microscopic system (upper part) we have to assign a universality class (right). However, since there is only a very limited set of different universality classes, while the number of systems is quasi-inifinite, different systems must exhibit identical transition behaviour. Further discussion, see text.

Imagine then, an experimentalist exploring a system that is known to exhibit a phase transition. As she must be keen to observe critical behaviour, available control parameters X_i (temperature, pressure, magnetic field, etc.) will be varied until the system begins to exhibit large fluctuations. On a theoretical level, the variation of the control parameters determines the initial values of the coupling constants of the model (as they functionally depend on the X_i's through their connection to the microscopic system Hamiltonian.)

In Fig. 9.9 the curve in coupling constant space defined in this way is indicated by γ. For system parameters corresponding to point above or below the critical manifold, the system asymptotically (i.e. when looked at at sufficiently large scales) falls either into the high or the low temperature regime (as indicated by the curves branching out from γ in Fig. 9.9.) However, eventually the parameter trajectory will meet the critical surface. For this particular value of the coupling constants, the system is critical. As we look at it on larger and larger length scales, it will be attracted by the fixed point sitting on S, i.e. it will display the universal behaviour characteristic for this particular point. This is the origin of universality: variation of the system parameters in a different manner (or for that matter considering a second system with different material constants) will generate a different trajectory $g_\alpha(\{X_i\}) = \gamma'$. However as long as the this trajectory intersects with S, it is guaranteed that critical behaviour of the same universal properties (viz. controlled by the unique fixed point) will be observed.

In fact a more farreaching statement can be made. Given that there is an infinity of systems exhibiting transition behaviour (symbolically indicated by the row of boxes in the upper part of Fig. 9.11) while there is only a very limited set of universality classes (the set of boxes on the left), many systems of *very* different microscopic morphology must share the same universal behaviour. More formally, different microscopic systems must map onto the same critical low energy theory. To illustrate the amazing consequences on just one example: it turns out (see the problem set) that the scaling behaviour discussed earlier in connection with the disordered Luttinger liquid, is also observed for a superconductor Josephson junction, i.e. a system of very different microscopic origin. Further coincidences of this type will be encountered below.

9.3.3 Scaling Theory

Above we have seen that the dynamical system of scaling fields encodes a wealth of information on the large scale structure and on the phases of a physical system. However, we have not yet established a connection between the concept of renormalization and *concrete*, i.e. exprimentally accessible data. This will be the subject of the present section.

Imagine then, we had represented some observable of experimental interest, X, in terms of the language of the functional integral. According to the discussion of the previous chapter this means that we have managed to express

$$X = \sum_{\mathbf{p}} C(p_i, g_\alpha),$$

as the sum over an n-point correlation function $C(p_i, g_\alpha) = \langle(\ldots)\phi\phi\ldots\phi\rangle_\phi$, where the (highly symbolic) notation indicates that C may depend on both the momentum scale at which it is evaluated (e.g. through the explicit momentum dependence of current operators, etc.) and on the coupling constants. The ellipses $(\ldots)$ stand for optional algebraic elements entering the definition of the correlation function.

We next build on our assumption of renormalizability of the theory, i.e. we use that we can evaluate C before or after an RG step, the result must be the same. On the other hand, the RG transformation will, of course, not leave the individual constituents entering

the definition of C invariant; it will change coupling consants, g_α, the momenta p_i, and the field amplitudes ϕ according to the prescriptions formulated in the previous section. Expressed in a single formula,

$$\boxed{C(p_i, g_\alpha) = b^{nd_\phi} C(p_i b, g_\alpha b^{\lambda_\alpha}),} \tag{9.31}$$

where we have simplified the notation by assuming that the coupling constants themselves scale. (Otherwise, the matrix elements of a linear transformation mediating between the coupling constants and the scaling fields would appear.) For notational convenience we also assume that the fixed point value of the coupling constants, $\mathbf{g}^* = 0$. The factor L^{nd_ϕ} accounts for the explicit rescaling of the n fields entering the definition of C.

Notice that Eq. (9.31) actually represents a very remarkable statement: although the three different elements (ϕ, p_i, g_α) contributing to the correlation function change under the transformation in a seemingly unrelated manner, the net result of the concerted rescaling is nil. Indeed, Eq. (9.31) serves as a starting point for the derivation of various relations of immediate practical relevance.

Scaling Functions

We get back to a principle already used in connection with the $1d$-Ising model. For concreteness, imagine that we are working under conditions where there is just a single relevant scaling field g_1, while all $g_{\alpha>1}$ are irrelevant (or marginal for that matter). We can then write

$$\begin{aligned} C(p_i, g_1, g_\alpha) &= b^{nd_\phi} C(p_i b, g_1 b^{\lambda_1}, g_\alpha b^{\lambda_\alpha}) = \\ &= g_1^{-nd_\phi/\lambda_1} C(p_i g_1^{-1/\lambda_1}, 1, g_\alpha g_1^{-\lambda_\alpha/\lambda_1}) \overset{g_1 \ll 1}{\approx} \\ &\overset{g_1 \ll 1}{\approx} g_1^{-nd_\phi/\lambda_1} C(p_i g_1^{-1/\lambda_1}, 1, 0) \equiv g_1^{-nd_\phi/\lambda_1} F(p_i g_1^{-1/\lambda_1}). \end{aligned}$$

Here, we have used the freedom of arbitrarily chosing the parameter b to set $g_1 b^{\lambda_1} = 1$. In the third equality we assumed that we are sufficiently close to the transition that the dependence of C on irrelevant scaling fields is inessential. The function F defined through

$$C(p_i, g_1) = g_1^{-nd_\phi/\lambda_1} F(p_i g_1^{-1/\lambda_1}) \tag{9.32}$$

is an example of a **scaling function**. Alternatively (e.g., if C represents a thermodynamic observable or a global transport coefficient) we might be interested in the correlation function $C(g_1, g_\alpha) \equiv C(p_i = 0, g_1, g_\alpha)$ at zero external momentum $p_i = 0$. In this case, a typical question to ask would be for the dependence of C on the most relevant, *and* the second most relevant control parameter g_2 (where we leave unspecified whether g_2 is relevant, marginal or irrelavant.) Following the same logics as above, we obtain

$$C(g_1, g_2) = g_1^{-nd_\phi/\lambda_1} \tilde{F}(g_2 g_1^{-\lambda_2/\lambda_1}),$$

with some different scaling function $\tilde{F}$.

▷ INFO. As an example particularly relevant to the comparison between analytical theory and numerics we mention the concept of **finite size scaling.** While analytical theories are most

conveniently formulated in the thermodynamic limit, numerical simulations are carried out for systems of still very limited size. (Typical system sizes are $\mathcal{O}(100-1000)$ for non-interacting models and $\mathcal{O}(10)$ for interacting models.) The need to compare between theory and numerical simulations motivates to explicitly keep track of the system size under renormalization. Indeed, the system size L has dimension [length][1] and, therefore, gets resaled as $L \to L/b$. Setting $L/b = 1$, we obtain a scaling function

$$G(g_\alpha, L) = L^{nd_\phi} F_{\rm fs}(g_\alpha L^{\lambda_\alpha}),$$

with explicit system size dependence.

While the construction of any particular scaling function may be context-dependent the principle behind the derivation is general: once the scaling behaviour of a correlation function is known, the arbitrariness of the scaling parameter b can be used to reduce the number of independent variables by one. The reduced correlation function is called a scaling function.

As with the response functions discussed in the previous chapter, scaling functions, too, represent a prime **interface between theory and experiment**. Experimentally, the measurement of an observable X in dependence on a number of relevant system parameters, t and h, say, results in a multi-parameter function $X(t,h)$. In fact, a better way to think about this object is as a *set* of one-dimensional functions $X_h(t)$ depending on a parameter h. (This is because in experiment one typically varies only a single control parameter, e.g. temperature at fixed magnetic field.) Scaling implies that all these functions collaps onto a generic one-dimensional[22] profile, if only the data is plotted as a function of the relevant scaling parameter th^x.

This mechanism can be made useful in several different ways. E.g., if there is not yet a theory of the transition phenomenon in question, the experimentalists may empirically identify the relevant scaling paramters and pose the explanation of the observed scaling exponent x – by construction a fully universal number – as a problem to the theorists[23] Conversely, theorists may suggest a scaling exponent which can be put to test by checking whether the experminental data collapses on this exponent. Sumarising, one of the great virtues of the concept of scaling is that it condenses the information exchange between experiment and therory (and analytical theory and numerics for that matter) into a small set of universal *numbers*.

▷ INFO. For the sake of completeness we mention that, especially in the field theoretical community, the information encapsulated in the scale dependent correlation functions is often represented in a different manner. Starting out from

$$C(p_i, g_\alpha) = e^{nld_\phi} C(p_i e^l, g_\alpha(l)),$$

[22] For an n-dimensional data set, the collaps is to an $(n-1)$ dimensional functional set.

[23] In parentheses we note that the empirical collapse of experimental data onto scaling functions requires a lot of skill. E.g. if the data set consists of a number of functional 'patches' of only limited overlap, it is quite 'easy' to construct a scaling function of, in fact, almost any desired power law dependence. Data of this type tends to contain a lot of statistical uncertainty which can easily lead to erroneous conclusions.

where we have set $b = \exp(l)$, we can use the l-independence of the lhs to write

$$0 = \frac{d}{dl} e^{nld_\phi} C(p_i e^l, g_\alpha(l)).$$

(Notice that here we do not require to be in the asymptotic scaling regime, i.e. for the sake of the present construction, the l-dependence of the coupling constants need not be explicitly exponential.) We next carry out the l-differentiation to obtain

$$\boxed{\left(n\left(d_{\mathrm{e},\phi} + \frac{\eta}{2}\right) + \partial_l + \beta_\alpha(g_\alpha)\partial_{g_\alpha}\right) C(p_i e^l, g_\alpha(l)) = 0.} \tag{9.33}$$

Here, $d_{\mathrm{e},\phi}$ is the engeneering dimension of the field ϕ and $\eta/2 = d_\phi - d_{\mathrm{e},\phi}$ its anomalous dimension. (Cf. the definition of η in the infobox on p 386.) Further, the partial derivative ∂_l acts on the explicit scale dependence of the momentum arguments (or any other explicitly scale dependent argument for that matter.) Finally, $\beta_\alpha(g_\alpha)$ is the β-function defined above.

Eq. (9.33) is known as a **renormalization group equation**. Both the RG equation and the scaling form we used to derive it equivalently express the scaling behaviour of the correlation function.

Scaling Functions and Critical Exponents

Another important aspect of scaling theory is that it can be used to disclose relations between the seemingly independent[24] critical exponents of the theory. For the sake of concreteness, let us consider the case of the ferromagnetic transition, i.e. a transition we had previously characterised in terms of six critical exponents $\alpha, \ldots, \eta$ (cf. p 388.) However, the flow in the vicinity of the magnetic fixed point is controlled by only two relevant scaling fields, the (reduced) temperature, t and the reduced magnetic field $h \equiv H/T$. Neglecting irrelevant perturbations, we thus conclude that under a renormalization group transformation, the reduced free energy $f = F/TL^d$ will behave as[25]

$$f(t, h) = b^{-d} f(tb^{\lambda_t}, hb^{\lambda_h}).$$

We next fix $tb^{\lambda_t} = 1$ to reduce the number of independent variables to one:

$$f(t, h) = t^{d/\lambda_t} \tilde{f}(h/t^{\lambda_h/\lambda_t}). \tag{9.34}$$

Containing the full thermodynamic information, Eq. (9.34) is all we need to compute the critical exponents. Indeed, comparing with the definitions summarized on pp 388 it is

[24] After all, the critical exponents describe the behaviour of quite different physical observables in the transition region.

[25] Here we used that the reduced free energy does not carry an anomalous dimension. By definition, the free energy $F = -T \ln \mathcal{Z}$ does not change under renormalization (which after all merely amounts to representing the *number* $\mathcal{Z}$ through functional integrals of different space/time resolution.) Thus, the scaling of the reduced free energy is entirely carried by the prefactor L^{-d}.

straightforward to show that

$$\alpha = 2 - \frac{d}{\lambda_t}, \qquad \beta = \frac{d-\lambda_h}{\lambda_t}, \qquad \gamma = \frac{2\lambda_h - d}{\lambda_t},$$
$$\delta = \frac{\lambda_h}{d-\lambda_h}, \qquad \nu = \frac{1}{d_t}, \qquad \eta = 2 + d - 2\lambda_h, \tag{9.35}$$

from where follow the cross-relations summarized in the table on p 389 by direct comparison. These relations illustrate our previous assertion that conceptually the dimensions of the relevant scaling fields have a status more fundamental than the critical exponents.

▷ EXERCISE. Verify these statements. To obtain the fifth relation, notice that under a change of scale, $\xi \to b\xi$. On the other hand, $t \sim \xi^{-1/\nu}$. The sixth relation is obtained from Eq. (9.5). Just substitute the definition of the spatial profile of the correlation function in terms of the critical exponent η into the integral to obtain a relation between the critical exponents γ and η (In fact, Fisher's scaling law.)

9.4 Example III: RG Analysis of the Ferromagnetic Transition

In the previous section, we have got acquainted with some fundamental elements of the structure of RG analyses, and their connection to the theory of second order phase transition. The discussion was kept on a fairly general level and, therefore, may have been at times somewhat abstract. To illustrate the concepts introduced above on a concrete problem, and to introduce some more elements of RG theory, we now turn to the discussion of our third example, the ferromagnetic transition.

In section 6.1.2 we had introduced ϕ^4-theory as an effective low energy model of that phase transition. However, we did not yet *apply* the model to explore its universal properties. Rather we left – see the discussion of the beginning of this chapter – the analysis of the model in a state of despair. However, by now we have all the machinery needed to actually do something useful with the model to our availability. Indeed, we shall see that RG methods, and *only* RG methods, can be applied to successfully understand much of the intriguing behaviour displayed by the $(d > 2)$-dimensional Ising model in the vicinity of its phase transition. We now chose to set $tb^{\lambda_t} = 1$ to reduce the number of independent variables to one:

$$f(t,h) = t^{d/\lambda_t} \tilde{f}(h/t^{\lambda_h/\lambda_t}).$$

9.4.1 Preliminary Dimensional Analysis

The first question we wish to address has somewhat technical status: What was our justification to represent the Ising model in terms of the action[26]

$$S[\phi] = \int d^d r \left(\frac{r}{2}\phi^2 + \frac{1}{2}\partial\phi\partial\phi + \frac{\lambda}{4!}\phi^4 - h\phi \right) \tag{9.36}$$

in the first place, i.e. why was it possible to neglect both higher powers of the field ϕ and/or gradients that surely *are* present in the exact reformulation of the Ising problem in terms of ϕ-variables?

To understand the neglect of these terms we proceed by dimensional analysis. Anticipating that (see below) the 'real' dimensions carried by the operators in the action will be not too far from their engeneering dimension, we begin by exploring the latter. We proceed along the lines of the general scheme outlined in the previous chapter and designate dimension unity to the leading gradient term $\int \partial\phi^2$ in the action. This entails $[\phi] = L^{(2-d)/2}$ from where it is straightforward to attribute engeneering dimensions to all other operators:

$$\begin{aligned} \left[\int \phi^2\right] &= L^2, \qquad \left[\int \phi^4\right] = L^{-d+4}, \\ \left[\int \phi^n\right] &= L^{d+(2-d)n/2}, \qquad \left[\int (\partial^m\phi)^2\right] = L^{2(1-m)}. \end{aligned} \tag{9.37}$$

These relations tell us a lot about the prospected significance of all structurally allowed operators:

- ▷ the engineering dimension of the non-gradient operator $\sim \phi^2$ is positive in all dimensions indicating general relevance.
- ▷ The $\sim \phi^4$ operator is relevant (irrelevant) in dimensions $d < 4$ ($d > 4$). This suggests that for $d > 4$ an harmonic approximation ($\lambda = 0$) of the model should be reasonable. It also gives us a preliminary clue as to how we might want to approach the ϕ^4-model on a technical level: while for dimensions $d = 2, 3$ 'much' smaller than $d = 4$ the interaction operator $\sim \phi^4$ is strongly relevant, dimension $d = 4$ is borderline. This suggests to analyse the model at $d = 4$, or maybe 'close'[27] to $d = 4$ where the ϕ^4 operator is not yet *that* virulent, and then try to extrapolate at what happens at the 'physical dimensions' $d = 2, 3$.
- ▷ Operators $\sim \phi^{n>4}$ become relevant only in dimensions $d < (1/n - 1/2)^{-1} < 4$. However, even below these threshold dimensions, operators of high powers in the field variable are much less relevant than the dominant un-harmonic operator $\sim$

[26] Generalising our discussion from section 6.1.2, we here add the coupling to a static magnetic field to the action. (Exercise: recapitulate the construction of 6.1.2 to convince yourself that, to lowest order in an expansion in terms of ϕ, coupling the system to a magnetic field leads to the fourth term of Eq. (9.36). In case you are too unpatient to do this: justify the structure of the term on physical grounds.)

[27] As we shall see momentarily, the analysis of the problem is readily generalized to non-integer dimensions.

$\int \phi^4$. This is the a posteriori justification of our neglect of operators $\sim \phi^{n>4}$ in the derivation of the model.

- ▷ Similarly, operators with more than two gradients are generally irrelevant and can be neglected in all dimensions.
- ▷ In contrast, the operator $\sim \int \phi$ coupling to the magnetic field carries dimension $1 + d/2$ and is therefore always strongly relevant.

Dimensional analysis provides us with some valuable hints (see, however, the info box below) as to the importance of various operators appearing in the theory. It also indicates that in the present context dimension $d = 4$ might play a special role. Guided by this information, we next proceed to analyse the model in a sequence of steps of increasing sophistication.

9.4.2 Mean-Field Theory

Given an action like (9.36), the first thing we might try is a mean field analysis. That is, assuming that our coupling constants r, λ are sufficiently large we assume that the functional integration over ϕ is centered around solutions of the equation $\frac{\delta S[\phi]}{\delta \phi} = 0$, or

$$r\bar{\phi} + \frac{\lambda}{12}\bar{\phi}^3 - h = 0, \tag{9.38}$$

where we used that mean field configurations of low energy will be spatially constant.

Just by looking at a plot of the potential part of the field-free ($h = 0$) Lagrangian, $\sim \frac{r}{2}\phi^2 + \frac{\lambda}{4!}\phi^4$ it is clear that, depending on the sign of r, the mean field equation possesses two fundamentally different types of solutions. For $r > 0$, the action has a global minimum at $\phi = 0$, implying that $\bar{\phi} = 0$ is the unique mean field. Noticing that the amplitude of ϕ represents a measure of the magnetization of the system (which is clear from the way the ϕ^4-action was derived from the Ising model on pp 188)), we identify $r > 0$ as a phase of zero net magnetism, the **paramagnetic phase**.

In contrast, for $r < 0$, the action has two degenerate minima at non-zero values, $\bar{\phi} = \pm\phi_0 \equiv \pm(12|r|/\lambda)^{1/2}$. The system then has to make a choice as to whether it wants to sit in the ground state configuration $\bar{\phi} = \phi_0$ or $\bar{\phi} = -\phi_0$. This is the state of spontaneous symmetry breaking indicative of the low temperature **ferromagnetic phase**. (Notice that upon switching on a small magnetic field, the degeneracy between the two ground states gets lifted and the system will populate a state of predetermined magnetization, $\bar{\phi} = \pm\phi_0$, depending on the sign of h.)

The preliminary analysis above indicates that r has the status of a fundamental parameter tuning the system through the ferromagnetic transition point. Indeed, our microscopic analysis in section 6.1.2 had indicated that $r \sim T - T_c$ was a function of temperature that changed sign at some critical temperature T_c, the mean-field critical temperature of the transition. However, even if we didn't know the microscopics, it would be clear that $r(T)$ is (i) *some* function of temperature which (ii) must have a zero at some temperature $T = T_c$ (Otherwise there would be no transition to begin with.) At any rate, in the vicinity of $T = T_c$, $r \sim T - T_c$ represents our prime measure of the distance to the transition

point. (This observation is, in fact, in perfect agreement with our earlier observation that the operator $\int \phi^2$ coupled to r is *relevant*, see the discussion in section 9.3.2.)

What can mean field theory say about the prime descriptors of the transition, the **critical exponents**. Identifying the amplitude of ϕ (alias the magnetization) with the order parameter of the transition, and referring back to our list of exponents on p 388, the low temperature profile

$$|\bar{\phi}| = (12|r|/\lambda)^{1/2} \sim |t|^{1/2}$$

implies $\beta = 1/2$. (Here we have introduced $t \equiv (T - T_c)/T_c$ as the reduced temperature of the transition. The exponent γ is obtained by differentiating (9.38) with respect to h. With $\chi \sim \partial_h \phi$, it is then we then straightforward to verify that approaching the transition point from both sides, high and low temperatures,

$$\chi \sim |t|^{-1},$$

or $\gamma = 1$. The action evaluated on the mean field configuration reads as

$$S[\bar{\phi}] = L^d \left(\frac{r}{2}\bar{\phi}^2 + \frac{\lambda}{4!}\bar{\phi}^4 \right) \sim \begin{cases} \lambda^{-1}t^2 & t < 0 \\ 0 & t > 0 \end{cases} \tag{9.39}$$

With the mean field free energy $F = TS[\bar{\phi}]$ we find that the specific heat $C = -T^2\partial_T^2 F \sim \partial_t^2 S$ behaves like a step function at the transition point: $\alpha = 0$.

Right at the critical temperature, $r = 0$, the mean field magnetisation depends on h as $\bar{\phi} \sim h^{1/3}$ implying that $\delta = 3$. Finally, the correlation length exponents ν, η cannot really be computed from plain mean field theory as they are tied to the spatial profile of *fluctuating* field configurations.

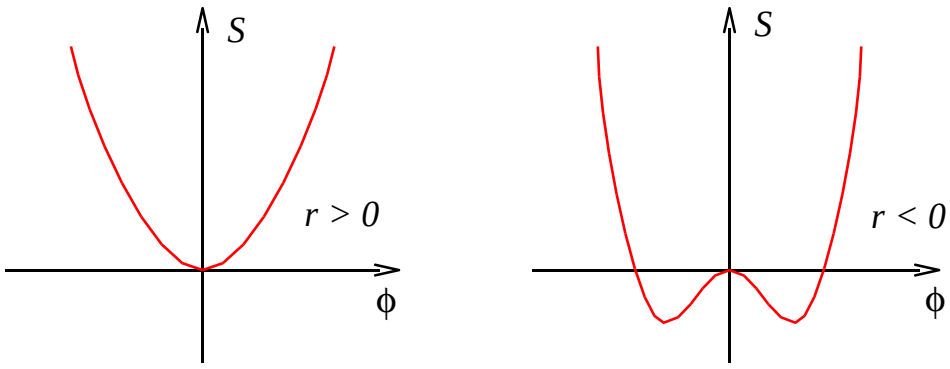

Figure 9.12: Action of the ϕ^4-theory evaluated on a constant field configuration above (left) and below (right) the transition point.

For the sake of later comparison, the mean field critical exponents are summarized in table 9.1. At first sight the differences between the experimentally observed exponents (first column) and the mean field exponents (second column) don't look dramatic – apparently the primitive mean field approach pursued here does not do *too* bad. Which, in view of the fact that the buildup of pronounced *fluctuations* is one of the hallmarks

of transition physics, should be a bit of a surprise. On the other hand we must keep in mind that the exponents describe singular power laws in the transition region. In view of that, the difference between 1.3 and 1 does look quite significant. At any rate, we should try to refine our theoretical understanding of the transition and explore whether better agreement with the experimental data can be achieved.

crit.exp.	experiment	mean field	Gaussian	ϵ^1	ϵ^5
α	0-0.14	0	1/2	1/3	.109
β	0.32-0.39	1/2	1/4	1/3	.327
γ	1.3-1.4	1	1	7/6	1.238
δ	4-5	3	5	4	4.786
ν	0.6-0.7	-	1/2	1	.631
η	0.05	-	0	0	.037

Table 9.1: Critical exponents of the ferromagnetic transition obtained through different methods. Experimental exponents represent cumulative data from various ferromagnetic substances.

9.4.3 Gaussian Model

The least we should do to improve on the mean field analysis is to integrate out quadratic fluctuations around the constant configuration $\bar{\phi}$. Approaching the transition point from above, we set $\bar{\phi} = 0$ and approximate the action through its quadratic expansion[28]

$$S[\phi] \approx \int d^d r \, \left(\frac{r}{2}\phi^2 + \frac{1}{2}\partial\phi\partial\phi - h\phi \right) \tag{9.40}$$

With this action, the further course of action seems to be clear. We should do the Gaussian integral and then evaluate the dependence of the free energy on the external parameters H and r. However, in anticipation of our analysis of the full problem below, we here pursue a slighly different, renormalization group oriented approach. I.e. pretending that we didn't know how to do the Gaussian integral, we will subject the quadratic action to a momentum shell RG analysis.

Proceeding along the lines of the canonical sheme, we split our field $\phi = \phi_s + \phi_f$ into a fast and a slow part, thereby causing the standard fragmentation of the action $S[\phi_s, \phi_f] = S_s[\phi_s] + S_f[\phi_f] + S_c[\phi_s, \phi_f]$. However, the crucial simplification characteristic for a Gaussian model is that the action S_c coupling fast and slow components, respectively, actually vanishes (why?), implying that the integration over fast field merely leads to an inessential constant. The effect of the RG step on the action is then entirely contained in the rescaling of the slow action. According to our previous discussion, the scaling factors

[28] The appearance of a linear term indicates that we are not expanding around the 'true' mean field, i.e. exact solution of (9.38), but rather around the solution $\bar{\phi} = 0$, of the field free system. However, in view of the fact that h has the status of an external perturbation, this choice of the reference configuration is quite natural.

thus appearing are determined by the *engineering* dimensions of the operators appearing in the action, i.e. (cf. Eq. (9.37)),

$$r \to b^2 r, \qquad h \to b^{d/2+1} h.$$

Using that $r \sim t$ we can then readily write down the two relevant scaling dimensions of the problem, $\lambda_t = 2$ and $\lambda_h = d/2 + 1$. Comparison with Eq. (9.35) finally leads to the list of exponents,

$$\alpha = 2 - \frac{d}{2}, \qquad \beta = \frac{d}{4} - \frac{1}{2}, \qquad \gamma = 1,$$
$$\delta = \frac{d+2}{d-2}, \qquad \nu = \frac{1}{2}, \qquad \eta = 0.$$

Notice that the exponents now explicitly depend on the dimensionality of the system, a natural consequence of the fact that they describe the effect of spatial flucutuations. The second column of table 9.1 contains the values of the exponents for a three dimensional system. We cannot really say that the results are any better than those obtained by mean field analysis. Some exponents (e.g. δ) agree better with the experimental data, others (e.g. α) decidedly worse.

As a corrolary to this section, we note that the Gaussian model possesses only one fixed point, viz. $r = h = 0$ which in the context of ϕ^4-theory is called the **Gaussin fixed point**.

9.4.4 Renormalization Group Analysis

In our so far analysis of the model, we have not really touched upon its principal source of complexity, the effect of the 'interaction operator' $\sim \phi^4$ on the fluctuation behaviour of the field. It is likely that the neglect of this aspect holds responsible for the comparatively poor predicitve power of both the straightforward mean field analysis and of the Gaussian model. Indeed, the dimensional analysis of section 9.4.1 indicated that the ϕ^4 addition to the action becomes relevant below four dimensions. A more physical argument to the same effect is given in the info box below.

Although the solution of the general problem posed by the action (9.36) still appears to be hopelessly difficult, there is one aspect we can turn to our advantage. While physical systems exist in integer dimensions $d = 1, \ldots, 4, \ldots$, there is actually no reason why we shouldn't be allowed to evaluate our theoretical model description, i.e. the functional integral with action (9.36), in *fractional dimensions*. In the present context, this seemingly academic freedom turns out to be of concrete practical relevance. The point is that we found the non-linear ϕ^4-operator to be marginal at $d = 4$ and relevant below. One may thus expect that in dimensions $d = 4 - \epsilon$, $\epsilon \ll 1$ the operator is relevant but not *that* relevant. I.e. the hope is that for sufficiently small deviations off the threshold dimension four, the theory knows of an expansion parameter, somehow related to ϵ, which will enable us to get the effect of the interaction operator under control. Of course, in the end of the day we will have to 'analytically contiune' to dimensions of interest, $\epsilon = 1$ or even $\epsilon = 2$, but for the moment we shall thrust aside that formidable perspective and see what we can learn from a $d = 4 - \epsilon$ representation of the theory.

▷ INFO. Our previous analysis relied on the presumption that the field integration is tightly bound to the vicinity of the extrema of the action. But let's now ask under what conditions, this assumption is actually justified. What we should do is develop some opinion as to the relative importance of the mean field content of the theory and of the **fluctuations around the mean field**, respectively. There are several ways of doing so, and the one we will pursue here is based on an analysis of the magnetic susceptibility of the system. (At this point, we should like to warn the reader that the arguments formulated below, while technically straightforward, are conceptually involved. I.e it is certainly well invested time to critically contemplate the logics of the construction in each of its steps.)

We recall that the susceptibility is defined by

$$\chi = -\partial_H^2 F \sim \int d^d r \langle \phi(\mathbf{r})\phi(0)\rangle_c \sim G(\mathbf{k}=0),$$

where we used that $\langle \phi(\mathbf{r})\phi(\mathbf{r}')\rangle = G(\mathbf{r}-\mathbf{r}')$ is the Green function of the model. Given this identification, we note that a formal criterion of the transition – divergent susceptibility! – is a singularity of the zero momentum Green function.

On the level of the Gaussian theory (see Eq. (9.40)) $G(\mathbf{k}) = (r+k^2)^{-1}$, i.e. $\chi \sim r^{-1}$. In foresight of troubling observations to come, we re-iterate that the mean field transition temperature is identified by the condition $r \sim t = 0$. Now, lets move on to explore corrections to the mean field susceptibility on the level of a perturbative one-loop calculation. To this end we remember that (if necessary, recapitulate the discussion of 6) that due to the presence of the ϕ^4 operator the Green function acquires a self energy which, at the one-loop level is given by

$$\Sigma = -\frac{\lambda}{2}\sum_{\mathbf{k}'}\frac{1}{r+k'^2}.$$

As a consequence, the susceptibility now estimates to

$$\chi^{-1} \sim (G(\mathbf{k}=0))^{-1} = r - \Sigma = r + \frac{\lambda}{2}\sum_{\mathbf{k}'}\frac{1}{r+k'^2}.$$

A first observation to be made is that non-Gaussian fluctuations (physically: interactions between harmonic fluctuations around the mean field amplitude) lower the transition amplitude, i.e. setting $r \sim T - T_c$ it now takes a smaller temperature T to reach the transition point; quite in accord with intuitive expectation, fluctuations tend to 'disorder' the system.

Irritatingly, we also observe that the cutoff Λ is needed to prevent the 'correction'

$$-\frac{\lambda}{2}\sum_{\mathbf{k}'}\frac{1}{r+k'^2} \sim \lambda\int^{\Lambda} d^d k' \frac{1}{r+k'^2}$$

from diverging in dimensions $d \geq 2$. To qualifiedly deal with this singularity, we have to realize that the effect of fluctuations is actually twofold: the transition temperature gets shifted *and* the temperature dependence of the inverse susceptibility is apparently no longer plain linear (by virtue of the r-dependence of the integrand.) The two effects can be disentangled by writing

$$\begin{aligned}\chi^{-1} &= \tilde{r} + \frac{\lambda}{2}\left(\frac{L}{2\pi}\right)^d \int^{\Lambda} d^d k' \left(\frac{1}{r+k'^2} - \frac{1}{k'^2}\right) = \\ &\approx \tilde{r} - \frac{\lambda\tilde{r}}{2}\left(\frac{L}{2\pi}\right)^d \int^{\Lambda} d^d k' \frac{1}{(\tilde{r}+k'^2)k'^2},\end{aligned} \tag{9.41}$$

where

$$\tilde{r} \equiv r + \frac{\lambda}{2}\left(\frac{L}{2\pi}\right)^d \int^{\Lambda} \frac{d^d k'}{k'^2}$$

represents the shifted transition temperature while the integral describing the deviation from the linear temperature dependence of the susceptibility is now UV-convergent in dimensions $d < 4$. Notice that in the second line of (9.41) we have replaced the parameter r in the integrand by the modified parameter $\tilde{r}$. To the accuracy of a one-loop calculation, this manipulation is permissible.

Naively, it looks as if our so-far manipulations have led us right away into a catastrophy: the flucutation-renormalized transition temperature appears to diverge as we send the cutoff to infinity, clearly a non-sensical prediction! However, a second thought shows us that this worry is based on prejudiced thinking. The point is that we had actually no justification to identify the *physical* transition temperature through the parameter r of the action in the first place. This identification was based on mean field theory alone, i.e. an approach to the problem altogether neglecting the key effect of fluctuations. However, the bare parameter r appearing in the action carries as little 'universal' meaning as the cutoff Λ or any other microscopic system parameter for that matter!

Once we have accepted this view on the problem, we should identify the transition temperature through the singularity of macroscopically observable system properties (e.g. divergence of the susceptibility $\rightsquigarrow$ (one-loop level) vanishing of modified parameter $\tilde{r}$) while the microscopic parameters carry now significance by themselves.

▷ EXERCISE. This interpretation of the problem actually closely parallels the philosophy of renormalization in high energy physics. There, the bare parameters of the action are *fundamentally* undetermined, while the inverse of the Green function at zero external momentum represents a physical observable, e.g. the mass of the electron. Since the loop corrections of to this latter quantity appear to be infinite (and the theory does not enjoy the luxury of the presence of a physically motivated cutoff), one *postulates* that the bare parameters of the action have been infinite by themselves. These singularities are deliberately adjusted so as to cancel the divergence of the fluctuation corrections and to produce finite 'physical' quantities.

Consult a textbook on renormalization in high energy physics (e.g. [**?**]) to get acquainted with the functioning of this strategy, and with the enormous success it had in the context of QED and other sub-branches of particle physics.

We next turn to the second effect of the fluctuation correction, viz. the deviation from the linear temperature dependence, as described by the integral contribution to (9.41). On dimensional grounds, the integral depends on the parameter $\tilde{r}$ as $\sim \lambda L^d \tilde{r}^{(d-2)/2}$. The (mean field + quadratic fluctuations) approach to the problem breaks down when this contribution becomes more important than the leading order contribution to the susceptibility, i.e. for dimensions $d \leq 4$. This observation is the essence of the so-called **Ginzburg criterion**. The criterion states that mean field theory becomes inapplicable below the so-called **upper critical dimension** $d_c = 4$. While we have derived this statement for the particular case of the ϕ^4 model, it is clear that similar estimates can be done for every non-linear field theory. I.e. Like the lower critical dimension, the upper critical dimension, too, represents an important threshold separating between mean field dominated $d > d_c$ and flucutation dominated $d < d_c$ behaviour. Also notice that the analysis above conforms with our previous observation that the non-linear ϕ^4-operator is relevant in dimensions $d < 4$. (Convince yourself that the two lines of arguments

reflect the same principle, viz. the dependence of fluctuations on the accessible phase volume, as determined by the dimensionality of the system.)

Before proceeding to the details of the RG program, let us try to predict a number of general elements of the ϕ^4 phase diagram on dimensional grounds. We saw that in dimensions $d > 4$ the ϕ^4-operator is irrelevant and the Gaussian model essentially dictates the behaviour of the system. Specifically, for $d > 4$ the Gaussian fixed point $r = \lambda = h = 0$ is the only fixed point of the system. Below four dimensions, the ϕ^4-operator becomes relevant and the emergence of a richer fixed point structure may be expected. However, for $\epsilon = 4 - d$ sufficiently small, we also expect that whatever new fixed points appear, they should be close to the Gaussian point. Which means that we can conduct our search for new fixed points within a double expansion in ϵ, and the small deviation of the coupling constants u, λ, h around the Gaussian fixed point. (In fact, we will momentarily identify a *third* expansion parameter, viz. the number of momentum loops appearing in fast field integration.)

Step I:

We next proceed to formulate the RG step in detail. To keep things simple, the RG transformation will be carried out to lowest order in a triple expansion in ϵ, the coupling constants, and the number of momentum loops. The rational behind the loop expansion can be best understood if we assume that the entire action[29] was multiplied by a large parameter (which, in the case of a quantum theory might be $\hbar^{-1}$.) The expansion in the number of loops is then equivalent to an expansion in the inverse of that parameter (for a quantum theory, an expansion away from the classical limit.)

▷ EXERCISE. Verify this statement. To this end, notice that a diagram of nth order in perturbation theory in the ϕ^4 vertex contains a prefactorial power a^n of our large parameter. On the other hand, each of the I internal lines, or propagators, contained by the diagrams contributes a factor a^{-1}, so that the overall power is a^{n-I}. Next relate the number of internal lines to the number L of loops. To this end, notice that each line corresponds to a momentum summation. However, the number of independent summations is constraint by the n δ-functions carried by the vertices. Use this information to show that the overall power of the graph is a^{-L+1}, i.e. an expansion in L is equivalent to an expansion in the inverse of a.

Having said this, we decompose our action in the standard manner, $S[\phi_s, \phi_f] = S_f[\phi_f] + S_s[\phi_s] + S_c[\phi_s, \phi_f]$, where

$$S_f[\phi_f] = \int d^d r \, \left(\frac{r}{2}\phi_f^2 + \frac{1}{2}\partial\phi_f \partial\phi_f \right),$$

$$S_s[\phi_s] = \int d^d r \, \left(\frac{r}{2}\phi_s^2 + \frac{1}{2}\partial\phi_s \partial\phi_s + \frac{\lambda}{4!}\phi_s^4 - h\phi_s \right),$$

$$S_c[\phi_s, \phi_f] = \frac{\lambda}{4} \int d^d r \, \phi_s^2 \phi_f^2 + \ldots .$$

[29] before we rescaled the fields so as to make the leading order coefficient equal $1/2$.

Several approximations related to the loop order of the expansion are imposed already at this level. We neglected terms of $\mathcal{O}(\phi_f^4)$ because their contration leads to two loop diagrams. The same for (think about it) terms of $\mathcal{O}(\phi_s\phi_f^3)$. Terms like of $\mathcal{O}(\phi_s^3\phi^f)$ do not arise because the addition of a fast momentum and three slow momenta can hardly add to zero total momentum.

Step II:

To simplify the notation, we rescale momentum according to $\mathbf{q} \to \mathbf{q}/\Lambda$ implying that coordinates are measured in units of the inverse cutoff $\mathbf{r} \to \mathbf{r}\Lambda$. With the coupling constants rescaled according to their engineering dimensions,

$$\begin{aligned} r &\to r\Lambda^2, \\ \lambda &\to \lambda\Lambda^{4-d}, \end{aligned}$$

the action remains unchanged, only that the fast and slow momenta are now integrated over the dimensionless intervals $|\mathbf{q}_s| \in [0, b^{-1}]$ and $|\mathbf{q}_f| \in [b^{-1}, 1]$, respectively.

We next construct an effective action by integration over the fast field:

$$\exp(-S_{\text{eff}}[\phi_s]) = \exp(-S_s[\phi_s]) \left\langle \exp(-S_c[\phi_s, \phi_f]) \right\rangle .$$

In doing the fast action average, $\langle \ldots \rangle$, we shall (a) retain only contributions of one-loop order while (b) neglecting terms which lead to the appearance of $\phi_s^{n>4}$ contributions in the action. (E.g., the contraction $\left\langle \left(\int \phi_s^2 \phi_f^2 \right)^3 \right\rangle$ would lead to such a term.) To this approximation (this step definitely asks for thorough contemplation!)

$$\exp(-S_{\text{eff}}[\phi_s]) = \exp(-S_s[\phi_s]) \exp\left(-\langle S_c[\phi_s, \phi_f] \rangle + \frac{1}{2} \left\langle S_c[\phi_s, \phi_f]^2 \right\rangle_c \right),$$

where, as usual, the subscript 'c' indicates a connected average. The two diagrams correspoding to the contractions $\langle S_c[\phi_s, \phi_f] \rangle$ and $\langle S_c[\phi_s, \phi_f]^2 \rangle_c$ are shown in the top and bottom part of the figure, respectively, where the sturdy line segments indicate the passive ϕ_s amplitudes. According to the standard rules of perturbation theory, the first of the two diagrams evaluates to

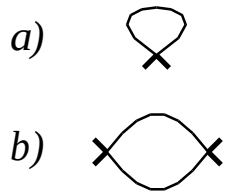

$$\langle S_c[\phi_s, \phi_f] \rangle = \frac{\lambda}{4} \int_f (dq') \frac{1}{r + q'^2} \int_s (dq) \phi_s(\mathbf{q}) \phi_s(-\mathbf{q}),$$

where we have introduced the shorthand notation $(dq) \equiv \frac{d^d q}{(2\pi)^d}$. We next consider the summation over fast momenta appearing in this expression. Using that we are in close vicinity to the transition, $r \ll b^{-1}$, and anticipating that we are interested in no more than the expansion of the β-function for small values of the coupling, we expand the integrand to first order in r,

$$\int_f (dq) \frac{1}{q^2 + r} = I_1 - r I_2,$$

where we have introduced the shorthand notation,

$$I_\alpha \equiv \int_f (dq) \frac{1}{q^{2\alpha}}.$$

These integrals are straightforwardly computed by switching to polar coordinates,

$$I_\alpha = \Omega_d \int_{b^{-1}}^{1} q^{d-2\alpha-1} dq = \frac{\Omega_d}{d-2\alpha}(1-b^{2\alpha-d}).$$

where $\Omega_d = (2\pi^{d/2}/\Gamma(d/2))/(2\pi)^d$ is the volume of the d-dimensional unit-sphere (measured in units of 2π). We thus find that after the integration over fast modes, and the standard rescaling operation,

$$\begin{aligned} q &\to bq, \\ \phi &\to b^{(d-2)/2}\phi, \end{aligned}$$

the quadratic part of the action reads as

$$S^{(2)}[\phi] = \frac{b}{2}\left(r + \frac{\lambda\Omega_d}{2(d-2)}(1-b^{2-d}) - \frac{r\lambda\Omega_d}{2(d-4)}(1-b^{4-d}) \right) \int d^d r\, \phi^2. \tag{9.42}$$

Turning to the diagram b) shown above, we notice that, owing to the presence of four external legs, its contribution will be proportional to ϕ_s^4. Further, momentum conservation implies that the momenta carried by the internal lines of the diagram will depend on both, the fast 'internal' momentum and the external momenta carried by the fields ϕ_s. However, we can simplify our life by neglecting the latter dependence from the outset. The reason is that integration over the internal momentum followed by Taylor expansion in the slow momenta would generate expressions of the architecture, $F(\mathbf{q}_1, \mathbf{q}_2, \mathbf{q}_3)\phi(\mathbf{q}_1)\phi(\mathbf{q}_2)\phi(\mathbf{q}_3)\phi(-\mathbf{q}_1-\mathbf{q}_2-\mathbf{q}_3)$, where $\mathbf{q}_{1,2,3}$ are slow momenta and F is some polynomial. Account for the small momenta would thus generate *derivatives* acting on an operator of fourth order in ϕ, a combination that we saw above is strongly irrelevant.

Neglecting the external momenta, diagram b) evaluates to

$$\frac{1}{2}\langle S_c[\phi_s, \phi_f]^2 \rangle \simeq \frac{\lambda^2}{8} \int d^d r\, \phi_s^4 \int_f (dq) \frac{1}{q^2+r} = \frac{\lambda^2 I_2}{8} \int d^d r\, \phi_s^4 + \mathcal{O}(\lambda^2 r).$$

Evaluating the integral and rescaling we find that the quartic contribution to the renormalized action reads as

$$S^{(4)}[\phi] = b^{4-d}\left(\frac{\lambda}{4!} - \frac{\lambda^2\Omega_d}{8}\frac{1-b^{4-d}}{d-4} \right) \int d^d r\, \phi^4.$$

Finally, there are no one-loop diagrams affecting the linear part of the action, i.e.

$$S^{(1)}[\phi] = h b^{d/2+1} \int d^d r\, \phi$$

rescales according to its engeneering dimension.

Combining everything, we find that to one loop order, the coupling constants change as

$$
\begin{aligned}
r &\to b^2 \left(r + \frac{\lambda \Omega_d}{(d-2)}(1-b^{2-d}) - \frac{r\lambda\Omega_d}{(d-4)}(1-b^{4-d}) \right) \\
\lambda &\to b^{4-d} \left(\lambda - 3\lambda^2 \Omega_d \frac{1-b^{4-d}}{d-4} \right) \\
h &\to h b^{d/2+1}.
\end{aligned}
$$

We next set $d = 4 - \epsilon$ and evaluate the rhs of these expressions to lowest order in an expansion in powers of ϵ. With $\Omega_{4-\epsilon} \approx \Omega_4 = \frac{1}{16\pi^2}$, we thus obtain

$$
\begin{aligned}
r &\to b^2 \left(r + \frac{\lambda \Omega_4}{2}(1-b^{-2}) - r\lambda\Omega_4 \ln b) \right) \\
\lambda &\to (1+\epsilon \ln b) \left(\lambda - 3\lambda^2 \Omega_4 \ln b \right) \\
h &\to h b^3.
\end{aligned}
$$

which, setting $b = \exp l$, leads to the **Gell-Mann-Low equations**

$$
\boxed{
\begin{aligned}
\frac{dr}{dl} &= 2r + \Omega_4 \lambda - \Omega_4 \lambda r \\
\frac{d\lambda}{dl} &= \epsilon\lambda - 3\Omega_4 \lambda^2 \\
\frac{dh}{dl} &= \frac{6-\epsilon}{2} h.
\end{aligned}
} \tag{9.43}
$$

These equations clearly illustrate the meaning of the ϵ-expansion. According to the second equation, a perturbation away from the Gaussian fixed point will initially grow at a rate set by the engeneering dimension ϵ. While on the level of the classical, zero loop theory, λ would grow indefinitely, the one-loop contribution $\sim \lambda^2$ stops the flow at a value $\lambda \sim \epsilon$.

Equating the rhs of (9.43) to zero (and temporarily ignoring the magnetic field), we indeed find that besides the Gaussian fixed point $(r_1^*, \lambda_1^*) = (0,0)$ a nontrivial second fixed point $(r_2^*, \lambda_2^*) = (-\frac{1}{6}\epsilon, \frac{1}{3\Omega_4}\epsilon)$ has appeared. Notice that, in accord with the schematic considerations made in the beginning of the section, the second fixed point is of $\mathcal{O}(\epsilon)$ and coagulates with the Gaussian fixed point as ϵ is sent to zero. Plotting the β-function for the coupling constant λ we further find that for $\epsilon > 0$, λ is relevant around the Gaussian fixed point but irrelevant at the non-trivial fixed point.

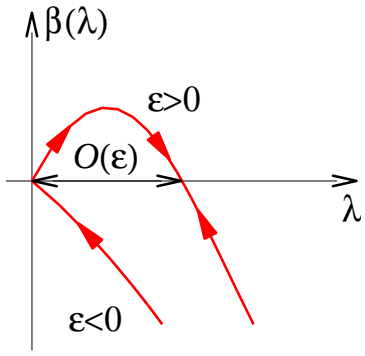

To understand the full flow diagram of the system, we linearize the β-function around both the Gaussian and the non-trivial fixed point. Denoting the linearized mappings by

$W_{1,2}$, we find

$$W_1 = \begin{pmatrix} 2 & \Omega_4 \\ 0 & \epsilon \end{pmatrix}, \qquad W_2 = \begin{pmatrix} 2 - \frac{1}{3}\epsilon & \Omega_4 \\ 0 & -\epsilon \end{pmatrix}.$$

Fig. 9.13 shows the flow in the vicinity of the two fixed points, as described by the matrices $W_{1,2}$ as well as the extrapolation to a global flow chart. Notice that the critical surface of the system – the straight line interpolating between the two fixed points – is tilted with respect to the $r \sim$ temperature axis of the phase diagram. Which implies that it is not the physical temperature alone that decides whether the system will eventually wind up in the paramagnetic ($r \gg 0$) or ferromagnetic ($r \ll 0$) sector of the phase diagram. We rather have to relate temperature ($\sim r$) to the strength of the non-linearity ($\sim \lambda$) to decide on which side of the critical surface we are. E.g. for λ strong enough, even a system with r initially negative may eventually flow towards the disordered phase. This type of behaviour cannot be predicted from the mean field analysis of the model (which would generally predict a ferromagnetic state for $r < 0$), it rather represents a non-trivial effect of fluctuations. Finally notice that while we can formally extend the flow into the lower portion of the diagram, $\lambda < 0$, this region is actually unphysical. The reason is that for $\lambda < 0$, the action is fundamentally unstable and does not describe a physical system.

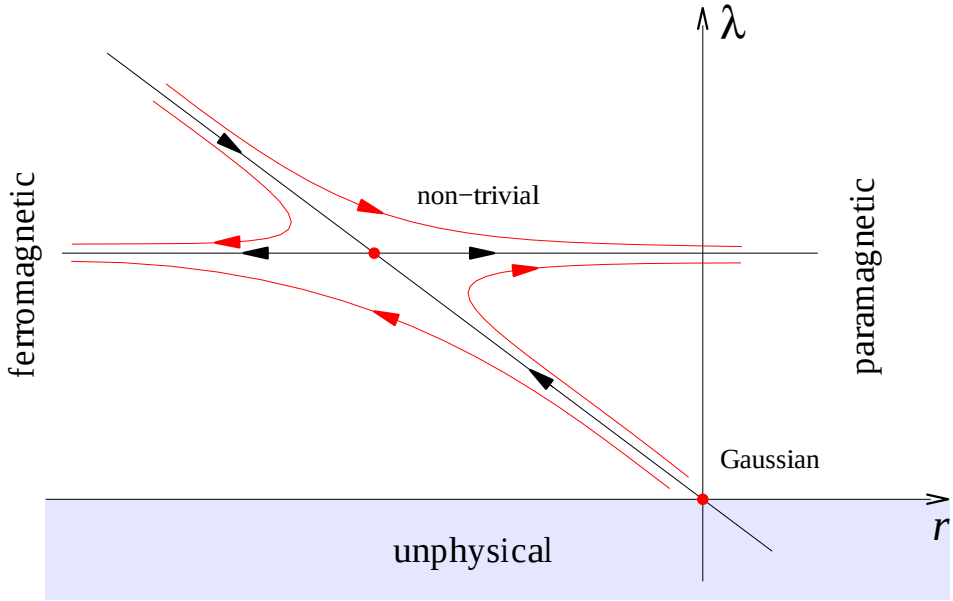

Figure 9.13: Phase diagram of the ϕ^4-model as obtained from the ϵ-expansion.

What are the crititical exponents of the one-loop approximation? Of the two eigenvalues of W_2, $2 - \epsilon/3$ and $-\epsilon$, only the former is relevant. As with the Gaussian fixed point, it is tied to the scaling of the coupling constant $r \sim t$, i.e. we have $\lambda_t = 2 - \epsilon/3$ and, as before, $\lambda_h = (d+2)/2 = (6-\epsilon)/2$. An expansion of the exponents summarized in Eq. (9.35) to first order in ϵ then yields the list

$$\alpha = \frac{\epsilon}{3}, \qquad \beta = \frac{1}{2} - \frac{\epsilon}{6}, \qquad \gamma = 1 + \frac{\epsilon}{6},$$
$$\delta = 3 + \epsilon, \qquad \nu = \frac{1}{2} + \frac{\epsilon}{2}, \qquad \eta = 0,$$

If we are now reckless enough to extend the radius of the expansion to $\epsilon = 1$, i.e. $d = 3$, we obtain the third column of table 9.1. Apparently the agreement with the experimental results has improved! And that in spite of the fact that we have driven the ϵ expansion far beyond its range of applicability. (For $\epsilon = 1$, terms of $\mathcal{O}(\epsilon^2)$ can our course no longer be neglected!)

How can we understand that the ϵ-expansion does so remarkably well? Trusting in the principle that good theories tend to work well beyond their regime of applicability, we might simply speculate that nature seems to be sympathetic to the concept of renormalization and the loop expansion. Of course, a more qualified approach to the question is to explore what happens at higher order in the ϵ-expansion. Needless to say that the price to be paid for this ambition is that at orders $\mathcal{O}(\epsilon^{n>1})$, things get quite laborious. Nonetheless, the success of ev, and therefore favourable results are obtaineden the first order expansion prompted people to drive the ϵ-expansion up to fifth order! The results of this analysis are summarized in the last column of table 9.1. In view of the fact that we are still extending a series beyond its radius of convergence[30] the level of agreement with the experimental data is absolutely striking. In fact, the exponents obtained by the ϵ-expansion even agree (to an accuracy better than one percent!) with the numerically observed exponents of the *two*-dimensional model, i.e. for a situation where the 'small' parameter ϵ has to be set to two.

However, it is important to realize that the ϵ-expansion is not just a comoputational tool for the calculation of exponents. On a more conceptual level, its merit is that it enables us to explore the phase diagram of non-linear theories in a more or less controlled manner. In fact, the ϵ-expansion is not only useful in the study of field theories close to the *upper* critical dimension (i.e. close to the mean field threshold) but can equally well applied to the analysis of systems in the vicinity of the *lower* critical dimension (the dimension marking the onset of global thermal disorder, see the problem set.)

With these remarks we conlude our preliminary discussion of the ϵ-expansion and its application to the ferromagnetic transition. We next turn to the RG analysis of an altogether different type of phase transitions, viz. *topological* transitions whose existence is limited to certain integer dimensions (and therefore not accessible in terms of ϵ-expansion schemes.)

9.5 Example IV: Berezinsky-Kosterlitz-Thouless Transition

Most of the theories discussed in previous chapters were defined on essentially structureless, target spaces – the real line, the complex plane, or, more generally, vector spaces of arbitrary dimensionality. Although we already met with a number of models with more complex target manifolds (e.g., the superconductor, or the Luttinger action with fields defined on the unit circle) the geometric structure of the target space never played that much of a role.

[30] Indeed, it is believed that we are dealing with a series that is only asymptotically convergent. I.e. beyond a certain order of the expansion, the agreement with the 'true' exponents will presumably become worse.

In fact, however, the large scale geometry, or topology of its field manifold may have striking influence on the long range behaviour of a system and it is one of the objectives of the present section to illustrate that phenomenon on a particular example. (A more comprehensive account of the role of geometry and topology in quantum field theory will be given in the next chapter.)

Consider, then, a two-dimensional square lattice with a phase like variable $\exp(i\phi_i) \in S_1$ defined on each of its sites i. Demanding that the action of the system be periodic in all ϕ_i^s and minimal on homogeneous field configurations, the most elementary action we can formulate reads as

$$S[\phi] = -J \sum_{\langle ij \rangle} \cos(\phi_i - \phi_j), \tag{9.44}$$

where $\sum_{\langle ij \rangle}$ is the usual sum over nearest neighbours. Eq. (9.44) is known as the action of the **two-dimensional xy-model**. To motivate this denotation, think of ϕ_i as an angle parameterizing the direction of a uni-modular vector (a classical 'spin') in the two-dimensional xy-plane. Indeed, the model (9.44) can be looked at as a two-dimensional descendent of the classical Heisenberg model, i.e. as a model where the Heisenberg spin is confined to a two dimensional plane (this condition *is*, in fact, realized for a number of magnetic materials.)

▷ INFO. Besides its natural occurance in magnetism, the xy-model finds a plenty of other **applications** in condensed matter physics. By way of example, we mention the physics of granulated metals and Josephson junction arrays.

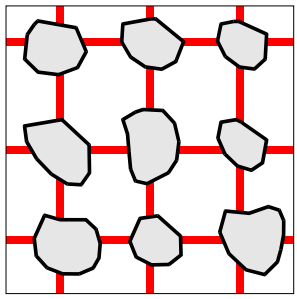

Imagine a system of small metallic (or superconducting) islands which are connected by poorly conducting tunneling barriers. (Arrays of this structure are believed to mimic the mesoscopic morphology of structurally disordered metals. However, they can also be manufactured artifically, with islands as small as several nm.) On a microscopic level, the state of the system is essentially determined by the number N_i of electronic charges populating each island i. However, unless the inter-grain tunneling conductance, g_T, is ultra-small (meaning $g_T < e^2/h$, the fundamental quantum unit of conductance), temporal fluctuations of the charge degrees of freedom are vast.

It is then more favourable to characterize the state of the system in terms of the variable canonically conjugate to the charge variable, i.e. the phase ϕ_i. (Remember that $[\phi_i, N_j] = \delta_{ij}$ form a canonically conjugate pair.) The model action $S[\phi]$ then of course depends on the microscopic structure of the system. However, for the case of a superconductor array in the classical limit ($\phi(\tau) = $ const.), and neglecting charging effects, the action collapses to the xy-action shown above. (Recapitulate the structure of the single-junction Josephson action to convince yourself that this is true.)

———————————————————

Q1 density-density correlation function of the $1d$-electron gas.

Q2 microscopic derivatsity correlation function of the $1d$-electron gas.

Q3 microscopic ion of the Luttinger action. ec

Q4 intuitive interpretation of the bosonic fermion representation.

Q5 Luttinger RG for strong backscattering.

Q6 RG analysis of $O(n)$-model